Universidad de Huelva

Departamento de Geología



Mineralogía, petrología y geoquímica de intrusiones sin-volcánicas en el distrito minero de Skellefte, Norte de Suecia
Mineralogy, petrology and geochemistry of syn-volcanic intrusions in the Skellefte mining district, Northern Sweden

Memoria para optar al grado de doctor
presentada por:

Manuel Jesús González Roldán

Fecha de lectura: 17 de marzo de 2010

Bajo la dirección de los doctores:

Emilio Pascual Martínez
Teodosio Donaire Romero
Rodney L. Allen

Huelva, 2010

ISBN: 978-84-92944-24-8
D.L.: H 253-2010

PARTE 2:

RESUMEN EN INGLÉS / ABSTRACT

I. INTRODUCTION 185

IV. GEOLOGICAL SETTING 186
IV.1. Geological History of Fennoscandia 186

IV.2. Skellefte Mining District 188
IV.2.1. Skellefte Group 188
IV.2.2. Vargfors Group 189
IV.2.3. Bothnian Group 189
IV.2.4. Arvidsjaur Group 189
IV.2.5. Intrusions in the Skellefte district 189

V. PETROGRAPHY 193
V.1. General Petrography 193
V.1.1. Hand specimen sample description 193
V.1.1.1. Modal study of intrusion in JGC 198

V.1.2. GI phase of JGC 199
V.1.2.1. Petrographic description of GI 199
V.1.2.2. Deformation of GI 201
V.1.2.3. Alteration of GI 201

V.1.2.4. Metamorphism of JGC 203
V.1.2.4.1. Metamorphic biotite in GI 203
V.1.2.4.2. Metamorphic amphibole in GI 204
V.1.2.4.3. Metamorphic quartz in GI 204

V.1.3. GII phase of JGC 204
V.1.3.1. Petrographic description of GII 204
V.1.3.2. Alteration of GII: uralitisation 205

V.1.4. GIII phase of JGC 206
V.1.5. GIV phase of JGC 206
V.1.6. Näsberget Layered Intrusion 206
V.1.7. Gabbros and diorites un-differentiated 207

V.1.8. Porphyritic Basalts 207
V.1.8.1. Andesite basalts: southern boundary 208
V.1.8.2. Andesite basalts deformation: southern dike 208

V.1.9. Gallejaur Monzonite 208

V.1.10. Viterliden Intrusive Complex 209
V.1.10.1. VIC deformation 209
V.1.10.2. VIC metamorphism 210

V.1.11. Revsund-type granitoids 210

V.1.12. Stavaträsk 211
V.1.12.1. Contact metamorphism of Stavaträsk pluton 211

V.3. Extension and phases of JGC 212
V.3.1. Limits of the Jörn Granitoid Complex 212
V.3.2. Southern boundary of JGC and Southern Dike 213
V.3.3. Phases distribution in the JGC 214

VI. LITHOGEOCHEMISTRY 216
VI.1. Major elements variation diagrams 217
VI.1.1. Harker diagrams 217

VI.1.2. Major elements classification 218
VI.1.2.1. Geochemical classification of granitoids 221

VI.1.3. Major element JGC and other intrusions comparison 222

VI.2. CIPW Norm Calculation 226

VI.3. Trace Elements Lithogeochemistry 229
VI.3.1. REE comparison of JGC and intrusions in Skellefte District 234
VI.3.2. Tectonic setting discrimination diagrams 239

VI.4. Isotopic Lithogeochemistry 241

VII. U-PB ZIRCON AND TITANITE DATING 245
VII.1. New U-Pb zircon and titanite dating in JGC 245
V.1.1. U-Pb zircon and titanite dating 246
V.1.2. Summary of the new U-Pb zircons and titanite dating 251

VII.2. Chemical mineralogy of zircons 253

VII.3. Chemical maps of zircons 253

VIII. DISCUSSION 255
VIII.1. Revision of Limits and Phases of Jörn Granitoid Complex 255
VIII.1.1. Distribution of phases in JGC 255
VIII.1.2. Lithogeochemical characteristics and age of JGC 256

VIII.2. Comparison of Phases in JGC with Intrusions in Skellefte District 257
VIII.2.1. Relationships between GI and satellite intrusions of JGC 257
VIII.2.2. The Hobergsliden and Antak intrusions in JGC 258
VIII.2.3. VIC and Stavaträsk intrusions compares with JGC 259

VIII.3. JGC and Volcanic Rocks of Skellefte Group 260
VIII.3.1. Comparison between JGC and Maurliden volcanic rocks 260
VIII.3.2. Comparison of JGC and volcanic rocks of Petikträsk South 261
VIII.3.3. Comparison between JGC and Tallberg 262
VIII.3.4. Age of volcanic rocks in the Skellefte mining district 262

VIII.4. Hydrothermal Alteration and Deformation of JGC 263

VIII.5. Characteristics of Metamorphism in JGC 264
VIII.5.1. Spread of metamorphism in the Skellefte Mining District 264
VIII.5.2. Mineralogical characteristics of metamorphism 264
VIII.5.3. Characteristics textures of metamorphism in JGC 265
VIII.5.4. Typology of metamorphism 266

VIII.6. Petrogenesis of JGC 266
VIII.6.1. Magmatic source of JGC 266
VIII.6.2. Process of crystallization and differentiation of JGC phases 268

VIII.7. Proposition of Regional Geological Evolution 270

I. INTRODUCTION

The mining industry has been active in the Skellefte mining district since 1924 with the first mine in the area: the Boliden ore deposit. The mining exploration starts during the base metal requirement during I World War when new holdings were created as very speculative companies. The Centralgruppen Emissionsbolag is the early origin of the Boliden Company (www.boliden.com). The Boliden ore deposit start operations in 1924 and has been active until 1967 as the biggest and richest gold mine in Europe. Three deposits are currently in operation in the Skellefte mining district: Kristineberg, Renström and Maurliden. The annual production of polymetallic ore is about 1.8 million tonnes of Cu, Zn, Pb, Ag and Au.

This project was initiated in 2002 focused on the improvement of the geological knowledge in some mineralizations and associated intrusions. The main objective of this work is the better understanding of the intrusions-volcanics relationships and the contributions to delineate a better geological history according to new petrography, lithogeochemical analyses, age determinations and mapping.

The Skellefte mining district is located in a Palaeo-Proterozoic domain in the Central-Svecofenian Province in the boundary with the Norr-Svecofenian Province (Weihed et al., 2005). It is dominated by island-arc volcanic rocks and subordinated calc-alkaline intrusions (Allen et al., 1996b; Weihed et al., 2005). It is a well-known base metal deposits area probably formed during the extension of the volcanic arc. Many different intrusions occur in the Skellefte mining district, where the most important in extension and number of facies is the early Proterozoic Jörn Granitoid Complex (JGC). These intrusions represent the subvolcanic intrusive activity during long magmatic periods.

The base of the Skellefte district is composed by the shallow-submarine felsic volcanics of the Skellefte Group, probably formed in a continental margin volcanic arc (Allen et al., 1996b). The Skellefte Group has been dated from 1900 to 1885 Ma (Billström and Weihed, 1996; Montelius, 2005; Skiold et al., 1993; Weihed and Schöberg, 1991). The sediments, lavas and mafic intrusions of Vargfors Group overlie the Skellefte Group, without unconformity between these two groups. Age determinations in the Vargfors Group indicate an age of 1875 Ma (Billström and Weihed, 1996; Skiold, 1988; Skiold et al., 1993), around 10 Ma younger than the Skellefte Group. Most of the Volcano Hosted Massive Sulphides (VHMS) deposits occur in the Skellefte Group but some of the mineralisations can be found in the upper Skellefte Group and lower Vargfors Group. The subaereal felsic volcanics of the Arvidsjaur Group is considered as the lateral equivalent of the Vargfors Group to the north (Allen et al., 1996b; Weihed et al., 2005). To the south of the Skellefte district the Bothnian basin metasediments occur, they were formed in a deep marine basin, and crop to the east of the JGC.

Important volumes of intrusions occur in the center of the Skellefte district, the JGC body is coeval with both the Skellefte and Vargfors Groups. The tonalites and subordinate trondhjemites of GI phase have been dated as coeval with the volcanics of the Skellefte Group volcanics with ages ranging from 1900 to 1888 Ma (Kathol et al., 2002; Lundström et al., 1997; Wilson et al., 1987). The granodiorites and qz-monzodiorites of GII phase of the JGC and Stavaträsk intrusions (diorites and granodiorites) are coeval with the Vargfors volcanics and intrusions (gabbros, diorites and monzonites) all of them with an age circa 1875 Ma (Bergström et al., 1999; Kathol et al., 2002; Kathol and Persson, 1997; Lundström et al., 1999; Lundström et al., 1997; Skiold, 1988; Skiold et al., 1993; Wilson et al., 1987). The rhyolites from the Arvidsjaur Group have gave the same age (1878 ±2 Ma) and are probably chemically related with the Antak granite (1879 +15/-12 Ma) of the same age (Skiold et al., 1993). In the westernmost part of the Skellefte district is located the Viterliden Intrusive Complex. This is a composite intrusion dominated by tonalites, trondhjemites and granites. It is deformed and metamorphosed as the hosting volcanics of Skellefte Group. The

hornblende tonalite (1907 ±12 Ma) is similar in age to some of the volcanics from Skellefte Group in Maurliden mine and Finnliden rhyolite porphyry (Montelius, 2005).

IV. GEOLOGICAL SETTING

The Skellefte mining district is part of the Fennoscandian or Baltic Shield. It is a complex long lived area that records geological activity from 3500 to 400 Ma (Huhma et al., 2004). The Baltic shield is the western area of the East European Craton and geographically encloses Norway, Sweden, Finland and northwest of Russia (Weihed et al., 2005). The evolution is complex and includes Archean to Proterozoic orogenies and continental growth processes (Condie, 2000; Condie, 2002a; Condie, 2002b; Condie, 2004).

IV.1. GEOLOGICAL HISTORY OF FENNOSCANDIA

Three main Archaean shields constitute the European Craton: Fennoscandia, Volgo-Uralia and Sarmatia. The Pachemel suture is the union between the segments Sarmatia and Volgo-Uralia in east Europe; and both welded to Fennoscandia by the Volhym-Central Russia suture. In Fennoscandia the Archaean rocks are in northern Finland and Kola, where two orogenic periods have been documented.

The Saamian orogenic period from 3.1 to 2.9 Ga constitutes the oldest stage of the Baltic Shield (Gaal and Gorbatschev, 1987; Gorbatschev and Bogdanova, 1993). The Lopian orogen is late Archean (2.9-2.6 Ga), producing most of the Archaean rocks in Baltic Shield by rifting and basic intrusions.

The main crustal growth of the Baltic Shield ocurred during the Svecofenian orogeny (1.90-1.75 Ga), simultaneously to the accretion of the Karelian Craton. The Baltic Shield is divided in three Provinces. Volcanosedimentary active continental-arc and volcanic-arc rocks mainly constitute the North-Svecofenian Province; the Skellefte mining district is located in this Province. The Central-Svecofenian Province is a deep marine sedimentary area of the Bothnia Basin. The South-Svecofenian Province is composed by island-arc volcanics, ocurred the Bergslagen minig district (**Fig. IV-3**). The accretion to the Archean continent ocurred firstly in the South- and Central-Svecofenian Provinces in Fenian orogen (1.87-1.86 Ga) later it is accreted to the north by the Jokkmokk-Luleå and Ladoga-Bothnia sutures, in Sweden and Finland respectively. Simultaneously the Keitele microcontinent was accreted to the Karelian Craton by the Ladoga-Bothnia suture at 1.89-1.88 Ga (Allen et al., 1996a; Allen et al., 1996b; Öhlander et al., 1993; Skiold and Ohlander, 1989; Weihed et al., 2005).

An important crustal growth happens in the MesoProterozoic, as evidenced by calc-alkaline A-type intrusions and felsic vulcanism of the TranScandinavian Igneous Belt (TIB) with activity peaks of 1.81-1.77 and 1.68-1.65 Ga (**Fig. IV-3**). Magmatism was related to an Andine continental margin with associated subduction of oceanic crust under the Svecofenian Domain. During the Gothian orogen (1.75 to 1.55 Ga) the TIB was accreted to the Fennoscandia (Balling, 2000; Gorbatschev and Bogdanova, 1993; Nironen, 1997; Nironen et al., 2000).

NeoProterozoic rocks dominate the southwest part of Sweden, formed during the Sveconorwegian Orogen (1.15-0.92 Ga). This was related to the Cordilleran type collisional event (Nironen, 1997; Plant et al., 2005; Weihed and Eilu, 2005). This area is dominated by gneisses of the Gothian Orogen and late stage granitoids (1.10-0.90 Ga). The younger intrusions in Fennoscandia are related to this period with the Bohus intrusion dated at 900 Ma. During the Cadomian Orogeny (650-550 Ma) Fennoscandia and the East European Craton formed the Baltica plate. The last geological process in Fennoscandia ocurred during the Caledonian Orogeny (450-400 Ma) with the collision of Baltica and Laurentia (North America and Greenland) plates after the closure of the Iapetus Ocean. The Norwegian territory display the thrusting of volcanosedimentary

NeoProterozoic to Silurian rocks of the Iapetus Ocean onto the Baltica continental plate (Aleksandrowski, 2003; Balling, 2000; Berthelsen, 1998; Berthelsen and Marker, 1986).

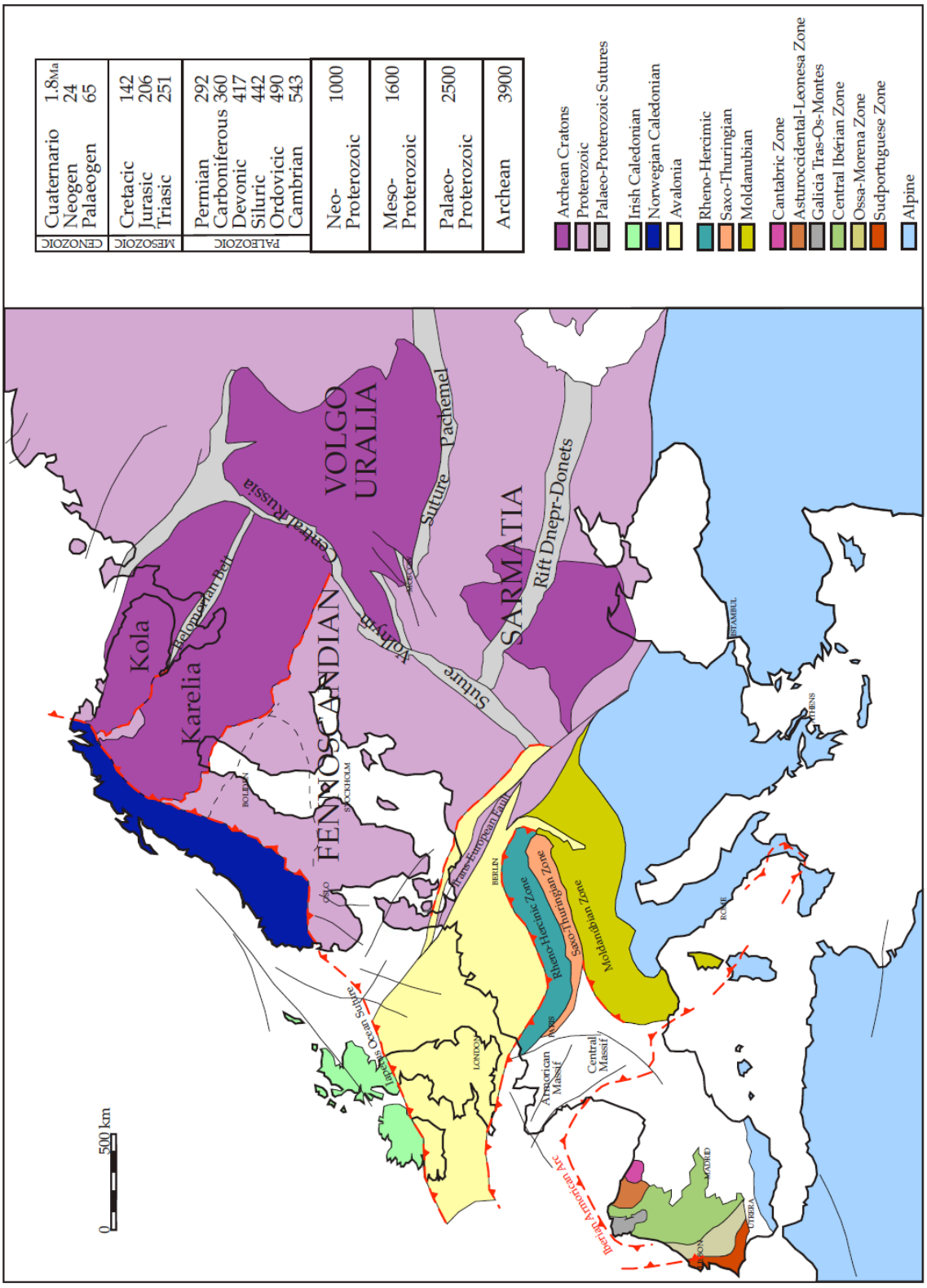

Fig. IV-1. European Geological Terrains.

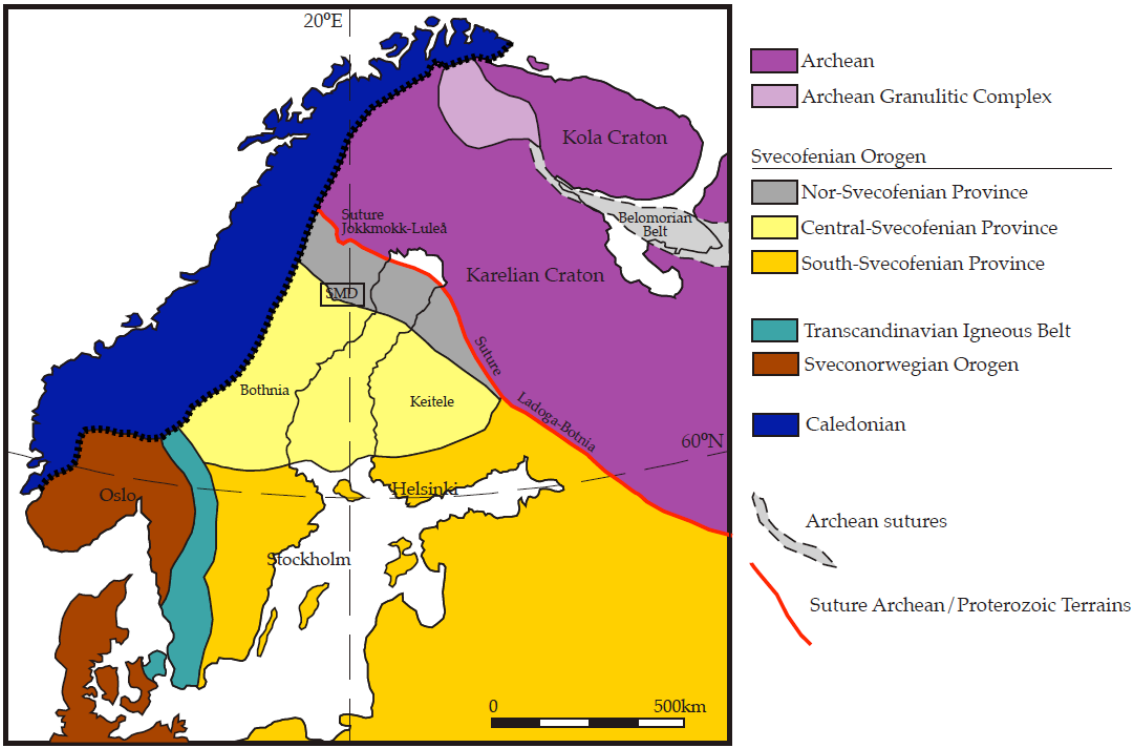

Fig. IV-3. Plot of the Fennoscandian geological parts. SMD: Skellefte mining district.

Orogenies	Age (Ma)	Process	Rocks generated
Archean evolution	3500-2500	Two Orogenic events	
Saamian	3100-2900	Constitution of Kola by collisions of proto-continents	Older Continental crust (trondhj, tonalites)
Lopian	2900-2600	Major volume of Archean rocks in the Baltic Shield	20 Greenstone belts of 100-150 km
Svecofenian	1900-1750	Nor-Svecofennian: volcanic-arc in a continental margin	Skellefte mining District and Norrboten
		Central-Svecofennian: deep marine sediments of Bothnia Basin	Deep marine sediments between arcs
		South-Svecofennian: island-arc	Bergslagen (VHMS and iron) mining district
Gothian	1750-1550	TranScandinavian Igneous Belt (TIB) of 1500 km long	A-type intrusions and calcalkaline felsic volcanism
Sveconorwegian	1150-920	Southwest of Baltic Shield during Cordilleran collision	Gneiss and granioids
Cadomian	650-550	Baltic plate and Thornqvist Sea	Rifting, no new rocks
Caledonian	450-400	Laurentia-Baltica collision, thrusting on Baltic Shield	Volcanosedimentary rocks from Iapetus Sea

Table IV-1. Summary of Orogenies in the Baltic Shield and related rocks.

IV.2. Skellefte Mining District

Three main volcanosedimentary groups have been documented in the Skellefte district. Many intrusive complexes are related to the igneous activity of each volcanic event.

IV.2.1. Skellefte Group

The basement of the Skellefte mining district is not known. The base of the Skellefte district is composed by the shallow-submarine felsic volcanics formed in a continental

margin volcanic arc. The maximum documented thickness of the volcanic series is 3 km in the Petikträsk area, in the central zone of the Skellefte district. The Skellefte Group series have been dated at 1884 ±6 Ma in Bjurvattnet at the east and 1889 ±3 Ma in Melestjärn at the center of the district (Billström and Weihed, 1996). The volcanic succession is mainly composed of volcaniclastic juvenile rocks, porphyrytic intrusions and lavas. The sedimentary successions are interbedded with the volcanic series, mainly composed by volcaniclastic siltstone, black and grey mudstone, sandstone and breccia-conglomerates. The volcanism is mainly rhyolitic (not bimodal), and most of the VHMS deposits occur in this group (Allen et al., 1996b).

IV.2.2. Vargfors Group

The sediments of the base of Vargfors Group are interbedded with the top of the Skellefte Group, without unconformity between these two groups. Many conglomerates are included in this group: the Menträsk conglomerate is composed of Skellefte Group clasts; the Abborrtjärn conglomerate is composed of GI; sandstones and Skellefte Group fragments; argillites and slates are abundant in the Elvaberg formation. Most of the VHMS deposits occur in the Skellefte Group but some of the mineralisations can be found in the upper Skellefte Group and lower Vargfors Group levels. Both the Skellefte and Vargfors Group show the same foliation, folding and intensity of deformation (Allen et al., 1996b; Weihed, 1992a). The lavas and intrusions in the group are stratigraphically located in the upper part of the Skellefte Group and in the Elvaberg formation as sills and dikes (Allen et al., 1996b). The minimum thickness of this group is 4 km in the Gallejaur and Nicknoret areas. The ages of the intrusions are 1876 ±4 Ma and 1873 ±10 Ma for gabbros and monzonites of Gallejaur, respectively; and 1875 ±4 Ma of the Nicknoret ignimbrite.

IV.2.3. Bothnian Group

The Central-Svecofennian Province is dominated by the Bothnia Basin metasediments. The Vargfors Group grade to paragneiss and migmatites of the Bothnian Group. The base of the Bothnian Group is unknown but intrusive Knafften granitoids are 1954 ±6 Ma. The thickness has been estimated as 10 km (Claesson, 1987; Claesson and Lundqvist, 1995; Lundqvist et al., 1998; Skiold and Rutland, 2006; Wasström, 1996; Wasström, 2005).

IV.2.4. Arvidsjaur Group

It is characterized by red and brown felsic to intermediate subaereal volcanism. It includes ignimbrites, ash falls layers and volcaniclastic rocks. Fragments of Arvidsjaur Group rocks are found in the upper beds of the Vargfors Group (not in the Skellefte or lower Vargfors Group), in the Abbortjärn and Dödmanberg conglomerates (Allen et al., 1996b). The Arvidsjaur is coeval with the Vargfors Group volcanics, rhyolites in the Skyträsket area have been dated at 1876 ±3 Ma and 1878 ±2 Ma, similar to the ages of the Gallejaur intrusions and Nicknoret ignimbrite of the Vargfors Group.

IV.2.5. Intrusions in the Skellefte district

Plutonic rocks in the Skellefte mining district are abundant and were emplaced during the long-lived igneous activity in the area, these intrusions outcrop in the central area and in the westernmost part of the district. The intrusions have been classified as syn-volcanics from 1.90 to 1.87 Ga and post-volcanics, generated after the Skellefte district volcanic activity (Allen et al., 1996b). The main syn-volcanic intrusions are the Jörn Granitoid Complex (JGC) and the Vitterliden Intrusive Complex (VIC), and the post-volcanics rocks are classified as Revsund type granitoids aged 1830-1775 Ma. The ages determinations of the JGC were achieved on the three main intrusives phases but the error in the determinations are too high to make an analysis of the relation with the volcanics. But the VIC has been dated as the older volcanics of the Skellefte Groups.

IV.2.5.1. Jörn Granitoid Complex (JGC)

It is the most important intrusion in volume in the Skellefte district. The JGC occupies the central area and is in contact with the Skellefte, Vargfors, Arvidsjaur and Bothnian Groups. It ranges in composition from gabbros to granites and four main phases has been determined GI to GIV (Wilson et al., 1987). The geologist Uno Svenson of the Boliden Mineral Company did the first work focused in the JGC in 1973, including a systematic geochemical work on 109 samples and a new mapping. The JGC was subdivided in three phases depending on the mineralogical composition: granodiorites, Jörn Granites, diorites and gabbros; including diabase dikes and sericitic altered zones (**Fig. IV-11**). The later four-fold division is (Wilson et al., 1987), for further descriptions see Petrography:

GI group: it is composed of quartz-porphyritic medium- to coarse-grained tonalites and less abundant trondhjemites. Hydrothermal alteration intensity is moderate to high, affecting the southern areas close to the Skellefte volcanic rocks. Amphibole and biotite group minerals are abundant but usually altered to secondary minerals. Plagioclase is the main feldspar, alkali-feldspar is related to alteration process.

GII group: it can further be divided in two subgroups, the granodiorites (GIIa) and qz-monzodiorites (GIIb) with microgranular enclaves. Plagioclase, quartz, biotite and hornblende are the main minerals with the poikilitic alkali feldspar. Some clinopyroxenes occur in the qz-monzodiorites as cores in amphiboles.

GIII group: it forms the main body of the central area of the JGC. It is composed by coarse-grained qz-porphyritic grey- to pink-coloured monzogranites. Biotite group minerals are lower than 5% in abundance, and amphibole does not occur.

GIV group: in the core of the GIII monzogranite a small pluton composed by medium- to fine-grained isogranular granodiorites occurs. It has not been dated yet.

Diorites and gabbros: many mafic rocks crops out in the JGC, but only in the border areas but they are never related to the GIII or GIV rock-types.

Most of the older datings in the JGC indicate that the Skellefte Group is coeval with GI intrusives while the Vargfors and Ardvidsjaur bodies are coeval with the GII and GIII groups. GI has been dated around 1885 Ma, and the GII-GIII was believed to be 10 Ma younger (Kathol and Persson, 1997; Wilson et al., 1987).

IV.2.5.2. The Stavaträsk intrusions

The Stavaträsk intrusion is located east of the JGC and it is composed by diorites and gabbros, and probably later coarse-grained granodiorites. The diorite has been dated at 1877 ±2 Ma, and the younger granodiorites are 1874 ±3 Ma old (Lundström et al., 1999; Lundström et al., 1997). The ages of this intrusion are similar to those obtained in the GII phase of the JGC.

IV.2.5.3. Tallberg porphyry

In the central south area of the JGC, in the porphyritic GI body is located the Tallberg porphyry copper. The Qz-Kfs porphyrytic rocks of Tallberg show mineralogical and geochemical similarities with the GI phase intrusions, and were dated at 1886 $^{+15}/_{-9}$ Ma (Weihed, 1992a; Weihed, 1992b; Weihed et al., 1992; Weihed and Schöberg, 1991). This could indicate the porphyry formation in the late magmatic GI stage.

IV.2.5.4. Hobergsliden

It is a medium- to fine-grained leuco-granodiorite located in the northeast of the GIII, Hobergsliden intrusion is probably a late-stage of the GIII magmas. The age of this intrusion is 1862 ±14 Ma (Lundström et al., 1997).

IV.2.5.5. Antak granite

It is an intrusion located in the west-northwest of the JGC that was emplaced prior to GIII. Its limits have been defined by the geophysical properties due to the absence of outcrops. The Antak granite can be related to the Arvidsjaur Group volcanics and is dated in 1879 $^{+15}/_{-12}$ Ma (Kathol and Persson, 1997).

IV.2.5.6. Gallejaur Monzonite and Gabbros

Southwest of JGC, the Gallejaur monzonites occur as a plate-shaped intrusion related by some authors to the impact of a meteorite (Lilljeqvist, 2002). Two main lithologies can be described in this intrusion: gabbros and monzonites. In the outer part of the intrusion occurs a medium-grained diorite and gabbronorite, 1876 ±4 Ma old (Skiold, 1988; Skiold et al., 1993). Some mafics that occur in the southern border of the JGC have been related to the Gallejaur suite. The age of the monzonite is 1873 ±10 Ma (Skiold, 1988; Skiold et al., 1993). The monzonite can be subdivided in rim and core monzonites that show significant differences. In the rim of the monzonitic phase occurs a fine- to medium-grained monzonite with hornblende. The idiomorphic amphiboles of the rim monzonite are well preserved but the acicular ones have been altered to chlorite, the plagioclase crystals show slight to medium degrees of alteration. The core of the monzonitic phase is characterised by a medium-grained monzonite with extensive symplectite texture with plagioclase and k-feldspars that crystallize around the plagioclase phenocrysts. The primary igneous mafic minerals (amphibole?) have been substituted by chlorite. Coarse-grained epidote is commonly found as secondary mineral in this rock-type.

IV.2.5.7. Viterliden Intrusive Complex (VIC)

VIC occurs in the westernmost part of the Skellefte district. Both VIC and JGC, are similar as they are composed by various intrusive phases ranging from tonalite to granite, and similar to the VIC 1907±12 Ma old (Bergström et al., 1999). It is strongly deformed by folds and faults according to the deformation in the Skellefte Group volcanics in that area. The Kribergstonalite occupies the core and the southeast of the complex. It is similar in composition to the GI phase and similar in mineralogy with the less altered GI at the west of the JGC. It has been affected by metamorphism and it is better defined as a quartz-amphibolite. Medium-grained phenocrysts of primary amphibole and plagioclase occur. The metamorphic layering is well defined with oriented crystals of fine grain metamorphic biotite and amphibole. In the central area is a band of strongly deformed tonalites and trondhjemites. Finally in the western and southeast boundary occurs porphyritic trondhjemites known as mine porphyry.

IV.2.5.8. Revsund type granitoids

This granitoids outcrop in many areas in the Skellefte district. It is characterised by a coarse grain porphyrytic A-type granitoids; in southern Skellefte district in Holmsfors the Revsund date is 1778 ±16 Ma (Skiold, 1988). The quartz show a characteristic bluish colour and occur with an average size of 5-10 mm. The subidiomorphic k-feldspars phenocrystals are very coarse size (5-30 mm). Plagioclase is poor in anortite and less abundant than k-felspars. The biotite group minerals are abundant (10-12 %) and occur disseminated pyrite. The enclaves and xenoliths are abundant in some areas, and at least have been differentiated three types of enclaves:

a. Enclaves usually rounded and 5 to 50 cm in size with the same mineralogical composition are common with the difference in the texture that in this case is granitic with a quite homogeneous size of the crystals of 2-4 mm but minor in size in the borders of the enclave with a size of 1-2 mm.

b. Mafic enclaves with a very fine-grained size are of 2-5 cm diameter, mainly composed of philosilicates and some opaque minerals.

c. Fine-grained enclaves with a high content of biotite and felspars, with some quartz. Corresponding to a microgranular enclave of the Revsund granite.

IV.2.5.9. Porphyrytic basalts (souther limit of JGC)

This lavas and intrusions are common in the southern of the JGC, it is related to the Vargfors Group volcanics. This lava-like intrusive dike draws the southern boundary of the GI with the Skellefte volcanics with a N110ºE orientation. This basic porphyrytic rocks (see petrography for textural description) occurs in many areas in the boundary of the JGC from south, in the Skellefte River close to Nicknoret, along the western boundary (Vitthaten) and in the northern of the JGC close o Ullricksberg. Field relationships indicate that GI is older than this basic lavas and intrusions.

V. PETROGRAPHY

A detailed petrographic description is really useful in any petrologic study. Actually the geochemical and isotopic analyses provide the best data in a geological work but this information without a detailed petrography can be difficult to solve or interpret.

V.1. GENERAL PETROGRAPHY

Each of the geological processes that occur to rocks since the crystallization until the sampling leaves a signal in the texture of the rock. In this way such geological magmatic event as any subsolidus processes leaves a signal in the rock that we must interpret that is partial information but at the same time is necessary. The total number of thin sections studied is 419, divided in: 105 of JGC collected by the geologist Uno Svenson 1973 sampling (Boliden Mineral AB); 9 from the Renström small pluton drill-core (REG-1280); 126 of the 2003 sampling of JGC, Gallejaur and mafics of southern Dike and 179 of the 2004 sampling including northern JGC and VIC.

V.1.1. HAND SPECIMEN SAMPLE DESCRIPTION

GI hand specimen:

The GI hand specimen textures are diverse and vary from holocrystaline equigranular to porphyritic. The GI tonalites are grey to white, medium to coarse grain. The quartz phenocrystals are xenomorphic usually bluish colored to intense blue in some areas. The quartz occurs as isolated crystals or grouped as quartz microcrystals aggregates. The plagioclase is white to green in the slightly to moderate altered areas of saussurite (epidote, chlorite, etc). The plagioclase crystals are usually subidiomorphic tabular, as medium grain aggregates. The mafic minerals are difficult to identify in many samples due to alteration (see next). The biotite is partially chloritised, green colored, forming microcrystals aggregates with decussate texture. The amphibole is dark green to black colored and occurs as subidiomorphic 3 mm crystals; it is partially substituted by chlorite and/or biotite. The biotite/chlorite aggregates also occurs in the amphibole boundary (**Photograph V-1a**).

The equigranular texture in tonalites is less common than the porphyritic ones; see the equigranular tonalite of Klockträsk GI-type (**Photograph V-1b**). The Klockträsk sample is moderately altered, as the plagioclase is moderately to strongly green due to the abundant epidote. The mafic minerals are less abundant and smaller than the usual GI-type samples, it suggest the higher hydrothermal alteration on this samples. The Tallberg porphyry copper generates GI-type granitoids, this granitoids are similar to the GI coarse grain and porphyrytic textures (**Photograph V-2a**).

In contrast, many subvolcanic intrusions in the JGC occur with different textures to the observed patterns in the GI tonalites. These subvolcanic intrusions are feldspar (+ quartz) porphyrytic, medium to coarse grain phenocrystals in a very fine matrix. The JO03-104 sample is located in the Skellefte group volcanics and is similar in texture to the GI granitoids. It is 15% plagioclase phenocrystals, subhedral, with xenomorphic medium to coarse quartz, matrix rich in plagioclase, quartz and poor in mafic minerals content (**Photograph V-2b**).

Litotype	Subtype	Classification	Mineralogy	Accesory	Texture	Comments
GI						
	Zone W	Tonalite	Pl, qz, bi, amph	Ap, zr, aln	Hip to xenomor. equi. Ø-medium	Chl and act secondary, biotite
	Zone SE	Tonalite	.	Ap, zr	Hip inequi to porfídica Ø-medium	metamorphic decussate
	Rengård	Tonalite	.	Ap, zr, tit	Idio equi a hip porf Ø-medium fine	Bi and amph metamorphic
	Klockträsk	Tonalite y trondhjemite	. Pl, qz		Hip granular to porf Ø-medium Hip to xenomor. Ø-medium fine	Dikes syn-intrusives Deformadas, abundante epidote
GII						
	GIIa	Granodiorite	Pl, kfs, qz, amph, bi	Tit, ap, zr	Idio to hip equi Ø-medium	Smoky Qz, abundant dikes
	GIIb	Quartz monzonite	Pl, kfs, px, amph, bi	Tit, ap, zr	Hip inequi porf Ø-medium matrix faneritic Ø-fine	Enclaves microgranulars, relicts of augite
GIII						
	GIII	Monzogranites	Qz, pl, kfs, bi	Tit, ap, aln	Hip inequi porf Ø-medium coarse	Pertites, pl en matrix
	Hobergsliden	Granites de Kfs	Qz, kfs, pl, bi	Tit, ap, aln	Hip inequi to porf Ø-medium	Pertites, mafic accessories
GIV		Monzogranites	Qz, pl, kfs, bi	Tit, ap, aln	Idio equi Ø-medium	Grey to yellow in outcrop
Näsberget		Gabbros and diorites	Px, pl, ol, amph, bi, mt	bi	Variable: intergranular, dolerite, ofitic, subofitic, accumulate	Layered, GI megablocks
Basalts Vargfors		Andesitic basalt	Px, pl,	Mt, sp	Afanitic porf Ø-medium	Massive to clastic/autoclastic? Southern limit of JGC
Gallejaur						
	Zone outer	Monzonite	Pl, bi, px, qz, kfs.	Mt, ap	Hip equi a porf Ø-medium fine	Px uralitisated, high mt
	Zone inner	Monzonite enclaves	Pl, px, qz, *s* kfs-qz	Mt, ap	idio-xeno Inequi porf simplectite Ø-medium fine	phenos of pl and matrix of simplectite of qz+kfs,
VIC						
	Tonalite	Quartz-amphibolite	Pl, qz, amph, bi	Zr, ap, tit, ep	Granolepidoblastic Ø-medium	Tonalite in amphibolite facies
	Trondhjemita	Trondhjemites	Pl, qz	Bi, chl, ap, zr	Xenomorfic ineq to porf Ø -medium fine	Absence of mafics, undeformed areas
Revsund						
	Monzogranites	Monzogranites	Pl, qz, kfs, amph, bi	Ap, tit, zr	Porf Ø-grueso, matriz pl-qz-bi	Abundant enclaves and xenos
	Granite	Granites of two micas	Pl, qz, kfs, bi, ms	Ap, tit, zr	Hip inequi to porf Ø-medium	Low mafic content
Stavaträsk		Granodiorite	Pl, kfs, qz, amph, bi	Ap, zr	Hip equi to inequi Ø-medium	Contact metamorphism on Bothnian sediments

Table V-1. Summary of characteristic textures of intrusions in the Skellefte mining district. Hip: hipidiomorfic; equi/inequi: equigranular/inequigranular; porf: porphyrytic; Ø: grain size.

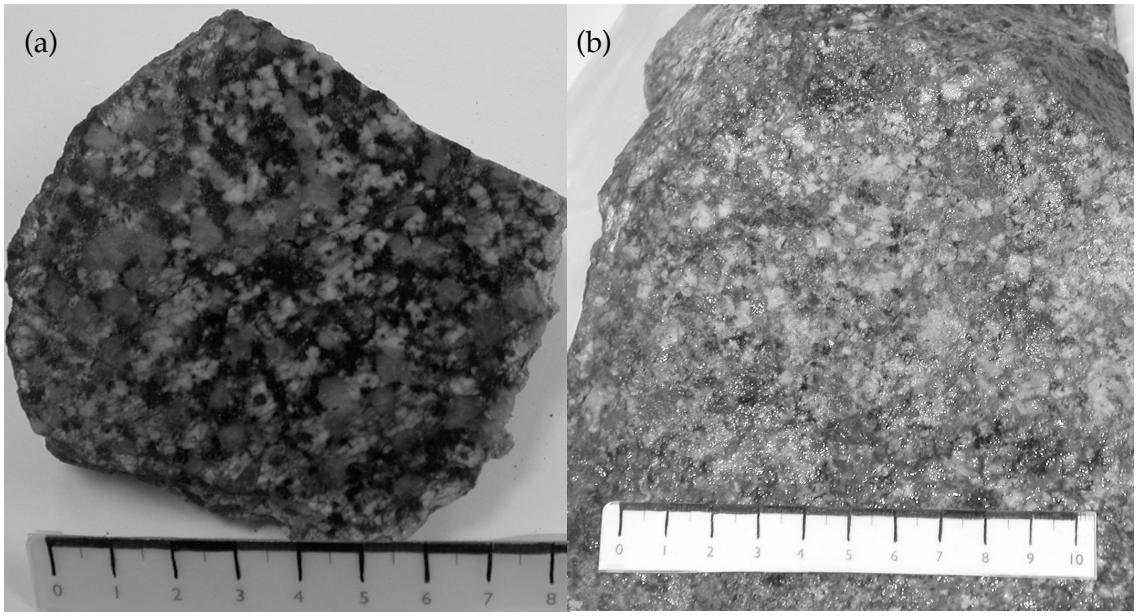

Photograph V-1: **(a)** GI hand specimen (sample JO03-55). **(b)** Klockträsk satellite GI-type intrusion (JO04-144). Scale in centimeters.

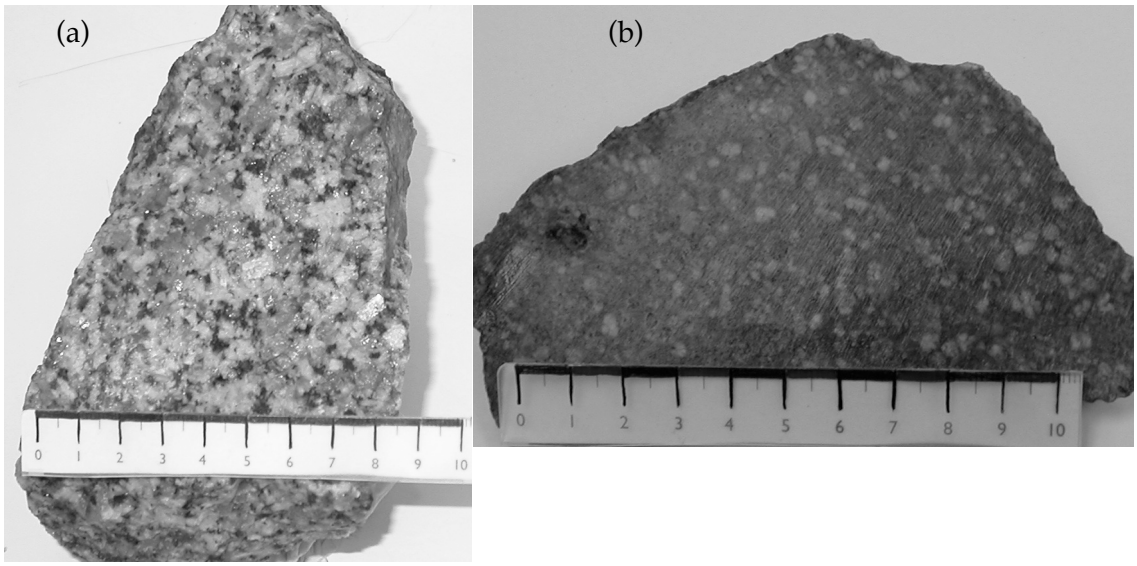

Photograph V-2: **(a)** Älgträsk dike tonalite. **(b)** Quartz + plagioclase porphyritic (JO03-104). Scale in centimeters.

GII hand specimen:

The GII simples can be divided in two groups: medium to coarse grain granodiorites and medium grain quartz-monzodiorites.

a) GIIa granodiorites: the hand specimen is grey with pinkish and yellow colors due to the alkali feldspars. The texture is medium grain holocrystaline equigranular to inequigranular. The main difference with the GI texture is the absence of plagioclase or quartz phenocrystals, in contrast it is common the occurrence of mafic "clots" mainly composed of amphibole and biotite. The quartz occurs as interstitial medium to fine grain crystals, xenomorfic as smoky quartz variety. The fine grain plagioclase is idiomorfic to subidiomorfic as tabular isolated or grouped crystals. The alkali feldspars

are medium grain size and occur as poikilocrystals hosting biotite, plagioclase and amphibole; alkali feldspars are identified as yellow to pink colored crystals. The fine grain biotite is black, easy to determine by hand specimen. The amphiboles occur as "clots" with biotite, occur as medium size crystals prismatic subidiomorfic, green colored. It is common the occurrence of microgranular enclaves.

b) GIIb quartz-monzodiorites: the color and textura are similar to the GIIa samples but smaller in crystal size. The microgranular enclaves are also abundant, with ellipsoidal geometry and size fom 5 to 30 cm (**Photograph V-3**).

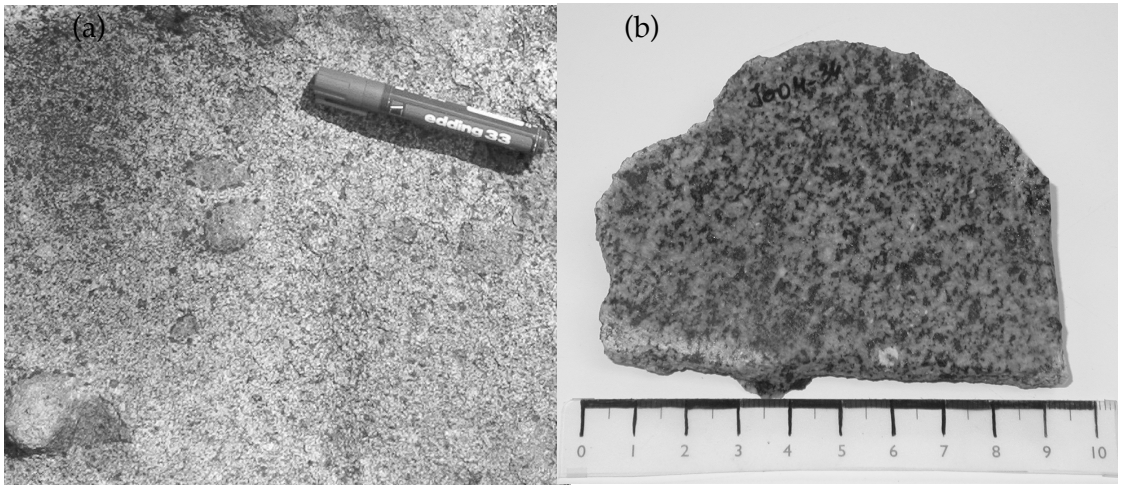

Photograph V-3: **(a)** GIIa outcrop with GIIb microgranular enclaves (in red). **(b)** GIIb hand sample (JO04-34). Scale in centimeters.

GIII:

Monzogranites and granodiorites of GIII are abundant in the core of the JGC. In hand specimen it is characterisd by intense orange pinkish to reddish rocks due to the abundant alkali feldspars; the bluish quartz is also characteristic in the GIII hand specimen (**Photograph V-4**). The general texture is holocrystaline porphyrytic with coarse grain size quartz and alkali feldspars phenocrystals, the matrix is rich in plagioclase and poor in biotite. The xenomorfic coarse grain size quartz phenocrystals are usually bluish and occur as isolated or polycrystalline aggregates. The alkali feldspar is usually poikilitic, medium to coarse grain size, red to orange colored; microcrystals of plagioclase (usually with Carlsbad twining) are hosted in the alkali feldspars. Idiomorfic to subidiomorfic plagioclase occurs as medium to fine grain size crystals, and occur as tabular prism. Biotite group minerals are low abundant, idiomorfic, black colored, of medium to fine grain size.

The granite to alkali granite of Hobergsliden occurs as a subphase of the GIII. The hand sample is similar to the GIII granites but richer in alkali feldspars and poorer in plagioclase, the biotite is less abundant in the Hobergsliden alkali granite. The grain size of the Hobergsliden granite is smaller than the GIII, but both shows similar textures.

GIV:

The small GIV body outcrops in the central area of the GIII intrusion. The GIV is a medium grain size granodiorite. The samples are white yellowish with very low abundant biotite. It is mainly holocrystaline inequigranular to porphyrytic with euhedral alkali feldspars phenocrystals of 1 mm, the carlsbad twining is common. The alkali feldspars are yellow to white. The quartz occurs as microgranular aggregates of 0,5-1 mm in size. The subhedral plagioclase is tabular, white yellowish, it occurs as

isolated crystals or glomeroporphytytic aggregates. The biotite is more abundant than the GIII, and similar to the GIIa; euhedral fine grain biotite is black.



Photograph V-4: GIII hand specimen (MG07-005). Scale in centimeters.

Gallejaur monzonite:

Two zones has been determined in Gallejaur intrusion: the outer and inner rims (see maps in the appendix).

a) Outer rim: it is a red fine grain holocrystaline inequigranular monzonite. The quartz is very fine and low abundant as disperse crystals in the matrix. The subhedral plagioclase is white to yellow. Alkali feldspars are subhedral of medium to fine grain size, the euhedral alkali feldspars phenocrystals are rare and are not widespread in the samples. Biotite group minerals occur as microaggregates. The pyroxene crystals are 1 mm long. It is relevant the intense magnetic susceptibility of this samples due to abundant magnetite. Microgranular enclaves rich in mafic minerals are common (pyroxene y biotite).

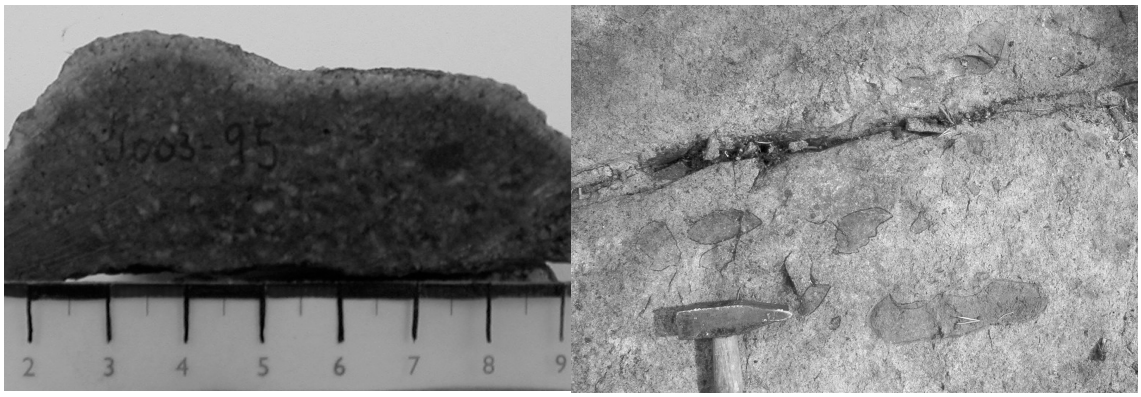

Photograph V-5: **(a)** Gallejaur monzonite (JO03-95). **(b)** Outcrop of Gallejaur monzonite of the inner zone, microgranular enclaves are abundant.

b) Inner zone: the hand sample are similar to the outer zone, the main difference is the absence of alkali feldspars phenocrystals. The rock is holocrystaline inequigranular medium to fine crystal size (**Photograph V-5a**). The idiomorfic tabular plagioclase is white yellowish smaller to 2 mm. Alkali felspars and quartz occur in the matrix as simplectites of qz + kfs (see appendix), it is red colored. Pyroxene and biotite, black colored, subidiomorfic and fine grain size. Pyroxene is prismatic, subidiomorfic; biotite is difficult to determine in hand specimen. Microgranular enclaves occur as elliptic to angular shape, 5-30 cm, margin transitional to chilled (**Photograph V-5b**). High magnetic susceptibility.

V.1.1.1. MODAL STUDY OF INTRUSIONS IN JGC

The modal calculations has been done using microphotographs (1x and 2x focus) and analysed with the ImageJ software of the National Institutes of Health of the United States.

GI:

The GI tonalites has been studied in two separate groups: the altered samples and the unaltered samples. The amphibole in altered samples has been altered to chlorites and biotites; it has been identified biotite/chlorite, plagioclase and quartz. In contrast the unaltered samples contain amphibole, biotite, plagioclase and quartz:

GI	(%)	amph	bi	pl	qz
altered		-	14,5	48,5	37
unaltered		9,6	5,8	39,1	45,5

GII:

It has been grouped in GIIa and GIIb. Quartz, plagioclase, alkali feldspars, biotite and amphibole occur in both groups, including relicts of pyroxene in GIIb, those have been included in the modal amphibole:

	(%)	amph	bi	pl	qz	kfs
GIIa		2,9	14,0	36,4	17	29,7
GIIb		11,6	9,4	50	16,3	12,7

GIII y GIV:

GIII, Hobergsliden and GIV contain quartz, plagioclase, alkali feldspars and biotite:

	(%)	bi	pl	qz	kfs
GIII		4,1	26,8	33,9	35,2
Hobergsliden		2,4	16,9	25,7	55,1
GIV		7,3	40,2	27,2	25,3

Gallejaur:

The Gallejaur intrusions modal study has differentiated two main groups: inner and outer zone. The simplectite (kfs + qz) texture is also included in the modal analyses:

(%)	bi	px	pl	qz	kfs	mt	simplectite
Anillo exterior	7	12,5	60,3	7,4	9	3,9	-
Anillo interior	5,3	10	53,5	6,6	1	3,2	20,4

V.1.2. GI phase of the Jörn Granitoid Complex

The most interesting granitoid from the geological view is the GI phase, it has been affected by many geological processes and outcrops closer to the Skellefte volcanics and mineralization than other JGC intrusions. The GI phase includes the satellite intrusions of Rengård and Klockträsk, and other subordinated qz+kfs porphyritic tonalites. The quartz-porphyritic and quartz+feldspars texture are dominant with phenocrysts grains of 5-10 mm, the quartz phenocrysts are usually made up of quartz microcrystals as polygonal mosaics. The mineral composition of GI is mainly classified as tonalites with some trondhjemites in subordinated areas. Generally GI is composed by quartz, andesine type plagioclase, hornblende type amphiboles and biotite. The zircon and apatite are the usual accessory minerals, with the occurrence of some allanite and magnetite. In the GI hydrothermal altered zones the main secondary minerals are chlorite, sericite, epidote, turmaline, kfs, qz and calcite. The GI texture is variable but in general is medium grain qz+kfs porphyritic tonalites, also occurs some bluish quartz.

V.1.2.1. Petrographic description of GI

Southwest of GI

GI tonalites are commonly medium-grained granitic to porphyritic tonalite with plagioclase and quartz phenocrystals. Microgranular qz crystals occur by re-crystallization of igneous quartz phenocrystals (**Pic V-1**). Plagioclase is medium-grain idiomorphic to subidomorphic, typically moderately to strongly altered to saussurite (sericite, epidote, albite). Igneous primary plagioclases are andesine to labradorite (45-55 % An).

Amphibole does not occur widespread in GI intrusions, and commonly is partially to totally substitute by secondary chlorite and biotite. The primary amphibole relicts are hornblende, but they are usually altered to actinolite group amphiboles. Igneous biotite (bi_1) group minerals are not often preserved and they occur commonly altered to chlorite (chl), so it is common to find qz+tit/rutile inclusions in the {001} sheet of the chloritized biotite crystals. Chlorite occurs as sheet bands or substituting the biotite crystals. Metamorphic biotite was usually crystallized substituting the mafic minerals, with minor size than the igneous biotite with decussated texture. These secondary biotites postdate the igneous minerals (amph and bi) and the secondary (hydrothermal alteration) chlorite (**Pic V-2**). In some samples is common the occurrence of the three minerals phases: primary biotite (bi_1), secondary chlorite (chl) and later metamorphic biotite (bi_2). Turmaline as secondary mineral is common. The microgranular fine-grained enclaves are usual with a similar Streckeisen composition than the host GI tonalites but higher proportion of mafic minerals.

Western GI

The GI tonalites at west and northwest of JGC are commonly medium-grained granitic and occur as qz+kfs porphyritic in the border areas of the JGC only. Plagioclases are moderately altered, partly albitized, epidotes occur as main alteration product (**Pic V-3**). The qz secondary crystals are usually crystallized as polygonal aggregates texture postdating the previous igneous phenocrystals.

The primary amphiboles are preserved as hornblende crystals but partly substituted by metamorphic biotite in many areas; these biotites crystallize along the double oblique cleavage system of the amphiboles (**Pic V-4**). Primary biotites are not usually altered to chlorite as occur in the southern areas of GI but they are commonly substituted by metamorphic biotites. It indicates that the hydrothermal alteration processes do not occur in the northwestern areas of GI but metamorphism reaches this area. The key identification of primary biotites respecting the metamorphic biotites is the textural characteristics of bi_2 that are usually decussated and much smaller in size than the bi_1.

Southeastern GI

The GI tonalites in the south-southeastern tonalites is medium- to coarse-grained qz+kfs porphyritic tonalites, qz phenocrystals of 5 mm size occur in many areas. The brittle deformation usually generates the elongation and fracture of qz crystals. The plagioclase is moderate to locally strongly altered to epidote and phyllosilicates.

The occurrences of mafic primary minerals are rare due to hydrothermal alteration. Igneous biotite and amphibole minerals group are not preserved, and they are commonly altered to chlorite. Most of the secondary chlorites have been substituted to metamorphic decussated biotites. Igneous biotite can be determined by the presence of qz and titanite lineation (in the {001} sheet of igneous biotite) related to chlorite alteration because they are overprinted by decussated biotite (**Pic V-5**). The secondary biotites also occur as minerals filling the fractures in the rock.

Rengård satellite intrusion

The Rengård intrusion is a medium-grained granitic to quartz porphyritic GI type tonalite. It is composed by the same mineral phases that occur in the northwestern tonalites of GI: qz, plagioclase, amphibole, biotite and zircons and apatite as accessory minerals. It is located in the surroundings of the Renström mine. It is elliptic in shape with the long axis to the NW, and it is truncated in the SE by a north-south fault. The Rengård intrusion is white to gray in hand specimen. The rim of the qz is usually crystallized as polygonal qz microcrystals (**Pic V-6**). The plagioclase crystals are slightly to moderate altered to saussurite but the igneous compositional zoning is preserved. Primary biotites are common, but occurrence os secondary titanite in the {001} or in the bending areas of the crystals are usual (**Pic V-7**). Secondary biotite overprinted on the primary biotite is common but smaller in size with decussated texture. Radial and acicular secondary biotite is common in the rim of igneous biotite and amphibole group minerals.

The amphiboles of the Rengård intrusion can be divided in two main groups. The igneous amphiboles are medium-grained and with the optical properties of common hornblende group minerals. The primary amphiboles are medium size isolated crystals or they crystallize as clots with the primary biotite. The metamorphic amphiboles are diverse and usually fine- to very fine-grained. These secondary amphiboles belong by the optical properties to the alkaline amphiboles group minerals, characterised by an intense bluish pleocroism tipiacal of the tschermakite and hastingsite minerals. The secondary amphiboles crystals overprint the igneous mafic minerals and probably crystallized coeval or later to the metamorphic biotite (**Pic V-8**). The very fine secondary amphiboles fill some intergranular areas of the rocks.

Kkockträsk intrusion

It is located in the southeast of the main JGC. It can be subdivided in two phases: common tonalites and trondhjemites characterized by the total absence of mafic minerals. It is a medium- to fine-grained granitic to qz+kfs porphyritic tonalites and trondhjemites. Microgranular enclaves and tonalitic dikes are common and show the same alteration than the host rocks.

The quartz of the granular tonalites is usually filling the interstitial zones rich in medium to fine plagioclase, amphibole and biotite with the occurrence of some plagioclase phenocrystal and poikilitic amphibole (**Pic V-9**). Euhedral plagioclase is usually in the matrix with slightly zoning and albite twins. The phenocrystals of plagioclase show continuous chemical zoning from core to rim. The amphiboles are euhedral to subhedral in the matrix and poikilitic as phenocrystals, they occur slight to moderately altered to actinolite group minerals or substituted by chlorite. Primary biotites also occur as relicts but they are usually altered to chlorite; secondary biotites

do not overprints/substitute completelly the primary biotites or secondary chlorites (**Pic V-10**).

V.1.2.2. Deformation of GI

The metamorphic re-crystallization overprints in most of the cases the brittle structures. The GI unit low temperature deformation is characterized by the development of a qz subgrains and bending of the biotites, it is associated to a very fine matrix of chlorite and carbonates. Deformation is widespread in the southern and southwestern boundary of JGC. Plagioclase or amphibole phenocrystals are commonly undeformed. The sericite rich bands are associated to fluid circulation during deformation.

The deformation in the south develops thin shear bands characterised by the quartz and plagioclase fragmentation from 2 mm to 50 μm size crystals and oriented biotite. Granoblasts of quartz are slightly oriented by deformation and show a characteristic intense undulating extinction. Secondary minerals are not associated to the deformation in this zone.

The ocelar mylonitic texture (Bard, 1985) is the usual texture of deformed GI, but rocks with a penetrative deformation contain quartz and plagioclase porphyroclasts (**Pic V-11**). Other areas with an incipient deformation, but not foliated or pressure shadow growth of minerals, show a protoclastic texture. The bending of the biotites is the most common character of the brittle-ductile deformation, but this texture is usually overprinted by hydrothermal alteration or metamorphism. The bending is sometimes documented in the igneous biotite relicts (**Pic V-12**) with a characteristic undulant interference color. The titanites and quartz as alteration-deformed products are associated to the sheet of altered biotites (see next in metamorphism). The dynamic crystallization of quartz is observed by the saw-like quartz boundaries (**Pic V-13**). The dynamic crystallization also occurs to plagioclase and generates the secondary twining (Shelley, 1993) oriented by the stress directions (**Pic V-14**).

V.1.2.3. Alteration of GI granitoids

Deformation and hydrothermal alteration textures suggest that both processes are coeval and, as happens with the deformation, it is limited to the GI unit. The alteration occurs in most of the GI rocks of the southern areas, but also occurs in the northwestern corner of the JGC.

Albitization

It is characterized by substitution of the Anortite molecule of calcic plagioclase by sodic plagioclase and is common in the GI unit. The unaltered GI plagioclase chemical composition average 40-50% An, but the altered plagioclase anortite content is lower to 15%. Two main type of albitization have been defined in GI rocks:

a) The anortite molecules have been partially substituted in the plagioclase crystals, the plagicoclase show different alteration degrees. The alteration develops a compositional zoning that is higer in the rim and in along the cleavage planes of the plagioclase crystals. Also in the plagioclase twins the albitization only substitutes the anortite in few crystals (**Pic V-15**).

b) The albitization also substitute complete crystals of plagioclase by aggregate of microcrystals of plagioclase with variable anortite content. This process usually occurs in association with the epidotization or saussuritation processes. The rims of the plagioclase crystals are usually substituted by albite (**Pic V-16**), and the core is substituted by the microcrystals of albite, epidote and sericite. The alteration products are usually oriented along the original crystals cleavage.

Epidotization/saussurite

This process is commonly associated to the albitization of the plagioclase. During the albitization process crystallize epidote. It is common the generation of epidote aggregates with the original shape of the plagioclases (**Pic V-17**). The epidote crystals occur in two main textures:

a) Epidote crystals substituting the cores of zoned plagioclase are generated in the more calcic zones. Although the whole plagioclase is altered, epidote crystals occur in the core of the plagioclase and the rim is usually substituted by albite (**Pic V-18**). The epidote in the less altered areas occur only in the weaker areas of the crystals such the cleavage planes (**Pic V-19**).

b) Associated to the fluid circulation the epidote crystallizes in fractures and substitute crystals that are not associated to the cation exchange of the epidotization. These epidotes are usually medium- to fine-grained and are abundant in the boundary of crystals as chlorite (**Pic V-20**). Epidote crystals are diverse in color, size, and shape and sometimes they are zoned (**Pic V-21**). The chemical composition of these epidote crystals is quite variable.

Chloritization

It is characterized by the introduction and replacement of chlorite crystals; the common reaction includes biotite but other minerals as plagioclase are needed (Eggleton and Banfield, 1985):

$$1\ bi + 0.21\ an + 1.64\ H_2O + 1.46\ H^+ + 0.08\ O_2 =$$

$$= 0.46\ chl + 0.11\ tit + 0.10\ ep + 0.56\ ms + 0.63\ qz + 0.02\ mt + 1.46\ K^+$$

The pyroxenes or amphiboles substitute the biotite in the reaction to generate chlorite. The chlorites occur in three main textures in the GI unit:

a) In veins associated to carbonates, sericite and sulphurs/oxides. These veins are generated during the deformation and hydrothermal alteration. The mafic minerals cross-cutted by these veins are altered to chlorite and but slightly altered or unaltered in the surroundings areas (**Pic V-22**).

b) The chlorite crystals usually substitute or fill the interstitial areas. The texture of these chlorites is decussated and usually associated with epidote (**Pic V-23**). Epidote crystals occur in association to the albitization of plagiclase.

c) One of the characteristics features of the GI unit is the chloritization of igneous biotite. The most usual occurrence of chlorite is by the substitution of biotite group minerals. The chlorite reaction starts with the brucite sheet substitution in the biotite layers (location of the K+ cation) (Banos and Amouric, 1984; Veblen and Ferry, 1983). The reaction occurs by the substitution of two biotite sheets by a simple chlorite sheets (Kogure and Banfield, 2000). The biotite crystals are totally or partially substituted by chlorite, if they are totally substituted the texture is commonly decussated. The Titanium is liberated as main constituent of secondary minerals, usually titanite crystallizes with the titanium of the biotite and calcium of the plagioclase; these titanite crystals occur in the {001} sheet of the igneous chloritized biotite and draw the igneous shape of the biotite crystals. If the intensity of the alteration is low the crystals of biotite are only partially substituted and they occur as "sandwich of chlorite" in the biotite (**Pic V-24**). The chloritization occur on biotite as low intensity of alteration, or prograde to amphiboles and pyroxenes in the strongly altered zones (**Pic V-25**).

V.1.2.4. Metamorphism of GI granitoids

The characteristics of the metamorphism in granitic rocks are usually difficult to define and sometimes a low metamorphism is not appreciable. The metamorphism in the intrusions is not homogeneous and the characteristics of metamorphism in JGC are completely different to those in the VIC. These differences are related to the metamorphic grade and the nature or origin of the metamorphism.

In JGC the metamorphism is exclusively limited to the GI phase as occurs with the hydrothermal alteration and deformation. The igneous minerals are not always identifiable of the secondary minerals or metamorphic. The deformation and hydrothermal alterations plays an important role as key identification of the metamorphism. The biotite group minerals are the main metamorphic minerals and the deformation and alteration overprinted on the igneous biotite make easier to differentiate the igneous and the metamorphic biotite. The metamorphic amphibole is poor but occurs in some areas of GI (Nör-Jörnsberget) and in the Rengård satellite intrusion.

V.1.2.4.1. Metamorphic biotite in JGC

The chlorite and igneous biotite (bi_1) minerals are the most important key for the identification of the metamorphism that overprints minerals with a newly formed biotite (bi_2) or amphibole. As previously documented, the chloritization products include many secondary minerals (qz, tit, mt, ep, ms), characterized by the crystallization of tit and qz in the {001} sheet of bi_1 (**Pic V-27**). The metamorphic biotite overprints the igneous biotite, chlorite and deformation textures (**Pic V-28**). This new biotite is much smaller (< 1 mm) than the previous biotite and/or chlorite, it crystallizes in decussated textures of several very fine-grained bi_2. Metamorphic biotite also occurs in veins or clots in the matrix of the rock, in this case decussated texture is widespread (**Pic V-30**).

Although the metamorphism is recognizable in previously altered rock, the criteria for the recognition vary for the unaltered areas of GI. The metamorphic biotites crystallize as very fine-grained crystals in the rims of igneous biotite (sizes 0.50-0.10 mm), also bi_2 crystallizes in the bending biotites along the deformed sheets (**Pic V-31**). The fractures surrounding igneous biotites are often filled with bi_2. The substitution of igneous biotite by metamorphic biotite minerals is usual and the crystals are commonly crystallized as fine-grained decussated metamorphic biotite (**Pic V-32**).

The metamorphism can overprint the chlorite, which previously altered the bi_1, and crystallizes a new biotite. This new metamorphic biotite has the same optical properties than the initial biotite but the crystallographic axis are changed or the new very fine grain biotite only growth in the dimensions of the previous igneous biotite (**Pic V-33**). The distinctive criterion is the presence of titanite and qz generated during the previous hydrothermal alteration.

Amphibole primary crystals are usually postdated by metamorphic biotite. The chlorite that altered the primary amphibole is partially or totally substituted to metamorphic biotite. The metamorphic biotite crystals do not substitute the relicts of amphiboles (**Pic V-34**). If the amphibole crystal was totally substituted by chlorite the metamorphic biotite crystals occurs as rhombohedra shape of the igneous amphibole. Some qz and chlorite also occurs as remnant of the hydrothermal alteration after metamorphism (**Pic V-35**).

The metamorphic biotites of the Rengård satellite intrusion occurs as in the other areas but the titanite inclusions generated during chloritization is usually transformed to oxide but with the rhombic shape of the original secondary titanites. These

transformed titanites to oxides during metamorphism also occur in the borders of the biotites (**Pic V-36**).

V.1.2.4.2. Metamorphic amphibole in JGC

The metamorphic amphibole crystals have been only detected in two locations: the Rengård intrusions and the Nör-Jörnsberget. It is smaller (< 0.50 mm) to the igneous amphibole (1-4 mm) but also occurs substituting the igneous crystals. The optical characteristic of the metamorphic amphiboles indicates the alkaline nature of the crystals (green to bluish pleocroism). These amphiboles are usually idiomorphic prismatic to acicular.

Three main amphiboles can be defined in the Rengård intrusions:

a) The igneous amphiboles are usually partially substituted by metamorphic amphiboles. It is pervasive in the rim of the crystals but the cores preserve the igneous character. Some of the amphiboles are totally substituted by a fine grain metamorphic amphibole aggregate (**Pic V-37**). The oblique cleavage system of amphiboles is usually filled of metamorphic amphiboles and also occurs magnetite inclusions.

b) A newly formed amphibole crystals characterize the second kind of metamorphic amphiboles. These very fine grain crystals (< 0.5-1 mm) are overprinted to igneous amphibole and biotite (**Pic V-38**). These are usually prismatic with a well-defined amphibole shape and cleavage. It usually crystallizes as decusated clots (**Pic V-39**).

c) The third kind of amphibole crystals does not occur in all the samples with metamorphic amphiboles. These are very fine grain amphiboles (5-50 μm) and occur filing fissures and microfractures in the minerals. These are usually grouped in the qz and kfs matrix (**Pic V-40**).

The amphiboles in the Nör-Jörnsberget have been only defined one kind of amphiboles. These are very fine grain crystals acicular or prismatic smaller than 0.50 mm. It usually occurs with the decussated biotite (**Pic V-41**). The igneous amphiboles are substituted in the rims but cores relicts of hornblende are common.

V.1.2.4.3. Metamorphic quartz in JGC

The quartz crystals of GI have evidence of metamorphism and usually it can be defined in hand specimen. The quartz is commonly re-crystallized as microgranular aggregates that substitutes the quartz phenocrystals (**Pic V-42**). The polygonal texture is usual. Isogranular polygonal quartz substitutes the phenocrystals but it is often heterogranular polygonal to saw-like textures. The cores of the quartz are usually not re-crystallized to polygonal microquartz (**Pic V-43**).

V.1.3. GII phase of the Jörn Granitoid Complex

This phase outcrops in the area of the city of Jörn and in the northern areas of JGC, this phase is subdivided in two subphases. The subphase GIIa is a medium grain granodiorite with amphibole and biotite. The GIIb is a medium to fine grain pyroxens bearing qz-monzodiorite. These intrusions are not deformed or altered.

V.1.3.1. Petrographic description of GII phase

GIIa subphase

This phase is homogeneous in mineralogy and textures as medium-grained granodiorite with granitic to porphyritic texture, white-colored in outcrop. Small

smoky quartz is characteristic in this phase. Idiomorphic to subidiomorphic K-feldspars and plagioclase are unaltered with the occurrence of some K-feldspars phenocrysts. Medium to fine grain hornblende is common and the biotite is usually sagenitic. In some areas can be determined a GIIa border phase with minor or absent hornblende than other areas. The plagioclase crystals are unaltered and ranges from oligoclase to andesine, these are subhedral tabular crystals with simple zoning and albite twins. Later poikilitic kfs crystals occur with pertite exsolutions. The amphiboles are euhedral to subhedral hornblende and occur as clots of amphibole and biotite (**Pic V-44**). The biotite is less abundant than amphibole and usually is observed as sagenitic textures. Apatite and titanite are relatively abundant accessory minerals, and particularly the titanite also occurs as subhedral crystals similar in size to biotite, titanite is many times associated to amphibole crystals. The apatite occurs as inclusions in the mafic minerals.

The microgranular enclaves are common with mineralogy similar to the host rocks. The enclaves are fine-grained granitic with absence or very low amphibole phenocrystals content. The interstitial quartz is less abundant than the host rock and the plagioclase is euhedral or glomeroporphyritic. Alkali feldspars are less abundant than the host rocks or absent in many areas of the microgranular enclave. Titanite is much less abundant than in the host rock but occur some magnetite. Mafic minerals are more abundant than in the host rocks.

GIIb subphase

It is an unaltered and undeformed medium- to fine-grained inequigranular qz-monzodiorite with kfs and pyroxene phenocrystals. Quartz in very low abundant and occur as interstitial crystals. The plagioclases are oligoclase to andesine and occur in a bimodal size distribution: occur some phenocrystals of plagioclase and as tabular euhedral to subhedral crystals in the matrix. Alkali feldspars are poikilitic with some small pertite. Accessory minerals are the same as GIIa but lower content of titanite and higher of magnetite.

The main character of GIIb is the occurrence of relicts of clynopyroxenes in the cores of some amphiboles, the uralite texture are common (**Pic V-46**). The pyroxenes usually occur with rutile exsolutions in the cleavage planes. In the boundary pyroxene-amphibole occur reaction textures. The pyroxenes only occur in the major sized amphiboles, and cannot be observed in the amphiboles of lower size. Amphiboles occur as clots and are smaller than the pyroxene crystals, it is medium size subhedral crystals. The clots of amphibole include biotite (sagenitic). The mafic minerals postdate the kfs and plagioclase.

The microgranular enclaves are commonly fine- to very fine-grained. Quartz is rare in the enclaves and also occurs amphiboles or relictic pyroxenes. Mafic minerals are more abundant than in the host rock (**Pic V-47**). In general the enclaves are fine grain isogranular monzonite (qz) and not reaction margins are developed (**Pic V-48**). The enclaves are centimetric to decimetric, rounded or elliptic with a variable abundance in the rocks (**Pic V-49**).

V.1.3.2. Alteration of GII: Uralitisation of pyroxenes

It is characterized in the substitution of pyroxene by pseudomorphic amphibole (usually hornblende). It has two possible processes (Shelley, 1993).

a) The uralite alteration can be related to metamorphism, and occurs tremolite or tremolitic hornblende that substitutes partial or totally the pyroxene crystals.

b) The intrusive fluids produce the second case, it is generated in the late stages of the intrusions (deuteric solutions). A continuous transformation from pyroxene to amphibole and it crystallizes with the amphibole shape crystals.

V.1.4. GIII phase of the Jörn Granitoid Complex

It occupies 1/3 of the total surface of JGC. It is the most homogeneous phase in mineralogy and texture. It is a medium- to coarse-grained qz+kfs porphyritic leuco-monzogranite to granodiorite and some areas of medium grain granitic texture. In hand specimen it is with to pink or orange with abundance of bluish quartz. The quartz is 3-6 mm with a usual undulating extinction. Alkali feldspars occur as 10 mm phenocrystals with biotite and plagioclase inclusions (**Pic V-51**). Plagioclase crystals occur with a bimodal distribution as a subhedral phenocrystals of 2-4 mm size and a glomeroporphyritic texture, and as 0.5-1 mm crystals in the matrix and included as inclusions in the poikilitic kfs. The small plagioclase crystals are not zoned or twined. A slight saussurite occur in plagioclase sometimes.

GIII is poor in biotite, lower of the 5% modal of the whole rock. The biotite crystals are 0.5-1 mm size and occur in association with apatite crystals. The titanite is relatively abundant as accessory minerals as occurs in GII with 0.5-1 mm to 2 mm size.

Hobergsliden subphase

It is a medium-grained granitic to qz+kfs porphyritic leuco syeno-granite. The pertitic exsolutions are pervasive in the alkali feldspars. The biotite minerals occur almost as accessory minerals and plagioclase is very low abundant (< 5% modal). It could represent the last igneous event of the GIII magmas.

V.1.5. GIV phase of the Jörn Granitoid Complex

The GIV pluton is located in the centre of the GIII phase. The mineral composition is similar to the GIII phase but lower in size and higher abundance of plagioclase. It is a grey medium- to fine-grained granitic equigranular leuco-monzogranite to granodiorite. The quartz is 3-5 mm and slightly elongated. The plagioclase is 2-4 mm but often occur relicts of plagioclase substituted by alkali feldspar during crystallization with skeletal texture (**Pic V-53**). Plagioclase 0.5-1 mm size crystals occur in the poikilitic kfs and as clots. The alkali feldspars are poikilitic 3-5 mm size. The biotite group minerals are more abundant than GIII (> 5% modal), and occur 0.2-0.5 mm size and clots. Titanites and apatites occur as accessory minerals, and also occur some white micas associated to plagioclase crystals.

V.1.6. Näsberg layered intrusion

It is a complex layered intrusion locates in the northern area of the JGC, but it is dominated by two main phases:

Näsberg Gabbronorites

This phase is often medium-grained and occurs with diverse textures. The most usual texture is the intergranular with the major abundance of plagioclase than pyroxenes. It is usual the subhedral to anhedral orthopyroxenes (hypersthene s.l.) with a pervasive fracturation developed on the double cleavage system, it is characteristic the pinkish to greenish pleocroism. The clynopyroxenes are medium-grained equigranular to the plagioclase, with common opx exsolutions in the cleavage (**Pic V-54**). Plagioclase is unaltered, usually tabular and subhedral. The boundary among plagioclases is filled by opx, also occur some biotite or amphibole but very low abundant. Reaction among plagioclase and pyroxenes with magnetite interstitial is common, and occur some rims of amphibole related to plagioclase-pyrxene reactions with magnetite (**Pic V-55**).

Ophitic textures are also abundant wit poikilitic cpx, 10 mm long, with unaltered plagioclase (**Pic V-56**). The cpx are anhedral and usually occur some opx exsolutions. The plagioclases occur with lobated margins. Plagioclase is tabular and subhedral with slight zoning and twins. Plagioclase crystals are not oriented. The opx is fine grain 0.5-1 mm. The biotite crystals are rare and occur in rim reaction with the magnetite crystals (1-2 mm). Amphibole crystals are kaersutite and hastingsite of 1-3 mm.

Näsberg Olivine Gabbronorites

It is medium-grained ophitic to subophitic and usually contains olivine, opx (hyperstene), cpx, plagioclase (labradorite to bytownite), amphibole and biotite, with some magnetite/spinel and ilmenite as accessory minerals.

The olivine is 1-2 mm, unaltered to serpentinized and usually reacts with opx as symplectite (**Pic V-57**). It is usual to occur an opx rim on olivine and inclusions associated to the fractures. The opx is subhedral to anhedral, 1-3 mm, colorless or slightly pleocroic. The opx crystals are moderately to strongly fractured parallel to the cleavage system, rutile inclusions are common. The cpx is poikilitic, 2-7 mm, and also occurs as fine grain crystals in the matrix. The opx exsolutions in cpx are widespread. Idiomorphic to subidiomorphic plagioclase is 2-4 mm with lobated boundaries in the poikilitic crystals. Amphibole and biotite are rare. The slightly altered zones usually produce serpentinizaton of olivine and chloritization of pyroxenes. Plagioclase is usually unaltered in the alteration zones.

V.1.6.1. Uralitisation of pyroxenes in Näsberget

The intrusive fluids generated in the late stages of the intrusions (deuteric solutions) produce uralitisation of pyroxenes. It generates a continuous transformation from pyroxene to amphibole and it crystallizes with the amphibole shape crystals.

V.1.7. Gabbros and diorites un-differentiated

Mafic intrusions are usual in the JGC and these are widespread in the whole complex: in the Älgträsk, south of the Jörntrasket, east of the central JGC. Also occur gabbros and diorites in the Stavaträsk intrusion or in Gallejaur. These intrusions are quite diverse but usually dominated by medium grain gabbronorites and diorites with ophitic to doleritic textures.

At the west of Jörn in the Hill Sör-Jörnsberget occur medium to fine (less) grain doleritic gabbronorites, it is usual the cpx and the sunhedral medium to fine grain plagioclase (**Pic V-58**). The reaction textures of plagioclase and magnetite are common. The actinolite-tremolite is usual as alteration products. Olivine has not been described but occurs some altered areas with probably bear some olivine crystals previous to the alteration. South of Jörn in Älträsk occurs gabbros similar to the Sör-Jörnsberget. Poikilitic kfs and plagioclase are usual but strongly altered to actinolite-tremolite, epidote and white micas.

The eastern gabbros and diorites are close to the boundary with the Bothnian metasediments in the area of the Klintån River. It is dominated by poikilitic textures with 5-10 mm amphiboles and smaller plagioclase (**Pic V-59**). Igneous pyroxenes are not preserved and usually altered to actinolite-tremolite, and occur some biotite.

V.1.8. Porphyritic basalts (Vargfors Group)

These rocks occur in a great diversity of textures and structures, the occurrence in Skellefte district is cited in the Geological Setting of this work. The usual texture is afanitic porphyritic with orthopyroxene and plagioclase. The opx phenocrystals are idiomorphic to subidiomorphic (**Pic V-61**) with lamellar twin and usually substituted by cpx and slightly to moderate altered. The plagioclase is phenocrystals are

moderately altered (**Pic V-62**), but higher alteration in the plagioclase of the matrix. Olivine crystals have not been observed but some morphological characteristics could indicate its initial presence.

V.1.8.1. Andesite basalts in the southern contact of JGC

The southern Dike of JGC has peculiarities that indicate its basaltic origin and autobrecciation. This area is usually more altered than the other basaltic porphyries and contains fragments of GI and autoclasts. The more foliated areas cannot be studied even by petrographic microscope. The most common textures are shown in the sample JO03-107 (**Pic V-63**). It is a fragment of porphyritic basalt with plagioclase and opx with a very fine matrix hosted in very fine chloritized basaltic rock with epidote actinolite and chlorite in the matrix (**Pic V-63**). This fragment is the same rock that can be observed in Ullricksberg, Vithatten or Nicknoret. The pyroxene is overprinted by the fine grain matrix rock, but the margin of both phases is lobated and chilled. The mafic crystals in the strongly altered rocks are usually altered to chlorite and epidote (**Pic V-64**). The plagioclase is usually altered to very fine grain sericite and epidote. Secondary amphibole is also substituting the magmatic pyroxene crystals.

V.1.8.2. Andesite basalts deformation (Southern dike)

The matrix of these basaltic rocks is very fine-grained and often strongly foliated. It is composed by altered plagioclase and amphibole, secondary epidote and chlorites and some magnetite/spinel (**Pic V-65**). The minerals of the matrix are not usually elongated or organized in a preferred orientation.

The southern Dike and GI associated rocks are the most deformed intrusions in the central area of the Skellefte mining district. A strong foliation occurs in the afanitic porphyritic basalts of the dike. In hand specimen the fragments are abundant (autoclast?) and range from 1 to 50 cm (**Pic V-66**). The fragments are rounded and elliptic oriented with the foliation (N110ºE/80-85ºN). The foliation usually does not modify the textures of the fragments that usually occur with chill margins. The deformation in the most deformed zones modifies the primary textures of phenocrystals with elongation and substitution by secondary chl, ep and amph. Less deformed areas preserve the original igneous phenocrystals of opx and pl with strongly foliated matrix (**Pic V-67**). GI tonalite fragments are not foliated (**Pic V-68**).

V.1.9. Gallejaur monzonite

It is located in the southwestern corner of the JGC. It is composed of quartz-monzonites but with important textural variations from inner core to outher rims. At the same time it is rounded by gabbros and diorites of the Vargfors Group.

Outer Rim of monzonites

The quartz monzonite is characterized by a medium- to fine-grained granitic to porphyritic texture, 0.5-2 mm, and some alkali feldspar phenocrystals of 15 mm. The modal quartz content is lower than 5% and it occur as very fine grain crystals. Alkali feldspars and plagioclase occur in the same amount as phenocrystals or matrix minerals. The biotite group minerals is acicular or occur as radial cumulates (**Pic V-70**). The medium grain idiomorphic to subidimorphic amphibole crystals are usual and rich in magnetite inclusions. Magnetite is an abundant accessory mineral, and magnetism is evident in hand specimen with the occurrence of bands rich in magnetite as fracture fillings. Magnetite also occurs as lineation of spotted crystals in the matrix (**Pic V-71**).

Inner Rim of monzonites

It is medium-grained quartz monzonites with plagioclase phenorystals (2-4 mm). The simplectitic texture of qz and kfs intergrowth occurs as rim around the plagioclase

phenocrystals. The simplectite texture is 1/3 of the whole rock (**Pic V-72**) and varies from fine grain to medium grain simplectite.

The plagioclase minerals are idiomorphic to subidiomorphic with 2-4 mm phenocrystals and 0.5-1 mm size in the matrix. Plagioclase is slightly altered and some epidote occurs associated to altered plagioclase. The quartz as non-simplectite is rare and occurs as very fine grain interstitial crystals in the matrix. The amphibole crystals are the same as in the outer rim but chloritized or altered to actinolite-tremolite. In the extent simplectite zones do not occur amphiboles and epidote and chlorite aggregates are abundant. Magnetites minerals are usual and occur bigger in size as the outer rim magnetites, but do not occur as lineation or spotted it occur as aggregates with epidotes and chlorites. Biotite crystals are less abundant than accessory magnetite.

The microgranular enclaves are abundant, and some outcrops are 15% modal enclaves. These enclaves are fragments of the outer rim quartz monzonite and occur with lobated margins. Some enclaves do not occur with chilled margins and occur as transition from host rock to enclave in texture and mineralogy. The enclaves are smaller in size than the host rock but contain more amphibole and plagioclase (**Pic V-73**). Biotite crystals do not occur in the enclaves.

V.1.10. Viterliden Intrusive Complex (VIC)

These intrusions are located in the westernmost part of the Skellefte district and comprise many intrusive phases. It contains manly tonalites, trondhjemites and granites. The deformation occurs in the intrusive and the host rocks as strain areas (High Strain Zone) and folding.

Hornblende tonalite

It is the main intrusive phase in the complex and is a medium-grained granitic to porphyritic tonalite but must be classified as quartz amphibolite. The felsic layers are 1-3 mm thick and comprise plagioclae and quartz, and the mafic layers of biotite and amphibole are 1 mm or less thickness (**Pic V-74**). The plagioclase and quartz in felsic layers occur in polygonal texture in a < 0.5 mm matrix. Plagioclase relicts of 1-2 mm also occur as granoblastic crystals but are not deformed (**Pic V-75**). Mafic layers are constituted by amphibole, biotite and epidote and some magnetite/ilmenite. Biotite and amphibole are oriented in the layers, some biotite is slightly altered to chlorite. Granoblastic amphibole is 1 mm and is usually not oriented with the deformation, these crystals are usually zoned and rich in rutile inclusions. The apatite and epidote occur as accessory minerals.

Trondhjemite

It is white medium- to fine-grained granitic equigranular to porphyritic trondhjemite. Only occur plagioclase and quartz as minerals. The quartz and plagioclase (subhedral tabular) are 1-2 mm but plagioclase also occurs in the matriz (**Pic V-76**). The plagioclase is slightly altered to sericite and less epidote. The chloritized biotite crystals occur as accessory mineral (< 1% modal).

V.1.10.1. VIC deformation

The deformation in the VIC is mainly ductile but with the occurrence of brittle shear areas as the High Strain Zone. It is defined by two main regional west-vergent anticlines. The northern charnel hosts the Kristineberg deposit. At mid-scale occurs chevron folds with crenulations associated to the mineralogical layering, charnels oriented in the N280ºE planes. The strong foliation associated to folding occurs oriented E-W/80-85ºN. The mineralogical layering is characteristic with the alternation of felsic (plagioclase+quartz) and mafic (amphibole+biotite) layers (**Pic V-77**). The porphyritic trondhjemites are usually undeformed or slightly foliated.

V.1.10.2. VIC Metamorphism

The metamorphism is characterized by a dynamic regional metamorphism that generates medium-grained layered qz-amphibolites. The metamorphism also occurs with a syn-metamorphic ductile deformation. The metamorphism is not developed in the whole phases of the VIC or the characteristics are not defined, in this case the trondhjemites does not indicates any kind of metamorphism.

The main metamorphic phase is a medium-grained metamorphic to tectonites qz-amphibolite, with granolepidoblastic to granoblastic plagioclase and amphibole. The melanocratic bands are porphyroblastic with medium grain porphyroblastic amphiboles (igneous relicts) in an intermediate lepidoblastic to nematoblastic fine grain matrix rich in amphiboles, biotites, chlorite and epidote. The felsic layers are granoblastic to porphyrogranoblastic medium grain, with plagioclase porphyroblast.

The mafic layers minerals are amphibole, epidote and biotite. The epidote is abundant close to the porphyroblast of amphibole. Epidote is smaller than 100 μm with idiomorphic prismatic shape **(Pic V-79**). The amphibole porphyroblasts are biotite inclusions rich (**Pic V-80**). The biotite and epidote minerals are 100 to 500 μm, and also occur some apatite and oxide inclusions.

In the Säter Salient (southern charnel of VIC) is located Skellefte Group metavolcanics. These rocks are composed of quartz, biotite, muscovite, and cordierite and less kyanite. It is a medium to fine grain inequigranular granitic metavolcanics with oriented phyllosilicates.

V.1.11. Revsund type granitoids

In the Skellefte mining district the Revsund granites are quite common, it is usually coarse-grained porphyritic granites with kfs phenocrystals. The mineralogy ranges from monzogranites (close to JGC) to alkali feldspars granites (close to VIC) (**Pic V-82**). In hand specimen the bluish quartz is usual and occur as aggregates of 5-12 mm. Alkali feldspars phenocrystals are 10-15 mm but sometimes bigger than 30 mm idiomorphic to subidiomorphic with pertite exsolutions. Plagioclase is an isogranular idiomorphic tabular albite of 2-4 mm. The biotite group minerals occur in the Revsund of the JGC and also occur some muscovite in the Revsund of the VIC area but are not always in this granite (**Pic V-83**).

In some areas of the Revsund (Renström area) it contains a great diversity of enclaves and xenoliths. Microgranular rounded or elliptic enclaves are 5-50 cm medium-grained porphyritic granites with same mineralogy as host rocks but higher amount of mafic minerals (**Pic V-84**), the boundaries of the enclaves are transitional to the host or chilled. The amphibole (hornblende) content of the enclaves is relatively high with zoning and subidiomorphic shape. The plagioclase is idiomorphic and tabular shaped and quartz or kfs are interstitial but abundant. Some alkali feldspar phenocrystal occurs in the enclaves and titanite as accessory mineral is 1-2 mm in size. Magnetite occurs associated to biotite.

The xenoliths of Revsund are abundant and ranges from 1 to 50 cm, up to 15% modal in some restricted areas. It occurs rounded, elliptical and angular in shapes. These are very fine grain with mafic phyllosilicates and some plagioclase, most of the xenoliths are covered by an oxide patina (**Pic V-85**). The areas of abundant xenoliths are related to dikes occurrence of fine grain quartz and kfs porphyritic leuco-granites. The areas rich in xenoliths are coarser grain than those where it is absent with kfs phenocrystals up to 60 mm and 30% modal of the rock. These areas are plagioclase poor and smaller with quartz lower than 20% and rich in mafic minerals (biotite and amphibole) 30% and completed percent with the xenoliths.

V.1.12. Stavaträsk

It is a pluton located 5 Km at the east of the JGC and composed by two well differentiated phases. The first is mainly composed by diorites and gabbros similar to those that can be found in the Näsberg intrusion. The second is a medium grain granitic to quartz and felspars porphyrytic tonalite similar to GIIa, it produced a contact metamorphism aureole on the metasediments of Skellefte Group.

V.1.12.1. Contact metamorphism of Stavaträsk pluton

The Stavaträsk granodiorite intrudes the metasediments of Bothnian Group, it is the only known outcrop where the intrusion-host sediments can be observed. In this area it is developed a thin contact metamorphism band. The andalucite (quastolite) crystals, 0.50 to 1.50 cm size, are abundant and also occur associated to biotite an alkali feldspars (**Pic V-86**). The general texture of the rock is layered with felsic qz+kfs and mafic biotite rich layers. The matrix crystals are 100 to 1 μm.

V.3. EXTENSION AND INTRUSIVE STAGES OF JÖRN GRANITOID COMPLEX

The number of phases and limits of the JGC have been changed with the improvements of new research in mapping and geochemistry. The first division of the JGC was Granodiorites, Jörn Granites and Diorites and Gabbros (**Fig. V-26**), and was completed with 109 lithochemical analyses (Svensson, 1970; Svensson, 1980). The Granodiorites was in the central area (actual GIII), the GII pluton in the city of Jörn and in the southern margin (actual defined as GI). The Jörn Granite included the northern area and some inner areas in the central-south area of the JGC, actually defined as GIIa. Diorites and gabbros are defined in the JGC since this time without any modification.

Using the new techniques in geophysics, mainly in airborne gravimetric analyses, by the Mining Companies, it was redefined the boundary and number of phases of the JGC. At this time is when GI-GIV nomenclature is accepted (**Fig. V-27**), and GIII or GIV is defined in the central area of the complex (Wilson et al., 1987). But the northern area of the JGC is determined as Sorsele Group granitoids that are the younger rocks in the Skellefte district (**Fig. V-27**), actually are not any dating of these rocks to check the age and compare it with the JGC phases. A regional mapping is defined in the Skellefte mining district in the late eighties (Rickard, 1986).

V.3.1. Limits of the Jörn Granitoid Complex

Most of the actual limits of the JGC are defined by tectonic structures, the intrusive structures of JGC on the host rocks are not preserved or actually can't be observed. The main eastern and western limits of the JGC can be traced by regional faults SSW-NNE (**Fig. V-28**). To the west the JGC limits with the subaereal rocks of the Arvidsjaur Group, in this border phase GI is characterised by qz+kfs porphyrytic tonalites. It is a straight boundary, but the absence of outcrops makes difficult the exact delineation. In contrast the eastern boundary is delimited by diverse faults and folding and includes diotites, GI tonalites, GII granodiorites, proterozoic sediments from Bothnia Group and Skellefte volcanics (**Fig. V-28**). The northern JGC limits with the Bothnian sediments in the east by regional faults in NW-SE direction, some megablocks of this metasediments can be found in the northern areas of JGC. To the west the limits with the Arvidsjaur volcanics are defined as in the central western areas by a porphyrytic tonalite.

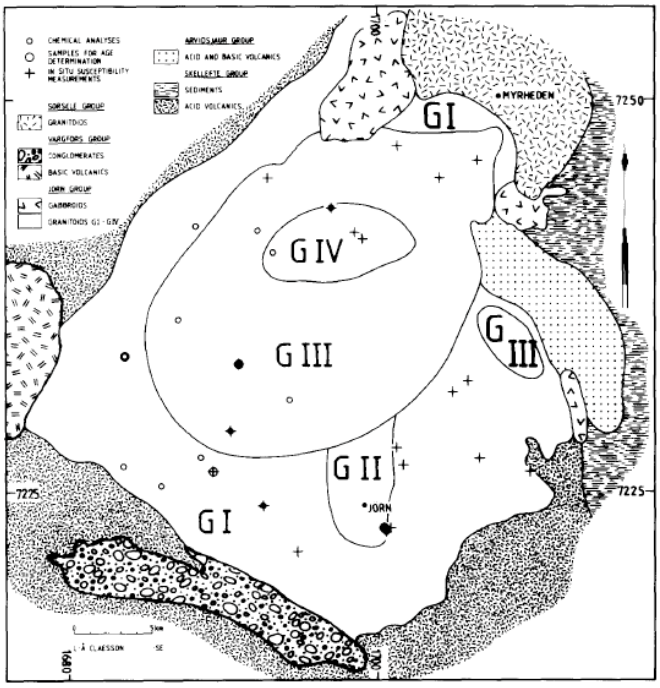

Fig. V-27. Wilson et al. (1987), geological map of the JGC. The northern area is defined as Sorsele Group granitoids.

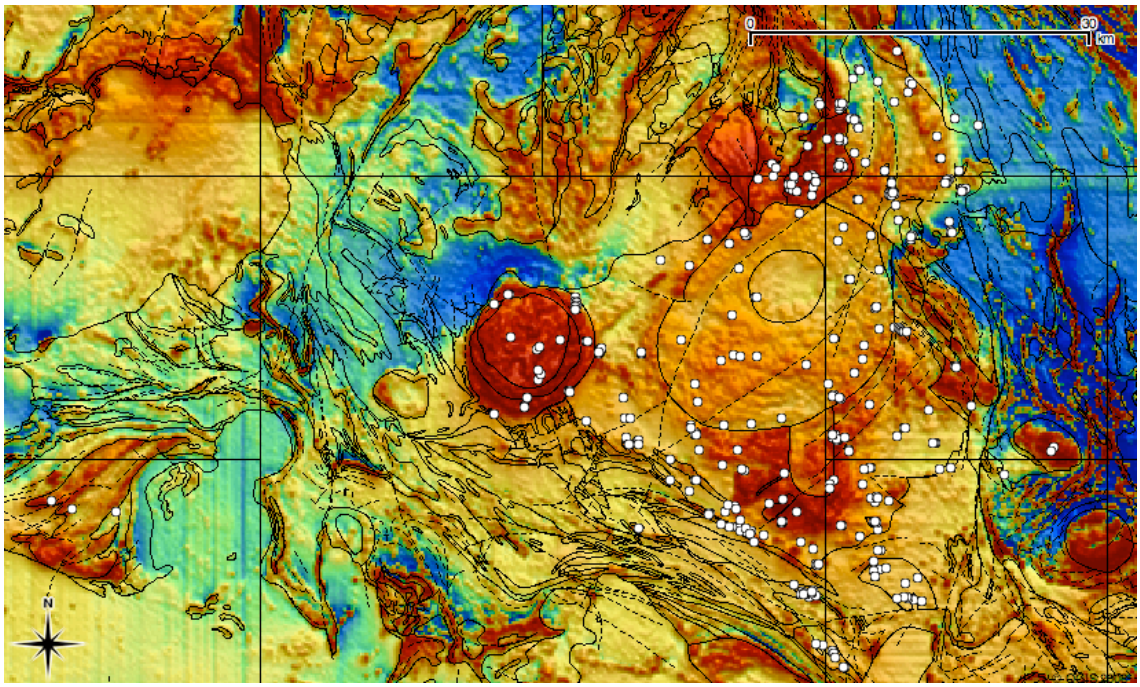

Fig. V-28. The Bouger anomaly map of the Skellefte mining district (SGU). The samples used in this study like white circles. Main structures in dashed lines and geology in line.

V.3.2. Southern boundary of JGC and Southern Dike

The southern limit is under controversy, but in this work we agree with the nature of this mafic rocks as a dike of Vargfors Group generated during extension of the basin (further description of these rocks in the Chapter about Petrography). The variety of rocks in the south of JGC comprises the Vargfors conglomerates and upper sedimentary series of Vargfors Group, and the Skellefte volcanics. In the Vargfors conglomerates at the south of GI can be found fragments from JGC only of the GI phase, any other JGC phases have not been observed. A detail of the southern boundary of GI with the mafic rocks of the Vargfors Group is exposed (**Fig. II-14**). Structural schemes of the rocks are drawn in the 3 and 104 outcrops, the jigsaw-fit texture with the mafic porphyrytic rock (same rock as can be examined from the central massive areas of the dike) intruding in the GI tonalite is similar in both cases. In this zone (**Fig. V-29**) the southern Dike is generally strongly foliated (N110ºE and average inclination 80º to north) and contains many fragments of GI tonalites and basic porphyrytic clasts (autoclasts?). These fragments are orientated with the foliation and occur with a diverse size and abundances. In the outcrops far from the boundary (1, 6, 7, 9 and 12) can only be determined mafic porphyrytic fragments some of them with decimetric sizes and igneous textures. Many inner areas of this Dike is characterised by the igneous texture as massive basaltic porphyrytic lava, an example are the outcrops 2 and 28 (geochemical samples has been obtained of this outcrop: JO04-154). In the outcrop 14 the GI phase is strongly foliated, parallel to the foliation of the mafic Dike in the outcrop 13 located to 50 m; the closer GI rocks to the mafics are characterised by cataclastic texture. Some rocks similar to diorites with chlorite alteration are located in the outcrops 29, it could be an internal zone of the mafic Dike.

In the southwest margin of the Dike occur the same igneous textures and structures as in the northeast side of the Dike but the Vargfors conglomerates cover most of the area. This mafic Dike occurs side to side of the southern margin of GI (N110ºE) with some of these structures in the outcrops. In the southwest corner of the JGC the mafic Dike is overprinted on the GI tonalites as a dike with an orientation of N130ºE (the dip of cleavage can not be determined), almost subparallel to the main Dike (sample JO03-71: N-7230983, E-1677360); this mafic porphyrytic rocks occur with igneous texture. In the

Vithhatten Hill the basalts occur with a similar igneous texture as in the massive areas of the southern Dike; some outcrops of the Vithatten Hill occur with similar clasts (autoclast?) of the southern Dike. This mafic porphyrytic rocks also occurs in the Skellefte River, south of the Gallejaur intrusions, and in the Ullbergträsket in the northwest of the JGC.

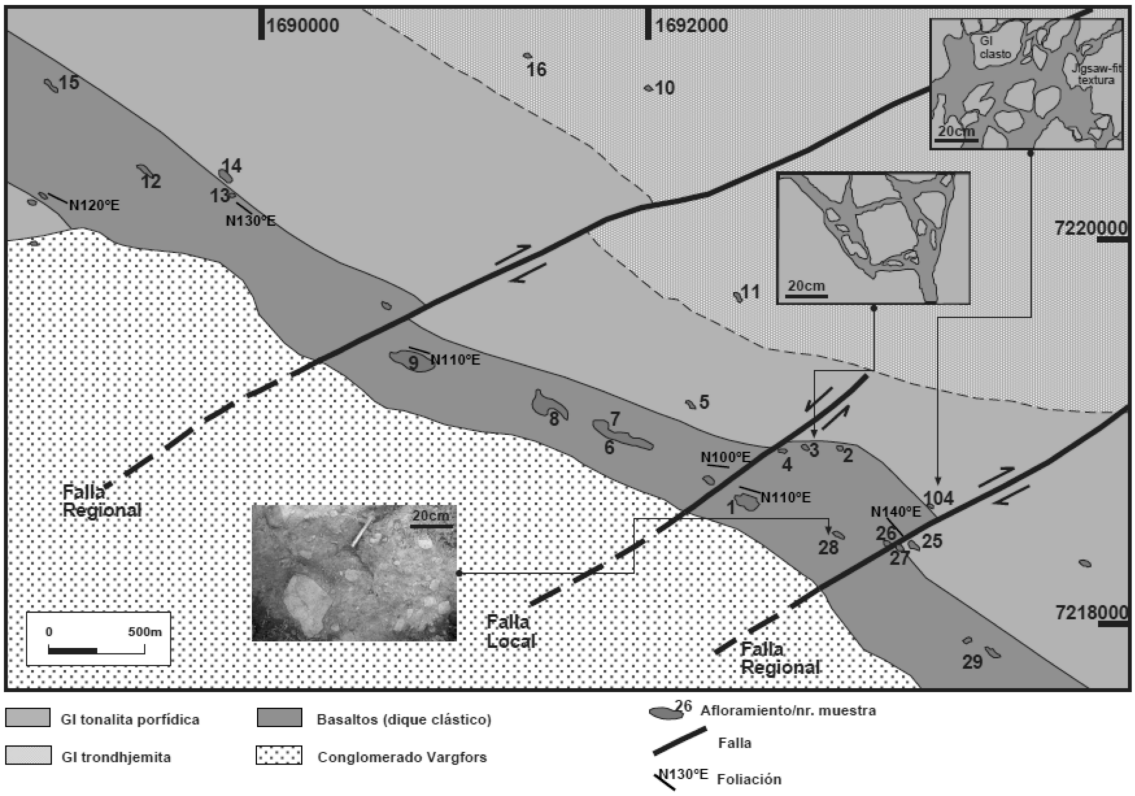

Fig. V-29. Detailed map of the GI-southern Dike rocks in the southern boundary of JGC.

V.3.3. Phases distribution in the JGC

The GI tonalites is the phase with a most complex distribution in the JGC, due to the different igneous textures (fine grain trondhjemites to coarse grain qz+kfs porphyrytic tonalites) as to the diverse process that occurs on this rocks and that modified the original textures. The old technical literature (Svensson, 1970; Svensson, 1980; Wilson et al., 1987), overestimated the presence of GI in the northern areas of JGC. In the north GI is located in the northwestern margin and in marginal areas close to the Näsberget layered intrusion. The main areas where the GI phase outcrops is in the southern and western borders of the JGC, and many areas in the southeaster area (**Fig. V-30**).

The northeast of the JGC, previously described as Jörn Granites or Sorsele granites (Svensson, 1970; Svensson, 1980; Wilson et al., 1987), is complex in the distribution of intrusive phases. As previously the GI occurs close to the east of the Näsberget layered intrusion and as megablocks into this basic intrusion. Although GI occurs in the north, this area in dominated by GII phases (**Fig. V-30**). In the GIIa of the northeast occur some megablocks of folded metasediments (sample JO04-141: N-7255080, E-1711453). In the south the GII phase occur in a small pluton close to the city of Jörn of GIIa subphase, but in other locations occur both phases GIIa and GIIb. In the boundary GIII-GI occurs some GIIa rocks but the absence of outcrops makes difficult the mapping of the real plutonic limits. In the next picture (**Fig. V-31)** is shown the outcrop with both subphases, GIIa and GIIb (sample JO04-147: N-7227111, E-1700632). The GIIb contain fragments of GIIa (left) and the mafic porphyrytic dike (right), abundant microgranular enclaves occur in the GIIb and other mafic dikes are intruding the GIIa in this area.

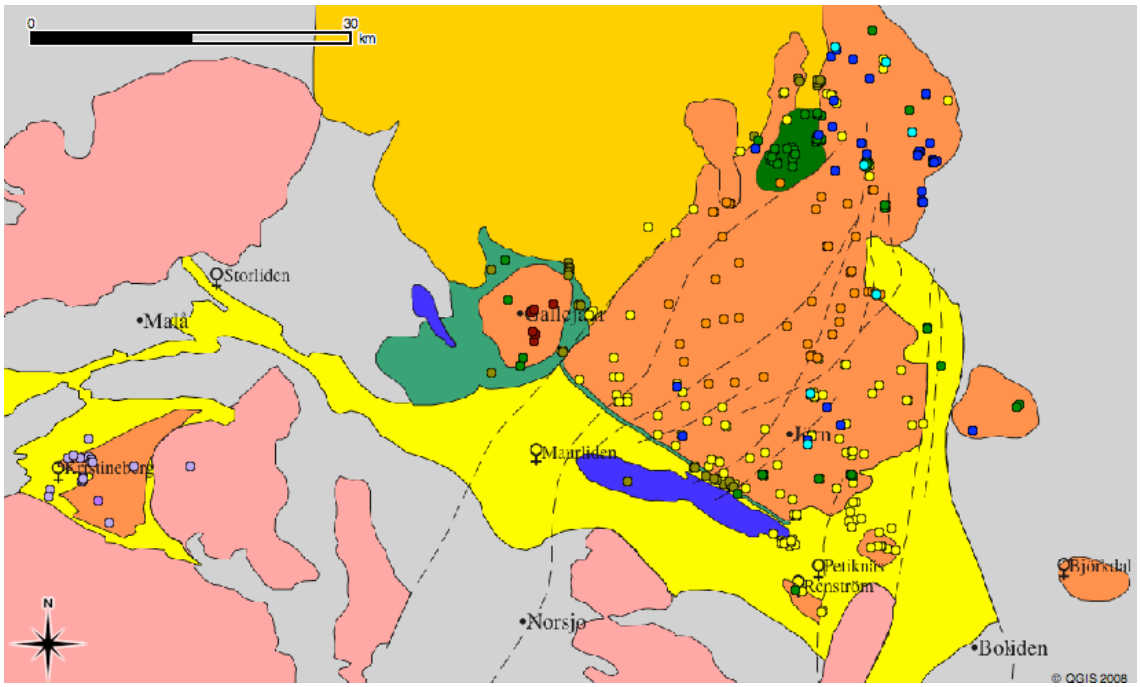

Fig. V-30. Regional geology with the locations of the samples used in this work. GI-yellow; GIIa-blue; GIIb-cyan; GIII-oranje; Monzonita-red; Gabbro-green; Basalts (dike)-dark green; VIC-violet.

The GIII phase outcrops in the centre of the JGC and occupies 1/3 of the whole JGC. It is postdating the GI and GII phases of JGC and the Antak of the Arvidsjaur (in the northwest). In the centre of the GIII is located the small GIV pluton. The Hobergsliden intrusion occurs in the northeast limit of GIII with the GII phases, it can be observed with simplectitic texture in the Ålsån River (N-7247958, E-1702888) with GII, mafic dikes and GI outcrops.

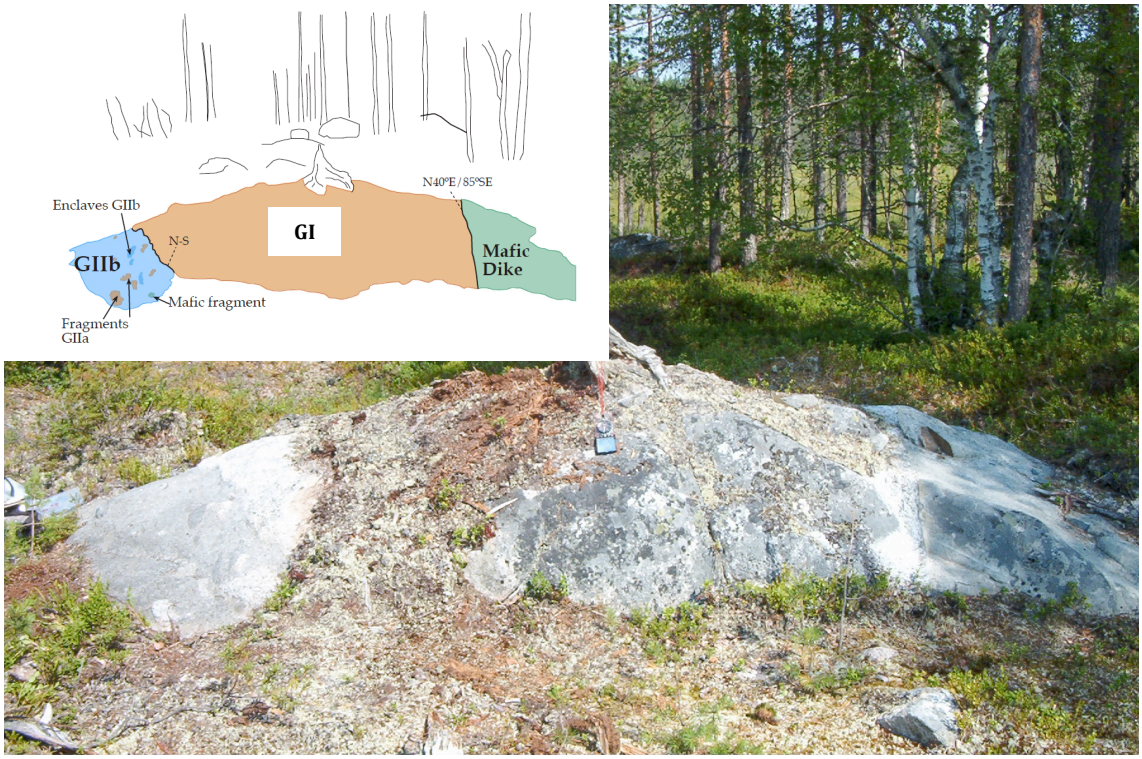

Fig. V-31. Picture of the GI and GIIb phases. Mafic dike in the right. Sample JO04-147 from the left.

VI. LITHOGEOCHEMISTRY

In the 2004 fieldwork 40 samples were collected to lithogeochemical analyses. The samples 94 and 147 have been duplicated using the standards procedures in the lithogeochemical analyses, it are from GI and GIIb phases of the JGC respectively. The 40 samples with the location in **table VI-1**, see **fig. VI-39** for location:

JO04-	N-coord	E-coord	Intrusive	Phase
03	7253287	1701197	Näsberg	Gabbronorite
06	7241282	1695737	JGC	GIV
07	7244764	1707754	JGC	GIII
23a	7247958	1702888	JGC	GIIa
24a	7250550	1705320	JGC	GIIa
34	7251600	1710192	JGC	GIIb
40	7258145	1707694	JGC	GIIb
51	7255290	1698135	JGC	GI
67	7252679	1698440	JGC	GI
75	7214608	1704438	JGC	GI
78	7218162	1703042	JGC	GI
83	7236331	1706834	JGC	GIIb
86	7221615	1704600	JGC	GI
88	7226455	1709570	JGC	GI
94	7215565	1699278	JGC	GI
100	7227773	1688105	JGC	GIIa
101	7223140	1688600	JGC	GIIa
107	7234447	1683768	JGC	GI
109	7242145	1688038	JGC	GI
112	7249993	1695395	JGC	GIIa
114	7254584	1702825	JGC	GIIa
115	7255023	1702688	Näsberg	Gabbronorite
119	7251284	1701333	JGC	GIIa
120	7227795	1707066	JGC	GI
122	7225725	1702132	JGC	GIIa
124	7208502	1699776	JGC	GI-Rengård
127	7213930	1697180	JGC	GI-Kläddberget
128	7222353	1700381	JGC	GIIb
130	7219375	1696165	JGC	GI
135	7226363	1683510	JGC	GI
136	7248480	1705649	JGC	GIIb
138	7248698	1712144	JGC	GIIa
139	7259567	1702957	JGC	GIIa
142	7255113	1711458	JGC	GIIa
144	7212435	1708579	JGC	GI-Klockträsk
145	7223625	1715795	Stavaträsk	Granodiorite
146	7213335	1698785	JGC	GI-Brannliden
147	7227111	1700632	JGC	GIIb
149	7219448	1704473	Gabro indif.	SörJörnsberget
154	7218420	1693130	Basalts	Southern Dike

Table VI-1. Lithogeochemical samples of JGC and other intrusions.

The lithogeochemistry is focused in the GI and GII phases of JGC, due to the textural and mineralogical variations of the GI and GII. The GI samples are collected according to the textural variation and proximity to the Skellefte volcanics (host of the main VHMS deposits). These have picked in the southern and western margins and covering the southeastern area. The satellite GI intrusions have been sampled, including: Rengård, Klockträsk and the small Brannliden and Klädberget.

The GII samples covered the two GII areas, the small pluton in the Jörn city area and the northern undifferentiated area. The Stavaträsk granodiorite is included with samples of diverse mafic intrusions and the poyphyritic basalt of the Vargfors Group. The GIII and GIV are homogeneous in mineralogy and chemical composition, so have been included one sample of each phase.

VI.1. MAJOR ELEMENTS VARIATION DIAGRAMS

Although some samples are of basic character 3, 115, 149 and 154; most of the rocks are granitoids so the same diagrams will be used for all the rocks excluding the basics. The major elements are listed in the **table VI-2**:

JO04	SiO_2	TiO_2	Al_2O_3	Fe_2O_3	MnO	MgO	CaO	Na_2O	K_2O	P_2O_5	LOI	Total
03	50,39	0,45	17,05	8,32	0,11	11,35	7,75	2,58	0,50	0,08	1,2	99,88
06	72,07	0,27	14,79	2,44	0,03	0,62	2,29	4,14	2,82	0,08	0,5	100,05
07	76,51	0,11	12,52	1,56	0,03	0,13	0,24	3,54	4,95	0,02	0,5	100,11
23a	65,01	0,50	17,56	4,03	0,05	1,19	3,91	4,91	1,90	0,16	0,8	100,03
24a	69,14	0,48	14,56	3,87	0,04	1,09	2,91	4,05	2,91	0,15	0,8	100,01
34	64,48	0,72	15,39	5,05	0,07	2,12	3,91	4,23	2,93	0,24	0,9	100,05
40	62,62	0,92	15,68	5,92	0,08	2,36	4,22	4,45	3,11	0,31	0,3	99,98
51	68,45	0,35	14,55	4,36	0,04	1,49	3,44	3,19	2,89	0,06	1,2	100,02
67	67,25	0,34	14,50	5,91	0,06	1,72	4,26	3,37	1,55	0,08	1,1	100,15
75	68,38	0,38	13,92	5,49	0,08	1,33	4,33	3,42	1,31	0,07	1,3	100,02
78	74,97	0,20	12,68	3,36	0,04	0,25	1,74	4,34	1,58	0,03	0,8	99,99
83	68,67	0,41	14,90	4,02	0,05	1,04	2,72	4,12	3,52	0,13	0,5	100,09
86	70,86	0,38	13,88	5,37	0,12	0,66	2,86	4,15	1,37	0,10	0,3	100,05
88	62,12	0,48	16,49	6,64	0,10	2,44	5,82	3,13	1,34	0,09	1,3	99,96
94	75,23	0,38	13,03	2,15	0,04	0,44	2,28	6,13	0,04	0,08	0,4	100,18
94*	74,99	0,38	13,24	2,01	0,03	0,45	2,28	6,21	0,04	0,07	0,5	100,18
100	70,91	0,28	15,17	3,24	0,05	0,92	3,21	4,03	1,65	0,07	0,5	100,03
101	68,85	0,26	15,67	3,03	0,05	1,18	3,06	4,92	1,40	0,09	1,5	100,01
107	68,18	0,37	13,84	5,42	0,08	2,08	3,44	3,03	1,92	0,06	1,5	99,93
109	70,26	0,32	13,39	4,65	0,08	1,12	3,64	3,10	2,46	0,05	0,9	99,97
112	64,52	0,40	16,95	4,62	0,07	1,87	4,94	3,57	1,21	0,11	1,7	99,96
114	67,70	0,49	16,12	3,73	0,05	1,01	3,06	4,04	2,49	0,16	1,1	99,95
115	55,78	0,80	16,50	8,36	0,12	4,16	7,08	3,84	1,01	0,26	2,1	100,02
119	69,55	0,24	16,35	3,05	0,05	0,75	4,12	4,42	0,76	0,10	0,6	100,00
120	68,02	0,32	15,66	4,52	0,07	1,73	3,86	3,54	1,61	0,07	0,6	100,01
122	71,75	0,23	15,32	2,86	0,04	0,58	3,28	4,35	1,01	0,09	0,5	100,01
124	70,21	0,26	14,89	4,55	0,05	0,78	3,43	3,67	1,03	0,09	1,0	99,97
127	75,57	0,19	12,48	2,64	0,04	2,09	0,75	3,10	1,02	0,03	2,1	100,01
128	67,44	0,57	15,45	4,22	0,06	1,29	2,94	4,14	3,24	0,18	0,5	100,03
130	73,01	0,24	13,43	4,00	0,06	0,63	3,03	3,34	1,64	0,04	0,5	99,92
135	65,43	0,36	15,30	6,31	0,10	1,85	5,09	2,84	1,35	0,06	1,2	99,89
136	68,13	0,53	15,20	3,92	0,05	1,27	3,05	4,07	2,98	0,17	0,6	99,99
138	69,80	0,35	15,83	2,88	0,03	0,98	3,46	4,61	1,66	0,12	0,3	100,01
139	68,93	0,52	14,73	4,03	0,05	1,24	2,67	4,03	3,44	0,17	0,2	100,01
142	69,99	0,34	15,86	2,86	0,03	0,92	3,13	3,77	2,44	0,11	0,5	99,96
144	73,41	0,30	13,11	3,10	0,04	0,84	2,39	4,63	0,61	0,08	1,5	100,02
145	70,76	0,26	15,40	2,56	0,03	0,85	2,70	4,69	2,02	0,10	0,6	99,98
146	72,28	0,24	13,63	4,02	0,05	0,52	2,65	4,02	1,09	0,06	1,4	99,96
147	61,47	0,85	16,61	6,07	0,15	2,60	5,03	4,65	1,87	0,28	0,4	99,98
147*	61,40	0,82	16,69	6,03	0,14	2,55	5,09	4,57	1,88	0,28	0,5	99,97
149	54,61	0,69	17,25	8,62	0,13	4,52	7,71	3,10	0,73	0,19	2,4	99,95
154	50,91	0,51	11,57	9,71	0,15	12,59	7,48	2,34	1,08	0,13	3,3	99,92

Table VI-2: major elements lithogeochemistry of the JGC, *repeated analysis.

VI.1.1. Harker diagrams

The granitic rocks occur with a great variation of major elements depending on the SiO_2 content (Harker, 1909). Harker diagrams of the JGC (**Fig. VI-1**). The differences among phases and subphases of the JGC are not always clear in major elements. Groups of tonalites of GI are usually the richest samples in SiO_2, around 5% higher, in comparison with the other phases excepting the sample of Hobergsliden. The Al_2O_3 vs. SiO_2 diagram indicates the occurrence of two main groups of rocks: the GI and the GII-GIV samples, with the exception of the Hobergsliden. The GI samples are poorer in Al_2O_3 and richer in SiO_2 in comparison with the other phases. The CaO and MgO variations with SiO_2 are identical for the phases in the JGC. The Fe_2O_3 vs. SiO_2 of the JGC separates two main trends with the same slope, GI is always richer in Fe_2O_3 than the GII at identical silica content. The K_2O and Na_2O vs. SiO_2 are dispersed and indicate

no relation in the content of these oxides with the silica variation (probably related to hydrothermal alteration). The TiO_2 vs. SiO_2 diagram plots two trends with different slopes, GI trend is almost parallel to silica axis that indicates the no variation of titanium with the silica content; the negative slope of the GII trend is dip and major in the GIIb samples that indicates the titanium variation with the silica content in GII subphases. The P_2O_5 Harker is identical to the TiO_2, both elements are related to the occurrence of titanite and apatite accessory minerals.

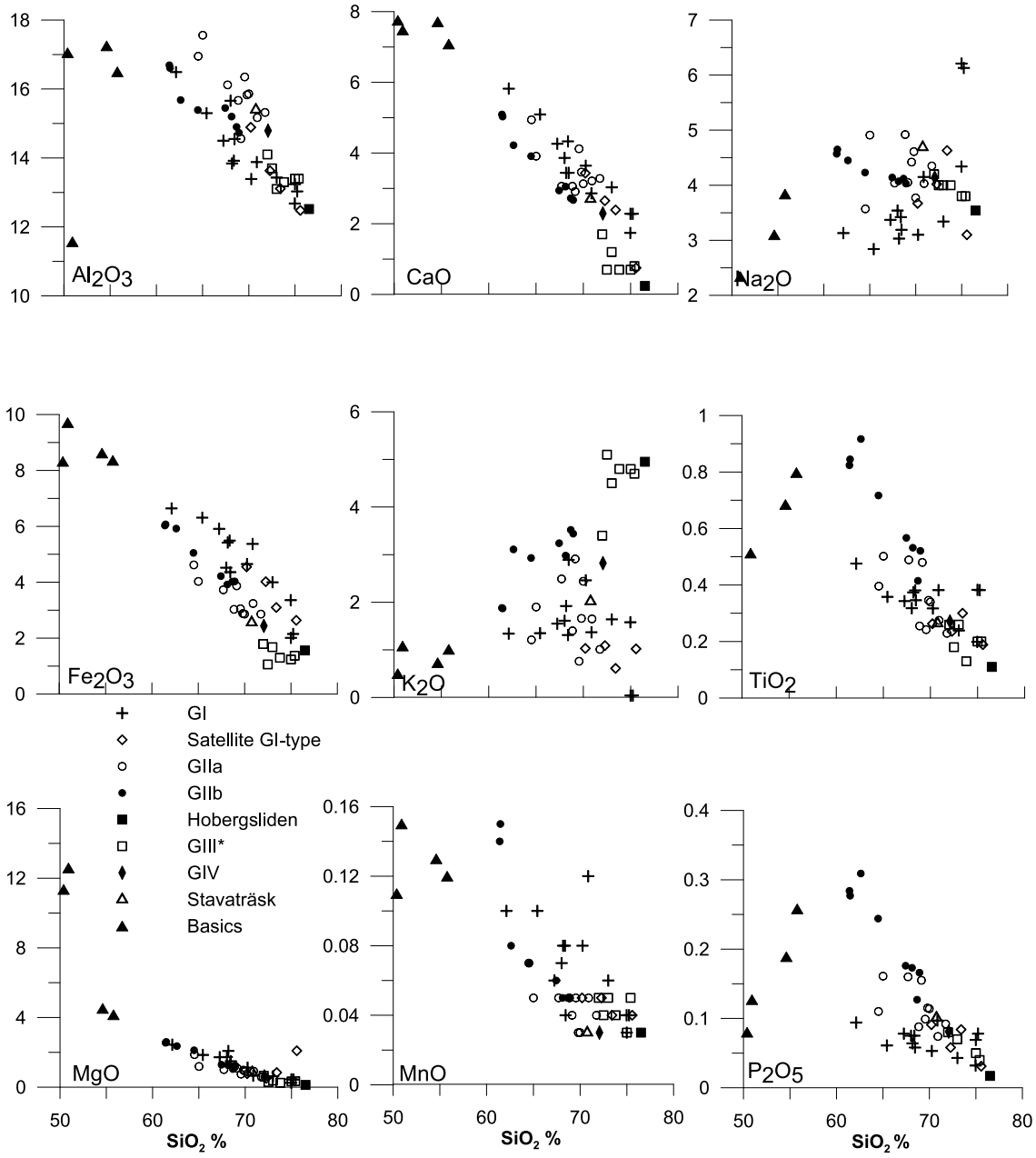

Fig. VI-1. Harker diagrams of JGC. GI-yellow rhombus; GIIa-blur circle; GIIb-red circle; GIII-square; GIV-filled circle; Rengard-cross; Stavaträsk-triangle.

VI.1.2. Major elements classification

The samples of GI phase are usually altered and difficult to classified using the mineral composition of the rock. The Fe2O3 vs. TiO2 plots the trends that differentiate the GI group from the GII-GIV samples (**Fig. VI-2**). The black line indicates the trend of the GII-GIV samples. It is a diminution of the Fe_2O_3 and TiO_2 from GIIb (qz-monzodiorites)

to GIIa (granodiorites) and GIII (alkali feldspars granite). The Stavaträsk sample is located in the GII-GIV trend. The titanium variation with the iron diminution is indicated by the yellow trend with a higher inclination than the GII samples. The Rengård sample is usually associated to the GI trends.

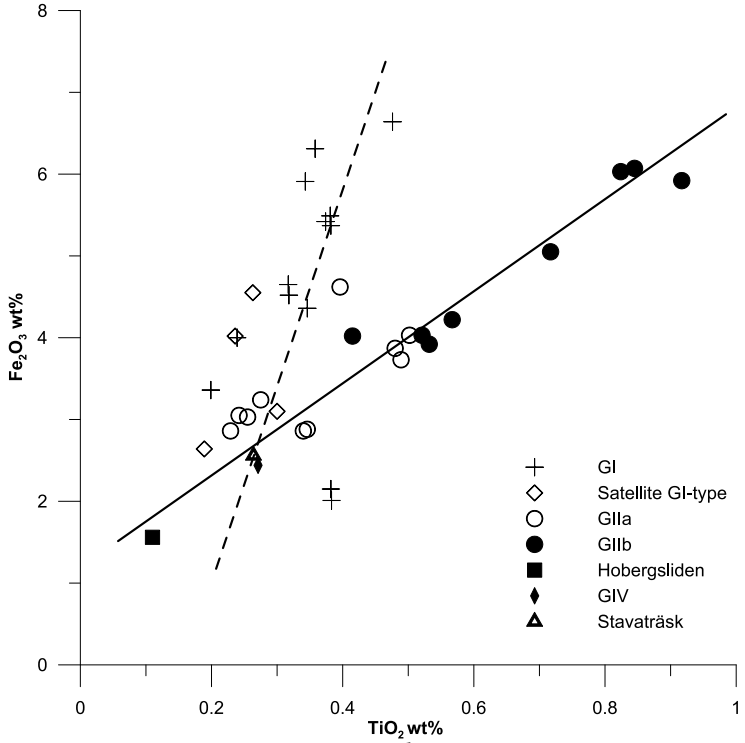

Fig. VI-2. Fe_2O_3 vs. TiO_2 diagram of the JGC samples.

The TAS (Total Alkali-Silica) diagram for igneous rocks (Cox et al., 1979) modified for plutonic rocks (Wilson, 1989), including the basic rocks analyzed of the JGC (**Fig. VI-3**).

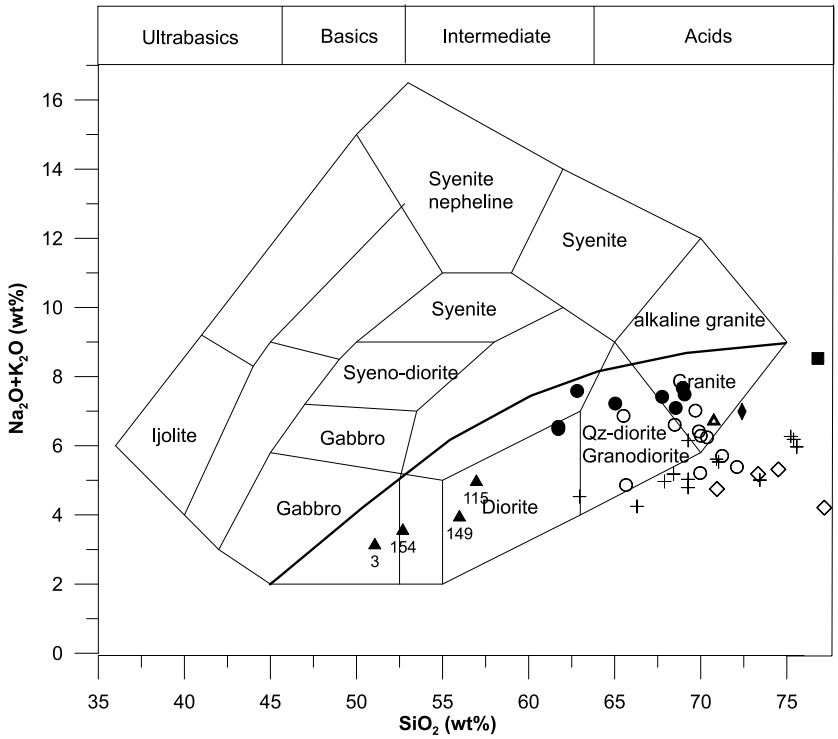

Fig. VI-3. TAS diagram of JGC, number of the GI samples are indicated, same legend as Fig VI-1

The Näsberg, basaltic dike and Sör-Jörnsberget mafic are classified as gabbros and diorites. Most of the GI samples are plotted out od the diagram but moved just parallel to the SiO_2 axis, in special is plotted out of the graphic the Kläddberget GI sample and the 78, 93, 130, 144 and 146 all these samples are located in the east-southeast of the JGC and satellite intrusions. The samples GIIa, GIIb, GIII, GIV and Stavaträsk are plotted in the area of their corresponding mineralogical composition. The whole samples are plotted under the subalkaline field (coarse black curved line) (**Fig. VI-3**).

The SiO_2 vs. K_2O diagram (**Fig. VI-4**) has been used to the discrimination of the intrusive series (Roberts and Clemens, 1993).

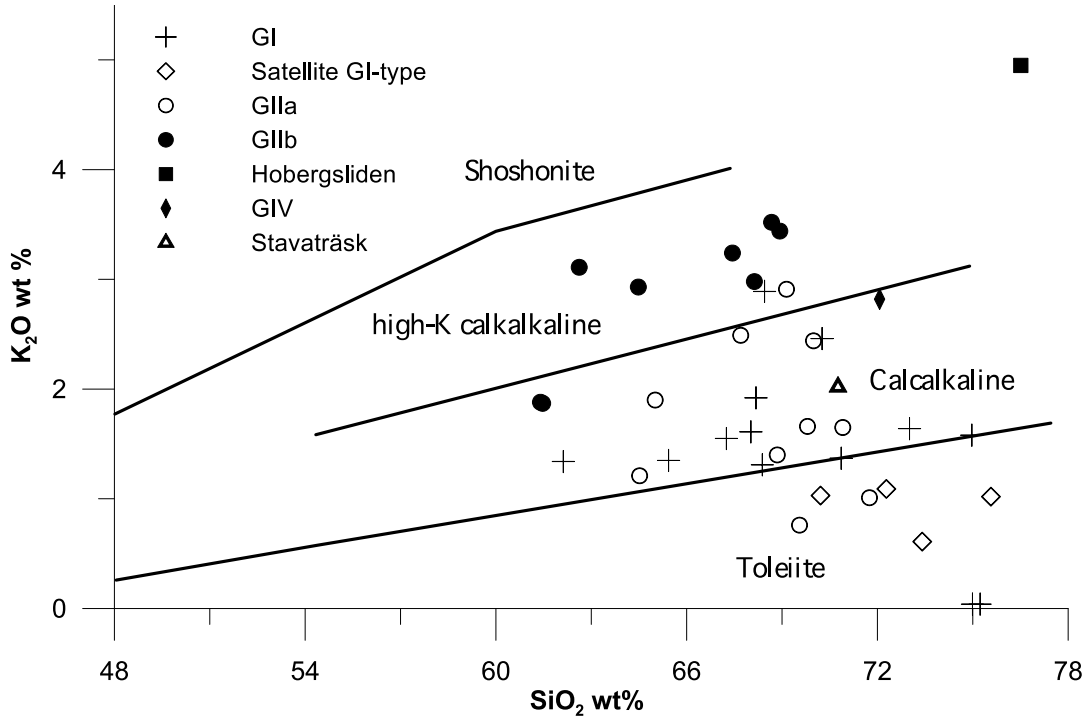

Fig. VI-4. Magmatic series classification diagram (Robert and Clemens, 1993).

The half of the GI samples plots in the toleiitic field, but these samples are characterized by the high silica content (78, 94, 127, 130, 144 and 146). Most of the samples with SiO_2 content lower than 72% are plot in the calcalkaline field. The Rengård sample plots in the transitional field from toleiitic to calcalkaline. The Stavaträsk and GIIa samples plot in the calcalkaline field with some samples as toleiitic or 24a close to the high K calalkaline field. The GIIb, GIII (Hobergsliden) and GIV plot in the High K calcalkaline field, the silica content of these samples is the similar or lower than GII or GIIa.

The AFM diagram indicates a trend of the GIIb, GIIa, GIII, GIV and Stavaträsk; the GI and Rengård samples are relatively dispersed but not lineated to the GII-GIV trend. The whole data plots as calcalkaline series (Fig. VI-5), like 85% of crustal rocks (Le Maitre, 1976), but alkali alteration can modify the original features. The black line is the calcalkaline-toleiite fields (Carmichael, 1964; Irvine and Baragar, 1971; Kuno, 1968). It is three possibilities about the F apex, Fe_2O_3 calculated as FeO has been used in this work, as the data were provided as Fe_2O_3. The MnO can be included in the F apex but no major changes are generated (Rickwood, 1989).

$F = (FeO + Fe_2O_3)$ as FeO_{total}
$F = FeO + 0.8998 \times Fe_2O_3$
$F = FeO + Fe_2O_3$ average

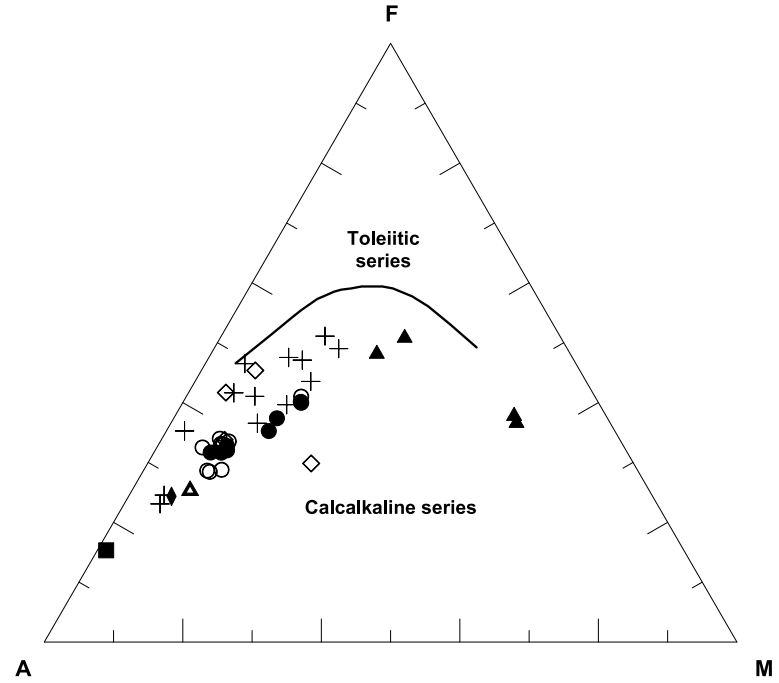

Fig. VI-5. AFM diagram of JGC granitoids. Same legend as fig. VI-1.

VI.1.2.1. Geochemical classification of granitoids

The classification of granitoids is based in three main variations (Frost et al., 2001): the Fe* index [$FeO^{tot}/(FeO^{tot} + MgO)$]; modified alkali index (MALI); and alumina saturation index (ASI).

The Fe* index differentiate the magmatic affinity between ferric and magnesian granitoids. Most of the JGC samples are located in the magnesian field, close to the ferric field. The phase distribution does not represent major difference in the ferric or magnesian affinity (**Fig. VI-6**) but the samples in the ferric field are higher than 70% of SiO_2 content (Frost et al., 2001). The field line between ferric and magnesian separates the toleiite (upper) from calc-alkaline (lower) after Miyashiro (1970). Most of the A-type granitoids are located in the ferric field.

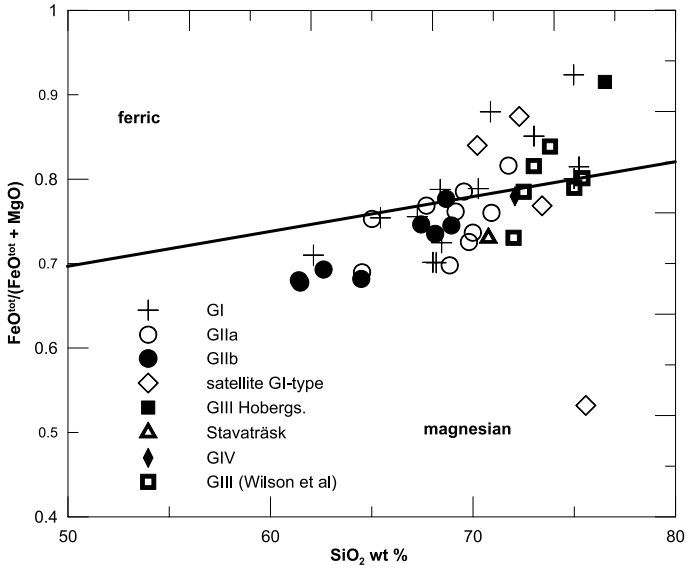

Fig. VI-6: Fe* diagram [$FeO^{tot}/(FeO^{tot} + MgO)$] vs SiO_2, for discrimination between ferric and magnesian granitoids. The GIII (Wilson et al) samples represent the Wilson et al. (1987) analyses.

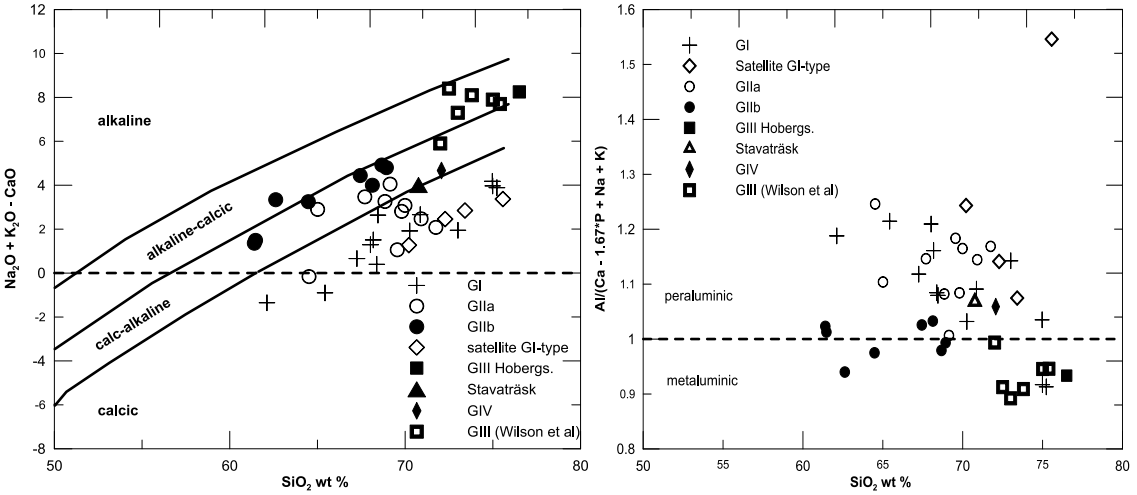

Fig. VI-7: **A:** MALI diagram for Modified Alcali-Lime Index of JGC. **B:** ASI diagram for Alumina Saturation Index of JGC. The GIII (Wilson et al) simples represents the Wilson et al. (1987) analyses.

The modified álcali lime index (MALI) diagram (**fig. VI-7a**) of Frost et al. (2001). The GI and satellite intrusions GI-type samples are classified in the field of calcic granitoids, and both plot as a trend from less evolved (GI) to silica rich (satellite GI-type). The GIIa samples plot in the calcic and calc-alkaline field, with similar values as some of the GI samples. GIIb samples plot in the calc-alkaline field close to the boundary of the alkaline-calcic field. The GIV and Stavaträsk samples plot in the transition from calc-alkaline to calcic. The GIII and GIII-Hobergsliden classifies as alkaline-calcic granitoids (**Fig. VI-7A**).

The ASI diagram (**Fig. VI-7B**) plots the alumina saturation index of granitoids using the Al/(Ca-1,67*P+Na+K) molecular vs SiO_2. The GI, GIIa, Stavaträsk, GIV and satellite GI-type intrusions plots in the peraluminic field, some of them close to the metaluminic field, excepting the strongly peraluminic JO04-94. The GIIb samples plot intermediate in the peraluminic and metaluminic field. The GIII and Hobergsliden samples plot in the metaluminic field (ASI < 0), with *(Na + K) > Al* molecular that indicates the peralkaline affinity of GIII (**Fig. VI-7B**).

VI.1.3. Major element JGC and other intrusions comparison

The VIC is a multiphase intrusion in the westernmost area of the Skellefte district, the chemical data have obtained from the Camiro Project. The Hornblende tonalites (qz-amphibolite) are classified in the granodiorites field without major compositional distribution. Most of the Mine porphyry and Trondhjemites plot similar to the GI phase including a relevant silica variation (**Fig. VI-8**).

The Revsund granites are in the margion of subalkaline to alkaline rocks classified as granites or alkaline granites. The GIII, Hobergsliden and Antak granite samples plot homogeneously in the granite field with higher silica contents than the other intrusions (**Fig. VI-9**). The GI samples from the Tallberg plots in the diorite field but the low silica content is related to the presence of minerallization. The Tallberg porphyry plots well with the GI samples and do not plots with higher or lower silica content than the unaltered GI rocks (**Fig. VI-9**). The samples of the VIC in the AFM are dispersed and only the Hbl tonalite occurs with a homogeneous pattern. The Hbl tonalite plots in the same trend than the GII-GIV samples (**Fig. VI-10**).

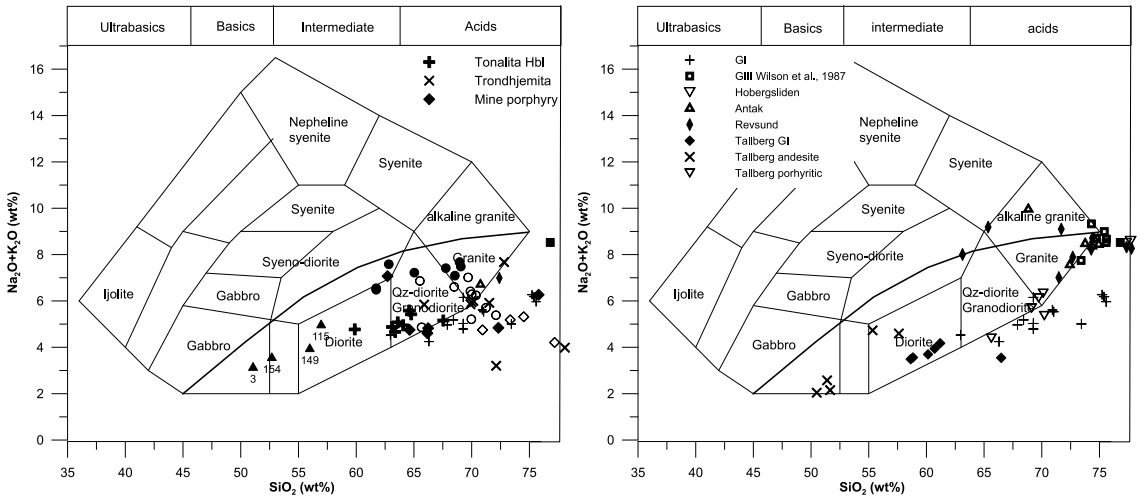

Figs. VI-8; VI-9. **VI-8 (left)**: TAS diagram VIC. **VI-9 (right):** TAS diagram of intrusions in Skellefte district: *Tallberg (Weihed, 1992b), *Revsund, Hobergsliden, Antak (SGU), GIII (Wilson et al., 1987). JGC legend in fig. VI-1.

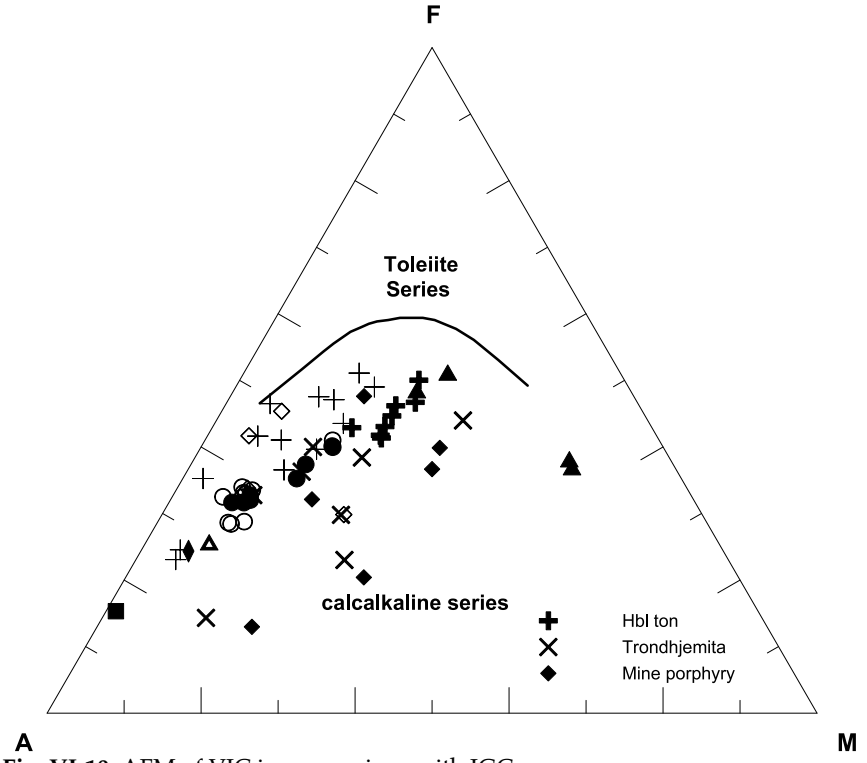

Fig. VI-10. AFM of VIC in comparison with JGC.

The GI samples of the Tallberg and the Petiknäs dacites plot in the GI and Rengård trend, but Talberg porphyry is correlated to the GII-GIV samples. The Petikträsk rhyolites correlate in a different trend of GI or GII-GIV (**Fig. VI-11**).

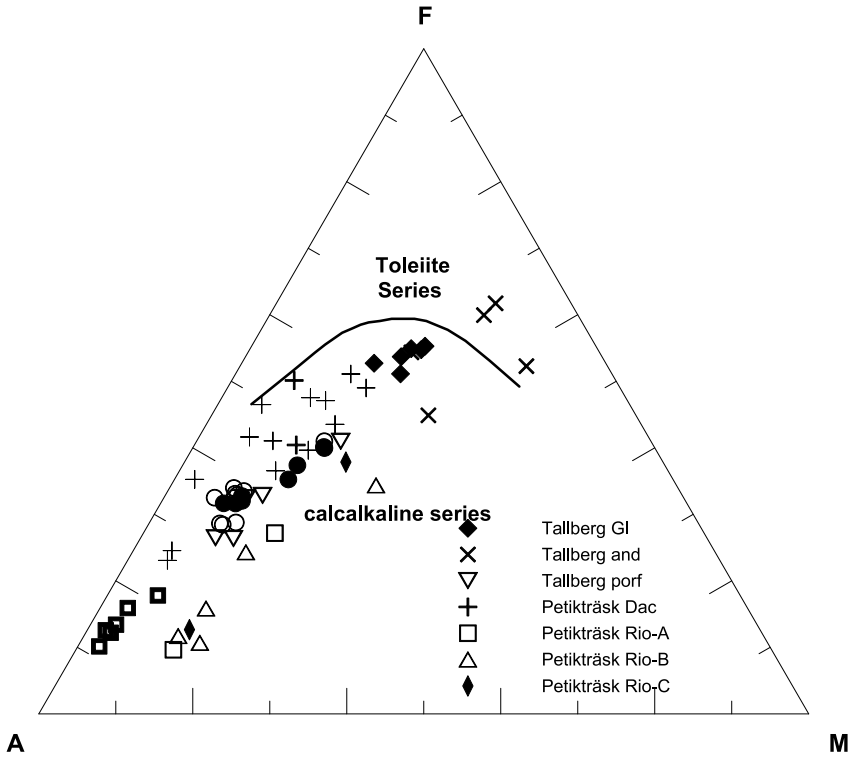

Fig. VI-11. AFM diagram of JGC, Petiknäs south volcanics and Tallberg (Schlatter, 2007; Weihed, 1992b; Wilson et al., 1987).

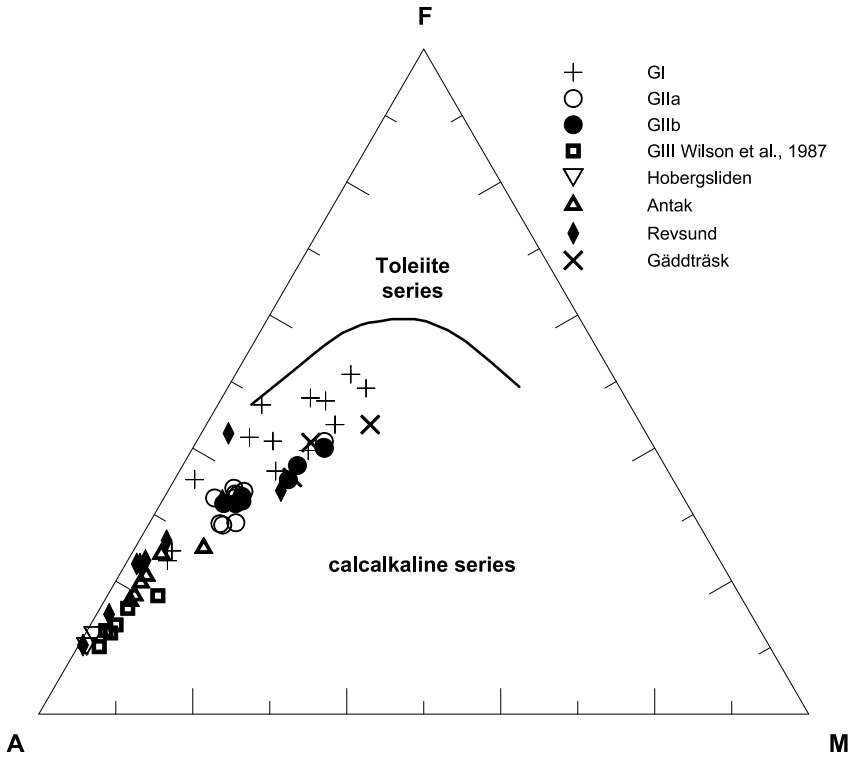

Fig. VI-12. AFM diagram of intrusions in the Skellefte district. Revsund, Hobergsliden, Antak and Gräddträsk (SGU); GIII (Wilson et el., 1987).

The Hobergsliden samples plots according to the more alkaline GIII samples. The Gräddträsk intrusion plots in the GIIb zone, the Antak fits in a intermediate area of GII and GIII (**Fig. VI-12**).

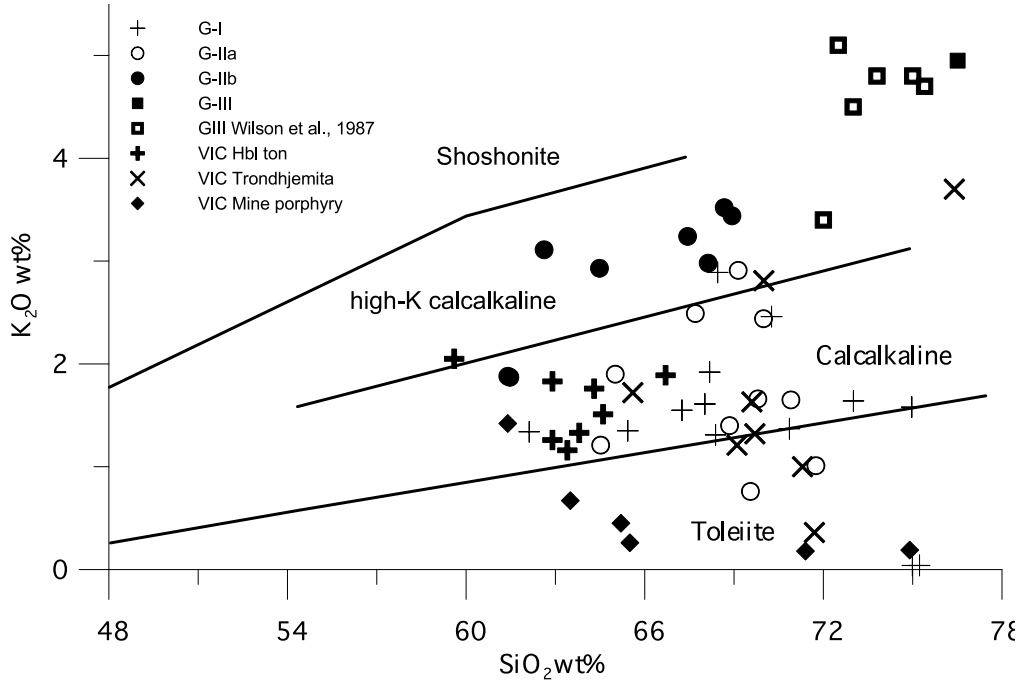

Fig. VI-13. K_2O vs. SiO_2 of VIC and JGC (Roberts and Clemens, 1993).

The Hornblende tonalite are classified in the calcalkaline field as the GI with lower silica content. Both, the Mine Porphyry and the Trondhjemite plot in the intermediate field of the calcalkaline and toleiite (**Fig. VI-13**).

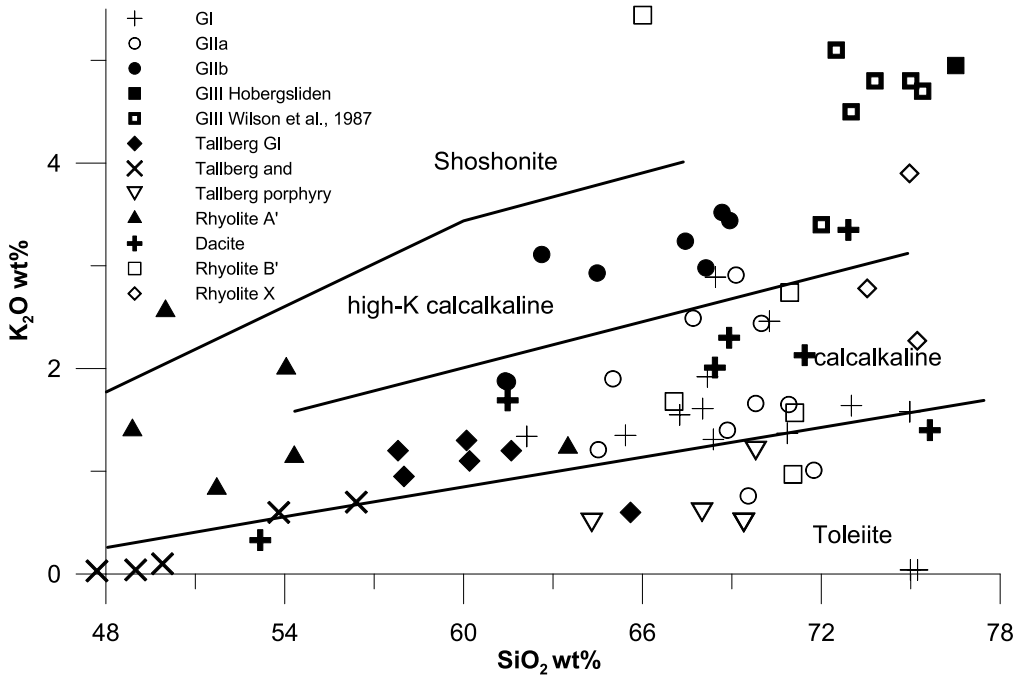

Fig. VI-14. K_2O vs. SiO_2 of Tallberg and Maurliden volcanics (Roberts and Clemens, 1993).

The GI samples of Tallberg plot as calcalkaline and the Pophyrytic in the toleiite field or intermediate to calcalkaline. The Maurliden rhyolite (A', B', X) and dacite plot in the calcalkaline field but the silica content of rhyolite A' is low (it is of the ore horizon).

The rhyolite B′ and dacite are calcalkaline but varies from intermediate calcalkaline-toleiite to calcalkaline-High K calcalkaline. The rhyolite X sills plot in the calcalkaline to High K calcalkaline.

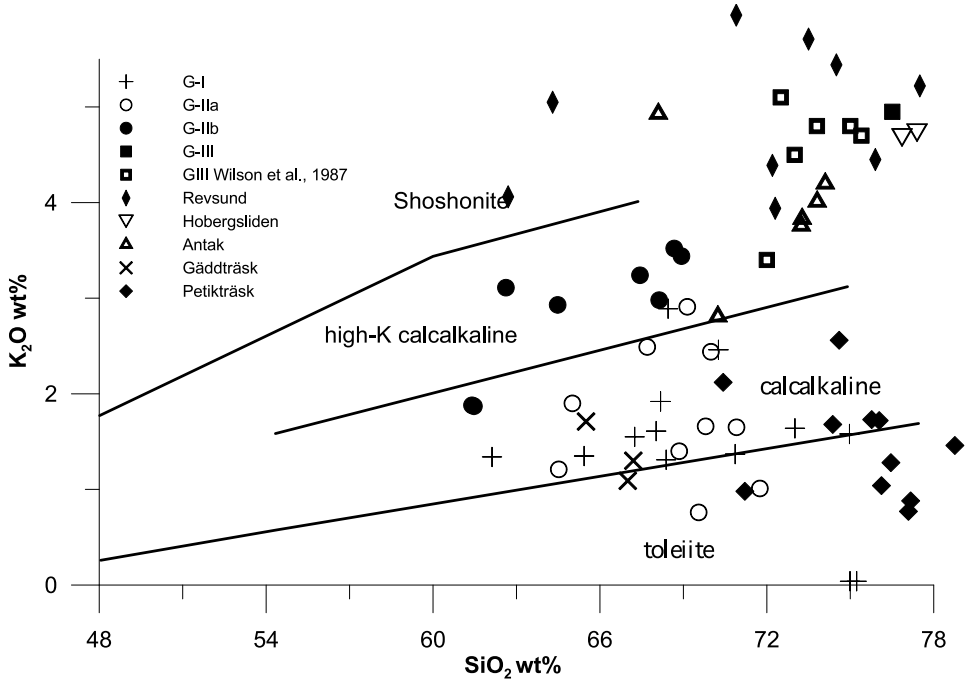

Fig. VI-15. K_2O vs. SiO_2 (Roberts and Clemens, 1993).of Revsund, Hobergsliden, Gräddträsk and Antak (SGU); and Petikträsk (Schlatter, 2007).

The Gräddträsk intrusion plots in the calcalkaline field as occur with the GIIa or the less silica rich samples of GI. The Revsund granite varies from shoshonitic to High K calcalkaline rocks. The Hobergsliden, GIII and the JO04-07 (Hobergsliden) plot as High K calcalkaline with similar silica or K_2O content. The Petikträsk volcanics plots in the intermediate area of toleiite to calcalkaline rocks with similar contents than the GI phase (**Fig. VI-15**).

VI.2. CIPW NORM CALCULATION

The hydrothermal alteration and minor deformation modify the texture and mineral composition of the rocks, in special on the GI phase. The CIPW of the lithogeochemical data generate a better classification of the rocks that this made using the mineral composition.

The Q′(F′)-ANOR diagram has been used for classification of the silica saturated (Q′) or silica unsaturated (F′) rocks (Streckeisen and Le Maitre, 1979). It indicates the silica saturation, but the main error occurs in the tonalites that is the dominant GI phase. This diagram plots:

X-axis: ANOR = 100xAn/(Or+An)

Y-axis: Q′ = Q/(Q+Or+Ab+An)
Y-axis: F′ = (Ne+Lc+Kp)/(Ne+Lc+Kp+Or+Ab+An)

JO04	Qtz	An	Dy	Hyp	Ab	Or	Ol	Apt	Ilm	Cor	Total
03	0,00	34,23	3,71	22,57	22,34	3,01	13,07	0,19	0,87	0,00	99,99
06	30,13	10,94	0,00	5,21	35,29	16,78	0,00	0,19	0,51	0,95	99,99
07	35,39	1,06	0,00	2,79	30,12	29,43	0,00	0,05	0,21	0,95	100,00
23a	16,98	18,60	0,00	8,98	42,05	11,35	0,00	0,37	0,97	0,70	100,00
24a	24,86	13,10	0,37	8,28	34,69	17,37	0,00	0,37	0,93	0,00	99,98
34	15,45	14,54	2,91	11,29	36,30	17,55	0,00	0,58	1,39	0,00	100,00
40	10,56	13,76	4,48	12,18	37,99	18,56	0,00	0,72	1,77	0,00	100,01
51	26,79	16,97	0,00	10,58	27,42	17,37	0,00	0,14	0,66	0,06	100,00
67	26,61	20,20	0,64	13,48	28,94	9,28	0,00	0,19	0,66	0,00	100,00
75	29,59	19,14	1,89	11,14	29,45	7,86	0,00	0,19	0,74	0,00	99,99
78	37,68	8,54	0,00	5,99	37,15	9,46	0,00	0,07	0,38	0,75	100,00
83	21,88	11,87	0,52	8,45	35,12	20,98	0,00	0,39	0,80	0,00	100,01
86	31,06	13,63	0,00	10,19	35,37	8,16	0,00	0,23	0,74	0,62	100,00
88	18,90	27,56	1,06	16,25	26,99	8,10	0,00	0,23	0,93	0,00	100,01
94	33,48	7,92	2,49	2,83	52,12	0,24	0,00	0,19	0,72	0,00	99,99
94*	32,87	8,19	2,31	2,71	52,80	0,24	0,00	0,16	0,72	0,00	100,00
100	31,09	15,62	0,00	7,35	34,35	9,81	0,00	0,16	0,53	1,09	100,00
101	25,10	14,89	0,00	7,76	42,39	8,45	0,00	0,21	0,49	0,71	100,01
107	29,69	16,96	0,00	13,95	26,23	11,58	0,00	0,16	0,72	0,70	99,99
109	31,13	15,61	2,03	9,21	26,57	14,71	0,00	0,12	0,61	0,00	99,98
112	23,33	24,33	0,00	12,03	30,89	7,33	0,00	0,25	0,76	1,06	99,99
114	24,95	14,38	0,00	8,09	34,69	14,95	0,00	0,37	0,95	1,62	100,01
115	5,14	25,54	7,38	20,10	33,51	6,15	0,00	0,63	1,56	0,00	100,00
119	29,36	19,98	0,00	6,68	37,74	4,55	0,00	0,23	0,46	1,01	100,00
120	27,68	18,83	0,00	11,51	30,29	9,63	0,00	0,19	0,61	1,28	100,01
122	33,20	15,83	0,00	5,90	37,06	6,03	0,00	0,21	0,44	1,33	99,99
124	33,86	16,68	0,00	9,25	31,56	6,21	0,00	0,21	0,51	1,74	100,01
127	48,29	3,62	0,00	9,55	26,82	6,15	0,00	0,07	0,36	5,11	99,98
128	20,60	13,56	0,00	9,44	35,37	19,32	0,00	0,42	1,08	0,20	100,00
130	37,47	14,92	0,00	7,98	28,52	9,81	0,00	0,09	0,46	0,75	99,99
135	26,16	25,36	0,00	14,91	24,54	8,16	0,00	0,14	0,70	0,04	100,01
136	22,76	14,17	0,00	8,93	34,78	17,79	0,00	0,39	1,03	0,15	99,99
138	26,29	16,48	0,00	6,74	39,26	9,87	0,00	0,28	0,66	0,44	100,02
139	22,73	12,04	0,17	8,97	34,27	20,45	0,00	0,39	0,99	0,00	100,00
142	29,27	14,96	0,00	6,59	32,15	14,54	0,00	0,25	0,65	1,59	100,00
144	36,57	11,47	0,00	6,92	39,85	3,66	0,00	0,21	0,59	0,73	100,00
145	27,48	12,84	0,00	6,01	40,02	12,06	0,00	0,23	0,51	0,84	100,00
146	36,19	13,00	0,00	7,79	34,69	6,56	0,00	0,14	0,46	1,18	100,01
147	10,34	19,11	3,57	13,78	39,77	11,17	0,00	0,65	1,61	0,00	99,99
147*	10,67	19,71	3,30	13,74	39,09	11,23	0,00	0,67	1,58	0,00	99,99
149	6,48	32,02	5,17	22,88	27,16	4,49	0,00	0,46	1,35	0,00	100,01
154	0,00	18,74	15,59	24,99	20,73	6,68	11,95	0,30	1,03	0,00	100,00

Table VI-3. CIPW norm of the JGC lithogeochemical analyses.

The whole samples are silica saturated, so it is only plotted the positive Y-axis (**Fig. VI-16**). Most of GI samples plot in tonalites, but some in granodiorite or trondhjmite fields. Stavaträsk and GIV are classified in the granodiorite field. The GIIb are plotted in qz-monzonites or qz-monzodiorites, the same field a by mineralogy. GIIa varies from granodiorites to tonalites. The basic samples plot in the corresponding diorite or gabbro field. The GIII (Wilson et al., 1987) plots in the Syeno-granite close to the alkali feldspars granite field.

The classification of granitic rocks can be determined by the molecular modal content of feldspars (Baker, 1979) with the ternary diabram Or-An-Ab (**Fig. VI-17**). This diagram represents the Qz-Ab-Or-An tetrahedron from the Qz-apex (O'Connor, 1965). In this case the tonalites are better represented than in the Q'-ANOR. The GI and the Rengård samples plot in the tonalite field exception 78, 94, 127 and 144 that plot in the trondhjemite field. Many of the GIIa plot in the granodiorite but most of them plot in the tonalite field (**Fig. VI-17**).

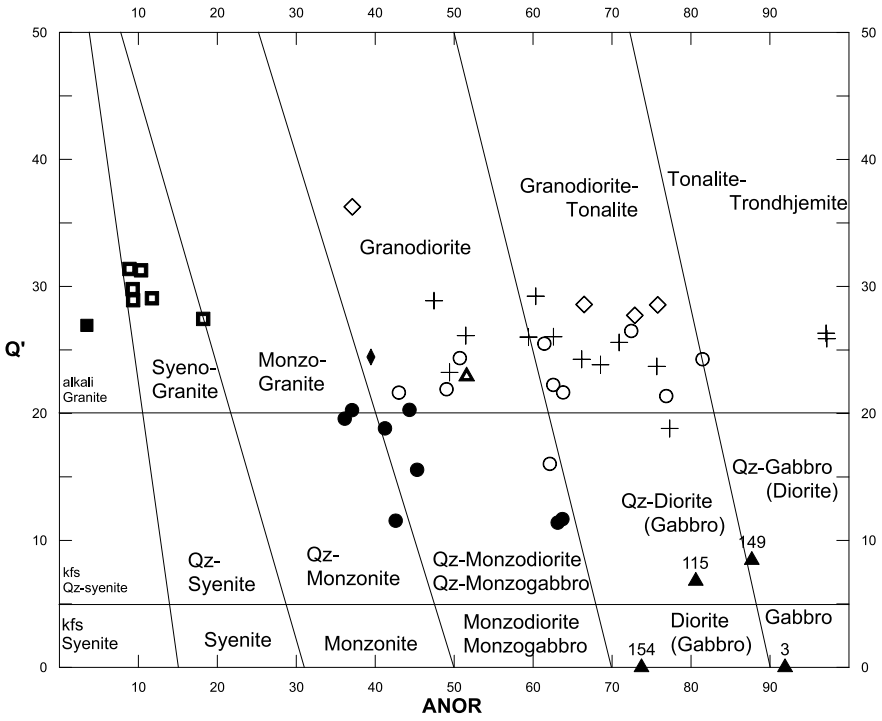

Fig. VI-16. Q'-ANOR diagram for plutonic rocks (Streckeisen and Le Maitre, 1979). Same legend as fig. VI-1; GIII-orange square (Wilson et al., 1987).

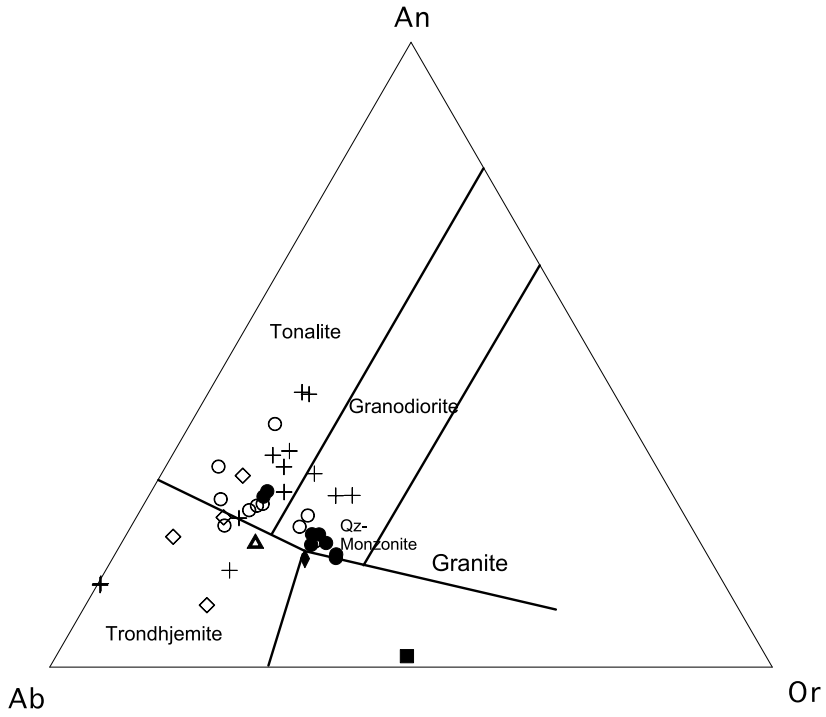

Fig. VI-17. Or-An-Ab diagram for granitoids (Baker, 1979), modified from O'Connor, 1965.

VI.3. TRACE ELEMENTS LITHOGEOCHEMISTRY

The different groups of chemical elements are represented in the **fig. VI-18**. Although the chemical character is similar in each group, many petrologic environments can modify the properties (Dunn, 1987; Green and Pearson, 1983; Rollinson, 1993; Ryerson and Hess, 1978; Watson, 1976), but most of the trace elements are immobile during alteration process, so it is helpful with the characterization of the GI samples. The whole chemical data are exposed in the Annexes.

$_{1}$H																	$_{2}$He
$_{3}$Li	$_{4}$Be																$_{10}$Ne
$_{11}$Na	$_{12}$Mg											$_{13}$Al	$_{14}$Si	$_{15}$P	$_{16}$S	$_{17}$Cl	$_{18}$Ar
$_{19}$K	$_{20}$Ca	$_{21}$Sc	$_{22}$Ti	$_{23}$V	$_{24}$Cr	$_{25}$Mn	$_{26}$Fe	$_{27}$Co	$_{28}$Ni	$_{29}$Cu	$_{30}$Zn	$_{31}$Ga	$_{32}$Ge	$_{33}$As	$_{34}$Se	$_{35}$Br	$_{36}$Kr
$_{37}$Rb	$_{38}$Sr	$_{39}$Y	$_{40}$Zr	$_{41}$Nb	$_{42}$Mo	$_{43}$Tc	$_{44}$Ru	$_{45}$Rh	$_{46}$Pd	$_{47}$Ag	$_{48}$Cd	$_{49}$In	$_{50}$Sn	$_{51}$Sb	$_{52}$Te	$_{53}$I	$_{54}$Xe
$_{55}$Cs	$_{56}$Ba	$_{57}$La*	$_{72}$Hf	$_{73}$Ta	$_{74}$W	$_{75}$Re	$_{76}$Os	$_{77}$Ir	$_{78}$Pt	$_{79}$Au	$_{80}$Hg	$_{81}$Tl	$_{82}$Pb	$_{83}$Bi	$_{84}$Po	$_{85}$At	$_{86}$Rn
$_{87}$Fr	$_{88}$Ra	$_{89}$Ac**	$_{104}$Rf	$_{105}$Ha													

*REE	$_{58}$Ce	$_{59}$Pr	$_{60}$Nd	$_{61}$Pm	$_{62}$Sm	$_{63}$Eu	$_{64}$Gd	$_{65}$Tb	$_{66}$Dy	$_{67}$Ho	$_{68}$Er	$_{69}$Tm	$_{70}$Yb	$_{71}$Lu
**actinoids	$_{90}$Th	$_{91}$Pa	$_{92}$U	$_{93}$Np	$_{94}$Pu	$_{95}$Am	$_{96}$Cm	$_{97}$Bk	$_{98}$Cf	$_{99}$Es	$_{100}$Fm	$_{101}$Md	$_{102}$No	$_{103}$Lw

Fig. VI-18. Periodic table of elements. Transition elements: orange; platinum group: blue; trace elements: grey and pink; REE: pink.

The chemical ratios of some trace elements have been plotted versus Ce and La in the **fig. VI-20**. According to the trace elements the samples of JGC can be separated in two main groups: the first group members are GI, Rengård and satellite intrusions (Brannliden, Klockträsk and Kläddberget) samples, and the second group is formed of the GIIa, GIIb, GIII, GIII (Hobergsliden), GIV and Stavaträsk samples. The trace elements plotted versus Ce have a clear differentiated trend for each the two groups, the diagrams plotted versus La are less clear but the two groups are clearly defined. It is an increase in the Ce and La content of the samples of Stavaträsk and GIIa granodiorites to the GIIb, GIII and Hobergsliden (**Fig. VI-20**). The major of the trace elements diagrams have a linear correlation excepting the Sr/La vs. Ce that plots in a logarithmic correlation. Both, the Lu and Y versus La plots similar correlation with an increase in the Lu and Y content of the GIIb samples, even higher than GIII/Hobergsliden that is the most evolved rocks in the JGC.

	(Haskin et al., 1968)	**(Nakamura, 1974)**
Método analítico	NAA	IDMS
Condrito	Compuesto	Compuesto
La	0.330	0.3290
Ce	0.880	0.8650
Pr	0.112	
Nd	0.600	0.6300
Sm	0.181	0.2030
Eu	0.069	0.0770
Gd	0.249	0.2760
Tb	0.047	
Dy		0.3430
Ho	0.070	
Er	0.200	0.2250
Tm	0.030	
Yb	0.200	0.2200
Lu	0.034	0.0339

Table VI-5. REE content of Chondritic meteorites.

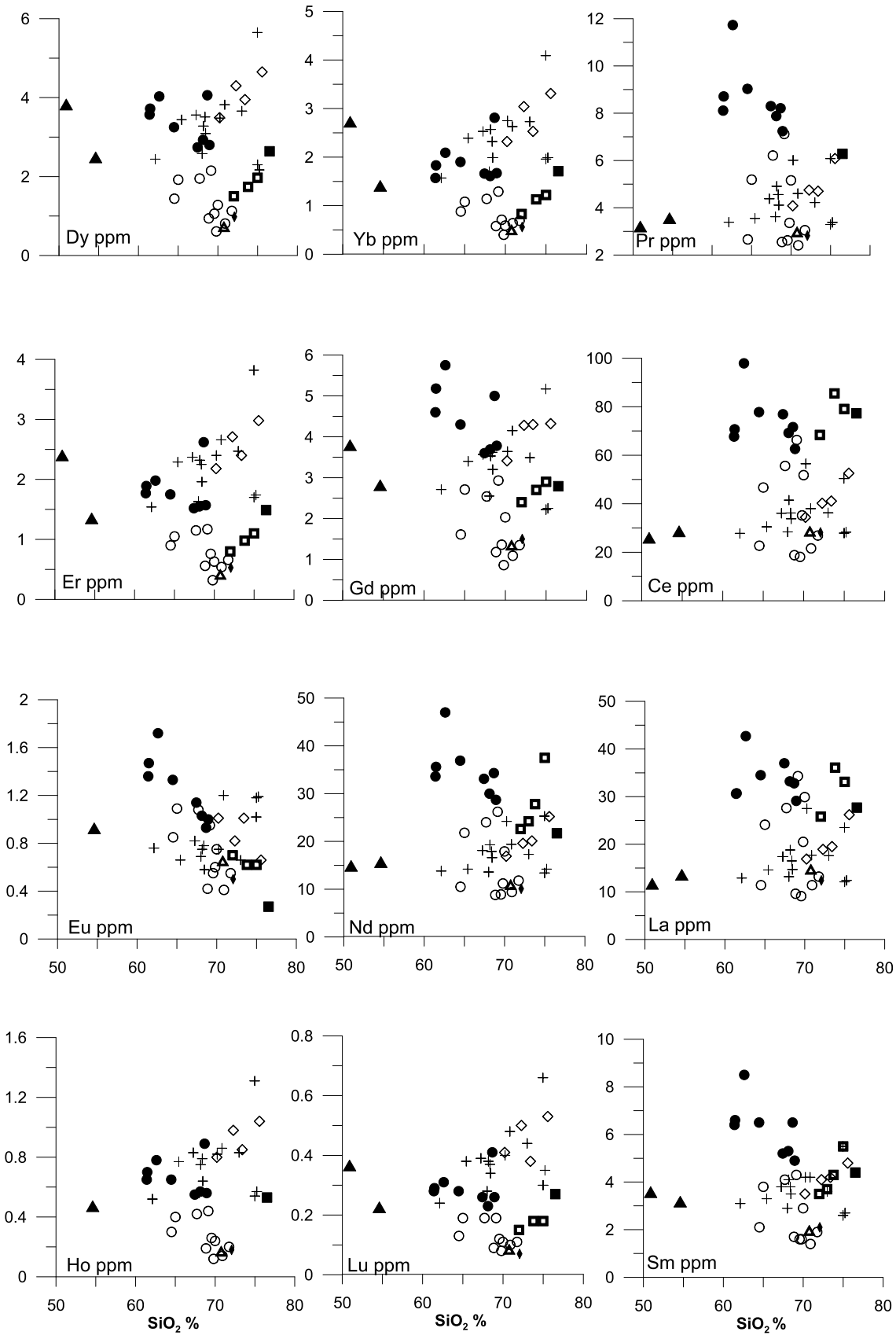

Fig. VI-19: Harker diagrams of REE vs. SiO2 of the JGC (Legend from fig. VI-1).

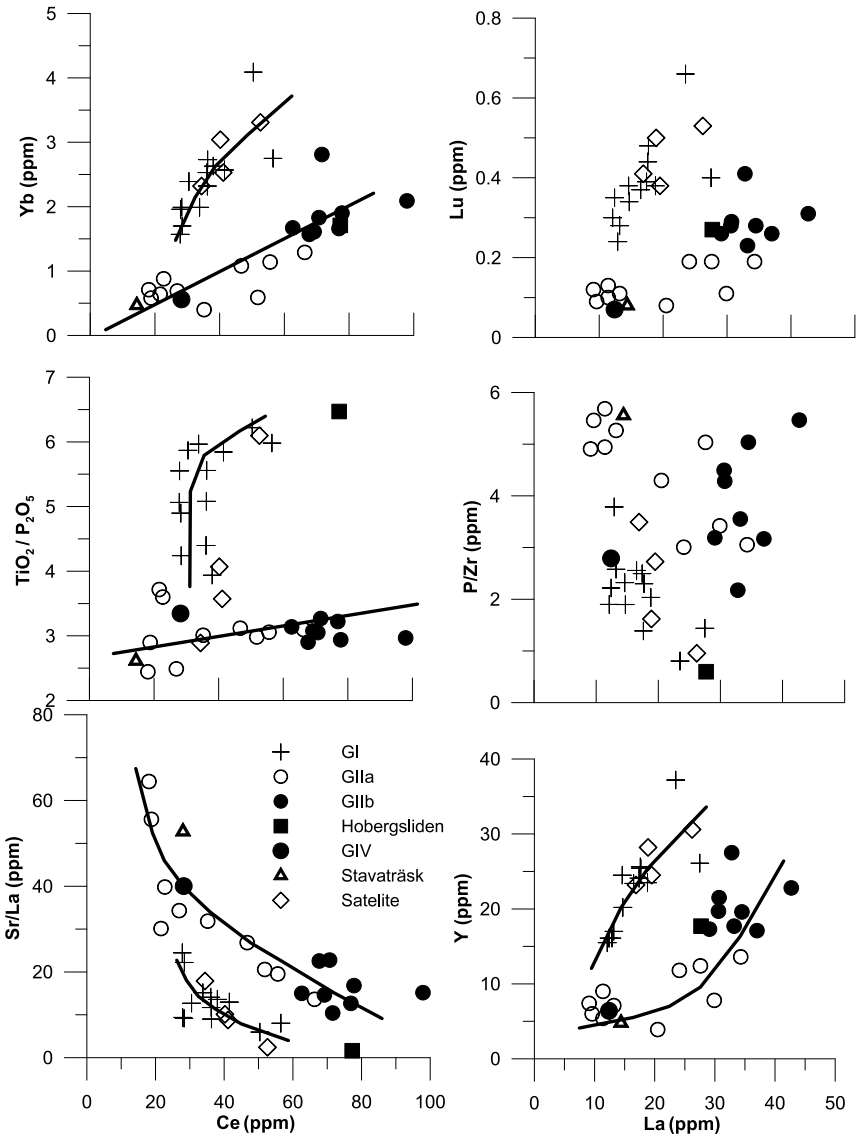

Fig. VI-20: Bivariate REE diagram of the JGC (Legend from fig. VI-1).

The REE diagrams represent the REE content of the samples normalized to the REE in Chondritic meteorites. In this work has been used the Nakamura chondrite (Nakamura, 1974) completed the Pr, Tb and Ho with Haskin et al. (1968) data that is the most accepted and certified Chondrites (**Table VI-5**). Nakamura (1974) used Isotope dilution mass spectrometer; and Haskin et al. (1968) used the Neutronic activation analyses method.

The LREE of the GI samples gentle dip from 100 to 20 (normalized values) to the Nd and Eu, with a small Eu negative anomaly. The HREE pattern of GI is parallel or subparallel to abscise axis with normalized values of 8 to 20, some HREE increase a bit from Dy to Lu (**Fig. VI-21**). The samples 94 and *94 (repeated) occurs with a small positive Eu anomaly.

The GIIa REE pattern is different to the GI pattern. In this case it is a descent of the normalized values from LREE to the Dy. In the GIIa pattern do not occur any Eu anomaly at any sample as occurs in the GI pattern. In contrast the samples 23a, 112, 114, 119, 138 and 145 patterns occur with a slight positive Eu anomaly (**Fig. VI-22**). The last HREE pattern is parallel to the abscise axis with values from 2 to 7 and a small positive Tm anomaly in some samples (**Fig. VI-22**).

The GIIb pattern is fairly similar to the pattern obtained with the GIIa samples. The first LREE elements (around 100 or higher normalized values) pattern is gentle dip that is increased from Nd to Eu (**Fig. VI-23**). The GIIb pattern end in Eu with a sligh negative anomaly and a gentle dip from Gd to Lu, a small Tm anomaly occurs in many samples (**Fig. VI-23**).

The characteristic pattern of the three main groups of rocks is shown in the **fig. VI-24**. The GIIa and GIIb patterns are similar but the GIIb REE content is always higher than the GIIa subphase (**Fig. VI-24**). The other intrusions and volcanic rocks will be compared with the characteristic REE diagram of GI and GII.

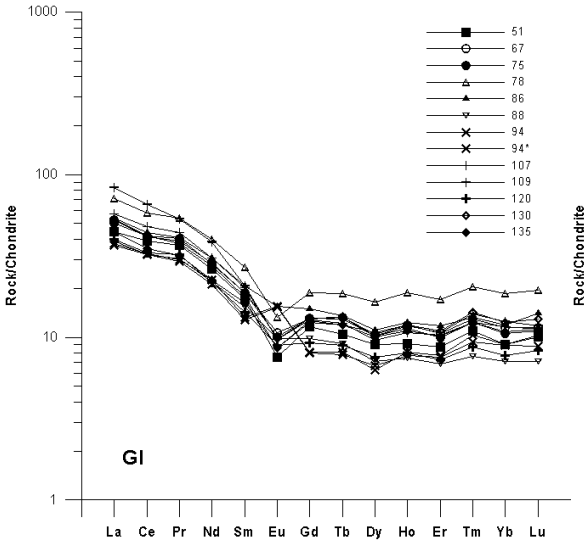

Fig. VI-21. REE pattern of GI group samples.

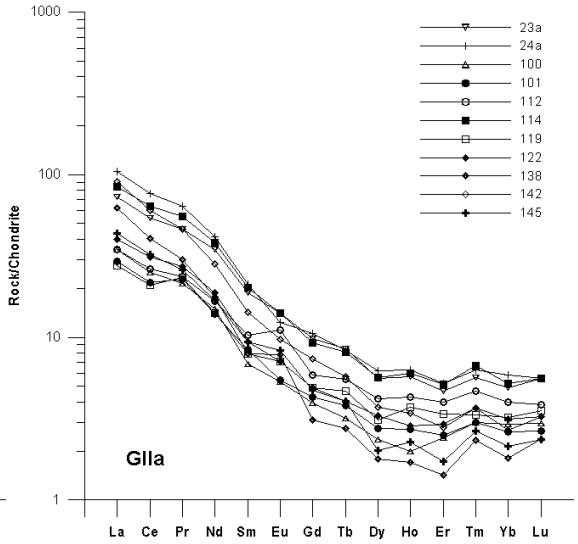

Fig. VI-22. REE pattern of GIIa subgroup samples.

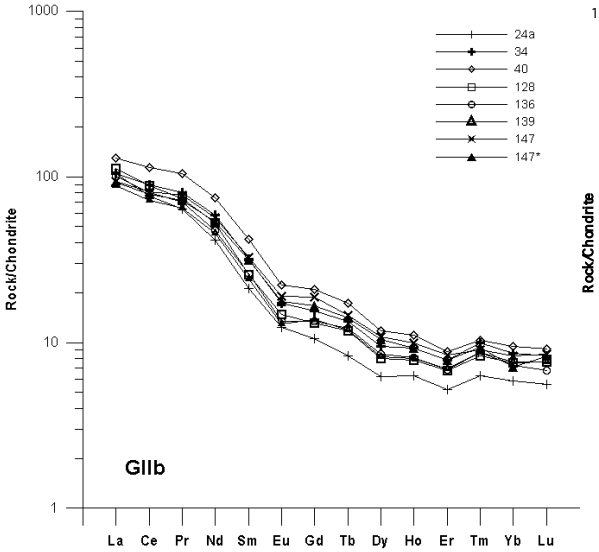

Fig. VI-23. REE pattern of GIIb subgroup samples.

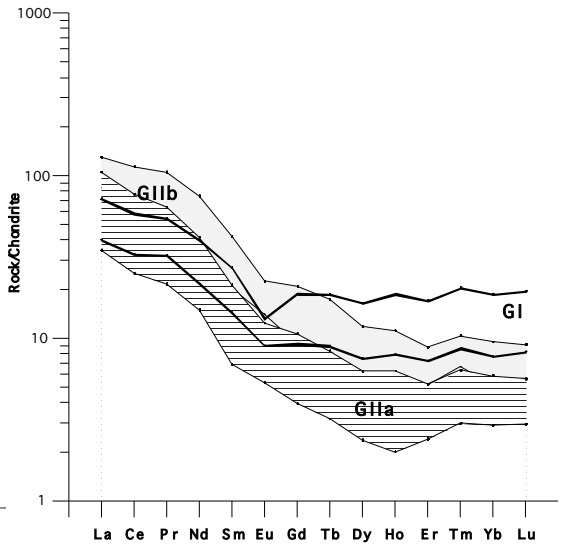

Fig. VI-24. Areas occurrence of REE pattern of JGC.

The REE patterns of satellite intrusions of GI (Rengård, Klockträsk, Brannliden and Kläddberget) fit in the area of GI (**Fig. VI-25**). The Rengård and Klockträsk intrusions fit in the REE GI pattern but occur without Eu anomaly or it is very slight. The

Brannliden and Klädberget fit with the GI pattern including the Eu anomaly. The 94 sample of the Flyggets local area (see coordinates) fits wit the GI but occur with a positive Eu anomaly; it is the only GI sample with this characteristic (**Fig. VI-25**). The REE pattern of GIV and Stavaträsk is fairly similar and occur as the lower REE samples of GIIa. The LREE and HREE of the GIII (Hobergsliden) fits with the GIIb pattern but close to the limit with GIIa pattern, but occur higher Eu negative anomaly (**Fig. VI-25**).

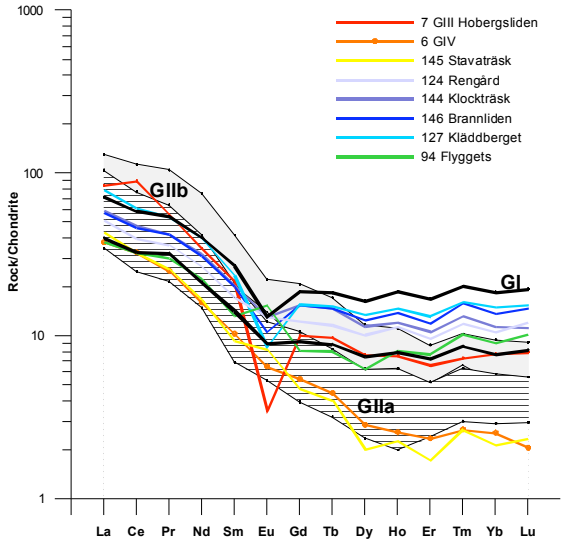

Fig. VI-25A. REE pattern of intrusions in JGC. JGC. *Numbers of samples referred in **table V-1**.

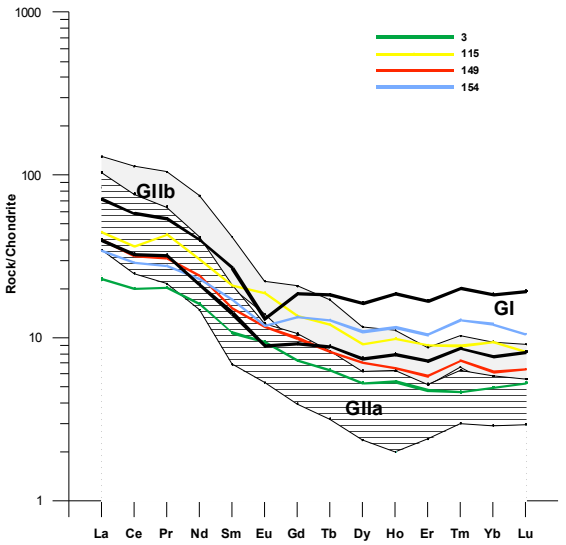

Fig. VI-25B. REE pattern of basic intrusions in the

The basic rocks of the JGC (Näsberg, Sör-Jörnsberget and the southern Dike) plot similar REE patterns. Both, the 3 and 115 samples of Näsberg are parallel but 115 with higher REE content. The REE pattern of 154 (southern Dike) is similar to GI but lower in LREE and a small negative Eu anomaly (**Fig. VI-25B**).

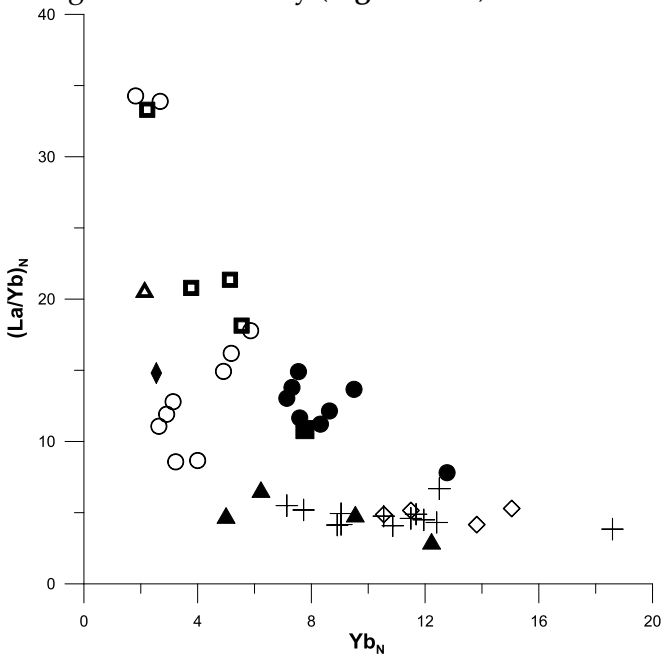

Fig. VI-26. $(La/Yb)_N$ vs. Yb_N diagram of REE fractionation in JGC. *Normalized REE data (Nakamura, 1974; Haskin et al., 1968).

According to REE fractionation the $(La/Yb)_N$ ratio does not varies with the increase of Yb_N in the GI and basic samples. The GII and GIII samples REE $(La/Yb)_N$ ratio decreases with the increase of Yb_N (brown arrow), it is a continuous descent of the LREE to the HREE in the GII-GIII groups. The $(La/Yb)_N$ ratios of GIV and Stavaträsk are similar to these of the GIIa samples but Hobergsliden is similar to the GIIb samples (**Fig. VI-26**).

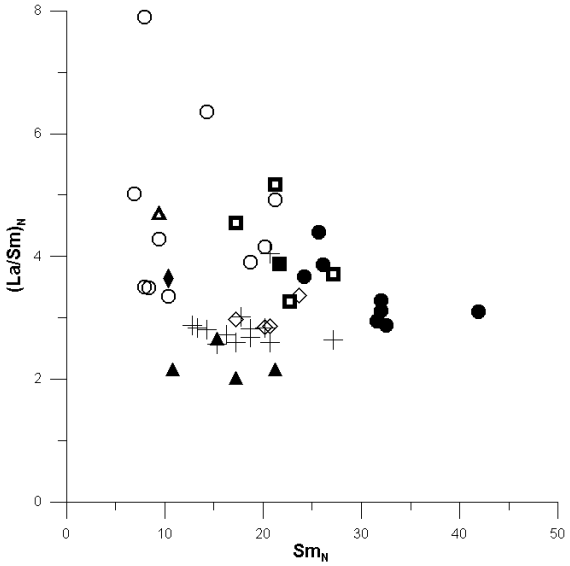

Fig. VI-27. $(La/Sm)_N$ vs. Sm_N diagram of HREE.

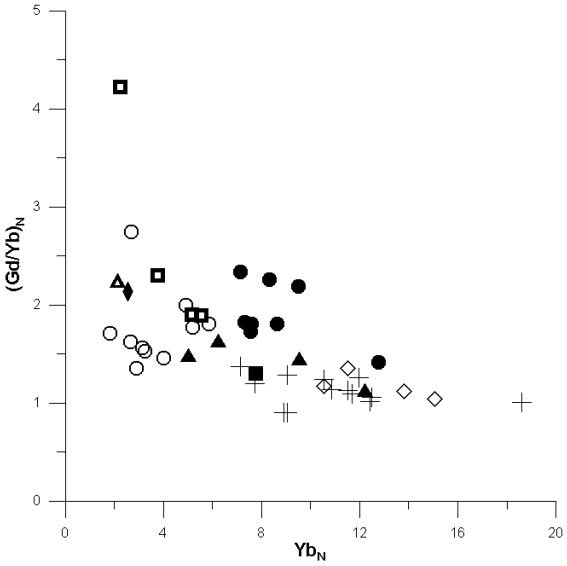

Fig. VI-28. $(Gd/Yb)_N$ vs. Yb_N diagram of HREE.

The LREE fractionation is shown in the **fig. VI-27** using the $(La/Sm)_N$ vs. Sm_N. the GI samples are not fractioned with the increase in the Sm_N (**Fig. VI-27**) as occurs in the REE fractionation diagram (**Fig. VI-26**). The $(La/Sm)_N$ ratio of the GII and GIII samples decreases with the Sm_N increase. As in the REE fractionation, the Rengård samples groups with the GI and the Stavaträsk, GIII and GIV are grouped with the GII-GIII trend (**Fig. VI-27**).

The GI $(Gd/Yb)_N$ ratio decreases with the Yb_N increase. The GII-GIII $(Gd/Yb)_N$ ratio variation with the Yb_N decrease do not occur as a clear trend, it is dispersed (**Fig. VI-28**).

VI.3.1. REE comparison of JGC and intrusions in the Skellefte district

The comparison of most of the intrusions associated to GI or occurring in the Skellefte mining district has been done with the REE diagram of GI-GIIa-GIIb obtained in this work (**Fig. VI-24**). Although many major elements data have been obtained, the REE patter have to be the better comparison due to the hydrothermal alteration. The GIII (Wilson et al., 1987) pattern is similar to the GIIa-GIIb patterns, with the LREE closer to the GIIb and the HREE closer to the GIIa. It also occurs a small negative Eu anomaly in the GIII samples (**Fig. VI-30B**). The GIII pattern is the same that the JO04-07 sample from Hobergsliden, but without such an important negative Eu anomaly (**Fig. VI-25**).

The Hobergsliden sample in the **fig. VI-30A** is also identical as the JO03-07 sample, and similar to the GIIa-GIIb patterns as occur in the GIII samples (**Fig. VI-30B**). The Antak granite (Arvidsjaur Group) LREE pattern is similar to the GIIb samples, but with a negative Eu anomaly and a successive positive Gd anomaly. The HREE pattern of Antak is parallel to the GII patterns but higher as the GI samples (**Fig. VI-30A**).

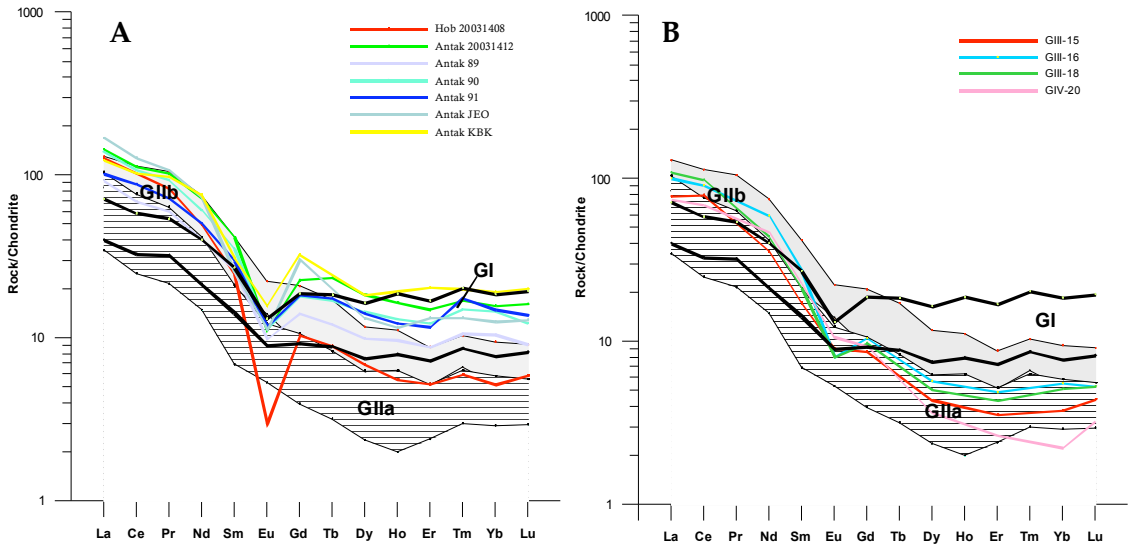

Fig. VI-30. REE normalized pattern of **A)** Hobergsliden and Antak (SGU) and **B)** GIII (Willson et al., 1987).

The REE diagram (normalized with Nakamura, 1974; Haskin et al., 1968) of the Tallberg porphyry copper samples (Weihed, 1992a) have been compared with the REE diagram of the JGC. The REE diagrams of the Tallberg GI samples plots similar to the GI area defined in this work, but slightly lower in LREE. The HREE pattern is roughtly the same of the GI but with a high variation of successive even to odd REE (**Fig. VI-31**).

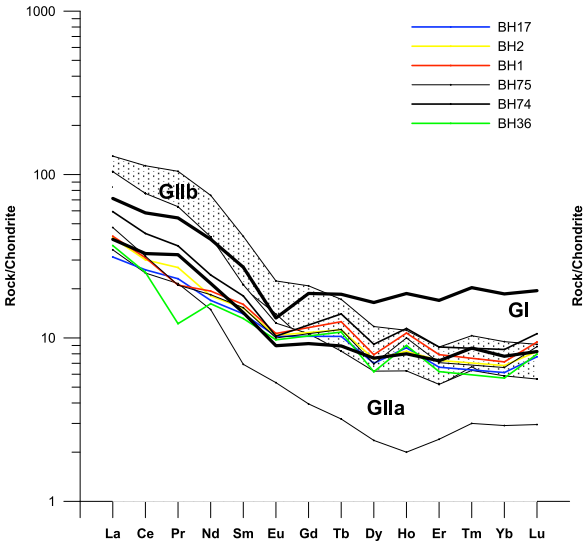

Fig. VI-31. REE of Tallberg GI (Weihed, 1992a). 1992a).

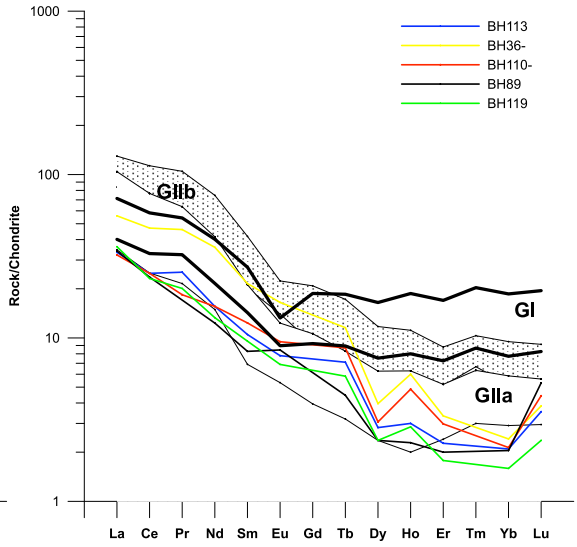

Fig. VI-32. REE of Tallberg porphyry (Weihed, 1992a).

The Tallberg porphyry REE diagram is similar to the GIIa samples in the LREE but the HREE variation in even and odd elements is too much high to determine any particular comparative relation to JGC phases but in general al lower than GI an similar to GIIa patterns (**Fig. VI-32**).

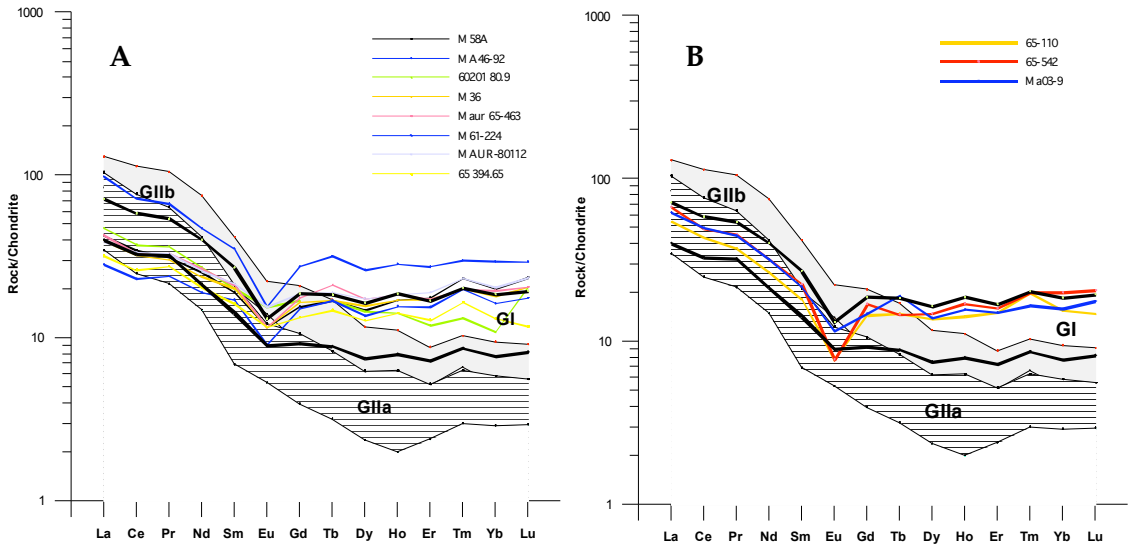

Fig. VI-33. REE patterns of **A)** Maurliden dacite and **B)** Maurliden Rhyolite X (Montelius, 2005).

The samples chosen for comparison with the JGC intrusions of the Maurliden volcanics are the porphyrithic dacites, rhyolite A', rhyolite B' and rhyolite X (Montelius, 2005). The REE pattern of the dacites of Maurliden is similar to the REE pattern defined by GI samples but with slightly lower LREE, it is a small negative Eu anomaly in the dacites as occur in the GI phase. The HREE pattern is the same as GI with higher REE normalized values. The MA46-92 pattern is parallel to the GI samples but it is systematically higher than the GI area (**Fig. VI-33A**). The rhyolite X REE define the same pattern than the GI samples, the only difference is defined by a negative Eu anomaly slight higher than the GI samples (**Fig. VI-33B**).

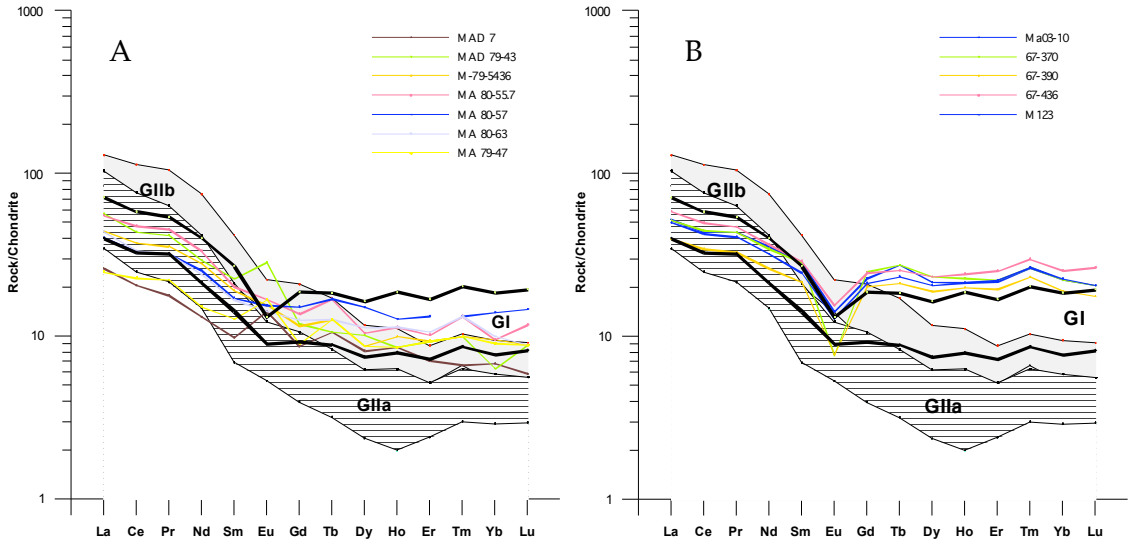

Fig. VI-34. REE patterns of **A)** Maurliden rhyolite A' and **B)** Maurliden Rhyolite B' (Montelius, 2005).

The REE rhyolite A' pattern fits with the GI LREE and HREE, but a positive Eu anomaly is characteristic of some of the rhyolite A' of the Maurliden volcanics (**Fig. VI-34A**). The rhyolite B' of Maurliden LREE fits with the GI area including the negative Eu anomaly, the HREE pattern is parallel to the GI but higher than the upper boundary defined by the GI samples (**Fig. VI-34B**). The negative Eu anomaly of the Maurliden rhyolita B' is slightly higher than the anomaly defined by the GI samples (**Fig. VI-34B**).

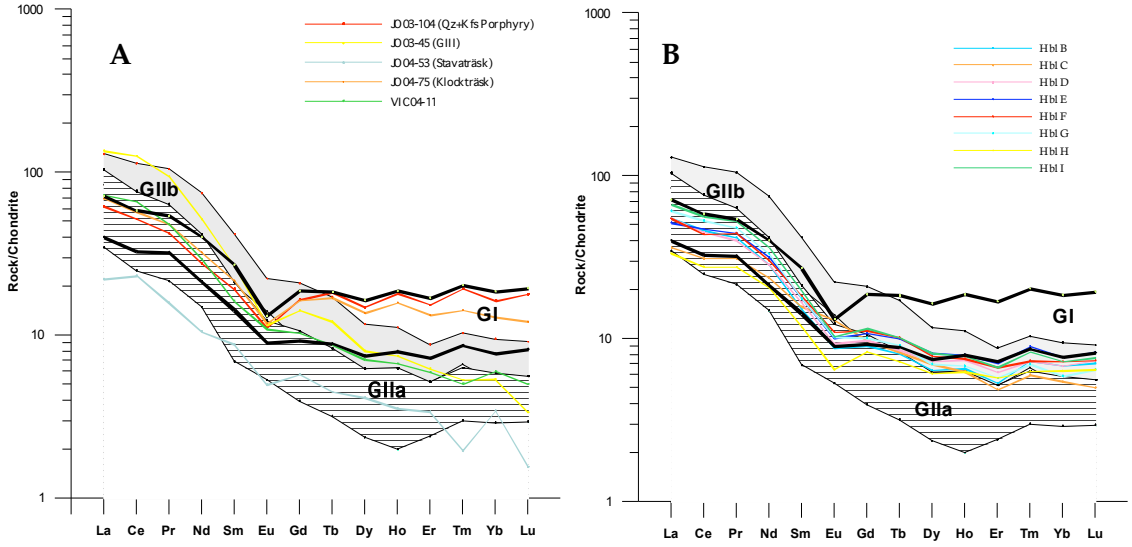

Fig. VI-35. REE patterns of **A)** intrusions associated to JGC (analyses done in the ICP-MS of the University of Huelva) and **B)** Hornblende tonalite of VIC (Camiro project).

The **fig. VI-35A** analyses include the samples of intrusions associated to JCG and that were used for Sm-Nd data (**table V-6**). The GI and GII (Sm-Nd) samples are not plotted because they fit exactly to the corresponding area. The JO03-104 sample is coarse grain qz+kfs porphyry in the Skellefte Group close to the Maurliden area and plots exact to the area pattern of the GI samples. The JO04-75 (Klockträsk) REE pattern is identical to the pattern of the JO03-104 qz+kfs porphyry, and plots exactly in the GI area. The JO03-45 (GIII) pattern is intermediate to the GIIb in the LREE and GIIa for the HREE, but similar to the other GIII and Hobergsliden patterns (**Figs. VI-25** and **VI-30**). The JO04-53 (Stavaträsk) REE pattern do not fit in any of the GI-GII areas, the LREE are lower than the whole of the samples and HREE similar to the GI. The VIC04-11 REE pattern is similar to the GI but HREE fits in the lower of the GI (**Fig. VI-35A**).

The hornblende tonalite of VIC REE have been plotted in the **fig. VI-35B**. The LREE pattern is identical to the GI samples including the negative Eu anomaly. The HREE pattern of Hbl tonalite is lower of GI, in special after the Dy but with similar values (**Fig. VI-35B**).

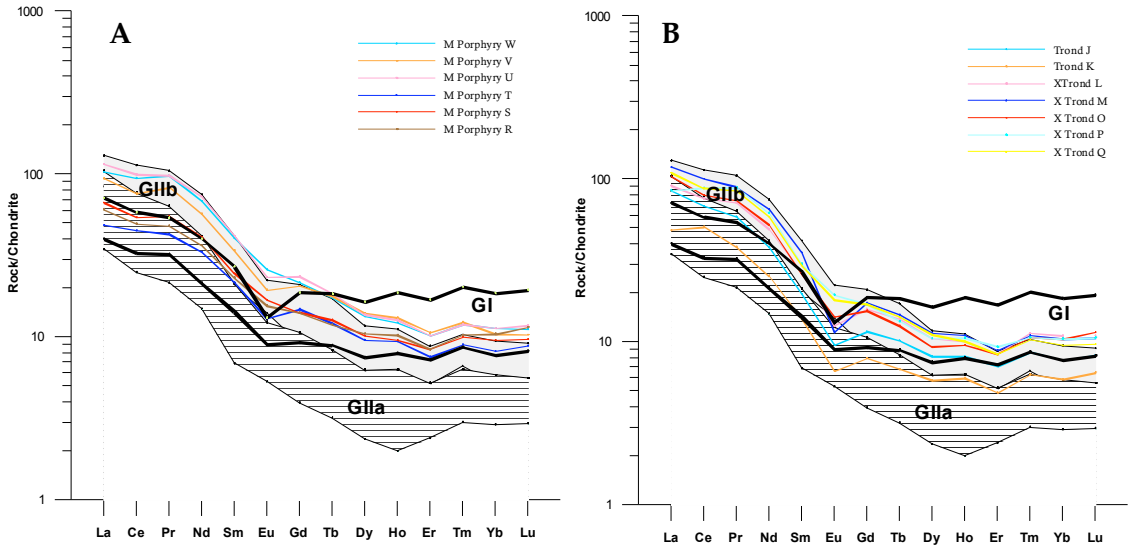

Fig. VI-36. REE patterns of **A)** Mine porphyry of VIC and **B)** Trondhjemites of VIC (Camiro project).

The Mine porphyry REE can be separated in two groups. The U, V and W samples fit with the GIIb subphase REE pattern. The R, S and T samples plot as the Hbl tonalites of VIC that is roughtly similar to the GI pattern (**Fig. VI-36A**). The trondhjemites and Xenolithic trondhjemites do no fit with any pattern of the GI but REE distribution is similar to the GI samples. In these trondhjemites the initial LREE are gentle dip with the increase of the dipping until the negative Eu anomaly, the HREE are parallel to abscise axis as the GI samples (**Fig. VI-36B**). The Petiknäs south deposit dacites and rhyolites (Schlatter, 2007) have been compared to the REE pattern of the JGC samples (**Fig. VI-37A** and **VI-37B**). The samples chosen are coherent dacites and rhyolites and juvenile clasts (McPhie et al., 1993), most of them from drill cores excepting the *Dacite II-13* (**Fig. VI-37A**). Excepting the *Rhy C II-9* with slight high HREE, all the samples plots in the GI pattern of JGC. All these samples have the same LREE and HREE patterns including the slight negative Eu anomaly.

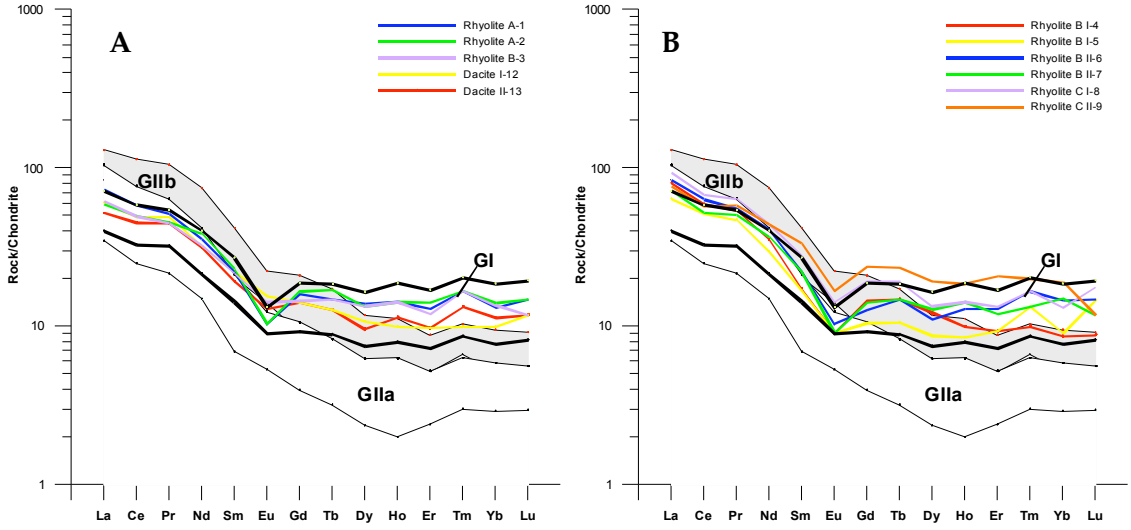

Fig. VI-37. REE patterns of Rhyolites and Dacites of the Petaiknäs south deposit (Schlatter, 2007).

The classification of volcanic rocks using immobile elements of the Petiknäs south and Maurliden (Schlatter, 2007; Montelius, 2005) are plotted in the **fig. VI-38**, the main JGC intrusions have been included. The rhyolites and dacites of the Petiknäs south deposit plot exactly on the GI tonalites in the rhyodacite and dacite field (**Fig. VI-38A**). The rhyolite A′ and X of Maurliden plot on the GI tonalites as rhyodacites and dacites, but the rhyolites B and dacites are lower in Nb/Y and plot in andesite field (**Fig. VI-38B**).

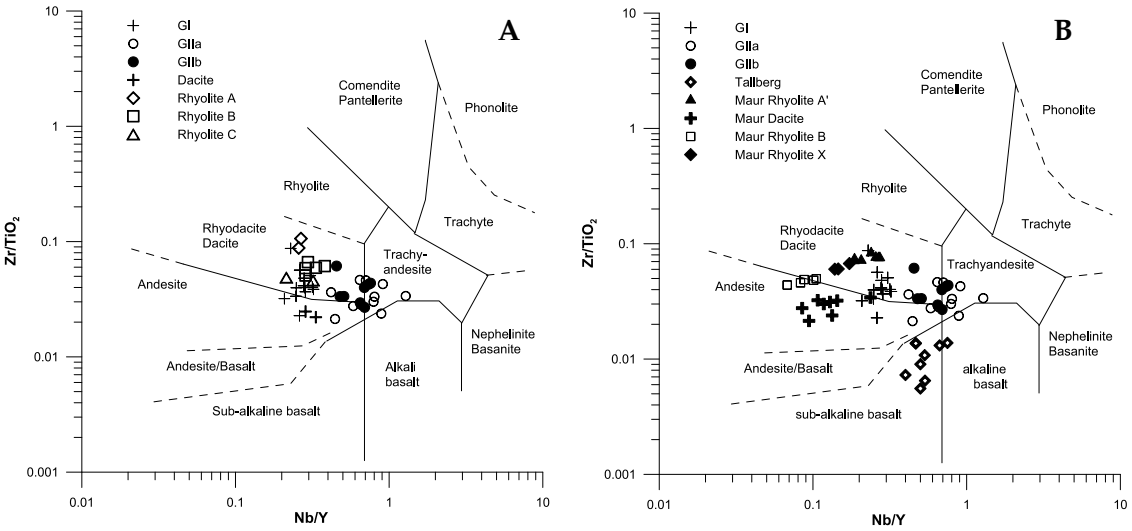

Fig. VI-38: Winchester and Floyd (1977) diagram of Petiknäs (Schlatter, 2007) and Maurliden (Montelius, 2005) volcanics and JGC samples.

VI.3.2. Tectonic setting discrimination diagrams

The classification of tectonic setting of the intrusions is obtained with the immobile trace elements Rb, Y, Nb and the equivalents Yb and Ta (Pearce and Cann, 1971; Pearce and Cann, 1973; Pearce et al., 1984). The four most used diagrams have been plotted with the same results (**Fig. VI-39**).

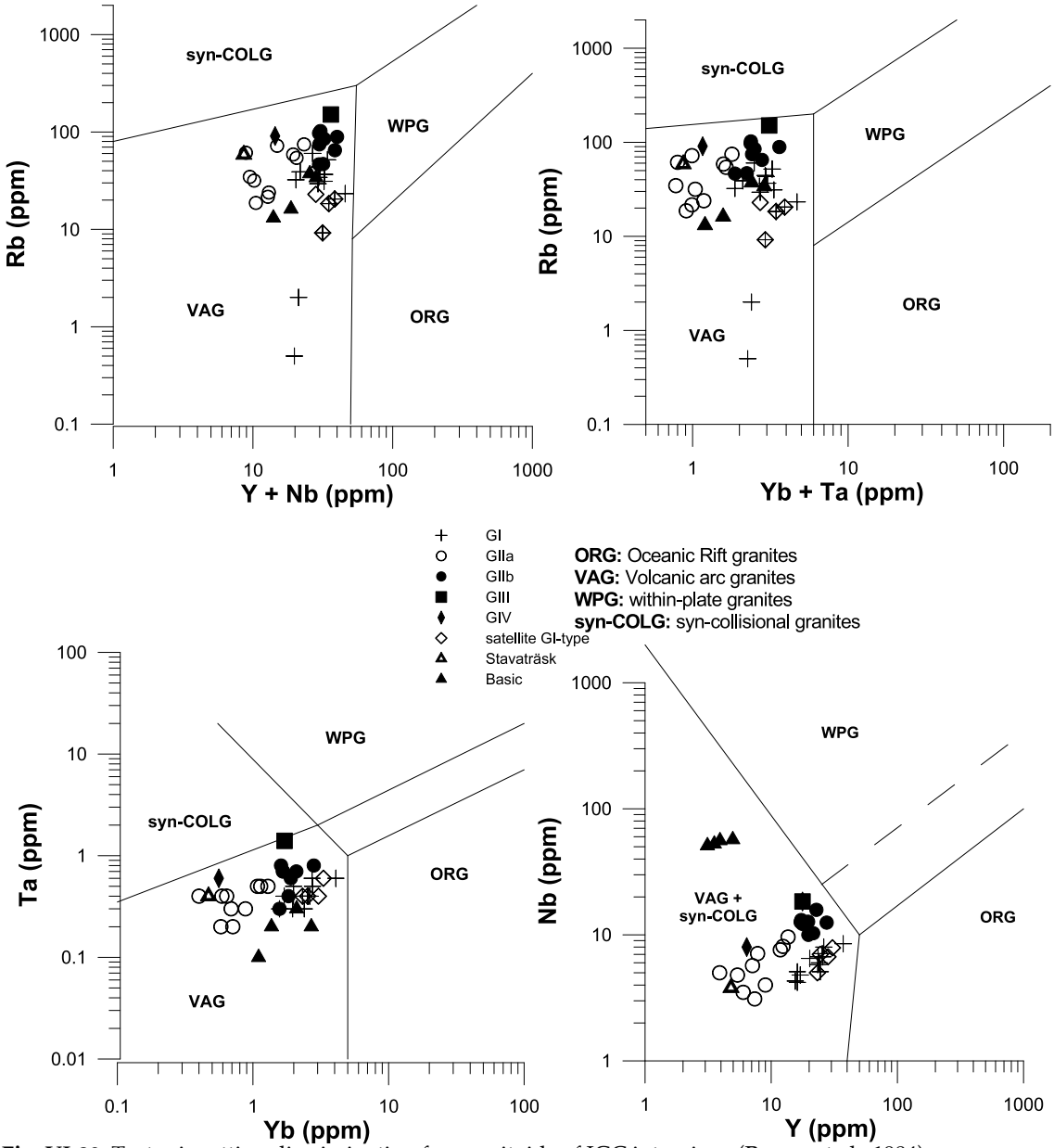

Fig. VI-39. Tectonic setting discrimination for granitoids of JGC intrusions (Pearce et al., 1984).

The basics intrusions are included in the **fig. VI-39** but the diagram is not useful for this type of rocks. In the four diagrams the JGC are plotted in the VAG (Volcanic Arc Granitoids) field. The GIII (Hobergsliden) sample always plots in the VAG but close to the boundary of the syn-collisional granitoids. The main phases are well grouped (GI, GIIa and GIIb), the Stavaträsk and GIV is usually plotted with the GIIa subphase; the Rengård sample is grouped with the GI samples (the satellite intrusions Klockträsk, Brannliden and Kläddberget are undifferentiated in the GI). The samples of GI in the Rb vs. Y+Nb(Yb+Ta) plotted out of the group is due to lower Rb content (altered samples?) (**Fig. VI-39**).

The ternary diagrams of tectonic setting for granitoids have been used (**Fig. VI-40**) but the results have to be less clear than the **fig. VI-39** due to the relevance of the Rb. The main utility in this diagram is the inclusion of the Tardi-post collisional setting, in this case the GIII (Hoberhsliden) is plotted in this field. The GII samples are plotted in the VAG, but most of the GI samples are plotted in the Intra-plate field but it is due to the Rb depletion of these rocks during hydrothermal alteration (**Fig. VI-40**).

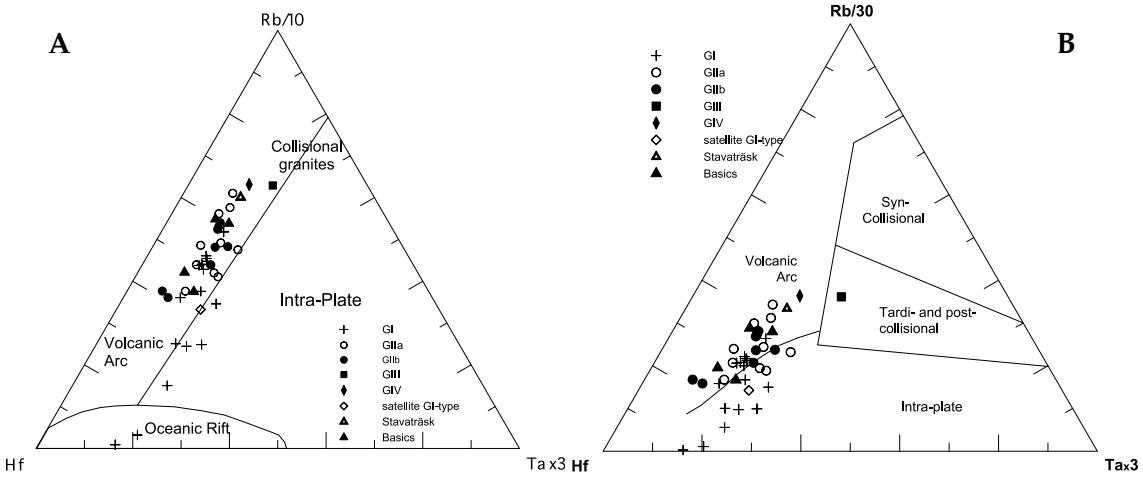

Fig. VI-40. Ternary diagrams for tectonic setting (Pearce et al., 1984).

The Hobergsliden and Antak intrusions have been plotted in the Nb vs. Y (ppm) diagram for tectonic setting. both, Hobergsliden and Antak plot in the VAG field grouped with the GIIb samples and close to the boundary WPG field (**Fig. VI-41A**). The three main phases of the VIC plot in the VAG field as the JGC, Hobergsliden and Antak (**Fig. VI-41B**). The Mine porphyry samples plots grouped intermediate to the GIIb and GI phases, and the trondhjemites on the GI samples area (**Fig. VI-41B**). The Hbl tonalites of VIC are not grouped and plots close to many of the different JGC intrusions (**Fig. VI-41B**).

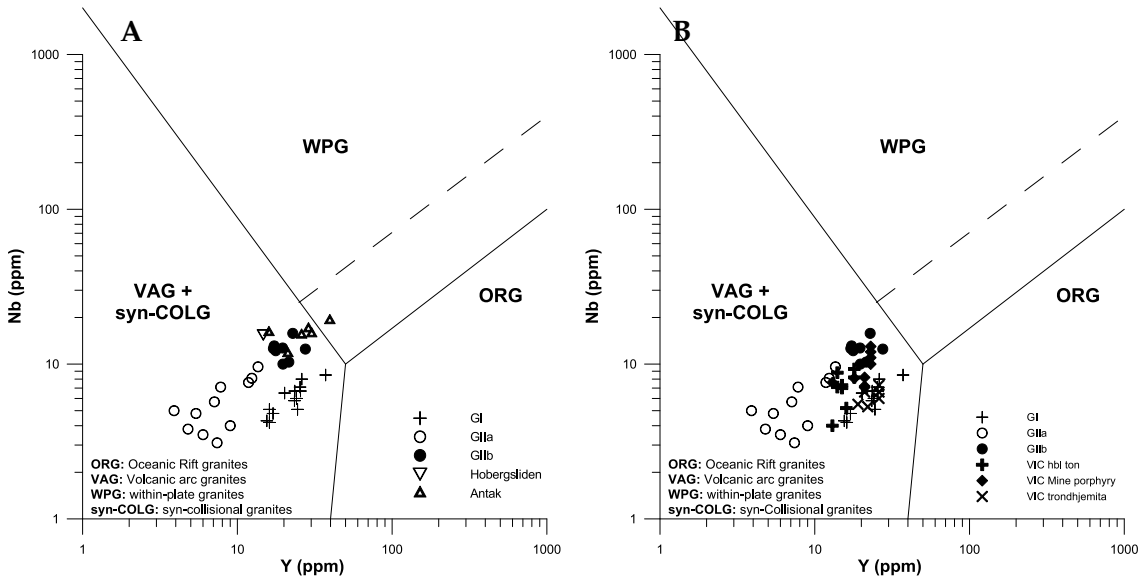

Fig. VI-41. Nb vs. Y (ppm) tectonic setting diagrams **A)** Hobergsliden and Antak (SGU) and **B)** Viterliden Intrusive Complex (Camiro project).

VI.4. ISOTOPIC LITHOGEOCHEMISTRY

The Samarium (Sm) and Neodymium (Nd) analyses have been realized on 12 samples that include the JGC phases, Klockträsk, Näsberg, Stavaträsk, qz+kfz porphyry and Hbl tonalite of VIC (**table VI-6**). Lithogeochemical analyses of the samples JO04-110, JO04-05, JO04-42, JO03-45, JO04-53 and VIC04-11 are included in this work (**table V-1**).

Sample	N-coord	E-coord	Intrusion	Phase
JO04-75	7214608	1704438	Klockträsk	GI (satellite)
JO04-86	7221615	1704600	JGC	GI (SE)
JO04-110	7244382	1689602	JGC	GI (NW)
JO04-135	7226363	1683510	JGC	GI (SW)
JO04-05	7253185	1701212	Näsberg	Gabronorite
JO04-34	7251600	1710192	JGC	GIIb (NE)
JO04-42	7259346	1703097	JGC	GIIa (N)
JO04-128	7222353	1700381	JGC	GIIb (Jörn)
JO03-45	7238400	1704300	JGC	GIII
JO04-53	7223590	1715814	Stavaträsk	Granodiorite
JO03-104	7221328	1676544	Mauriden	Dacite
VIC04-11	7221260	1631550	VIC	Hbl tonalite

Table VI-6. Samples analyzed for Sm and Nd data of intrusions in the Skellefte mining distric.

The Sm/Nd ratio in the chondritic uniform reservoir (CHUR) and the $^{143}Nd/^{144}Nd$ ratio with time and the epsilon Neodymium-$\varepsilon_{Nd(t)}$ [1] are the main reference to characterize the terrestrial reservoir (DePaolo, 1978; DePaolo and Wasserburg, 1976).

$$\varepsilon_{Nd(t)}=\left[\frac{\left(^{143}Nd/_{144}Nd\right)_{roca(t)}}{\left(^{143}Nd/_{144}Nd\right)_{CHUR(t)}}-1\right]\times 10000 \qquad [1]$$

During the analytical process is obtained the Sm, Nd concentrations and $^{143}Nd/^{144}Nd$ ratioare measured that allow to define the $\varepsilon_{Nd(t)}$. The $\varepsilon_{Nd(t)}$ is referred to the line deviation of CHUR in time of rock formation, and the next parameter are needed $^{147}Sm/^{144}Nd$ [2], $CHUR_{(t)}$ and $^{143}Nd/^{144}Nd_{(t)}$ [3]

$$\frac{^{147}Sm}{^{143}Nd}=\left[\frac{^{143}Nd}{^{144}Nd_{CHUR}}+\left(\frac{^{147}Sm}{^{144}Nd_{CHUR}}\times\frac{^{143}Nd}{^{144}Nd}\right)\right]\times\frac{Sm(ppm)}{Nd(ppm)} \qquad [2]$$

$$\frac{^{143}Nd}{^{144}Nd}(t)=\frac{^{143}Nd}{^{144}Nd}-\left[\frac{^{147}Sm}{^{144}Nd}\times\left(e^{X}-1\right)\right] \qquad [3]$$

$$X=6.54\times10^{-12t}$$

CHUR(t); is defined by the time evolution of CHUR.

The approximate age is obtained [4]. It is obtained depending on two suppositions. The ^{147}Sm and ^{143}Nd have been determined and λ is the constant ^{147}Sm (λ=6.54x10^{-12} years).

$$\left(^{143}Nd/_{144}Nd\right) = \left(^{143}Nd/_{144}Nd\right)_{(0)} + \left(^{147}Sm/_{144}Nd\right)\left(e^{\lambda t} - 1\right) \qquad [4]$$

The first supposition assumes that the rock has the initial Sm, Nd and $^{143}Nd/^{144}Nd$ content than the CHUR and the mantle. It is the Nd (*Nd model age*) and the age is the T_{CHUR} [5], and it is estimation about the time that a rock is in the crust in a closed system without Sm and Nd transferences. The age is the intersection of the Sm-Nd line with the CHUR (**Fig. VI-42**).

$$T_{CHUR} = \frac{1}{\lambda} \times \ln\left[1 + \frac{\left(^{143}Nd/_{144}Nd\right)_{rock} - \left(^{143}Nd/_{144}Nd\right)_{CHUR}}{\left(^{147}Sm/_{144}Nd\right)_{rock} - \left(^{147}Sm/_{144}Nd\right)_{CHUR}}\right] \qquad [5]$$

In this work is assumed the second supposition, the Depleted Mantle model age. It is a continuous Nd/Sm ratio enrichment in the crust (**Fig. VI-42**), it is due to the major incompatibility of the Nd. The mantle is continuously depleted in Nd referred to Sm (DePaolo, 1978; DePaolo et al., 1991; DePaolo and Wasserburg, 1976). Sm/Nd and $^{143}Nd/^{144}Nd$ for depleted mantle using MORB analyses, and is used the expression [4] to obtain the age [6]. The $^{143}Nd/^{144}Nd$ CHUR at 1900 Ma is 0,510179.

$$T_{DM} = \frac{1}{\lambda} \times \ln\left[1 + \frac{\left(^{143}Nd/_{144}Nd\right)_{rock} - \left(^{143}Nd/_{144}Nd\right)_{DM}}{\left(^{147}Sm/_{144}Nd\right)_{rock} - \left(^{147}Sm/_{144}Nd\right)_{DM}}\right] \qquad [6]$$

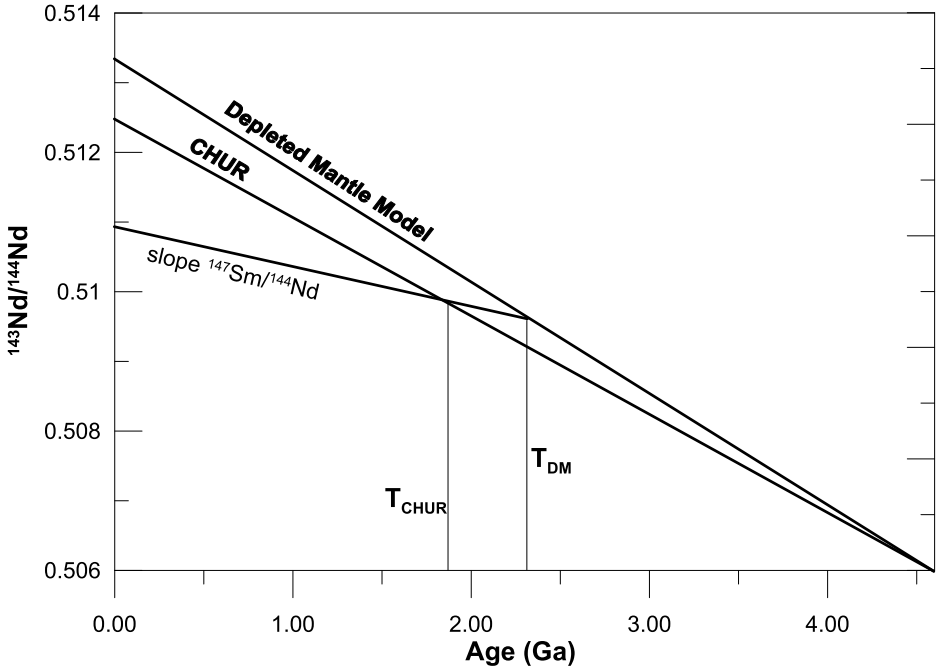

Fig. VI-42. Scheme of the CHUR and Depleted Mantle model (Modelo Manto Empobrecido) ages. Analyzed $^{147}Sm/^{144}Nd$: green; Depleted Mantle Model: red; CHUR model age: blue. Intersection in abscises axis is Time calculated by CHUR or Depleted mantle model.

The data obtained of $\varepsilon_{Nd(t)}$ and ages using the Depleted Mantle Model T_{DM} in **table V-7**.

nr	Samples	Phase	Sm	Nd	$^{147}Sm/^{144}Nd$	$^{143}Nd/^{144}Nd$	$\varepsilon_{Nd(0)}$	$\varepsilon_{Nd(t)}$	T_{DM}
1	**J004-86**	GI (SE)	4,70	26,8	0,1059	0,511644	- 19,4	**2,7**	1.98
2	**J004-110**	GI (NW)	3,83	16,6	0,1398	0,512117	- 10,2	**3,8**	1.91
3	**J004-135**	GI (SW)	3,10	14,6	0,1286	0,511936	- 13,7	**3,0**	1.99
4	**J004-75**	Klockträsk	4,11	19,5	0,1275	0,511965	- 13,2	**3,8**	1.91
5	**J004-05**	Näsberg	2,07	9,41	0,1333	0,512003	- 12,4	**3,2**	1.98
6	**J004-128**	GIIa (Jörn)	5,64	33,1	0,1030	0,511613	- 20,0	**2,9**	1.97
7	**J004-34**	GIIb (NE)	6,30	35,4	0,1076	0,511674	- 18,8	**2,9**	1.97
8	**J004-42**	GIIa (N)	4,94	30,3	0,0985	0,511557	- 21,1	**2,9**	1.97
9	**J003-45**	GIII (E)	3,77	23,2	0,0982	0,511542	- 21,4	**2,6**	1.99
10	**J004-53**	Stavaträsk	1,40	5,36	0,1574	0,512115	- 10,2	**-0,7**	2.54
11	**J003-104**	Maurliden	4,21	18,4	0,1388	0,512090	- 10,7	**3,6**	1.94
12	**VIC04-11**	VIC	3,43	17,6	0,1179	0,511756	- 17,2	**2,0**	2.05

Table VI-7: Isotopic Sm-Nd data of intrusions in the Skellefte district using the Depleted mantle model: T_{DM} (DePaolo, 1978; DePaolo and Wasserburg, 1976). Samples location in **fig. VI-43**. Sm and Nd concentrations (ppm) as measured by isotope dilution.

The GI samples $\varepsilon_{Nd(t)}$ is upper than 3,0 excepting the sample of Nör-Jörnsberget that is 2,7. The Klockträsk satellite intrusion and the JO04-110 $\varepsilon_{Nd(t)}$ are the higher values (3,8). The qz+kfs porphyritic dacite of the Maurliden $\varepsilon_{Nd(t)}$ is similar to the Klockträsk and JO04-110 samples of GI (**table VI-7**). The GII $\varepsilon_{Nd(t)}$ values are lower than GI and associated rocks and are homogeneous in the 2,9 value. It is not differences in $\varepsilon_{Nd(t)}$ values from north (JO04-34 and -42) to south (JO04-128) or comparing GIIa and GIIb. The GIII $\varepsilon_{Nd(t)}$ is 2,6 that is lower than the GI and GII samples. The hornblende tonalite of VIC04-11 $\varepsilon_{Nd(t)}$ is 2,0 that is much lower than GI or GII. The Näsberg gabbro $\varepsilon_{Nd(t)}$ value (3,2) is higher than the GII and similar to the GI phase. The Stavaträsk granodiorites $\varepsilon_{Nd(t)}$ = -0,7 is the only sample with negative value.

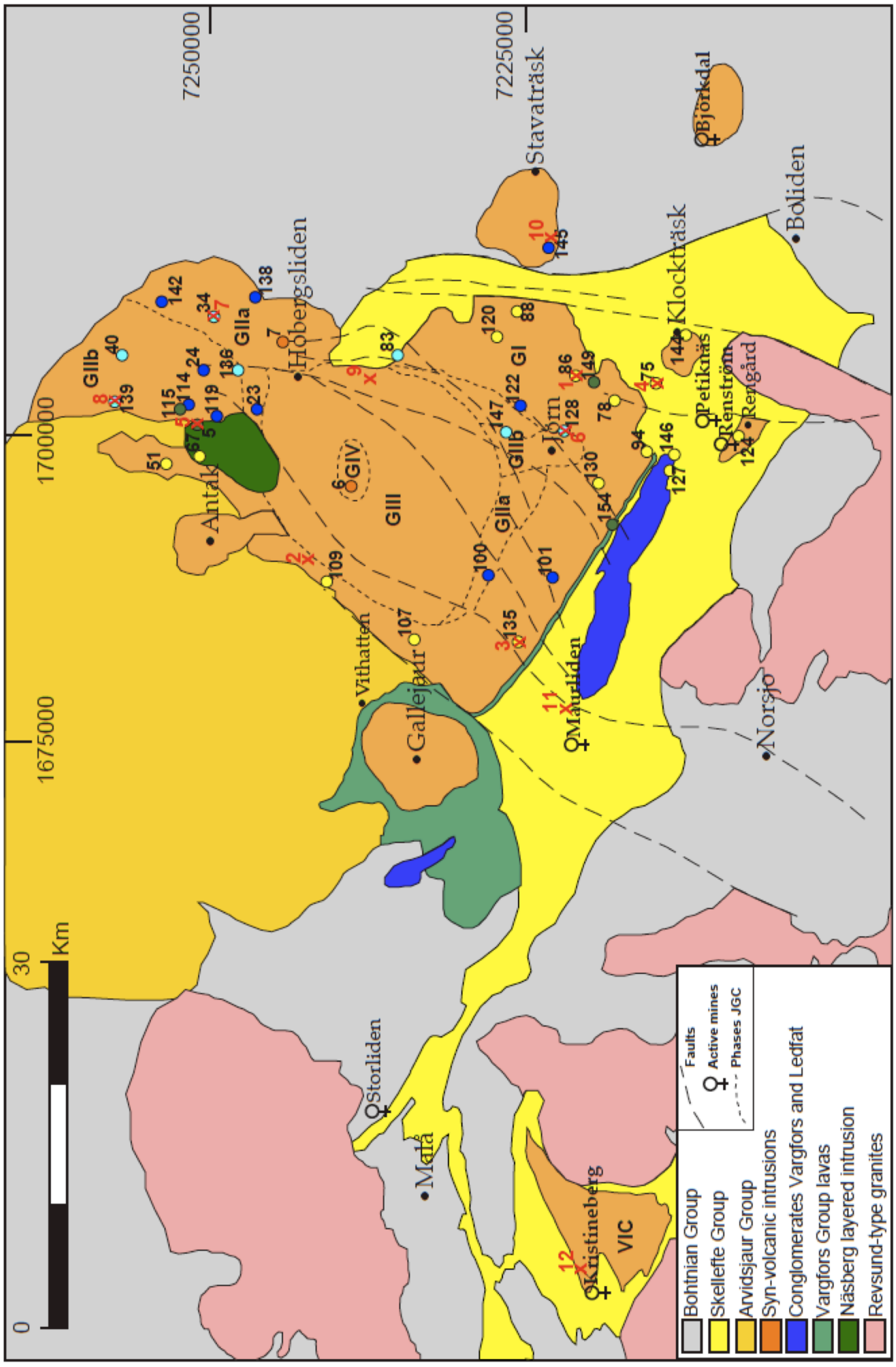

Fig. VI-43: Location of the lithogeochemical analyses (**table V-1**) including color of the phase. The location of the isotopic Sm/Nd analyses in red crosses and number in **table VI-7**.

VII. U-Pb Zircon and Titanite Dating and Chemical Analysis of Zircons

It is many U-Pb zircons dating of intrusions in the Skellefte mining district. It includes the JGC, Sravaträsk, Gallejaur, VIC and other minor intrusions and volcanics (**Table VII-1** and **fig. VII-7**). The major problem with the old datings of the rocks is that the analytical error in most of the cases is higher than 10 Ma.

	Intrusion/Zone	Rock	Author	N	E	Age Ma
1	JGC *Hobergsliden*	GIII	Lundström et al., 1997	7247600	1706800	1862±14
2	Stavaträsk	Diorite	Lundström et al., 1997	7226380	1721900	1877±2
3	Stavaträsk	Granodiorite	Lundström et al., 1999	7223500	1715820	1874±3
4	JGC *Skidbäcken*	GIIb	Wilson et al., 1987	7222590	1700400	1874^{+48}_{-26}
5	JGC (E)	GI	Wilson et al., 1987	7234560	1683680	1888^{+20}_{-14}
6	Tallberg porp.	GI type	Weihed and Schöberg, 1991	7221000	1693000	1886^{+15}_{-9}
7	Antak *Kåtaselet*	Granite	Kathol and Persson, 1997	7254650	1691940	1879^{+15}_{-12}
8	Gallejaur	Monzonite	Skiold, 1988	7235500	1676900	1873±10
9	JGC	GIII	Wilson et al., 1987	7233890	1691940	1873^{+18}_{-14}
10	Gallejaur	Gabro	Skiold et al., 1993	7233300	1669900	1876±4
11	VIC *N-Svanaberget*	Tonalite	Bergström et al., 1999	7216930	1634140	1907±12
12	GI *Halmyrtjärnen*	GI	Kathol et al., 2002	7226872	1682720	1898±11
13	Bjurvattnet	Peperite	Billström and Weihed, 1996	7202590	1708540	1884±6
14	Melestjärn	Porphyry	Billström and Weihed, 1996	7213410	1685530	1889±3
15	Vargfors	Ignimbrite	Billström and Weihed, 1996	7229200	1670500	1875±4
16	Maurliden	Rhyolite B	Montelius et a., 2007	-	-	1885±3
16	Maurliden	Rhyolite A	Montelius et a., 2007	-	-	1902±21
16	Maurliden	Rhyolite A	Montelius et a., 2007	-	-	1885±6
17	Finnliden	Rhyolite A	Montelius et a., 2007	-	-	1901±3
18	Petikträsk	Mass-flow	Billström and Weihed, 1996	7225200	1681250	1847±3
19	Arvidsjaur (Skyt.)	Rhyolite	Skiold et al., 1993	7256150	1693450	1878±2

Table VII-1. U-Pb dating of intrusions and volcanics in the Skellefte mining district.

VII.1. New U-Pb zircon and titanite dating in JGC

The samples of JGC have been dated using zircons and titanites. The GI samples used for dating are located in the southwest and western area of JGC and two satellite intrusions have been dated, the Klockträsk (tit) and Rengård (zr). The GII phase have been dated in the south (city of Jörn) and the north (Kåtaberget) of the JGC, it have been dated with zircons and titanites. The date of the GIII sample has been determined using zircons and titanites (**Table VII-2**). EPMA microanalyses of the zircons have been done to determine the zircon analyses that have to be refused to obtain a better and realistic age determination. Chemical maps of some zircons are used to determine alteration on zircons.

Sample	Phase	Mineral	N-coord	E-coord	Zone	Lithogeochemical equivalence
23J28	GI	Zr	7226850	1682350	South (Hålmyrtj)	JO04-135
JO03-55a	GI	Zr	7226550	1683350	South (Hålmyrtj)	JO04-135
MG07-001	GII	Zr+tit	7222681	1700310	Jörn (Skidbacken)	JO04-128
MG07-004	GI	Zr	7242143	1688028	W (Järpkullen)	JO04-109
MG07-005	GIII	Zr+tit	7235755	1702913	Centre (Storklinta)	-
MG07-006	GI	Tit	7214250	1707070	Klockträsk(Vänträsk)	JO04-75
MG07-007	GI	Zr	7207970	1700790	Rengård	JO04-124
MG07-008	GII	Zr+tit	7251600	1710203	NE (Kåtaberget)	JO04-34

Table VII-2. Samples and minerals used for U-Pb dating.

VII.1.1. U-Pb zircon and titanite dating

The complete lines of zircons are shown in the **figs VII-1** and **VII-2**.

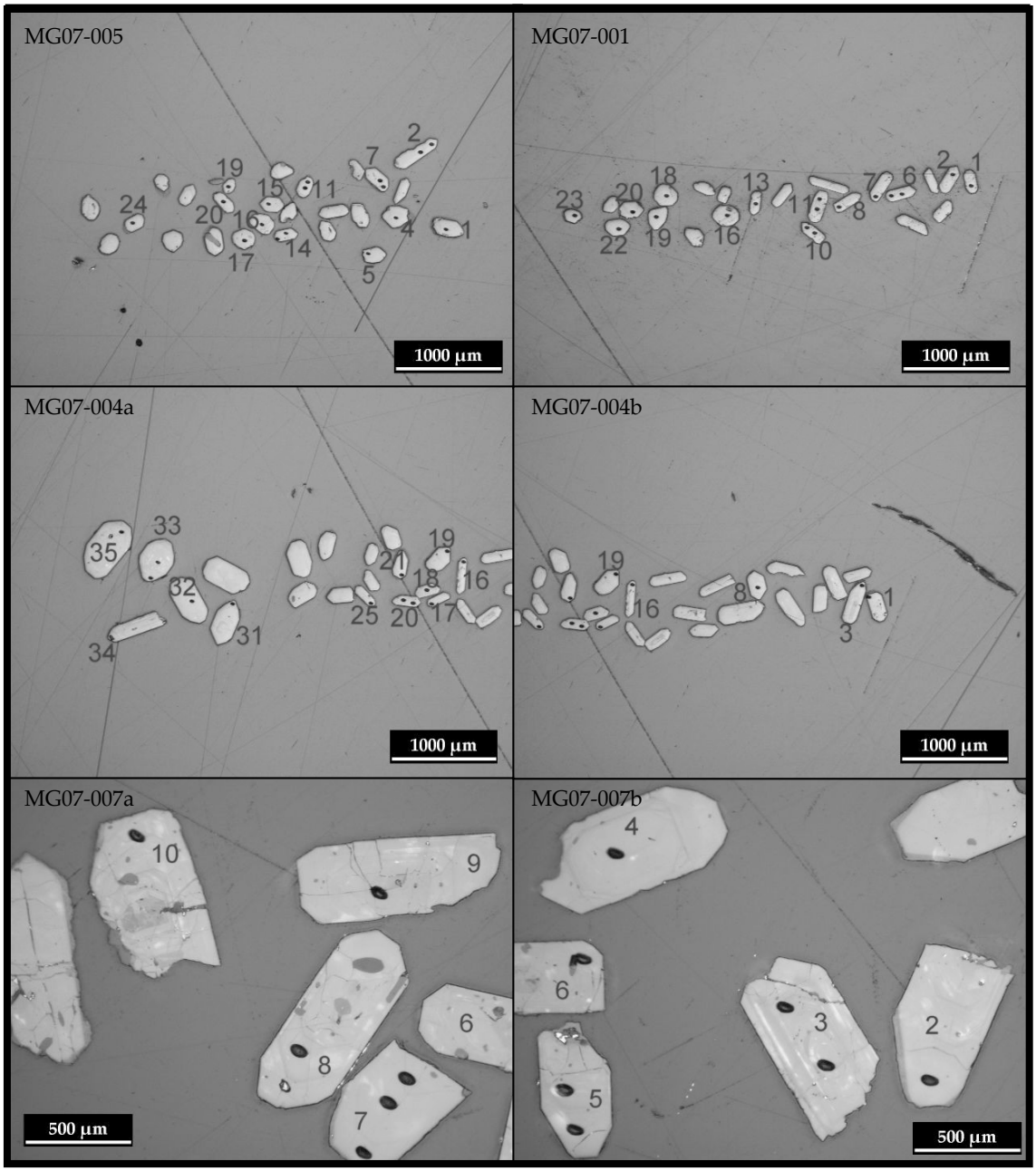

Fig. VII-1. Microphotography of zircons using reflected light petrography microscope. Samples MG07-001, MG07-004, MG07-005 and MG07-007.

The ellipsoidal black dots are the areas that have been analyzed by the NORDSIM ionic microprobe. The red numbers are referred in the Annex data as the number of the zircons analyzed in each sample. If zircons have been dated using more than a dot of analysis it is named from Xa, Xb, … Xn, from core to rim. The zircons size of MG07-001, MG07-005 and JO03-55 samples is 63-125 μm. The zircons size of MG07-007 and MG07-008 is 125-250 μm. The two ranges of zircons sizes (63-125 μm and 125-250 μm) are used in the samples MG07-004 and 23J28. The usual shape of the 63-125 μm zircons is prismatic or elongated prism but never acicular, it can be classified as P2 and P3 for

the elongated and S10 and S15 for the prismatic (Pupin, 1980). The 125-250 μm zircons shape group is the S14 and S19 (Pupin, 1980).

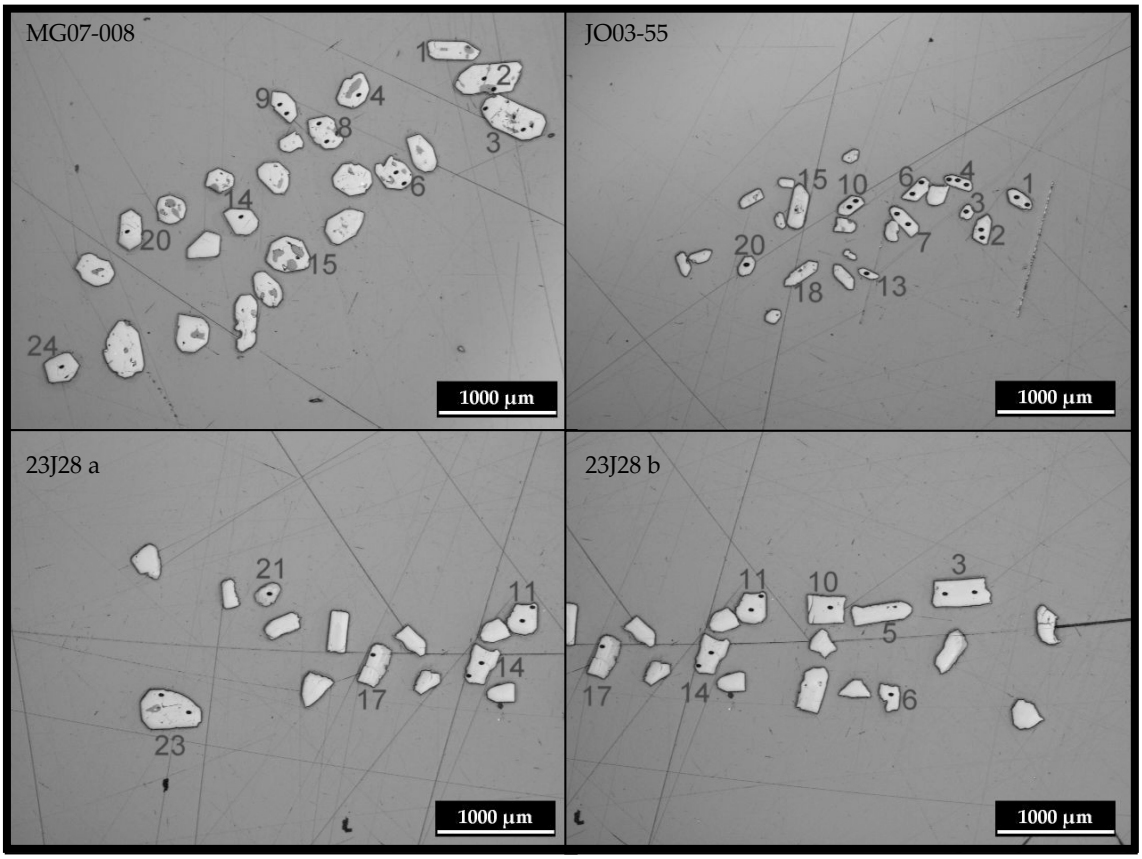

Fig. VII-2. Microphotography of zircons using reflected light petrography microscope. Samples MG07-008, 23J28 and JO03-55.

The samples dated using titanites are defined in **table V-9**. The titanites size is 125-250 μm range. The error in the age determination is higher than the U-Pb zircons dating but the age determined for each phase is the same than the zircon analyses. Microphotographs of the titanite crystals in **fig. VII-3**. As occurs in the zircons microphotograph th ellipsoidal black dots are the areas that have been analyzed by the NORDSIM ionic microprobe. The red numbers are referred in the Annex data as the number of the titanites analyzed in each sample. If titanites have been dated using more than a dot of analysis it is named from Xa, Xb, … Xn, from core to rim.

The ages have been obtained with the intersection with the Concordia line of the ratios $^{206}Pb/^{238}U$ and $^{207}Pb/^{235}U$ for each single zircon data. Most of the isotopic analyses were later complemented with a microprobe analysis for zircons that do not plot in the intersection line with the Concordia. These zircons and titanites analyses were studied and reasonably eliminated to obtain a lower error in the age determination. The whole data have been represented in the table 3, only two zircons have been eliminated of the Concordia calculation: the 14a of the 23J28 and the 2b of the MG07-008, both of them due to comprise altered zones or mixture of different zones in the crystal. The analysis on the titanite crystals shows that the dating on it is more difficult than with zircons, at least for the samples of JGC. Regarding on the titanites of the JGC samples, two of the samples show a lot of analysis that plot a bad result, the MG07-006 and the MG07-005. The whole of these titanite analyses that have been eliminated from the final calculus are due to do the analysis in boundary between inclusions or zoning with the titanite. It is the 1c, 3a, 5a, 5b and 7a of the MG07-006, and the 3b, 6a, 8b, 10a, 10b of the MG07-005.

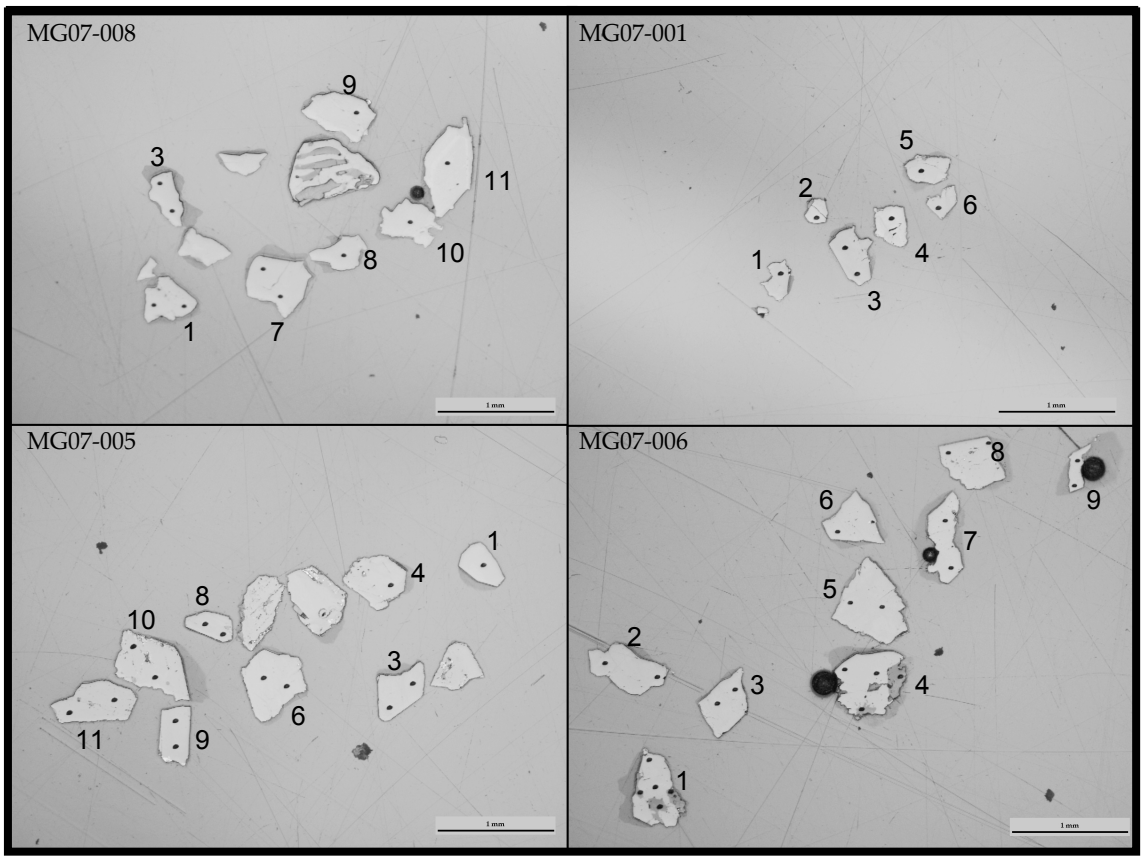

Fig. VII-3. Microphotography of titanites using reflected light petrography microscope. Samples MG07-001, MG07-005, MG07-006 and MG07-008.

The zircons age obtained for the GI phase of the JGC main body is quite homogeneous around 1885 Ma. In the western boundary, close to the limit with the Arvidsjaur Group volcanics the age of the MG07-004 is 1886,4 ±3,3 Ma (MSWD = 0.68). Other age determinations in the main GI body come from the southern area, both samples plot a similar age but lower for the 23J28 (1880 ±3,9 Ma; MSWD = 1.6) but the age error overlaps with the age of JO03-55 (1884,7 ±4,8 Ma; MSWD = 1.6). In the dating of these GI samples have been included analyses on the two size fractions of zircons, completed with a detailed petrography in the location of the analytical spots. This spots include inner zones, borders and cores of the zircon crystals. The zircon analyses of MG07-007 have shown the lower GI-type age (1879 ±5,0 Ma; MSWD = 1.14), the Rengård intrusion is stratigraphycally over the mineralization of Petiknäs deposit. The zircons of Rengård show a complex zoning, lot of inclusions and fractures, have been analyzed cores, inner zones and rims without difference among zones. (**Fig. VII-4**).

The age of GII (**Fig. VII-5**) comprises the two mineralogical subphases defined in this intrusive phase; the first is the GIIa (granodiorite) that is represented by the MG07-001 with an age of 1871 ±4,0 Ma (MSWD = 1.3). The zircons of the MG07-001 are quite homogeneous in size, shape and do not shows complex zoning. The later GIIb subphase (qz-monzodiorite) MG07-008 of the north of JGC has been aged as 1874 ±6,5 Ma (MSWD = 1.3), in this case the zircons are heterogeneous in zoning and inclusions rich, with some inherited cores. The zircon dating of the younger phase of JGC shows an age of 1862,8 ±4,7 Ma (MSWD = 1.17), similar to the previous age of the GIII-type Hobergsliden intrusion (Lundström et al., 1997). The zircons are zoned and contain inclusions, but there is not difference from cores to rim in the analyses.

Regarding to titanite ages the error in the determinations is bigger than data obtained with zircons. The older dating in a GI-type phase is the 1897 ±10 Ma (MSWD = 2.3) of

the MG07-006 of the Klockträsk intrusion (**Fig. VII-4**), half of the data are not useful due to the presence of small inclusions. The titanite ages of the GII samples are similar to the ages of the zircons analyses but the error is higher for the MG07-001 (1878 ±10 Ma; MSWD = 4.3); for the MG07-008 the ages of titanites (1874,3 ±4,2 Ma; MSWD = 1.5) is almost identical to the age obtained with the zircons. As happens with the MG07-006, the titanites of the MG07-005 contain lot of inclusions that produce interferences in the age determinations. The dating with titanites of GIII (**Fig. VII-6**) on MG07-005 (1864 ±46 Ma; MSWD = 3.0) is coherent with this of the zircons but the error is extremely high to make further consideration.

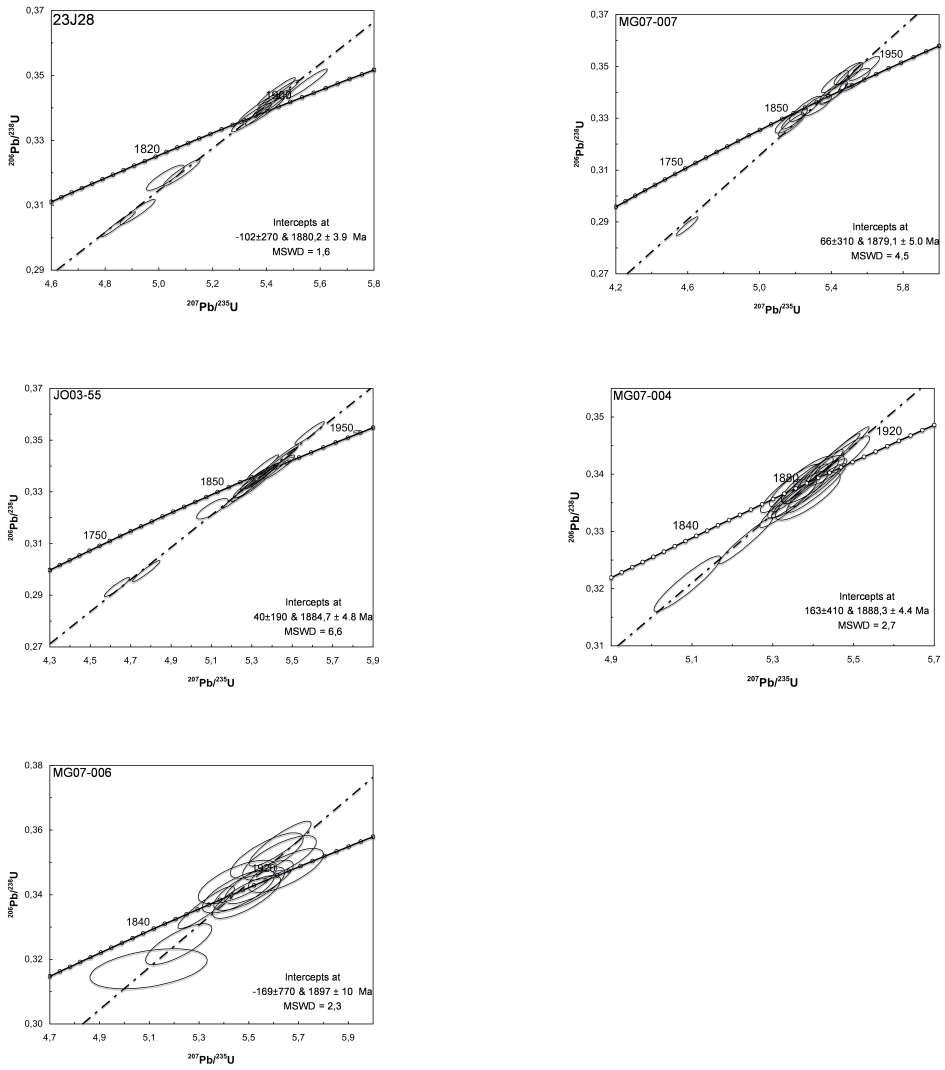

Fig. 4. Age determinations of GI tonalites and GI type satellite intrusions of JGC. All samples dated using U-Pb in zircons excepting the MG07-006 dated using U-Pb in titanites.

The Skellefte Group volcanics and related intrusions belong to a long live igneous activity that starts at least on 1900 Ma and is active until 1885 Ma for the younger intrusions and volcanism. The older phases have been developed from east to west Skellefte mining district, although, it shows a 10 Ma error in the date, in the east the Klockträsk satellite GI-type intrusion is the oldest igneous body in the eastern area of the district (1897 ±10 Ma). The Finnliden rhyolite porphyry and GI tonalite in Halmyrtjärnen crop in the central area of the Skellefte district with an age reaching the 1900 Ma, representing the hosting volcanics of the Skelelfte Group and the related intrusions respectively. The westernmost part of the district is represented by the

hornblende tonalite of the VIC, it is coeval with the Skellefte Group volcanics where it is hosted, and it is the oldest rock that has been dated in the district.

Most of the ages determinations of the Skellefte Group volcanics and the GI type rocks are dated circa 1885 Ma. It comprises volcanics rocks in the easternmost part of the district Bjurvattnet and Rengård intrusion and a most of the dating in the central area of the Skellefte Group volcanics, it is the Melestjärn porphyry, Maurliden rhyolites and most of the GI dating. Some of these are related to mineralization and Rengård intrusion that is over de Petikträsk South deposits.

The second main period of igneous activity is related to the Vargfors and Arvidsjaur Group with circa 1875 Ma. Both groups look coeval, with Arvidsjaur as the subaereal northern equivalent to the Vargfors Group volcanics and intrusions. It comprises different intrusions and volcanics with rocks of diverse nature. Among the intrusions the most important are those related to the GII phases of the JGC (granodiorites and qz-monzodiorites). Related to the Vargfors Group are found the Gallejaur gabbros, monzonites and ignimbrite in the southwestern corner of the JGC, all these rocks with an dating fairly close to 1875 Ma. To the north the Antak granite and the Arvidsjaur volcanics shows an age similar to the GII and the Vargfors Group rocks. At the east of JGC, the Stavaträsk intrusions are dated in this intrusive period in its diorites and granodiorites. At the western area do not are any dates of this intrusive stage.

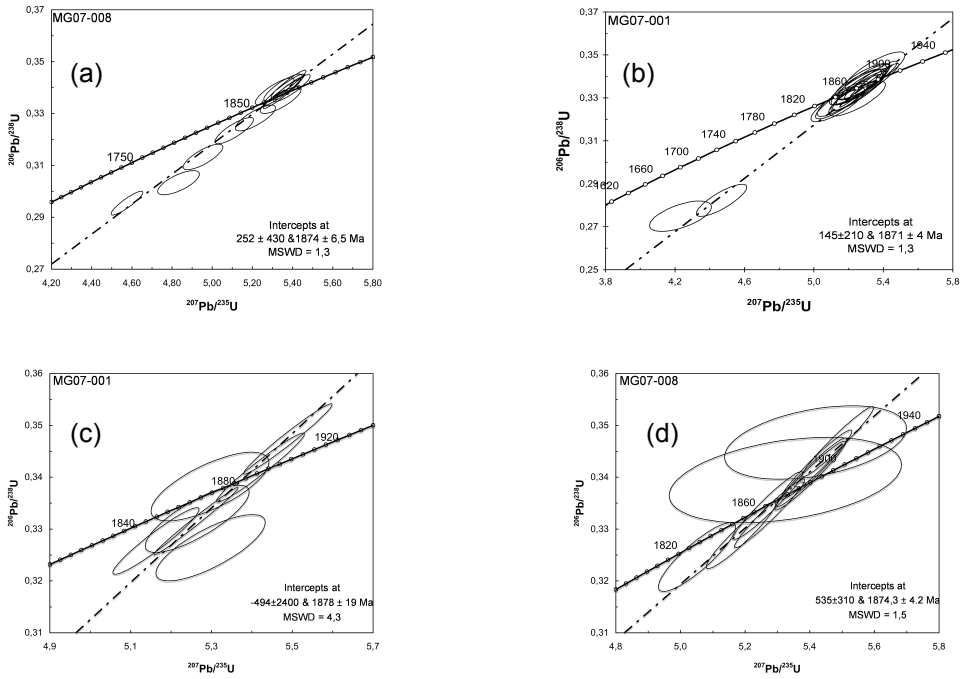

Fig. VII-5: Age determinations of GII granodiorites and quartzmonzonites. (a) and (b) dated using U-Pb in zircons; (c) and (d) dated using U-Pb in titanites.

The last igneous event is related to the GIII monzogranites and the Hobergsliden Kfs-rich granites, both crops in the central JGC and occupies the main surface of this composite intrusion. The GIII U-Pb zircons age is 1862,8 ±4,7 Ma, and a similar ages was obtained with the Hobergsliden intrusion in 1862 ±10 Ma that is probably to the most evolved magmas that produce this intrusion. No other intrusions are associated to this event excepting the small GIV pluton located in the center of the GIII intrusion, it has not been yet dated.

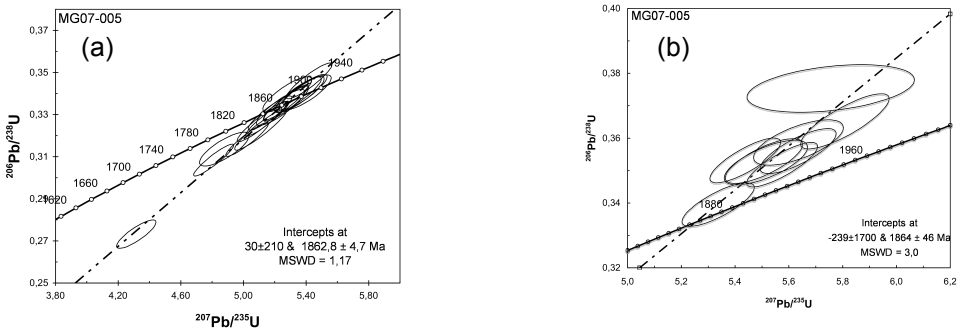

Fig. VII-6: Age determinations of GIII granites in Storklinta. (a) dated using U-Pb in zircons and (b) dated using U-Pb in titanites.

VII.1.3. Summary of the new U-Pb zircons and titanite dating

The total new analyses of U-Pb of JGC samples are 153 (105 of zircons and 48 of titanites) obtained on 11 samples (eight different samples). The dates of seven samples have been determined using zircons and four using titanites (**Table VII-3**).

Sample	Phase	Location	Mineral	Age (Ma)
MG07-004	GI	Järpkullen	Zr	1886,4 ± 3,3
JO03-55	GI	Hålmyrtj	Zr	1884,7 ± 4,8
23J28	GI	Hålmyrtj	Zr	1880,0 ± 3,9
MG07-007	GI satellite	Rengård	Zr	1879,0 ± 5,0
MG07-001	GII	Skidbäcken	Zr	1871,0 ± 4,0
MG07-008	GIIb	Kåtaberget	Zr	1874,0 ± 6,5
MG07-005	GIII	Storklinta	Zr	1862,8 ± 4,7
MG07-006	GI satellite	Klockträsk	Tit	1897,0 ± 10
MG07-001	GII	Skidbäken	Tit	1878,0 ± 19
MG07-008	GIIb	Kåtaberget	Tit	1874,3 ± 4,2
MG07-005	GIII	Storklinta	Tit	1864,0 ± 46

Table VII-3. U-Pb zircons and titanites age determinations.

The GI age determinations are homogeneous from different locations in the JGC. The date of samples in the southwest of GI 23J28 and JO03-55, 1880,0 ±3,9 Ma and 1884,7 ±4,8 Ma respectively, and the central western margin GI MG07-004 is 1886,4 ±3,3 Ma. The Rengård satellite intrusion date 1879 ±5,0 Ma is slightly lower than the GI average. The date of the Klockträsk satellite intrusion is 1897 ±10 Ma, around 10 Ma older than the GI samples and 15 Ma older than the Rengård intrusion.

The date of GII samples from the North and the South are almost identical. The U-Pb zircon date of GII samples in Skidbäcken and GIIb in Kåtaberget are 1871,0 ±4,0 Ma and 1874,0 ±6,5 Ma respectively. The titanite date of GII Skidbäcken and GIIb in Kåtaberget are 1878,0 ±19 Ma and 1874,3 ±4,2 Ma respectively. The titanites and zircons age determination indicates that the GII is at least 10 Ma younger than the GI average.

The U-Pb zircon date of GIII is 1862,8 ±4,7 Ma, that is similar to the date using titanites (1864,0 ±46 Ma) but the error using titanites limit the comparison. The zircon date of GIII indicates that it is 10 Ma younger than GII and at least 20-25 Ma older than the GI average date.

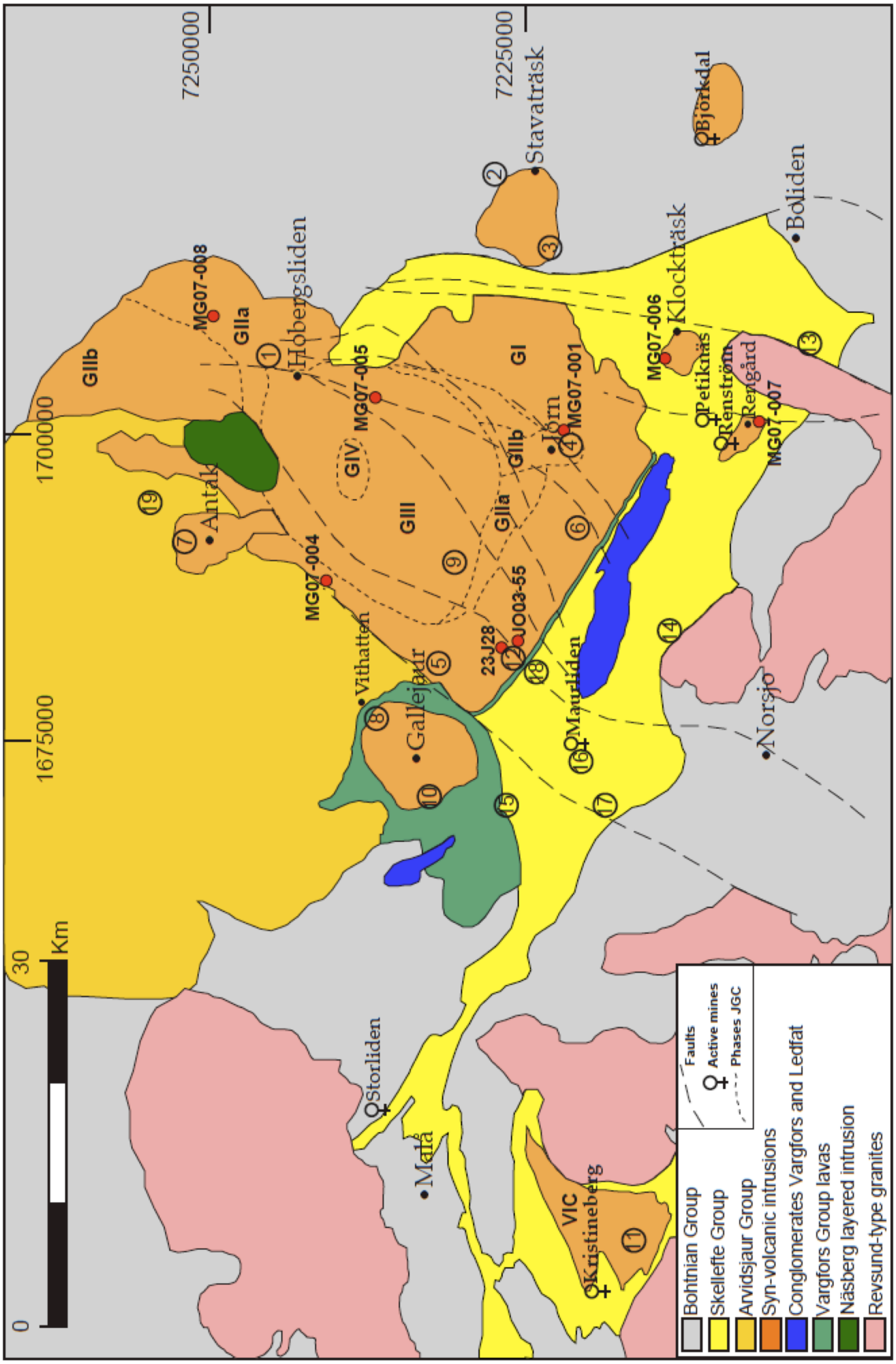

Fig. VII-7. Location of the samples dated in this work as red dot (**Table VII-3**) and ages of the bibliography in circle numbers (**Table VII-1**).

VII.2. Chemical Mineralogy of Zircons

Zircons of the seven dated samples have been analyzed in EPMA microprobe. The zircons microphotographs are in **Figs. VII-8** to **VII-14**. The numbered red circles are the EPMA analyses (see Annex), in white the number of zircons of each samples.
The EPMA analisis nr 5 of MG07-001 is the 11a U-Pb analysis of zircon nr 11. The nr 5 analysis is Y, U and Th richer than the other zircons. The zircons 11 and 20 plotted out of the grouped analyses in the U-Pb determination (**Fig. VII-7**).

The EPMA analyses of the MG07-004 is quite homogeneous, with only variation of higher Y values in the data in the core of the zircons 3, 33 and 35 (EPMA analyses nr 8, 9, 16 and 17). The zircon 3 is U richer than the others, with the core high in Th.

The chemical composition of the zircons is quite homogeneous with the only higher Y values in the zircons 2 and 16 (**Fig. VII-10**).

The EPMA analyses of the MG07-007 indicate that these zircons contain the higher Y values of the samples analyzed but in general the composition is homogeneous. It only occur a slight difference in the ZrO_2 % in the core that in the rim.

The zircons of the MG07-008 sample contain lot of quartz intrusions and it is characteristic a lower Y content in the rim than in the core of the crystals (**Fig. VII-12**).

The major and minor components of the JO03-55 zircons do not change from crystals or zonings. The JO03-55 zircons are usually zoned (**Fig. VII-13**).

The 17 and 21 zircons in the 23J28 sample are strongly altered, the altered zones are U and Th rich in comparison to the other zircons. The alteration occurs in the rim and in the fractures and the products are ZrO_2 and SiO_2 poor (**Fig. VII-14**).

VII.3. Chemical Maps of Zircons

The Chemical Maps of zircons obtained with the EPMA provide images of relative abundance of elements. The scale is increased from deep blue to red, and image of the zircon is included in the centre of the picture. The elements chosen are Zr, Th, P, Si, Ce, Y, Gd and Ca. The zircons analyzed are the nr 17 of the 23J28, the nr 11 of the MG07-001, the nr 3 of the MG07-004, the nr 8 of the MG07-005 and the nr 8 of the MG07-008.

In the central area of the zircon is the ellipsoidal mark of the microprobe U-Pb analysis nr 17a of the sample 23J28 (**Fig. VII-15**). The altered area is poor in Si and Zr content, the alteration increases the Ca content of the crystal.

The 11a and 11b U-Pb analyses for age determination in the central image (**Fig. VII-16**). The central are is not an older zircon, the rim area around the core is related to alteration process. The radial fractures starts in the core and reaches the rim of the zircon (**Fig. VII-16**). The EPMA nr 5 and nr 6 analyses are done in the core and rim of this zircon. The core is richer in Th and slightly richer in P compared to the rim. Ce and Ca rich (Si and Zr poor) minerals have been crystallized in the core-rim boundary and fractures. The Ca and P very rich area define the apatite inclusions in the zircon (**Fig. VII-16**).

The texture of zircon nr 3 of MG07-004 (**Fig. VII-17**) sample is similar to the texture observed in the zircon 11 of the MG07-001 sample (**Fig. VII-16**). As previously observed the radial fractures occur from core to rim. The very fine rim and fractures are Ca rich, the core is slightly richer in Th and P than the rim crystal. The U-Pb nr 3 analyses is located in the lower corner, this analysis was not used in the Concordia calculation for age determination because it is probably contaminated by the fracture (**Fig. VII-17**).

The alteration in the zircon nr 8 of MG07-005 (**Fig. VII-18**) is similar to the zircon nr 17 of 23J28 (**Fig. VII-15**). The altered areas are Ca, Gd, Ce and Th richer (Zr and Si poor) than the unaltered areas. The core of the zircon is slightly richer in P than the rim or altered areas. It also occurs some apatite inclusions (**Fig. VII-18**).

The zircon nr 8 of MG07-008 is zoned as can be seen in the central Compo image, but the chemical composition of the crystal is homogeneous. It is not defined any heterogeneity in the analyzed chemical elements. The crystals contain some quartz and apatite inclusions defined by the Si and P-Ca anomalies respectively (**Fig. VII-19**). The U-Pb 8a and 8b analyses are located in core and rim of the zircon.

VIII. DISCUSSION

VIII.1. REVISION OF LIMITS AND INTRUSIVE STAGES OF JÖRN GRANITOID COMPLEX

The cartographical and lithogeochemical initial studies of the Jörn Granitoid Complex were published in the early eighties and nineties of XXth century (Richard, 1986; Weihed, 1992; Wilson et al., 1985; Wilson et al., 1987), those works are monographies on the JGC; it is also used the lithogeochemical database of the Boliden Mineral Company (Svensson, 1970; Svensson, 1980). The early works established three main phases of JGC: *granodiorites*, *Jörn granites* and *Gabbros-diorites* (**Fig. V-18**). The actual maps only preserve the original intrusions of gabbros-diorites. The old phase "granodiorites", in the central area is dominated by the GIII intrusion, and the southern boundary corresponding to GI. The "Jörn granite", in the inner southern and SW-NW areas, including the northern areas of JGC, belongs to GI and GII phases of JGC. Svensson included sericited areas in the maps (**Fig. V-18**).

The borders and numbers of phases of JGC have been modified using the new airborne geophysical techniques. In the Wilson et al (1987) were included the GIV phase and the actual names were re-defined (GI to GIV), GIII is determined in the central area of JGC (**Fig. V-19**). The NE area, established as Jörn granite by Svensson, is related with the Sorsele granites (**Fig. V-19**), as the youngest intrusions in the Skellefte mining district but still the age was not determined. The regional scale geological map of the Skellefte district (Richard, 1986) is used as the base map for regional mapping with many modifications.

VIII.1.2. Distribution of phases in JGC

The Wilson et al (1987) work has been used as the main reference for this work, for the use of rocks nomenclature (GI to GIV). It is the terminology used by the mineral companies that occupies the exploration and exploitation areas of the Skellefte district and by the Swedish Geological Survey SGU (Sveriges Geologiska Undersökning).

The extension and distribution of the GI phase is the most complex of the JGC due to: variations in texture (fine-medium grained trondhjemites to coarse qz+fs porphyritic tonalites), and the process that overprints the original characteristic of the rocks. The area occupied by this phase is smaller than previously determined in Wilson et al (1987) (**Fig. V-19**), is relevant the absence of great GI outcrops in the northeastern area of JGC at the E of the Näsberget layered intrusions. The NE of JGC, determined as "Jörn granites" or "Sorsele granites" by early publications, is complex in the phase distributions but mainly dominated by GIIa and GIIb subphases. In the surroundings of Näsberget and inner the gabbros or GII is common the presence of GI megablocks. The **fig. V-30** plots the studied samples and the phases. The complexity of the NE area of JGC, dominated by GII and some GI and gabbros, is evident.

The GII phase is located in the south of JGC, in the surroundings of Jörn village, and occurs as a small pluton, it is not possible to plot the exact margins and the GIIa-GIIb dominance due to the absence of outcrops. Both GIIa and GIIb are present in most of the areas were GII occurs. The **fig. V-31** represents an outcrop where both subphases are in connection. The GIIb contains fragments of GIIa and the mafic dike; it also contains microgranular enclaves (defined and photographed in the petrografical descriptions). The GIIa subphase is more abundant in the NE of JGC. Megablocks of metapelitic rocks in the northeastern area (JO04-141 coordinates) hosted in the GIIa subphase also occur

In the central area of JGC, the GIII granites outcrop. GIII is overprinted on the GI from the SE to the N; and over GII in the south and NE of central JGC. The most evolved plutonic body of GIII is located in the NE of GIII, in the Hobergsliden area, dominated

by leuco-alkali granites. The GIV small pluton is located in the middle of the GIII intrusion.

VIII.1.3. Lithogeochemical characteristics and age of JGC

The timing of emplacement and the plutonic relationships are among the main targets of this work. The hydrothermal alteration occurs on the GI rocks, in this case the use of immobile elements is essential, in particular REE. The major elements AFM diagram (**Fig. VI-5**) of GII, GIII, GIV and Stavaträsk form a trend from less evolved (qz-monzodiorite GIIb) to late intrusions (alkali granites of GIII-Hobergsliden). The GI and satellite intrusions are disperse, but not associated with the GII-GIV trend.

The Harker diagram (**Fig. VI-1**) separates trends of GI and GII in two separate and unrelated groups; the satellite intrusions are associated to GI and Stavaträsk, GIII, GIV are associated to the GII magmatic trend. The major elements in K_2O vs. SiO_2 diagram (Roberts and Clemens, 1993) has been used to discrimination of magmatic series. The GI samples are calcalkaline partially plotted in the tholeiitic field, specially the satellite intrusions, those samples are the highest in SiO_2 content and could be related with alteration processes. Many samples of GII plot in the calcalkaline field, and are transitional to high K calcalkaline. GIIb, GIII, GIV, Stavaträsk and GIII-Hobergsliden samples are high K calcalkaline. Those data suggest a change in the magmatic affinity of the intrusions from tholeiitic (transitional) to calcalkaline and finally high K calcalkaline for the younger intrusions (**Fig. VI-4**).

The granite classification of Frost et al. (2001), indicates that most of the samples plot as magnesian or in the ferric-magnesian transition of the Fe* vs. SiO_2 (**Fig. VI-6**). It indicates the tholeiitic to calcalkaline transition (Miyashiro, 1970). The GI and satellite intrusions of JGC plot as calcic granitoids in the MALI diagram; the GIIa samples are disperse in the calcic and calc-alkaline, in contrast with GIIb, Stavaträsk and GIV that plot as calc-alkaline in transition to alkaline-calcic; finally GIII and GIII-Hobergsliden plot as alkaline-calcic (**Fig. VI-7A**). GI, GIIa, GIIb, GIV and Stavaträsk plot as metaluminous, excepting GIIb in the transition to peraluminous (**Fig. VI-7B**); the GIII and Hobergsliden sample plot in the peraluminous field (ASI < 0) but classify as peralkaline due to *(Na+K) > Al* molecular (**Fig. VI-7B**).

The REE diagrams of JGC have allowed to separate the rocks in two groups: GI and GII (GIIa and GIIb). The REE patterns of GII (GIIa granodiorites and GIIb qz-monzodiorites) are parallel but GIIb samples are systematically higher in REE content (**Fig. VI-24**). The GIII, GIV and GIII-Hobergsliden fit in the REE pattern of GIIa (**Figs. VI-25** y **VI-30**), with the particular *Eu* negative anomaly for the Hobergsliden sample. The Hobergsliden leuco-alkali granite has been determined as the most evolved magma of the GIII granites, and the *Eu* negative anomaly suggests the prior fractionation of plagioclase in the magmatic reservoir parental to this intrusion. The mineralogy of Hobergsliden is similar to GIII, but poorer in plagioclase and mafic minerals and richer in alkali feldspars.

The isotopic $^{143}Nd/^{144}Nd$ have been used for magmatic discrimination among the intrusions in the Skellefte district (**Fig. VIII-1**). The isotopic data suggest geochemical differences of GII and GIII relative to the GI samples (**Table VI-7**). The $\varepsilon_{Nd(t)}$ values of GII samples are homogeneous around 2,9. The $\varepsilon_{Nd(t)}$ = 2,6 of GIII is slightly lower to GII and similar to the old Sm-Nd data obtained by Wilson et al. (1987) with 2,4 and 2,7 of the samples GIII-13 y GIII-16 respectively (table VI in Wilson et al., 1987); in this study, $\varepsilon_{Nd(t)}$ = 3,2 for GIV (sample GIV-20). The $\varepsilon_{Nd(t)}$ value of GI samples is slightly heterogeneous, the data suggest small variations in the magmatic source. The Sm-Nd of GI varies from $\varepsilon_{Nd(t)}$ = 2,7 for JO04-86 (SE), 3,0 for JO04-135 (SW), up to 3,8 for JO04-110 (WNW) of JGC. The Sm-Nd data of Wilson et al. (1987) are quite variable so they have not been used for comparison. The Klockträsk satellite intrusion isotopic character is identical to GI in the WNW area ($\varepsilon_{Nd(t)}$ = 3,8). The "Maurliden" subvolcanic

qz+fs porphyry Sm-Nd is $\varepsilon_{Nd(t)}$ = 3,6, similar to GI as occurs with satellite intrusion of Klockträsk. The Näsberget gabbro isotopic values are smaller than some of GI but slightly higher than GII. Stavaträsk samples Sm-Nd is close to $\varepsilon_{Nd(t)}$ = 0 (see next petrogenesis).

The lithogeochemical and isotopic data suggest a change in the magmatic affinity in the rocks from G to GII and GIII-GIV. The isotopic data are similar, all corresponding to magmas derived from mantle sources that were depeted in Nd relative to Sm on a time integrated basis, but GII-GIII are homogeneous, at variance with the GI that varies from $\varepsilon_{Nd(t)}$ = 2,7 to 3,2.

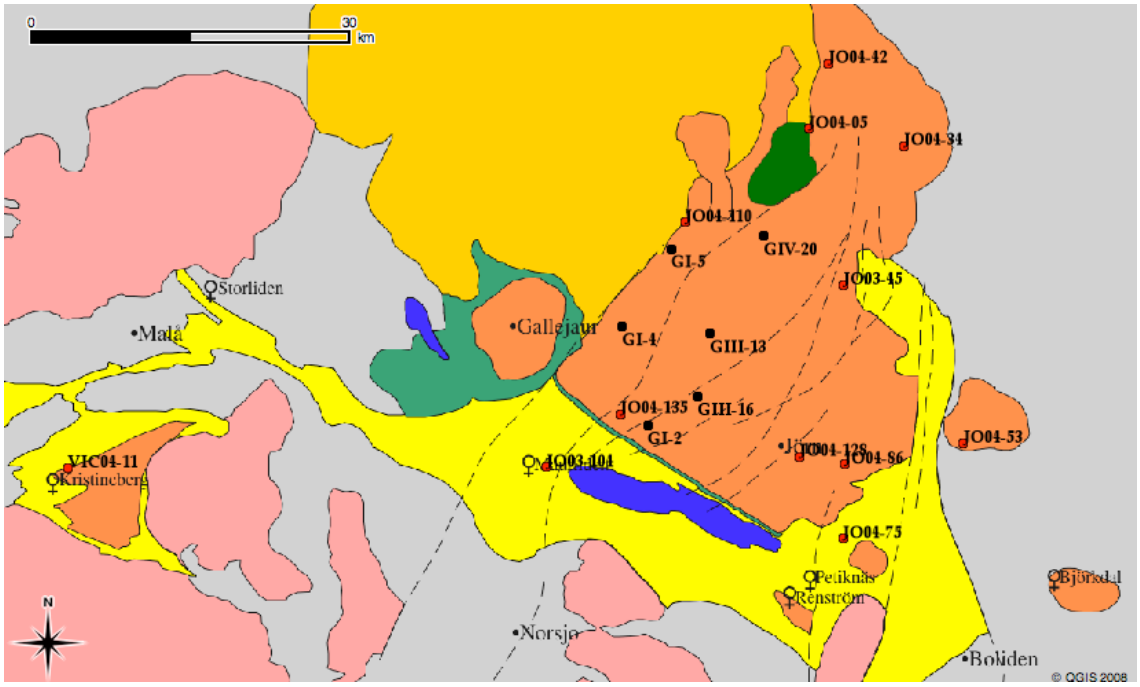

Fig. VIII-1. Location of the samples used in the Sm-Nd of this work (in red); Wilson et al. (1987) as black dots.

The possible change in the magmatic character is added to the possible time differences of the different phases in the JGC. **Table VII-2** is the summary of age determinations for JGC; GI samples vary from 1880 to 1886 Ma with errors around ±4 Ma. This array allows a time gap between GI and GII of 10 Ma, as the average age is 1874 (±5) Ma. The late stage of magmatic activity, alkaline-calcic character, is dominated by the GIII intrusions (Storklinta: 1865±5 and 1864±5 Ma) ca. 20 Ma younger than GI, and 10 Ma younger than GII. Location of samples in **fig. VII-7**.

VIII.2. Comparison of Units of JGC with Intrusions in Skellefte District

It is not only important to define the units but also the relationships between the JGC and the intrusions in the Skellefte district. These intrusions include the satellite intrusions of JGC and the intrusive complexes as VIC or Stavaträsk.

VIII.2.1. Relationships between GI unit and satellite intrusions of JGC

Many plutons located in the surroundings of JGC and with tonalitic-trondhjemitic nature are considered as GI satellite intrusions. The petrographical characteristics are complex as observed in GI, there are variations in the crystal size, texture, mineralogy, degree of alteration, etc. The absence of a clear pattern of occurrence among these intrusions might have several causes: they are formed in different magmatic events; the intrusions were at different crustal levels; the cooling and nucleation process were not homogeneous for the different plutons. The GI type intrusion of major area is

Klockträsk, it outcrops in two main facies, the first is trondhjemitic and the second is a granitic medium-grained tonalites with abundant syn-intrusive porphyritic dikes. The medium-grained porphyritic tonalites of Kläddberget and Råberget in the southern boundary of JGC, their textures are similar to subvolcanic dacitic intrusions of the Skellefte Group. The Brännliden small pluton is a granitic isogranular medium grained tonalite (**Fig. VI-43**). The Rengård intrusion is similar in texture to the western areas of GI, but different in minealogy. These associated satellite GI type intrusions are located in the southern boundary of JGC inside the volcanosedimentary rocks of Skellefte Goup.

The deformation of GI satellite intrusions cannot be observed in hand specimen, excepting some southern areas of JGC as the small pluton of Klädberget (penetrative brittle-ductile deformation). The metamorphic biotites occur in most of the satellite intrusions, excepting Rengård pluton with the occurrence of metamorphic amphibole (tschermakite and hastingsite). The data suggest a higher metamorphic degree for the Rengård intrusion in comparison with the main GI body or satellite intrusions.

The major elements of satellite intrusions suggest the magmatic link to the GI of JGC. The magmatic affinity as calcic and peraluminous intrusions and classification of GI and satellite intrusions are identical. In the modal classification Or-An-Ab diagram, the satellite intrusions plot as tonalite to trondhjemite (**Fig. VI-17**).

The satellite intrusions are moderately altered as also observed in the GI tonalites. The REE normalized diagram of satellite intrusions fit in the GI field. The black lines represent the GI area defined in this work (**Fig. VIII-2**). The identical REE pattern, mineralogy, alteration and metamorphic textures are added to the major element similarities. The JO04-94 sample of the southern boundary of JGC has been included in the comparison due to the proximity to satellite intrusions (**Fig. VI-43**); this sample is the poorest in K_2O (almos absent) and Fe_2O_3 but the richest in Na_2O and SiO_2 of GI, it plots a Eu positive anomaly. The Normal CIPW diagram (**Fig. VI-17**) and textures indicate that it is a trondhjemite by mineralogy and lithogeochemistry.

The Klockträsk (Vänträsk) and Rengård age determinations, samples MG07-006 and MG07-007 respectively (**Table VII-2**), indicate the coeval emplacement of satellite intrusions and the main GI body of JGC. The Rengård pluton is 1879 ± 5 Ma that is slightly younger than the average age of GI. The Klockträsk intrusion is 1897 ± 10 Ma that is moderately older than the average age of the GI intrusion; the higher error respecting the GI could be determined by the use of titanites in the age determination. The data could indicate a long-lived activity of the GI type magmatism around 10 Ma, but it is an unsupported supposition due to the larger analytical error in the age determinations; older age determinations of GI (Halmyrtjärnen) indicates 1898 ± 11 Ma (Kathol et al., 2002). Other age determinations in the Halmyrtjärnen area in this work (23J28 and JO03-55 samples) provide younger data of 1880 ± 4 Ma and 1885 ± 5 Ma respectively (**Table VII-2**).

VIII.2.2. The Hobergsliden and Antak intrusions in JGC

The Hobergsliden intrusion is a late pluton in the NE of GIII, in contrast, the Antak granite and GIII intrusions emplacement relationships remain unclear. The mineralogy and lithogeochemistry of Hobergsliden refer to a leuco-alkali granite (**Fig. VI-16**). The Antak and Hobergsliden intrusions have affinity with GIII, all of them as high K calc-alkaline rocks (alkaline calcic granites) (**Fig. VI-15**). The REE normalized pattern in **fig. VI-25** of GIII (JO04-07) belongs to Hobergsliden pluton, identical to the Hobergsliden database in the SGU (**Fig. VI-30A**). Both samples of Hobergsliden REE pattern fit with the GIII (**Fig. VI-30B**), but with an Eu negative anomaly (as previously: it suggests the plagioclase crystallization in the magmatic reservoir of this intrusion). The Antak REE patterns (**Fig. VI-30A**) do not fit with any of the JGC intrusive stages (GI to GIV).

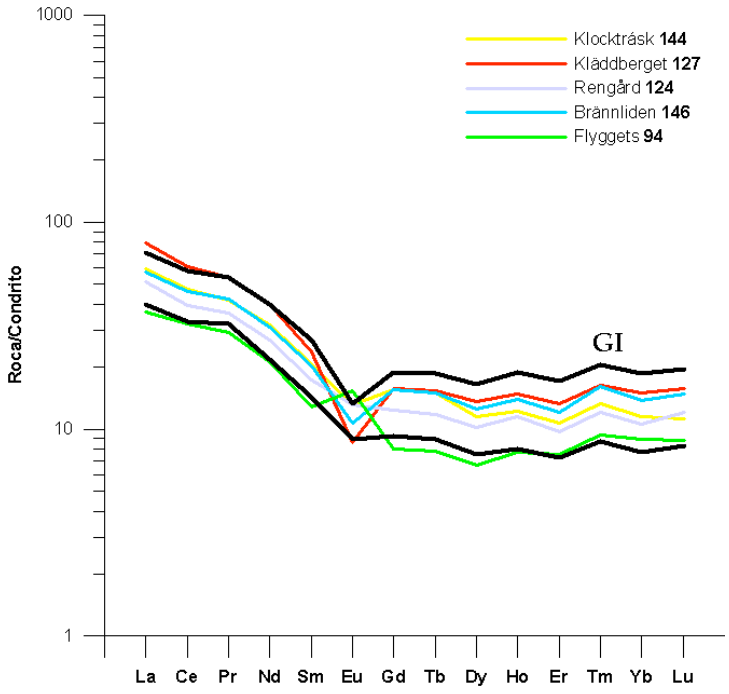

Fig. VIII-2. REE chondrite normalized pattern of satellite intrusions of JGC in comparison with the GI field. Lithogeochemical analyses of 2004, **Table VI-1**.

The age determinations of Antak and Hobergsliden (**Table VIII-3**) provide different a time gap between both intrusions. The Hobergsliden age (Lundström et al., 1997) suggests that is coeval with GIII. The Antak granite is older, 1879 $^{+15}/_{-12}$ Ma (Kathol and Persson, 1997), than GIII and could be coeval with the GII intrusions, but the analytical error is bigger than the time gap between GII and GIII events. The Bouguer anomaly map (**Fig. V-28**) is unclear but seems to indicate that GIII overprints the Antak granite.

VIII.2.3. VIC and Stavaträsk intrusions compared with JGC

The mineralogy of igneous minerals of Stavaträsk intrusion is similar to the GIIa granodiorites but biotites are usually substituted by chlorite, in contrast with is observed in the GII. The JO04-145 lithogeochemical analysis belongs to a Stavaträsk granodiorite. The major elements of Stavaträsk plot associated preferably with the GIIa samples and GIV (**Figs. VI-1** and **VI-2**). It is classified in the calcalkaline field as GIIa (**Figs. VI-4** and **VI-5**). Trace elements variation diagram of Stavaträsk plot in the GIIa group and similar to GIV (**Fig. V-19** and **V-20**). The REE patterns for Stavaträsk fit in the GIIa field, and identical to GIV (**Fig. VI-30B**). The Stavaträsk age determinations of 1874 ± 3 Ma (Lundström et al., 1999), suggest that this pluton is coeval with the GII event of JGC (**Table VII-2**) and 10 Ma older to GIII, Hobergsliden (**Table VIII-3**) and probably GIV.

The Viterliden intrusive complex is the more complex and widespread in the western area of the Skellefte district. VIC and volcanosedimentary rocks are strongly deformed, faulted and folded. It is a composite intrusion with different units of diverse mineralogy, texture and lithogeochemistry. The main phase of VIC is the hornblende tonalite (qz-amphibolite), similar to some GI tonalites. These also occur trondhjemites and the Mine porphyry that is also of trondhjemitic character; both phases are not similar to any of the JGC units. The hornblende tonalite are calcalkaline (**Fig. VI-13**), but the SiO_2% is lower than GI samples. The Mine porphyry and Trondhjemite are tholeiitic to transition to calcalkaline. In the AFM diagram VIC does not plot as a trend of rocks, excepting the tonalites that plot calcalkaline as JGC (**Fig. VI-10**). There are

some similarities in the REE patterns of VIC and JGC phases; the tonalite of VIC plot in the GI tonalite field but slightly lower in the HREE (**Fig. VI-35B**); the Trondhjemite and Mine porphyry do not fit with any of REE field of JGC (**Fig. VI-36B**) excepting some of the Mine porphyry that plot as GIIb (**Fig. VI-36A**). The age determination of VIC hornblende tonalite is 1907 ±12 Ma (Bergström et al., 1999), older than JGC GI average age obtained in this work, but similar to some of the GI and Klockträsk (1897 ±10 Ma) (**Table VII-2**).

VIII.3. JÖRN GRANITOID COMPLEX AND VOLCANIC ROCKS OF SKELLEFTE GROUP

It is relevant to establish the igneous relationships among the volcanic rocks of the Skellefte Group and the intrusions of JGC. The lithogeochemical analyses of the Manurliden volcanics (Montelius, 2005), Petikträsk South (Schletter, 2007) and Tallberg porphyry copper (Weihed, 1992) have been used to compare with the JGC intrusions, in particular with GI tonalites. It has been also included the lithogeochemical and isotopic analyses of the sample JO03-104 that is a subvolcanic intrusion (dacite-porphyritic tonalite) in the Skellefte Group.

VIII.3.1. Comparison between JGC and Maurliden volcanic rocks

The lithogeochemical analyses of the Maurliden volcanics in the Ph-D Thesis Montelius (2005) have been used. The Rhyolite A' belongs to the mineralized horizons and are pre- or syn-ore formation. In contrast, the Rhyolite B and Dacite are pre-ore; the first in the footwall of the deposit and the second occurs as domes or cryptodomes. The Rhyolite X is an post-ore formation intrusive unit (Montelius, 2005).

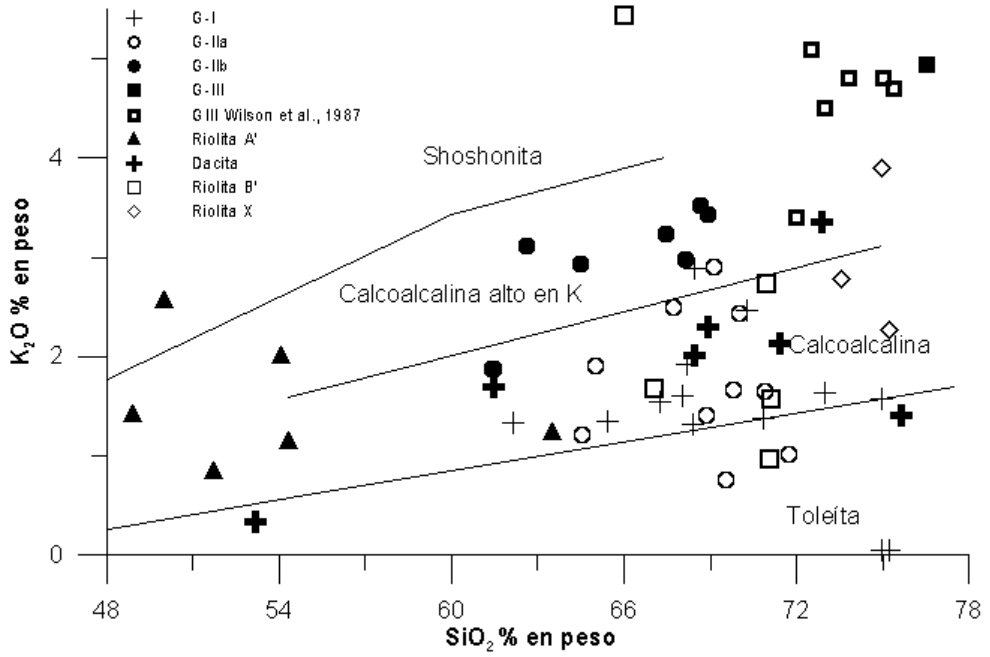

Fig. VIII-3: Magmatic series discrimination diagram (Roberts and Clemens, 1993) of volcanic rocks for the Maurliden volcanics (Montelius, 2005).

The major elements of Dacite and Rhyolite B plots in the calcalkaline field as observed for the GI and GIIa samples. Some samples plot in the transitional domain to high K calcalkaline granitoids (**Fig. VIII-3**). The SiO_2 content of the Rhyolite A' is lower than any of the JGC samples due to the sulphide mineralization (**Fig. VIII-3**). The Rhyolite X post-ore intrusions in Maurliden plot in the calcalkaline field as the GI and GIIa samples (**Fig. VIII-3**).

The immobile elements Zr/TiO_2 *vs.* Nb/Y classification diagram (Winchester and Floyd, 1977) was used to classify the volcanics and also the main plutonic rocks of JGC. Both Rhyolite A' and Rhyolite X samples are homogeneous groups and plot in the same areas than the GI samples. Dacite and Rhyolite B do not fit in the JGC classification fields (**Fig. VI-38B**).

The Rhyolite X (post-ore intrusions) REE patterns plot in the field of GI samples (**Fig. VI-33**), added to the lithogeochemical data, it suggest that probably intruded associated to the GI event. The Dacite and Rhyolite B (pre-ore volcanic rocks) REE diagram are similar to those of GI tonalites but slightly higher in the HREE values (**Fig. VI-33** and **VI-34**). The Rhyolite A' REE diagram, that classified as GI using immobile elements, plot with an irregular pattern, most of the samples with *Eu* positive anomaly (MAD 7; MAD 79-43 and MA 79-47) that fit with the JO04-94 GI trondhjemite of the southern boundary of JGC (**Fig. VI-34** and **VIII-2**); the immobile element classification and the REE pattern of Rhyolite A' suggest similarities with subordinated rocks in the GI southern tonalite-trondhjemite.

The JO03-104 is a coarse-grained qz+fs porphyrytic dacite, 2 km SE of the Maurliden Openpit. The Sm/Nd isotopic study obtained a $\boldsymbol{\varepsilon_{Nd(1.9)}= 3.6}$; it is the same as obtained for GI satellite intrusion Klockträsk (JO04-75) and GI at NW (JO04-110) (**Table VI-7**). The REE data (**VI-35A**) and isotopic data suggest that Klockträsk, GI and the JO03-104 dacite intruded from a similar magmatic source during the same magmatic event.

The age determinations on the Maurliden volcanic rocks suggest that they are coeval with the main Skellefte Group volcanic activity and the GI event. The DH 80 001 sample age determination error is too high to make any comparison with the other intrusions (**Table VIII-1**). The Finnliden Rhyolite (10 km SW of Maurliden mineralization) is slightly older than the average GI but coeval with Klockträsk (**Table VII-2**) and hornblende tonalite of VIC (Bergström et al., 1999).

Sample	Rock type	Age (Ma)
DH 68	Rhyolite B (porphyry)	1885 ± 3
DH 80 001	Rhyolite A (pumice)	1902 ± 21
Open pit (Maurliden)	Rhyolite A (pumice)	1885 ± 6
Finnliden	Rhyolite A (cryptodome)	1901 ± 3

Table VIII-1. Age determinations of the volcanic rocks of Maurliden; DH-Drill hole, Open-pit (wall of Openpit in Maurliden). Montelius (2005).

VIII.3.2. Comparison of JGC and the volcanic rocks of Petikträsk South

The Rengård GI-type satellite intrusion is located in the Petikträsk South mineralization area. The samples chosen for the comparison with the igneous rocks of JCG are the unaltered volcanic rocks or lower hydrothermal alteration [Table 2 I manuscript of Ph-D Thesis D. Schlatter (2007)]. The samples form a coherent group of volcanic rocks excepting the Dacite II-13 that is a juvenil volcanoclastic rock.

The magmatic affinity of the Petikträsk volcanic rocks is calcalkaline, these samples plot in the field of the GI samples (**Fig. VI-15**), but higher in the SiO_2%. The AFM diagram of Petikträsk Dacite plot in the GI trend; the rhyolites define a calcalkaline trend parallel to GI or GII samples but higher in MgO content (**Fig. VI-11**).

The volcanic samples of Petikträsk have been classified using immobile elements Zr/TiO2 *vs.* Nb/Y (Winchester and Floyd, 1977). The Dacite and rhyolites (Rhyolite A, B and C) plot in the GI field (**Fig. VI-38A**). The trace elements of Petikträsk have been plotted in the JGC REE normalized patterns fields (**Fig. VI-37A**). The complete set of

volcanic samples plot in the GI field including the small *Eu* negative anomaly and flat distribution of HREE.

The classification diagrams based on major elements and REE data suggest that the Petikträsk volcanic rocks and the GI tonalites share the same magmatic origin.

The Rengård satellite intrusion occurs in the area of the Petikträsk South deposit. The age determination of Rengård is 1879 ±5 Ma (**Table VII-2**), 5 Ma younger than the average GI. The age of Petikträsk volcanics has not been determined but the field data imply that they are coeval to or slightly older than Rengård.

VIII.3.3. Comparison between JGC and Tallberg porphyry copper deposit

The Tallberg porphyry copper is located at the south of JGC in the GI tonalites (Weihed, 1992). The rocks used for the comparison with the JGC are GI-type tonalites, andesites and porphyritic rocks.

The major element lithogeochemistry of Tallberg correlates with the GI tonalites. The AFM diagram of Tallberg (**Fig. V-11**) indicates that the GI-type of Tallberg plots as the less evolved GI samples of JGC. In contrast, the porphyritic samples plot in the GII trend. The K_2O *vs.* SiO_2 diagram of GI-type indicates that Tallberg tonalites are lower in SiO_2 than GI but have the same content of K_2O (**Fig. VI-14**). The porphyry and andesites (very low SiO_2 and K_2O) plot as transitional tholeiitic to calcalkaline or calcalkaline (**Fig. VI-14**).

The REE elements *Gd* and *Er* have not been included in the old analyses (Weihed, 1992). However, the tonalites in Tallberg and GI must plot in the same field, the GI of Tallberg are systematically poorer in LREE (**Fig. VI-31**). The *Tb*, *Dy* and *Ho* occur as serrated distribution in the HREE field. Unlike the GI, the Tallberg porphyry REE pattern fit in the GIIa field (**Fig. VII-32**) and similar to GIII (**Fig. VI-30B**); the *Dy* and *Yb* elements are very low compared to GII samples.

The age determination of the Tallberg porphyry is $1886^{+15}/_{-9}$ Ma (Weihed and Schöberg, 1991), it is coeval with the average age of GI (**Table VII-2**). The sample was taken in a drill core log of a qz+fs porphyritic rock.

VIII.3.4. Age of the volcanic rocks in Skellefte mining district

Besides the intrusions and volcanics age determinations (**Table VIII-3**) there are more Skellefte Group volcanic rocks age determinations to complete the whole area of the Skellefte district (**Table VII-2**); this rocks were analyzed to establish the provenance of mineralizations (Billström and Weihed, 1996). The volcanic rocks age determinations are distributed in the western, central and eastern areas of Skellefte district.

Zone	Rock type	Age (Ma)
Melestjärn	qz + fs porphyry	1889 ± 3
Bjurvattnet	Peperite	1884 ± 6
Vargfors	Ignimbrite	1875 ± 4
Petikträsk	Mass-flow	1847 ± 3

Table VIII-2. Age of volcanic rocks in the Skellefte district (Billström and Weihed, 1996).

A peperite of the Bjurvattnet area, at the south of the main Boliden mineralization is located in the extreme south-east of the Skellefte ming district (**Fig. VI-7**), with a radiometric age of 1884 ±6 Ma. The qz+fs porphyry in the Melestjärn zone, 1889 ±3 Ma, is located in the middle zone of the mining district. Both, Bjurvattnet and Melestjärn,

data suggest a coeval evolution of the acid volcanic rocks and GI tonalites of JGC (**Tables VII-2** and **VIII-2**).

The Vargfors group volcanics age has been determined on an ignimbrite at Nicknoret location, as 1875 ±4 Ma (**Table VIII-2**). The GII magmatic event, determined as 1874 Ma (**Table VII-2**), and the Vargfors of Nicknoret age determinations imply a coeval evolution of the GII phases and the Vargfors Group volcanic rocks.

The samples used in the comparison are represented in **fig. VII-7**, age, type of rocks and coordinates are represented in **Table VIII-3**. The sample identified as "4" belongs to the same MG07-001 (of this work) outcrop. The "12" sample are located in the 23J28 and JO03-35 of this work (**Fig. VII-7**).

	Intrusion/Zone	Rock/Phase	Author	N	E	Age Ma
1	JGC *Hobergsliden*	GIII	Lundström et al., 1997	7247600	1706800	1862±14
2	Stavaträsk	Diorite	Lundström et al., 1997	7226380	1721900	1877±2
3	Stavaträsk	Granodiorite	Lundström et al., 1999	7223500	1715820	1874±3
4	JGC *Skidbäcken*	GIIb	Wilson et al., 1987	7222590	1700400	1874^{+48}_{-26}
5	JGC (E)	GI	Wilson et al., 1987	7234560	1683680	1888^{+20}_{-14}
6	Porphyry Tallberg	Type GI	Weihed and Schöberg, 1991	7221000	1693000	1886^{+15}_{-9}
7	Antak *Kåtaselet*	Granite	Kathol and Persson, 1997	7254650	1691940	1879^{+15}_{-12}
8	Gallejaur	Monzonite	Skiold, 1988	7235500	1676900	1873±10
9	JGC	GIII	Wilson et al., 1987	7233890	1691940	1873^{+18}_{-14}
10	Gallejaur	Gabbro	Skiold et al., 1993	7233300	1669900	1876±4
11	VIC *N-Svanaberget*	Tonalite	Bergström et al., 1999	7216930	1634140	1907±12
12	GI *Halmyrtjärnen*	GI	Kathol et al., 2002	7226872	1682720	1898±11
13	Bjurvattnet	Peperite	Billstrom and Weihed, 1996	7202590	1708540	1884±6
14	Melestjärn	Porphyry	Billstrom and Weihed, 1996	7213410	1685530	1889±3
15	Vargfors	Ignimbrite	Billstrom and Weihed, 1996	7229200	1670500	1875±4
16	Maurliden	Rhyolite B	Montelius et al., 2007	-	-	1885±3
16	Maurliden	Rhyolite A	Montelius et al., 2007	-	-	1902±21
16	Maurliden	Rhyolite A	Montelius et al., 2007	-	-	1885±6
17	Finnliden	Rhyolite A	Montelius et al., 2007	-	-	1901±3
18	Petikträsk	Mass-flow	Billstrom and Weihed, 1996	7225200	1681250	1847±3
19	Arvidsjaur (Skyt.)	Rhyolite	Skiold et al., 1993	7256150	1693450	1878±2

Table VIII-3. Age determinations of intrusions and volcanic rocks in the Skellefte mining district.

VIII.4. HYDROTHERMAL ALTERATION AND DEFORMATION OF JGC

The hydrothermal alteration process in JGC has been only determined in the GI unit. The intensity of alteration increases to the southern areas in the boundary with the volcanic rocks of the Skellefte Group. The alteration characteristics include the plagioclase saussuritization, and the substitution of mafic minerals (amphibole and biotite) to chlorite, epidote, etc. The altered minerals are overprinted by low-grade metamorphism. The chloritization (see Petrography) of biotite, and minor amphiboles, occurs in most of the samples of GI, including satellite intrusions as Klockträsk. The chlorites are usually substituted by secondary biotite during metamorphism. However, metamorphism is pervasively overprinted on alteration, and also occur chlorite and newly grown biotite. The most intensely altered GI tonalites are located in the south, specially in the surroundings of Tallberg. The northern areas are less metamorphosed, and the high degree of alteration has not been overprinted in the northwestern areas.

The deformation features are not usual in macroscopic scale, and cannot be determined in most of the outcrops. Macroscopic strain is only observed in the most altered areas in the southern boundary of GI; it is characterized by an intense foliation parallel to the boundary (usual close to the Southern Dike). However, steep or relatively flat deformation is commonly observed in thin sections, and is widespread in the whole GI. Deformation in thin sections is characterized by oriented biotite-chlorite layers, folding of crystals and/or elongation of the alteration products of the chloritized biotite (appendix: **pic. V-12**). The textures imply that microscopic deformation overprinted the hydrothermal alteration (see Petrography for deep descriptions).

VIII.5. CHARACTERISTICS OF METAMORPHISM IN JGC

The metamorphism in the Skellefte district has been studied in geological works, focused on the volcanic rocks or Viterliden Intrusive Complex. The metamorphic transition between green schist to amphibolite facies is defined in the southern boundary of the Skellefte district [Fig. 14 in (Bergman-Weihed, 2000)]. Regional metamorphism degree increases towards the southern proterozoic metasediments.

The metamorphic textures are determined in the *V. Petrography* and have been included microphotographs in the appendix of this work. It includes samples of metamorphic textures extensive in the whole GI of JGC.

VIII.5.1. Extent of metamorphism in the Skellefte Mining District

The main subject of this work is the JGC but the metamorphic textures have been studied in most of the intrusions in the district as VIC. The metamorphic mineral phases that have been defined in thin section (or polished section) include amphibole, biotite and epidote. They have been found only in GI phase of JGC, and the satellite intrusions Klockträsk and Rengård. The northwestern GI rocks are not metamorphosed, suggesting that the metamorphic event did not reach this area or that the intensity was not enough to modify the igneous textures. VIC hornblende tonalites are metamorphosed, but metamorphic textures have not been observed in trondhjemites. The volcanosedimentary host rocks of VIC metamorphism have been observed in the surroundings of the intrusion.

The JGC post-GI units and sub-units (GII to GIV) have not been metamorphosed, or the Stavaträsk intrusion or the porphyritic basalts of southern dike. Näsberget gabbros-diorites and Gallejaur monzonite-gabbros textures and minerals are igneous, and have not been determined any metamorphic characteristic. The data imply that the metamorphic event occur between 1885 Ma (age of GI or Skellefte Group) and the younger GII magmatic event at 1875 Ma.

VIII.5.2. Mineralogical characteristics of metamorphism

The biotite and amphibole group minerals have been identified as metamorphic crystals postdating both igneous and hydrothermal alteration products. Metamorphic biotite is widespread in most of the GI samples; amphiboles are restricted to a few locations in Rengård satellite intrusion and southern JGC Nör-Jörnsberget area (JO04-84).

Although the chemical composition of GI metamorphic biotites is homogeneous, there are some differences depending on the areal distribution. The central, eastern or western GI biotites are slightly different in the $Fe_t/(Fe_t+Mg)$ ratio, but Al^{IV} apfu variation is similar in most of the analyzed samples (**Fig. V-1**). The satellite intrusions (Klockträsk and Rengård) biotite chemical composition is analogous.

The chemical composition of igneous and metamorphic biotites can be differentiated regarding to Fe and Mg apfu in crystals. The Mg/Fe ratio has been used to separate two main groups of biotites: Mg/Fe > 1 include the post-metamorphic biotites of GII-

GIV; in contrast, the metamorphic biotites Mg/Fe ratio is less than 1. Klockträsk and Rengård satellite intrusions show Mg/Fe < 1 (**Fig. V-2**).

Amphibole group tschermakite and hastingsite are usually observed as metamorphic products. The metamorphic amphiboles of JO04-84 are poorer in $Mg/(Mg+Fe^{2+})$ ratio compared with Rengård amphiboles. The size and texture of amphibole are diverse: acicular, tabular, prismatic, euhedral, etc., suggesting various crystallization processes as substitution or newly formed amphiboles. The newly formed amphiboles are smaller than igneous and post-date biotite. Those are usually 0.5-1 mm size hastingsite $[(Na+K)_A > 0.50]$ or ferro-tschermakite $[(Na+K)_A < 0.50]$. The Rengård JO03-110 sample hosts very fine-grained metamorphic amphiboles in cavities or mineral inter-phases ferro-pargasitic in composition (**Fig. V-9A**). In contrast, the igneous amphiboles are determined by optical and chemical composition as magnesio- or ferro-hornblendes (**Fig. V-9B**).

The VIC hornblende tonalite is mainly composed of metamorphic minerals. The biotite and amphibole group minerals are very different in chemical composition compares to the GI minerals. The $Mg/(Mg+Fe^{2+})$ ratio of biotites of VIC is higher than 1, in contrast to GI tonalites (**Fig. V-2**). The amphiboles of VIC hornblende tonalite classify as tschermakite and tschermakitic hornblende. Although the Si apfu of VIC is lower to GI, the amphibole chemical characteristics of VIC and JGC are very similar (**Fig. V-7**).

VIII.5.3. Characteristics textures of metamorphism in JGC

The secondary (metamorphic) biotite group minerals (bi_2) have been the subject of the main petrographical studies of the metamorphism in GI. The metamorphic biotite overprints the previous deformation and/or hydrothermal alteration processes in the JGC; the new biotite growth "cross-cuts" or encloses the altered and/or deformed minerals (**pic. V-28**). The metamorphic biotite (bi_2) is smaller than the igneous biotite (bi_1) (**pic. V-29**) and they usually form decussated clots of minerals. Decussated textures suggest the static character (contact metamorphism?) of the crystal growth event. The metamorphic crystals occur on the previously altered biotites and/or amphiboles, and usually substitute the igneous mafic minerals. The re-crystallization of quartz is also observed as very fine-grained microcrystalline granoblastic aggregates (**pic. V-1**). It is also common to observe in quartz preserved igneous core surrounded by a microgranular granoblastic rim.

The metamorphic amphiboles of Rengård and Nör-Jörnsberget (**pic. V-41**), as also observed with the GI biotite, post-date the alteration and deformation in JGC. These are subhedral to euhedral and overprint mafic minerals or occur as disperse crystals in the matrix of the rocks. The most common texture is the substitution of igneous hornbende (**pic. V-38**). The inter-crystalline amphiboles (very fine-grained ferro-pargaites) have been identified in the Rengård satellite intrusion only; the ferro-pargasite crystals correspond to the late stage of crystal growth during metamorphism (**pic. V-40**). The metamorphic amphibole crystals do not showed any fabric; the crystal growth is random or decussated; these also have been oriented like the igneous overprinted crystals.

The VIC hornblende tonalite textures are completely different regarding the GI metamorphic textures. The alternance of mafic and felsic crystals layers is commonly observed. The mafic layers are biotite, amphibole and minor epidote; felsic layers are feldspar rich with very low granoblastic quartz content. The mafic minerals are strongly oriented in the layers with the occurrence of amphibole and plagioclase porphyroblast (**pic. V-80**). In contrast to GI tonalites, the data suggest a dynamic regional metamorphism.

VIII.5.4. Typology of metamorphism

The characteristics determined in the rocks of the GI phase suggest that the metamorphic event occur under static conditions (or the dynamic process do not produce effects on GI during metamorphism). The dynamic regional metamorphism effects (layering, crystal orientation, pressure shadow, etc.) have not been observed on GI biotites and amphiboles. The fact of the metamorphic amphibole are restricted to Rengård and Jörn areas imply the higher degree of metamorphism in the central-southern GI and south of JGC (Petikträsk area); the metamorphic grade decreases to the west and north where only occur biotite; at northwest of JGC the samples are not metamorphosed and chlorite (alteration of igneous biotite) is the mafic mineral. The data suggest a thermal static event that can be defined as Regional Contact Metamorphism (Spear, 1995).

VIC is representative of the metamorphism on intrusions in the western area of Skellefte mining district. The hornblende tonalites have been metamorphosed to layered qz-amphibolites; chevron type folds are usually developed on the mafic and felsic layering. Another characteristic that differentiates the VIC and GI is that the hornblende tonalites deformation is consistent with that documented in the Skellefte Group.

The age differences of GI and VIC could determine the differences in the process of deformation and metamorphism, but the Klockträsk intrusion, that is older as VIC, is not deformed or metamorphosed. The actual data suggests that deformation and metamorphism in the central and western area are coeval, implying that VIC experienced a dynamic regional metamorphism while the GI intrusions domain was undeformed and there only occurs a thermal event.

VIII.6. PETROGENESIS OF JGC

VIII.6.1. Magmatic source of JGC

The ε_{Nd} isotopic data of the analyzed intrusions is always positive, they vary in from +2,0 to +3,8, excepting JO04-53 sample of the Stavaträsk intrusion that is ε_{Nd} = -0,7. It implies a magmatic source in the time-integrated depleted mantle for JGC, satellite intrusions, VIC, Näsberget and "Maurliden" subvolcanic qz+fs porhyry (**Table VIII-4**).

A depleted mantle source was tapped during Early Meso-Proterozoic, approximate 1900 Ma, and it generates intense igneous activity at global scale (DePaolo, 1981). During the Proterozoic a great number of granitoids are generated in the northern Sweden with ε_{Nd} and REE depleted mantle character (Wilson et al., 1983; Skiöld and Cliff, 1984); in particular a great volume of granitoid with calc-alkaline affinity was generated in the southern margin of Karelia during 1.90-1.84 Ga (Wilson et al., 1985). The boundary of the Archean crustal participation is determined by ε_{Nd} of Sweden intrusions and named APB (Archean-Proterozoic Boundary). To the north of APB the ε_{Nd} is negative due to the Archean crust; in contrast, south of the APB, where the JGC is located, the ε_{Nd} are positive (Wilson et al., 1987; Sköld et al., 1993; Öhlander et al. 1999, Mellqvist et al., 1999; Juhlin, 2002), indicative of crustal growth.

The similarities in Sm-Nd isotope signature, lithogeochemical character and REE indicate the same magmatic origin for the different phases of JGC, excepting the GI tonalites (different magmatic character and REE patterns). The magmatic source, in the depleted mantle model, have to be received the small participation of Archean crustal material (Mansfeld, 2001). The ε_{Nd} and participation of Archean crustal material have been the subject of some investigations (Patchett and Bridgewater, 1984; Mellqvist et al., 1999). To calculate the crustal participation in the generation of JGC intrusions has been applied the formula previously used in Melqvist et al. (1999), the ε_{Nd} = -11,5 for Archean crust at 1.9 Ga of Öhlander and Skiöld (1994), 31 ppm is the Nd concentration

in Archean crust (Öhlander et al., 1987); it has been assumed the value of 10 ppm of Nd for the mantle-derived melt. The applied equation:

$$X = \frac{C_{Nd(DM)}}{C_{Nd(CC)}} \frac{\varepsilon_{Nd(sample)} - \varepsilon_{Nd(DM)}}{\varepsilon_{Nd(CC)} - \varepsilon_{Nd(sample)}}; \% \text{ crustal participation: } \% = \frac{100 \times X}{1 + X}$$

$C_{Nd(DM)}$= 10 ppm
$C_{Nd(CC)}$= -11,5 ppm
CC= continental crust
DM= depleted mantle (depleted mantle model: DePaolo, 1981)

Sample	Phase	Sm	Nd	$^{147}Sm/^{144}Nd$	$^{143}Nd/^{144}Nd$	$\varepsilon_{Nd(0)}$	$\varepsilon_{Nd(t)}$	T_{DM}
J004-86	GI (SE)	4,70	26,80	0,1059	0,511644	- 19,4	**+2,7**	1.98
J004-110	GI (NW)	3,83	16,60	0,1398	0,512117	- 10,2	**+3,8**	1.91
J004-135	GI (SW)	3,10	14,60	0,1286	0,511936	- 13,7	**+3,0**	1.99
J004-75	Klockträsk	4,11	19,50	0,1275	0,511965	- 13,2	**+3,8**	1.91
J004-05	Näsberget	2,07	9,41	0,1333	0,512003	- 12,4	**+3,2**	1.98
J004-128	GIIa	5,64	33,10	0,1030	0,511613	- 20,0	**+2,9**	1.97
J004-34	GIIb (NE)	6,30	35,40	0,1076	0,511674	- 18,8	**+2,9**	1.97
J004-42	GIIa (N)	4,94	30,30	0,0985	0,511557	- 21,1	**+2,9**	1.97
J003-45	GIII (E)	3,77	23,20	0,0982	0,511542	- 21,4	**+2,6**	1.99
J004-53	Stavaträsk	1,40	5,36	0,1574	0,512115	- 10,2	**-0,7**	2.54
J003-104	Maurliden	4,21	18,40	0,1388	0,512090	- 10,7	**+3,6**	1.94
VIC04-11	VIC	3,43	17,60	0,1179	0,511756	- 17,2	**+2,0**	2.05

Table VIII-4. Isotopic data of Sm, Nd and ε_{Nd} of JGC, VIC, Stavaträsk, Klockträsk, Näsberget intrusions, and "Maurliden" qz+fs porphyry.

The crustal participation data of Skellefte district intrusions have been summarized in the **table VIII-5** of this work. It has been determined a participation of 0-5% for the whole set of samples, excepting the JO04-53 of the Stavaträsk intrusion. The data of Stavaträsk indicate a 10% continental crust (**Table VIII-5**).

Sample	Phase	$\varepsilon_{Nd(t)}$	% crustal
J004-86	GI (SE)	**+2,7**	2,9
J004-110	GI (NW)	**+3,8**	0,4
J004-135	GI (SW)	**+3,0**	2,2
J004-75	Klockträsk	**+3,8**	0,4
J004-05	Näsberget	**+3,2**	1,7
J004-128	GIIa	**+2,9**	2,4
J004-34	GIIb (NE)	**+2,9**	2,4
J004-42	GIIa (N)	**+2,9**	2,4
J003-45	GIII (E)	**+2,6**	3,1
J004-53	Stavaträsk	**-0,7**	12,3
J003-104	Maurliden	**+3,6**	0,8
VIC04-11	VIC	**+2,0**	4,6

Table VIII-5. Inferred Archaean crustal participation in the magmatic source of JGC intrusions. Calculation using$v\varepsilon_{Nd}$ and Nd concentrations in Archean Crust (CC) and depleted mantle (DM). After Patchett and Bridgewater (1984) and Mellqvist et al. (1999).

VIII.6.2. Process of crystallization and differentiation of JGC igneous units

The age determinations of JGC intrusions (**Table VII-2**) imply that each of the phases of JGC developed during three discrete magmatic events: GI, GII and GIII. The differences of the three magmatic events determine the absence of differentiation or fractional crystallization processes among the units, but not between sub-units of each magmatic event like GIIa-GIIb or GIII-Hobergsliden.

GIIa and GIIb samples in Harker diagram (**Fig. VI-1**) define an inverse linear trend of P_2O_5, TiO_2, MnO, Fe_2O_3 and MgO versus SiO_2 increase. Most of the GIIb samples are less evolved than GIIa, without any compositional gap between GII samples. Chemical data of MnO, Fe_2O_3 and MgO suggest pyroxene and amphibole crystallization in GIIb magmatic source, including accessories to correlate the variation of de P_2O_5 and TiO_2 in Harker diagram. The petrographical study supports the crystallization of py+amph, because the GIIb samples are rich in cpx (augite) and amph (hornblende) as major components, and titanite and apatite accessory minerals for GIIa. Harker diagrams for Al_2O_3 and CaO are identical for GIIa y GIIbl, implying that feldspars (alkali feldspars and plagioclase) did not fractionate or differentiate in GIIb to generate GIIa; Na_2O and K_2O Harker diagrams are inconclusive (**Fig. VI-1**). Modal analyses of GII show that the relative plagioclase content of GIIa and GIIb is similar, but the alkali feldspars are more abundant in the GIIb sub-unit.

Harker diagrams magmatic trends for GIII (GIII, GIV and Hobergsliden) group samples are restricted to a short SiO_2 compositional range (**Fig. VI-1**). GIII samples trend is inverse linear for K_2O, Al_2O_3 and CaO vs. SiO_2. GIV is located in the less evolved GIII group; and Hobergsliden as the more evolved intrusion, GIII samples plot in the medium area between GIV and Hobergsliden (**Fig. VI-1**). Harker diagram of Na_2O, TiO_2, P_2O_5, Fe_2O_3 and MgO plot inverse lineal correlation but GIV and GIII overlap.

REE diagram of GIII group samples display differences in *Eu* anomaly. Hobergsliden samples have large *Eu* negative anomalies; in contrast, the GIV samples REE pattern is smooth without *Eu* anomaly. GIII samples REE diagram plot a small *Eu* negative anomaly (**Fig. VIII-4A**). These data and the previously described lithogeochemical, isotopic and age determinations suggest for GIII and GIV the intrusion from the same magmatic source with different degrees of mineral fractionation. Hobergsliden constitutes a melt of GIII after plagioclase separation, as supported petrographically by the enrichment in alkali feldspar and the depletion in plagioclase and mafic minerals (**Fig. VIII-4**). The Ba *vs*. Sr diagram for GIII samples with the crystallization vectors of plagioclase, biotite and alkali feldspars, shows that only the alkali feldspar crystallization vector can explain the generation of the GIII, GIV and Hobergsliden intrusions (**Fig. VIII-4B**).

Basic and ultrabasic intrusions are associated to the GI and GII intrusions, the bigger area is outcropped by the Näsberget layered intrusion at the northwest of the JGC. The generation of granitoids can be related with the generation and ascent of basic magmas, or otherwise the generation from the same source of basic and felsic granitoids. The big volumes of basic rocks could indicate the first option.

Basic intrusions in the GI tonalites are not abundant, but geophysical studies have suggested that huge volumes of basic rocks occur in deep in the south and east of Jörn. The Gq-149 sample belongs to a gabbronorite at the east of Jörn villa, its REE pattern are similar to the GI field, especially regarding to LREE (**Fig. VIII-5A**).

There are no age determinations in the gabbro-diorites of Näsberget, but Näsberget contains megablocks of GI and the southern boundary is limited by the GIII intrusion; this suggests a broadly similar age to GII intrusions (Vargfors Group). The eastern boundary is truncated by regional faults that link Näsberget with GII intrusions. The

31-34 and 216-220 outcrops, of 2004 sampling, document the relation of GII and gabbros, the limits are warped, and suggest that both magmas ocurried as melts and partly mixed; these data imply that both rocks are coeval, and even that GII can be formed from Näsberget gabbros. Näsberget intrusions are mainly composed in this area of gabbronorites and hbl+px gabbros, usually occurs some quartz and olivine (**pic. VIII-1A**). Close to Näsberget (Stop 38 of 2004) the GII intrusions qz-monzodiorites host a high proportion of grabbroic enclaves, the structure and texture of which suggest that both lithologies were intermingled (**pic. VIII-1B**).

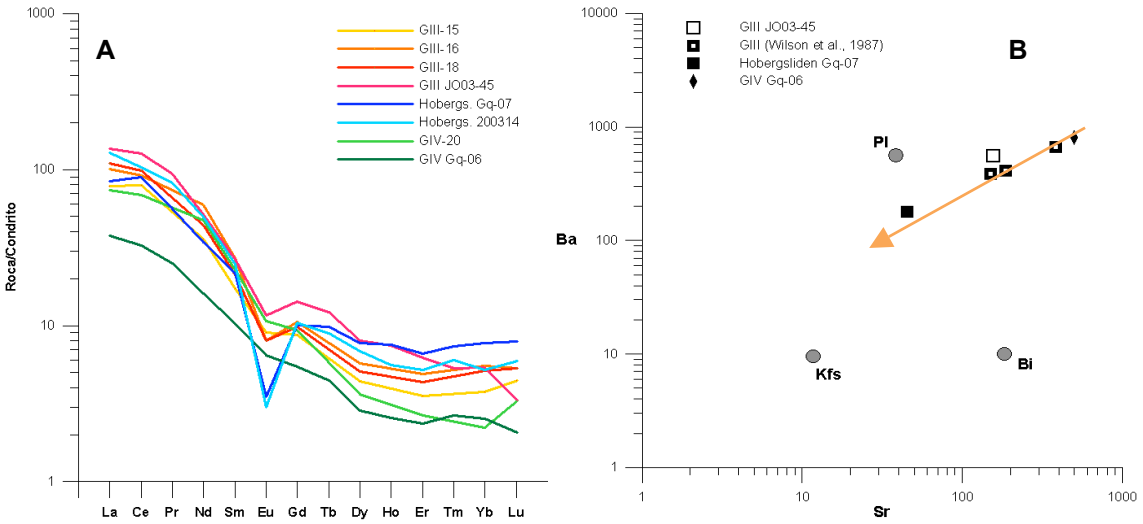

Fig. VIII-4. **A**: REE diagram of GIII group samples (GIII, Hobergsliden and GIV). Samples GIII-15, -16, -17 and GIV-20 of Wilson et al (1987); Hobergsliden sample 200314 of SGU. **B**: diagram Ba *vs*. Sr for GIII samples, crystallization vectors of alkali feldspars (Kfs), plagioclase (Pl) y biotite (Bi). The orange arrow delineates the crystallization of plagioclase in the GIII group samples.

REE normalized pattern of separated samples under low melt degree is characterized to be enriched in LREE (fig. 6 Ph-D Thesis of DePaolo, 1978). It has been determined in Näsberget samples of the eastern areas (Lower zone) respecting the central area (Main layered zone) of the intrusion. GII REE patterns fit with those of the gabbro of the eastern area of Näsberget (Lower zone) (**Fig. VIII-5B**).

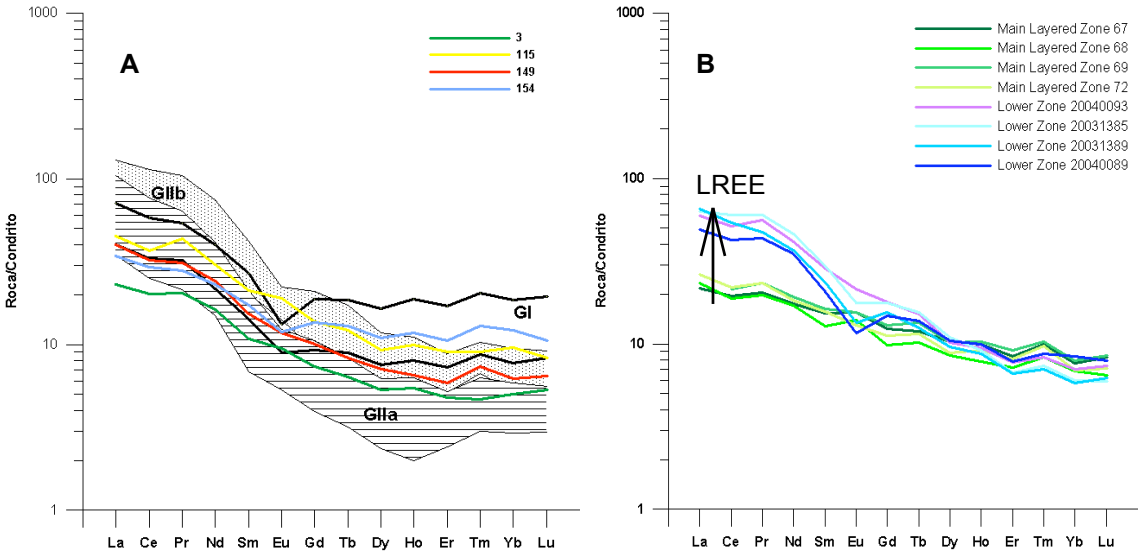

Fig VIII-5: **A**: REE diagram for basic samples in comparison wit hthe JGC intrusions. Gq-03 and -115 samples of Näsberget gabbros, Gq-149 intrusive gabbro in GI and Gq-154 porphyritic basalts. **B**: REE diagram of Näsberget samples: Main Layered Zone (green) and Lower Zone (blue).

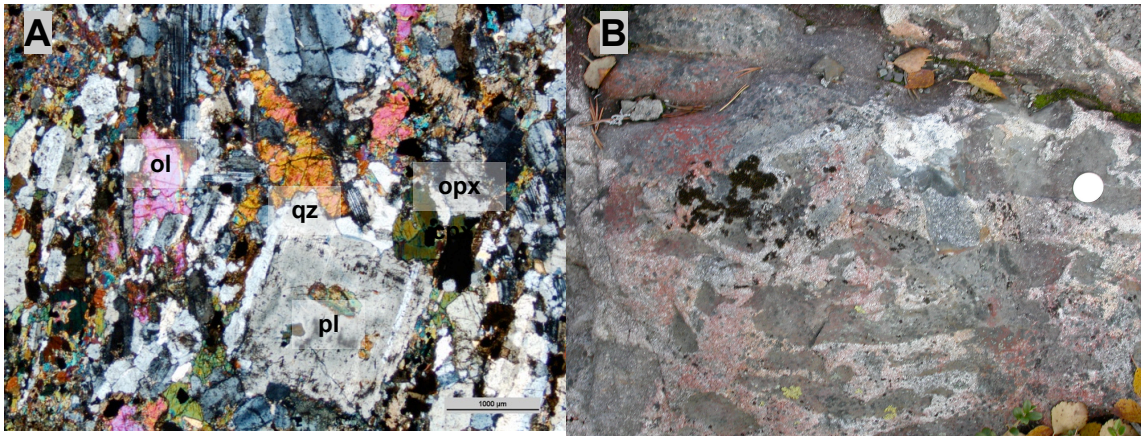

Pic. VIII-1: **A**: microphotography of JO04-117 crossed polars (pl + opx + cpx + ol ± qz ± il/mt). **B**: GII outcrop with gabbroic enclaves (possible Näsberget).

VIII.7. INFERRED REGIONAL GEOLOGICAL EVOLUTION

A volcanic island-arc is the regional setting for the Skellefte mining district. The continental margin could be located on a subductive plate that displace to the actual north under continental zone (BABEL, 1990; Gaal and Gorbatschev, 1987; Korja et al., 1993). The base of the Skellefte district is unknown, but can be formed by 1.95 Ga intrusive series (Wasström, 1996; Wasström, 2005).

1. The basement of the Skellefte mining district is composed by the submarine volcanic rocks of the Skellefte Group, such rocks have been developed in an extensional environment intra-arc on a continental crust or mature island arc (Weihed at al., 2005; Weihed and Eliu, 2005). Most of the mineral deposits are located in the Skellefte Group, but Vargfors Group volcanics also host some mineralizations. Volcanosedimentary rocks of Skelelfte Group are 1.90-1.88 Ga. GI intrusions of the JGC are associated to the Skelletfe Group volcanism. Age determinations and lithogeochemistry suggest that the GI and Skellefte Group were generated from the same or equivalent magmatic source. GI intrusions are supposed to be the subvolcanic to deep magmatic activity of the Skellefte Group.

2. Hydrothermal alteration, deformation and metamorphic processes occur exclusively in the GI and GI-type satellite intrusions, these processes have not been documented in GII or later intrusions. Alteration, deformation and metamorphism are constrained to have ocurred later than 1885 Ma (GI) but prior to 1874 Ma (GII). Secondary minerals generated during hydrothermal alteration are usually deformed, it imply that deformation ocurred syn- or post-alteration. The metamorphism postdates the hydrothermal alteration and deformation, because metamorphic textures overprint the previous igneous or secondary minerals and deformation. GII or later intrusions do not show metamorphic overprinting, implying that the thermal event was pre- or syn- the GII intrusive event (see next paragraph).

3. The sedimentary, volcanic and intrusive rocks of the Vargfors Group stratigraphically overlie the Skellefte Group (Allen et al., 1996). Sediments from the Skellefte Group and GI tonalitic clasts dominate the upper materials of the Vargfors Group. These data suggest the formation during an extension process of the Skellefte basin. The Vargfors Group ignimbrite in Nicknoret is 1875 ±4 Ma (Billström and Weihed, 1996). Sediments with detritus of GII or later intrusions have not been observed in the Vargfors sediments, these could not outcrop during erosive process or be located in unexposed or unpreserved basins. Mafic rocks associated to Vargfors sediments are common, including the Gallejaur gabbros, diorites and Basalts of the Southern Dike of JGC (**Fig. V-29**). The Southern Dike could be intruded along regional

Southern Dike of JGC (**Fig. V-29**). The Southern Dike could be intruded along regional faults during extension of the basin, and the conglomerates with Skellefte Group and GI sediments could have been deposited during this process. GII intrusions (GIIa and GIIb) are coeval with the volcanic and intrusive rocks of the Vargfors Group; and with Stavaträsk granodiorite and diorites. The lithogeochemistry of GII group suggests a variation in the magmatic affinity comparing to GI intrusions; the rocks vary from calcalkaline (calcic granitoids) GI to high-K calalkaline (alkaline calcic granitoids) GII and Stavaträsk. As previously defined, the metamorphism overprinted the GI intrusions, but is older than GII; the thermal event (Regional Contact Metamorphism) could be related to the volume of intrusions generated during the Vargfors Group episode as diorites and gabbros of Gallejaur and Näsberget, Southern Dike type porphyritic basalts, and the GII intrusions. These intrusions probably acted as the "thermal engine" that generated the metamorphism in the JGC.

4. Subaerial felsic volcanism of the Arvidsjaur Group, north and northwest of the Skellefte mining district, is coeval with the Vargfors Group and GII intrusions. The age determinations of Arvidsjaur rocks, 1878 ±2 Ma, of Skyberget and Gråträsk rhyolites (Skiöld et al., 1993), correlates with those obtained for the GII intrusions in N and S of JGC (**Table VII-2**) and the Vargfors ignimbrite of Nicknoret (**Table VIII-3**). These data suggest that aerial volcanism of Arvidsjaur is the subaerial expression of the magmatic event that generated the submarine Vargfors Group and GII intrusions.

5. The last plutonic event in the JGC is recorded by the GIII, Hobergsliden and GIV intrusions. The age of these intrusions have been determinated in 1863 ±5 Ma (**Tables VII-2** and **VIII-3**). GIII, GIV and Hobergsliden intrusions magmas reflect a new change in the magmatic affinity to high-k calcalkaline (alkaline calcic granitoids), but REE content are consistent with those of the GIIa intrusion in most samples.

IX. CONCLUSIONS

- Three main plutonic facies have been determined in the Jörn Granitoid Complex, regarding to three differentiated intrusive stages. The first intrusive stage is related to GI and GI-type satellite intrusions; the second is composed by the GII intrusions and, possibly, the Näsberget layered intrusions; the GIII and GIV intrusions corresponding to a late intrusive stage. The differences among the intrusive facies are systematic, regarding to mineralogy, texture, alteration, metamorphism, lithogeochemical character and age. In particular, the lithogeochemical differences suggest an important variation in the magma type.

- The lithogeochemical character, petrographical properties and age of the rocks of the GI group can establish a direct relationships with the satellite intrusions of Klockträsk and Rengård, including the small plutons of Kläddberget and Brannliden at south and southeast of JGC, respectively.

- The volcanic rocks of the Skellefte Group, including the host rocks of the mineralization of Petikträsk, Maurliden and Tallberg porphyry copper, occur during the GI intrusions intrusive stage.

- VIC tonalite and GI intrusions show similarities in the lithogeochemical character, both VIC and JGC are postdated by alteration and deformation (different intensity) related to the ore deposits, the age determinations of these rocks suggest a coeval evolution. As well both, JGC and VIC show intrusive stages that postdate the hydrothermal alteration as GII-GIV in JGC and porphyritic trondhjemites in VIC.

- The trondhjemites of VIC are correlated with the GII intrusions of JGC in lithogeochemical character, and are strongly different to the GI stage. These data suggest a relevant change in the lithogeochemical character of the magmas in the early JGC, VIC and Skellefte Group, in contrast to the late intrusive stages. We suggest that this change could be represented in the volcanic rocks in the transition from the submarine volcanism of Skellefte Group to the subaerial Arvidsjaur Group.

- The nature of magmas varies in time from the initial GI calcic tonalites, the transition calcic to calc-alkaline of the GIIa granodiorites, the calc-alkaline GIIb qz-monzodiorites; finally the GIII-Hobergsliden intrusions are alkaline-calcic. The rocks are peraluminious, excepting the GIII classified as peralkaline [(Na+K)>Al].

- A Volcanic Arc Granitoid (VAG) is the geotectonic setting of JGC, VIC, Hobergsliden and Antak granitoids. Intrusions have been emplaced in sub-volcanic levels in an extensive basin.

- Deformation, hydrothermal alteration and metamorphism occur exclusively on the GI rocks; these processes can be dated in the time gap among the GI (ca. 1885 Ma) and GII (ca. 1875 Ma) intrusive stages. It is a significant time gap that can be correlated with the lithogeochemical variation of the JGC intrusions, suggesting an important geological event between the GI and GII emplacement.

- Hydrothermal alteration is extended on the GI intrusions, where the most intense alteration is located in the southern and northwestern areas of JGC; the central-western area is the less altered and deformed part of the GI. Deformation process post-dates the hydrothermal alteration, and show brittle to britlle-ductile low temperature character; these textures are generalized in GI, in particular, the southern areas are characterized by a pervasive foliation parallel to the intrusive boundary.

- The presented data suggest that hydrothermal alteration and mineralizations in the Skellefte Group volcanics are related with thermal anomalies associated to the magma generation. These indicate the direct or secondary relationships between the generation and/or emplacement of late calc-alkaline plutons represented by the shallow intrusions of GII and the Näsberget basic intrusions.

- The P-T conditions of the Rengård intrusions indicates that the equilibrium during metamorphism reaches the 800 ºC and 4 kbar, in contrast to the GI tonalites that have been calculated in 760 ºC and 2.5 kbar. The GII intrusions emplacement P-T conditions have been determined in 690 ºC and 1.66 kbar for GIIa, and 720 ºC and 2.7 Kbar for the GIIb intrusions and microgranular enclaves.

- Textural evidences suggest that the metamorphism postdates the deformation and alteration reaching the anphibolite field towards the S in the Petikträsk area and Rengård tonalites. The static metamorphic textures truncate systematically those related to the hydrothermal alteration or deformation. However, stages of alteration and metamorphism could be the expression of the same regional thermal event. The GI rocks of the northern JGC do not show metamorphic textures.

- The metamorphism on intrusions in the westernmost part of Skellefte district shows pattern of a dynamic regional metamorphism, the same ductile structures can be observed in both VIC and the Skellefte Group volcanics. The VIC hornblende tonalites (quartz amphibolites) are deformed and metamorphosed under regional dynamic metamorphism. Both static and dynamic metamorphism occurrence suggest different tectonic regimes in the area or differences in the propagation of deformation in the JGC and VIC.

- The ε_{Nd} (+2,0 a +3,8) isotopic data indicate the occurrence of an Archaean depleted mantle source for the JGC intrusions, satellite intrusions, VIC, Näsberget and the subvolcanic porphyritic dacite of Maurliden. Stavaträsk pluton with a negative ε_{Nd} (-0,7) indicates a marginal Archaean crustal material.

- The three differentiated intrusive stages have been summarized in:

  a) The first intrusive stage implies the emplacement of GI pluton and satellite intrusions (Rengård y Klockträsk), these rocks show calcic affinity and are associated to the Skellefte Group volcanics. The igneous activity is at least active from 1900 Ma to 1885 Ma, it includes the plutonic, volcanic and volcanosedimentary rocks. The older plutons are located in the western margin of Skellefte district (Viterliden intrusive complex) as well as the eastern area represented by the Klockträsk satellite intrusion (1897 ±10 Ma). The central Skellefte district intrusive bodies have been dated at 1900 Ma in the Finnliden rhyolite and GI tonalite of Halmyrtjärnen. Most of the GI intrusions have been dated ca. 1885 Ma, including the Rengård satellite intrusion.

  b) The second intrusive stage implies the emplacement of GII intrusions, Näsberget (?) and Stavaträsk pluton at 1875 Ma, these intrusions show calc-alkaline affinity. The age determinations of these intrusions include samples from the north, south and east of the JGC.

  c) Third intrusive stage is determined by the intrusion of alkaline-calcic to alkaline granitoids of GIII, GIV and Hobergsliden, at 1865 Ma. Most of these plutons are located in the centre of JGC.

PARTE 3:

ANEXOS / APPENDIX

ANEXO I. ABREVIATURAS *ABBREVIATIONS* 1

ANEXO II. QUÍMICA MINERAL *MINERAL CHEMISTRY* 3
A-II.1. Micas *Micas* 3
A-II.2. Anfíbol *Amphibole* 19
A-II.3. Piroxeno *Pyroxene* 33
A-II.4. Feldespatos *Feldspars* 39
A-II.5. Epidota *Epidote* 45
A-II.6. Olivino *Olivine* 46
A-II.7. Accesorios *Accesory* 47

ANEXO III. LITOGEOQUÍMICA *LITHOGEOCHEMISTRY* 49

ANEXO IV. ANÁLISIS ISOTÓPICO *ISOTOPIC ANALYSES* 57

ANEXO V. DATACIONES *AGE DETERMINATIONS* 59

ANEXO VI. QUÍMICA MINERAL DE CIRCONES *ZIRCONS MINERAL CHEMISTRY* 65

ANEXO VII. LOCALIZACIÓN DE MUESTRAS *SAMPLES LOCATION* 69
A-VII.1. Muestras de 2003 *2003 samples* 69
A-VII.2. Muestras de 2004 *2004 samples* 72

ANEXO VIII. FOTOS PETROGRAFÍA *PETROGRAPHY MICROPHOTOGRAPHS* 77

ANEXO IX. FOTOS QUÍMICA MINERAL *MINERAL CHEMISTRY MICROPHOTOGRAPHS* 103

ANEXO X. MAPAS *MAPS* 115
A-X.1. Mapa Regional (Mapa 0) 115
A-X.2. Gallejaur (Mapa 1) 116
A-X.3. Zona de Jörn (Mapa 2) 118
A-X.4. Zona E (Mapa 3) 120
A-X.5. Zona ENE (Mapa 4) 122
A-X.6. Contacto GI, GII, GIII (Mapa 5) 124
A-X.7. Zona norte de JGC y Näsberget (Mapa 6) 126
A-X.8. Ulbergträsket (Mapa 7) 134
A-X.9. Dique Sur (Mapa 8) 136

ANEXO I. ABREVIATURAS
ABBREVIATIONS

Abr.	Mineral
Ab	Albita / Albite
Act	Actinolita / Actinolite
Aln	Alanita / Alanite
And	Andalucita / Andalusite
Amph	Anfíbol / Amphibole
An	Anortita / Anortite
Aug	Augita / Augite
Ap	Apatito / Apatite
Brz	Bronzita / Bronzite
Bt	Biotita / Biotite
Cal	Calcita / Calcite
Ccp	Calcopirita / Chalcopyrite
Chl	Clorita / Chlorite
Cpx	Clinopiroxeno / Clinopyroxene
Di	Diópsido / Diopside
Ed	Edenita / Edenite
En	Enstatita / Enstatite
Ep	Epidota / Epidote
Fa	Fatalita / Fayalite
Fo	Forsterita / Forsterite
Fs	Ferrosilita / Ferrosilite
Gr	Grafito / Graphite
Hbl	Hornblenda / Hornblende
Hem	Hematites / Hematites

Abr.	Mineral
Hs	Hastingsita / Hastingsite
Hyp	Hiperstena / Hyperstene
Ilm	Ilmenita / Ilmenite
Kfs	Feldespato alcalino / Alkali felds
Krs	Kaersutita / Kaersutite
Ky	Distena / Kyanite
Mag	Magnetita / Magnetite
Ms	Moscovita / Muscovite
Ol	Olivino / Olivine
Or	Ortosa / Orthoclase
Opx	Ortopiroxeno / Orthopyroxene
Phl	Flogopita / Phlogopite
Pl	Plagioclasa / Plagioclase
Prg	Pargasita / Pargasite
Py	Pirita / Pyrite
Qz	Cuarzo / Quartz
Rt	Rutilo / Rutile
Ser	Sericita / Sericite
Sil	Silimanita / Sillimanite
Spl	Espinela / Spinel
Tit	Titanita / Titanite
Ts	Tschermaquita / Tschermakite
Zr	Circón / Zircon

Original	Español/Spanish
Bothnia Basin	Cuenca de Botnia
Cadomian Orogen	Orogenia Cadomiana
Caledonian Origen	Orogenia Caledoniana
Fennoscandian Shield	Escudo Fenoescandinavo
Gothian Orogen	Orogenia Gotiana (Gótica)
Iapetus Ocean	Océano Jápeto
Jörn Granitoid Complex	Complejo de Granitoides de Jörn
Karelian Craton	Cratón Kareliano
Kola Craton	Cratón de Kola
Mid Ocean Ridge Basalts-MORB	Basaltos de Dorsal Oceánica
Näsberget Layered Intrusion	Complejo Bandeado Näsberget
Skellefte Mining District	Distrito Minero de Skellefte
Svecofennian Orogen	Orogenia Svecofeniana
Sveconorwegian Orogen	Orogenia Sveconoruega
Transcandinavian Igneous Belt	Cinturón Ígneo Transescandinavo
Viterliden Intrusive Complex	Complejo Intrusivo Viterliden

ANEXO II. QUÍMICA MINERAL

MINERAL CHEMISTRY

Fase	GI							GI												
Litotipo	tonalita grano medio							tonalita grano medio												
Muestra	23j28							23j29												
Análisis	2	3	11	12	15	18	19	1	2	3	4	5	6	7	8	9	10	11	12	13
Mineral	chl	bi	bi	chl	bi	bi	chl	bi	bi	bi	bi	bi	bi	bi	bi	chl	bi	bi	bi	chl
SiO_2	25,95	35,17	35,90	26,21	36,70	37,43	25,73	35,44	35,67	34,81	35,77	35,57	37,33	35,73	34,87	26,14	35,59	34,81	36,45	25,91
TiO_2	0,10	1,62	1,35	0,19	1,81	1,84	0,07	1,02	1,49	1,51	1,69	1,75	1,54	1,12	1,52	0,08	1,79	1,79	2,13	0,03
Al_2O_3	18,72	15,57	15,85	19,31	16,36	17,59	19,53	16,39	16,80	16,35	15,99	16,67	16,50	16,35	16,04	20,00	17,25	16,09	17,56	20,72
FeO	27,35	21,45	21,35	27,36	20,96	21,33	28,36	20,98	21,07	21,02	21,23	20,80	21,35	23,46	21,23	27,67	21,77	20,74	22,02	27,59
MnO	0,45	0,21	0,40	0,68	0,30	0,30	0,72	0,30	0,40	0,47	0,53	0,25	0,64	0,43	0,37	0,53	0,46	0,32	0,18	0,94
MgO	13,64	9,68	9,51	13,59	9,76	9,90	12,65	9,10	9,24	8,84	9,20	9,19	9,25	9,41	9,50	13,88	9,23	9,13	8,89	13,87
CaO	0,09	0,10	0,03	0,07	0,03	0,13	0,45	0,13	0,04	0,15	0,10	0,20	0,00	0,21	0,51	0,07	0,01	0,15	0,10	0,04
Na_2O	0,22	0,46	0,58	0,40	0,56	0,50	0,16	0,48	0,23	0,17	0,33	0,52	0,28	0,20	0,31	0,37	0,16	0,85	0,32	0,35
K_2O	0,02	8,99	8,85	0,00	9,08	9,25	0,00	8,71	9,18	8,94	9,17	8,48	9,18	8,89	8,19	0,17	9,11	9,04	9,40	0,03
Total	86,54	93,25	93,82	87,81	95,56	98,27	87,67	92,55	94,12	92,26	94,01	93,43	96,07	95,80	92,54	88,91	95,37	92,92	97,05	89,48
Si	4,42	5,56	5,62	4,40	5,62	5,56	4,36	5,61	5,56	5,55	5,60	5,56	5,69	5,53	5,53	4,34	5,49	5,52	5,52	4,27
Al^{IV}	3,58	2,44	2,38	3,60	2,38	2,44	3,64	2,39	2,44	2,45	2,40	2,44	2,31	2,47	2,47	3,66	2,51	2,48	2,48	3,73
Al^{VI}	0,18	0,46	0,55	0,22	0,57	0,64	0,26	0,67	0,65	0,62	0,55	0,64	0,65	0,51	0,53	0,25	0,62	0,53	0,65	0,30
Ti	0,01	0,19	0,16	0,02	0,21	0,21	0,01	0,12	0,17	0,18	0,20	0,21	0,18	0,13	0,18	0,01	0,21	0,21	0,24	0,00
Fe^{2+}	3,90	2,84	2,80	3,84	2,68	2,65	4,02	2,78	2,75	2,80	2,78	2,72	2,72	3,04	2,82	3,84	2,81	2,75	2,79	3,80
Mn	0,06	0,03	0,05	0,10	0,04	0,04	0,10	0,04	0,05	0,06	0,07	0,03	0,08	0,06	0,05	0,07	0,06	0,04	0,02	0,13
Mg	3,47	2,28	2,22	3,40	2,23	2,19	3,19	2,15	2,15	2,10	2,15	2,14	2,10	2,17	2,25	3,43	2,12	2,16	2,01	3,41
Ca	0,02	0,02	0,01	0,01	0,00	0,02	0,08	0,02	0,01	0,03	0,02	0,03	0,00	0,03	0,09	0,01	0,00	0,03	0,02	0,01
Na	0,07	0,14	0,18	0,13	0,17	0,14	0,05	0,15	0,07	0,05	0,10	0,16	0,08	0,06	0,10	0,12	0,05	0,26	0,09	0,11
K	0,00	1,81	1,77	0,00	1,77	1,75	0,00	1,76	1,83	1,82	1,83	1,69	1,78	1,76	1,66	0,04	1,79	1,83	1,81	0,01
Cl	0,00	0,00	0,00	0,00	0,00	0,00	0,00	0,00	0,00	0,00	0,00	0,00	0,00	0,00	0,00	0,00	0,00	0,00	0,00	0,00
F	0,00	0,00	0,00	0,00	0,00	0,00	0,00	0,00	0,00	0,00	0,00	0,00	0,00	0,00	0,00	0,00	0,00	0,00	0,00	0,00
Total	15,72	15,77	15,73	15,73	15,67	15,64	15,71	15,69	15,67	15,67	15,69	15,62	15,59	15,76	15,66	15,77	15,66	15,81	15,63	15,77

Fase	GI									GI			GI							
Litotipo	tonalita grano medio									tonalita grano medio			tonalita grano medio							
Muestra	23j31									23k09			23k37							
Análisis	5	10	11	12	13	14	15	19	20	3	7	8	1	2	5	6	7	9	10	11
Mineral	bi	bi	chl	bi	bi	chl	bi	bi	bi	bi	bi	bi	chl	bi	bi	bi	bi	bi	bi	bi
SiO_2	36,43	36,41	25,41	36,11	36,7	26,69	35,65	37,05	36,81	36,31	35,63	34,80	27,85	35,69	35,63	31,43	36,65	37,6	37,26	37,47
TiO_2	2,31	2,04	0,09	1,74	2,42	0,11	1,88	2,19	2,28	2,19	1,68	1,23	0,47	1,35	2,13	1,36	1,9	1,5	1,68	1,74
Al_2O_3	15,76	15,24	20,05	15,99	16,02	20,59	15,79	16,19	15,45	15,78	15,52	16,39	18,29	15,79	16,49	17,41	16,56	15,07	16,24	17,02
FeO	19,55	19,48	24,72	20,99	19,58	24,63	19,86	19,65	20,24	23,68	23,64	22,95	23,06	19,05	18,8	21,25	19,92	18,03	19	18,81
MnO	0,53	0,41	0,86	0,6	0,5	1,02	0,59	0,42	0,42	0,45	0,36	0,33	0,53	0,48	0,26	0,5	0,22	0,3	0,36	0,39
MgO	10,05	10,16	14,68	10,01	10,86	15,62	10,44	10,35	10,30	8,31	9,25	9,68	14,97	10,97	10,63	13,36	10,83	12,22	11,96	11,43
CaO	0,08	0,02	0	0,15	0,04	0,35	0,05	0,16	0,09	0,07	0,12	0,16	0,28	0,02	0,16	0,13	0,01	0,19	0,13	0,02
Na_2O	0,25	0,4	0,26	0,35	0,39	0,13	0,38	0,29	0,13	0,53	0,68	0,55	0,26	0,4	0,32	0,15	0,62	0,54	0,39	0,7
K_2O	8,89	8,96	0	9,03	9,26	0,07	8,86	9,65	9,41	8,99	8,41	8,06	1,23	8,65	8,89	4,64	9,19	8,93	8,85	9,16
Total	93,85	93,12	86,07	94,97	95,77	89,21	93,5	95,95	95,13	96,31	95,29	94,15	86,94	92,4	93,31	90,23	95,9	94,38	95,87	96,74
Si	5,65	5,69	4,30	5,58	5,58	4,34	5,57	5,63	5,65	5,60	5,55	5,46	4,64	5,61	5,54	5,05	5,56	5,74	5,62	5,60
Al^{IV}	2,35	2,31	3,70	2,42	2,42	3,66	2,43	2,37	2,35	2,40	2,45	2,54	3,36	2,39	2,46	2,95	2,44	2,26	2,38	2,40
Al^{VI}	0,52	0,50	0,30	0,49	0,45	0,29	0,48	0,53	0,45	0,46	0,40	0,49	0,23	0,54	0,56	0,34	0,53	0,45	0,50	0,59
Ti	0,27	0,24	0,01	0,20	0,28	0,01	0,22	0,25	0,26	0,25	0,20	0,15	0,06	0,16	0,25	0,16	0,22	0,17	0,19	0,20
Fe^{2+}	2,53	2,55	3,50	2,71	2,49	3,35	2,60	2,50	2,60	3,05	3,08	3,01	3,21	2,50	2,44	2,85	2,53	2,30	2,40	2,35
Mn	0,07	0,05	0,12	0,08	0,06	0,14	0,08	0,05	0,05	0,06	0,05	0,04	0,07	0,06	0,03	0,07	0,03	0,04	0,05	0,05
Mg	2,32	2,37	3,71	2,31	2,46	3,79	2,43	2,34	2,36	1,91	2,15	2,26	3,72	2,57	2,46	3,20	2,45	2,78	2,69	2,55
Ca	0,01	0,00	0,00	0,02	0,01	0,06	0,01	0,03	0,01	0,01	0,02	0,03	0,05	0,00	0,03	0,02	0,00	0,03	0,02	0,00
Na	0,08	0,12	0,09	0,10	0,11	0,04	0,12	0,09	0,04	0,16	0,21	0,17	0,08	0,12	0,10	0,05	0,18	0,16	0,11	0,20
K	1,76	1,79	0,00	1,78	1,80	0,01	1,77	1,87	1,84	1,77	1,67	1,61	0,26	1,73	1,76	0,95	1,78	1,74	1,70	1,75
Cl	0,00	0,00	0,00	0,00	0,00	0,00	0,00	0,00	0,00	0,00	0,00	0,00	0,00	0,00	0,00	0,00	0,00	0,00	0,00	0,00
F	0,00	0,00	0,00	0,00	0,00	0,00	0,00	0,00	0,00	0,00	0,00	0,00	0,00	0,00	0,00	0,00	0,00	0,00	0,00	0,00
Total	15,56	15,62	15,73	15,70	15,66	15,70	15,69	15,65	15,63	15,68	15,77	15,77	15,68	15,70	15,63	15,64	15,72	15,68	15,66	15,68

Fase	Näsberg			GII									GII		GI				
Litotipo	gabro norita			granodiorita grano medio									granodiorita		tonalita cuarzo porfídica grano grueso				
Muestra	23j84			24k104									JO03-67		JO03-35a				
Análisis	9	18	20	1	3	5	10	11	12	15	16	19	3	12	1	2	3	8	9
Mineral	bi	bi	bi	bi	chl	ms	bi	bi	bi	chl	chl	ms	bi	bi	bi	bi	chl	bi	chl
SiO_2	37,19	35,55	35,75	37,9	25,94	48,26	37,66	37,35	38,25	25,97	26,47	47,43	38,58	37,72	35,48	35,05	25,93	34,88	25,35
TiO_2	4,10	1,90	3,26	0,75	0,06	0	1,08	1,08	1,36	0,03	0,04	0,13	1,45	2,61	1,70	1,56	0,01	1,96	0,12
Al_2O_3	13,42	13,24	13,83	15,26	18,98	29,36	14,11	14,72	15,02	18,93	19,86	33,79	15,01	14,78	16,21	16,44	18,60	16,52	18,27
FeO	20,90	16,30	17,50	19,27	25,29	4,21	17,5	17,96	18,33	24,32	25,41	1,03	16,62	18,22	25,46	25,39	34,27	25,95	32,51
MnO	0,04	0,23	0,13	0,21	0,36	0,05	0,28	0,19	0,44	0,26	0,57	0,09	0,60	0,26	0,55	0,59	1,06	0,78	0,80
MgO	10,97	13,09	12,45	13,24	15,29	1,29	12,42	12,71	13,09	16	15,87	0,27	14,25	13,36	6,52	7,05	10,60	6,87	10,45
CaO	0,07	0,48	0,14	0,14	0,29	0,01	0,07	0,01	0,08	0,01	0,3	0,19	0,03	0,09	0,14	0,11	0,02	0,03	0,01
Na_2O	0,48	0,41	0,44	0,5	0,09	0,32	0,2	0,28	0,27	0,12	0,25	0,21	0,26	0,28	0,23	0,55	0,27	0,34	0,51
K_2O	8,41	7,78	8,40	9,61	0,03	10,41	9,3	9,09	9,12	0,01	0,02	10,71	8,13	9,10	9,27	9,06	0,02	9,08	0,04
Total	95,58	88,98	91,90	96,88	86,33	93,91	92,62	93,39	95,96	85,65	88,79	93,85	94,93	96,42	95,56	95,80	90,78	96,41	88,06
Si	5,68	5,73	5,61	5,68	4,38	7,92	5,86	5,76	5,74	4,40	4,34	6,39	5,77	5,64	5,58	5,50	4,37	5,46	4,39
Al^{IV}	2,32	2,27	2,39	2,32	3,62	0,08	2,14	2,24	2,26	3,60	3,66	1,61	2,23	2,36	2,42	2,50	3,63	2,54	3,61
Al^{VI}	0,10	0,24	0,17	0,38	0,16	2,86	0,44	0,44	0,40	0,17	0,18	3,75	0,42	0,25	0,58	0,54	0,07	0,50	0,11
Ti	0,47	0,23	0,39	0,08	0,01	0,00	0,13	0,13	0,15	0,00	0,00	0,01	0,16	0,29	0,20	0,18	0,00	0,23	0,02
Fe^{2+}	2,67	2,20	2,30	2,42	3,57	0,00	2,28	2,32	2,30	3,44	3,49	0,12	2,08	2,28	3,35	3,33	4,83	3,39	4,70
Mn	0,01	0,03	0,02	0,03	0,05	0,00	0,04	0,02	0,06	0,04	0,08	0,01	0,08	0,03	0,07	0,08	0,15	0,10	0,12
Mg	2,50	3,14	2,91	2,96	3,85	0,23	2,88	2,92	2,93	4,04	3,88	0,05	3,18	2,98	1,53	1,65	2,67	1,60	2,70
Ca	0,01	0,08	0,02	0,02	0,05	0,32	0,01	0,00	0,01	0,00	0,05	0,03	0,00	0,01	0,02	0,02	0,00	0,01	0,00
Na	0,14	0,13	0,13	0,15	0,03	2,38	0,06	0,08	0,08	0,04	0,08	0,05	0,08	0,08	0,07	0,17	0,09	0,10	0,17
K	1,64	1,60	1,68	1,84	0,01	0,00	1,84	1,79	1,75	0,00	0,00	1,84	1,55	1,74	1,86	1,81	0,00	1,81	0,01
Cl	0,00	0,00	0,00	0,00	0,00	0,00	0,00	0,00	0,00	0,00	0,00	0,00	0,00	0,00	0,00	0,00	0,00	0,00	0,00
F	0,00	0,00	0,00	0,00	0,00	0,00	0,00	0,00	0,00	0,00	0,00	0,00	0,00	0,00	0,00	0,00	0,00	0,00	0,00
Total	15,53	15,65	15,63	15,87	15,74	13,80	15,68	15,71	15,69	15,73	15,77	13,87	15,55	15,67	15,68	15,79	15,82	15,75	15,83

Fase	GI							GI					GI							
Litotipo	tonalita cuarzo porfídica grano grueso							tonalita grano medio					tonalita grano medio							
Muestra	JO03-35a							JO03-80b					JO03-80a							
Análisis	11	12	18	19	20	23	24	1	2	3	4	5	1	2	4	5	7	9	11	12
Mineral	bi	bi	bi	chl	bi	chl	bi	bi	bi	bi	bi	bi	bi	bi	bi	bi	bi	bi	bi	chl
SiO_2	25,28	35,78	34,04	24,63	34,43	34,60	25,20	35,06	34,68	35,55	34,69	35,64	34,98	35,74	35,64	36,11	35,49	34,69	37,30	26,12
TiO_2	0,09	1,45	1,44	0,08	1,82	1,53	0,02	1,47	1,39	1,42	1,13	1,45	1,38	0,98	1,64	1,57	1,48	1,40	1,58	0,00
Al_2O_3	17,98	16,38	15,82	18,16	15,55	16,51	17,16	15,57	15,50	15,59	16,19	15,21	15,40	15,41	15,87	15,69	15,61	15,91	15,71	18,96
FeO	32,48	25,38	25,58	32,97	25,04	25,82	32,40	26,13	25,58	25,98	25,54	24,64	25,75	25,63	25,51	26,96	25,71	25,94	24,90	33,10
MnO	0,61	0,55	0,48	1,04	0,56	0,50	0,97	0,35	0,42	0,25	0,15	0,35	0,43	0,33	0,49	0,53	0,54	0,42	0,41	0,56
MgO	9,87	6,88	6,63	9,30	6,77	6,79	9,56	7,20	7,68	7,82	8,38	8,11	7,78	7,88	7,70	8,03	7,72	8,66	8,76	11,09
CaO	0,15	0,21	0,13	0,03	0,02	0,04	0,01	0,02	0,08	0,07	0,03	0,01	0,12	0,01	0,20	0,04	0,10	0,14	0,05	0,09
Na_2O	0,49	0,41	0,38	0,25	0,30	0,23	0,27	0,33	0,42	0,62	0,39	0,31	0,35	0,45	0,28	0,53	0,39	0,17	0,43	0,58
K_2O	0,08	8,83	8,53	0,09	8,94	8,85	0,12	9,11	8,65	8,88	8,38	8,96	8,53	8,69	8,41	8,80	8,98	7,21	9,21	0,09
Total	87,03	95,87	93,03	86,55	93,43	94,87	85,71	95,24	94,40	96,18	94,88	94,68	94,72	95,12	95,74	98,26	96,02	94,54	98,35	90,59
Si	4,43	5,59	5,51	4,37	5,54	5,49	4,50	5,55	5,53	5,47	5,63	5,56	5,55	5,63	5,57	5,54	5,56	5,47	5,65	4,38
Al^{IV}	3,57	2,41	2,49	3,63	2,46	2,51	3,50	2,45	2,47	2,53	2,37	2,44	2,45	2,37	2,43	2,46	2,44	2,53	2,35	3,62
Al^{VI}	0,14	0,60	0,53	0,16	0,50	0,57	0,11	0,46	0,44	0,48	0,46	0,43	0,43	0,49	0,49	0,37	0,44	0,43	0,45	0,13
Ti	0,01	0,17	0,18	0,01	0,22	0,18	0,00	0,18	0,17	0,13	0,17	0,17	0,16	0,12	0,19	0,18	0,17	0,17	0,18	0,00
Fe^{2+}	4,76	3,31	3,46	4,89	3,37	3,42	4,83	3,46	3,41	3,37	3,25	3,40	3,42	3,38	3,33	3,46	3,37	3,42	3,15	4,64
Mn	0,09	0,07	0,07	0,16	0,08	0,07	0,15	0,05	0,06	0,02	0,05	0,03	0,06	0,04	0,06	0,07	0,07	0,06	0,05	0,08
Mg	2,58	1,60	1,60	2,46	1,63	1,61	2,54	1,70	1,82	1,97	1,91	1,82	1,84	1,85	1,79	1,84	1,80	2,04	1,98	2,77
Ca	0,03	0,04	0,02	0,01	0,00	0,01	0,00	0,00	0,01	0,01	0,00	0,01	0,02	0,00	0,03	0,01	0,02	0,02	0,01	0,02
Na	0,17	0,12	0,12	0,09	0,09	0,07	0,09	0,10	0,13	0,12	0,09	0,19	0,11	0,14	0,08	0,16	0,12	0,05	0,13	0,19
K	0,02	1,76	1,76	0,02	1,84	1,79	0,03	1,84	1,76	1,69	1,80	1,77	1,73	1,75	1,68	1,72	1,79	1,45	1,78	0,02
Cl	0,00	0,00	0,00	0,00	0,00	0,00	0,00	0,00	0,00	0,00	0,00	0,00	0,00	0,00	0,00	0,00	0,00	0,00	0,00	0,00
F	0,00	0,00	0,00	0,00	0,00	0,00	0,00	0,00	0,00	0,00	0,00	0,00	0,00	0,00	0,00	0,00	0,00	0,00	0,00	0,00
Total	15,79	15,68	15,74	15,78	15,72	15,72	15,76	15,79	15,80	15,79	15,74	15,82	15,76	15,76	15,66	15,80	15,78	15,63	15,72	15,85

Fase	GI									GI										Näsberg
Litotipo	tonalita grano medio									tonalita grano medio										norita
Muestra	JO03-81									JO03-87a										A55
Análisis	1	2	3	4	5	6	7	8	9	1	2	3	4	5	6	9	10	11	12	10
Mineral	bi	bi	chl	bi	chl	bi	chl	bi	chl	bi	bi	bi	bi	chl	bi	bi	bi	bi	chl	bi
SiO_2	37,10	36,80	26,10	36,68	26,83	38,56	25,26	37,45	25,01	31,71	33,84	34,67	34,74	30,65	35,50	37,34	36,93	36,73	28,52	34,48
TiO_2	1,73	1,41	0,05	1,56	0,05	1,44	0,02	1,56	0,37	1,17	1,60	1,63	1,75	0,08	1,60	1,71	1,66	1,86	0,11	2,59
Al_2O_3	16,20	15,72	19,04	16,49	19,78	16,23	19,07	16,14	18,09	18,37	15,96	15,19	15,31	15,38	16,44	15,26	16,26	16,59	14,68	14,90
FeO	22,19	21,79	30,28	22,70	31,02	21,54	30,31	21,91	29,80	19,97	18,12	18,15	17,70	24,11	19,36	18,99	18,71	18,93	25,65	25,73
MnO	0,36	0,56	0,67	0,48	0,60	0,23	0,82	0,23	0,69	0,36	0,43	0,25	0,22	0,48	0,40	0,46	0,43	0,44	0,60	0,45
MgO	9,73	9,79	12,46	9,51	12,50	10,51	11,53	9,94	11,26	11,82	10,60	10,96	11,21	16,55	11,48	11,39	11,68	11,63	15,63	6,50
CaO	0,21	0,27	0,12	0,09	0,09	0,16	0,19	0,10	0,49	0,02	0,23	0,07	0,06	0,07	0,12	0,06	0,10	0,10	0,41	0,00
Na_2O	0,20	0,30	0,34	0,31	0,27	0,31	0,30	0,17	0,31	0,38	0,17	0,28	0,36	0,44	0,26	0,44	0,42	0,33	0,39	0,00
K_2O	9,65	9,53	0,01	9,30	0,00	9,42	0,00	9,28	0,04	6,57	7,93	8,53	8,52	1,17	8,70	9,11	8,85	8,96	0,13	7,89
Total	97,37	96,17	89,07	97,12	91,14	98,40	87,50	96,78	86,06	90,37	88,88	89,73	89,87	88,93	93,86	94,76	95,04	95,57	86,12	92,54
Si	5,61	5,64	4,39	5,57	4,40	5,72	4,34	5,67	4,38	5,10	5,51	5,60	5,59	4,99	5,50	5,71	5,62	5,71	4,85	5,59
Al^{IV}	2,39	2,36	3,61	2,43	3,60	2,28	3,66	2,33	3,62	2,90	2,49	2,40	2,41	2,95	2,50	2,29	2,38	2,29	2,94	2,41
Al^{VI}	0,50	0,48	0,16	0,53	0,22	0,56	0,21	0,55	0,11	0,58	0,57	0,49	0,49	0,00	0,50	0,47	0,53	0,47	0,00	0,43
Ti	0,20	0,16	0,01	0,18	0,01	0,16	0,00	0,18	0,05	0,14	0,20	0,20	0,21	0,01	0,19	0,20	0,19	0,20	0,01	0,32
Fe^{2+}	2,81	2,79	4,26	2,88	4,25	2,67	4,36	2,77	4,36	2,68	2,47	2,45	2,38	3,28	2,51	2,43	2,38	2,43	3,65	3,49
Mn	0,05	0,07	0,10	0,06	0,08	0,03	0,12	0,03	0,10	0,05	0,06	0,03	0,03	0,07	0,05	0,06	0,06	0,06	0,09	0,06
Mg	2,20	2,24	3,12	2,15	3,06	2,32	2,95	2,24	2,94	2,83	2,57	2,64	2,69	4,02	2,65	2,60	2,65	2,60	3,96	1,57
Ca	0,03	0,04	0,02	0,01	0,02	0,03	0,03	0,02	0,09	0,00	0,04	0,01	0,01	0,01	0,02	0,01	0,02	0,01	0,07	0,00
Na	0,06	0,09	0,11	0,09	0,09	0,09	0,10	0,05	0,11	0,12	0,05	0,09	0,11	0,14	0,08	0,13	0,12	0,13	0,13	0,00
K	1,86	1,86	0,00	1,80	0,00	1,78	0,00	1,79	0,01	1,35	1,65	1,76	1,75	0,24	1,72	1,78	1,72	1,78	0,03	1,63
Cl	0,00	0,00	0,00	0,00	0,00	0,00	0,00	0,00	0,00	0,00	0,00	0,00	0,00	0,00	0,00	0,00	0,00	0,00	0,00	0,00
F	0,00	0,00	0,00	0,00	0,00	0,00	0,00	0,00	0,00	0,00	0,00	0,00	0,00	0,00	0,00	0,00	0,00	0,00	0,00	0,00
Total	15,70	15,75	15,78	15,72	15,72	15,64	15,77	15,63	15,77	15,75	15,61	15,68	15,68	15,71	15,71	15,67	15,66	15,67	15,74	15,49

Fase	GI												Rengård, tipo GI			Rengård, tipo GI				
Litotipo	tonalita grano medio												tonalita grano medio			tonalita grano medio				
Muestra	JO03-87b												JO03-108			JO03-109				
Análisis	1	2	3	4	5	6	7	8	9	10	11	12	2	10	12	5	9	23	25	27
Mineral	bi	bi	bi	bi	bi	bi	bi	bi	bi	bi	bi	bi	bi	bi	bi	bi	bi	bi	bi	bi
SiO_2	38,29	37,15	38,22	37,89	37,08	36,91	37,67	37,26	37,63	33,89	36,73	37,10	35,75	34,78	34,95	36,22	34,92	34,30	34,99	32,71
TiO_2	1,90	1,97	1,87	1,66	1,68	1,85	1,66	1,85	1,64	1,50	1,52	1,69	2,33	2,26	2,15	2,28	2,29	2,10	2,16	1,95
Al_2O_3	17,12	16,87	16,94	16,90	16,61	15,19	16,60	16,37	16,70	16,31	16,96	16,19	16,14	15,69	15,12	16,93	16,19	15,72	16,17	15,52
FeO	19,15	20,05	19,96	19,59	18,07	18,62	19,38	19,76	18,82	20,41	19,37	19,85	23,14	22,04	23,44	21,81	23,25	21,13	21,60	21,99
MnO	0,47	0,42	0,37	0,07	0,25	0,19	0,23	0,64	0,34	0,53	0,26	0,36	0,71	0,62	0,47	0,27	0,04	0,18	0,26	0,17
MgO	12,24	11,86	12,42	12,53	11,66	11,56	11,80	11,83	12,17	11,68	11,80	11,49	7,73	7,13	7,03	7,98	8,45	7,53	7,39	7,89
CaO	0,06	0,13	0,00	0,17	0,01	0,32	0,11	0,11	0,06	0,28	0,11	0,06	0,22	0,14	0,16	0,20	0,08	0,05	0,09	0,01
Na_2O	0,15	0,19	0,41	0,34	0,39	0,43	0,50	0,45	0,48	0,02	0,26	0,30	0,43	0,15	0,36	0,24	0,40	0,12	0,17	0,04
K_2O	9,74	9,19	9,26	9,69	9,13	8,83	8,72	9,52	8,85	6,73	8,88	8,77	8,89	8,34	8,39	8,60	7,65	8,27	8,28	7,33
Total	99,12	97,83	99,45	98,84	94,88	93,90	96,67	97,79	96,69	91,35	95,89	95,81	95,34	91,15	92,07	94,53	93,27	89,40	91,11	87,61
Si	5,59	5,52	5,57	5,56	5,63	5,69	5,62	5,55	5,61	5,39	5,54	5,62	5,56	5,63	5,64	5,61	5,51	5,63	5,63	5,50
Al^{IV}	2,41	2,48	2,43	2,44	2,37	2,31	2,38	2,45	2,39	2,61	2,46	2,38	2,44	2,37	2,36	2,39	2,49	2,37	2,37	2,50
Al^{VI}	0,53	0,47	0,48	0,48	0,60	0,44	0,55	0,43	0,54	0,44	0,56	0,50	0,53	0,62	0,52	0,70	0,53	0,67	0,70	0,58
Ti	0,21	0,22	0,20	0,18	0,19	0,21	0,19	0,21	0,18	0,18	0,17	0,19	0,27	0,28	0,26	0,27	0,27	0,26	0,26	0,25
Fe^{2+}	2,34	2,49	2,43	2,40	2,29	2,40	2,42	2,46	2,35	2,71	2,44	2,51	3,01	2,98	3,17	2,82	3,07	2,90	2,91	3,09
Mn	0,06	0,05	0,05	0,01	0,03	0,02	0,03	0,08	0,04	0,07	0,03	0,05	0,09	0,09	0,06	0,04	0,01	0,03	0,04	0,02
Mg	2,66	2,63	2,70	2,74	2,64	2,65	2,63	2,63	2,70	2,77	2,65	2,59	1,79	1,72	1,69	1,84	1,99	1,84	1,77	1,98
Ca	0,01	0,02	0,00	0,03	0,00	0,05	0,02	0,02	0,01	0,05	0,02	0,01	0,04	0,02	0,03	0,03	0,01	0,01	0,02	0,00
Na	0,04	0,05	0,12	0,10	0,11	0,13	0,14	0,13	0,14	0,01	0,08	0,09	0,13	0,05	0,11	0,07	0,12	0,04	0,05	0,01
K	1,81	1,74	1,72	1,81	1,77	1,74	1,66	1,81	1,68	1,36	1,71	1,69	1,77	1,72	1,73	1,70	1,54	1,73	1,70	1,57
Cl	0,00	0,00	0,00	0,00	0,00	0,00	0,00	0,00	0,00	0,00	0,00	0,00	0,00	0,00	0,00	0,00	0,00	0,00	0,00	0,00
F	0,00	0,00	0,00	0,00	0,00	0,00	0,00	0,00	0,00	0,00	0,00	0,00	0,00	0,00	0,00	0,00	0,00	0,00	0,00	0,00
Total	15,66	15,68	15,69	15,75	15,64	15,65	15,63	15,77	15,65	15,59	15,67	15,64	15,63	15,48	15,58	15,47	15,54	15,48	15,45	15,51

Fase	Rengård, tipo GI			Rengård, tipo GI										Näsberg	Näsberg				Näsberg
Litotipo	tonalita grano medio			tonalita grano medio										norita	gabro norita				norita
Muestra	JO03-109			JO03-110										A28	S110				S30
Análisis	31	32	34	6	7	10	14	22	24	25	28	32	42	12	9	14	19	20	3
Mineral	bi	bi	bi	bi	bi	bi	bi	bi	bi	bi	bi	bi	bi	bi	bi	bi	bi	bi	bi
SiO_2	26,99	31,24	33,71	34,59	33,71	34,70	34,32	36,33	35,08	36,17	34,12	31,47	35,02	35,80	38,70	37,16	38,31	37,89	38,17
TiO_2	1,07	1,34	2,10	2,38	1,99	2,18	2,19	2,59	2,32	2,50	2,39	2,12	2,78	6,55	4,85	3,59	5,26	4,30	2,15
Al_2O_3	16,81	16,49	15,80	15,64	15,76	16,05	16,68	17,01	15,94	16,94	15,63	15,74	16,46	13,27	13,77	13,69	13,85	13,93	13,41
FeO	23,96	24,73	20,87	22,65	22,29	22,42	21,84	22,86	24,15	23,33	21,77	21,78	22,08	15,18	8,05	7,84	9,01	8,92	20,56
MnO	0,35	0,18	0,29	0,55	0,34	0,07	0,33	0,47	0,22	0,22	0,47	0,50	0,26	0,00	0,00	0,00	0,00	0,00	0,48
MgO	9,37	9,02	8,19	6,42	6,94	6,80	6,97	7,52	6,52	7,05	7,07	6,68	6,87	12,53	19,61	19,06	18,96	18,61	10,39
CaO	0,49	0,55	0,05	0,08	0,08	0,01	0,04	0,18	0,01	0,18	0,13	0,05	0,08	0,00	0,00	0,00	0,00	0,00	0,00
Na_2O	0,46	0,16	0,41	0,38	0,22	0,32	0,23	0,48	0,09	0,38	0,60	0,02	0,13	0,00	1,28	1,27	1,31	1,23	0,00
K_2O	1,34	3,96	7,74	8,12	8,06	8,18	8,30	8,71	8,40	8,70	8,14	7,22	8,53	8,52	7,76	7,17	7,73	7,99	8,83
Total	80,84	87,67	89,16	90,81	89,39	90,73	90,90	96,15	92,73	95,47	90,32	85,58	92,21	91,85	94,02	89,78	94,43	92,87	93,99
Si	4,89	5,24	5,54	5,64	5,58	5,63	5,56	5,57	5,62	5,59	5,58	5,44	5,59	5,56	5,63	5,65	5,58	5,62	5,91
Al^{IV}	3,11	2,76	2,46	2,36	2,42	2,37	2,44	2,43	2,38	2,41	2,42	2,56	2,41	2,43	2,36	2,35	2,38	2,38	2,09
Al^{VI}	0,48	0,50	0,60	0,64	0,65	0,70	0,74	0,64	0,63	0,67	0,59	0,65	0,68	0,00	0,00	0,10	0,00	0,05	0,36
Ti	0,15	0,17	0,26	0,29	0,25	0,27	0,27	0,30	0,28	0,29	0,29	0,28	0,33	0,76	0,53	0,41	0,58	0,48	0,25
Fe^{2+}	3,63	3,47	2,87	3,09	3,08	3,04	2,96	2,93	3,23	3,01	2,98	3,15	2,95	1,97	0,98	1,00	1,10	1,11	2,66
Mn	0,05	0,03	0,04	0,08	0,05	0,01	0,05	0,06	0,03	0,03	0,07	0,07	0,04	0,00	0,00	0,00	0,00	0,00	0,06
Mg	2,53	2,25	2,01	1,56	1,71	1,65	1,68	1,72	1,56	1,62	1,72	1,72	1,63	2,90	4,25	4,32	4,12	4,11	2,40
Ca	0,10	0,10	0,01	0,01	0,01	0,00	0,01	0,03	0,00	0,03	0,02	0,01	0,01	0,00	0,00	0,00	0,00	0,00	0,00
Na	0,16	0,05	0,13	0,12	0,07	0,10	0,07	0,14	0,03	0,11	0,19	0,01	0,04	0,00	0,36	0,37	0,37	0,35	0,00
K	0,31	0,85	1,62	1,69	1,70	1,69	1,71	1,70	1,72	1,71	1,70	1,59	1,74	1,69	1,44	1,39	1,44	1,51	1,75
Cl	0,00	0,00	0,00	0,00	0,00	0,00	0,00	0,00	0,00	0,00	0,00	0,00	0,00	0,00	0,00	0,00	0,00	0,00	0,00
F	0,00	0,00	0,00	0,00	0,00	0,00	0,00	0,00	0,00	0,00	0,00	0,00	0,00	0,00	0,00	0,00	0,00	0,00	0,00
Total	15,41	15,41	15,54	15,47	15,53	15,46	15,48	15,52	15,47	15,49	15,56	15,48	15,42	15,31	15,56	15,60	15,56	15,62	15,48

Fase	Näsberg		Näsberg		Näsberg	GI													
Litotipo	gabro norita		gabro norita		norita	tonalita grano medio													
Muestra	S128		S134		S217	23j28 epma													
Análisis	9	14	5	13	5	1	2	5	7	8	20	22	23	25	26	28	30	33	34
Mineral	bi	bi	bi	bi	bi	bi	bi	chl	chl	bi	bi	bi	bi	bi	bi	chl	chl	bi	chl
SiO_2	37,68	36,40	37,08	36,58	38,01	36,23	36,04	26,34	26,54	35,59	35,48	35,40	34,99	35,27	35,77	26,36	25,15	35,28	25,72
TiO_2	5,96	5,29	5,63	5,23	4,77	1,34	1,26	0,07	0,05	1,20	1,41	1,54	1,45	1,27	1,17	0,11	0,12	1,32	0,05
Al_2O_3	13,49	13,34	13,43	12,54	13,34	16,85	16,88	20,06	19,96	17,07	17,75	18,38	17,13	17,05	16,89	20,16	20,25	17,27	20,28
FeO	11,78	10,86	18,32	22,46	17,04	20,72	20,87	26,04	26,03	20,90	20,90	19,30	20,38	20,86	20,57	26,25	25,92	20,00	26,63
MnO	0,00	0,00	0,00	0,00	0,00	0,16	0,22	0,45	0,44	0,26	0,22	0,22	0,22	0,20	0,20	0,43	0,42	0,21	0,46
MgO	16,60	16,21	13,19	9,85	13,47	9,62	9,43	13,59	13,93	9,81	9,38	9,58	9,32	9,83	9,77	14,08	14,08	10,13	11,95
CaO	0,00	0,00	0,00	0,00	0,00	0,15	0,27	0,10	0,10	0,22	0,09	0,04	0,11	0,12	0,14	0,05	0,15	0,11	0,32
Na_2O	1,28	1,05	0,00	0,54	0,00	0,03	0,04	0,00	0,03	0,06	0,05	0,01	0,06	0,08	0,07	0,00	0,00	0,07	0,07
K_2O	8,06	7,61	8,94	8,55	8,90	10,11	9,72	0,03	0,04	10,02	10,21	10,46	9,83	10,06	10,19	0,02	0,03	10,27	0,05
Total	94,85	90,76	96,59	95,75	95,53	95,19	94,72	86,67	87,11	95,14	95,47	94,93	93,49	94,74	94,76	87,46	86,11	94,65	85,51
Si	5,56	5,58	5,55	5,64	5,70	5,59	5,58	4,43	4,44	5,51	5,47	5,45	5,50	5,48	5,55	4,40	4,27	5,47	4,41
Al^{IV}	2,34	2,41	2,37	2,28	2,30	2,41	2,42	3,57	3,56	2,49	2,53	2,55	2,50	2,52	2,45	3,60	3,73	2,53	3,59
Al^{VI}	0,00	0,00	0,00	0,00	0,05	0,65	0,66	0,41	0,38	0,62	0,69	0,78	0,67	0,61	0,64	0,36	0,33	0,63	0,51
Ti	0,66	0,61	0,63	0,61	0,54	0,15	0,15	0,01	0,01	0,14	0,16	0,18	0,17	0,15	0,14	0,01	0,02	0,15	0,01
Fe^{2+}	1,45	1,39	2,29	2,90	2,14	2,67	2,70	3,66	3,64	2,70	2,69	2,48	2,68	2,71	2,67	3,66	3,68	2,59	3,82
Mn	0,00	0,00	0,00	0,00	0,00	0,02	0,03	0,06	0,06	0,03	0,03	0,03	0,03	0,03	0,03	0,06	0,06	0,03	0,07
Mg	3,65	3,71	2,94	2,26	3,01	2,21	2,18	3,41	3,47	2,26	2,16	2,20	2,18	2,28	2,26	3,50	3,57	2,34	3,06
Ca	0,00	0,00	0,00	0,00	0,00	0,02	0,05	0,02	0,02	0,04	0,01	0,01	0,02	0,02	0,02	0,01	0,03	0,02	0,06
Na	0,37	0,31	0,00	0,16	0,00	0,01	0,01	0,00	0,01	0,02	0,01	0,00	0,02	0,02	0,02	0,00	0,00	0,02	0,02
K	1,52	1,49	1,71	1,68	1,70	1,99	1,92	0,01	0,01	1,98	2,01	2,05	1,97	1,99	2,02	0,00	0,01	2,03	0,01
Cl	0,00	0,00	0,00	0,00	0,00	0,00	0,00	0,00	0,00	0,00	0,00	0,00	0,00	0,00	0,00	0,00	0,00	0,00	0,00
F	0,00	0,00	0,00	0,00	0,00	0,00	0,00	0,00	0,00	0,00	0,00	0,00	0,00	0,00	0,00	0,00	0,00	0,00	0,00
Total	15,55	15,50	15,49	15,53	15,44	15,73	15,70	15,58	15,60	15,79	15,77	15,74	15,74	15,81	15,79	15,61	15,69	15,82	15,55

Fase	GI													
Litotipo	tonalita grano medio													
Muestra	23j28 epma													
Análisis	1	2	5	7	8	20	22	23	25	26	28	30	33	34
Mineral	bi	bi	chl	chl	bi	bi	bi	bi	bi	bi	chl	chl	bi	chl
SiO_2	36,23	36,04	26,34	26,54	35,59	35,48	35,40	34,99	35,27	35,77	26,36	25,15	35,28	25,72
TiO_2	1,34	1,26	0,07	0,05	1,20	1,41	1,54	1,45	1,27	1,17	0,11	0,12	1,32	0,05
Al_2O_3	16,85	16,88	20,06	19,96	17,07	17,75	18,38	17,13	17,05	16,89	20,16	20,25	17,27	20,28
FeO	20,72	20,87	26,04	26,03	20,90	20,90	19,30	20,38	20,86	20,57	26,25	25,92	20,00	26,63
MnO	0,16	0,22	0,45	0,44	0,26	0,22	0,22	0,22	0,20	0,20	0,43	0,42	0,21	0,46
MgO	9,62	9,43	13,59	13,93	9,81	9,38	9,58	9,32	9,83	9,77	14,08	14,08	10,13	11,95
CaO	0,15	0,27	0,10	0,10	0,22	0,09	0,04	0,11	0,12	0,14	0,05	0,15	0,11	0,32
Na_2O	0,03	0,04	0,00	0,03	0,06	0,05	0,01	0,06	0,08	0,07	0,00	0,00	0,07	0,07
K_2O	10,11	9,72	0,03	0,04	10,02	10,21	10,46	9,83	10,06	10,19	0,02	0,03	10,27	0,05
F	0	0	0	0	0	0	0	0	0	0	0	0	0	0
Total	95,19	94,72	86,67	87,11	95,14	95,47	94,93	93,49	94,74	94,76	87,46	86,11	94,65	85,51
Si	5,59	5,58	4,43	4,44	5,51	5,47	5,45	5,50	5,48	5,55	4,40	4,27	5,47	4,41
Al^{IV}	2,41	2,42	3,57	3,56	2,49	2,53	2,55	2,50	2,52	2,45	3,60	3,73	2,53	3,59
Al^{VI}	0,65	0,66	0,41	0,38	0,62	0,69	0,78	0,67	0,61	0,64	0,36	0,33	0,63	0,51
Ti	0,15	0,15	0,01	0,01	0,14	0,16	0,18	0,17	0,15	0,14	0,01	0,02	0,15	0,01
Fe^{2+}	2,67	2,70	3,66	3,64	2,70	2,69	2,48	2,68	2,71	2,67	3,66	3,68	2,59	3,82
Mn	0,02	0,03	0,06	0,06	0,03	0,03	0,03	0,03	0,03	0,03	0,06	0,06	0,03	0,07
Mg	2,21	2,18	3,41	3,47	2,26	2,16	2,20	2,18	2,28	2,26	3,50	3,57	2,34	3,06
Ca	0,02	0,05	0,02	0,02	0,04	0,01	0,01	0,02	0,02	0,02	0,01	0,03	0,02	0,06
Na	0,01	0,01	0,00	0,01	0,02	0,01	0,00	0,02	0,02	0,02	0,00	0,00	0,02	0,02
K	1,99	1,92	0,01	0,01	1,98	2,01	2,05	1,97	1,99	2,02	0,00	0,01	2,03	0,01
Cl	0,00	0,00	0,00	0,00	0,00	0,00	0,00	0,00	0,00	0,00	0,00	0,00	0,00	0,00
F	0,00	0,00	0,00	0,00	0,00	0,00	0,00	0,00	0,00	0,00	0,00	0,00	0,00	0,00
Total	15,73	15,70	15,58	15,60	15,79	15,77	15,74	15,74	15,81	15,79	15,61	15,69	15,82	15,55

Fase	Rengård, tipo GI										Rengård, tipo GI											
Litotipo	tonalita grano medio										tonalita grano medio											
Muestra	JO03-109 epma										JO03-110 epma											
Análisis	8	9	17	18	19	20	32	35	36	37	6	7	12	18	19	20	24	27	32	34	37	42
Mineral	bi	bi	bi	bi	bi	bi	bi	bi	bi	bi	bi	bi	bi	bi	bi	bi	bi	bi	bi	bi	bi	bi
SiO_2	35,36	34,53	33,82	34,76	35,07	35,13	34,88	35,06	34,88	35,09	35,02	35,06	34,91	33,54	31,73	33,25	34,55	34,96	34,60	34,50	34,18	34,90
TiO_2	1,87	1,82	2,02	1,91	2,06	1,90	1,89	1,84	1,83	1,85	2,40	2,33	2,54	2,28	2,39	2,29	2,28	2,23	2,25	2,12	2,00	2,16
Al_2O_3	16,52	17,12	16,59	16,78	16,59	16,36	16,50	16,77	16,50	16,59	16,90	16,80	16,96	16,20	15,67	15,78	16,49	17,11	16,79	17,10	17,13	16,73
FeO	22,78	23,37	24,04	22,73	23,19	23,36	22,94	22,47	22,67	22,93	24,33	24,24	23,47	22,75	24,10	23,56	24,41	23,89	23,48	22,90	22,86	23,80
MnO	0,20	0,18	0,15	0,20	0,16	0,19	0,21	0,17	0,18	0,19	0,29	0,29	0,28	0,28	0,29	0,25	0,28	0,30	0,24	0,33	0,31	0,30
MgO	8,37	8,36	8,62	8,55	8,29	8,24	8,42	8,63	8,67	8,72	6,91	7,16	7,13	6,85	7,25	7,06	6,87	6,99	7,13	7,09	6,83	7,17
CaO	0,09	0,07	0,14	0,07	0,05	0,02	0,04	0,06	0,01	0,01	0,05	0,04	0,03	0,01	0,02	0,02	0,03	0,02	0,04	0,07	0,08	0,03
Na_2O	0,10	0,06	0,04	0,06	0,07	0,09	0,05	0,05	0,07	0,05	0,04	0,05	0,05	0,01	0,05	0,06	0,08	0,04	0,01	0,05	0,02	0,04
K_2O	9,85	9,26	8,47	9,62	9,82	9,94	9,71	9,69	10,04	10,07	9,91	10,08	10,16	9,86	9,74	9,64	10,20	10,04	10,10	10,07	9,84	10,05
F	0	0	0	0	0	0	0	0	0	0	0	0	0	0	0	0	0	0	0	0	0	0
Total	95,13	94,77	93,88	94,67	95,29	95,22	94,63	94,73	94,85	95,50	95,84	96,06	95,51	91,78	91,22	91,90	95,19	95,58	94,61	94,23	93,25	95,18
Si	5,52	5,42	5,37	5,45	5,48	5,50	5,48	5,48	5,47	5,47	5,47	5,47	5,46	5,47	5,46	5,44	5,47	5,28	5,47	5,46	5,47	5,49
Al^{IV}	2,48	2,58	2,63	2,55	2,52	2,50	2,52	2,52	2,53	2,53	2,53	2,53	2,54	2,53	2,54	2,56	2,53	2,72	2,53	2,54	2,53	2,51
Al^{VI}	0,56	0,58	0,47	0,56	0,53	0,52	0,54	0,58	0,52	0,52	0,58	0,56	0,53	0,62	0,59	0,48	0,58	0,35	0,60	0,65	0,69	0,59
Ti	0,22	0,22	0,24	0,23	0,24	0,22	0,22	0,22	0,22	0,22	0,28	0,27	0,27	0,26	0,30	0,28	0,28	0,30	0,27	0,25	0,24	0,26
Fe^{2+}	2,97	3,06	3,19	2,98	3,03	3,06	3,02	2,94	2,97	2,99	3,18	3,16	3,23	3,12	3,07	3,22	3,10	3,35	3,10	3,03	3,06	3,13
Mn	0,03	0,02	0,02	0,03	0,02	0,02	0,03	0,02	0,02	0,03	0,04	0,04	0,04	0,04	0,04	0,03	0,04	0,04	0,03	0,04	0,04	0,04
Mg	1,95	1,96	2,04	2,00	1,93	1,92	1,97	2,01	2,03	2,03	1,61	1,67	1,62	1,63	1,66	1,72	1,66	1,80	1,68	1,67	1,63	1,68
Ca	0,01	0,01	0,02	0,01	0,01	0,00	0,01	0,01	0,00	0,00	0,01	0,01	0,00	0,00	0,01	0,00	0,00	0,00	0,01	0,01	0,01	0,01
Na	0,03	0,02	0,01	0,02	0,02	0,03	0,01	0,02	0,02	0,02	0,01	0,02	0,02	0,01	0,01	0,02	0,00	0,01	0,00	0,01	0,01	0,01
K	1,96	1,85	1,71	1,92	1,96	1,98	1,95	1,93	2,01	2,00	1,97	2,01	2,06	2,00	2,03	2,01	2,05	2,07	2,04	2,03	2,01	2,02
Cl	0,00	0,00	0,00	0,00	0,00	0,00	0,00	0,00	0,00	0,00	0,00	0,00	0,00	0,00	0,00	0,00	0,00	0,00	0,00	0,00	0,00	0,00
F	0,00	0,00	0,00	0,00	0,00	0,00	0,00	0,00	0,00	0,00	0,00	0,00	0,00	0,00	0,00	0,00	0,00	0,00	0,00	0,00	0,00	0,00
Total	15,73	15,72	15,70	15,74	15,74	15,77	15,75	15,73	15,80	15,80	15,68	15,72	15,77	15,70	15,70	15,77	15,72	15,93	15,72	15,71	15,69	15,72

Fase	GIII								GI								GIV			
Litotipo	granodiorita								tonalita								granito alcalino			
Muestra	JO03-67 epma								23J31epma								23J58 epma			
Análisis	26	28	29	30	39	40	47	48	7	9	12	14	15	16	17	8	29	31	32	34
Mineral	bi	bi	bi	bi	bi	bi	bi	bi	bi	bi	bi	bi	bi	bi	bi	chl	bi	bi	bi	bi
SiO_2	35,35	36,69	36,95	37,31	37,65	36,56	35,87	33,28	36,16	36,08	36,58	36,26	36,02	35,92	35,43	25,47	35,55	35,80	35,84	32,40
TiO_2	1,25	1,63	1,61	2,01	1,53	1,58	1,32	0,93	1,19	1,41	2,49	2,36	1,61	1,37	1,91	0,05	1,83	1,77	2,12	1,44
Al_2O_3	16,21	15,59	15,47	15,39	15,47	15,47	16,69	17,28	17,11	17,19	16,53	16,68	17,78	17,92	16,87	20,87	16,18	17,37	16,80	0,30
FeO	17,03	16,27	16,05	16,39	16,18	16,00	15,97	17,18	19,33	19,60	19,62	19,72	19,35	19,28	19,29	24,16	21,04	19,60	19,87	0,89
MnO	0,43	0,37	0,46	0,44	0,46	0,42	0,36	0,43	0,44	0,40	0,45	0,45	0,44	0,36	0,50	0,72	0,35	0,32	0,37	0,00
MgO	13,83	13,33	13,17	13,07	13,69	13,56	13,29	15,45	10,50	10,09	9,87	10,26	10,13	10,00	10,17	14,95	8,84	9,72	9,54	0,05
CaO	0,33	0,29	0,04	0,07	0,07	0,12	0,04	0,15	0,08	0,06	0,02	0,02	0,04	0,03	0,13	0,03	0,06	0,00	0,01	1,04
Na_2O	0,10	0,12	0,24	0,15	0,10	0,09	0,10	0,06	0,05	0,01	0,05	0,07	0,03	0,05	0,08	0,01	0,05	0,03	0,03	0,00
K_2O	6,51	7,78	9,30	8,86	9,19	9,06	9,54	5,61	9,75	9,67	9,47	9,61	9,74	9,74	9,57	0,00	9,51	9,89	9,65	0,04
F	0,61	0,57	0,96	0,46	0,91	0,55	0,65	0,72	0,33	0,55	0,46	0,21	0,11	0,30	0,31	0,00	0,00	0,00	0,00	0,00
Total	91,64	92,64	94,24	94,14	95,25	93,41	93,83	91,09	94,92	95,18	96,03	96,26	95,52	95,02	94,59	86,35	93,66	95,34	94,86	36,21
Si	5,51	5,66	5,67	5,69	5,70	5,63	5,52	5,23	5,57	5,56	5,60	5,54	5,51	5,52	5,51	4,28	5,60	5,53	5,56	4,36
Al^{IV}	2,49	2,34	2,33	2,31	2,30	2,37	2,48	2,77	2,43	2,44	2,40	2,46	2,49	2,48	2,49	3,72	2,40	2,47	2,44	0,43
	0,00	0,00	0,00	0,00	0,00	0,00	0,00	0,00												
Al^{VI}	0,49	0,50	0,47	0,46	0,46	0,44	0,55	0,43	0,67	0,69	0,58	0,55	0,71	0,76	0,59	0,41	0,60	0,69	0,63	0,00
Ti	0,15	0,19	0,19	0,23	0,17	0,18	0,15	0,11	0,14	0,16	0,29	0,27	0,18	0,16	0,22	0,01	0,22	0,21	0,25	3,96
Fe^{2+}	2,22	2,10	2,06	2,09	2,05	2,06	2,06	2,26	2,49	2,53	2,51	2,52	2,48	2,48	2,51	3,39	2,77	2,53	2,58	0,18
Mn	0,06	0,05	0,06	0,06	0,06	0,05	0,05	0,06	0,06	0,05	0,06	0,06	0,06	0,05	0,07	0,10	0,05	0,04	0,05	0,01
Mg	3,22	3,07	3,01	2,97	3,09	3,11	3,05	3,62	2,41	2,32	2,25	2,34	2,31	2,29	2,36	3,74	2,08	2,24	2,20	0,00
Ca	0,05	0,05	0,01	0,01	0,01	0,02	0,01	0,02	0,01	0,01	0,00	0,00	0,01	0,01	0,02	0,01	0,01	0,00	0,00	4,53
Na	0,03	0,04	0,07	0,04	0,03	0,03	0,03	0,02	0,02	0,00	0,02	0,02	0,01	0,01	0,03	0,00	0,01	0,01	0,01	0,00
K	1,30	1,53	1,82	1,72	1,77	1,78	1,87	1,12	1,91	1,90	1,85	1,87	1,90	1,91	1,90	0,00	1,91	1,95	1,91	0,03
Cl	0,00	0,00	0,00	0,00	0,00	0,00	0,00	0,00	0,00	0,00	0,00	0,00	0,00	0,00	0,00	0,00	0,00	0,00	0,00	0,00
F	0,30	0,28	0,46	0,22	0,44	0,27	0,32	0,36	0,16	0,27	0,22	0,10	0,05	0,14	0,15	0,00	0,00	0,00	0,00	0,50
Total	15,51	15,51	15,69	15,58	15,65	15,68	15,76	15,64	15,71	15,66	15,56	15,63	15,66	15,66	15,69	15,66	15,65	15,66	15,62	13,49

Fase	GIIII					GIIII				Vargfors								GIII	
Litotipo	granodiorita					granodiorita				basalto andesítico porfídico								granodiorita	
Muestra	JO03-45 epma					JO03-58 epma				JO03-124 epma								JO04-34 epma	
Análisis	25	27	26	28	29	1	2	3	7	2	5	8	12	9	10	13	4	27	29
Mineral	bi	bi	chl	chl	chl	bi	bi	bi	bi	bi	bi	bi	bi	chl	chl	chl	chl	bi	bi
SiO_2	46,27	45,94	28,43	28,70	28,74	38,04	38,07	37,07	37,81	38,63	39,04	39,35	38,14	28,93	28,38	28,41	29,13	37,65	37,85
TiO_2	0,14	0,20	0,08	0,03	0,11	1,19	0,92	1,26	1,52	0,83	0,83	0,71	1,00	0,06	0,03	0,04	0,05	1,10	1,31
Al_2O_3	29,70	30,47	19,56	19,17	19,49	15,09	15,83	16,33	15,69	15,02	14,72	14,64	15,54	18,86	19,34	19,99	18,46	14,68	15,09
FeO	4,67	4,76	21,29	20,35	20,95	16,83	16,74	17,73	16,74	12,25	12,62	12,49	13,38	14,27	14,27	14,46	13,76	17,79	17,43
MnO	0,04	0,09	0,89	0,82	0,87	0,73	0,74	0,74	0,81	0,13	0,15	0,12	0,13	0,17	0,19	0,22	0,18	0,21	0,20
MgO	1,86	1,74	16,56	16,99	16,55	12,89	12,62	12,21	12,20	16,34	16,42	16,79	16,59	24,17	23,51	23,68	24,76	13,03	12,71
CaO	0,00	0,00	0,09	0,12	0,18	0,00	0,02	0,04	0,00	0,01	0,04	0,01	0,04	0,05	0,27	0,20	0,04	0,08	0,07
Na_2O	0,19	0,13	0,01	0,02	0,01	0,07	0,05	0,04	0,05	0,02	0,02	0,05	0,07	0,03	0,03	0,02	0,00	0,04	0,04
K_2O	11,10	11,19	0,05	0,02	0,07	10,09	9,94	9,16	9,98	10,25	10,13	10,17	10,13	0,04	0,06	0,18	0,04	9,71	9,51
F	0,22	0,21	0,32	0,15	0,21	1,15	0,91	0,15	1,06	0,10	0,00	0,11	0,08	0,00	0,00	0,08	0,29	0,01	0,06
Total	94,20	94,92	87,30	86,45	87,14	95,65	95,56	94,71	95,76	94,24	94,74	95,41	95,50	87,34	86,94	87,63	87,34	94,28	94,26
Si	6,39	6,32	4,64	4,69	4,67	5,77	5,76	5,64	5,74	5,81	5,84	5,86	5,68	4,56	4,51	4,46	4,59	5,76	5,77
Al^{IV}	1,61	1,68	3,36	3,31	3,33	2,23	2,24	2,36	2,26	2,19	2,16	2,14	2,32	3,44	3,49	3,54	3,41	2,24	2,23
Al^{VI}	3,23	3,26	0,39	0,39	0,41	0,47	0,59	0,58	0,55	0,47	0,44	0,43	0,40	0,07	0,13	0,16	0,02	0,41	0,49
Ti	0,01	0,02	0,01	0,00	0,01	0,14	0,10	0,14	0,17	0,09	0,09	0,08	0,11	0,01	0,00	0,01	0,01	0,13	0,15
Fe^{2+}	0,54	0,55	2,90	2,78	2,85	2,14	2,12	2,26	2,12	1,54	1,58	1,55	1,66	1,88	1,90	1,90	1,81	2,28	2,22
Mn	0,01	0,01	0,12	0,11	0,12	0,09	0,09	0,10	0,10	0,02	0,02	0,02	0,02	0,02	0,03	0,03	0,02	0,03	0,03
Mg	0,38	0,36	4,02	4,14	4,01	2,92	2,85	2,77	2,76	3,66	3,66	3,73	3,68	5,68	5,57	5,54	5,82	2,97	2,89
Ca	0,00	0,00	0,02	0,02	0,03	0,00	0,00	0,01	0,00	0,00	0,01	0,00	0,01	0,01	0,05	0,03	0,01	0,01	0,01
Na	0,05	0,03	0,00	0,01	0,00	0,02	0,01	0,01	0,01	0,00	0,01	0,01	0,02	0,01	0,01	0,01	0,00	0,01	0,01
K	1,96	1,96	0,01	0,00	0,01	1,95	1,92	1,78	1,93	1,97	1,93	1,93	1,92	0,01	0,01	0,04	0,01	1,90	1,85
Cl	0,00	0,00	0,00	0,00	0,00	0,00	0,00	0,00	0,00	0,00	0,00	0,00	0,00	0,00	0,00	0,00	0,00	0,00	0,00
F	0,10	0,09	0,16	0,08	0,11	0,55	0,43	0,07	0,51	0,05	0,00	0,05	0,04	0,00	0,00	0,04	0,15	0,00	0,03
Total	14,18	14,19	15,48	15,46	15,45	15,73	15,69	15,64	15,66	15,75	15,74	15,75	15,82	15,69	15,69	15,71	15,69	15,74	15,65

Fase	GII																						
Litotipo	granodiorita																						
Muestra	JO04-42 epma																						
Análisis	5	6	11	25	26	27	28	35	37	38	40	43	44	46	47	48	49	50	51	52	53	54	55
Mineral	bi	bi	bi	bi	bi	bi	bi	bi	bi	bi	bi	bi	bi	bi	bi	bi	bi	bi	bi	bi	bi	bi	bi
SiO_2	37,63	36,87	36,20	36,83	36,96	37,18	37,44	36,57	36,70	37,01	36,79	36,58	36,39	37,09	36,50	36,11	37,08	36,69	36,44	36,60	37,03	37,32	36,86
TiO_2	1,18	1,14	1,17	1,93	1,87	1,27	1,24	1,48	1,52	1,47	1,39	1,39	1,33	1,41	1,11	1,16	1,59	2,18	2,16	1,64	1,76	1,37	2,18
Al_2O_3	14,42	15,22	14,67	14,36	14,44	14,53	14,74	14,89	15,24	14,59	14,81	14,83	15,12	14,67	15,41	15,12	14,27	14,34	14,44	14,37	14,56	14,40	14,34
FeO	20,27	20,97	21,78	22,19	21,72	21,33	21,50	21,17	21,06	21,05	21,16	21,55	21,12	21,26	21,61	21,40	21,72	21,59	21,86	21,52	21,55	21,84	21,45
MnO	0,28	0,35	0,33	0,33	0,28	0,28	0,26	0,26	0,23	0,25	0,25	0,31	0,26	0,31	0,27	0,24	0,28	0,28	0,32	0,29	0,23	0,28	0,27
MgO	11,95	11,35	11,26	10,32	10,76	11,07	11,14	11,08	11,20	11,30	10,94	10,93	10,81	11,11	10,89	10,92	10,88	10,44	10,34	10,81	10,64	11,08	10,47
CaO	0,00	0,03	0,02	0,00	0,03	0,02	0,01	0,02	0,05	0,05	0,03	0,04	0,05	0,03	0,04	0,02	0,00	0,02	0,00	0,00	0,00	0,00	0,01
Na_2O	0,05	0,03	0,04	0,04	0,07	0,10	0,05	0,06	0,08	0,03	0,06	0,04	0,06	0,07	0,03	0,07	0,02	0,04	0,01	0,05	0,09	0,03	0,03
K_2O	9,92	9,98	9,47	9,73	9,54	9,69	9,82	9,74	9,70	9,81	9,79	9,63	9,77	9,68	9,39	9,82	9,80	9,60	9,57	9,61	9,91	9,73	9,78
F	1,26	1,47	1,27	0,80	1,11	1,11	0,96	1,10	1,00	1,27	1,35	0,99	1,06	1,05	1,07	1,09	0,92	1,05	0,91	1,00	0,91	1,15	1,26
Total	96,62	97,00	95,90	96,47	96,94	96,31	96,93	96,06	96,65	96,50	96,17	95,97	95,66	96,47	95,97	95,66	96,59	96,89	96,87	96,25	96,38	97,35	96,86
Si	5,75	5,65	5,63	5,69	5,69	5,73	5,72	5,65	5,63	5,69	5,68	5,66	5,64	5,70	5,63	5,62	5,72	5,68	5,66	5,69	5,70	5,72	5,69
Al^{IV}	2,25	2,35	2,37	2,31	2,31	2,27	2,28	2,35	2,37	2,31	2,32	2,34	2,36	2,30	2,37	2,38	2,28	2,32	2,34	2,31	2,30	2,28	2,31
Al^{VI}	0,35	0,40	0,32	0,30	0,31	0,36	0,38	0,36	0,38	0,34	0,38	0,36	0,41	0,36	0,44	0,39	0,31	0,30	0,30	0,32	0,34	0,33	0,30
Ti	0,14	0,13	0,14	0,22	0,22	0,15	0,14	0,17	0,17	0,17	0,16	0,16	0,16	0,16	0,13	0,14	0,18	0,25	0,25	0,19	0,20	0,16	0,25
Fe^{2+}	2,59	2,69	2,83	2,87	2,80	2,75	2,75	2,73	2,70	2,71	2,73	2,79	2,74	2,73	2,79	2,78	2,80	2,80	2,84	2,80	2,77	2,80	2,77
Mn	0,04	0,05	0,04	0,04	0,04	0,04	0,03	0,03	0,03	0,03	0,03	0,04	0,03	0,04	0,03	0,03	0,04	0,04	0,04	0,04	0,03	0,04	0,04
Mg	2,72	2,59	2,61	2,38	2,47	2,54	2,54	2,55	2,56	2,59	2,52	2,52	2,50	2,55	2,51	2,53	2,50	2,41	2,39	2,50	2,44	2,53	2,41
Ca	0,00	0,00	0,00	0,00	0,00	0,00	0,00	0,00	0,01	0,01	0,01	0,01	0,01	0,00	0,01	0,00	0,00	0,00	0,00	0,00	0,00	0,00	0,00
Na	0,01	0,01	0,01	0,01	0,02	0,03	0,02	0,02	0,02	0,01	0,02	0,01	0,02	0,02	0,01	0,02	0,00	0,01	0,00	0,01	0,03	0,01	0,01
K	1,93	1,95	1,88	1,92	1,87	1,90	1,91	1,92	1,90	1,93	1,93	1,90	1,93	1,90	1,85	1,95	1,93	1,90	1,89	1,90	1,95	1,90	1,93
Cl	0,00	0,00	0,00	0,00	0,00	0,00	0,00	0,00	0,00	0,00	0,00	0,00	0,00	0,00	0,00	0,00	0,00	0,00	0,00	0,00	0,00	0,00	0,00
F	0,61	0,71	0,62	0,39	0,54	0,54	0,47	0,54	0,49	0,62	0,66	0,48	0,52	0,51	0,52	0,53	0,45	0,52	0,44	0,49	0,44	0,56	0,61
Total	15,79	15,82	15,84	15,74	15,73	15,77	15,77	15,79	15,78	15,78	15,78	15,78	15,79	15,77	15,76	15,84	15,77	15,71	15,72	15,77	15,76	15,77	15,72

Fase	GII										GI							
Litotipo	tonalita										tonalita							
Muestra	JO04-75 epma										JO04-86 epma							
Análisis	42	44	45	46	52	53	54	55	56	57	19	21	24	25	29	31	33	37
Mineral	bi	bi	bi	bi	bi	bi	chl	bi	bi	bi	bi	bi	bi	bi	bi	bi	bi	bi
SiO_2	35,31	34,97	34,58	35,07	35,95	35,46	28,45	35,60	35,28	34,95	34,94	35,07	34,35	34,29	34,47	34,22	34,47	34,48
TiO_2	1,25	1,46	1,46	1,27	1,26	1,31	0,48	1,42	1,21	1,11	1,95	1,95	2,21	2,08	2,39	2,11	2,05	1,95
Al_2O_3	16,23	16,26	16,46	15,89	15,93	16,15	18,56	15,92	16,48	15,95	16,90	17,14	16,67	16,67	16,63	17,70	18,06	17,36
FeO	25,06	24,74	25,21	25,26	24,80	25,13	29,45	24,72	24,41	24,63	27,27	27,15	27,86	27,39	27,95	26,81	26,77	27,17
MnO	0,23	0,27	0,24	0,24	0,20	0,28	0,46	0,25	0,29	0,29	0,65	0,62	0,66	0,69	0,72	0,63	0,63	0,64
MgO	8,16	7,92	7,60	8,35	8,33	8,11	9,80	8,16	8,21	8,45	4,80	4,81	4,68	4,88	4,71	4,47	4,43	4,67
CaO	0,12	0,06	0,03	0,03	0,00	0,05	0,16	0,03	0,07	0,13	0,02	0,01	0,00	0,05	0,06	0,01	0,06	0,08
Na_2O	0,01	0,03	0,02	0,04	0,00	0,03	0,01	0,04	0,03	0,03	0,07	0,04	0,02	0,03	0,05	0,03	0,03	0,06
K_2O	9,37	9,51	9,67	9,18	9,73	9,60	2,53	9,70	9,26	8,78	9,84	9,95	9,59	9,54	9,50	9,53	9,65	9,66
F	0,63	0,37	0,36	0,32	0,14	0,37	0,00	0,14	0,32	0,24	0,29	0,50	0,23	0,46	0,32	0,17	0,29	0,49
Total	96,22	95,69	95,74	95,54	96,55	96,60	90,12	96,07	95,79	94,69	96,95	97,25	96,54	96,15	97,01	96,17	96,67	96,77
Si	5,52	5,51	5,46	5,52	5,59	5,53	4,75	5,56	5,53	5,53	5,51	5,50	5,46	5,46	5,45	5,43	5,43	5,45
Al^{IV}	2,48	2,49	2,54	2,48	2,41	2,47	3,25	2,44	2,47	2,47	2,49	2,50	2,54	2,54	2,55	2,57	2,57	2,55
Al^{VI}	0,52	0,52	0,53	0,46	0,51	0,50	0,40	0,50	0,57	0,51	0,65	0,68	0,58	0,59	0,55	0,74	0,78	0,69
Ti	0,15	0,17	0,17	0,15	0,15	0,15	0,06	0,17	0,14	0,13	0,23	0,23	0,26	0,25	0,28	0,25	0,24	0,23
Fe^{2+}	3,28	3,26	3,33	3,32	3,22	3,28	4,11	3,23	3,20	3,26	3,59	3,56	3,70	3,65	3,70	3,56	3,52	3,59
Mn	0,03	0,04	0,03	0,03	0,03	0,04	0,07	0,03	0,04	0,04	0,09	0,08	0,09	0,09	0,10	0,09	0,08	0,09
Mg	1,90	1,86	1,79	1,96	1,93	1,89	2,44	1,90	1,92	1,99	1,13	1,12	1,11	1,16	1,11	1,06	1,04	1,10
Ca	0,02	0,01	0,00	0,00	0,00	0,01	0,03	0,00	0,01	0,02	0,00	0,00	0,00	0,01	0,01	0,00	0,01	0,01
Na	0,00	0,01	0,01	0,01	0,00	0,01	0,00	0,01	0,01	0,01	0,02	0,01	0,01	0,01	0,01	0,01	0,01	0,02
K	1,87	1,91	1,95	1,84	1,93	1,91	0,54	1,93	1,85	1,77	1,98	1,99	1,94	1,94	1,92	1,93	1,94	1,95
Cl	0,00	0,00	0,00	0,00	0,00	0,00	0,00	0,00	0,00	0,00	0,00	0,00	0,00	0,00	0,00	0,00	0,00	0,00
F	0,31	0,18	0,18	0,16	0,07	0,18	0,00	0,07	0,16	0,12	0,14	0,25	0,12	0,23	0,16	0,09	0,15	0,24
Total	15,77	15,77	15,81	15,79	15,77	15,79	15,64	15,78	15,74	15,74	15,69	15,68	15,69	15,70	15,68	15,63	15,63	15,68

Fase	GII											GIII										
Litotipo	tonalita											granodiorita										
Muestra	JO04-110 epma											JO04-128 epma										
Análisis	65	66	67	68	69	71	72	79	84	85	94	99	100	101	106	107	118	119	128	129	130	131
Mineral	bi	bi	bi	bi	bi	bi	chl	bi	bi	bi	bi	bi	bi	bi	chl	bi	bi	chl	bi	bi	bi	bi
SiO_2	35,24	35,26	35,31	35,24	34,80	35,20	35,26	35,49	35,12	35,00	34,02	36,90	36,41	37,36	25,62	37,26	36,87	36,61	37,70	37,04	37,25	36,33
TiO_2	1,29	1,30	1,17	1,35	1,24	1,27	1,07	1,31	1,18	1,44	1,18	2,70	1,20	1,99	0,09	2,22	1,54	1,21	1,17	2,31	2,00	1,65
Al_2O_3	17,07	16,60	16,68	16,50	16,89	16,62	16,69	16,72	16,59	17,25	17,12	13,97	14,93	14,15	19,48	14,47	14,91	14,41	14,28	14,33	14,49	15,05
FeO	22,48	21,71	22,46	21,89	23,08	22,70	21,58	21,89	22,49	22,18	22,19	21,71	20,55	21,81	28,42	21,58	21,38	20,65	19,88	21,28	21,11	20,96
MnO	0,35	0,35	0,32	0,31	0,36	0,34	0,31	0,35	0,33	0,26	0,28	0,34	0,24	0,24	0,54	0,26	0,33	0,28	0,28	0,30	0,31	0,26
MgO	9,48	9,90	9,92	9,82	9,52	9,41	9,50	9,89	9,46	9,45	9,67	10,70	11,46	11,23	13,60	10,54	11,32	11,81	12,19	10,83	11,06	10,69
CaO	0,03	0,04	0,07	0,06	0,02	0,01	0,06	0,06	0,05	0,04	0,11	0,02	0,01	0,02	0,07	0,05	0,01	0,12	0,07	0,02	0,00	0,06
Na_2O	0,09	0,05	0,01	0,04	0,06	0,03	0,04	0,07	0,02	0,03	0,05	0,04	0,02	0,06	0,01	0,03	0,08	0,07	0,02	0,11	0,06	0,01
K_2O	9,61	9,75	9,32	9,72	9,59	9,89	9,59	9,60	9,57	9,71	8,68	9,77	9,89	9,93	0,05	9,83	9,94	9,28	9,95	9,73	9,96	9,65
F	0,39	0,23	0,30	0,33	0,39	0,60	0,23	0,28	0,34	0,11	0,00	0,72	1,37	1,09	0,00	0,70	0,56	0,98	1,05	0,85	1,27	0,73
Total	96,36	95,31	95,80	95,44	96,13	96,18	94,51	95,87	95,26	95,84	93,60	96,81	95,64	97,73	88,00	96,89	96,79	95,23	96,43	96,61	97,19	95,25
Si	5,46	5,49	5,48	5,49	5,42	5,48	5,53	5,49	5,49	5,43	5,38534	5,67	5,65	5,70	4,32	5,70	5,64	5,68	5,77	5,68	5,69	5,64
Al^{IV}	2,54	2,51	2,52	2,51	2,58	2,52	2,47	2,51	2,51	2,57	2,61	2,33	2,35	2,30	3,68	2,30	2,36	2,32	2,23	2,32	2,31	2,36
Al^{VI}	0,57	0,53	0,53	0,52	0,52	0,53	0,61	0,55	0,55	0,59	0,578615	0,20	0,38	0,24	0,19	0,31	0,32	0,32	0,34	0,27	0,30	0,40
Ti	0,15	0,15	0,14	0,16	0,15	0,15	0,13	0,15	0,14	0,17	0,140119	0,31	0,14	0,23	0,01	0,25	0,18	0,14	0,13	0,27	0,23	0,19
Fe^{2+}	2,91	2,83	2,92	2,85	3,01	2,95	2,83	2,83	2,94	2,88	2,937158	2,79	2,67	2,78	4,01	2,76	2,73	2,68	2,54	2,73	2,70	2,72
Mn	0,05	0,05	0,04	0,04	0,05	0,04	0,04	0,05	0,04	0,03	0,037802	0,04	0,03	0,03	0,08	0,03	0,04	0,04	0,04	0,04	0,04	0,03
Mg	2,19	2,30	2,30	2,28	2,21	2,18	2,22	2,28	2,21	2,19	2,281808	2,45	2,65	2,55	3,42	2,41	2,58	2,73	2,78	2,48	2,52	2,48
Ca	0,01	0,01	0,01	0,01	0,00	0,00	0,01	0,01	0,01	0,01	0,018992	0,00	0,00	0,00	0,01	0,01	0,00	0,02	0,01	0,00	0,00	0,01
Na	0,03	0,02	0,00	0,01	0,02	0,01	0,01	0,02	0,01	0,01	0,014729	0,01	0,01	0,02	0,00	0,01	0,02	0,02	0,01	0,03	0,02	0,00
K	1,90	1,94	1,84	1,93	1,90	1,96	1,92	1,90	1,91	1,92	1,75209	1,91	1,96	1,93	0,01	1,92	1,94	1,84	1,94	1,90	1,94	1,91
Cl	0,00	0,00	0,00	0,00	0,00	0,00	0,00	0,00	0,00	0,00	0	0,00	0,00	0,00	0,00	0,00	0,00	0,00	0,00	0,00	0,00	0,00
F	0,19	0,11	0,15	0,16	0,19	0,30	0,11	0,14	0,17	0,05	0	0,35	0,67	0,52	0,00	0,34	0,27	0,48	0,51	0,41	0,61	0,36
Total	15,80	15,81	15,78	15,81	15,85	15,83	15,77	15,79	15,80	15,79	15,76131	15,72	15,83	15,78	15,74	15,70	15,82	15,79	15,79	15,72	15,75	15,75

Fase	Hbl tonalite					Hbl ton									X trondhjemite								
Litotipo	tonalita (cuarzo anfibolita)					tonalita									trondhjemita								
Muestra	VIC04-01 epma					VIC04-07 epma									VIC04-11 epma								
Análisis	3	7	9	26	27	29	30	32	37	39	41	43	45	46	1	2	3	4	11	12	13	14	19
Mineral	bi	bi	bi	bi	bi	bi	chl	chl	bi	bi	chl	bi	bi	bi	chl	bi	bi	chl	bi	bi	chl	bi	bi
SiO_2	35,76	36,14	36,02	36,47	35,20	40,30	26,51	24,97	36,47	37,14	26,63	37,05	36,49	37,77	26,99	38,42	38,18	26,91	37,755	37,828	27,398	38,433	38,137
TiO_2	1,86	1,82	1,94	1,61	1,44	1,51	0,05	0,06	1,55	1,64	0,05	1,81	1,86	1,65	0,06	1,72	2,03	0,08	1,631	1,764	0,06	1,579	1,597
Al_2O_3	16,73	16,49	16,40	16,31	16,23	18,56	20,34	22,45	16,10	16,39	20,27	15,60	16,28	15,92	21,18	15,93	16,18	21,12	15,539	15,803	20,03	15,909	15,784
FeO	18,45	18,54	18,99	18,30	18,88	12,20	17,96	19,07	16,73	15,51	18,94	16,23	16,00	16,05	18,00	14,14	14,88	18,02	14,056	14,372	17,614	14,315	14,245
MnO	0,24	0,30	0,25	0,25	0,22	0,09	0,23	0,21	0,13	0,10	0,20	0,10	0,09	0,16	0,31	0,15	0,18	0,34	0,196	0,151	0,317	0,181	0,166
MgO	11,29	11,41	11,39	11,16	11,69	10,53	19,66	18,48	12,97	13,46	19,64	13,70	13,65	13,46	20,31	14,56	14,00	20,56	15,098	14,211	20,816	14,674	14,611
CaO	0,05	0,05	0,03	0,01	0,00	1,11	0,10	0,04	0,02	0,03	0,03	0,01	0,00	0,02	0,00	0,05	0,07	0,00	0,064	0,056	0	0,101	0,08
Na_2O	0,11	0,10	0,14	0,15	0,12	2,22	0,07	0,03	0,11	0,08	0,00	0,09	0,09	0,08	0,03	0,00	0,00	0,01	0,029	0	0,001	0	0
K_2O	9,54	9,34	9,26	9,65	9,48	7,34	0,08	0,01	9,29	9,72	0,01	9,61	9,36	9,72	0,03	9,80	9,96	0,01	9,378	9,696	0,025	9,493	9,63
F	0,00	0,00	0,00	0,00	0,00	0,00	0,00	0,00	0,00	0,00	0,00	0,00	0,00	0,00	0,00	0,00	0,00	0,00	0	0	0	0	0
Total	94,02	94,18	94,40	93,90	93,26	93,87	85,01	85,31	93,35	94,05	85,77	94,19	93,82	94,81	86,90	94,76	95,46	87,04	93,746	93,881	86,261	94,685	94,25
Si	5,52	5,56	5,54	5,62	5,50	5,92	4,36	4,12	5,60	5,63	4,36	5,63	5,56	5,69	4,33	5,73	5,68	4,31	5,69	5,71	4,42	5,73	5,72
Al^{IV}	2,48	2,44	2,46	2,38	2,50	2,08	3,64	3,88	2,40	2,37	3,64	2,37	2,44	2,31	3,67	2,27	2,32	3,69	2,31	2,29	3,58	2,27	2,28
Al^{VI}	0,56	0,55	0,51	0,59	0,49	1,14	0,30	0,48	0,52	0,56	0,26	0,43	0,48	0,51	0,33	0,53	0,52	0,30	0,45	0,52	0,23	0,53	0,51
Ti	0,22	0,21	0,22	0,19	0,17	0,17	0,01	0,01	0,18	0,19	0,01	0,21	0,21	0,19	0,01	0,19	0,23	0,01	0,18	0,20	0,01	0,18	0,18
Fe^{2+}	2,38	2,38	2,44	2,36	2,47	1,50	2,47	2,63	2,15	1,97	2,59	2,06	2,04	2,02	2,41	1,76	1,85	2,41	1,77	1,81	2,38	1,79	1,79
Mn	0,03	0,04	0,03	0,03	0,03	0,01	0,03	0,03	0,02	0,01	0,03	0,01	0,01	0,02	0,04	0,02	0,02	0,05	0,03	0,02	0,04	0,02	0,02
Mg	2,60	2,62	2,61	2,57	2,72	2,31	4,82	4,54	2,97	3,04	4,79	3,11	3,10	3,02	4,86	3,24	3,10	4,91	3,39	3,20	5,01	3,26	3,27
Ca	0,01	0,01	0,00	0,00	0,00	0,18	0,02	0,01	0,00	0,00	0,00	0,00	0,00	0,00	0,00	0,01	0,01	0,00	0,01	0,01	0,00	0,02	0,01
Na	0,03	0,03	0,04	0,05	0,04	0,63	0,02	0,01	0,03	0,02	0,00	0,03	0,03	0,02	0,01	0,00	0,00	0,00	0,01	0,00	0,00	0,00	0,00
K	1,88	1,83	1,82	1,90	1,89	1,38	0,02	0,00	1,82	1,88	0,00	1,86	1,82	1,87	0,01	1,86	1,89	0,00	1,80	1,87	0,01	1,81	1,84
Cl	0,00	0,00	0,00	0,00	0,00	0,00	0,00	0,00	0,00	0,00	0,00	0,00	0,00	0,00	0,00	0,00	0,00	0,00	0,00	0,00	0,00	0,00	0,00
F	0,00	0,00	0,00	0,00	0,00	0,00	0,00	0,00	0,00	0,00	0,00	0,00	0,00	0,00	0,00	0,00	0,00	0,00	0,00	0,00	0,00	0,00	0,00
Total	15,70	15,67	15,68	15,68	15,80	15,31	15,68	15,70	15,69	15,67	15,68	15,71	15,69	15,66	15,67	15,61	15,62	15,69	15,65	15,62	15,67	15,60	15,62

Fase	GI		GI	Näsberg					GI					GII		
Litotipo	tonalita		tonalita	gabro norita					tonalita					granodiorita		
Muestra	23j28		23j31	23j84					23k09					24k104		
Análisis	16	17	23	4	5	6	7	10	1	2	4	5	6	13	14	17
Mineral	Mg-Hbl	Mg-Hbl	Fe-Ed	Mg-hst	Mg-hst	Mg-hst	Prg	Mg-hst	Mg-Hbl	Mg-Hbl	Mg-Hbl	Mg-Hbl	Mg-Hbl	Mg-Hbl	Mg-Hbl	Act
SiO_2	46,15	45,42	44,31	42,75	43,98	42,89	43,78	42,74	46,36	47,15	48,1	45,95	46,20	50,04	47,52	52,50
TiO_2	1,50	1,64	4,00	3,84	3,43	3,86	3,7	3,54	1,57	1,36	1,53	1,68	1,55	0,26	0,79	0,12
Al_2O_3	7,14	7,64	16,48	9,61	10,59	10,06	10	9,49	5,78	5,93	6,4	6,22	6,10	3,20	6,09	0,92
Cr_2O_3	0,12	0,07	0,00	0,19	0,1	0,19	0,12	0,02	0,01	0,02	0,05	0,07	0,01	0,10	0,10	0,06
FeO	20,42	20,64	9,63	12,25	11,86	12,49	11,56	11,93	18,82	17,94	18,55	20,72	18,94	17,12	19,48	15,06
MnO	0,51	0,66	0,20	0,21	0,09	0,21	0,2	0,19	0,39	0,52	0,38	0,42	0,35	0,65	0,82	0,12
MgO	9,70	9,12	1,49	13,41	13,72	13,4	13,47	13,51	10,59	11,5	11,26	9,51	10,57	11,98	10,03	14,08
CaO	11,35	11,15	12,49	11,72	11,95	11,72	11,98	11,66	10,73	10,57	10,94	10,87	10,79	11,06	11,12	12,51
Na_2O	1,08	0,84	1,88	2,37	1,87	2,35	2,04	2,51	1,83	1,71	1,49	2,07	1,89	1,15	1,39	0,44
K_2O	0,61	0,78	1,33	0,92	1,04	0,94	0,84	0,91	0,38	0,34	0,35	0,52	0,36	0,28	0,44	0,22
Total	98,58	97,96	91,81	97,27	98,63	98,11	97,69	96,50	96,46	97,04	99,05	98,03	96,76	95,84	97,78	96,03
Si	6,84	6,78	6,78	6,35	6,38	6,31	6,44	6,40	6,99	6,98	6,99	6,91	6,95	7,49	7,08	7,81
Al^{IV}	1,16	1,22	1,22	1,65	1,62	1,69	1,56	1,60	1,01	1,02	1,01	1,09	1,05	0,51	0,92	0,16
T	8,00	8,00	8,00	8,00	8,00	8,00	8,00	8,00	8,00	8,00	8,00	8,00	8,00	8,00	8,00	7,97
Al^{VI}	0,08	0,12	1,76	0,03	0,19	0,05	0,18	0,07	0,02	0,02	0,09	0,01	0,03	0,06	0,14	0,00
Ti	0,17	0,18	0,46	0,43	0,37	0,43	0,41	0,40	0,18	0,15	0,17	0,19	0,18	0,03	0,09	0,01
Cr	0,01	0,01	0,00	0,02	0,01	0,02	0,01	0,00	0,00	0,00	0,01	0,01	0,00	0,01	0,01	0,01
Fe^{3+}	0,70	0,77	0,00	0,15	0,23	0,23	0,03	0,10	0,56	0,78	0,69	0,49	0,58	0,44	0,56	0,03
Fe^{2+}	1,83	1,81	1,23	1,37	1,21	1,31	1,39	1,40	1,81	1,44	1,56	2,12	1,80	1,70	1,87	1,84
Mn	0,06	0,08	0,03	0,03	0,01	0,03	0,02	0,02	0,05	0,07	0,05	0,05	0,04	0,08	0,10	0,02
Mg	2,14	2,03	0,34	2,97	2,97	2,94	2,95	3,01	2,38	2,54	2,44	2,13	2,37	2,67	2,23	3,12
C	5,00	5,00	3,81	5,00	5,00	5,00	5,00	5,00	5,00	5,00	5,00	5,00	5,00	5,00	5,00	5,03
Ca	1,80	1,78	2,05	1,86	1,86	1,85	1,89	1,87	1,73	1,68	1,70	1,75	1,74	1,77	1,77	1,99
Na	0,20	0,22	-0,05	0,14	0,14	0,15	0,11	0,13	0,27	0,32	0,30	0,25	0,26	0,23	0,23	0,01
B	2,00	2,00	2,00	2,00	2,00	2,00	2,00	2,00	2,00	2,00	2,00	2,00	2,00	2,00	2,00	2,00
Na	0,11	0,03	0,61	0,55	0,38	0,52	0,47	0,60	0,27	0,17	0,12	0,35	0,29	0,11	0,18	0,12
K	0,12	0,15	0,26	0,17	0,19	0,18	0,16	0,17	0,07	0,06	0,06	0,10	0,07	0,05	0,08	0,04
A	0,23	0,17	0,87	0,72	0,58	0,69	0,63	0,77	0,34	0,23	0,19	0,45	0,36	0,16	0,26	0,16

Fase	Rengård, tipo GI				Rengård, tipo GI													
Litotipo	tonalita				tonalita													
Muestra	JO03-108				JO03-109													
Análisis	1	6	9	15	1	2	3	4	6	7	8	10	12	13	15	16	17	18
Mineral	Fe-Hbl	Fe-Hbl	Fe-Hbl	Fe-Hbl	Fe-Ts	Fe-Hbl	Fe-Ts	Fe-Ts	Fe-Ts	Fe-Hbl	Fe-Ts	Fe-Ts	Fe-Hbl	Fe-Ts	Fe-Ts	Fe-Ts	Fe-Ts	Fe-Ts
SiO_2	45,61	44,29	43,56	44,68	40,22	43,82	41,45	42,41	40,40	44,97	40,24	42,44	43,36	38,80	40,06	41,88	39,74	39,15
TiO_2	0,98	0,88	0,89	0,84	0,25	0,38	0,17	0,40	0,31	0,33	0,59	0,59	0,60	0,30	0,06	0,36	0,20	0,27
Al_2O_3	7,24	6,88	7,06	7,40	15,22	11,91	15,49	14,29	15,15	9,46	14,66	14,05	9,99	15,05	15,36	13,20	14,86	14,91
Cr_2O_3	0,00	0,00	0,00	0,00	0,00	0,00	0,00	0,00	0,00	0,00	0,00	0,00	0,00	0,00	0,00	0,00	0,00	0,00
FeO	21,41	20,87	21,35	20,73	22,13	21,53	22,05	21,66	21,63	21,45	22,74	21,09	20,58	20,46	21,27	21,78	20,61	21,60
MnO	0,68	0,81	0,87	0,85	0,54	0,55	0,49	0,48	0,41	0,42	0,49	0,47	0,56	0,39	0,44	0,37	0,18	0,40
MgO	7,45	7,18	6,59	7,14	4,72	6,63	4,82	5,35	4,51	7,13	4,84	5,56	6,62	4,36	4,55	5,68	4,49	4,36
CaO	10,89	10,70	10,70	10,86	11,25	11,14	11,28	11,45	11,34	11,03	11,24	11,21	10,38	10,61	11,29	11,04	10,85	10,76
Na_2O	1,11	1,17	0,91	1,16	1,40	1,43	1,29	1,32	1,69	1,18	1,36	1,64	1,06	1,47	1,31	1,38	1,54	1,50
K_2O	0,55	0,67	0,66	0,69	0,47	0,40	0,46	0,46	0,47	0,32	0,41	0,50	0,45	0,38	0,49	0,44	0,45	0,56
Total	95,92	93,45	92,59	94,35	96,20	97,79	97,50	97,82	95,91	96,29	96,57	97,55	93,60	91,82	94,83	96,13	92,92	93,51
Si	7,02	7,03	6,99	7,02	6,20	6,59	6,28	6,41	6,28	6,85	6,18	6,43	6,78	6,25	6,26	6,43	6,34	6,22
Al^{IV}	0,98	0,97	1,01	0,98	1,80	1,41	1,72	1,59	1,72	1,15	1,82	1,57	1,22	1,75	1,74	1,57	1,66	1,78
T	8,00	8,00	8,00	8,00	8,00	8,00	8,00	8,00	8,00	8,00	8,00	8,00	8,00	8,00	8,00	8,00	8,00	8,00
Al^{VI}	0,33	0,32	0,33	0,39	0,96	0,70	1,04	0,95	1,05	0,55	0,84	0,94	0,62	1,11	1,09	0,82	1,13	1,01
Ti	0,11	0,11	0,11	0,10	0,03	0,04	0,02	0,05	0,04	0,04	0,07	0,07	0,07	0,04	0,01	0,04	0,02	0,03
Cr	0,00	0,00	0,00	0,00	0,00	0,00	0,00	0,00	0,00	0,00	0,00	0,00	0,00	0,00	0,00	0,00	0,00	0,00
Fe^{3+}	0,39	0,31	0,36	0,24	0,55	0,55	0,52	0,37	0,22	0,50	0,66	0,27	0,57	0,37	0,35	0,55	0,20	0,47
Fe^{2+}	2,37	2,46	2,51	2,48	2,30	2,15	2,27	2,37	2,59	2,23	2,26	2,40	2,12	2,39	2,43	2,25	2,55	2,40
Mn	0,09	0,11	0,12	0,11	0,07	0,07	0,06	0,06	0,05	0,05	0,06	0,06	0,07	0,05	0,06	0,05	0,02	0,05
Mg	1,71	1,70	1,58	1,67	1,08	1,49	1,09	1,21	1,04	1,62	1,11	1,26	1,54	1,05	1,06	1,30	1,07	1,03
C	5,00	5,00	5,00	5,00	5,00	5,00	5,00	5,00	5,00	5,00	5,00	5,00	5,00	5,00	5,00	5,00	5,00	5,00
Ca	1,80	1,82	1,84	1,83	1,86	1,79	1,83	1,85	1,89	1,80	1,85	1,82	1,74	1,83	1,89	1,82	1,85	1,83
Na	0,20	0,18	0,16	0,17	0,14	0,21	0,17	0,15	0,11	0,20	0,15	0,18	0,26	0,17	0,11	0,18	0,15	0,17
B	2,00	2,00	2,00	2,00	2,00	2,00	2,00	2,00	2,00	2,00	2,00	2,00	2,00	2,00	2,00	2,00	2,00	2,00
Na	0,13	0,18	0,12	0,18	0,28	0,21	0,21	0,24	0,40	0,15	0,26	0,30	0,06	0,29	0,29	0,23	0,33	0,29
K	0,11	0,14	0,14	0,14	0,09	0,08	0,09	0,09	0,09	0,06	0,08	0,10	0,09	0,08	0,10	0,09	0,09	0,11
A	0,23	0,32	0,26	0,32	0,37	0,29	0,30	0,33	0,49	0,21	0,34	0,40	0,15	0,37	0,39	0,31	0,42	0,41

Fase	Rengård, tipo GI												Rengård, tipo GI					
Litotipo	tonalita												tonalita					
Muestra	JO03-109 cont.												JO03-110					
Análisis	19	20	21	22	24	26a	26b	28	29	30	33	36	1	2	4	5	8	9
Mineral	Fe-Hbl	Fe-Ts	Fe-Ts	Fe-Hbl	Fe-Ts	Fe-Ts	Fe-Ts	Fe-Ts	Fe-Ts	Fe-Ts	Fe-Ts	Fe-Ts	Fe-Ts	Fe-Hbl	Fe-Ts	Fe-Ts	Fe-Ts	Fe-Hbl
SiO_2	43,53	39,66	39,80	42,62	39,85	39,93	39,10	39,51	40,11	39,06	40,24	38,09	45,32	39,56	40,14	39,49	43,86	41,05
TiO_2	0,77	0,40	0,35	0,52	0,24	0,09	0,28	0,30	0,30	0,25	0,35	0,37	1,17	0,37	0,32	0,36	1,47	0,51
Al_2O_3	9,71	15,26	14,43	10,38	15,02	17,17	14,94	14,73	15,12	14,89	14,73	15,75	7,53	13,71	13,11	15,62	7,20	12,82
Cr_2O_3	0,00	0,00	0,00	0,00	0,00	0,00	0,00	0,00	0,00	0,00	0,00	0,00	0,00	0,00	0,00	0,00	0,00	0,00
FeO	21,32	20,78	20,37	19,73	20,71	20,69	21,38	20,90	20,84	21,37	21,14	20,85	18,96	21,84	21,84	21,37	19,47	21,48
MnO	0,51	0,51	0,43	0,52	0,74	0,36	0,66	0,55	0,52	0,48	0,27	0,61	0,78	0,64	0,80	0,82	0,77	0,78
MgO	6,66	4,83	4,96	6,74	4,82	4,07	4,62	4,47	4,63	4,74	4,85	3,84	8,82	4,69	4,68	3,97	7,82	5,16
CaO	10,08	10,97	10,69	10,78	10,38	10,82	10,63	10,57	11,06	10,65	10,51	10,79	10,46	10,88	10,64	10,72	9,70	10,62
Na_2O	1,19	1,34	1,58	1,30	1,30	1,44	1,69	1,42	1,54	1,26	1,55	1,56	0,98	1,62	1,30	1,37	1,14	1,52
K_2O	0,53	0,55	0,42	0,36	0,39	0,45	0,49	0,56	0,48	0,54	0,47	0,48	0,45	0,67	0,67	0,48	0,46	0,47
Total	94,30	94,30	93,03	92,95	93,45	95,02	93,79	93,01	94,60	93,24	94,11	92,34	94,47	93,98	93,50	94,20	91,89	94,41
Si	6,76	6,22	6,32	6,74	6,25	6,19	6,18	6,29	6,29	6,18	6,30	6,14	6,95	6,29	6,38	6,21	6,95	6,44
Al^{IV}	1,24	1,78	1,68	1,26	1,75	1,81	1,82	1,71	1,71	1,82	1,70	1,86	1,05	1,71	1,62	1,79	1,05	1,56
T	8,00	8,00	8,00	8,00	8,00	8,00	8,00	8,00	8,00	8,00	8,00	8,00	8,00	8,00	8,00	8,00	8,00	8,00
Al^{VI}	0,53	1,03	1,02	0,67	1,03	1,32	0,96	1,05	1,08	0,96	1,02	1,14	0,31	0,86	0,84	1,11	0,29	0,81
Ti	0,09	0,05	0,04	0,06	0,03	0,01	0,03	0,04	0,04	0,03	0,04	0,04	0,14	0,04	0,04	0,04	0,18	0,06
Cr	0,00	0,00	0,00	0,00	0,00	0,00	0,00	0,00	0,00	0,00	0,00	0,00	0,00	0,00	0,00	0,00	0,00	0,00
Fe^{3+}	0,71	0,46	0,37	0,34	0,70	0,36	0,57	0,44	0,28	0,69	0,50	0,32	0,65	0,43	0,54	0,47	0,67	0,50
Fe^{2+}	2,06	2,27	2,34	2,26	2,02	2,32	2,25	2,34	2,45	2,14	2,27	2,50	1,79	2,47	2,37	2,34	1,91	2,32
Mn	0,07	0,07	0,06	0,07	0,10	0,05	0,09	0,07	0,07	0,06	0,04	0,08	0,10	0,09	0,11	0,11	0,10	0,10
Mg	1,54	1,13	1,17	1,59	1,13	0,94	1,09	1,06	1,08	1,12	1,13	0,92	2,02	1,11	1,11	0,93	1,85	1,21
C	5,00	5,00	5,00	5,00	5,00	5,00	5,00	5,00	5,00	5,00	5,00	5,00	5,00	5,00	5,00	5,00	5,00	5,00
Ca	1,68	1,84	1,82	1,83	1,74	1,80	1,80	1,80	1,86	1,81	1,76	1,86	1,72	1,85	1,81	1,81	1,65	1,79
Na	0,32	0,16	0,18	0,17	0,26	0,20	0,20	0,20	0,14	0,19	0,24	0,14	0,28	0,15	0,19	0,19	0,35	0,21
B	2,00	2,00	2,00	2,00	2,00	2,00	2,00	2,00	2,00	2,00	2,00	2,00	2,00	2,00	2,00	2,00	2,00	2,00
Na	0,03	0,25	0,31	0,22	0,14	0,23	0,32	0,24	0,33	0,19	0,23	0,35	0,01	0,35	0,21	0,22	0,00	0,25
K	0,10	0,11	0,09	0,07	0,08	0,09	0,10	0,11	0,10	0,11	0,09	0,10	0,09	0,14	0,14	0,10	0,09	0,09
A	0,14	0,36	0,39	0,30	0,22	0,32	0,42	0,35	0,42	0,30	0,33	0,45	0,10	0,49	0,35	0,32	0,09	0,34

Fase	Rengård, tipo GI																				
Litotipo	tonalita																				
Muestra	JO03-110 cont.																				
Análisis	12	13	17	18	19	20	21	23	26	27	29	30	31	33	34	35	38	39	40	43	44
Mineral	Fe-Ts	Fe-Ts	Fe-Hbl	Fe-Ts	Fe-Hbl	Fe-Ts	Fe-Ts	Fe-Ts	Fe-Ts	Fe-Ts	Fe-Ts	Fe-Ts	Fe-Ts	Fe-Ts	Fe-Ts	Fe-Ts	Fe-Ts	Fe-Ts	Fe-Hbl	Mg-Hbl	Mg-Hbl
SiO_2	39,02	39,09	44,10	40,58	42,85	40,40	40,72	41,37	41,69	39,34	40,03	38,13	38,43	39,22	38,35	37,77	39,59	40,23	43,28	39,34	43,93
TiO_2	0,19	0,15	0,66	0,35	0,71	0,37	0,29	0,26	0,37	0,23	0,33	0,46	0,47	0,43	0,37	0,47	0,52	0,48	1,55	0,54	1,46
Al_2O_3	15,43	14,28	9,76	14,26	11,51	15,17	14,51	15,23	15,46	15,53	13,55	12,94	14,80	14,31	14,85	13,59	14,89	12,09	7,47	13,64	7,31
Cr_2O_3	0,00	0,00	0,00	0,00	0,00	0,00	0,00	0,00	0,00	0,00	0,00	0,00	0,00	0,00	0,00	0,00	0,00	0,00	0,00	0,00	0,00
FeO	22,30	21,01	21,12	21,71	21,05	22,11	22,77	22,39	23,01	22,22	21,22	21,29	20,82	21,79	20,87	21,77	21,00	21,67	19,67	22,02	19,02
MnO	0,80	0,87	0,49	0,57	1,00	0,61	0,70	0,88	0,74	0,76	0,57	0,82	0,58	0,67	0,90	0,59	0,59	0,58	0,99	0,63	0,76
MgO	3,68	4,10	6,72	4,48	6,19	4,11	4,47	4,35	4,62	4,18	4,67	4,21	3,88	4,35	4,31	4,18	4,20	4,95	7,43	3,99	8,77
CaO	10,95	10,57	11,05	11,06	11,03	11,13	11,16	11,42	11,37	10,76	10,91	10,38	10,52	10,72	10,26	10,53	10,78	10,44	9,90	10,59	9,61
Na_2O	1,56	1,62	1,06	1,61	1,54	1,44	1,67	1,08	1,63	1,47	1,35	1,45	1,46	1,23	1,52	1,31	1,45	1,46	1,06	1,59	1,05
K_2O	0,68	0,52	0,47	0,73	0,39	0,66	0,59	0,64	0,60	0,60	0,72	0,64	0,42	0,66	0,31	0,57	0,48	0,44	0,41	0,59	0,38
Total	94,61	92,21	95,43	95,35	96,27	96,00	96,88	97,62	99,49	95,09	93,35	90,32	91,38	93,38	91,74	90,78	93,50	92,34	91,76	92,93	92,29
Si	6,17	6,32	6,81	6,36	6,58	6,28	6,28	6,29	6,23	6,14	6,39	6,31	6,25	6,24	6,17	6,21	6,29	6,47	6,89	6,34	6,86
Al^{IV}	1,83	1,68	1,19	1,64	1,42	1,72	1,72	1,71	1,77	1,86	1,61	1,69	1,75	1,76	1,83	1,79	1,71	1,53	1,11	1,66	1,14
T	8,00	8,00	8,00	8,00	8,00	8,00	8,00	8,00	8,00	8,00	8,00	8,00	8,00	8,00	8,00	8,00	8,00	8,00	8,00	8,00	8,00
Al^{VI}	1,05	1,04	0,59	0,99	0,67	1,05	0,91	1,02	0,96	1,00	0,94	0,84	1,09	0,93	0,99	0,84	1,08	0,76	0,30	0,93	0,20
Ti	0,02	0,02	0,08	0,04	0,08	0,04	0,03	0,03	0,04	0,03	0,04	0,06	0,06	0,05	0,04	0,06	0,06	0,06	0,19	0,07	0,17
Cr	0,00	0,00	0,00	0,00	0,00	0,00	0,00	0,00	0,00	0,00	0,00	0,00	0,00	0,00	0,00	0,00	0,00	0,00	0,00	0,00	0,00
Fe^{3+}	0,40	0,34	0,39	0,22	0,42	0,32	0,44	0,46	0,50	0,64	0,30	0,45	0,33	0,56	0,67	0,59	0,30	0,51	0,65	0,34	0,99
Fe^{2+}	2,55	2,50	2,34	2,63	2,28	2,56	2,49	2,39	2,38	2,26	2,54	2,50	2,50	2,34	2,14	2,41	2,49	2,41	1,97	2,63	1,50
Mn	0,11	0,12	0,06	0,08	0,13	0,08	0,09	0,11	0,09	0,10	0,08	0,12	0,08	0,09	0,12	0,08	0,08	0,08	0,13	0,09	0,10
Mg	0,87	0,99	1,55	1,05	1,42	0,95	1,03	0,99	1,03	0,97	1,11	1,04	0,94	1,03	1,03	1,02	0,99	1,19	1,76	0,96	2,04
C	5,00	5,00	5,00	5,00	5,00	5,00	5,00	5,00	5,00	5,00	5,00	5,00	5,00	5,00	5,00	5,00	5,00	5,00	5,00	5,00	5,00
Ca	1,86	1,83	1,83	1,86	1,82	1,85	1,84	1,86	1,82	1,80	1,87	1,84	1,83	1,83	1,77	1,85	1,83	1,80	1,69	1,83	1,61
Na	0,14	0,17	0,17	0,14	0,18	0,15	0,16	0,14	0,18	0,20	0,13	0,16	0,17	0,17	0,23	0,15	0,17	0,20	0,31	0,17	0,32
B	2,00	2,00	2,00	2,00	2,00	2,00	2,00	2,00	2,00	2,00	2,00	2,00	2,00	2,00	2,00	2,00	2,00	2,00	2,00	2,00	1,93
Na	0,33	0,34	0,15	0,35	0,27	0,29	0,34	0,18	0,29	0,24	0,28	0,31	0,29	0,21	0,24	0,27	0,28	0,25	0,02	0,32	0,00
K	0,14	0,11	0,09	0,15	0,08	0,13	0,12	0,12	0,11	0,12	0,15	0,14	0,09	0,13	0,06	0,12	0,10	0,09	0,08	0,12	0,08
A	0,47	0,44	0,24	0,49	0,35	0,42	0,46	0,30	0,41	0,36	0,43	0,44	0,38	0,34	0,31	0,39	0,38	0,34	0,10	0,44	0,08

Fase	GII						GII							GII				
Litotipo	granodiorita						granodiorita							granodiorita				
Muestra	JO03-38b						JO03-67							JO03-80b				
Análisis	1	2	3	8	9	12	1	2	3	8	9	13	14	6	7	8	9	10
Mineral	Mg-Hbl	Ed	Mg-Hbl	Mg-Hbl	Mg-Hbl	Mg-Hbl	Mg-Hbl	Mg-Hbl	Mg-Hbl	Mg-Hbl	Mg-Hbl	Mg-Hbl	Mg-Hbl	Mg-Hbl	Mg-Hbl	Mg-Hbl	Mg-Hbl	Mg-Hbl
SiO_2	49,84	50,72	49,48	46,75	46,65	46,84	49,14	49,22	48,63	50,02	52,26	49,20	48,75	49,06	46,96	46,23	46,15	44,71
TiO_2	1,22	0,88	1,62	1,49	1,24	1,35	1,25	1,32	1,07	0,28	0,61	1,05	1,41	0,74	1,56	1,34	1,54	1,58
Al_2O_3	5,45	4,09	5,62	5,53	5,21	5,98	5,63	5,43	5,48	4,82	3,52	5,22	5,55	3,76	5,96	5,65	5,82	5,69
Cr_2O_3	0,06	0,14	0,09	0,10	0,13	0,01	0,09	0,08	0,08	0,07	0,20	0,19	0,06	0,09	0,16	0,01	0,05	0,14
FeO	13,48	12,15	14,38	13,21	13,93	14,63	13,46	13,60	14,51	14,54	11,71	13,01	14,29	20,25	18,12	21,56	18,5	20
MnO	1,00	1,07	0,90	0,81	0,81	0,78	1,07	0,81	1,01	0,75	0,94	1,07	0,93	0,40	0,31	0,67	0,35	0,26
MgO	14,34	13,71	14,16	13,16	13,17	13,33	14,44	14,33	13,77	13,48	15,10	14,48	14,14	10,78	11,34	8,91	10,77	9,61
CaO	12,39	15,35	12,25	11,56	11,63	11,58	12,09	12,32	12,38	12,51	14,02	11,92	11,63	10,92	10,77	10,43	10,6	10,33
Na_2O	1,15	0,69	0,94	0,97	1,04	1,02	1,17	1,40	0,89	0,84	0,59	1,28	1,14	1,13	1,50	1,37	2,13	1,55
K_2O	0,52	0,46	0,78	0,62	0,54	0,66	0,67	0,59	0,58	0,18	0,34	0,47	0,62	0,39	0,39	0,59	0,39	0,51
Total	99,45	99,26	100,22	94,20	94,35	96,18	99,01	99,10	98,40	97,49	99,29	97,89	98,52	97,52	97,07	96,76	96,30	94,38
Si	7,14	7,33	7,05	7,08	7,07	6,95	7,06	7,10	7,07	7,32	7,47	7,13	7,02	7,29	6,97	7,01	6,97	6,92
Al^{IV}	0,86	0,67	0,94	0,92	0,93	1,04	0,94	0,90	0,93	0,68	0,53	0,87	0,94	0,66	1,03	0,99	1,03	1,04
T	8,00	8,00	7,99	8,00	8,00	7,99	8,00	8,00	8,00	8,00	8,00	8,00	7,97	7,95	8,00	8,00	8,00	7,96
Al^{VI}	0,06	0,03	0,00	0,07	0,00	0,00	0,01	0,03	0,00	0,15	0,07	0,03	0,00	0,00	0,01	0,01	0,01	0,00
Ti	0,13	0,10	0,17	0,17	0,14	0,15	0,14	0,14	0,12	0,03	0,07	0,11	0,15	0,08	0,17	0,15	0,18	0,18
Cr	0,01	0,02	0,01	0,01	0,02	0,00	0,01	0,01	0,01	0,01	0,02	0,02	0,01	0,01	0,02	0,00	0,01	0,02
Fe^{3+}	0,31	0,00	0,47	0,34	0,45	0,67	0,47	0,27	0,47	0,27	0,00	0,44	0,67	0,70	0,72	0,77	0,53	0,74
Fe^{2+}	1,31	1,47	1,24	1,33	1,32	1,15	1,14	1,37	1,29	1,51	1,40	1,14	1,05	1,81	1,52	1,96	1,81	1,84
Mn	0,12	0,13	0,11	0,10	0,10	0,10	0,13	0,10	0,12	0,09	0,11	0,13	0,11	0,05	0,04	0,09	0,04	0,03
Mg	3,06	2,96	3,01	2,97	2,98	2,95	3,09	3,08	2,98	2,94	3,22	3,13	3,04	2,39	2,51	2,01	2,43	2,22
C	5,00	4,70	5,01	5,00	5,00	5,01	5,00	5,00	5,00	5,00	4,89	5,00	5,03	5,05	5,00	5,00	5,00	5,04
Ca	1,90	2,38	1,87	1,88	1,89	1,84	1,86	1,90	1,93	1,96	2,15	1,85	1,80	1,74	1,71	1,69	1,72	1,71
Na	0,10	-0,38	0,13	0,12	0,11	0,16	0,14	0,10	0,07	0,04	-0,15	0,15	0,20	0,26	0,29	0,31	0,28	0,29
B	2,00	2,00	2,00	2,00	2,00	2,00	2,00	2,00	2,00	2,00	2,00	2,00	2,00	2,00	2,00	2,00	2,00	2,00
Na	0,22	0,57	0,13	0,16	0,19	0,13	0,19	0,30	0,18	0,20	0,31	0,21	0,11	0,06	0,14	0,10	0,34	0,18
K	0,10	0,08	0,14	0,12	0,10	0,12	0,12	0,11	0,11	0,03	0,06	0,09	0,11	0,07	0,07	0,11	0,08	0,10
A	0,32	0,66	0,27	0,28	0,30	0,26	0,31	0,40	0,29	0,23	0,37	0,30	0,23	0,14	0,22	0,21	0,42	0,28

Fase	GII		Näsberg	Näsberg		Näsberg		Näsberg			Näsberg	Näsberg	GI				
Litotipo	granodiorita		norita	gabro norita		gabro norita		gabro norita			norita	norita	tonalita de grano medio				
Muestra	JO03-80a		A28	A53		A80		S110			S128	S128	23j28 epma				
Análisis	14	15	11	9	12	14	15	4	10	27	19	2	19	21	24	31	32
Mineral	Mg-Hbl	Mg-Hbl	Prg	Prg	Fe-Hbl	Mg-Hs	Mg-Hbl	Krs	Krs	Krs	Mg-Hs	Mg-Hs	Mg-Hbl	Mg-Hbl	Mg-Hbl	Mg-Hbl	Mg-Hbl
SiO_2	46,15	44,42	41,17	42,35	45,64	42,77	46,14	41,42	43,12	41,89	42,29	44,50	44,65	43,59	44,27	44,44	45,07
TiO_2	1,26	1,36	3,82	3,74	0,00	3,41	2,21	4,44	4,56	4,74	3,86	3,22	1,40	1,56	1,53	0,23	1,40
Al_2O_3	4,84	5,08	9,58	10,45	8,31	9,71	7,99	9,52	10,41	9,71	10,42	9,97	8,19	7,95	8,18	8,21	7,97
Cr_2O_3	0,00	0,00	0,00	0,00	0,00	0,00	0,00	0,62	0,00	0,77	0,00	0,00	0,05	0,00	0,00	0,03	0,06
FeO	19,69	19,13	11,83	12,20	19,64	12,49	12,28	9,34	9,25	9,55	11,38	14,84	19,58	19,90	19,86	20,67	20,06
MnO	0,58	0,38	0,00	0,00	0,32	0,00	0,00	0,00	0,00	0,00	0,00	0,00	0,36	0,47	0,47	0,46	0,46
MgO	10,07	9,53	12,23	12,48	9,17	12,71	13,85	13,66	14,58	13,88	13,45	12,49	9,63	9,10	9,04	8,52	9,23
CaO	9,82	10,33	10,95	11,70	11,69	11,39	11,56	11,37	11,66	11,54	11,53	11,99	10,59	10,75	10,69	11,61	10,77
Na_2O	1,67	1,40	1,97	2,44	1,87	1,81	1,04	2,60	2,61	2,63	2,24	1,95	1,23	1,02	1,16	0,97	0,94
K_2O	0,31	0,43	0,93	0,99	0,00	0,71	0,69	0,84	0,85	0,86	0,92	0,96	0,77	0,73	0,74	0,70	0,74
Total	94,39	92,06	92,48	96,35	96,64	95,00	95,76	93,81	97,04	95,57	96,09	99,92	96,44	95,07	95,93	95,83	96,68
Si	7,08	7,05	6,41	6,36	6,92	6,45	6,81	6,33	6,34	6,29	6,32	6,45	6,72	6,69	6,73	6,82	6,77
Al^{IV}	0,87	0,95	1,59	1,64	1,08	1,55	1,19	1,67	1,66	1,71	1,68	1,55	1,28	1,31	1,27	1,18	1,23
T	7,95	8,00	8,00	8,00	8,00	8,00	8,00	8,00	8,00	8,00	8,00	8,00	8,00	8,00	8,00	8,00	8,00
Al^{VI}	0,00	0,00	0,17	0,21	0,40	0,18	0,19	0,04	0,14	0,01	0,15	0,15	0,17	0,12	0,19	0,31	0,19
Ti	0,15	0,16	0,45	0,42	0,00	0,39	0,25	0,51	0,50	0,54	0,43	0,35	0,16	0,18	0,17	0,03	0,16
Cr	0,00	0,00	0,00	0,00	0,00	0,00	0,00	0,07	0,00	0,09	0,00	0,00	0,01	0,00	0,00	0,00	0,01
Fe^{3+}	0,90	0,61	0,09	0,00	0,34	0,25	0,43	0,00	0,00	0,00	0,15	0,25	0,87	0,85	0,76	0,57	0,83
Fe^{2+}	1,63	1,93	1,45	1,53	2,15	1,33	1,09	1,19	1,14	1,20	1,27	1,55	1,59	1,71	1,76	2,08	1,69
Mn	0,08	0,05	0,00	0,00	0,04	0,00	0,00	0,00	0,00	0,00	0,00	0,00	0,05	0,06	0,06	0,06	0,06
Mg	2,30	2,25	2,84	2,79	2,07	2,86	3,05	3,11	3,19	3,11	2,99	2,70	2,16	2,08	2,05	1,95	2,07
C	5,05	5,00	5,00	4,96	5,00	5,00	5,00	4,94	4,97	4,95	5,00	5,00	5,00	5,00	5,00	5,00	5,00
Ca	1,61	1,76	1,83	1,88	1,90	1,84	1,83	1,86	1,84	1,86	1,84	1,86	1,71	1,77	1,74	1,91	1,73
Na	0,39	0,24	0,17	0,12	0,10	0,16	0,17	0,14	0,16	0,14	0,16	0,14	0,29	0,23	0,26	0,09	0,27
B	2,00	2,00	2,00	2,00	2,00	2,00	2,00	2,00	2,00	2,00	2,00	2,00	2,00	2,00	2,00	2,00	2,00
Na	0,11	0,19	0,42	0,59	0,45	0,37	0,12	0,63	0,58	0,62	0,49	0,41	0,07	0,07	0,08	0,20	0,01
K	0,06	0,09	0,18	0,19	0,00	0,14	0,13	0,16	0,16	0,16	0,18	0,18	0,15	0,14	0,14	0,14	0,14
A	0,17	0,27	0,61	0,78	0,45	0,51	0,25	0,80	0,74	0,79	0,67	0,59	0,21	0,21	0,23	0,33	0,15

Fase	GII																
Litotipo	granodiorita																
Muestra	JO03-67 epma																
Análisis	14	15	16	17	18	19	20	21	24	25	27	31	32	34	35	36	51
Mineral	Mg-Hbl	Mg-Hbl	Mg-Hbl	Mg-Hbl	Mg-Hbl	Mg-Hbl	Mg-Hbl	Mg-Hbl	Mg-Hbl	Mg-Hbl	Mg-Hbl	Mg-Hbl	Mg-Hbl	Mg-Hbl	Ed	Ed	Mg-Hbl
SiO_2	48,53	48,26	48,15	49,20	47,02	49,53	47,37	48,08	46,69	49,30	47,62	47,53	48,34	48,16	49,91	49,12	46,53
TiO_2	0,65	0,71	1,04	0,51	1,02	0,45	1,17	0,13	1,43	0,49	1,00	1,16	1,04	1,15	0,45	0,37	1,11
Al_2O_3	5,83	5,91	5,47	4,78	6,43	5,03	6,25	5,58	6,73	5,07	6,15	5,70	5,76	5,86	2,87	2,58	6,70
Cr_2O_3	0,00	0,13	0,02	0,00	0,02	0,04	0,06	0,06	0,07	0,01	0,00	0,00	0,09	0,00	0,41	0,42	0,00
FeO	13,34	13,75	12,47	12,69	13,51	12,37	13,00	13,07	13,15	12,44	13,73	12,75	13,12	13,76	10,29	9,55	13,90
MnO	0,61	0,65	0,76	0,67	0,71	0,70	0,72	0,59	0,63	0,64	0,68	0,68	0,73	0,74	0,75	0,84	0,69
MgO	13,37	13,92	14,48	13,52	13,59	14,50	13,66	13,85	13,64	14,77	13,39	14,43	14,36	13,24	14,26	13,07	13,56
CaO	11,84	11,46	11,65	11,94	11,74	11,93	11,52	12,73	11,57	12,01	11,92	11,12	11,79	12,09	16,25	19,35	11,72
Na_2O	0,60	0,51	0,75	0,49	0,79	0,47	0,78	0,55	0,75	0,59	0,59	1,15	0,63	0,59	0,49	0,50	0,72
K_2O	0,49	0,49	0,53	0,34	0,61	0,51	0,65	0,33	0,66	0,38	0,58	0,59	0,52	0,59	0,21	0,17	0,62
Total	95,26	95,77	95,30	94,13	95,43	95,54	95,18	94,98	95,32	95,68	95,66	95,12	96,38	96,17	95,87	95,96	95,54
Si	7,21	7,08	7,11	7,39	6,98	7,28	7,04	7,19	6,93	7,23	7,06	7,03	7,06	7,13	7,43	7,37	6,90
Al^{IV}	0,79	0,92	0,89	0,61	1,02	0,72	0,96	0,81	1,07	0,77	0,94	0,97	0,94	0,87	0,50	0,46	1,10
T	8,00	8,00	8,00	8,00	8,00	8,00	8,00	8,00	8,00	8,00	8,00	8,00	8,00	8,00	7,93	7,82	8,00
Al^{VI}	0,23	0,10	0,06	0,24	0,11	0,16	0,13	0,18	0,11	0,11	0,14	0,03	0,06	0,15	0,00	0,00	0,07
Ti	0,07	0,08	0,11	0,06	0,11	0,05	0,13	0,01	0,16	0,05	0,11	0,13	0,11	0,13	0,05	0,04	0,12
Cr	0,00	0,01	0,00	0,00	0,00	0,01	0,01	0,01	0,01	0,00	0,00	0,00	0,01	0,00	0,05	0,05	0,00
Fe^{3+}	0,38	0,81	0,60	0,21	0,60	0,47	0,55	0,29	0,62	0,53	0,50	0,72	0,68	0,35	0,00	0,00	0,74
Fe^{2+}	1,28	0,87	0,94	1,39	1,08	1,06	1,06	1,35	1,01	0,99	1,20	0,86	0,93	1,36	1,28	1,20	0,99
Mn	0,08	0,08	0,09	0,08	0,09	0,09	0,09	0,08	0,08	0,08	0,09	0,09	0,09	0,09	0,09	0,11	0,09
Mg	2,96	3,04	3,19	3,03	3,01	3,18	3,03	3,09	3,02	3,23	2,96	3,18	3,13	2,92	3,16	2,92	3,00
C	5,00	5,00	5,00	5,00	5,00	5,00	5,00	5,00	5,00	5,00	5,00	5,00	5,00	5,00	4,64	4,32	5,00
Ca	1,88	1,80	1,84	1,92	1,87	1,88	1,83	2,04	1,84	1,89	1,89	1,76	1,85	1,92	2,59	3,11	1,86
Na	0,12	0,15	0,16	0,08	0,13	0,12	0,17	-0,04	0,16	0,11	0,11	0,24	0,15	0,08	-0,59	-1,11	0,14
B	2,00	1,95	2,00	2,00	2,00	2,00	2,00	2,00	2,00	2,00	2,00	2,00	2,00	2,00	2,00	2,00	2,00
Na	0,06	0,00	0,06	0,06	0,10	0,01	0,06	0,20	0,06	0,06	0,06	0,09	0,03	0,09	0,73	1,26	0,07
K	0,09	0,09	0,10	0,06	0,12	0,10	0,12	0,06	0,12	0,07	0,11	0,11	0,10	0,11	0,04	0,03	0,12
A	0,15	0,09	0,16	0,13	0,21	0,11	0,18	0,26	0,18	0,13	0,17	0,20	0,12	0,20	0,77	1,29	0,19

Fase	GII											Rengård, tipo GI						
Litotipo	enclave en granodiorita											tonalita						
Muestra	JO03-67 epma											JO03-109						
Análisis	2	3	5	6	7	10	11	41	45	50	55	3	5	10	11	12	14	22
Mineral	Mg-Hbl	Mg-Hbl	Mg-Hbl	Mg-Hbl	Mg-Hbl	Mg-Hbl	Mg-Hbl	Mg-Hbl	Mg-Hbl	Mg-Hbl	Mg-Hbl	Fe-Ts	Fe-Ts	Fe-Ts	Fe-Ts	Fe-Ts	Mg-Hbl	Fe-Ts
SiO_2	47,46	47,41	48,92	48,36	46,67	47,61	42,37	49,12	46,08	45,97	47,41	40,04	40,61	39,62	40,56	39,18	44,01	39,23
TiO_2	1,28	1,12	0,92	1,06	1,33	1,31	0,91	0,98	1,25	1,26	0,49	0,26	0,27	0,28	0,24	0,24	0,70	0,49
Al_2O_3	6,77	6,68	5,68	6,51	6,82	6,40	5,68	6,19	6,68	6,77	5,87	15,81	15,01	15,78	14,12	16,10	9,38	15,67
Cr_2O_3	0,00	0,04	0,04	0,01	0,01	0,00	0,02	0,06	0,00	0,05	0,00	0,01	0,03	0,00	0,00	0,05	0,08	0,01
FeO	12,82	13,82	12,52	12,97	13,29	13,01	12,62	13,35	13,03	13,63	13,39	22,41	22,19	22,80	22,48	22,05	21,76	22,37
MnO	0,62	0,74	0,66	0,69	0,70	0,77	0,70	0,66	0,77	0,75	0,65	0,38	0,46	0,40	0,44	0,45	0,50	0,37
MgO	13,56	13,27	14,54	13,87	13,45	14,11	12,63	13,16	13,55	13,69	13,60	4,95	5,36	4,80	5,56	4,65	7,91	4,89
CaO	11,77	11,76	11,92	11,85	11,59	11,50	11,74	11,81	11,58	11,60	12,14	11,36	11,08	11,24	11,06	11,20	10,68	11,21
Na_2O	0,73	0,69	0,72	0,71	0,91	0,98	0,65	0,66	0,87	0,85	0,58	1,41	1,47	1,40	1,41	1,44	1,13	1,35
K_2O	0,63	0,62	0,52	0,58	0,65	0,66	0,52	0,54	0,74	0,64	0,40	0,55	0,42	0,69	0,43	0,65	0,41	0,62
Total	95,64	96,15	96,43	96,61	95,42	96,33	87,84	96,51	94,55	95,20	94,54	97,18	96,90	97,01	96,29	96,01	96,56	96,21
Si	7,02	6,99	7,14	7,07	6,94	6,98	6,91	7,21	6,91	6,84	7,11	6,10	6,18	6,06	6,22	6,05	6,65	6,04
Al^{IV}	0,98	1,01	0,86	0,93	1,06	1,02	1,09	0,79	1,09	1,16	0,89	1,90	1,82	1,94	1,78	1,95	1,35	1,96
T	8,00	8,00	8,00	8,00	8,00	8,00	8,00	8,00	8,00	8,00	8,00	8,00	8,00	8,00	8,00	8,00	8,00	8,00
Al^{VI}	0,20	0,16	0,12	0,19	0,13	0,08	0,00	0,28	0,10	0,03	0,14	0,94	0,87	0,90	0,77	0,99	0,32	0,89
Ti	0,14	0,12	0,10	0,12	0,15	0,14	0,11	0,11	0,14	0,14	0,06	0,03	0,03	0,03	0,03	0,03	0,08	0,06
Cr	0,00	0,00	0,00	0,00	0,00	0,00	0,00	0,01	0,00	0,01	0,00	0,00	0,00	0,00	0,00	0,01	0,01	0,00
Fe^{3+}	0,43	0,56	0,50	0,49	0,56	0,64	0,45	0,28	0,59	0,78	0,49	0,66	0,76	0,74	0,83	0,63	1,00	0,73
Fe^{2+}	1,16	1,14	1,03	1,10	1,09	0,95	1,27	1,36	1,05	0,91	1,19	2,19	2,06	2,18	2,05	2,22	1,75	2,15
Mn	0,08	0,09	0,08	0,09	0,09	0,10	0,10	0,08	0,10	0,09	0,08	0,05	0,06	0,05	0,06	0,06	0,06	0,05
Mg	2,99	2,92	3,16	3,02	2,98	3,08	3,07	2,88	3,03	3,04	3,04	1,12	1,21	1,10	1,27	1,07	1,78	1,12
C	5,00	5,00	5,00	5,00	5,00	5,00	5,00	5,00	5,00	5,00	5,00	5,00	5,00	5,00	5,00	5,00	5,00	5,00
Ca	1,87	1,86	1,86	1,86	1,84	1,81	2,05	1,86	1,86	1,85	1,95	1,85	1,81	1,84	1,82	1,85	1,73	1,85
Na	0,13	0,14	0,14	0,14	0,16	0,19	-0,05	0,14	0,14	0,15	0,05	0,15	0,19	0,16	0,18	0,15	0,27	0,15
B	2,00	2,00	2,00	2,00	2,00	2,00	2,00	2,00	2,00	2,00	2,00	2,00	2,00	2,00	2,00	2,00	2,00	2,00
Na	0,08	0,06	0,07	0,06	0,11	0,08	0,26	0,05	0,12	0,09	0,12	0,27	0,24	0,26	0,23	0,29	0,06	0,25
K	0,12	0,12	0,10	0,11	0,12	0,12	0,11	0,10	0,14	0,12	0,08	0,11	0,08	0,14	0,08	0,13	0,08	0,12
A	0,19	0,17	0,17	0,17	0,23	0,21	0,37	0,15	0,26	0,21	0,19	0,38	0,32	0,39	0,32	0,41	0,14	0,37

Fase	Rengård, tipo GI										Rengård, tipo GI							
Litotipo	tonalita										tonalita							
Muestra	JO03-109 epma cont.										JO03-110 epma							
Análisis	23	24	25	27	28	29	30	31	33	34	1	2	3	4	5	8	14	15
Mineral	Fe-Ts	Fe-Ts	Fe-Ts	Fe-Ts	Fe-Ts	Fe-Ts	Fe-Ts	Fe-Hbl	Fe-Ts	Fe-Ts	Fe-Hbl	Mg-Hbl	Fe-Ts	Fe-Ts	Fe-Prg	Fe-Prg	Fe-Prg	Hs
SiO_2	40,16	39,73	40,02	39,93	40,10	39,78	39,17	43,34	39,66	39,79	45,07	44,95	39,63	39,24	37,66	37,84	39,42	37,53
TiO_2	0,34	0,14	0,32	0,48	0,28	0,16	0,23	0,31	0,09	0,29	1,49	1,43	0,46	0,21	0,14	0,09	0,00	0,36
Al_2O_3	14,48	16,06	15,56	15,17	16,13	16,03	16,97	10,51	16,14	15,61	7,97	7,79	14,84	15,52	25,23	24,70	24,74	13,18
Cr_2O_3	0,00	0,00	0,03	0,02	0,00	0,00	0,00	0,06	0,02	0,00	0,05	0,04	0,00	0,06	0,00	0,00	0,00	0,01
FeO	22,37	22,20	22,32	22,26	22,37	22,34	21,80	21,61	22,18	22,73	21,49	21,22	23,65	23,11	9,60	10,61	9,91	23,45
MnO	0,39	0,40	0,42	0,45	0,43	0,39	0,37	0,40	0,47	0,47	0,74	0,78	0,59	0,65	0,23	0,25	0,23	0,65
MgO	5,39	4,79	5,21	5,07	4,82	4,95	4,28	7,41	4,86	4,32	8,12	8,58	4,53	4,40	0,03	0,08	0,02	4,67
CaO	11,22	11,13	11,24	11,12	11,21	11,25	11,34	11,19	11,16	11,05	10,89	10,72	11,28	11,09	22,76	22,59	21,89	11,10
Na_2O	1,32	1,34	1,40	1,49	1,28	1,48	1,26	1,25	1,37	1,37	1,01	1,10	1,31	1,38	0,00	0,02	0,70	1,53
K_2O	0,58	0,53	0,51	0,48	0,52	0,51	0,66	0,35	0,60	0,45	0,47	0,49	0,77	0,73	0,09	0,03	0,02	0,78
Total	96,25	96,32	97,02	96,47	97,16	96,88	96,07	96,44	96,54	96,07	97,28	97,09	97,06	96,38	95,74	96,21	96,93	93,24
Si	6,18	6,09	6,09	6,13	6,09	6,07	6,04	6,59	6,07	6,14	6,79	6,76	6,10	6,06	5,67	5,69	5,84	6,06
Al^{IV}	1,82	1,91	1,91	1,87	1,91	1,93	1,96	1,41	1,93	1,86	1,21	1,24	1,90	1,94	2,33	2,31	2,16	1,94
T	8,00	8,00	8,00	8,00	8,00	8,00	8,00	8,00	8,00	8,00	8,00	8,00	8,00	8,00	8,00	8,00	8,00	8,00
Al^{VI}	0,80	0,99	0,88	0,87	0,98	0,96	1,13	0,48	0,98	0,98	0,20	0,14	0,79	0,89	2,14	2,07	2,16	0,57
Ti	0,04	0,02	0,04	0,06	0,03	0,02	0,03	0,04	0,01	0,03	0,17	0,16	0,05	0,02	0,02	0,01	0,00	0,04
Cr	0,00	0,00	0,00	0,00	0,00	0,00	0,00	0,01	0,00	0,00	0,01	0,00	0,00	0,01	0,00	0,00	0,00	0,00
Fe^{3+}	0,74	0,73	0,77	0,70	0,74	0,72	0,52	0,77	0,75	0,66	0,77	0,90	0,75	0,77	0,00	0,00	0,00	0,79
Fe^{2+}	2,13	2,12	2,07	2,15	2,11	2,13	2,29	1,98	2,09	2,27	1,94	1,77	2,29	2,22	1,21	1,33	1,23	2,37
Mn	0,05	0,05	0,05	0,06	0,05	0,05	0,05	0,05	0,06	0,06	0,09	0,10	0,08	0,08	0,03	0,03	0,03	0,09
Mg	1,23	1,10	1,18	1,16	1,09	1,13	0,98	1,68	1,11	0,99	1,82	1,92	1,04	1,01	0,01	0,02	0,01	1,12
C	5,00	5,00	5,00	5,00	5,00	5,00	5,00	5,00	5,00	5,00	5,00	5,00	5,00	5,00	3,40	3,46	3,42	5,00
Ca	1,85	1,83	1,83	1,83	1,82	1,84	1,87	1,82	1,83	1,83	1,76	1,73	1,86	1,84	3,67	3,64	3,47	1,92
Na	0,15	0,17	0,17	0,17	0,18	0,16	0,13	0,18	0,17	0,17	0,24	0,27	0,14	0,16	-1,67	-1,64	-1,47	0,08
B	2,00	2,00	2,00	2,00	2,00	2,00	2,00	2,00	2,00	2,00	2,00	2,00	2,00	2,00	2,00	2,00	2,00	2,00
Na	0,24	0,23	0,25	0,27	0,20	0,28	0,25	0,19	0,24	0,24	0,05	0,05	0,25	0,25	1,67	1,65	1,68	0,40
K	0,11	0,10	0,10	0,09	0,10	0,10	0,13	0,07	0,12	0,09	0,09	0,09	0,15	0,14	0,02	0,01	0,00	0,16
A	0,36	0,33	0,34	0,36	0,30	0,37	0,38	0,26	0,35	0,32	0,14	0,14	0,40	0,39	1,69	1,65	1,68	0,56

Fase	Rengård, tipo GI											Vargfors				
Litotipo	tonalita											basaltos andesíticos porfíficos				
Muestra	JO03-110 epma cont.											JO03-124 epma				
Análisis	16	17	23	26	28	31	35	36	38	40	41	1	3	7	14	15
Mineral												Act	Act	Act	Act	Act
SiO_2	36,51	36,90	39,16	39,60	39,22	39,79	40,16	43,80	39,34	44,70	39,29	40,04	40,61	39,62	40,56	39,18
TiO_2	0,33	0,46	0,35	0,42	0,42	0,36	0,09	1,56	0,37	1,76	0,36	0,26	0,27	0,28	0,24	0,24
Al_2O_3	14,02	13,16	14,92	14,25	15,14	14,81	14,81	8,04	14,27	7,72	15,29	15,81	15,01	15,78	14,12	16,10
Cr_2O_3	0,00	0,00	0,07	0,01	0,05	0,00	0,05	0,00	0,06	0,10	0,01	0,01	0,03	0,00	0,00	0,05
FeO	23,23	23,46	23,77	23,57	23,28	23,08	22,98	22,33	23,27	20,20	22,85	22,41	22,19	22,80	22,48	22,05
MnO	0,65	0,66	0,65	0,66	0,62	0,59	0,63	0,80	0,54	0,67	0,63	0,38	0,46	0,40	0,44	0,45
MgO	4,27	4,58	4,55	4,57	4,50	4,43	4,48	7,08	4,57	8,87	4,45	4,95	5,36	4,80	5,56	4,65
CaO	10,99	11,02	11,16	11,17	11,18	11,17	11,10	10,71	11,12	10,38	11,14	11,36	11,08	11,24	11,06	11,20
Na_2O	1,45	1,50	1,39	1,40	1,40	1,29	1,41	0,94	1,38	1,04	1,38	1,41	1,47	1,40	1,41	1,44
K_2O	0,72	0,75	0,80	0,83	0,79	0,81	0,51	0,49	0,84	0,46	0,72	0,55	0,42	0,69	0,43	0,65
Total	92,19	92,50	96,80	96,49	96,59	96,33	96,21	95,75	95,75	95,89	96,11	97,18	96,90	97,01	96,29	96,01
Si	5,96	6,01	6,04	6,14	6,06	6,16	6,20	6,75	6,15	6,77	6,09	7,70	7,79	7,71	7,61	7,55
Al^{IV}	2,04	1,99	1,96	1,86	1,94	1,84	1,80	1,25	1,85	1,23	1,91	0,24	0,18	0,24	0,39	0,41
T	8,00	8,00	8,00	8,00	8,00	8,00	8,00	8,00	8,00	8,00	8,00	7,95	7,98	7,95	8,00	7,95
Al^{VI}	0,66	0,54	0,75	0,75	0,82	0,87	0,90	0,21	0,77	0,14	0,88	0,00	0,00	0,00	0,02	0,00
Ti	0,04	0,06	0,04	0,05	0,05	0,04	0,01	0,18	0,04	0,20	0,04	0,00	0,00	0,00	0,00	0,00
Cr	0,00	0,00	0,01	0,00	0,01	0,00	0,01	0,00	0,01	0,01	0,00	0,05	0,02	0,03	0,03	0,05
Fe^{3+}	0,85	0,85	0,86	0,71	0,73	0,63	0,67	0,76	0,68	0,92	0,68	0,36	0,23	0,37	0,34	0,46
Fe^{2+}	2,32	2,34	2,21	2,34	2,27	2,36	2,30	2,11	2,36	1,64	2,28	0,49	0,61	0,48	0,64	0,60
Mn	0,09	0,09	0,08	0,09	0,08	0,08	0,08	0,10	0,07	0,09	0,08	0,02	0,02	0,02	0,01	0,02
Mg	1,04	1,11	1,05	1,06	1,04	1,02	1,03	1,63	1,06	2,00	1,03	4,13	4,14	4,14	3,95	3,91
C	5,00	5,00	5,00	5,00	5,00	5,00	5,00	5,00	5,00	5,00	5,00	5,05	5,02	5,05	5,00	5,05
Ca	1,92	1,92	1,84	1,86	1,85	1,85	1,84	1,77	1,86	1,68	1,85	1,93	1,96	1,94	1,94	1,94
Na	0,08	0,08	0,16	0,14	0,15	0,15	0,16	0,23	0,14	0,30	0,15	0,07	0,04	0,05	0,06	0,06
B	2,00	2,00	2,00	2,00	2,00	2,00	2,00	2,00	2,00	1,99	2,00	2,00	2,00	1,99	2,00	2,00
Na	0,38	0,40	0,26	0,28	0,27	0,24	0,26	0,05	0,28	0,00	0,27	0,00	0,00	0,00	0,04	0,03
K	0,15	0,16	0,16	0,16	0,16	0,16	0,10	0,10	0,17	0,09	0,14	0,01	0,01	0,01	0,02	0,02
A	0,53	0,55	0,41	0,44	0,43	0,40	0,36	0,14	0,44	0,09	0,41	0,01	0,01	0,01	0,06	0,05

Fase	GIIb					GI				GI							
Litotipo	cuarzo monzodiorita					tonalita				tonalita							
Muestra	JO04-34 epma					JO04-75 epma				JO04-86 epma							
Análisis	22	24	26	28	35	41	47	48	49	23	27	28	32	34	35	36	38
Mineral	Mg-Hbl	Mg-Hbl	Act	Mg-Hbl	Mg-Hbl	Mg-Hbl	Mg-Hbl	Fe-Hbl	Mg-Hbl	Fe-Hbl	Hast	Fe-Hbl	Fe-Ts	Fe-Ts	Fe-Ts	Fe-Ts	Fe-Hbl
SiO_2	50,11	46,60	51,87	46,53	44,93	46,21	46,48	46,76	45,69	42,45	39,36	43,91	41,25	41,20	39,82	40,48	41,61
TiO_2	0,70	1,31	0,45	1,29	1,74	1,46	1,41	0,09	1,58	0,85	0,34	1,13	0,79	0,77	0,86	0,92	0,91
Al_2O_3	4,85	6,64	3,12	6,96	6,93	6,69	6,51	5,80	7,10	9,25	12,75	7,69	10,00	9,58	11,12	10,67	9,47
Cr_2O_3	0,22	0,01	0,31	0,06	0,05	0,04	0,00	0,02	0,16	0,06	0,05	0,00	0,08	0,07	0,12	0,08	0,00
FeO	11,60	16,65	13,13	16,49	16,76	18,29	19,20	24,49	18,75	26,71	27,33	25,82	27,11	27,60	27,66	27,19	27,32
MnO	0,30	0,39	0,31	0,39	0,37	0,30	0,30	0,51	0,30	1,01	0,93	1,13	0,95	1,05	1,01	1,01	1,03
MgO	14,90	11,57	14,68	11,58	11,35	11,51	10,74	6,88	11,29	4,30	2,96	5,02	3,67	3,73	3,21	3,36	3,80
CaO	12,13	11,45	11,85	11,71	11,08	10,48	10,45	11,90	10,61	11,22	11,19	11,08	10,91	10,75	11,06	10,86	10,81
Na_2O	0,86	1,31	0,62	1,16	1,39	1,60	1,52	0,44	1,83	0,94	1,16	0,95	0,98	1,21	1,07	1,16	1,13
K_2O	0,39	0,82	0,31	0,82	1,03	0,39	0,39	0,31	0,44	1,05	1,36	0,66	1,21	1,18	1,47	1,39	1,14
Total	96,18	96,76	96,68	97,14	95,70	97,66	97,18	97,32	98,11	98,03	97,53	97,50	97,06	97,34	97,41	97,26	97,35
Si	7,34	6,97	7,55	6,94	6,82	6,83	6,90	7,16	6,74	6,60	6,19	6,81	6,49	6,48	6,28	6,39	6,53
Al^{IV}	0,66	1,03	0,45	1,06	1,18	1,17	1,10	0,84	1,23	1,40	1,81	1,19	1,51	1,52	1,72	1,61	1,47
T	8,00	8,00	8,00	8,00	8,00	8,00	8,00	8,00	7,97	8,00	8,00	8,00	8,00	8,00	8,00	8,00	8,00
Al^{VI}	0,18	0,14	0,09	0,17	0,06	0,00	0,04	0,21	0,00	0,29	0,55	0,21	0,34	0,26	0,35	0,37	0,28
Ti	0,08	0,15	0,05	0,14	0,20	0,16	0,16	0,01	0,18	0,10	0,04	0,13	0,09	0,09	0,10	0,11	0,11
Cr	0,03	0,00	0,04	0,01	0,01	0,00	0,00	0,00	0,02	0,01	0,01	0,00	0,01	0,01	0,01	0,01	0,00
Fe^{3+}	0,17	0,38	0,29	0,36	0,52	0,99	0,90	0,50	0,96	0,68	0,79	0,62	0,75	0,84	0,79	0,71	0,77
Fe^{2+}	1,26	1,70	1,31	1,70	1,61	1,27	1,48	2,63	1,35	2,80	2,80	2,73	2,81	2,79	2,86	2,88	2,81
Mn	0,04	0,05	0,04	0,05	0,05	0,04	0,04	0,07	0,04	0,13	0,12	0,15	0,13	0,14	0,13	0,13	0,14
Mg	3,26	2,58	3,19	2,58	2,57	2,54	2,38	1,57	2,48	1,00	0,69	1,16	0,86	0,87	0,75	0,79	0,89
C	5,00	5,00	5,00	5,00	5,00	5,00	5,00	5,00	5,03	5,00	5,00	5,00	5,00	5,00	5,00	5,00	5,00
Ca	1,90	1,84	1,85	1,87	1,80	1,66	1,66	1,95	1,68	1,87	1,88	1,84	1,84	1,81	1,87	1,84	1,82
Na	0,10	0,16	0,15	0,13	0,20	0,34	0,34	0,05	0,32	0,13	0,12	0,16	0,16	0,19	0,13	0,16	0,18
B	2,00	2,00	2,00	2,00	2,00	2,00	2,00	2,00	2,00	2,00	2,00	2,00	2,00	2,00	2,00	2,00	2,00
Na	0,15	0,22	0,02	0,21	0,21	0,12	0,10	0,08	0,20	0,15	0,24	0,12	0,14	0,18	0,20	0,19	0,16
K	0,07	0,16	0,06	0,16	0,20	0,07	0,07	0,06	0,08	0,21	0,27	0,13	0,24	0,24	0,30	0,28	0,23
A	0,22	0,37	0,08	0,36	0,41	0,19	0,17	0,14	0,28	0,36	0,51	0,26	0,38	0,42	0,49	0,47	0,39

Fase	GII																GI
Litotipo	granodiorita																tonalita
Muestra	JO04-42 epma																JO04-110
Análisis	1	2	3	4	9	10	13	31	32	33	34	36	39	42	45	58	73
Mineral	Mg-Hbl	Mg-Hbl	Mg-Hbl	Mg-Hbl	Mg-Hbl	Mg-Hbl	Mg-Hbl	Mg-Hbl	Mg-Hbl	Mg-Hbl	Mg-Hbl	Mg-Hbl	Mg-Hbl	Mg-Hbl	Ed	Ed	Mg-Hbl
SiO_2	45,66	46,72	45,32	45,86	45,47	45,98	52,39	45,58	48,19	46,78	46,55	46,51	45,23	45,44	45,15	45,80	49,427
TiO_2	1,59	1,42	1,48	1,07	1,47	1,47	0,03	1,41	0,81	1,54	1,50	1,44	1,53	1,58	1,58	1,66	0,405
Al_2O_3	7,01	6,15	7,21	6,59	6,81	6,83	1,85	6,92	5,73	6,15	6,45	6,25	7,08	6,83	7,12	6,75	4,334
Cr_2O_3	0,00	0,09	0,10	0,12	0,03	0,00	0,00	0,00	0,05	0,01	0,04	0,00	0,05	0,00	0,06	0,04	0,124
FeO	19,06	17,99	18,85	18,52	18,86	18,53	16,10	18,56	17,81	18,12	18,23	17,65	18,91	19,12	19,07	18,40	17,374
MnO	0,49	0,48	0,45	0,40	0,42	0,44	0,36	0,41	0,43	0,44	0,46	0,39	0,47	0,47	0,46	0,43	0,525
MgO	10,32	10,98	10,37	10,53	10,70	10,80	13,74	10,62	11,86	11,39	10,97	11,69	10,18	10,52	10,30	10,98	12,297
CaO	11,06	11,06	11,33	11,25	10,84	11,01	12,35	11,00	10,57	10,98	11,18	10,98	11,17	11,19	11,23	10,99	12,037
Na_2O	1,75	1,53	1,55	1,47	1,86	1,54	0,26	1,73	1,86	1,68	1,36	1,71	1,53	1,50	1,47	1,59	0,591
K_2O	0,84	0,74	0,74	0,76	0,77	0,79	0,14	0,85	0,35	0,71	0,76	0,73	0,87	0,82	0,90	0,80	0,328
Total	97,99	97,41	97,78	96,89	97,60	97,50	97,53	97,57	98,15	98,18	97,78	97,82	97,36	97,82	97,57	97,82	97,56
Si	6,83	6,99	6,80	6,93	6,82	6,86	7,67	6,85	7,08	6,94	6,93	6,91	6,82	6,81	6,79	6,83	7,2816581
Al^{IV}	1,17	1,01	1,20	1,07	1,18	1,14	0,32	1,15	0,92	1,06	1,07	1,09	1,18	1,19	1,21	1,17	0,7183419
T	8,00	8,00	8,00	8,00	8,00	8,00	7,99	8,00	8,00	8,00	8,00	8,00	8,00	8,00	8,00	8,00	8
Al^{VI}	0,07	0,07	0,08	0,10	0,02	0,06	0,00	0,08	0,07	0,01	0,06	0,01	0,08	0,02	0,05	0,02	0,0341209
Ti	0,18	0,16	0,17	0,12	0,17	0,16	0,00	0,16	0,09	0,17	0,17	0,16	0,17	0,18	0,18	0,19	0,0448759
Cr	0,00	0,01	0,01	0,01	0,00	0,00	0,00	0,00	0,01	0,00	0,00	0,00	0,01	0,00	0,01	0,00	0,0144422
Fe^{3+}	0,52	0,49	0,54	0,50	0,66	0,63	0,37	0,55	0,76	0,60	0,56	0,63	0,51	0,63	0,58	0,65	0,5500077
Fe^{2+}	1,86	1,76	1,83	1,84	1,71	1,69	1,60	1,79	1,43	1,64	1,71	1,56	1,88	1,77	1,81	1,65	1,5902644
Mn	0,06	0,06	0,06	0,05	0,05	0,06	0,04	0,05	0,05	0,05	0,06	0,05	0,06	0,06	0,06	0,05	0,0655034
Mg	2,30	2,45	2,32	2,37	2,39	2,40	3,00	2,38	2,60	2,52	2,43	2,59	2,29	2,35	2,31	2,44	2,7007854
C	5,00	5,00	5,00	5,00	5,00	5,00	5,01	5,00	5,00	5,00	5,00	5,00	5,00	5,00	5,00	5,00	5
Ca	1,77	1,77	1,82	1,82	1,74	1,76	1,94	1,77	1,66	1,74	1,78	1,75	1,81	1,80	1,81	1,76	1,8997927
Na	0,23	0,23	0,18	0,18	0,26	0,24	0,06	0,23	0,34	0,26	0,22	0,25	0,19	0,20	0,19	0,24	0,1002073
B	2,00	2,00	2,00	2,00	2,00	2,00	2,00	2,00	2,00	2,00	2,00	2,00	2,00	2,00	2,00	2,00	2
Na	0,28	0,22	0,27	0,25	0,28	0,21	0,01	0,28	0,19	0,23	0,18	0,24	0,25	0,23	0,24	0,22	0,0685886
K	0,16	0,14	0,14	0,15	0,15	0,15	0,03	0,16	0,06	0,13	0,14	0,14	0,17	0,16	0,17	0,15	0,0616381
A	0,44	0,36	0,41	0,40	0,43	0,36	0,04	0,44	0,26	0,36	0,32	0,38	0,42	0,39	0,41	0,37	0,1302266

Fase	Hbl tonalite									Hbl tonalite							
Litotipo	tonalita (cuarzo anfibolita)									tonalita (cuarzo anfibolita)							
Muestra	VIC04-01 epma									VIC04-07 epma							
Análisis	2	8	10	20	21	22	24	25	28	33	34	35	36	38	40	42	44
Mineral	Ts	Ts	Ts	Mg-Hbl	Mg-Hbl	Mg-Hbl	Mg-Hbl	Ts	Mg-Hbl	Fe-Hbl	Hast	Fe-Hbl	Fe-Ts	Fe-Ts	Fe-Ts	Fe-Ts	Fe-Hbl
SiO_2	42,21	41,88	41,50	40,85	45,07	40,34	41,59	42,43	40,94	42,85	42,58	43,23	41,71	42,01	42,91	43,34	43,62
TiO_2	0,54	0,46	0,48	0,51	0,32	0,55	0,56	0,47	0,51	0,46	0,36	0,37	0,54	0,32	0,72	0,34	0,32
Al_2O_3	11,48	11,24	11,58	11,90	8,79	12,36	11,31	11,13	11,53	13,21	13,55	13,17	13,97	13,54	13,44	12,09	13,08
Cr_2O_3	0,00	0,04	0,02	0,03	0,00	0,02	0,00	0,00	0,00	0,16	0,00	0,17	0,00	0,01	0,18	0,00	0,00
FeO	19,11	19,21	19,53	19,09	17,34	19,51	19,27	19,15	19,20	15,98	15,63	15,48	16,21	15,93	16,00	15,88	15,74
MnO	0,27	0,34	0,30	0,32	0,33	0,34	0,34	0,35	0,33	0,20	0,27	0,27	0,27	0,25	0,30	0,32	0,36
MgO	9,08	8,65	8,81	8,71	10,96	8,43	8,74	8,72	8,85	10,05	10,35	10,38	9,85	10,41	10,00	10,92	10,22
CaO	11,70	11,67	11,63	11,73	11,94	11,81	11,71	11,75	11,71	11,16	11,19	11,06	11,21	11,18	11,24	11,04	10,74
Na_2O	1,15	1,13	1,25	1,16	0,92	1,18	1,15	1,11	1,21	1,53	1,47	1,57	1,52	1,58	1,57	1,56	1,76
K_2O	1,07	1,13	1,08	1,18	0,70	1,16	1,23	1,12	1,16	0,32	0,33	0,26	0,32	0,28	0,32	0,18	0,22
Total	96,61	95,77	96,22	95,51	96,54	95,74	95,92	96,26	95,45	96,00	95,93	96,02	95,66	95,58	96,70	95,74	96,07
Si	6,39	6,42	6,33	6,28	6,28	6,75	6,21	6,47	6,38	6,37	6,32	6,40	6,23	6,26	6,34	6,45	6,43
Al^{IV}	1,61	1,58	1,67	1,72	1,72	1,25	1,79	1,53	1,62	1,63	1,68	1,60	1,77	1,74	1,66	1,55	1,57
T	8,00	8,00	8,00	8,00	8,00	8,00	8,00	8,00	8,00	8,00	8,00	8,00	8,00	8,00	8,00	8,00	8,00
Al^{VI}	0,44	0,46	0,41	0,44	0,44	0,30	0,45	0,47	0,42	0,69	0,69	0,70	0,69	0,63	0,68	0,72	0,54
Ti	0,06	0,05	0,05	0,06	0,06	0,04	0,06	0,05	0,06	0,05	0,04	0,04	0,06	0,04	0,08	0,04	0,04
Cr	0,00	0,00	0,00	0,00	0,00	0,00	0,00	0,00	0,00	0,02	0,00	0,02	0,00	0,00	0,02	0,00	0,00
Fe^{3+}	0,71	0,62	0,77	0,71	0,71	0,64	0,74	0,56	0,64	0,76	0,86	0,79	0,87	0,96	0,73	0,81	0,97
Fe^{2+}	1,71	1,85	1,72	1,75	1,75	1,53	1,76	1,88	1,83	1,23	1,08	1,12	1,15	1,03	1,25	1,13	1,00
Mn	0,03	0,04	0,04	0,04	0,04	0,04	0,04	0,05	0,04	0,02	0,03	0,03	0,03	0,03	0,04	0,04	0,04
Mg	2,05	1,98	2,00	2,00	2,00	2,45	1,93	1,98	2,00	2,23	2,29	2,29	2,19	2,31	2,20	2,25	2,41
C	5,00	5,00	5,00	5,00	5,00	5,00	5,00	5,00	5,00	5,00	5,00	5,00	5,00	5,00	5,00	5,00	5,00
Ca	1,90	1,92	1,90	1,93	1,93	1,92	1,95	1,92	1,92	1,78	1,78	1,75	1,79	1,78	1,78	1,70	1,75
Na	0,10	0,08	0,10	0,07	0,07	0,08	0,05	0,08	0,08	0,22	0,22	0,25	0,21	0,22	0,22	0,30	0,25
B	2,00	2,00	2,00	2,00	2,00	2,00	2,00	2,00	2,00	2,00	2,00	2,00	2,00	2,00	2,00	2,00	2,00
Na	0,23	0,25	0,27	0,28	0,28	0,18	0,30	0,25	0,26	0,22	0,20	0,21	0,23	0,24	0,23	0,20	0,20
K	0,21	0,22	0,21	0,23	0,23	0,13	0,23	0,22	0,24	0,06	0,06	0,05	0,06	0,05	0,06	0,04	0,03
A	0,44	0,47	0,48	0,51	0,51	0,32	0,53	0,47	0,50	0,28	0,27	0,25	0,30	0,29	0,29	0,25	0,23

Fase	GII											
Litotipo	granodiorita											
Muestra	JO04-128 epma											
Análisis	97	98	111	112	114	115	117	120	122	123	126	127
Mineral	Mg-Hbl	Mg-Hbl	Mg-Hbl	Mg-Hbl	Mg-Hbl	Mg-Hbl	Act	Mg-Hbl	Mg-Hbl	Mg-Hbl	Mg-Hbl	Mg-Hbl
SiO_2	50,75	46,09	48,72	46,10	49,57	46,12	51,71	49,49	51,00	46,22	46,53	50,78
TiO_2	0,19	1,50	0,49	1,50	0,30	1,18	0,09	0,24	0,16	1,57	1,62	0,19
Al_2O_3	3,19	6,58	4,39	6,42	3,93	6,19	2,44	3,83	2,99	6,66	6,46	3,09
Cr_2O_3	0,00	0,00	0,05	0,09	0,00	0,10	0,00	0,00	0,13	0,00	0,03	0,05
FeO	16,78	17,93	17,41	18,18	17,13	18,25	16,91	17,29	16,59	17,81	17,79	16,68
MnO	0,44	0,42	0,41	0,46	0,47	0,44	0,49	0,42	0,43	0,47	0,47	0,44
MgO	13,12	11,28	12,25	11,01	12,89	11,36	13,13	12,64	13,32	11,28	10,84	12,98
CaO	12,01	10,93	11,79	11,27	11,77	11,33	12,14	11,88	12,01	10,78	10,84	12,00
Na_2O	0,66	1,63	0,99	1,40	0,78	1,47	0,36	0,75	0,50	1,56	1,34	0,55
K_2O	0,25	0,79	0,44	0,74	0,35	0,76	0,20	0,36	0,23	0,76	0,76	0,27
Total	97,60	97,37	97,37	97,39	97,45	97,51	97,66	97,12	97,62	97,19	97,00	97,13
Si	7,44	6,88	7,24	6,90	7,29	6,90	7,57	7,32	7,46	6,88	6,97	7,48
Al^{IV}	0,55	1,12	0,76	1,10	0,68	1,09	0,42	0,67	0,52	1,12	1,03	0,52
T	8,00	8,00	8,00	8,00	7,97	7,99	7,99	7,99	7,98	8,00	8,00	8,00
Al^{VI}	0,00	0,03	0,01	0,03	0,00	0,00	0,00	0,00	0,00	0,05	0,11	0,02
Ti	0,02	0,17	0,05	0,17	0,03	0,13	0,01	0,03	0,02	0,18	0,18	0,02
Cr	0,00	0,00	0,01	0,01	0,00	0,01	0,00	0,00	0,02	0,00	0,00	0,01
Fe^{3+}	0,51	0,64	0,51	0,56	0,67	0,64	0,47	0,58	0,56	0,69	0,55	0,46
Fe^{2+}	1,55	1,60	1,65	1,71	1,44	1,64	1,60	1,56	1,47	1,52	1,68	1,59
Mn	0,06	0,05	0,05	0,06	0,06	0,06	0,06	0,05	0,05	0,06	0,06	0,05
Mg	2,87	2,51	2,71	2,46	2,83	2,53	2,87	2,79	2,91	2,50	2,42	2,85
C	5,00	5,00	5,00	5,00	5,03	5,01	5,01	5,01	5,02	5,00	5,00	5,00
Ca	1,89	1,75	1,88	1,81	1,86	1,81	1,90	1,88	1,88	1,72	1,74	1,89
Na	0,11	0,25	0,12	0,19	0,14	0,19	0,10	0,12	0,12	0,28	0,26	0,11
B	2,00	2,00	2,00	2,00	2,00	2,00	2,00	2,00	2,00	2,00	2,00	2,00
Na	0,08	0,22	0,16	0,21	0,08	0,24	0,01	0,10	0,02	0,17	0,13	0,05
K	0,05	0,15	0,08	0,14	0,06	0,15	0,04	0,07	0,04	0,14	0,15	0,05
A	0,12	0,37	0,25	0,35	0,14	0,39	0,04	0,17	0,07	0,31	0,27	0,10

Fase	Näsberg											GII				Dique sur		
Litotipo	gabro norita											granodiorita				basalto andesítico		
Muestra	23j84											JO03-38b				JO03-103b		
Análisis	1	2	11	12	14	15	16	21	23	24	27	6	7	10	11	1	2	3
Mineral	Hyp	Hyp	Hyp	Brz	Aug	Hyp	Aug	Aug	Hyp	Aug	S-Aug	Di	Di	Di	Di	Aug	Aug	Aug
SiO_2	54,88	54,20	54,01	62,44	51,91	56,63	50,54	53,26	53,62	50,38	51,90	53,70	52,78	53,23	52,59	52,25	55,31	51,85
TiO_2	0,19	0,25	0,30	0,12	0,37	0,09	0,00	0,10	0,17	0,37	0,13	0,11	0,03	0,06	0,23	0,32	0,08	0,49
Al_2O_3	0,25	0,19	0,16	0,61	1,11	0,88	4,70	1,20	0,35	0,89	0,93	0,07	0,22	0,02	0,24	2,29	1,64	1,84
Cr_2O_3	0,01	0,01	0,04	0,02	0,23	0,05	0,06	0,16	0,18	0,44	0,05	0,08	0,19	0,34	0,14	0,59	0,51	0,69
FeO	19,09	19,23	19,67	8,86	8,19	9,92	12,58	10,77	19,46	8,74	15,72	8,38	7,98	8,60	8,55	8,63	7,25	8,06
MnO	0,68	0,48	0,59	0,09	0,51	0,24	0,40	0,46	0,71	0,18	1,14	0,98	0,92	0,86	0,83	0,26	0,33	0,15
MgO	24,71	23,76	24,10	27,54	14,72	22,65	14,63	17,23	23,97	13,88	15,43	13,20	12,66	13,31	12,76	16,41	19,44	16,30
CaO	1,16	1,16	1,26	0,23	21,48	0,47	11,59	12,08	1,38	20,00	8,98	25,02	24,43	23,96	23,74	18,80	12,65	20,23
Na_2O	0,43	0,25	0,06	0,41	0,64	0,27	0,79	0,39	0,21	0,32	0,35	0,29	0,34	0,73	0,71	0,70	0,37	0,35
K_2O	0,00	0,00	0,02	0,37	0,04	0,03	0,01	0,00	0,08	0,12	0,01	0,10	0,02	0,10	0,06	0,02	0,04	0,00
Total	101,40	99,53	100,21	100,69	99,20	91,23	95,30	95,65	100,13	95,32	94,64	101,93	99,57	101,21	99,85	100,27	97,62	99,96
Si	1,99	2,00	1,99	2,13	1,95	2,15	1,95	2,03	1,98	1,97	2,04	1,98	1,99	1,98	1,98	1,93	2,03	1,92
Al^{IV}	0,01	0,00	0,01	-0,13	0,05	-0,15	0,05	-0,03	0,02	0,03	-0,04	0,00	0,01	0,00	0,01	0,07	-0,03	0,08
Al^{VI}	0,00	0,01	0,00	0,16	0,00	0,19	0,17	0,08	0,00	0,01	0,08	0,00	0,00	0,00	0,00	0,03	0,10	0,00
Fe^{3+}	0,05	0,00	0,01	0,00	0,10	0,00	0,00	0,00	0,05	0,02	0,00	0,07	0,04	0,12	0,09	0,08	0,00	0,07
Cr	0,00	0,00	0,00	0,00	0,01	0,00	0,00	0,00	0,01	0,01	0,00	0,00	0,01	0,01	0,00	0,02	0,01	0,02
Ti	0,01	0,01	0,01	0,00	0,01	0,00	0,00	0,00	0,00	0,01	0,00	0,00	0,00	0,00	0,01	0,01	0,00	0,01
Fe^{2+}	0,53	0,59	0,59	0,26	0,16	0,33	0,41	0,35	0,55	0,27	0,52	0,19	0,21	0,15	0,18	0,18	0,23	0,18
Mn	0,02	0,02	0,02	0,00	0,02	0,01	0,01	0,01	0,02	0,01	0,04	0,03	0,03	0,03	0,03	0,01	0,01	0,00
Mg	1,34	1,31	1,32	1,40	0,83	1,28	0,84	0,98	1,32	0,81	0,90	0,73	0,71	0,74	0,72	0,90	1,06	0,90
Ca	0,05	0,05	0,05	0,01	0,87	0,02	0,48	0,49	0,05	0,84	0,38	0,99	0,99	0,96	0,96	0,74	0,50	0,80
Na	0,03	0,02	0,00	0,03	0,05	0,02	0,06	0,03	0,02	0,02	0,03	0,02	0,02	0,05	0,05	0,05	0,03	0,03
K	0,00	0,00	0,00	0,02	0,00	0,00	0,00	0,00	0,00	0,01	0,00	0,00	0,00	0,00	0,00	0,00	0,00	0,00
Suma	4,01	4,00	4,00	3,88	4,03	3,85	3,97	3,96	4,01	4,01	3,96	4,02	4,01	4,04	4,03	4,03	3,94	4,02
Wo	2,24	2,32	2,48	0,49	0,90	0,21	1,59	0,00	0,00	0,00	0,00	48,88	49,26	46,86	47,42	37,75	27,28	40,53
En	66,50	66,03	66,13	82,40	30,75	31,17	15,51	68,34	68,62	82,90	31,66	35,88	35,52	36,23	35,47	45,86	58,33	45,44
Fs	29,75	30,75	31,17	15,51	68,34	68,62	82,90	31,66	31,38	17,10	68,34	14,22	13,98	14,33	14,54	13,84	12,95	12,76
Act	1,50	0,90	0,21	1,60	0,00	0,00	0,00	0,00	0,00	0,00	0,00	1,03	1,24	2,58	2,57	2,54	1,44	1,27

Fase	Dique sur													Näsberg						
Litotipo	basalto andesítico													gabro norita						
Muestra	JO03-103b cont.													A3						
Análisis	4	5	11	14	15	16	17	18	19	20	22	23	24	5	6	13	14	2	3	10
Mineral	Aug	Aug	Aug	Aug	Aug	Aug	Aug	Aug	Aug	Aug	Aug	Aug	Aug	Hyp	Hyp	Hyp	Hyp	Aug	Di	Di
SiO_2	53,49	51,83	51,57	51,59	51,97	55,22	52,26	53,25	51,81	52,31	52,28	54,92	52,08	54,40	53,95	52,59	52,81	52,64	52,50	51,11
TiO_2	0,37	0,40	0,58	0,39	0,40	0,36	0,43	0,10	0,73	0,26	0,29	0,37	0,29	0,00	0,61	0,59	0,56	0,54	0,84	0,62
Al_2O_3	1,76	1,73	3,61	1,50	2,76	2,46	1,71	3,40	1,67	1,83	1,58	1,81	2,66	0,84	0,66	0,90	0,68	1,68	2,31	1,65
Cr_2O_3	0,32	0,49	0,18	0,27	0,41	0,79	0,40	0,17	0,07	0,49	0,80	0,52	0,83	0,00	0,00	0,00	0,00	0,58	0,56	0,00
FeO	8,25	7,00	11,80	7,08	7,81	9,08	7,69	9,32	8,99	8,01	7,88	8,24	7,21	19,65	19,45	18,51	18,58	6,88	6,08	7,76
MnO	0,19	0,36	0,20	0,41	0,35	0,15	0,37	0,25	0,28	0,33	0,08	0,09	0,29	0,63	0,58	0,54	0,39	0,00	0,00	0,42
MgO	16,69	16,21	17,63	16,18	16,53	18,74	15,31	17,32	15,06	17,26	16,43	17,69	16,53	24,17	23,19	23,78	23,68	16,41	15,82	13,96
CaO	19,80	20,32	11,72	19,81	19,80	12,18	21,00	12,54	20,21	19,99	19,74	13,19	20,34	1,59	1,98	2,29	2,04	21,06	22,30	21,73
Na_2O	0,43	0,43	0,60	0,56	0,40	0,57	0,67	0,53	0,57	0,51	0,60	0,41	0,41	0,00	0,00	0,52	0,00	0,82	0,00	0,00
K_2O	0,03	0,09	0,03	0,02	0,07	0,03	0,08	0,11	0,04	0,12	0,10	0,18	0,05	0,00	0,00	0,00	0,00	0,00	0,00	0,00
Total	101,33	98,86	97,92	97,81	100,50	99,58	99,92	96,99	99,43	101,11	99,78	97,42	100,69	101,28	100,42	99,72	98,74	100,61	100,41	97,25
Si	1,95	1,94	1,93	1,95	1,91	2,00	1,94	1,99	1,94	1,92	1,94	2,03	1,91	1,98	1,98	1,95	1,97	1,93	1,93	1,95
Al^{IV}	0,05	0,06	0,07	0,05	0,09	0,00	0,06	0,01	0,06	0,08	0,06	-0,03	0,09	0,02	0,02	0,04	0,03	0,07	0,07	0,05
Al^{VI}	0,03	0,01	0,09	0,01	0,03	0,11	0,02	0,14	0,01	0,00	0,01	0,11	0,03	0,01	0,01	0,00	0,00	0,01	0,03	0,03
Fe^{3+}	0,04	0,07	0,00	0,07	0,08	0,00	0,08	0,00	0,07	0,14	0,09	0,00	0,08	0,01	0,00	0,10	0,00	0,11	0,00	0,00
Cr	0,01	0,01	0,01	0,01	0,01	0,02	0,01	0,01	0,00	0,01	0,02	0,02	0,02	0,00	0,00	0,00	0,00	0,02	0,02	0,00
Ti	0,01	0,01	0,02	0,01	0,01	0,01	0,01	0,00	0,02	0,01	0,01	0,01	0,01	0,00	0,02	0,02	0,02	0,01	0,02	0,02
Fe^{2+}	0,21	0,15	0,37	0,15	0,16	0,28	0,15	0,29	0,21	0,10	0,15	0,26	0,14	0,59	0,60	0,46	0,57	0,10	0,19	0,25
Mn	0,01	0,01	0,01	0,01	0,01	0,00	0,01	0,01	0,01	0,01	0,00	0,00	0,01	0,02	0,02	0,02	0,01	0,00	0,00	0,01
Mg	0,91	0,90	0,99	0,91	0,91	1,01	0,85	0,96	0,84	0,94	0,91	0,98	0,90	1,31	1,27	1,31	1,32	0,90	0,87	0,80
Ca	0,77	0,81	0,47	0,80	0,78	0,47	0,84	0,50	0,81	0,79	0,78	0,52	0,80	0,06	0,08	0,09	0,08	0,83	0,88	0,89
Na	0,03	0,03	0,04	0,04	0,03	0,04	0,05	0,04	0,04	0,04	0,04	0,03	0,03	0,00	0,00	0,04	0,00	0,06	0,00	0,00
K	0,00	0,00	0,00	0,00	0,00	0,00	0,00	0,01	0,00	0,01	0,00	0,01	0,00	0,00	0,00	0,00	0,00	0,00	0,00	0,00
Suma	4,01	4,02	3,99	4,02	4,02	3,95	4,03	3,96	4,02	4,04	4,03	3,93	4,02	4,00	3,99	4,03	4,00	4,03	3,99	3,99
Wo	39,31	41,16	25,08	40,30	39,71	26,14	42,19	27,77	40,91	38,91	39,59	29,20	40,76	3,11	3,97	4,48	4,10	41,54	45,45	45,69
En	46,11	45,69	52,50	45,80	46,14	55,97	42,81	53,37	42,43	46,76	45,86	54,50	46,09	65,89	64,63	64,79	66,17	45,04	44,87	40,85
Fs	13,04	11,58	20,09	11,83	12,70	15,67	12,56	16,74	14,57	12,53	12,37	14,65	11,66	30,99	31,41	28,88	29,73	10,50	9,69	13,46
Act	1,54	1,58	2,32	2,06	1,45	2,21	2,44	2,12	2,09	1,80	2,18	1,64	1,49	0,00	0,00	1,84	0,00	2,93	0,00	0,00

Fase	Näsberg															Näsberg				
Litotipo	norita olivínica															norita olivínica				
Muestra	A28															A53B				
Análisis	1	13	15	19	24	20	25	27	3	9	18	21	22	23	26	1	3	4	11	18
Mineral	Hyp	Hyp	Hyp	Hyp	Hyp	Hyp	Hyp	Hyp	Aug	Aug	Aug	Aug	Aug	Aug	Aug	Aug	Aug	Aug	Di	Aug
SiO_2	54,23	54,46	53,54	54,44	52,29	52,82	49,46	53,00	51,66	50,59	50,99	51,47	50,17	51,29	51,70	52,26	51,61	52,50	53,61	51,30
TiO_2	0,30	0,00	0,45	0,00	0,64	0,42	0,40	0,00	0,61	0,66	0,68	0,76	1,20	1,24	0,51	0,76	0,85	0,97	0,30	0,99
Al_2O_3	0,00	0,00	0,60	1,49	0,98	0,59	2,49	0,74	1,11	1,89	3,30	1,39	7,54	2,20	1,42	1,80	1,78	1,76	0,00	2,32
Cr_2O_3	0,00	0,00	0,00	0,00	0,00	0,00	0,00	0,00	0,00	0,00	0,00	0,00	0,00	0,00	0,00	0,00	0,00	0,00	0,00	0,51
FeO	19,94	20,12	19,73	19,02	18,60	19,36	16,37	19,74	8,75	9,25	10,39	9,52	9,80	10,66	9,11	9,32	9,22	8,71	7,96	8,88
MnO	0,39	0,49	0,43	0,46	0,61	0,61	0,00	0,57	0,45	0,40	0,61	0,00	0,00	0,00	0,00	0,00	0,00	0,00	0,00	0,00
MgO	24,00	23,79	23,93	22,57	22,88	22,38	19,73	23,63	14,22	14,14	14,02	14,46	11,84	15,15	14,59	14,30	13,89	14,20	14,56	13,87
CaO	1,48	1,37	1,88	1,67	1,93	3,27	5,33	1,46	21,16	19,72	18,99	20,31	16,32	18,92	21,24	21,21	21,13	21,07	23,18	20,98
Na_2O	0,00	0,00	0,00	0,00	0,00	0,00	0,59	0,00	0,00	0,00	0,73	0,00	1,27	0,59	0,50	0,00	0,00	0,00	0,00	0,63
K_2O	0,00	0,00	0,00	0,00	0,00	0,00	0,00	0,00	0,00	0,00	0,00	0,00	0,00	0,00	0,00	0,00	0,00	0,00	0,00	0,00
Total	100,34	100,23	100,56	99,65	97,93	99,45	94,37	99,14	97,96	96,65	99,71	97,91	98,14	100,05	99,07	99,65	98,48	99,21	99,61	99,48
Si	1,99	2,00	1,97	2,00	1,97	1,97	1,94	1,97	1,96	1,95	1,91	1,96	1,88	1,92	1,95	1,95	1,95	1,96	2,00	1,92
Al^{IV}	0,00	0,00	0,03	0,00	0,03	0,03	0,06	0,03	0,04	0,05	0,09	0,04	0,12	0,08	0,05	0,05	0,05	0,04	0,00	0,08
Al^{VI}	0,00	0,00	0,00	0,07	0,01	0,00	0,05	0,01	0,01	0,03	0,06	0,02	0,21	0,01	0,01	0,03	0,03	0,04	0,00	0,03
Fe^{3+}	0,00	0,00	0,02	0,00	0,00	0,02	0,05	0,03	0,00	0,00	0,07	0,00	0,00	0,07	0,07	0,00	0,00	0,00	0,00	0,04
Cr	0,00	0,00	0,00	0,00	0,00	0,00	0,00	0,00	0,00	0,00	0,00	0,00	0,00	0,00	0,00	0,00	0,00	0,00	0,00	0,02
Ti	0,01	0,00	0,01	0,00	0,02	0,01	0,01	0,00	0,02	0,02	0,02	0,02	0,03	0,03	0,01	0,02	0,02	0,03	0,01	0,03
Fe^{2+}	0,61	0,62	0,58	0,59	0,59	0,59	0,48	0,58	0,28	0,30	0,26	0,30	0,31	0,26	0,21	0,29	0,29	0,27	0,25	0,24
Mn	0,01	0,02	0,01	0,01	0,02	0,02	0,00	0,02	0,01	0,01	0,02	0,00	0,00	0,00	0,00	0,00	0,00	0,00	0,00	0,00
Mg	1,31	1,30	1,31	1,24	1,28	1,24	1,15	1,31	0,81	0,81	0,78	0,82	0,66	0,84	0,82	0,80	0,78	0,79	0,81	0,78
Ca	0,06	0,05	0,07	0,07	0,08	0,13	0,22	0,06	0,86	0,81	0,76	0,83	0,66	0,76	0,86	0,85	0,86	0,84	0,93	0,84
Na	0,00	0,00	0,00	0,00	0,00	0,00	0,04	0,00	0,00	0,00	0,05	0,00	0,09	0,04	0,04	0,00	0,00	0,00	0,00	0,05
K	0,00	0,00	0,00	0,00	0,00	0,00	0,00	0,00	0,00	0,00	0,00	0,00	0,00	0,00	0,00	0,00	0,00	0,00	0,00	0,00
Suma	4,00	4,00	4,01	3,97	3,99	4,00	4,02	4,01	3,99	3,99	4,02	3,99	3,97	4,02	4,02	3,99	3,99	3,97	3,99	4,01
Wo	2,92	2,71	3,69	3,45	3,96	6,54	11,44	2,91	43,95	42,00	39,26	42,42	38,12	38,34	42,90	43,82	44,31	44,19	46,67	43,41
En	65,80	65,45	65,44	64,88	65,25	62,30	58,95	65,55	41,10	41,91	40,34	42,03	38,49	42,73	41,00	41,11	40,54	41,45	40,79	39,94
Fs	31,28	31,84	30,87	31,67	30,79	31,15	27,31	31,54	14,95	16,09	17,67	15,56	18,03	16,77	14,27	15,07	15,15	14,36	12,53	14,30
Act	0,00	0,00	0,00	0,00	0,00	0,00	2,29	0,00	0,00	0,00	2,73	0,00	5,37	2,16	1,83	0,00	0,00	0,00	0,00	2,36

Fase	Näsberg								Näsberg						Näsberg			
Litotipo	gabro norita								norita olivínica						gabro norita			
Muestra	A55								A80						S30			
Análisis	1	2	5	11	12	15	16	17	1	2	8	10	3	9	1	8	9	12
Mineral	Hyp	Hyp	Aug	Aug	Aug	Aug	Aug	Aug	Di	Di	Aug	Di	S-Aug	Hyp	Di	Aug	Aug	Aug
SiO_2	53,61	53,94	51,86	50,74	51,56	50,17	51,41	52,38	53,54	53,84	53,05	53,35	55,19	55,52	53,57	51,01	54,38	53,79
TiO_2	0,53	0,65	1,18	0,87	1,00	0,62	0,63	0,88	0,00	0,36	0,27	0,00	0,33	0,11	0,00	0,63	0,44	0,56
Al_2O_3	0,66	0,00	1,80	1,50	2,48	2,16	1,55	1,70	0,54	0,47	0,69	0,75	0,96	0,28	0,90	0,91	1,43	1,20
Cr_2O_3	0,00	0,00	0,00	0,00	0,00	0,00	0,00	0,00	0,00	0,00	0,00	0,00	0,00	0,00	0,00	0,00	0,00	0,42
FeO	20,78	21,14	9,99	15,00	10,53	11,14	9,72	10,56	8,78	8,17	8,50	8,50	12,47	19,95	8,19	10,90	12,07	12,93
MnO	0,65	0,50	0,00	0,28	0,00	0,00	0,00	0,00	0,00	0,00	0,00	0,00	0,42	0,88	0,68	0,54	0,39	0,00
MgO	22,50	23,01	13,70	16,27	13,89	14,30	13,92	14,21	14,60	14,45	14,92	14,67	17,34	20,50	14,60	14,45	14,92	14,67
CaO	1,81	1,28	21,09	12,77	20,95	18,56	20,07	20,04	22,43	22,71	21,89	22,37	10,64	1,40	23,59	20,61	12,48	12,45
Na_2O	0,00	0,00	0,00	0,00	0,00	0,00	0,00	0,00	0,00	0,00	0,46	0,58	0,00	0,11	0,00	0,00	0,46	0,58
K_2O	0,00	0,00	0,00	0,00	0,00	0,00	0,00	0,00	0,00	0,00	0,00	0,00	0,05	0,00	0,00	0,00	0,00	0,00
Total	100,54	100,52	99,62	97,43	100,41	96,95	97,30	99,77	99,89	100,00	99,78	100,22	97,40	98,75	101,53	99,05	96,57	96,60
Si	1,98	1,99	1,94	1,95	1,92	1,93	1,97	1,96	1,99	2,00	1,98	1,98	2,06	2,07	1,97	1,94	2,06	2,05
Al^{IV}	0,02	0,00	0,06	0,05	0,08	0,07	0,03	0,04	0,01	0,00	0,02	0,02	-0,06	-0,07	0,03	0,04	-0,06	-0,05
Al^{VI}	0,01	0,00	0,02	0,02	0,03	0,03	0,04	0,03	0,02	0,02	0,01	0,01	0,10	0,08	0,01	0,00	0,12	0,10
Fe^{3+}	0,00	0,00	0,00	0,00	0,00	0,00	0,00	0,00	0,00	0,00	0,05	0,07	0,00	0,00	0,03	0,06	0,00	0,00
Cr	0,00	0,00	0,00	0,00	0,00	0,00	0,00	0,00	0,00	0,00	0,00	0,00	0,00	0,00	0,00	0,00	0,00	0,01
Ti	0,01	0,02	0,03	0,03	0,03	0,02	0,02	0,02	0,00	0,01	0,01	0,00	0,01	0,00	0,00	0,02	0,01	0,02
Fe^{2+}	0,64	0,65	0,31	0,48	0,33	0,36	0,31	0,33	0,27	0,25	0,21	0,19	0,40	0,63	0,22	0,28	0,39	0,42
Mn	0,02	0,02	0,00	0,01	0,00	0,00	0,00	0,00	0,00	0,00	0,00	0,00	0,01	0,03	0,02	0,02	0,01	0,00
Mg	1,24	1,27	0,77	0,93	0,77	0,82	0,79	0,79	0,81	0,80	0,83	0,81	0,97	1,14	0,80	0,82	0,84	0,83
Ca	0,07	0,05	0,85	0,53	0,84	0,77	0,82	0,80	0,89	0,90	0,87	0,89	0,43	0,06	0,93	0,84	0,51	0,51
Na	0,00	0,00	0,00	0,00	0,00	0,00	0,00	0,00	0,00	0,00	0,03	0,04	0,00	0,01	0,00	0,00	0,03	0,04
K	0,00	0,00	0,00	0,00	0,00	0,00	0,00	0,00	0,00	0,00	0,00	0,00	0,00	0,00	0,00	0,00	0,00	0,00
Suma	3,99	3,99	3,98	3,99	4,00	4,00	3,98	3,98	4,00	3,98	4,02	4,02	3,92	3,94	4,01	4,02	3,92	3,93
Wo	3,63	2,55	43,95	26,96	43,19	39,36	42,64	41,67	45,21	46,14	43,70	44,36	23,61	3,00	46,42	41,55	28,36	28,17
En	62,77	63,75	39,73	47,80	39,85	42,20	41,16	41,11	40,95	40,85	41,45	40,48	53,55	61,12	39,98	40,54	47,17	46,19
Fs	33,60	33,70	16,32	25,24	16,96	18,45	16,20	17,22	13,83	13,01	13,19	13,08	22,84	35,45	13,60	17,92	22,58	23,27
Act	0,00	0,00	0,00	0,00	0,00	0,00	0,00	0,00	0,00	0,00	1,66	2,08	0,00	0,43	0,00	0,00	1,89	2,37

Fase	Näsberg					Näsberg					Näsberg						
Litotipo	norita olivínica					norita olivínica					norita olivínica						
Muestra	S110					S128					S134						
Análisis	1	3	11	17	21	1	3	12	6	11	6	7	15	17	1	16	14
Mineral	Brz	Brz	Brz	Brz	En	Hyp	Hyp	Aug	Aug	Aug	Hyp	Hyp	Hyp	Hyp	Aug	Aug	Di
SiO_2	55,34	55,07	55,27	54,88	60,97	53,88	53,81	50,93	51,89	56,39	54,14	52,91	52,66	52,60	53,33	51,65	53,26
TiO_2	0,30	0,49	0,42	0,43	0,11	0,48	2,05	0,51	0,75	0,09	0,30	0,00	0,40	0,59	0,52	0,63	0,00
Al_2O_3	0,42	0,54	0,45	0,86	0,15	0,48	0,99	0,00	1,20	0,00	0,64	0,00	0,74	0,64	0,98	1,71	0,68
Cr_2O_3	0,00	0,00	0,00	0,00	0,00	0,00	0,00	0,00	0,00	0,11	0,00	0,00	0,00	0,00	0,58	0,56	0,00
FeO	13,05	13,33	13,46	12,95	4,55	17,62	17,97	8,81	9,27	5,52	22,27	23,62	22,27	22,69	10,27	9,72	9,31
MnO	0,42	0,48	0,44	0,24	0,23	0,00	0,43	0,00	0,00	0,00	0,00	0,00	0,54	0,59	0,00	0,00	0,48
MgO	28,60	29,19	28,50	27,99	27,86	24,97	24,92	14,72	15,60	21,32	21,74	21,14	20,86	21,21	14,51	13,91	14,00
CaO	1,29	1,18	1,21	2,00	0,09	1,99	0,00	19,70	19,43	12,44	1,02	1,86	2,34	1,59	20,87	21,88	22,84
Na_2O	0,35	0,00	0,00	0,00	0,26	0,00	0,00	0,63	0,00	0,24	0,00	0,00	0,00	0,00	0,59	0,00	0,00
K_2O	0,00	0,00	0,00	0,00	0,01	0,00	0,00	0,00	0,00	0,00	0,00	0,00	0,00	0,00	0,00	0,00	0,00
Total	99,77	100,28	99,75	99,35	94,23	99,42	100,17	95,30	98,14	96,11	100,11	99,53	99,81	99,91	101,65	100,06	100,57
Si	1,98	1,96	1,98	1,97	2,17	1,98	1,96	1,99	1,96	2,08	2,01	2,00	1,98	1,97	1,96	1,93	1,98
Al^{IV}	0,02	0,02	0,02	0,03	-0,17	0,02	0,04	0,00	0,04	-0,08	-0,01	0,00	0,02	0,03	0,04	0,07	0,02
Al^{VI}	0,00	0,00	0,00	0,01	0,18	0,00	0,00	0,00	0,01	0,08	0,03	0,00	0,01	0,00	0,01	0,01	0,01
Fe^{3+}	0,04	0,03	0,00	0,00	0,00	0,00	0,00	0,06	0,00	0,00	0,00	0,01	0,00	0,00	0,04	0,01	0,01
Cr	0,00	0,00	0,00	0,00	0,00	0,00	0,00	0,00	0,00	0,00	0,00	0,00	0,00	0,00	0,02	0,02	0,00
Ti	0,01	0,01	0,01	0,01	0,00	0,01	0,06	0,01	0,02	0,00	0,01	0,00	0,01	0,02	0,01	0,02	0,00
Fe^{2+}	0,35	0,36	0,40	0,39	0,14	0,54	0,55	0,23	0,29	0,17	0,69	0,73	0,70	0,71	0,27	0,30	0,28
Mn	0,01	0,01	0,01	0,01	0,01	0,00	0,01	0,00	0,00	0,00	0,00	0,00	0,02	0,02	0,00	0,00	0,02
Mg	1,53	1,55	1,52	1,50	1,48	1,37	1,35	0,86	0,88	1,17	1,20	1,19	1,17	1,19	0,80	0,78	0,78
Ca	0,05	0,05	0,05	0,08	0,00	0,08	0,00	0,82	0,79	0,49	0,04	0,08	0,09	0,06	0,82	0,88	0,91
Na	0,02	0,00	0,00	0,00	0,02	0,00	0,00	0,05	0,00	0,02	0,00	0,00	0,00	0,00	0,04	0,00	0,00
K	0,00	0,00	0,00	0,00	0,00	0,00	0,00	0,00	0,00	0,00	0,00	0,00	0,00	0,00	0,00	0,00	0,00
Suma	4,01	4,01	4,00	4,00	3,84	4,00	3,97	4,02	3,99	3,93	3,98	4,00	4,00	4,00	4,01	4,00	4,00
Wo	2,47	2,25	2,34	3,90	0,21	3,94	0,00	40,90	40,15	26,51	2,09	3,74	4,76	3,23	41,64	44,82	45,71
En	76,23	77,29	76,67	75,99	89,70	68,81	70,53	42,53	44,86	63,22	62,02	59,20	59,01	59,87	40,29	39,65	38,99
Fs	20,08	20,47	20,99	20,11	9,00	27,25	29,47	14,20	14,98	9,35	35,88	37,06	36,23	36,90	15,94	15,53	15,29
Act	1,21	0,00	0,00	0,00	1,09	0,00	0,00	2,37	0,00	0,93	0,00	0,00	0,00	0,00	2,13	0,00	0,00

Fase	Näsberg									GII					GII					
Litotipo	gabro norita									granodiorita					cuarzo monzonita					
Muestra	S217									JO03-67 epma					JO04-34 epma					
Análisis	1	8	14	2	6	9	10	15	16	12	13	33	37	38	21	23	25	30	37	38
Mineral	Hyp	Hyp	Hyp	Di	Aug	Aug	Aug	Aug	Aug	Di	Aug	Aug	Di	Di	Aug	Aug	Aug	Di	S-Aug	Di
SiO_2	54,03	53,82	53,27	52,70	52,33	51,30	50,40	52,11	50,38	52,39	52,20	52,65	51,71	49,84	51,35	50,89	52,09	50,89	48,38	52,86
TiO_2	0,43	0,00	0,00	0,90	0,72	0,77	1,09	0,87	0,72	0,16	0,39	0,07	0,15	0,24	0,49	0,53	0,38	0,36	0,91	0,14
Al_2O_3	0,55	0,61	0,67	1,96	3,09	2,02	2,34	3,54	2,25	1,05	2,19	1,43	0,94	0,95	2,90	3,14	1,96	2,32	4,87	0,70
Cr_2O_3	0,00	0,00	0,00	0,00	0,00	0,00	0,00	0,00	0,00	0,26	0,19	0,18	0,29	0,07	0,37	0,52	0,45	0,39	0,06	0,03
FeO	18,80	19,97	19,24	9,01	12,08	10,25	10,40	9,79	9,80	8,21	10,29	11,24	8,19	8,42	10,88	11,03	8,99	10,87	15,25	10,60
MnO	0,57	0,56	0,61	0,00	0,00	0,58	0,00	0,00	0,00	0,92	0,73	0,73	0,84	0,81	0,36	0,38	0,40	0,39	0,31	0,48
MgO	23,86	23,37	23,71	13,90	16,58	15,28	14,88	14,01	15,20	13,38	15,70	15,64	13,09	12,34	13,20	13,15	13,64	12,59	12,86	11,91
CaO	1,79	1,90	1,65	22,12	13,56	19,26	18,97	18,39	19,48	21,95	14,32	13,45	22,64	22,48	17,86	18,01	20,24	19,81	11,90	22,77
Na_2O	0,00	0,00	0,00	0,00	0,84	0,53	0,55	0,81	0,00	0,37	0,28	0,17	0,51	0,39	0,64	0,65	0,61	0,52	0,68	0,48
K_2O	0,00	0,00	0,00	0,00	0,00	0,00	0,00	0,00	0,00	0,05	0,15	0,05	0,00	0,00	0,26	0,24	0,11	0,23	0,56	0,00
Total	100,03	100,23	99,15	100,59	99,20	99,99	98,63	99,52	97,83	98,73	96,44	95,59	98,35	95,54	98,38	98,65	98,90	98,39	95,87	100,04
Si	1,98	1,98	1,98	1,95	1,95	1,92	1,91	1,94	1,92	1,98	1,99	2,02	1,97	1,96	1,95	1,93	1,96	1,95	1,90	1,99
Al^{IV}	0,02	0,02	0,02	0,05	0,05	0,08	0,09	0,06	0,08	0,02	0,01	-0,02	0,03	0,04	0,05	0,07	0,04	0,05	0,10	0,01
Al^{VI}	0,01	0,01	0,01	0,04	0,08	0,01	0,01	0,09	0,02	0,03	0,09	0,09	0,01	0,01	0,08	0,07	0,05	0,05	0,13	0,02
Fe^{3+}	0,00	0,01	0,02	0,00	0,00	0,10	0,08	0,00	0,03	0,01	0,00	0,00	0,06	0,07	0,00	0,01	0,01	0,03	0,00	0,01
Cr	0,00	0,00	0,00	0,00	0,00	0,00	0,00	0,00	0,00	0,01	0,01	0,01	0,01	0,00	0,01	0,02	0,01	0,01	0,00	0,00
Ti	0,01	0,00	0,00	0,03	0,02	0,02	0,03	0,02	0,02	0,00	0,01	0,00	0,00	0,01	0,01	0,02	0,01	0,01	0,03	0,00
Fe^{2+}	0,58	0,61	0,58	0,28	0,38	0,22	0,25	0,31	0,28	0,25	0,33	0,37	0,20	0,21	0,35	0,34	0,28	0,31	0,50	0,32
Mn	0,02	0,02	0,02	0,00	0,00	0,02	0,00	0,00	0,00	0,03	0,02	0,02	0,03	0,03	0,01	0,01	0,01	0,01	0,01	0,02
Mg	1,31	1,28	1,31	0,77	0,92	0,85	0,84	0,78	0,86	0,75	0,89	0,90	0,74	0,72	0,75	0,74	0,77	0,72	0,75	0,67
Ca	0,07	0,08	0,07	0,88	0,54	0,77	0,77	0,73	0,79	0,89	0,58	0,55	0,92	0,95	0,73	0,73	0,82	0,81	0,50	0,92
Na	0,00	0,00	0,00	0,00	0,06	0,04	0,04	0,06	0,00	0,03	0,02	0,01	0,04	0,03	0,05	0,05	0,04	0,04	0,05	0,04
K	0,00	0,00	0,00	0,00	0,00	0,00	0,00	0,00	0,00	0,00	0,01	0,00	0,00	0,00	0,01	0,01	0,01	0,01	0,03	0,00
Suma	3,99	4,00	4,00	3,98	4,00	4,03	4,02	3,99	4,01	4,00	3,96	3,95	4,02	4,02	4,00	4,00	4,00	4,01	4,00	4,00
Wo	3,57	3,77	3,29	45,58	28,49	38,62	38,92	39,12	40,36	45,39	31,56	29,90	46,39	47,29	38,66	38,83	42,47	42,12	27,55	46,61
En	66,21	64,47	65,83	39,86	48,48	42,63	42,49	41,47	43,83	38,49	48,17	48,39	37,33	36,14	39,79	39,46	39,84	37,23	41,45	33,91
Fs	30,22	31,76	30,88	14,56	19,83	16,83	16,55	16,30	15,81	14,74	19,14	21,04	14,40	15,11	19,02	19,19	15,37	18,64	28,15	17,69
Act	0,00	0,00	0,00	0,00	3,19	1,92	2,04	3,12	0,00	1,38	1,12	0,66	1,88	1,47	2,52	2,52	2,32	2,01	2,85	1,78

Fase	GI					GI										Näsberg
Litotipo	tonalita					tonalita										norita
Muestra	23j28					23j31										23j84
Análisis	5	6	8	9	10	3	6	7	8	9	16	17	18	28	29	13
Mineral	Pl	Pl	Kfs	Pl	Pl	Pl	Kfs	Kfs	Kfs	Kfs	Kfs	Kfs	Pl	Pl	Pl	Kfs
SiO_2	55,29	61,06	64,22	57,26	67,14	64,65	62,72	62,93	64,72	63,12	64,11	62,14	67,04	57,28	65,62	56,07
Al_2O_3	27,40	23,67	18,15	27,28	21,23	21,08	18,08	18,10	18,13	18,40	17,88	18,10	19,56	26,17	22,42	27,63
FeO	0,16	0,04	0,04	0,18	0,04	0,12	0,14	0,12	0,42	0,08	0,01	0,11	0,14	0,21	0,27	0,00
CaO	10,71	5,96	0,13	10,08	1,85	2,52	0,17	0,10	0,03	0,24	0,02	0,09	0,76	8,84	3,17	0,29
Na_2O	5,38	8,09	0,55	6,17	9,49	9,62	0,77	0,83	0,42	0,98	1,01	0,98	10,44	6,56	9,77	10,44
K_2O	0,10	0,07	15,81	0,07	0,36	0,04	14,46	14,09	15,31	14,65	14,75	13,43	0,10	0,26	0,27	5,71
BaO	-	-	-	-	-	0,00	2,17	2,10	0,04	2,11	0,69	3,16	0,00	0,00	0,00	0,20
Total	99,04	98,89	98,90	101,04	100,11	98,03	98,51	98,27	99,07	99,58	98,47	98,01	98,04	99,32	101,52	100,34
An	52,08	28,82	0,65	47,26	9,51	12,62	0,91	0,54	0,16	1,23	0,10	0,50	3,84	42,05	14,97	1,12
Ab	47,34	70,78	4,99	52,35	88,29	87,15	7,42	8,17	4,00	9,11	9,42	9,93	95,55	56,47	83,51	72,72
Or	0,58	0,40	94,36	0,39	2,20	0,24	91,68	91,28	95,85	89,65	90,48	89,56	0,60	1,47	1,52	26,17

Fase	GII						GI			GII				Rengård, tipo GI			Rengård
Litotipo	granodiorita						tonalita			granodiorita				tonalita			tonalita
Muestra	24k104						JO03-35a			JO03-67				JO03-108			JO03-109
Análisis	4	6	7	8	9	18	13	14	17	4	5	10	11	3	4	8	14
Mineral	Pl	Kfs	Kfs	Pl	Pl	Pl	Pl	Kfs	Kfs	Pl	Pl	Pl	Pl	Pl	Pl	Pl	Pl
SiO_2	65,80	64,14	64,97	71,15	65,27	65,66	65,51	67,10	64,38	59,06	62,77	60,84	64,08	63,46	63,14	57,84	55,66
Al_2O_3	20,80	18,07	17,64	17,95	21,80	21,66	18,70	20,50	17,96	25,09	23,8	24,47	23,21	23,19	24,07	26,14	24,29
FeO	0,04	0,23	0,09	0,18	0,10	0,10	0,05	0,29	0,03	0,37	0,25	0,09	0,61	0,08	0,43	0,17	0,13
CaO	2,47	0,02	0,37	0,95	3,35	2,91	0,06	1,29	0,01	8,00	5,59	6,85	5,06	4,76	4,82	7,74	6,98
Na_2O	10,21	0,63	0,75	10,27	9,46	10,12	0,44	9,79	0,40	7,33	8,62	7,63	8,92	8,65	8,5	6,74	6,48
K_2O	0,03	15,08	15,37	0,13	0,05	0,10	15,78	1,31	15,76	0,12	0,15	0,17	0,18	0,05	0,08	0,13	0,01
BaO	-	-	-	-	-	-	-	-	-	-	-	-	-	-	-	-	-
Total	99,35	98,17	99,19	100,63	100,03	100,55	100,54	100,28	98,54	99,97	101,18	100,05	102,06	100,19	101,04	98,76	93,55
An	11,77	0,10	1,85	4,82	16,32	13,63	0,31	6,27	0,05	37,37	26,16	32,84	23,63	23,25	23,75	38,52	37,29
Ab	88,06	5,96	6,78	94,39	83,39	85,81	4,05	86,14	3,71	61,96	73,00	66,19	75,37	76,46	75,78	60,71	62,65
Or	0,17	93,93	91,38	0,79	0,29	0,56	95,64	7,58	96,24	0,67	0,84	0,97	1,00	0,29	0,47	0,77	0,06

Fase	GI		Rengård, tipo GI				Rengård, tipo GI		Rengård, tipo GI							
Litotipo	tonalita		tonalita				tonalita		tonalita							
Muestra	JO03-87		JO03-110				JO03-109 epma		JO03-110 epma							
Análisis	7	8	16	36	37	41	1	2	10	11	13	21	22	29	30	39
Mineral	Pl	Pl	Pl	Pl	Pl	Pl	Pl	Pl	Pl	Pl	Pl	Pl	Pl	Pl	Pl	Pl
SiO_2	62,64	56,14	58,96	59,89	59,01	63,46	59,58	60,36	66,17	60,29	60,27	61,19	59,77	66,70	60,32	64,54
Al_2O_3	23,26	27,19	24,90	22,12	23,14	20,04	24,35	24,01	21,09	24,88	24,68	23,61	25,22	20,36	24,47	21,11
FeO	0,07	0,16	0,07	0,17	0,22	0,08	0,03	0,13	0,00	0,07	0,42	0,05	0,05	0,02	0,00	0,02
CaO	5,37	10,38	6,98	4,28	5,29	1,81	5,45	5,17	1,60	6,04	5,78	4,82	6,59	1,22	6,04	1,73
Na_2O	8,29	5,74	7,49	8,42	7,31	9,59	7,96	8,02	10,68	8,13	8,12	8,61	7,47	10,76	8,04	10,27
K_2O	0,02	0,12	0,05	0,03	0,03	0,1	0,07	0,07	0,05	0,06	0,13	0,05	0,05	0,05	0,07	0,05
BaO	-	-	-	-	-	-	-	-	0,00	0,04	0,07	0,02	0,04	0,06	0,03	0,11
Total	99,65	99,73	98,45	94,91	95	95,08	97,43	97,75	99,59	99,51	99,47	98,34	99,20	99,17	98,95	97,85
An	26,33	49,64	33,89	21,89	28,51	9,39	27,33	26,15	7,63	29,00	28,04	23,55	32,68	5,88	29,20	8,51
Ab	73,55	49,68	65,82	77,93	71,30	90,00	72,27	73,42	92,07	70,66	71,23	76,19	67,03	93,82	70,41	91,18
Or	0,12	0,68	0,29	0,18	0,19	0,62	0,40	0,43	0,30	0,33	0,73	0,26	0,29	0,30	0,39	0,32

Fase	GI														
Litotipo	tonalita														
Muestra	23j28 epma														
Análisis	9	10	11	12	13	14	15	16	17	18	35	36	37	39	40
Mineral	Pl	Pl	Pl	Pl	Pl	Pl	Pl	Pl	Pl	Pl	Pl	Pl	Kfs	Pl	Pl
SiO_2	60,59	54,43	57,45	54,40	60,33	54,55	54,42	60,14	59,37	54,81	55,87	63,46	48,10	55,03	54,36
Al_2O_3	24,37	28,84	26,75	28,88	24,41	28,49	28,32	24,79	25,11	28,61	27,69	22,53	30,87	28,22	28,55
FeO	0,06	0,13	0,10	0,13	0,08	0,18	0,10	0,11	0,11	0,06	0,21	0,05	2,54	0,12	0,08
CaO	5,83	10,82	8,38	10,74	6,01	10,87	10,01	6,11	6,44	10,14	9,55	3,39	0,18	10,32	10,55
Na_2O	8,20	5,16	6,68	5,27	8,14	5,34	5,59	7,85	7,77	5,82	6,02	9,65	0,35	5,45	5,41
K_2O	0,04	0,06	0,06	0,08	0,07	0,06	0,07	0,07	0,08	0,07	0,05	0,04	11,58	0,05	0,07
BaO	0,00	0,05	0,04	0,07	0,00	0,08	0,07	0,03	0,00	0,00	0,00	0,06	0,13	0,00	0,04
Total	99,08	99,48	99,46	99,55	99,05	99,56	98,59	99,09	98,87	99,50	99,38	99,18	93,77	99,19	99,05
An	28,15	53,50	40,81	52,76	28,85	52,76	49,53	29,97	31,24	48,87	46,58	16,23	1,25	50,98	51,67
Ab	71,60	46,17	58,85	46,80	70,73	46,92	50,06	69,64	68,29	50,74	53,15	83,56	4,36	48,72	47,93
Or	0,25	0,34	0,33	0,44	0,42	0,32	0,41	0,39	0,47	0,39	0,27	0,21	94,39	0,30	0,40

Fase	GII						GII				GIV						
Litotipo	enclave en granodiorita						granodiorita				monzogranito						
Muestra	JO03-67 epma						JO03-67 epma				23J58 epma						
Análisis	1	4	8	9	52	53	22	23	44	49	22	23	24	25	26	27	30
Mineral	Pl	Pl	Pl	Pl	Pl	Pl	Pl	Pl	Pl	Pl	Pl	Pl	Pl	Pl	Pl	Pl	Kfs
SiO_2	60,91	59,95	60,40	60,42	60,52	55,44	61,09	60,48	53,14	60,20	61,36	63,82	59,90	64,01	65,64	63,24	62,91
Al_2O_3	24,97	25,02	24,82	24,40	24,60	26,99	24,49	24,36	28,63	24,05	23,71	22,63	24,50	18,77	20,39	22,72	18,93
FeO	0,31	0,21	0,11	0,18	0,09	0,14	0,22	0,20	0,19	0,23	0,11	0,04	0,01	0,05	0,01	0,09	0,00
CaO	5,70	6,23	5,84	5,46	5,62	8,65	5,50	5,45	10,37	4,94	4,25	2,98	4,91	0,00	0,23	3,19	0,00
Na_2O	8,05	7,70	7,96	8,16	8,09	6,34	8,14	7,82	5,31	8,51	9,17	10,03	8,82	0,25	11,50	9,68	0,32
K_2O	0,10	0,08	0,08	0,09	0,06	0,08	0,10	0,14	0,15	0,09	0,07	0,05	0,08	16,55	0,11	0,08	16,51
BaO	-	-	-	-	-	-	-	-	-	-	0,00	0,04	0,00	0,01	0,00	0,00	0,00
Total	100,04	99,19	99,21	98,71	98,99	97,65	99,54	98,45	97,79	98,02	98,67	99,59	98,22	99,63	97,88	99,00	98,67
An	27,96	30,75	28,71	26,86	27,64	42,78	27,02	27,55	51,47	24,18	20,29	14,07	23,41	0,00	1,07	15,31	0,00
Ab	71,49	68,76	70,82	72,62	72,01	56,74	72,39	71,60	47,66	75,32	79,30	85,64	76,13	2,24	98,34	84,24	2,83
Or	0,55	0,49	0,47	0,52	0,35	0,48	0,59	0,85	0,87	0,50	0,41	0,29	0,45	97,76	0,59	0,45	97,16

Fase	GIV															
Litotipo	monzogranito															
Muestra	JO03-58 epma															
Análisis	5	6	8	9	10	11	12	13	14	15	16	17	18	19	20	21
Mineral	Pl	Pl	Pl	Pl	Pl	Pl	Kfs	Pl	Kfs	Kfs	Pl	Pl	Pl	Kfs	Pl	Kfs
SiO_2	63,86	62,78	67,39	63,58	63,35	65,58	63,82	63,60	63,49	61,88	63,72	62,66	66,88	62,18	65,38	63,22
Al_2O_3	22,14	23,09	20,17	22,06	22,96	20,24	19,08	22,01	18,94	19,12	22,11	22,30	20,18	18,51	21,00	18,88
FeO	0,04	0,10	0,07	0,14	0,14	0,06	0,11	0,00	0,00	0,00	0,11	0,14	0,06	0,06	0,03	0,04
CaO	2,62	3,56	0,20	2,32	3,25	0,06	0,00	2,00	0,00	0,00	2,27	3,49	0,29	0,00	1,05	0,00
Na_2O	10,09	9,45	11,47	10,21	9,83	11,85	0,48	10,58	0,46	0,48	10,14	9,52	11,48	0,53	11,12	0,50
K_2O	0,06	0,05	0,07	0,09	0,08	0,04	16,01	0,10	16,21	16,07	0,07	0,06	0,04	16,06	0,10	16,34
BaO	0,00	0,00	0,00	0,02	0,00	0,05	0,56	0,04	0,22	0,56	0,02	0,03	0,00	0,35	0,00	0,15
Total	98,80	99,03	99,37	98,41	99,61	97,87	100,06	98,33	99,31	98,12	98,44	98,20	98,92	97,69	98,67	99,12
An	12,50	17,17	0,95	11,09	15,37	0,30	0,00	9,39	0,00	0,00	10,94	16,80	1,36	0,00	4,91	0,00
Ab	87,15	82,54	98,66	88,42	84,17	99,50	4,36	90,04	4,12	4,38	88,64	82,85	98,43	4,78	94,53	4,40
Or	0,35	0,28	0,40	0,49	0,46	0,20	95,64	0,57	95,88	95,62	0,43	0,35	0,21	95,22	0,56	95,60

Fase	Hbl tonalite											GIIb				
Litotipo	tonalite (cuarzo anfibolita)											cuarzo monzodiorita				
Muestra	VIC04-01 epma											JO04-34 epma				
Análisis	4	5	11	12	13	14	17	18	19	52	53	31	32	33	34	36
Mineral	Pl	Pl	Pl	Pl	Pl	Pl	Pl	Pl	Pl	Pl	Pl	Pl	Pl	Pl	Pl	Pl
SiO_2	59,11	58,53	59,23	57,61	49,33	57,11	58,22	58,16	59,37	60,52	55,44	63,11	62,45	58,29	61,78	62,76
Al_2O_3	25,11	25,65	25,22	25,96	16,49	25,73	25,89	25,82	25,00	24,60	26,99	18,24	22,26	24,82	22,51	17,82
FeO	0,09	0,30	0,04	0,03	11,03	0,05	0,09	0,07	0,08	0,09	0,14	0,03	0,06	0,10	0,02	0,02
CaO	6,32	6,69	6,41	7,06	9,59	6,89	7,08	6,97	6,72	5,62	8,65	0,00	4,06	7,21	4,26	0,00
Na_2O	7,86	7,70	7,83	7,50	4,28	7,53	7,49	7,47	7,67	8,09	6,34	0,54	9,02	7,28	8,95	0,35
K_2O	0,15	0,11	0,07	0,07	0,51	0,07	0,06	0,10	0,13	0,06	0,08	15,50	0,06	0,14	0,09	16,04
BaO	0,00	0,00	0,00	0,02	0,00	0,05	0,04	0,22	0,56	0,02	0,03	0,00	0,00	0,00	0,02	0,00
Total	98,63	98,97	98,79	98,24	91,22	97,42	98,86	98,81	99,54	99,01	97,67	97,42	97,92	97,84	97,63	96,99
An	30,49	32,26	31,03	34,07	53,45	33,46	34,20	33,82	32,39	27,64	42,78	0,00	19,85	35,10	20,72	0,00
Ab	68,67	67,14	68,57	65,56	43,19	66,17	65,47	65,60	66,88	72,01	56,74	5,01	79,79	64,10	78,74	3,20
Or	0,83	0,60	0,40	0,37	3,37	0,38	0,33	0,58	0,73	0,35	0,48	94,99	0,35	0,79	0,54	96,80

Fase	Tonalite	Hbl tonalite									GI		Vargfors
Litotipo	tonalite	tonalita									tonalita		basalto
Muestra	VIC04-07	VIC04-11 epma									JO04-86 epma		JO03-124
Análisis	31	5	6	7	8	9	10	15	16	17	20	16	17	6
Mineral	Pl	Pl	Pl	Pl	Pl	Pl	Pl	Pl	Pl	Pl	Pl	Pl	Pl	Pl
SiO_2	58,04	65,38	64,41	65,21	64,90	64,91	64,35	63,77	63,69	64,27	63,62	63,34	55,72	66,91
Al_2O_3	25,63	21,74	22,40	21,88	21,95	21,91	22,22	22,46	21,86	22,02	22,60	22,87	28,24	19,82
FeO	0,10	0,00	0,02	0,01	0,03	0,02	0,00	0,00	0,02	0,00	0,03	0,07	0,09	0,10
CaO	5,75	9,99	9,61	9,83	9,61	9,87	9,66	9,45	9,63	9,49	9,21	4,07	10,13	0,31
Na_2O	8,73	2,89	3,58	3,04	3,30	3,12	3,36	3,75	3,36	3,45	3,96	8,97	5,41	10,83
K_2O	0,03	0,08	0,08	0,07	0,06	0,06	0,07	0,08	0,07	0,05	0,07	0,07	0,10	0,07
BaO	0	0,00	0,00	0,00	0,02	0,00	0,00	0,00	0,00	0,00	0,00	0,04	0,05	0,029
Total	98,29	100,08	100,10	100,03	99,87	99,90	99,65	99,52	98,62	99,28	99,49	99,49	99,89	98,23
An	26,62	65,29	59,37	63,80	61,36	63,33	61,09	57,85	60,98	60,13	55,95	19,96	50,55	1,57
Ab	73,19	34,12	40,05	35,66	38,16	36,21	38,41	41,54	38,50	39,50	43,51	79,64	48,88	98,03
Or	0,19	0,58	0,58	0,54	0,48	0,46	0,50	0,61	0,52	0,37	0,54	0,40	0,56	0,40

Fase	GI								GII								
Litotipo	tonalita								qz-monzodiorita								
Muestra	23J31 epma								JO04-128								
Análisis	1	2	3	4	5	6	10	11	102	103	104	105	116	132	133	134	135
Mineral	Pl	Pl	Pl	Pl	Pl	Kfs	Kfs	Kfs	Pl	Pl	Pl	Kfs	Pl	Pl	Pl	Pl	Pl
SiO_2	65,20	57,28	68,08	63,72	68,02	64,00	63,73	62,37	66,92	60,90	62,06	64,23	62,97	63,55	67,86	63,70	64,49
Al_2O_3	21,74	26,83	19,90	22,89	20,07	18,75	18,53	19,31	19,86	24,21	23,55	18,50	18,53	22,37	19,67	22,37	22,20
FeO	0,14	0,14	0,00	0,12	0,02	0,03	0,42	0,47	0,06	0,12	0,11	0,19	0,00	0,18	0,02	0,15	0,02
CaO	2,37	8,38	0,31	3,55	0,37	0,00	0,00	0,00	0,27	5,33	4,70	0,00	0,00	3,39	0,16	3,46	2,89
Na_2O	9,80	6,40	10,73	8,96	10,61	0,41	0,27	0,33	11,08	8,20	8,67	0,37	0,31	9,37	11,29	9,23	9,83
K_2O	0,07	0,08	0,05	0,12	0,12	16,31	16,49	15,45	0,10	0,08	0,13	16,61	16,67	0,21	0,07	0,21	0,10
BaO	0,00	0,00	0,07	0,00	0,00	0,00	0,04	2,36	0,00	0,09	0,08	0,19	0,05	0,06	0,00	0,06	0,06
Total	99,47	99,25	99,26	99,44	99,32	99,59	99,68	100,39	98,77	99,16	99,54	100,33	98,73	99,24	99,17	99,39	99,83
An	11,75	41,80	1,56	17,84	1,90	0,00	0,00	0,00	1,34	26,27	22,89	0,00	0,00	16,48	0,79	16,94	13,88
Ab	87,84	57,71	98,14	81,46	97,38	3,64	2,42	3,18	98,08	73,25	76,38	3,31	2,73	82,33	98,83	81,83	85,53
Or	0,41	0,49	0,31	0,70	0,72	96,36	97,58	96,82	0,59	0,48	0,73	96,69	97,27	1,20	0,37	1,23	0,60

Fase	GIII							GI									
Litotipo	monzogranito							tonalita									
Muestra	JO03-45 epma							JO04-75 epma									
Análisis	18	19	20	21	22	23	25	39	40	58	59	60	61	62	63	64	65
Mineral	Kfs	Pl	Pl	Pl	Kfs	Pl	Pl	Pl	Pl	Pl	Kfs	Pl	Pl	Pl	Pl	Pl	Pl
SiO_2	64,38	66,91	67,87	64,97	63,95	66,69	67,30	64,45	65,06	57,52	62,03	57,43	56,22	67,27	57,64	57,48	55,05
Al_2O_3	18,65	20,00	19,84	21,57	18,75	20,64	20,01	21,98	21,82	26,29	23,62	26,43	27,18	20,01	25,96	26,10	27,95
FeO	0,07	0,00	0,08	0,04	0,09	0,04	0,05	0,14	0,15	0,32	0,19	0,30	0,29	0,02	0,29	0,30	0,33
CaO	0,00	0,29	0,10	2,24	0,00	1,01	0,31	2,80	2,48	8,34	4,76	8,41	9,21	0,60	8,01	8,33	10,29
Na_2O	0,24	10,58	10,57	9,35	0,53	10,25	10,27	9,46	9,44	6,22	8,34	6,28	5,64	10,52	6,40	6,13	5,22
K_2O	16,53	0,11	0,05	0,09	15,92	0,08	0,08	0,12	0,16	0,26	0,14	0,18	0,23	0,05	0,29	0,25	0,23
BaO	0,00	0,00	0,04	0,00	0,47	0,02	0,00	0,02	0,02	0,06	0,11	0,00	0,05	0,00	0,00	0,00	0,00
Total	99,96	98,04	98,65	98,44	99,79	99,02	98,18	99,07	99,21	99,14	99,37	99,10	99,16	98,58	98,84	98,75	99,18
An	0,00	1,50	0,51	11,64	0,00	5,16	1,64	13,96	12,55	41,92	23,76	42,06	46,78	3,05	40,16	42,23	51,44
Ab	2,19	97,83	99,17	87,83	4,83	94,36	97,87	85,32	86,46	56,56	75,40	56,85	51,82	96,64	58,09	56,26	47,18
Or	97,81	0,68	0,32	0,53	95,17	0,48	0,49	0,72	0,98	1,53	0,84	1,09	1,40	0,31	1,75	1,51	1,37

Fase	GI												
Litotipo	tonalita												
Muestra	JO04-110 epma												
Análisis	59	60	61	62	63	74	75	76	77	89	90	91	92
Mineral	Pl	Pl	Pl	Pl	Pl	Kfs	Kfs	Kfs	Kfs	Pl	Pl	Pl	Kfs
SiO_2	65,20	66,39	66,51	64,61	68,11	63,72	62,87	64,15	62,93	63,45	67,58	65,69	64,20
Al_2O_3	21,40	20,35	20,29	21,63	19,74	18,60	18,81	18,59	18,94	22,47	19,73	21,14	18,43
FeO	0,15	0,01	0,00	0,09	0,05	0,05	0,07	0,05	0,10	0,17	0,02	0,01	0,08
CaO	2,25	1,01	0,81	2,60	0,16	0,01	0,00	0,00	0,00	3,51	0,16	1,66	0,00
Na_2O	10,42	10,94	10,96	10,18	11,26	0,45	0,38	0,46	0,64	9,49	11,44	10,41	0,31
K_2O	0,09	0,03	0,04	0,09	0,07	16,32	15,91	16,34	15,61	0,11	0,06	0,05	16,57
BaO	0,00	0,11	0,07	0,04	0,00	0,30	1,61	0,55	1,52	0,09	0,06	0,03	0,00
Total	99,60	99,02	98,83	99,41	99,50	99,57	99,82	100,18	99,88	99,64	99,10	99,16	99,63
An	10,62	4,83	3,93	12,32	0,77	0,02	0,00	0,00	0,00	16,86	0,78	8,06	0,00
Ab	88,88	94,98	95,86	87,19	98,82	4,02	3,48	4,10	5,87	82,53	98,85	91,63	2,74
Or	0,50	0,19	0,20	0,49	0,42	95,96	96,52	95,90	94,13	0,61	0,36	0,31	97,26

Fase	GII														
Litotipo	qz-monzodiorita														
Muestra	JO04-42 epma														
Análisis	7	8	14	15	16	17	18	19	20	21	22	23	24	56	57
Mineral	Kfs	Pl	Kfs	Pl	Pl	Pl	Pl	Pl	Pl	Pl	Pl	Kfs	Kfs	Pl	Pl
SiO_2	64,32	63,55	64,38	68,21	63,88	61,76	63,45	67,70	98,44	63,08	66,66	63,79	64,19	61,37	61,11
Al_2O_3	18,64	22,83	18,59	19,96	22,57	24,12	22,96	19,93	0,02	23,15	20,26	18,49	18,48	23,28	23,97
FeO	0,09	0,13	0,16	0,01	0,10	0,12	0,05	0,01	0,04	0,12	0,03	0,11	0,10	0,20	0,13
CaO	0,00	3,51	0,00	0,08	3,37	5,01	3,81	0,22	0,00	3,99	0,68	0,00	0,00	4,36	4,96
Na_2O	0,50	9,92	0,35	11,97	10,05	8,81	9,67	11,75	0,01	9,49	11,64	0,58	0,68	8,93	8,63
K_2O	16,38	0,09	16,57	0,11	0,07	0,09	0,06	0,10	0,01	0,14	0,06	16,32	16,20	0,05	0,12
BaO	0,00	0,00	0,00	0,02	0,08	0,09	0,00	0,00	0,02	0,00	0,05	0,05	0,11	0,13	0,00
Total	100,00	100,28	100,12	100,41	100,23	100,12	100,14	99,93	98,60	100,02	99,46	99,44	99,93	98,45	99,12
An	0,00	16,28	0,00	0,37	15,59	23,79	17,83	1,02	0,00	18,70	3,13	0,00	0,00	21,18	23,94
Ab	4,43	83,21	3,07	99,02	84,04	75,68	81,82	98,43	55,43	80,53	96,53	5,15	6,01	78,53	75,37
Or	95,57	0,51	96,93	0,61	0,37	0,53	0,36	0,55	44,57	0,77	0,35	94,85	93,99	0,29	0,69

Fase	GI tonalita				GI tonalita						GI tonalita			GI tonalita				GI trondhj.	
Muestra	23J28				23J31						23K37			JO03-35				JO03-80	
Análisis	1	7	13	14	4	2	21	21b	22	15ep	3	4	8	5	10	16	21	3	13
Mineral	ep	ep	ep	ep	ep	ep	ep	ep	ep	ep	ep	ep	ep	ep	ep	ep	ep	ep	ep
SiO_2	37,43	37,71	37,24	37,49	36,81	37,31	38,50	38,25	37,84	37,56	37,53	37,82	38,64	37,70	37,95	39,20	38,18	38,48	38,64
TiO_2	0,23	0,14	0,03	0,21	0,12	0,26	0,08	0,10	0,16	0,09	0,12	0,10	0,12	0,16	0,03	0,13	0,14	0,22	0,24
Al_2O_3	22,31	25,69	21,03	24,72	21,58	22,22	23,79	23,03	22,13	23,92	24,50	22,70	24,89	21,51	22,36	26,25	23,38	23,74	24,65
FeO	13,15	8,16	14,74	9,09	12,52	12,41	12,36	12,03	13,13	11,99	8,89	11,49	10,09	13,20	13,73	9,13	11,95	11,40	11,90
MnO	0,45	0,28	0,33	0,10	0,48	0,48	0,81	0,93	0,35	0,43	0,23	0,04	0,08	0,16	0,17	0,12	0,35	0,15	0,45
MgO	0,05	0,13	0,23	0,05	0,12	0,19	0,30	0,02	0,08	0,01	0,12	0,13	0,10	0,29	0,14	0,21	0,07	0,12	0,14
CaO	23,37	23,62	23,37	23,71	23,14	13,81	23,74	23,67	23,64	23,15	23,44	22,93	23,87	24,12	24,08	24,51	23,80	23,27	24,59
Na_2O	0,32	0,47	0,18	0,27	0,20	0,22	0,31	0,22	0,14	0,02	0,22	0,24	0,19	0,10	0,38	0,29	0,35	0,32	0,40
K_2O	0,06	0,04	0,05	0,03	0,11	0,13	0,03	0,06	0,08	0,08	0,09	0,03	0,06	0,06	0,04	0,08	0,08	0,14	0,03
Suma	97,37	96,24	97,20	95,67	95,08	87,03	99,92	98,31	97,55	97,26	95,14	95,48	98,04	97,30	98,88	99,92	98,30	97,84	101,04
Si	2,98	2,99	2,98	3,00	3,00	3,20	2,98	3,01	3,00	2,97	3,02	3,04	3,02	3,01	2,98	3,00	3,00	3,02	2,95
Ti	0,01	0,01	0,00	0,01	0,01	0,02	0,00	0,01	0,01	0,01	0,01	0,01	0,01	0,01	0,00	0,01	0,01	0,01	0,01
Al	2,09	2,40	1,99	2,33	2,07	2,25	2,17	2,14	2,07	2,23	2,32	2,15	2,29	2,02	2,07	2,37	2,16	2,20	2,22
Fe^{+3}	0,88	0,54	0,99	0,61	0,85	0,89	0,80	0,79	0,87	0,79	0,60	0,77	0,66	0,88	0,90	0,58	0,78	0,75	0,76
Mn	0,03	0,02	0,02	0,01	0,03	0,03	0,05	0,06	0,02	0,03	0,02	0,00	0,01	0,01	0,01	0,01	0,02	0,01	0,03
Mg	0,01	0,02	0,03	0,01	0,01	0,02	0,03	0,00	0,01	0,00	0,01	0,02	0,01	0,03	0,02	0,02	0,01	0,01	0,02
Ca	1,99	2,01	2,01	2,03	2,02	1,27	1,97	2,00	2,01	1,96	2,02	1,98	2,00	2,06	2,03	2,01	2,00	1,96	2,01
Na	0,05	0,07	0,03	0,04	0,03	0,04	0,05	0,03	0,02	0,00	0,03	0,04	0,03	0,02	0,06	0,04	0,05	0,05	0,06
K	0,01	0,00	0,01	0,00	0,01	0,01	0,00	0,01	0,01	0,01	0,01	0,00	0,01	0,01	0,00	0,01	0,01	0,01	0,00
H	1,00	1,00	1,00	1,00	1,00	1,00	1,00	1,00	1,00	1,00	1,00	1,00	1,00	1,00	1,00	1,00	1,00	1,00	1,00

Fase	Näsberget			Näsberget		Näsberget					Näsberget		
Muestra	A28			A53B		S110					S128		
Análisis	2	4	7	13	14	2	8	12	18	24	2	4	7
Mineral	ol	ol	ol	ol	ol	ol	ol	ol	ol	ol	ol	ol	ol
SiO_2	37,01	36,56	35,09	36,71	36,97	38,73	38,55	38,85	38,85	38,92	37,1	36,85	37,66
TiO_2	0,01	0,00	0,00	0,00	0,00	0,00	0,00	0,00	0,00	0,00	0	0,00	0,00
Al_2O_3	0,13	0,00	0,00	0,00	0,00	0,00	0,00	0,00	0,00	0,00	0	0,00	0,00
Cr_2O_3	0,00	0,00	0,00	0,00	0,00	0,00	0,10	0,00	0,00	0,00	0,00	0,00	0,00
FeO	32,74	32,74	31,52	33,63	34	21,14	21,45	21,70	22,42	21,26	30,39	30,84	30,17
MnO	0,82	0,53	0,9	0,59	0,66	0,40	0,37	0,49	0,00	0,00	0,00	0,00	0,00
MgO	30,56	29,97	28,26	29,71	29,69	39,24	39,50	39,08	37,86	39,01	31,83	31,66	31,86
CaO	0,16	0,00	0,00	0,00	0,00	0,00	0,00	0,00	0,00	0,00	0,00	0,00	0,00
Suma	101,43	99,80	95,77	100,64	101,32	99,51	99,97	100,12	99,13	99,19	99,32	99,35	99,69
Te	0,9	0,6	1,1	0,7	0,8	0,4	0,4	0,5	0,0	0,0	0,0	0,0	0,0
Fo	61,7	61,6	60,8	60,7	60,4	76,5	76,3	75,8	75,1	76,6	65,1	64,7	65,3
Fa	37,1	37,8	38,1	38,6	38,8	23,1	23,3	23,6	24,9	23,4	34,9	35,3	34,7
Ca-Ol	0,2	0,0	0,0	0,0	0,0	0,0	0,0	0,0	0,0	0,0	0,0	0,0	0,0

Litotipo	GI	GI				GII	GI	Rengård, tipo GI		Rengård, tipo GI		
muestra	23J28	JO03-35				JO03-67	JO03-80	JO03-109		JO03-110		
analisis	4	4	6	7	15	9	6	11	35	3	11	15
mineral	tit	ap	mt/spl	tit	tit	ilm	ilm	mt/spl	ilm	ilm	ilm	ap
SiO_2	30,65	0,43	0,33	30,79	30,73	0,35	0,17	0,11	0,00	0,26	0,08	0,21
TiO_2	29,63	0,01	0,14	38,86	34,25	51,74	51,72	0,24	47,50	47,04	44,22	0,10
Al_2O_3	6,17	0,03	0,10	1,93	4,60	0,09	0,12	0,14	0,00	0,07	0,03	0,10
FeO	1,57	0,52	89,86	1,24	0,52	42,33	46,92	84,77	40,80	38,72	38,37	0,29
MnO	0,06	0,04	0,22	0,04	0,06	7,34	3,89	0,07	3,18	4,05	4,27	0,29
MgO	0,05	0,12	0,09	0,31	0,06	0,17	0,13	0,16	0,00	0,04	0,05	0,02
CaO	29,20	55,81	0,49	29,36	29,20	0,13	0,03	0,05	0,00	0,20	0,06	52,32
Na_2O	0,38	0,19	0,92	0,19	0,26	0,53	0,96	0,42	0,00	0,03	0,45	0,20
K_2O	0,13	0,14	0,06	0,04	0,03	0,04	0,05	0,02	0,00	0,02	0,07	0,10
P_2O_5												37,27
Suma	34,65	57,29	92,21	102,76	99,71	102,72	103,99	85,98	91,48	90,43	87,60	90,90
Si			0,013					0,005				
Ti			0,004					0,008				
Al			0,005					0,007				
Cr			0,000					0,000				
Fe^{3+}			1,961					1,969				
Fe^{2+}			1,005					1,000				
Mn			0,007					0,002				
Mg			0,005					0,010				

Litotipo	Näsberget				Näsberget	Näsberget			Näsberget		Näsberget
muestra	A55				A80	A53B			S128		S134
analisis	6a	6b	8	9	7	6	17	8	7	15	10
mineral	mt/spl	ilm	?	mt/spl	mt/spl	mt/spl	mt/spl	mt/spl	mt/spl	mt/spl	mt/spl
SiO_2							0,33	0,21			
TiO_2	1,63	52,68		0,41		3,91	1,00	0,61	0,97	2,55	3,39
Al_2O_3			14,02		0,33	0,88	0,34	1,71	0,94	2,46	
Cr_2O_3						0,53	1,10	0,40	4,99	7,71	0,79
FeO	88,33	46,93	43,76	87,67	89,12	84,88	88,45	85,49	82,26	78,93	89,03
MnO			1,23								
MgO											
CaO				0,61	0,25						
Na_2O						0,85		0,53			0,81
K_2O											
V_2O_5	1,35	0,73		1,34	1,05	1,47	2,13	1,74	1,34	1,67	1,66
Suma	91,31	100,34	59,01	90,03	90,75	92,52	93,35	90,69	90,50	93,32	95,68
Si	0,000			0,000	0,000	0,000	0,013	0,008	0,000	0,000	0,000
Ti	0,049			0,013	0,000	0,117	0,030	0,018	0,029	0,075	0,099
Al	0,000			0,000	0,016	0,041	0,016	0,081	0,045	0,113	0,000
Cr	0,000			0,000	0,000	0,017	0,034	0,013	0,159	0,238	0,024
Fe^{3+}	1,902			1,975	1,984	1,708	1,865	1,852	1,738	1,500	1,779
Fe^{2+}	1,049			1,013	1,000	1,117	1,043	1,027	1,029	1,075	1,099
Mn	0,000			0,000	0,000	0,000	0,000	0,000	0,000	0,000	0,000
Mg	0,000			0,000	0,000	0,000	0,000	0,000	0,000	0,000	0,000

Litotipo	Näsberget					Näsberget		Näsberget			Näsberget	
muestra	23J84					A3		A28			S110	
analisis	3	17	19	22	25	15	16	5	6	7	13	25
mineral	mt/spl	mt/spl	mt/spl	mt/spl	ilm	mt/spl	ilm	ilm	mt/spl	mt/spl	mt/spl	mt/spl
SiO_2	2,68	0,74	0,13	0,34	0,27	0,20						
TiO_2	0,01	8,86	0,29	0,04	51,56	0,53	50,04	50,88	1,80	1,43	2,67	
Al_2O_3	0,02	0,50	0,11	0,19	0,03				1,10		2,10	0,41
Cr_2O_3	0,00	1,95	1,10	0,23	0,14				2,47	1,66	12,48	11,63
FeO	70,52	77,23	84,98	87,41	43,57	86,57	45,96	43,44	81,77	86,33	75,18	78,62
MnO	0,22	1,05	0,40	0,10	3,25		1,33	2,12	0,48			
MgO	0,23	0,22	0,06	0,00	0,15							
CaO	0,06	0,09	0,08	0,08	0,02				0,24			
Na_2O	1,06	0,48	0,38	0,46	0,48	0,83					0,63	0,92
K_2O	0,09	0,26	0,06	0,05	0,01							
V_2O_5						2,34	0,59		1,26	2,04	0,80	
Si	0,129	0,029	0,005	0,014		0,008			0,000	0,000	0,000	0,000
Ti	0,000	0,265	0,009	0,001		0,016			0,055	0,043	0,078	0,000
Al	0,001	0,023	0,005	0,009		0,000			0,053	0,000	0,096	0,019
Cr	0,000	0,061	0,036	0,007		0,000			0,080	0,053	0,383	0,366
Fe^{3+}	1,740	1,326	1,930	1,954		1,951			1,757	1,861	1,365	1,615
Fe^{2+}	1,104	1,246	0,997	1,012		1,025			1,039	1,043	1,078	1,000
Mn	0,009	0,035	0,014	0,003		0,000			0,017	0,000	0,000	0,000
Mg	0,017	0,013	0,004	0,000		0,000			0,000	0,000	0,000	0,000

litotipo	GIII epma	GII epma				VIC epma			
muestra	JO03-58	JO03-67				VIC04-01			
analisis	4	42	43	46	54	1	6	23	18
mineral	?	ilm	mt/spl	ap	ap	?	ap	tit	mt/spl
SiO_2	32,18	3,52	2,12	20,14	0,18	32,84	0,15	29,31	0,04
TiO_2	0,00	46,56	0,07	0,03	0,04	0,04	0,01	36,97	0,03
Al_2O_3	0,10	0,26	0,96	8,26	0,03	0,02	0,00	1,21	0,02
FeO	0,23	34,79	83,89	0,19	0,06	0,00	0,14	0,84	89,81
MnO	0,00	6,70	0,13	0,06	0,10	0,04	0,02	0,07	0,06
MgO	0,00	0,31	0,66	0,02	0,02	0,00	0,00	0,03	0,00
CaO	0,38	2,82	0,45	38,83	54,56	0,01	54,71	27,85	0,04
Na_2O	0,00	0,00	0,29	3,96	0,06	0,00	0,03	0,00	0,04
K_2O	0,01	0,02	0,01	0,04	0,00	0,00	0,00	0,01	0,00
Suma	32,91	94,98	88,58	71,52	55,04	32,95	55,06	96,29	90,05
Si			0,085						0,002
Ti			0,002						0,001
Al			0,046						0,001
Cr			0,000						0,000
Fe^{3+}			1,779						1,994
Fe^{2+}			1,043						1,001
Mn			0,004						0,002
Mg			0,040						0,000

ANEXO III. LITOGEOQUÍMICA
LITHOGEOCHEMISTRY

Muestra	Gq-51	Gq-67	Gq-75	Gq-78	Gq-86	Gq-88	Gq-94	RE Gq-94	Gq-107	Gq-109	Gq-120
Fase	GI	GI	GI	GI	GI	GI	GI	GI	GI	GI	GI
E-coord.	1698135	1698440	1704438	1703042	1704600	1709570	1699278	1699278	1683768	1688038	1707066
N-coord.	7255290	7252679	7214608	7218162	7221615	7226455	7215565	7215565	7234447	7242145	7227795
SiO_2 [%]	68,45	67,25	68,38	74,97	70,86	62,12	75,23	74,99	68,18	70,26	68,02
TiO_2	0,35	0,34	0,38	0,20	0,38	0,48	0,38	0,38	0,37	0,32	0,32
Al_2O_3	14,55	14,50	13,92	12,68	13,88	16,49	13,03	13,24	13,84	13,39	15,66
Fe_2O_3	4,36	5,91	5,49	3,36	5,37	6,64	2,15	2,01	5,42	4,65	4,52
MnO	0,04	0,06	0,08	0,04	0,12	0,10	0,04	0,03	0,08	0,08	0,07
MgO	1,49	1,72	1,33	0,25	0,66	2,44	0,44	0,45	2,08	1,12	1,73
CaO	3,44	4,26	4,33	1,74	2,86	5,82	2,28	2,28	3,44	3,64	3,86
Na_2O	3,19	3,37	3,42	4,34	4,15	3,13	6,13	6,21	3,03	3,10	3,54
K_2O	2,89	1,55	1,31	1,58	1,37	1,34	0,04	0,04	1,92	2,46	1,61
P_2O_5	0,06	0,08	0,08	0,03	0,10	0,09	0,08	0,07	0,06	0,05	0,08
tot C	0,01	0,02	0,01	0,03	0,02	0,03	0,02	0,02	0,07	0,01	0,01
S	0,01	0,08	0,01	0,01	0,01	0,01	0,01	0,01	0,01	0,01	0,01
LOI	1,20	1,10	1,30	0,80	0,30	1,30	0,40	0,50	1,50	0,90	0,60
Total	100,02	100,15	100,02	99,99	100,05	99,96	100,18	100,18	99,93	99,97	100,01
Recalculado	98,82	99,05	98,72	99,19	99,75	98,66	99,78	99,68	98,43	99,07	99,41
Zr [ppm]	133,3	136,3	127,9	173,6	183,9	108,3	153,4	158,4	137,2	160,7	126,8
Y	20,2	24,1	23,4	37,2	25,4	16,1	16,1	15,5	23,5	26,1	17,0
Nb	6,5	6,0	5,8	8,5	7,1	4,2	5,1	4,3	6,7	8,0	4,8
Y+Nb	26,7	30,1	29,2	45,7	32,5	20,3	21,2	19,8	30,2	34,1	21,8
Ba	743,0	563,2	406,2	775,7	515,4	442,2	35,3	30,9	646,9	805,0	570,8
Rb	60,2	44,4	29,5	23,3	36,7	32,3	2,0	0,5	43,3	51,9	39,0
Sr	222,7	245,6	193,0	140,3	240,8	315,6	114,2	113,6	243,8	221,3	293,2
Co	10,2	13,3	7,9	2,0	3,7	16,2	2,1	1,7	10,8	9,4	9,7
Cr_2O_3	10	20	10	10	10	30	10	10	30	20	20
Ni	7,1	4,7	3,3	2,9	2,0	8,9	3,0	3,2	6,0	6,3	6,6
Cu	23,8	124,1	13,8	10,7	9,5	37,9	12,1	12,3	45,0	19,6	10,8
Pb	3,8	3,1	2,3	1,0	2,2	2,3	1,6	1,7	10,4	12,9	2,5
Zn	21,0	31,0	25,0	28,0	74,0	53,0	18,0	18,0	72,0	64,0	43,0
As	1,0	3,1	3,4	1,3	1,8	2,6	2,8	2,8	7,0	2,6	1,0
Ag	<.1	0,1	<.1	<.1	<.1	<.1	<.1	<.1	0,1	0,1	<.1
Au	2,2	1,9	1,1	1,0	1,6	3,9	1,8	0,9	1,6	1,1	0,6
Fe_2O_3/MgO	2,93	3,44	4,13	13,44	8,14	2,72	4,89	4,47	2,61	4,15	2,61
Zr/ TiO_2	0,04	0,04	0,03	0,09	0,05	0,02	0,04	0,04	0,04	0,05	0,04
Ti/Zr	15,56	15,09	17,86	6,87	12,45	26,35	14,93	14,50	16,34	11,83	15,03
Zr/ Al_2O_3	9,16	9,40	9,19	13,69	13,25	6,57	11,77	11,96	9,91	12,00	8,10
Al_2O_3 /TiO_2	42,05	42,27	36,54	63,72	36,34	34,64	34,11	34,57	37,01	42,24	49,25
Zr/ P_2O_5	0,23	0,17	0,17	0,54	0,19	0,12	0,20	0,23	0,21	0,30	0,17
P/Zr	1,90	2,50	2,56	0,80	2,30	3,79	2,22	1,90	2,03	1,44	2,58
TiO_2/P_2O_5	5,97	4,40	5,08	6,22	3,94	5,06	4,90	5,55	5,84	5,98	4,24
Zr/Y	6,60	5,66	5,47	4,67	7,24	6,73	9,53	10,22	5,84	6,16	7,46
Zr/Nb	20,51	22,72	22,05	20,42	25,90	25,79	30,08	36,84	20,48	20,09	26,42
Nb/Y	0,32	0,25	0,25	0,23	0,28	0,26	0,32	0,28	0,29	0,31	0,28
Sr/La	15,15	14,11	11,70	5,97	13,60	24,47	9,21	9,39	12,97	8,05	22,21
Cu+Zn/ Na_2O	14,04	46,02	11,35	8,92	20,12	29,04	4,91	4,88	38,61	26,97	15,20
Ishik. A.I.	39,78	30,00	25,41	23,14	22,46	29,69	5,40	5,46	38,20	34,69	31,10
Modif. A.I.	40,71	32,67	27,85	17,41	19,65	37,65	3,77	3,80	39,76	36,61	32,05

Muestra	Gq-51	Gq-67	Gq-75	Gq-78	Gq-86	Gq-88	Gq-94	RE Gq-94	Gq-107	Gq-109	Gq-120
Fase	GI	GI	GI	GI	GI	GI	GI	GI	GI	GI	GI
Be [ppm]	1	1	1	1	<1	<1	<1	1	<1	<1	1
Bi	<.1	0,1	<.1	<.1	<.1	<.1	<.1	<.1	0,1	0,1	<.1
Cd	0,1	<.1	<.1	0,1	0,1	0,1	0,1	0,1	0,2	0,2	<.1
Cs	0,6	1,1	1,0	0,4	1,3	1,1	0,5	<.1	1,2	2,7	0,9
Ga	16,0	16,1	14,0	16,1	17,2	17,4	16,0	16,1	14,0	13,5	16,9
Hf	4,1	4,5	3,7	5,4	5,3	3,2	4,8	4,7	4,0	4,9	4,0
Hg	<.01	<.01	0,02	0,01	0,01	<.01	<.01	<.01	0,01	<.01	<.01
Mo	0,9	2,2	0,6	0,8	1,1	0,8	0,6	0,5	0,9	1,1	0,5
Sb	0,3	0,3	0,2	0,2	0,2	0,6	0,4	0,3	1	1,1	0,3
Sc	12	17	17	9	17	18	11	11	16	12	10
Se	<.5	<.5	<.5	<.5	0,5	<.5	0,5	<.5	<.5	<.5	0,5
Sn	2	1	1	1	1	<1	1	<1	1	1	<1
Ta	0,5	0,4	0,4	0,6	0,4	0,3	0,4	0,3	0,4	0,5	0,4
Tl	0,2	0,3	0,1	0,1	0,2	0,2	<.1	<.1	0,3	0,3	0,3
Th	8,1	5,5	4,5	5,7	4,3	4,6	5,0	4,4	7,1	8,2	5,9
U	3,4	2,6	1,4	2,3	1,6	1,7	1,4	1,3	2,9	3,2	1,5
V	63,0	78,0	61,0	<5	10,0	106,0	25,0	25,0	77,0	56,0	59,0
W	0,6	1,0	0,3	0,4	0,1	1,8	0,3	0,7	1,5	0,5	0,4
La	14,70	17,40	16,50	23,50	17,70	12,90	12,40	12,10	18,80	27,50	13,20
Ce	33,80	36,10	36,20	50,40	38,00	27,80	28,30	27,90	41,50	56,50	28,40
Pr	4,11	4,38	4,56	6,08	4,60	3,39	3,38	3,29	4,91	6,01	3,62
Nd	16,60	18,10	17,90	25,30	19,40	13,80	14,20	13,40	19,30	24,20	13,60
Sm	3,50	3,80	3,80	5,50	4,20	3,10	2,70	2,60	4,10	4,20	2,90
Eu	0,58	0,82	0,78	1,02	1,20	0,76	1,19	1,18	0,75	0,75	0,69
Gd	3,20	3,57	3,62	5,17	4,15	2,71	2,25	2,22	3,53	3,64	2,55
Tb	0,49	0,62	0,62	0,87	0,64	0,43	0,38	0,37	0,57	0,61	0,42
Dy	3,09	3,56	3,51	5,65	3,82	2,44	2,17	2,30	3,28	3,48	2,58
Ho	0,64	0,83	0,79	1,31	0,86	0,52	0,57	0,54	0,75	0,82	0,56
Er	1,96	2,37	2,25	3,82	2,66	1,54	1,74	1,70	2,32	2,40	1,63
Tm	0,33	0,39	0,37	0,61	0,40	0,23	0,31	0,28	0,37	0,42	0,26
Yb	1,99	2,53	2,32	4,09	2,63	1,57	1,99	1,96	2,57	2,75	1,70
Lu	0,34	0,39	0,37	0,66	0,48	0,24	0,35	0,30	0,38	0,40	0,28
La/Yb	7,39	6,88	7,11	5,75	6,73	8,22	6,23	6,17	7,32	10,00	7,76

Muestra	Gq-127	Gq-130	Gq-135	Gq-144	Gq-146	Gq-23a	Gq-24a	Gq-100	Gq-101	Gq-112	Gq-114
Fase	GI	GI	GI	GI	GI	GIIa	GIIa	GIIa	GIIa	GIIa	GIIa
E-coord.	1697180	1696165	1683510	1708579	1698785	1702888	1705320	1688105	1688600	1695395	1702825
N-coord.	7213930	7219375	7226363	7212435	7213335	7247958	7250550	7227773	7223140	7249993	7254584
SiO_2 [%]	75,57	73,01	65,43	73,41	72,28	65,01	69,14	70,91	68,85	64,52	67,70
TiO_2	0,19	0,24	0,36	0,30	0,24	0,50	0,48	0,28	0,26	0,40	0,49
Al_2O_3	12,48	13,43	15,30	13,11	13,63	17,56	14,56	15,17	15,67	16,95	16,12
Fe_2O_3	2,64	4,00	6,31	3,10	4,02	4,03	3,87	3,24	3,03	4,62	3,73
MnO	0,04	0,06	0,10	0,04	0,05	0,05	0,04	0,05	0,05	0,07	0,05
MgO	2,09	0,63	1,85	0,84	0,52	1,19	1,09	0,92	1,18	1,87	1,01
CaO	0,75	3,03	5,09	2,39	2,65	3,91	2,91	3,21	3,06	4,94	3,06
Na_2O	3,10	3,34	2,84	4,63	4,02	4,91	4,05	4,03	4,92	3,57	4,04
K_2O	1,02	1,64	1,35	0,61	1,09	1,90	2,91	1,65	1,40	1,21	2,49
P_2O_5	0,03	0,04	0,06	0,08	0,06	0,16	0,16	0,07	0,09	0,11	0,16
tot C	0,18	0,03	0,07	0,25	0,10	0,02	0,01	0,03	0,12	0,05	0,02
S	0,01	0,01	0,01	0,01	0,01	0,01	0,10	0,01	0,02	0,03	0,01
LOI	2,10	0,50	1,20	1,50	1,40	0,80	0,80	0,50	1,50	1,70	1,10
Total	100,01	99,92	99,89	100,02	99,96	100,03	100,01	100,03	100,01	99,96	99,95
Recalculado	97,91	99,42	98,69	98,52	98,56	99,23	99,21	99,53	98,51	98,26	98,85
Zr [ppm]	141,7	135,2	114,6	134,3	156,3	233,5	221,3	65,3	70,3	84,4	138,6
Y	30,6	25,6	24,5	24,5	28,2	11,8	13,6	5,4	6,0	9,0	12,4
Nb	7,9	6,7	5,1	7,0	6,7	7,6	9,6	4,8	3,5	4,0	8,1
Y+Nb	38,5	32,3	29,6	31,5	34,9	19,4	23,2	10,2	9,5	13,0	20,5
Ba	246,8	463,0	425,4	148,4	412,9	996,3	1243,5	673,0	856,6	707,5	1124,1
Rb	20,5	31,2	34,2	9,2	18,4	58,8	74,7	31,7	34,6	23,9	54,2
Sr	64,1	158,6	185,6	171,1	191,0	646,7	467,2	343,4	533,7	453,9	539,1
Co	2,7	5,2	13,9	2,8	5,0	7,4	9,3	5,1	7,2	9,8	6,9
Cr_2O_3	10	10	10	10	10	20	20	10	50	10	10
Ni	3,0	3,6	5,7	2,9	2,5	8,5	11,4	4,4	25,4	12,6	6,5
Cu	12,2	11,8	40,4	10,8	12,4	8,4	64,1	11,9	24,0	72,8	15,6
Pb	2,0	2,7	1,8	0,7	3,7	2,9	4,2	3,1	2,3	20,2	3,1
Zn	14,0	36,0	52,0	14,0	21,0	55,0	43,0	43,0	32,0	80,0	45,0
As	2,3	1,7	2,0	1,5	4,7	0,9	0,8	1,2	3,5	2,5	1,0
Ag	<.1	<.1	0,1	<.1	<.1	<.1	<.1	<.1	<.1	0,1	<.1
Au	0,9	1,8	0,9	1,7	1,4	1,3	1,2	0,5	0,5	2,3	0,6
Fe_2O_3/MgO	1,26	6,35	3,41	3,69	7,73	3,39	3,55	3,52	2,57	2,47	3,69
Zr/ TiO_2	0,07	0,06	0,03	0,04	0,07	0,05	0,05	0,02	0,03	0,02	0,03
Ti/Zr	8,00	10,60	18,73	13,39	9,05	12,89	13,00	25,25	21,75	28,13	21,15
Zr/ Al_2O_3	11,35	10,07	7,49	10,24	11,47	13,30	15,20	4,30	4,49	4,98	8,60
Al_2O_3 /TiO_2	66,03	56,19	42,74	43,70	57,75	34,98	30,33	55,16	61,45	42,80	32,97
Zr/ P_2O_5	0,46	0,31	0,19	0,16	0,27	0,15	0,14	0,09	0,08	0,08	0,09
P/Zr	0,95	1,39	2,32	2,73	1,62	3,01	3,06	4,94	5,46	5,69	5,04
TiO_2/P_2O_5	6,10	5,56	5,87	3,57	4,07	3,12	3,10	3,72	2,90	3,60	3,06
Zr/Y	4,63	5,28	4,68	5,48	5,54	19,79	16,27	12,09	11,72	9,38	11,18
Zr/Nb	17,94	20,18	22,47	19,19	23,33	30,72	23,05	13,60	20,09	21,10	17,11
Nb/Y	0,26	0,26	0,21	0,29	0,24	0,64	0,71	0,89	0,58	0,44	0,65
Sr/La	2,45	9,01	12,71	8,77	10,11	26,83	13,62	30,12	55,59	39,82	19,53
Cu+Zn/ Na_2O	8,45	14,31	32,54	5,36	8,31	12,91	26,44	13,62	11,38	42,80	15,00
Ishik. A.I.	44,68	26,27	28,75	17,12	19,44	25,94	36,50	26,20	24,43	26,57	33,02
Modif. A.I.	33,40	25,36	36,04	13,54	16,68	23,93	33,06	24,18	20,77	30,14	30,22

Muestra	Gq-127	Gq-130	Gq-135	Gq-144	Gq-146	Gq-23a	Gq-24a	Gq-100	Gq-101	Gq-112	Gq-114
Fase	GI	GI	GI	GI	GI	GIIa	GIIa	GIIa	GIIa	GIIa	GIIa
Be [ppm]	1	<1	1	<1	<1	2	1	<1	1	1	1
Bi	0,1	<.1	<.1	0,1	0,1	<.1	<.1	<.1	0,1	<.1	<.1
Cd	<.1	<.1	<.1	<.1	<.1	<.1	<.1	<.1	<.1	0,4	<.1
Cs	0,9	0,9	0,9	0,2	0,6	2,6	2,2	0,7	0,6	0,9	1,1
Ga	12,4	15,2	16,1	16,5	17,0	22,9	19,7	17,8	17,7	20,0	19,0
Hf	4,4	4,1	3,1	4,0	4,3	6,0	6,4	2,3	2,1	2,4	4,1
Hg	0,07	0,01	<.01	0,02	0,01	<.01	<.01	<.01	<.01	<.01	<.01
Mo	0,8	0,8	0,6	0,7	1,2	1,1	1,2	0,6	0,5	0,7	0,7
Sb	0,3	0,2	0,3	0,3	1,4	0,2	0,2	0,4	0,8	0,7	0,2
Sc	10	13	22	13	12	8	6	4	5	9	6
Se	<.5	0,5	<.5	0,5	<.5	<.5	0,5	<.5	<.5	<.5	<.5
Sn	3	2	2	1	3	1	1	<1	<1	2	<1
Ta	0,6	0,6	0,3	0,4	0,4	0,5	0,5	0,4	0,2	0,3	0,5
Tl	<.1	0,1	0,3	<.1	<.1	0,4	0,4	0,2	0,1	0,1	0,1
Th	6,3	5,9	6,2	3,7	3,7	4,9	9,9	3,5	1,7	3,2	6,3
U	3,7	1,9	1,3	2,1	2,3	3,8	5,5	1,0	0,8	1,4	3,1
V	21,0	32,0	105,0	16,0	19,0	46,0	48,0	30,0	35,0	65,0	42,0
W	0,6	0,2	0,3	1,0	0,7	0,5	0,3	0,1	0,2	0,7	0,3
La	26,20	17,60	14,60	19,50	18,90	24,10	34,30	11,40	9,60	11,40	27,60
Ce	52,60	36,30	30,50	41,10	40,20	46,70	66,30	21,60	18,80	22,70	55,60
Pr	6,08	4,22	3,55	4,70	4,75	5,19	7,12	2,41	2,55	2,66	6,21
Nd	25,20	17,30	14,20	20,10	19,60	21,80	26,20	9,40	8,80	10,50	24,00
Sm	4,80	3,60	3,30	4,20	4,10	3,80	4,30	1,40	1,70	2,10	4,10
Eu	0,66	0,66	0,66	1,01	0,82	1,09	0,95	0,41	0,42	0,85	1,08
Gd	4,32	3,49	3,40	4,30	4,28	2,71	2,93	1,09	1,18	1,61	2,54
Tb	0,72	0,56	0,56	0,70	0,70	0,40	0,39	0,15	0,18	0,26	0,38
Dy	4,65	3,66	3,44	3,95	4,30	1,92	2,15	0,81	0,94	1,44	1,95
Ho	1,04	0,83	0,77	0,85	0,98	0,40	0,44	0,14	0,19	0,30	0,42
Er	2,98	2,47	2,29	2,40	2,71	1,05	1,17	0,54	0,56	0,90	1,15
Tm	0,49	0,43	0,37	0,40	0,48	0,17	0,19	0,09	0,09	0,14	0,20
Yb	3,31	2,73	2,39	2,53	3,04	1,08	1,29	0,64	0,58	0,88	1,14
Lu	0,53	0,44	0,38	0,38	0,50	0,19	0,19	0,10	0,09	0,13	0,19
La/Yb	7,92	6,45	6,11	7,71	6,22	22,31	26,59	17,81	16,55	12,95	24,21

Muestra	Gq-119	Gq-122	Gq-138	Gq-142	Gq-145	Gq-34	Gq-40	Gq-83	Gq-128	Gq-136	Gq-139
Fase	GIIa	GIIa	GIIa	GIIa	GIIa	GIIb	GIIb	GIIb	GIIb	GIIb	GIIb
E-coord.	1701333	1702132	1712144	1711458	1715795	1710192	1707694	1706834	1700381	1705649	1702957
N-coord.	7251284	7225725	7248698	7255113	7223625	7251600	7258145	7236331	7222353	7248480	7259567
SiO_2 [%]	69,55	71,75	69,80	69,99	70,76	64,48	62,62	68,67	67,44	68,13	68,93
TiO_2	0,24	0,23	0,35	0,34	0,26	0,72	0,92	0,42	0,57	0,53	0,52
Al_2O_3	16,35	15,32	15,83	15,86	15,40	15,39	15,68	14,90	15,45	15,20	14,73
Fe_2O_3	3,05	2,86	2,88	2,86	2,56	5,05	5,92	4,02	4,22	3,92	4,03
MnO	0,05	0,04	0,03	0,03	0,03	0,07	0,08	0,05	0,06	0,05	0,05
MgO	0,75	0,58	0,98	0,92	0,85	2,12	2,36	1,04	1,29	1,27	1,24
CaO	4,12	3,28	3,46	3,13	2,70	3,91	4,22	2,72	2,94	3,05	2,67
Na_2O	4,42	4,35	4,61	3,77	4,69	4,23	4,45	4,12	4,14	4,07	4,03
K_2O	0,76	1,01	1,66	2,44	2,02	2,93	3,11	3,52	3,24	2,98	3,44
P_2O_5	0,10	0,09	0,12	0,11	0,10	0,24	0,31	0,13	0,18	0,17	0,17
tot C	0,01	0,05	0,01	0,03	0,02	0,02	0,02	0,03	0,01	0,01	0,02
S	0,01	0,04	0,01	0,01	0,01	0,01	0,01	0,01	0,01	0,01	0,01
LOI	0,60	0,50	0,30	0,50	0,60	0,90	0,30	0,50	0,50	0,60	0,20
Total	100,00	100,01	100,01	99,96	99,98	100,05	99,98	100,09	100,03	99,99	100,01
Recalculado	99,40	99,51	99,71	99,46	99,38	99,15	99,68	99,59	99,53	99,39	99,81
Zr [ppm]	88,0	76,2	116,7	145,4	79,3	211,3	246,6	254,7	242,3	212,4	227,1
Y	7,4	7,1	3,9	7,8	4,8	19,6	22,8	27,5	17,1	17,7	17,3
Nb	3,1	5,7	5,0	7,1	3,8	12,7	15,8	12,5	12,6	12,2	13,1
Y+Nb	10,5	12,8	8,9	14,9	8,6	32,3	38,6	40,0	29,7	29,9	30,4
Ba	468,4	520,2	495,6	732,8	751,7	1029,2	1092,9	816,6	1052,6	1031,3	941,0
Rb	18,7	21,6	61,2	72,1	58,7	84,9	65,0	89,1	97,0	74,7	102,1
Sr	586,3	452,9	652,9	615,4	759,6	580,1	647,7	341,8	468,8	486,1	436,8
Co	4,7	3,5	5,9	4,8	5,7	13,4	13,5	6,8	8,5	10,0	7,6
Cr_2O_3	10	10	20	10	10	60	70	10	30	30	20
Ni	5,0	2,5	5,7	4,8	8,3	22,6	16,0	8,4	12,2	10,0	9,7
Cu	9,7	19,0	14,1	10,0	9,9	39,7	35,4	14,3	20,9	12,9	20,4
Pb	0,9	3,1	3,5	5,2	5,1	5,5	5,4	6,1	5,0	5,2	5,4
Zn	49,0	35,0	50,0	46,0	53,0	51,0	42,0	34,0	51,0	46,0	42,0
As	0,7	5,8	0,6	1,8	1,7	4,3	3,9	1,8	1,8	1,1	1,3
Ag	<.1	<.1	<.1	<.1	<.1	<.1	<.1	<.1	<.1	<.1	<.1
Au	<.5	3,5	1,6	1,5	1,1	0,8	0,9	3,2	1,4	1,9	1,7
Fe_2O_3/MgO	4,07	4,93	2,94	3,11	3,01	2,38	2,51	3,87	3,27	3,09	3,25
Zr/ TiO_2	0,04	0,03	0,03	0,04	0,03	0,03	0,03	0,06	0,04	0,04	0,04
Ti/Zr	16,49	18,02	17,77	14,02	19,96	20,34	22,29	9,77	14,03	15,02	13,75
Zr/ Al_2O_3	5,38	4,97	7,37	9,17	5,15	13,73	15,73	17,09	15,68	13,97	15,42
Al_2O_3 /TiO_2	67,56	66,90	45,75	46,65	58,33	21,46	17,10	35,90	27,25	28,57	28,27
Zr/ P_2O_5	0,09	0,08	0,10	0,13	0,08	0,09	0,08	0,20	0,14	0,12	0,14
P/Zr	4,91	5,27	4,30	3,42	5,56	5,04	5,47	2,18	3,17	3,55	3,19
TiO_2/P_2O_5	2,44	2,49	3,01	2,98	2,61	2,94	2,97	3,27	3,22	3,08	3,14
Zr/Y	11,89	10,73	29,92	18,64	16,52	10,78	10,82	9,26	14,17	12,00	13,13
Zr/Nb	28,39	13,37	23,34	20,48	20,87	16,64	15,61	20,38	19,23	17,41	17,34
Nb/Y	0,42	0,80	1,28	0,91	0,79	0,65	0,69	0,45	0,74	0,69	0,76
Sr/La	64,43	34,31	31,85	20,58	52,75	16,81	15,17	10,42	12,67	14,64	15,01
Cu+Zn/ Na_2O	13,28	12,41	13,90	14,85	13,41	21,44	17,39	11,72	17,37	14,47	15,48
Ishik. A.I.	15,02	17,25	24,65	32,75	27,97	38,29	38,68	40,00	39,02	37,38	41,12
Modif. A.I.	14,59	15,45	22,26	30,83	23,43	37,38	38,07	35,63	35,36	34,30	36,73

Muestra	Gq-119	Gq-122	Gq-138	Gq-142	Gq-145	Gq-34	Gq-40	Gq-83	Gq-128	Gq-136	Gq-139
Fase	GIIa	GIIa	GIIa	GIIa	GIIa	GIIb	GIIb	GIIb	GIIb	GIIb	GIIb
Be [ppm]	1	1	1	1	1	2	2	2	3	1	1
Bi	<.1	0,1	<.1	<.1	<.1	0,1	0,1	0,1	<.1	<.1	<.1
Cd	<.1	<.1	<.1	0,1	0,1	<.1	<.1	0,1	0,1	<.1	<.1
Cs	0,9	1,0	1,6	3,2	2,7	3,0	1,5	1,3	2,3	1,9	2,9
Ga	17,5	19,7	22,9	23,7	22,4	21,8	20,7	21,2	20,1	21,1	20,4
Hf	2,5	2,2	3,3	3,4	2,7	5,7	6,2	7,2	6,7	5,6	6,6
Hg	<.01	<.01	<.01	<.01	<.01	<.01	<.01	<.01	0,01	<.01	<.01
Mo	0,7	0,6	0,4	7,4	0,5	0,7	0,8	2,4	2	1,2	2
Sb	0,2	0,4	0,1	0,1	0,2	0,5	0,4	0,2	0,2	0,1	0,1
Sc	4	4	4	5	3	10	12	7	7	8	7
Se	<.5	<.5	<.5	<.5	<.5	<.5	0,5	0,5	<.5	0,5	<.5
Sn	<1	<1	2	2	1	2	2	2	2	2	3
Ta	0,2	0,3	0,4	0,4	0,4	0,6	0,7	0,8	0,7	0,8	0,7
Tl	0,1	0,2	0,4	0,3	0,3	0,5	0,3	0,3	0,5	0,4	0,4
Th	1,0	1,7	9,5	6,8	4,0	9,2	5,8	11,2	9,3	9,7	11,3
U	0,5	0,8	3,3	2,3	1,9	2,9	2,0	5,3	2,5	2,6	5,4
V	23,0	16,0	40,0	34,0	30,0	84,0	89,0	39,0	58,0	52,0	48,0
W	0,5	0,3	1,0	0,3	0,1	1,0	0,7	1,9	0,4	0,4	0,6
La	9,10	13,20	20,50	29,90	14,40	34,50	42,70	32,80	37,00	33,20	29,10
Ce	18,10	26,90	35,20	51,80	28,00	77,80	97,90	71,60	76,90	69,20	62,60
Pr	2,62	3,05	3,36	5,16	2,91	9,03	11,73	8,21	8,30	7,88	7,24
Nd	8,90	11,80	11,20	17,90	10,60	36,90	47,00	34,30	33,10	30,00	28,70
Sm	1,60	1,90	1,60	2,90	1,90	6,50	8,50	6,50	5,20	5,30	4,90
Eu	0,55	0,55	0,60	0,75	0,64	1,33	1,72	0,93	1,14	1,03	1,00
Gd	1,36	1,35	0,86	2,03	1,31	4,30	5,75	5,00	3,60	3,69	3,78
Tb	0,22	0,19	0,13	0,27	0,19	0,63	0,81	0,73	0,55	0,57	0,56
Dy	1,06	1,13	0,61	1,28	0,69	3,25	4,03	4,06	2,74	2,93	2,80
Ho	0,26	0,20	0,12	0,24	0,16	0,65	0,78	0,89	0,55	0,57	0,56
Er	0,76	0,66	0,32	0,63	0,39	1,75	1,98	2,62	1,52	1,55	1,57
Tm	0,10	0,11	0,07	0,11	0,08	0,30	0,31	0,43	0,25	0,26	0,26
Yb	0,71	0,69	0,40	0,59	0,47	1,90	2,09	2,81	1,66	1,61	1,67
Lu	0,12	0,11	0,08	0,11	0,08	0,28	0,31	0,41	0,26	0,23	0,26
La/Yb	12,82	19,13	51,25	50,68	30,64	18,16	20,43	11,67	22,29	20,62	17,43

Muestra	Gq-147	RE Gq-147	Gq-07	Gq-06	Gq-154	Gq-115	Gq-03	Gq-149	Gq-124
Fase	GIIb	GIIb	GIII	GIV	Basalt	Näsberg	Näsberg	Gabbro	Rengård
E-coord.	1700632	1700632	1707754	1695737	1693130	1702688	1701197	1704473	1699776
N-coord.	7227111	7227111	7244764	7241282	7218420	7255023	7253287	7219448	7208502
SiO_2 [%]	61,47	61,40	76,51	72,07	50,91	55,78	50,39	54,61	70,21
TiO_2	0,85	0,82	0,11	0,27	0,51	0,80	0,45	0,69	0,26
Al_2O_3	16,61	16,69	12,52	14,79	11,57	16,50	17,05	17,25	14,89
Fe_2O_3	6,07	6,03	1,56	2,44	9,71	8,36	8,32	8,62	4,55
MnO	0,15	0,14	0,03	0,03	0,15	0,12	0,11	0,13	0,05
MgO	2,60	2,55	0,13	0,62	12,59	4,16	11,35	4,52	0,78
CaO	5,03	5,09	0,24	2,29	7,48	7,08	7,75	7,71	3,43
Na_2O	4,65	4,57	3,54	4,14	2,34	3,84	2,58	3,10	3,67
K_2O	1,87	1,88	4,95	2,82	1,08	1,01	0,50	0,73	1,03
P_2O_5	0,28	0,28	0,02	0,08	0,13	0,26	0,08	0,19	0,09
tot C	0,02	0,02	0,01	0,08	0,09	0,07	0,04	0,04	0,04
S	0,01	0,01	0,01	0,01	0,01	0,02	0,09	0,01	0,02
LOI	0,40	0,50	0,50	0,50	3,30	2,10	1,20	2,40	1,00
Total	99,98	99,97	100,11	100,05	99,92	100,02	99,88	99,95	99,97
Recalculado	99,58	99,47	99,61	99,55	96,62	97,92	98,68	97,55	98,97
Zr [ppm]	282,1	275,6	124,2	126,6	78,4	81,7	56,5	72,6	113,7
Y	21,5	19,7	17,7	6,4	24,4	19,9	11,3	14,1	23,2
Nb	10,3	10,0	18,4	8,0	3,9	5,6	2,7	4,6	5,0
Y+Nb	31,8	29,7	36,1	14,4	28,3	25,5	14,0	18,7	28,2
Ba	1237,2	1253,4	178,8	810,7	286,8	455,7	271,6	431,2	447,6
Rb	46,9	46,5	151,0	90,8	34,0	37,3	13,1	16,2	22,9
Sr	699,0	690,3	45,0	496,3	387,8	550,0	519,6	570,2	302,6
Co	9,9	9,2	1,0	3,7	48,6	29,6	55,8	27,4	5,6
Cr_2O_3	60	60	10	10	1130	30	670	50	10
Ni	17,9	17,8	3,4	5,4	162,3	19,9	176,6	13,6	2,1
Cu	8,4	9,2	12,3	12,2	42,4	20,6	129,5	51,2	392,5
Pb	1,9	1,9	13,0	7,3	2,0	5,0	3,9	1,6	1,2
Zn	52,0	54,0	16,0	45,0	38,0	48,0	23,0	60,0	55,0
As	1,5	1,3	2,6	0,8	3,0	1,9	1,5	3,1	1,3
Ag	<.1	<.1	<.1	<.1	<.1	<.1	0,1	<.1	0,3
Au	0,7	0,9	3,1	2,1	0,9	<.5	3,4	2,1	0,9
Fe_2O_3/MgO	2,33	2,36	12,00	3,94	0,77	2,01	0,73	1,91	5,83
Zr/ TiO_2	0,03	0,03	0,11	0,05	0,02	0,01	0,01	0,01	0,04
Ti/Zr	17,96	17,92	5,31	12,83	39,23	58,56	47,43	56,56	13,87
Zr/ Al_2O_3	16,98	16,51	9,92	8,56	6,78	4,95	3,31	4,21	7,64
Al_2O_3 /TiO_2	19,66	20,25	113,82	54,58	22,55	20,68	38,14	25,18	56,62
Zr/ P_2O_5	0,10	0,10	0,73	0,16	0,06	0,03	0,07	0,04	0,12
P/Zr	4,28	4,49	0,60	2,79	7,07	13,77	6,18	11,36	3,49
TiO_2/P_2O_5	3,05	2,90	6,47	3,35	4,04	3,09	5,59	3,62	2,89
Zr/Y	13,12	13,99	7,02	19,78	3,21	4,11	5,00	5,15	4,90
Zr/Nb	27,39	27,56	6,75	15,83	20,10	14,59	20,93	15,78	22,74
Nb/Y	0,48	0,51	1,04	1,25	0,16	0,28	0,24	0,33	0,22
Sr/La	22,77	22,56	1,62	40,02	34,32	37,16	68,37	43,20	17,91
Cu+Zn/ Na_2O	12,99	13,83	7,99	13,82	34,36	17,86	59,11	35,87	121,93
Ishik. A.I.	31,59	31,44	57,34	34,85	58,19	32,13	53,43	32,69	20,31
Modif. A.I.	32,46	32,65	41,78	29,35	74,50	40,23	69,66	45,85	19,78

Muestra	Gq-147	RE Gq-147	Gq-07	Gq-06	Gq-154	Gq-115	Gq-03	Gq-149	Gq-124
Fase	GIIb	GIIb	GIII	GIV	Basalt	Näsberg	Näsberg	Gabbro	Rengård
Be [ppm]	1	1	2	2	1	<1	1	<1	1
Bi	<.1	<.1	0,1	0,1	<.1	<.1	0,1	0,1	0,2
Cd	<.1	0,1	0,1	0,1	<.1	0,1	0,1	<.1	0,1
Cs	1,7	1,6	1,3	2,1	1,0	0,8	0,9	1,0	1,1
Ga	23,2	23,6	17,2	22,0	14,2	18,6	15,5	22,8	17,9
Hf	7,1	6,8	4,7	3,5	2,2	2,3	1,5	2,1	3,4
Hg	<.01	<.01	<.01	<.01	0,02	<.01	<.01	0,01	0,02
Mo	0,5	0,5	0,9	1,1	0,3	0,5	0,4	0,6	2
Sb	0,2	0,2	0,2	0,1	0,2	0,2	0,2	0,2	0,2
Sc	13	13	1	3	30	22	12	24	7
Se	<.5	<.5	<.5	<.5	<.5	<.5	0,5	<.5	0,6
Sn	2	2	2	2	2	1	<1	2	<1
Ta	0,4	0,3	1,4	0,6	0,2	0,3	0,1	0,2	0,4
Tl	0,3	0,3	0,1	0,4	0,1	<.1	0,3	<.1	0,2
Th	2,9	2,7	27,8	10,6	3,4	2,0	0,6	1,6	1,1
U	2,4	2,1	7,1	2,1	1,2	1,3	0,6	0,8	0,5
V	96,0	93,0	<5	28,0	179,0	166,0	80,0	174,0	22,0
W	0,9	0,9	0,7	0,4	0,5	0,7	0,6	0,3	0,3
La	30,70	30,60	27,70	12,40	11,30	14,80	7,60	13,20	16,90
Ce	70,70	67,70	77,30	28,20	25,20	31,90	17,40	27,90	34,40
Pr	8,71	8,11	6,28	2,82	3,13	4,85	2,30	3,48	4,08
Nd	35,60	33,60	21,70	10,10	14,50	19,20	10,30	15,30	16,90
Sm	6,60	6,40	4,40	2,10	3,50	4,30	2,20	3,10	3,50
Eu	1,47	1,36	0,27	0,50	0,92	1,47	0,73	0,91	1,01
Gd	5,18	4,60	2,79	1,50	3,75	3,78	2,03	2,77	3,41
Tb	0,69	0,66	0,46	0,21	0,61	0,57	0,30	0,39	0,55
Dy	3,72	3,57	2,64	0,98	3,78	3,18	1,83	2,44	3,49
Ho	0,70	0,65	0,53	0,18	0,82	0,70	0,38	0,46	0,80
Er	1,89	1,77	1,49	0,53	2,37	2,04	1,08	1,32	2,18
Tm	0,27	0,28	0,22	0,08	0,39	0,27	0,14	0,22	0,36
Yb	1,83	1,57	1,71	0,56	2,69	2,10	1,10	1,37	2,32
Lu	0,29	0,28	0,27	0,07	0,36	0,28	0,18	0,22	0,41
La/Yb	16,78	19,49	16,20	22,14	4,20	7,05	6,91	9,64	7,28

ANEXO IV. ANÁLISIS ISOTÓPICO
ISOTOPIC ANALYSES

Muestra	J004-05	J004-34	J004-42	J003-45	J004-53	J004-75	J004-86	J003-104	J004-110	J004-128	J004-135	VIC04-11
Fase	Näsberg	GII	GI	GIII	GII	GI	GI	Mau	GI	GII	GI	VIC
E-coord	1701212	1710192	1703097	1704500	1715814	1704438	1704600		1689602	1700381	1683510	1631550
N-coord	7253185	7251600	7259346	7238490	7223590	7214608	7221615		7244382	7222353	7226363	7221260
Zr	49,46	138,05	133,08	120,09	63,37	114,55	78,76	122,12	77,49	109,90	85,98	110,30
Y	7,78	19,81	17,00	14,02	8,38	25,79	21,17	28,57	16,67	10,22	20,46	13,04
Nb	2,70	13,08	13,25	10,94	7,70	6,83	5,33	5,16	4,82	9,33	4,18	7,10
Ba	241,54	660,02	605,40	557,10	492,82	325,70	348,86	231,38	311,72	428,82	291,67	312,12
Rb	11,38	66,21	97,06	69,28	45,17	30,13	23,99	20,38	32,32	67,60	29,65	8,65
Sr	411,27	499,88	336,11	155,18	369,88	146,60	144,90	89,17	95,57	183,08	124,44	162,80
Co	11,25	14,16	9,47	3,55	3,95	11,66	3,94	4,80	6,49	6,61	14,26	4,99
Cr	31,44	87,20	142,14	129,33	114,13	97,49	84,41	100,80	75,32	52,99	113,55	81,80
Ni	1,03	28,08	10,71	3,54	4,52	2,88	1,17	1,34	2,81	7,40	4,38	1,84
Cu	17,01	42,62	10,43	1,58	12,53	7,89	0,81	10,28	1,69	10,49	31,21	17,35
Pb	29,83	48,23	44,24	39,94	46,62	31,66	43,04	35,41	24,15	24,91	31,64	27,18
Zn	97,09	69,26	50,73	30,14	29,85	31,48	56,34	51,00	38,37	36,63	52,67	11,12
As	0,95	5,55	1,53	1,00	3,98	2,45	1,87	3,36	0,93	1,38	1,47	0,86
B	831,20	233,51	245,79	178,61	126,58	190,07	359,19	251,08	238,41	509,51	69,20	399,38
Be	0,50	1,91	2,17	1,34	1,92	0,78	0,79	0,70	0,41	1,15	0,62	0,97
Bi	-0,17	-0,18	-0,30	-0,31	-0,27	-0,26	-0,34	-0,09	-0,22	-0,32	-0,32	-0,22
Cd	0,28	0,45	0,42	0,36	0,36	0,32	0,28	0,37	0,27	0,12	0,33	0,27
Cs	0,64	3,16	4,02	0,71	2,42	0,69	0,64	0,27	1,26	2,09	0,80	0,21
Ga	27,51	52,82	52,12	45,59	46,30	30,32	31,76	24,19	22,40	32,60	26,77	27,83
Ge	0,58	0,64	0,61	0,50	0,14	0,60	0,61	0,41	0,37	0,53	0,64	0,46
Hf	1,62	4,92	4,79	3,68	2,88	4,13	2,64	4,55	2,64	3,52	2,69	3,82
Li	6,86	13,19	29,87	6,57	12,88	6,39	7,71	9,33	9,97	17,04	12,65	4,37
Mo	0,25	-0,47	0,59	-0,33	2,60	-0,68	-0,72	-0,34	-1,22	-1,24	-0,96	-1,28
Sb	0,48	0,94	-0,02	-0,35	0,07	0,43	0,05	2,13	1,19	0,10	0,73	-0,38
Sc	19,79	11,34	8,08	2,32	3,23	19,36	14,68	9,98	10,16	6,55	20,99	9,86
Se	0,36	0,55	0,29	0,40	0,13	1,13	0,51	0,59	0,34	0,20	0,56	0,19
Sn	0,32	1,75	1,44	0,76	0,26	1,08	0,61	1,09	0,85	0,75	1,29	0,90
Ta	2,84	1,82	1,46	1,08	1,98	0,93	1,06	1,58	1,30	0,77	2,15	0,74
Th	0,75	10,23	12,11	10,50	9,06	4,50	6,11	4,29	5,16	4,77	4,66	5,29
Tl	0,07	0,56	0,82	0,61	0,27	0,10	0,11	0,44	0,24	0,44	0,23	-0,06
U	0,42	3,26	6,04	3,35	5,13	1,89	1,70	2,61	2,46	1,52	1,34	2,48
V	203,08	79,49	51,68	15,54	16,38	67,80	9,24	21,57	38,84	39,00	89,39	42,48
W	0,13	0,91	0,49	0,23	0,10	0,12	-0,07	0,64	0,00	-0,15	0,13	0,02
La	9,12	43,68	48,85	44,78	7,30	22,79	48,29	20,40	20,63	28,41	19,60	23,93
Ce	20,67	95,22	92,16	109,52	20,12	49,57	88,16	44,99	45,08	59,08	41,76	57,32
Pr	2,02	10,73	9,70	10,57	1,77	5,41	8,84	4,74	4,50	6,03	3,99	5,37
Nd	7,80	36,89	31,06	32,49	6,64	20,41	27,88	17,33	15,40	19,75	14,07	18,52
Sm	1,57	6,42	4,98	5,40	1,78	4,40	4,43	3,90	2,92	3,27	2,91	3,30
Eu	0,85	1,61	1,14	0,90	0,38	0,91	1,04	0,86	0,51	0,75	0,64	0,84
Gd	1,53	5,17	4,04	3,94	1,60	4,53	4,24	4,57	2,79	2,64	3,08	2,85
Tb	0,21	0,80	0,58	0,57	0,21	0,80	0,67	0,87	0,48	0,35	0,54	0,41
Dy	1,37	3,81	3,01	2,76	1,42	4,71	3,82	5,12	2,90	1,96	3,43	2,44
Ho	0,28	0,82	0,61	0,52	0,25	1,11	0,88	1,27	0,66	0,36	0,82	0,47
Er	0,80	2,11	1,72	1,41	0,76	2,99	2,45	3,47	1,84	1,04	2,32	1,34
Tm	0,07	0,28	0,23	0,16	0,06	0,43	0,33	0,58	0,27	0,10	0,31	0,15
Yb	0,71	1,88	1,67	1,18	0,76	2,83	2,38	3,59	1,77	0,97	2,27	1,33
Lu	0,06	0,27	0,23	0,11	0,05	0,41	0,34	0,61	0,26	0,10	0,32	0,17

muestra	roca	Sm	Nd	$^{147}Sm/^{144}Nd$	$^{143}Nd/^{144}Nd$	$\varepsilon Nd_{(0)}$	$\varepsilon Nd_{(1.9\ Ga)}$	T_{DM} (Ga)
J004-86	GI (SE)	4,70	26,80	0,1059	0,511644	- 19.4	+2,7	1.98
J004-110	GI (NW)	3,83	16,60	0,1398	0,512117	- 10.2	+3,8	1.91
J004-135	GI (SW)	3,10	14,60	0,1286	0,511936	- 13.7	+3,0	1.99
J004-75	GI (Klöckträsk)	4,11	19,50	0,1275	0,511965	- 13.2	+3,8	1.91
J004-05	Näsberg	2,07	9,41	0,1333	0,512003	- 12.4	+3,2	1.98
J004-128	GIIa (Jörn)	5,64	33,10	0,103	0,511613	- 20.0	+2,9	1.97
J004-34	GIIb (NE)	6,30	35,40	0,1076	0,511674	- 18.8	+2,9	1.97
J004-42	GIIa (N)	4,94	30,30	0,0985	0,511557	- 21.1	+2,9	1.97
J003-45	GIII (E)	3,77	23,20	0,0982	0,511542	- 21.4	+2,6	1.99
J004-53	Stavaträsk	1,40	5,36	0,1574	0,512115	- 10.2	-0,7	2.54
J003-104	Maurliden	4,21	18,40	0,1388	0,512090	- 10.7	+3,6	1.94
VIC04-11	VIC	3,43	17,6	0,1179	0,511756	- 17.2	+2,0	2.05

ANEXO V. DATACIONES

AGE DETERMINATIONS

	$^{207}Pb/^{235}U$	±σ %	$^{206}Pb/^{238}U$	±σ %	ρ	$^{208}Pb/^{232}Th$	±σ %	Disc. % conv.	Disc. % 2σ lim.
Zr					**MG07-004; GI**				
01a	5,233	1,04	0,328	1,00	0,964	0,09	2,79	-3,522	-1,20
03a	5,088	1,32	0,321	1,23	0,929	0,09	3,37	-5,221	-1,98
08a	5,399	1,19	0,339	1,01	0,855	0,10	3,03	-0,301	
16a	5,387	1,22	0,336	1,01	0,825	0,10	2,92	-1,870	
17a	5,399	1,14	0,340	1,10	0,964	0,10	2,71	0,111	
18a	5,439	1,16	0,342	1,14	0,983	0,10	2,72	0,917	
19a	5,461	1,17	0,344	1,14	0,976	0,10	2,70	1,169	
20a	5,361	1,13	0,336	1,00	0,888	0,10	3,04	-1,174	
20b	5,338	1,08	0,335	1,01	0,933	0,09	2,68	-1,694	
21a	5,465	1,13	0,342	1,03	0,913	0,10	2,90	0,399	
25a	5,380	1,27	0,337	1,22	0,960	0,10	3,00	-0,914	
31a	5,367	1,06	0,338	1,01	0,955	0,09	2,72	-0,553	
32a	5,343	1,13	0,338	1,02	0,901	0,09	2,85	-0,116	
33a	5,407	1,12	0,338	1,04	0,932	0,10	2,75	-1,405	
33b	5,371	1,20	0,339	1,06	0,885	0,09	3,01	0,062	
35a	5,412	1,09	0,338	1,02	0,936	0,10	2,77	-0,931	

Zr					**MG07-007; Rengård**				
02a	5,420	1,14	0,344	1,01	0,884	0,098	2,97	2,403	
03a	5,178	1,18	0,328	1,07	0,903	0,086	6,26	-2,959	
03b	5,495	1,04	0,347	1,01	0,966	0,098	2,64	2,632	0,22
04a	5,166	1,27	0,328	1,01	0,795	0,095	3,09	-2,166	
05a	5,411	1,19	0,340	1,01	0,847	0,094	3,25	0,027	
05b	5,254	1,37	0,334	1,20	0,879	0,088	3,30	-0,703	
06a	5,195	1,14	0,330	1,00	0,881	0,086	3,11	-1,850	
07a	5,531	1,26	0,345	1,05	0,828	0,096	3,28	0,598	
07b	5,583	1,26	0,349	1,09	0,870	0,098	3,07	2,248	
07c	5,318	1,29	0,335	1,01	0,782	0,086	3,34	-1,113	
08a	5,495	1,20	0,347	1,01	0,841	0,096	3,11	2,801	
09a	4,597	1,08	0,288	1,02	0,943	0,104	3,41	-15,281	-12,90
10a	5,409	1,11	0,339	1,00	0,900	0,094	2,88	-0,283	

	$^{207}Pb/^{235}U$	±σ %	$^{206}Pb/^{238}U$	±σ %	ρ	$^{208}Pb/^{232}Th$	±σ %	Disc. % conv.	Disc. % 2σ lim.
Zr					**23J28; GI**				
03a	5,372	1,17	0,340	1,11	0,943	0,098	2,79	0,691	
03b	5,419	1,06	0,341	1,01	0,954	0,099	2,75	0,754	
06a	5,443	1,16	0,344	1,11	0,959	0,097	3,00	1,784	
10a	5,438	1,05	0,345	1,01	0,959	0,098	2,70	2,641	0,15
11a	5,085	1,10	0,320	1,04	0,947	0,084	4,99	-5,656	-3,10
11b	5,344	1,14	0,337	1,07	0,941	0,089	3,06	-0,430	
14a	4,984	1,04	0,321	1,00	0,961	0,095	3,36	-3,102	-0,74
14b	4,850	1,06	0,304	1,04	0,977	0,093	2,75	-10,670	-8,55
17a	5,552	1,10	0,348	1,05	0,957	0,101	2,71	1,848	
21a	4,921	1,09	0,308	1,03	0,939	0,095	6,34	-9,790	-7,26
23a	5,023	1,15	0,319	1,00	0,875	0,024	8,18	-5,358	-2,18
23b	5,394	1,11	0,339	1,06	0,954	0,096	2,71	-0,174	
Zr					**JO03-55; GI**				
01a	4,777	1,17	0,299	1,11	0,955	0,110	3,77	-12,202	-9,70
01b	5,264	1,05	0,330	1,00	0,960	0,093	2,74	-2,994	-0,63
02a	4,632	1,10	0,293	1,03	0,935	0,064	3,73	-13,033	-10,50
02b	5,315	1,12	0,335	1,07	0,952	0,097	2,96	-1,083	
03a	5,442	1,27	0,342	1,25	0,983	0,100	2,75	0,711	
04a	5,390	1,07	0,338	1,03	0,961	0,099	3,51	-0,960	
04b	5,585	1,07	0,353	1,02	0,956	0,105	2,74	4,362	1,78
04c	5,450	1,21	0,343	1,18	0,972	0,103	2,85	1,245	
06a	5,291	1,30	0,333	1,21	0,930	0,086	3,30	-2,176	
06b	5,104	1,25	0,324	1,01	0,807	0,071	14,90	-3,920	-0,01
07a	5,432	1,20	0,340	1,12	0,939	0,101	2,92	-0,645	
07b	5,297	1,20	0,332	1,11	0,926	0,027	4,61	-2,504	
10a	5,364	1,05	0,337	1,05	0,995	0,099	3,44	-1,150	
10b	5,234	1,22	0,328	1,19	0,980	0,091	4,29	-3,490	-0,94
13a	5,356	1,18	0,340	1,14	0,961	0,100	2,78	0,927	
20a	5,349	1,26	0,336	1,22	0,967	0,103	2,77	-1,091	

	$^{207}Pb/^{235}U$	±σ %	$^{206}Pb/^{238}U$	±σ %	ρ	$^{208}Pb/^{232}Th$	±σ %	Disc. % conv.	Disc. % 2σ lim.
Zr					**MG07-008; GIIb**				
02a	4,987	1,39	0,324	1,00	0,723	0,090	3,52	-0,970	
02b	12,670	66,97	0,518	9,64	0,144	no data	no data	2,826	
03a	4,954	1,32	0,313	1,04	0,784	0,093	3,96	-7,183	-2,97
03b	5,310	1,20	0,339	1,01	0,838	0,096	2,88	1,223	
04a	5,356	1,25	0,339	1,18	0,938	0,094	2,78	0,654	
06a	5,347	1,16	0,338	1,11	0,958	0,096	2,73	-0,140	
06b	5,352	1,17	0,340	1,01	0,858	0,092	2,77	1,279	
08a	5,380	1,07	0,342	1,01	0,950	0,091	3,90	1,603	
08b	5,215	1,27	0,328	1,00	0,792	0,082	3,07	-3,210	
09a	5,109	1,24	0,323	1,04	0,832	0,091	2,85	-4,053	-0,30
09b	5,396	1,13	0,340	1,01	0,898	0,095	2,71	0,204	
14a	5,341	1,26	0,335	1,02	0,804	0,094	3,32	-1,529	
20a	4,832	1,42	0,303	1,02	0,714	0,089	4,11	-10,843	-5,96
24a	4,575	1,14	0,295	1,03	0,898	0,093	2,78	-10,369	-7,41
Zr					**MG07-005; GIII**				
01a	5,023	1,11	0,318	1,03	0,931	0,090	2,75	-5,546	-2,86
02a	5,237	1,20	0,333	1,05	0,873	0,093	2,75	-0,467	
02b	5,271	1,13	0,335	1,02	0,903	0,092	2,70	-0,061	
04a	4,877	1,33	0,314	1,05	0,791	0,090	2,79	-5,334	-1,09
05a	5,380	1,17	0,341	1,02	0,874	0,093	2,75	1,021	
07a	5,152	1,10	0,328	1,03	0,938	0,092	2,80	-2,054	
07b	5,279	1,21	0,340	1,01	0,833	0,095	2,75	2,536	
11a	5,272	1,10	0,336	1,02	0,926	0,093	2,71	0,298	
11b	5,419	1,10	0,346	1,00	0,911	0,096	2,77	3,619	0,64
14a	4,315	1,19	0,273	1,01	0,844	0,061	2,87	-18,932	-15,59
14b	5,348	1,14	0,340	1,01	0,886	0,094	2,69	1,033	
15a	5,358	1,20	0,340	1,04	0,864	0,092	2,82	0,862	
16a	4,809	1,08	0,308	1,01	0,928	0,086	2,70	-7,176	-4,54
17a	5,119	1,28	0,327	1,20	0,938	0,098	2,84	-2,211	
19a	5,110	1,33	0,323	1,25	0,935	0,091	2,84	-4,368	-1,15
20a	5,170	1,10	0,331	1,00	0,912	0,089	2,76	-0,728	
24a	5,399	1,21	0,341	1,00	0,829	0,095	2,76	0,568	

	$^{207}Pb/^{235}U$	±σ %	$^{206}Pb/^{238}U$	±σ %	ρ	$^{208}Pb/^{232}Th$	±σ %	Disc. % conv.	Disc. % 2σ lim.
Zr					MG07-001; GII				
01a	5,158	1,18	0,328	1,02	0,870	0,094	2,92	-1,924	
02a	5,137	1,23	0,327	1,01	0,815	0,068	3,16	-2,431	
06a	5,256	1,23	0,333	1,13	0,914	0,095	2,85	-1,019	
06b	5,351	1,32	0,342	1,07	0,815	0,095	2,86	2,803	
07a	5,348	1,08	0,338	1,01	0,937	0,098	2,70	-0,097	
08a	5,238	1,17	0,335	1,01	0,857	0,098	3,07	0,557	
10a	5,256	1,15	0,333	1,04	0,898	0,095	2,86	-1,323	
10b	5,327	1,17	0,338	1,08	0,930	0,093	2,77	0,615	
11a	4,231	1,72	0,275	1,05	0,611	0,032	5,24	-16,016	-9,50
11b	5,283	1,04	0,334	1,03	0,989	0,092	2,63	-1,031	
13a	5,284	1,16	0,337	1,01	0,864	0,092	2,94	1,040	
16a	5,248	1,27	0,330	1,01	0,791	0,092	2,99	-2,996	
18a	5,278	1,22	0,338	1,00	0,822	0,095	2,87	1,366	
19a	5,250	1,18	0,335	1,02	0,866	0,095	2,96	0,274	
20a	4,468	1,32	0,282	1,08	0,819	0,062	3,42	-16,407	-12,51
22a	5,167	1,18	0,330	1,01	0,853	0,099	2,91	-1,453	
23a	5,275	1,13	0,335	1,01	0,888	0,097	2,83	-0,066	

	$^{207}Pb/^{235}U$	±σ %	$^{206}Pb/^{238}U$	±σ %	ρ	$^{208}Pb/^{232}Th$	±σ %	Disc. % conv.	Disc. % 2σ lim.
Tit					**MG07-005; GIII**				
01a	5,514	2,30	0,353	1,60	0,694	no data	no data	5,691	
03a	5,336	2,06	0,340	1,62	0,786	no data	no data	1,265	
03b	8,288	12,81	0,490	2,69	0,210	no data	no data	35,057	
04a	5,437	1,98	0,353	1,60	0,807	no data	no data	7,806	1,28
06a	5,667	6,92	0,397	1,75	0,253	no data	no data	32,587	
06b	5,755	4,42	0,375	1,60	0,362	no data	no data	15,130	
08a	5,635	2,42	0,359	1,60	0,658	no data	no data	7,027	
08b	6,229	13,00	0,388	3,84	0,296	no data	no data	13,298	
09a	5,634	2,05	0,356	1,60	0,777	no data	no data	5,395	
09b	5,574	1,93	0,352	1,60	0,825	no data	no data	4,005	
10a	5,689	2,18	0,350	1,60	0,731	no data	no data	0,831	
10b	4,996	22,82	0,316	2,12	0,093	no data	no data	-6,158	
11a	5,808	2,32	0,365	1,91	0,822	no data	no data	7,523	0,11
11b	5,507	2,13	0,353	1,60	0,748	no data	no data	6,132	
Tit					**MG07-008; GII**				
01a	5,324	5,51	0,339	1,98	0,360	no data	no data	1,487	
01b	5,417	4,24	0,347	1,67	0,393	no data	no data	4,085	
03a	5,421	1,66	0,342	1,60	0,964	no data	no data	1,336	
03b	5,404	1,65	0,341	1,60	0,968	no data	no data	0,737	
07a	5,487	1,65	0,347	1,60	0,968	no data	no data	2,732	
07b	5,271	1,67	0,335	1,60	0,958	no data	no data	-0,466	
08a	5,275	1,68	0,333	1,63	0,968	no data	no data	-1,519	
09a	5,051	1,93	0,325	1,67	0,867	no data	no data	-2,063	
10a	5,187	1,69	0,329	1,60	0,947	no data	no data	-2,326	
11a	5,401	1,65	0,340	1,60	0,967	no data	no data	0,419	

	$^{207}Pb/^{235}U$	±σ %	$^{206}Pb/^{238}U$	±σ %	ρ	$^{208}Pb/^{232}Th$	±σ %	Disc. % conv.	Disc. % 2σ lim.
Tit				**MG07-006; Klockträsk**					
01a	5,218	2,09	0,325	1,60	0,765	no data	no data	-5,492	
01b	5,329	1,75	0,336	1,60	0,914	no data	no data	-0,727	
01e	5,908	6,44	0,325	1,91	0,296	no data	no data	-16,528	
02a	5,541	2,03	0,344	1,60	0,784	no data	no data	-0,146	
02b	5,502	2,12	0,342	1,61	0,759	no data	no data	-0,643	
03a	5,572	2,15	0,352	1,63	0,758	no data	no data	4,238	
03b	5,786	2,01	0,350	1,60	0,793	no data	no data	-0,950	
04c	5,097	3,78	0,317	1,60	0,423	no data	no data	-7,720	
05a	6,237	2,29	0,361	1,60	0,698	no data	no data	-2,776	
05b	5,619	2,14	0,336	1,60	0,745	no data	no data	-6,293	
06a	5,649	2,19	0,348	1,60	0,730	no data	no data	-0,099	
07a	5,744	2,23	0,346	1,60	0,715	no data	no data	-2,915	
07b	5,626	1,81	0,356	1,60	0,881	no data	no data	5,424	0,19
08a	5,458	2,18	0,341	1,60	0,733	no data	no data	-0,310	
08b	5,623	2,15	0,351	1,60	0,741	no data	no data	2,754	
09a	5,491	2,04	0,339	1,60	0,786	no data	no data	-1,976	
09b	5,454	2,36	0,344	1,60	0,676	no data	no data	1,592	

Tit				**MG07-001; GII**					
01a	5,421	1,64	0,342	1,60	0,972	no data	no data	0,972	
02a	5,265	2,00	0,332	1,60	0,799	no data	no data	-1,955	
03a	5,262	1,62	0,332	1,61	0,990	no data	no data	-2,169	
03b	5,489	1,63	0,347	1,60	0,979	no data	no data	3,011	
04a	5,298	2,09	0,326	1,60	0,765	no data	no data	-6,016	
05a	5,296	2,25	0,338	1,60	0,710	no data	no data	1,295	
06a	5,163	1,69	0,328	1,60	0,949	no data	no data	-2,501	

ANEXO VI. QUÍMICA MINERAL DE CIRCONES

ZIRCONS MINERAL CHEMISTRY

Muestra	MG07-001 GII					MG07-004 GI										
Coordenada	E: 7222681; N:1700310					E: 1688028; N: 7242143										
Nr	3	4	5	6	7	8	9	10	11	12	13	14	15	16	17	18
Y_2O_3	0,020	0,122	0,369	0,009	0,018	0,175	0,888	0,037	0,039	0,039	0,046	0,058	0,037	0,349	0,151	0,083
ZrO_2	68,27	66,53	65,90	66,63	67,20	65,99	65,37	67,23	67,14	67,31	66,54	66,72	66,83	66,65	66,94	66,78
Nd_2O_3	-	0,002	-	0,016	-	-	0,004	0,004	-	0,015	-	-	0,001	0,007	0,011	0,002
SiO_2	32,15	31,85	31,53	31,88	31,88	31,36	31,53	31,63	31,98	31,51	31,97	31,88	32,01	31,97	31,98	32,26
P_2O_5	-	-	-	-	-	-	-	-	-	-	-	-	-	-	-	-
Pr_2O_3	0,014	0,012	0,031	0,008	0,008	-	-	0,005	-	-	0,01	0,036	0,016	0,018	0,022	-
HfO_2	1,314	1,294	1,12	1,602	1,268	1,535	1,265	1,386	1,388	1,717	1,292	1,443	1,441	1,3	1,328	1,469
CaO	0,006	0,011	0,012	-	0,012	0,021	0,020	0,011	-	0,015	0,007	0,009	0,002	0,012	0,001	0,011
ThO_2	0,013	0,026	0,403	0,007	0,015	0,035	0,134	0,006	-	0,007	0,003	0,01	0,013	0,027	0,017	0,007
Sm_2O_3	-	-	-	-	-	-	0,001	0,004	-	0,006	0,017	-	-	-	-	0,013
Lu_2O_3	0,012	0,006	0,013	0,006	-	0,02	0,056	0,007	0,011	0,007	0,01	0,007	0,003	0,028	0,01	0,004
La_2O_3	-	-	-	0,001	-	-	-	0,005	-	-	-	-	-	-	-	0,008
UO_2	0,026	0,032	0,46	0,034	0,017	0,127	0,293	0,027	0,021	0,071	0,03	0,027	0,042	0,071	0,044	0,041
Gd_2O_3	-	0,011	0,008	-	-	-	0,013	-	0,006	-	-	0,024	0,001	-	-	-
Yb_2O_3	-	-	0,037	-	-	0,031	0,226	-	-	-	-	-	-	0,072	-	-
Ce_2O_3	0,015	-	-	-	-	-	-	-	-	-	-	-	-	-	-	-
Ho_2O_3	-	-	-	-	0,002	-	0,01	-	-	-	-	-	-	-	-	-
Tb_2O_3	-	-	0,005	-	0,001	-	-	0,001	0,005	-	-	-	-	-	-	-
Al_2O_3	-	0,005	-	-	-	-	-	-	-	0,005	-	-	-	0,003	0,006	-
FeO	0,014	-	-	0,002	0,011	0,027	0,02	0,006	-	-	0,012	0,006	0,005	-	-	0,013
Eu_2O_3	-	-	0,003	0,002	-	-	-	0,009	0,018	-	0,004	-	-	0,003	-	0,01
Tm_2O_3	-	0,003	-	-	-	0,015	0,002	-	-	-	-	-	-	0,002	-	-
MnO	0,003	-	-	-	0,008	0,016	-	-	0,013	-	0,008	0,012	-	-	-	-
TiO_2	0,039	0,036	0,02	0,036	0,048	0,039	0,03	0,04	0,036	0,049	0,04	0,05	0,043	0,049	0,026	0,048
MgO	-	0,009	-	-	-	-	-	0,001	0,003	-	0,001	0,005	-	-	-	0,006
Total	101,90	99,95	99,91	100,23	100,49	99,40	99,85	100,41	100,66	100,75	99,99	100,29	100,44	100,56	100,53	100,76

Muestra	MG07-005 GIII							MG07-008 GII								
Coordenada	E: 1702913; N: 7235755							E: 1710203; N: 7251600								
Nr	19	20	21	22	23	24	25	29	30	31	32	33	34	35	36	37
Y_2O_3	0,153	0,041	0,053	0,19	0,056	0,017	0,059	0,079	-	0,118	0,053	0,053	-	0,024	0,085	0,081
ZrO_2	66,97	66,79	67,39	67,18	66,81	67,00	66,20	66,52	0,02	66,88	66,25	66,91	67,34	66,94	66,83	66,43
Nd_2O_3	0,011	0,014	-	0,009	-	-	0,023	0,002	-	0,022	0,005	0,013	0,001	-	0,018	0,009
SiO_2	32,07	32,21	32,05	32,03	32,04	32,01	31,94	32,00	91,52	31,85	31,78	32,14	32,25	31,62	31,76	31,71
P_2O_5	-	-	-	-	-	-	-	-	0,003	-	-	-	-	-	-	-
Pr_2O_3	0,011	-	-	-	-	-	-	-	0,004	0,002	-	0,01	-	0,015	-	-
HfO_2	1,201	1,306	1,249	1,103	1,268	1,181	1,274	1,284	0,073	1,362	1,71	1,356	1,673	1,599	1,265	1,396
CaO	0,022	0,006	0,013	0,008	0,009	-	0,021	0,004	0,011	0,013	0,01	-	0,021	0,010	0,011	-
ThO_2	0,031	0,010	0,019	0,037	0,016	0,009	0,02	-	0,004	0,014	0,024	0,017	0,01	0,018	0,003	0,015
Sm_2O_3	0,005	0,007	-	0,012	-	0,002	0,005	-	-	-	0,002	0,001	-	0,004	-	-
Lu_2O_3	-	0,006	-	0,025	0,011	0,005	-	0,011	-	0,007	0,008	0,002	0,01	0,008	0,017	-
La_2O_3	-	0,003	-	0,019	-	-	-	0,008	-	-	-	-	0,012	-	-	0,008
UO_2	0,036	0,037	0,035	0,057	0,034	0,017	0,037	0,022	0,003	0,031	0,084	0,022	0,088	0,039	0,053	0,025
Gd_2O_3	0,005	0,014	-	0,014	-	-	-	-	0,003	-	-	0,007	-	-	0,002	0,008
Yb_2O_3	0,003	-	-	-	-	-	-	-	-	-	-	-	-	-	-	-
Ce_2O_3	0,007	-	-	0,006	-	-	-	-	-	-	-	-	-	-	-	-
Ho_2O_3	0,009	-	-	0,039	0,014	-	-	-	-	-	-	0,009	-	-	-	0,012
Tb_2O_3	0,001	-	0,004	0,007	-	-	-	-	-	0,016	-	-	0,01	-	-	-
Al_2O_3	-	0,002	-	0,001	-	0,007	0,024	-	0,014	0,01	-	0,002	0,006	-	-	-
FeO	-	0,01	0,008	0,028	0,006	0,007	0,045	0,017	0,002	0,002	0,013	0,002	0,009	-	0,016	-
Eu_2O_3	-	0,024	0,018	-	-	-	-	-	-	0,006	0,003	-	0,007	-	0,012	0,003
Tm_2O_3	0,011	-	0,003	-	0,001	0,002	0,004	-	-	0,003	-	-	-	-	0,017	0,005
MnO	0,008	-	0,004	0,002	-	0,006	-	-	-	0,008	0,001	-	-	0,009	0,001	-
TiO_2	0,037	0,047	0,046	0,022	0,028	0,034	0,048	0,042	0,007	0,032	0,051	0,037	0,033	0,052	0,036	0,029
MgO	0,001	-	-	0,003	-	-	0,003	-	0,002	-	-	-	0,003	0,003	0,002	0,003
Total	100,59	100,53	100,89	100,79	100,29	100,30	99,71	99,98	91,67	100,38	99,99	100,57	101,46	100,35	100,13	99,73

Muestra	MG07-007 Rengard			JO03-55a GI					23J28 GI							
Coordenada	E: 1700790; N: 7207970			E: 1683350; N: 7226550					E: 1682350; N: 7226850							
Nr	26	27	28	38	39	40	41	42	43	44	45	46	47	48	49	50
Y_2O_3	0,077	0,05	0,415	0,098	0,104	0,13	0,044	0,129	0,205	0,193	0,067	0,09	0,078	0,063	0,049	0,021
ZrO_2	67,36	66,22	66,41	66,50	66,29	66,77	66,89	66,20	66,33	66,48	65,39	66,72	58,76	58,15	66,45	55,23
Nd_2O_3	0,003	0,01	0,008	-	0,037	-	0,008	-	-	0,014	0,018	0,015	-	-	0,015	-
SiO_2	31,81	31,95	31,53	31,87	31,74	31,92	32,30	32,23	32,29	32,21	32,62	32,29	29,53	29,48	32,16	29,67
P_2O_5	-	-	-	-	-	-	-	-	-	-	-	-	-	-	-	-
Pr_2O_3	0,012	0,018	-	0,024	-	-	-	0,003	-	-	-	0,019	-	-	-	-
HfO_2	1,364	1,466	1,426	1,575	1,555	1,561	1,537	1,353	1,474	1,496	1,634	1,455	1,5	1,501	1,524	1,503
CaO	-	0,004	0,027	0,010	0,040	0,010	0,006	0,003	0,007	0,007	-	-	3,009	4,608	0,018	5,322
ThO_2	0,009	0,003	0,042	0,017	0,029	0,012	0,008	0,012	0,014	0,014	0,026	0,006	0,068	0,029	0,042	0,112
Sm_2O_3	0,002	0,002	0,001	0,002	0,007	0,004	0,002	0,012	0,012	-	0,008	-	-	-	0,001	0,005
Lu_2O_3	0,008	0,004	0,025	0,007	-	-	0,004	0,009	0,018	0,014	0,008	0,006	0,015	0,014	0,023	0,009
La_2O_3	-	0,01	-	-	-	-	-	-	-	0,014	-	-	-	-	-	-
UO_2	0,02	0,018	0,076	0,072	0,061	0,07	0,034	0,061	0,079	0,084	0,13	0,039	0,365	0,347	0,261	0,522
Gd_2O_3	-	0,012	0,002	0,001	0,018	-	-	0,004	-	-	0,011	-	-	-	-	-
Yb_2O_3	-	-	0,063	-	-	-	-	-	-	0,015	-	-	-	-	-	-
Ce_2O_3	-	-	-	-	0,003	-	-	-	-	-	-	-	-	-	-	-
Ho_2O_3	0,009	-	-	-	-	0,01	0,01	0,014	-	0,002	0,001	-	-	-	0,001	-
Tb_2O_3	0,007	0,013	-	0,006	0,006	0,008	0,017	0,012	0,018	0,001	0,011	0,011	0,004	-	0,002	-
Al_2O_3	0,003	0,002	0,002	0,006	0,059	0,007	0,002	-	0,003	0,003	-	-	0,143	0,103	-	0,48
FeO	0,004	0,004	0,031	-	0,062	-	-	0,005	-	0,02	-	0,002	0,369	0,58	-	0,302
Eu_2O_3	-	0,023	0,003	-	-	-	0,012	-	-	0,002	-	-	-	0,054	-	0,002
Tm_2O_3	-	0,007	-	-	-	-	-	0,005	-	-	-	-	-	-	-	-
MnO	-	-	-	0,011	0,009	-	-	-	0,009	-	0,005	-	0,04	0,155	-	0,09
TiO_2	0,034	0,036	0,037	0,039	0,048	0,047	0,056	0,045	0,029	0,041	0,037	0,05	0,053	0,037	0,029	0,029
MgO	-	0,005	-	0,004	0,01	-	-	-	0,004	-	-	-	-	-	-	0,008
Total	100,73	99,85	100,10	100,24	100,08	100,55	100,93	100,10	100,50	100,61	99,97	100,70	93,93	95,12	100,57	93,30

ANEXO VII. LOCALIZACIÓN DE MUESTRAS
SAMPLES LOCATION

JO03-	Fecha	Stop n°	Estructuras	E-coord	N-coord	Comentario
1,2,3	06-jul-03	1	fol-N110E/70N	1692500	7218600	basaltos zonas masivas, acumulados y foliadas/basalts foliated, massive and cummulates
	06-jul-03	2				basaltos zona porfídica-fenos de px/basalts porphyrytic area, pyroxene crystals
4	06-jul-03	3	Jigsaw-fit	1692820	7218840	Venas de tonalíta sobre diorita/felsic veins in diorite
5	06-jul-03	4		1692720	7218820	Metabasita, anfibolita, plano de falla?/metabasite-amphibolite, fault?
6	06-jul-03	5		1692210	7219060	tonalita cuarzo porfidica/quartz porphyrytic tonalite
	07-jul-03	6	brecha			Clastos de basaltos 0.2-15 cm; monomícticos/basalt fragments(0.2-15 cm), monomictic
7	07-jul-03	7	brecha	1691790	7219000	Brecha basaltos no deformada, monomíctica/undeformed (auto?) breccia (monomictic)
8	07-jul-03	8	brecha	1691530	7219030	Clastos de basaltos 0.2-40 cm; monomícticos/basalt fragments(0.2-40 cm), monomictic
9	07-jul-03	9	fol-N110E	1690800	7219310	basaltos fenocristales orientados por deformación/px crystals foliated and elongated
10	07-jul-03	10		1692010	7220810	GI, leuco-trondjhemita/ GI trondhjemite
11	07-jul-03	11		1692440	7219650	GI, leuco-trondjhemita/ GI trondhjemite
	08-jul-03	12	fol-N110E			clastos de 2-3 cm, foliada a masiva/basalt foliated to massive, 2-3 cm fragments
	08-jul-03	13	fol-N115E/76N			idem Stop 12
12	08-jul-03	14	fol-N30E/80SE	1689800	7220280	variaciones de porfídica a masiva de GI/ GI porphyrytic to granitic texture
	08-jul-03	15				idem Stop 12
13	08-jul-03	16		1691390	7220910	GI, leuco-trondjhemita/ GI trondhjemite
14	09-jul-03	17		1698890	7212400	brecha máfica, cantos de la tonalita y máfica/polymictic mafic breccia with GI clasts
	09-jul-03	18				Riolita/Rhyolite
	09-jul-03	19				Riolita, horizontes vesiculados y otros soldados/Rhyolite, vesicule and welded areas
15	09-jul-03	20		1698630	7212785	GI porfídica/qz+plg porphyritic rock
	09-jul-03	21				Pórfido de plg, no GI?/feldspar porphyrytic, GI?
16	09-jul-03	22		1698980	7213380	GI porfídica/qz+plg porphyritic rock
	09-jul-03	23				Conglomerado/Conglomerate
17	09-jul-03	24		1699210	7212940	Riolita masiva/massive Rhyolite
18	11-jul-03	25		1693250	7218340	GI porfídica/qz+plg porphyritic rock
19	11-jul-03	26'				GI porfídica/qz+plg porphyritic rock
20	11-jul-03	26''	fol-N140E	1693350	7218340	brecha máfica, cantos de la tonalita y máfica/polymictic mafic breccia with GI clasts
21	11-jul-03	27	Jigsaw-fit?			Contacto entre básica porfídica y tonalita/tonalite and mafic boundary
22	11-jul-03	28	Venas	1693100	7218550	venas de aplita en roca máfica/aplite breccia in basalt
23	11-jul-03	29		1693750	7217720	Gabro masivo a porfídico/porphyrytic gabbro
24	12-jul-03	30				
	12-jul-03	31				
25-27	12-jul-03	32				
28	14-jul-03	33				
29-31	14-jul-03	34		1699360	7215600	limite de GI al sur/GI southern boundary
32	16-jul-03	35		1697950	7213270	GI porfídica/qz+plg porphyritic rock
	16-jul-03	36				GI porfídica a granular/qz + plg porphyritic to granitic rock
	16-jul-03	37				GI porfídica a granular/qz + plg porphyritic to granitic rock
33	16-jul-03	38		1698130	7213000	GI porfídica a granular/qz + plg porphyritic to granitic rock
	16-jul-03	39				GI porfídica/qz+plg porphyritic rock
34	17-jul-03	40				no afloramiento/no outcrop
35a+b+c	17-jul-03	41		1696170	7219520	dioritas y tonalitas tipo GI/Coarse grained GI tonalite + gabbro
36	18-jul-03	42		1700900	7227170	Tonalita GI/tonalite
37	18-jul-03	43	Diq-N110E	1700640	7226940	Tonalita GI/tonalite
	18-jul-03	44				Tonalita GI/tonalite
38b+B	18-jul-03	45	Cnt-N-S	1700620	7227120	contacto GI-GII + dique máfico N40E/GII-GI contact ans mafic dike
	18-jul-03	46	diq-N40E			Tonalita GI/tonalite
	18-jul-03	47	diq-N40E			Tonalita GI/tonalite
39+40	18-jul-03	48	Diq-N30E	1701020	7226700	Tonalita GI/tonalite
41	18-jul-03	49		1701012	7226758	dacita, dique sin-intrusivo/ dacite, syn-intrusive dike
	18-jul-03	50				Tonalita GI/tonalite
	19-jul-03	51				Tonalita GI/tonalite
42	19-jul-03	52	diq-N50E	1701740	7226920	Tonalita GI/tonalite
	19-jul-03	53				Tonalita GI/tonalite
	19-jul-03	54				Tonalita GI/tonalite
	19-jul-03	55	diq-N40E			Tonalita GI/tonalite

JO03-	Fecha	Stop n°	Estructuras	E-coord	N-coord	Comentario
43	21-jul-03	56	diq-N40E	1701410	7230340	Tonalita GI/tonalite
44	21-jul-03	57		1700610	7230580	Granodiorita a monzogranito GIII/ granodiorite to monzogranite GIII
	21-jul-03	58				Granodiorita a monzogranito GIII/ granodiorite to monzogranite GIII
	21-jul-03	59				Granodiorita a monzogranito GIII/ granodiorite to monzogranite GIII
	21-jul-03	60				Granodiorita a monzogranito GIII/ granodiorite to monzogranite GIII
101	21-jul-03	61		1702610	7232670	Granodiorita a monzogranito GIII/ granodiorite to monzogranite GIII
	21-jul-03	62				Granodiorita a monzogranito GIII/ granodiorite to monzogranite GIII
	21-jul-03	63				Granodiorita a monzogranito GIII/ granodiorite to monzogranite GIII
	21-jul-03	64				Granodiorita a monzogranito GIII/ granodiorite to monzogranite GIII
	22-jul-03	65				Granodiorita a monzogranito GIII/ granodiorite to monzogranite GIII
	22-jul-03	66				Granodiorita a monzogranito GIII/ granodiorite to monzogranite GIII
	22-jul-03	67				Granodiorita a monzogranito GIII/ granodiorite to monzogranite GIII
45	22-jul-03	68		1704500	7238490	Granodiorita a monzogranito GIII/ granodiorite to monzogranite GIII
	22-jul-03	69				Granodiorita a monzogranito GIII/ granodiorite to monzogranite GIII
46	22-jul-03	70				Granodiorita a monzogranito GIII/ granodiorite to monzogranite GIII
47	24-jul-03	71		1698800	7250190	Gabro/Gabbro
48	24-jul-03	72		1698910	7249090	Gabro/Gabbro
49	24-jul-03	73		1699060	7249870	Gabro/Gabbro
	24-jul-03	74				Gabro/Gabbro
	24-jul-03	75				Gabro/Gabbro
	24-jul-03	76				Diorita/diorite
50	24-jul-03	77		1698450	7250000	Diorita-gabro/diorite-Gabbro
51	24-jul-03	78		1697230	7249830	gabro grano fino/fine grain gabbro
52	25-jul-03	79				Conglomerados con GI/conglomerate with GI fragments
53	25-jul-03	80				conglomerado volcánico/volcanoclastic conglomerate
54	25-jul-03	81				Conglomerados con GI/conglomerate with GI fragments
55a+b	25-jul-03	82				Tonalita GI/tonalite
56	25-jul-03	83	fol-N-S			GI porfídica/qz+plg porphyritic rock
57	25-jul-03	84		1700340	7222730	GII
	26-jul-03	85				zona porfídica-fenos de px/porphyrytic area, pyroxene crystals
	26-jul-03	86	fol-N130E			Clastos basálticos de 0.2-15 cm; monomícticos/basalt fragments(0.2-15 cm), monomictic
	26-jul-03	87				GI porfídica/qz+plg porphyritic rock
	26-jul-03	88	diq-N40E/75W			GI tonalita/ tonalite
	26-jul-03	89	fol-N140E/80SW			GI tonalita/ tonalite
58	28-jul-03	90				Granodiorita a monzogranito GIII/ granodiorite to monzogranite GIII
59	29-jul-03	91		1697080	7242130	GI tonalita/ tonalite
60	29-jul-03	92	Dike	1697090	7242230	idem Stop 49, Stop 176, Stop 179
61	29-jul-03	93	Dike mafN50E	1697050	7242310	GI tonalita/ tonalite
	29-jul-03	94	Dike mafN50E			GI tonalita/ tonalite
62	29-jul-03	95	Dk monzonita	1697055	7242010	dique de monzonita/monzonite dike
	29-jul-03	96	Dike			idem Stop 49, Stop 176, Stop 179
	29-jul-03	97				GI tonalita/ tonalite
63	29-jul-03	98	Dike féls-N100E	1695110	7241420	GI porfídica/qz+plg porphyritic rock
	29-jul-03	99	Dike féls-N90E			GI porfídica/qz+plg porphyritic rock
	31-jul-03	100				Granodiorita a monzogranito GIII/ granodiorite to monzogranite GIII
64	31-jul-03	101		1702130	7240930	Granodiorita a monzogranito GIII/ granodiorite to monzogranite GIII
65	31-jul-03	102		1702230	7240850	Granodiorita a monzogranito GIII/ granodiorite to monzogranite GIII
66+67	31-jul-03	103	cnt-N-S	1700632	7227111	contacto GI-GII + dique máfico N40E/GII-GI contact ans mafic dike
	1-Ago-03	104	Contacto			GI brechificado por máfica porfídica/ tonalite breccia and basalt
	1-Ago-03	105	fol-N130E			brecha basaltica con fragmentos de tonalita y basalto/ GI bearing basaltic breccia
	1-Ago-03	106	Jigsaw-fit			brecha de basalto andesítico/andesite basalt breccia
	1-Ago-03	107				GI tonalita/ tonalite
	1-Ago-03	108				GI tonalita/ tonalite
68	2-Ago-03	109	Dike máf-N40E	1703516	7251218	GIIa con dique máfico/ mafic dike in granodiorite
	2-Ago-03	110				GIIa con enclaves microgranudos/ microgranular enclaves
	2-Ago-03	111				GIIa con enclaves microgranudos/ microgranular enclaves
69	2-Ago-03	112		1701681	7253132	gabro-olivínico con fragmento de tonalita/olivine gabbro with tonalite fragment
	2-Ago-03	113	Dike féls-N-S			tonalita a granodiorita porfídica GI-GII?/qz porphyritic rock, fined grained
	2-Ago-03	114	fol-N120E			Diorita/diorite
	5-Ago-03	115	Xenos máficos			Tonalita GI, textura granular, qz azul/tonalite, granitic texture, bluish qz
	5-Ago-03	116	Xenos máficos	1683430	7226636	Tonalita GI, textura granular, qz azul/tonalite, granitic texture, bluish qz
	5-Ago-03	117	Brecha	1682607	7226326	roca félsica microgranuda brechificada por tonalita/felsic breccia, tonalite veins
70	5-Ago-03	118		1682810	7226297	Tonalita GI, textura granular, altered/tonalite, granitic texture, altered
	5-Ago-03	119		1677320	7231011	GI tonalita/ tonalite, granular, no xenos
71	5-Ago-03	120	Dike máf-N130E	1677360	7230983	GI intruido por dique de máfica porfídica tipo Vithatten/ tonalite
	6-Ago-03	121		1678932	7235409	basaltos zonas masivas y brechificadas/basalts foliated, massive and breccia
	6-Ago-03	122		1678888	7235378	basaltos zonas masivas y brechificadas/basalts foliated, massive and breccia
	6-Ago-03	123		1680034	7234470	Tonalita GI, plg alteradas/ tonalite altered plagioclase
	6-Ago-03	124	fol-N130E	1680050	7234663	GI tonalita alterada/ tonalite, altered
	6-Ago-03	125	fol-N110E	1680057	7234728	GI, tonalita porfídica/qz porphyritic rock, qz<5%
72	6-Ago-03	126		1680118	7234704	GI, tonalita porfídica/qz porphyritic rock, qz=35%
73	6-Ago-03	127	Dk sienítico	1680177	7234665	monzonita de granular a porfídica/monzonite
74	6-Ago-03	128	Dike máf-N50E	1679960	7234393	GI tonalita porfídica/qz + plg porphyritic rock, 35% de cristales
	6-Ago-03	129	Brecha	1679916	7234448	GI tonalita intruye a volcánica félsica/ tonalite hosted in felsic volcanic rock
	6-Ago-03	130		1680191	7234805	GI tonalita porfídica/qz + plg porphyritic rock
75	7-Ago-03	131	cnt-E-W	1673425	7229657	gabro en contacto con máfica porfídica/basalt-gabbro boundary
76	7-Ago-03	132	Brecha	1673395	7229639	gabro brechifica a máfica porfídica/intrusive gabbro in basalt breccia
	7-Ago-03	133	Brecha	1673364	7229626	gabro brechifica a máfica porfídica/intrusive gabbro in basalt breccia
	7-Ago-03	134		1673698	7230459	diorita, variaciones a grano muy fino/diorite, fine to medium grain
77	7-Ago-03	135		1673674	7230433	diorita/diorite

JO03-	Fecha	Stop n°	Estructuras	E-coord	N-coord	Comentario
79	8-Ago-03	1H		1708590	7212420	GI tonalita porfídica/ tonalite porphyrytic
80	8-Ago-03	2H		1704441	7214607	GI tonalita enclaves microgranulares/ tonalite enclaves máficos
81	8-Ago-03	3H	Dike tonalita	1704252	7215099	GI tonalita, diques sin-intrusivos/ tonalite syn-intrusive dike
82	8-Ago-03	4H	Contacto	1704351	7215933	GI tonalita intrusiva sobre roca félsica/ tonalite intrusive on felsic rock
83	8-Ago-03	5H		1703054	7218162	GI tonalita margen sur de JGC/ tonalite southern margin
	8-Ago-03	6H		1700633	7227102	idem stop 45, stop 103
84	8-Ago-03	7H		1710083	7224125	GI tonalita porfídica/ tonalite porphyrytic
	8-Ago-03	8H		1711140	7224226	GI tonalita porfídica/ tonalite porphyrytic
85	9-Ago-03	136		1674657	7231989	Gallejaur monzonita/monzonite
	9-Ago-03	137		1674825	7232558	Gallejaur monzonita/monzonite
	9-Ago-03	138		1674598	7232855	Gallejaur monzonita con enclaves/monzonite with enclaves
86	9-Ago-03	139		1674485	7234738	Gallejaur monzonita con enclaves/monzonite with enclaves
	9-Ago-03	140		1674754	7234947	Gallejaur monzonita con enclaves/monzonite with enclaves
87	10-Ago-03	141		1683748	7234387	GI tonalita textura granítica/ tonalite granitic texture
78	10-Ago-03	"129"	Brecha	1679917	7234448	GI tonalita intruye a volcánica félsica/ tonalite hosted in felsic volcanic rock
	15-Ago-03	142	dike felsicos	1706604	7205848	Revsund granite
	15-Ago-03	143	dike felsicos	1707226	7205530	Revsund granite
88	15-Ago-03	144		1705686	7209280	Revsund granite
89	15-Ago-03	145		1705786	7209280	Revsund granite
	15-Ago-03	146	Falla-N30E	1707404	7205412	Revsund granite, high in xenolits
	16-Ago-03	147		1705008	7206784	Revsund granite, high in xenolits
	16-Ago-03	148		1704869	7208865	Andesita?
	16-Ago-03	149		1705064	7208853	Andesita?
	16-Ago-03	150		1705243	7208798	Andesita?
	16-Ago-03	151		1705479	7208659	Revsund granite
	16-Ago-03	152		1706261	7209269	Revsund granite
90	16-Ago-03	153		1705668	7209281	Andesita?
	16-Ago-03	154				Andesita?
	17-Ago-03	155				Gallejaur monzonita/monzonite
91	17-Ago-03	156				Gallejaur monzonita/monzonite, enclaves
92	18-Ago-03	157		1677923	7239280	Basálto andesítico porfídico con fenos de px/andesite basalt massive, px phenos.
	18-Ago-03	158		1677930	7238908	Basálto andesítico porfídico con fenos de px/andesite basalt massive, px phenos.
	18-Ago-03	159		1678036	7238849	Basálto andesítico porfídico con fenos de px/andesite basalt massive, px phenos.
	18-Ago-03	160		1678074	7238780	basalto andesítico brechificado/andesite basalt breccia
	18-Ago-03	161		1678005	7238543	Basálto andesítico porfídico con fenos de px/andesite basalt massive, px phenos.
93	18-Ago-03	162		1677933	7238430	Basálto andesítico porfídico con fenos de px y pl/andesite basalt massive, px+ pl
94	18-Ago-03	163		1677930	7238203	Basálto andesítico porfídico con fenos de px y pl/andesite basalt massive, px+ pl
95	19-Ago-03	164		1676558	7235507	Gallejaur monzonita/monzonite
96	19-Ago-03	165	Dk sienítico,N70	1672204	7235830	Diorita a gabro/diorite-Gabbro
97	19-Ago-03	166		1671988	7239542	Diorita a gabro/diorite-Gabbro
98+99	19-Ago-03	167	Fall-N80E	1671962	7239525	basalto andesítico, venas félsicas/ andesite basalt, felsic veins
100	21-Ago-03	168		1701200	7230450	Granodiorita a monzogranito GIII/ granodiorite to monzogranite GIII
101	21-Ago-03	169		1695678	7241262	GIV Granodiorita/Granodiorite
102*	21-Ago-03	170		1701673	7240719	no afloramiento/no outcrop
	22-Ago-03	171				Secuencia sedimentaria, Vargforsdamm/sediments
	22-Ago-03	172				Conglomerados, GI y volcánicas/Vargfors conglomerate
	22-Ago-03	173				Basálto andesítico porfídico con fenos de px y pl/andesite basalt massive, px+ pl
	22-Ago-03	174				Conglomerados, GI y volcánicas/Vargfors conglomerate
103	22-Ago-03	175		1670724	7228954	Basálto andesítico porfídico con fenos de px y pl/andesite basalt massive, px+ pl
104	22-Ago-03	176		1676544	7221328	pórfido de qz+pl, tipo GI?/ qz+plg porphyritic rock, Maurliden related
105	23-Ago-03	177		1704409	7219468	Gabro/gabbro
106	23-Ago-03	178		1704349	7219452	GI tonalita textura granítica/ tonalite granitic texture
107	23-Ago-03	179		1688532	7223120	pórfido de qz+pl, tipo GI?/ qz+plg porphyritic rock, Maurliden related
	23-Ago-03	180		1700570	7207955	Rengård tonalita/tonalite
108	23-Ago-03	181		1700692	7208010	Rengård tonalita/tonalite
	23-Ago-03	182	Dike máf-EW			Rengård tonalita/tonalite
109	23-Ago-03	183		1700777	7207839	Rengård tonalita/tonalite
110	23-Ago-03	184		1700946	7207443	Rengård tonalita/tonalite
111	24-Ago-03	185	cnt-N50E	1672015	7239522	Basálto andesítico porfídico con fenos de px/andesite basalt massive, px phenos
	24-Ago-03	186	Fluidos sieníticos			Basálto andesítico porfídico con fenos de px/andesite basalt massive, px phenos.
	24-Ago-03	187	fol-N70E			Basálto andesítico porfídico con fenos de px/andesite basalt massive, px phenos.
112	24-Ago-03	188		1670729	7238677	Basálto andesítico porfídico con fenos de px/andesite basalt massive, px phenos.
113	25-Ago-03	189		1706360	7227033	GI tonalita textura granítica/ tonalite granitic texture
114	25-Ago-03	190	cnt-N100E	1715670	7223676	Stavaträsk, aureola metamórfica (quiastolito)/metamorphic aureole (kyastolite)
115	25-Ago-03	191		1715755	7223707	GI tonalita textura granítica/ tonalite granitic texture
116	25-Ago-03	192		1712877	7229701	Gabro de grano medio a fino/medium to fine grain gabbro
	25-Ago-03	193				Gabro de grano medio a fino, fluidos pegmatíticos/medium to fine grain gabbro, pegm.
	25-Ago-03	194				Gabro de grano medio a fino/medium to fine grain gabbro
117	25-Ago-03	195		1711526	7233189	Gabro/Gabbro
118	25-Ago-03	196		1711622	7233202	Gabro/Gabbro
119	25-Ago-03	197		1711571	7233161	Gabro/Gabbro
120-122	26-Ago-03	198	Contacto	1704441	7214607	GI tonalita/ tonalite
123	26-Ago-03	199				GI tonalita textura/ tonalite qz+plg porphyritic rock
	26-Ago-03	200	falla?	1693306	7218481	brecha polimictica GI-basalto, falla?/ basalt-GI polimictic fault? Breccia
124	26-Ago-03	201		1689718	7220170	basalto porfídico (auto?)brecha/andesite basalt (auto?)breccia
	26-Ago-03	202				Dolerita porfídica, rica en plg de grano fino/dolerite, high pl content
125	8-ago-03	*H		1700340	7222730	GII

JO04-	Fecha	Stop n°	Estructuras	E-coord	N-coord	Comentario
1	03-jul-04	1		1703515	7251219	GIIa con dique máfico/ mafic dike in granodiorite
2	03-jul-04	2		1701681	7253132	GI? Tonalita en gabro/tonalite fragment in gabbro
3*Gq	03-jul-04	3		1701197	7253287	Gabro con microenclaves/cummulate gabbro with microenclaves
4	03-jul-04	4		1701202	7253247	Gabro con pirrotina/gabbro with pyrrotite
5	03-jul-04	5		1701212	7253185	Contacto gabro con GI?/gabbro-GI? Boundary
6*Gq	03-jul-04	6		1695737	7241282	GIV
	07-jul-04	7	lin-N20E	1707634	7244428	GIII Hobergsliden
7*Gq	07-jul-04	8		1707754	7244764	GIII Hobergsliden
8	07-jul-04	9		1707622	7244426	Diorita-gabro alterado/diorite-Gabbro altered
9	07-jul-04	10		1707578	7244679	Diorita-gabro alterado/diorite-Gabbro altered
	07-jul-04	11		1706440	7246129	GIII
10	07-jul-04	12		1706517	7246109	GIII
11	07-jul-04	13		1706188	7247462	GII granodiorita/granodiorite
	07-jul-04	14		1705977	7248715	dique máfico en GII/mafic dike
12	07-jul-04	15		1705937	7248704	dique máfico en GII/mafic dike
	07-jul-04	16		1705945	7248677	dique máfico en GII/mafic dike
	07-jul-04	17		1705735	7248741	GII
	07-jul-04	18		1705753	7248458	GII, dique máfico/ mafic dike
13	07-jul-04	19		1705779	7248456	GII
14	07-jul-04	20	diq-N50E	1705760	7248407	GII, dique máfico/ mafic dike
15	07-jul-04	21		1705807	7248350	GII, dique máfico/ mafic dike
	07-jul-04	22		1705873	7248376	GII, dique máfico/ mafic dike
	08-jul-04	23		1705951	7248580	GII, dique máfico/ mafic dike
	08-jul-04	24	diq-N20E	1705980	7248597	GII
	08-jul-04	25		1705995	7248566	GII
	08-jul-04	26		1706033	7248556	GII
	08-jul-04	27		1706036	7248540	GII
16	08-jul-04	28	diq-N60E/65N	1706047	7248515	GII
17	08-jul-04	29		1706114	7248507	GII
	08-jul-04	30	diq-N50E	1706167	7248457	GII
	08-jul-04	31	diq-N40E	1701168	7250713	GII, dique máfico/ mafic dike
18	08-jul-04	32		1701546	7250850	Diorita-gabro/diorite-Gabbro
19	08-jul-04	33		1701649	7250853	GII en gabro/GII in gabbro (megablock?)
20	08-jul-04	34		1701587	7250861	Diorita-gabro grano grueso/diorite-Gabbro coarse grain
	09-jul-04	35	diq-	1705849	7249518	GI tonalita y dique máfico/tonalite and mafic dike
21a	09-jul-04	36	diq-?	1705869	7249497	GI
21b	09-jul-04	37		1705858	7249425	dique máfico/mafic dike
22	09-jul-04	38	enclaves	1705905	7249449	GII enclaves microgranulares/ microgranular enclaves
	09-jul-04	39		1705875	7249323	GI tonalita y dique máfico/tonalite and mafic dike
23a+b	09-jul-04	40		1702888	7247958	GII-GIII
24a*Gq-	09-jul-04	41	diq-N50E	1705320	7250550	GII, dique máfico/ mafic dike
25+26	10-jul-04	42		1710969	7249788	GII enclaves microgranulares/ microgranular enclaves
	10-jul-04	43		1710873	7249698	GII
	10-jul-04	44		1710758	7249698	GII
	10-jul-04	45		1710702	7249444	GII
	10-jul-04	46		1710651	7249399	GII
27	10-jul-04	47		1712098	7248747	GII
	10-jul-04	48		1712093	7248937	GII
	10-jul-04	49		1712244	7248875	GII
28	10-jul-04	50		1712439	7248891	GII
29	10-jul-04	51		1712948	7248626	GI deformado/deformed GI tonalite
30	11-jul-04	52		1710117	7246338	GI deformado/deformed GI tonalite
31	11-jul-04	53		1710763	7246720	GI deformado/deformed GI tonalite
	11-jul-04	54		1710924	7246317	GI deformado/deformed GI tonalite
	11-jul-04	55		1711025	7245986	GII
	11-jul-04	56		1711127	7245030	GII
	11-jul-04	57		1711106	7245000	GII
32	11-jul-04	58		1711100	7245132	GII
33	11-jul-04	59		1711184	7245012	GII
34*Gq	13-jul-04	60	dik-N40E	1710192	7251600	GII
35	13-jul-04	61		1711807	7250480	GII
36	14-jul-04	62		1709894	7253595	Diorita-gabro/diorite-Gabbro
37	14-jul-04	63		1711000	7257161	Metasedimentos/sediments
38	14-jul-04	64		1706358	7261140	Diorita-gabro/diorite-Gabbro
39	14-jul-04	65		1707494	7258380	GI
40*Gq	14-jul-04	66		1707694	7258145	GII
41	14-jul-04	67		1707380	7257434	GI
42	15-jul-04	68		1703097	7259346	GII
43	15-jul-04	69		1701585	7256365	basalto andesítico porfídico pl+px/andeseite basalt porphyrytic pl+px
	15-jul-04	70		1701428	7256153	basalto andesítico porfídico pl+px/andeseite basalt porphyrytic pl+px
	15-jul-04	71		1701349	7256121	basalto andesítico porfídico pl+px/andeseite basalt porphyrytic pl+px
	15-jul-04	72		1701290	7256000	basalto andesítico porfídico pl+px/andeseite basalt porphyrytic pl+px
	15-jul-04	73		1701307	7256268	basalto andesítico porfídico pl+px/andeseite basalt porphyrytic pl+px
44	15-jul-04	74		1701259	7256500	basalto andesítico porfídico pl+px/andeseite basalt porphyrytic pl+px
	15-jul-04	75		1701466	7256495	basalto andesítico porfídico pl+px/andeseite basalt porphyrytic pl+px
45a+b	15-jul-04	76		1702337	7256845	GIIa+facies de borde/border facies of GIIa

JO04-	Fecha	Stop n°	Estructuras	E-coord	N-coord	Comentario
46	16-jul-04	77		1700155	7258760	qz+pl porfídica/qz+pl porphyrytic rock
	16-jul-04	78		1699271	7259219	qz+pl porfídica/qz+pl porphyrytic rock
	16-jul-04	79		1699285	7259237	qz+pl porfídica/qz+pl porphyrytic rock
47	16-jul-04	80		1699234	7259272	qz+pl porfídica/qz+pl porphyrytic rock
48	16-jul-04	81		1698590	7258410	qz+pl porfídica/qz+pl porphyrytic rock
49	16-jul-04	82		1697252	7259344	qz+pl porfídica/qz+pl porphyrytic rock
	16-jul-04	83		1699658	7258027	qz+pl porfídica/qz+pl porphyrytic rock
50a+b	16-jul-04	84		1698000	7255155	GI tonalita y dique máfico/tonalite and mafic dike
	16-jul-04	85	diq-N45E	1698102	7255279	GI tonalita y dique máfico/tonalite and mafic dike
51*Gq	16-jul-04	86		1698135	7255290	GI
	16-jul-04	87		1699485	7256620	GI tonalita y dique máfico/tonalite and mafic dike
52	16-jul-04	88		1699466	7256580	basalto andesítico porfídico pl+px/andeseite basalt porphyrytic pl+px
	16-jul-04	89		1699565	7256365	basalto andesítico porfídico pl+px/andeseite basalt porphyrytic pl+px
	17-jul-04	90		1715818	7223730	GI
	17-jul-04	91	Cnt-N100E	1715721	7223705	Contacto granodiorita-metasedimentos/sediments-granodiorite contact aureole
	17-jul-04	92		1715746	7223673	Contacto granodiorita-metasedimentos/sediments-granodiorite contact aureole
53	17-jul-04	93		1715814	7223590	Contacto granodiorita-metasedimentos/sediments-granodiorite contact aureole
	17-jul-04	94	fol-N80E/80N	1714450	7224700	Metasedimentos/sediments
	17-jul-04	95	fol-N135E/85S	1714540	7224810	Metasedimentos/sediments
54	17-jul-04	96		1714780	7224743	Pórfido de plg/pl porphyrytic rock
55	17-jul-04	97		1715539	7226842	Pórfido de plg/pl porphyrytic rock
56	17-jul-04	98		1715980	7227147	Pórfido de plg/pl porphyrytic rock
57	17-jul-04	99		1715803	7227147	Metasedimentos/sediments
58	17-jul-04	100		1719782	7224653	GI con xenolitos de encajante/GI hosting xenoliths of the host rock
59	17-jul-04	101		1720207	7226006	Máfica, acumulado de minerales máficos/mafic cummulate
60	17-jul-04	102		1719960	7225725	Diorita a gabro/diorite-Gabbro
	17-jul-04	103		1720680	7228797	Metasedimentos/sediments
	17-jul-04	104	fol-N92E/80N	1720570	7228665	granitoide arenizado/arenized granitoid
	17-jul-04	105		1720650	7228627	Metasedimentos/sediments
61	17-jul-04	106	Cnt	1720604	7228646	granitoide arenizado/arenized granitoid
62	21-jul-04	107	diques maf	1690949	7244816	GI tonalita/ tonalite
63	21-jul-04	108		1691520	7244113	Granodiorita a monzogranito GIII/ granodiorite to monzogranite GIII
	21-jul-04	109		1692979	7444802	Granodiorita a monzogranito GIII/ granodiorite to monzogranite GIII
64	21-jul-04	110		1692810	7244984	Granodiorita a monzogranito GIII/ granodiorite to monzogranite GIII
65	21-jul-04	111		1695704	7250780	Diorita a gabro/diorite-Gabbro
66	21-jul-04	112		1695302	7251178	basalto andesítico porfídico pl+px/andeseite basalt porphyrytic pl+px
67*Gq	21-jul-04	113		1698440	7252679	GI tonalita porfídica/qz + plg porphyritic rock
68	22-jul-04	114	fol-N120E/80S	1685039	7223315	Riolita a riodacita, intensa foliación/Rhyolite-rhyodacite, strongly foliated
	22-jul-04	115		1684055	7223729	Riolita a riodacita, intensa foliación/Rhyolite-rhyodacite, strongly foliated
	22-jul-04	116	fol-N130E	1683837	7224352	Riolita a riodacita, intensa foliación/Rhyolite-rhyodacite, strongly foliated
	22-jul-04	117		1683752	7224447	Riolita a riodacita, matriz qz/Rhyolite-rhyodacite, qz matrix
	22-jul-04	118	fol-N105E/75N	1683585	7224725	Riolita a riodacita, intensa foliación/Rhyolite-rhyodacite, strongly foliated
	22-jul-04	119		1683592	7224770	Riolita a riodacita, sferulites/Rhyolite-rhyodacite, sferulites
	22-jul-04	120		1683535	7224867	Riolita a riodacita, qz+pl porfídica/Rhyolite-rhyodacite pl+qz porphyrytic
69	22-jul-04	121	fol-N110E	1683490	7224877	Riolita a riodacita, qz+pl porfídica/Rhyolite-rhyodacite pl+qz porphyrytic
70	22-jul-04	122		1683500	7218880	basalto andesítico porfídico pl+px/andeseite basalt porphyrytic pl+px
	24-jul-04	123		1708190	7214465	GI tonalita porfídica/ tonalite porphyrytic
71	24-jul-04	124		1707769	7212526	GI tonalita porfídica/ tonalite porphyrytic
72	24-jul-04	125		1707334	7212725	GI tonalita porfídica/ tonalite porphyrytic
	24-jul-04	126		1707200	7212767	GI tonalita porfídica/ tonalite porphyrytic
	24-jul-04	127		1706935	7212770	GI tonalita porfídica/ tonalite porphyrytic
73	24-jul-04	128		1706335	7212683	GI tonalita porfídica deformada/ tonalite porphyrytic, deformed
74	24-jul-04	129		1707035	7214030	GI tonalita porfídica/ tonalite porphyrytic
75*Gq	26-jul-04	130		1704438	7214608	GI tonalita/ tonalite
76	26-jul-04	131	def-N50E/50NW	1704923	7216906	GI tonalita porfídica/ tonalite porphyrytic
77	26-jul-04	132		1704642	7216932	GI tonalita porfídica/ tonalite porphyrytic
78*Gq	26-jul-04	133		1703042	7218162	GI tonalita porfídica/ tonalite porphyrytic
79	26-jul-04	134		1701325	7219090	dique máfico/mafic dike
80	26-jul-04	135		1703395	7224095	GII
81	26-jul-04	136		1703515	7224100	GI tonalita porfídica/ tonalite porphyrytic
	26-jul-04	137		1704012	7224267	GI tonalita porfídica/ tonalite porphyrytic
	26-jul-04	138		1703940	7224270	GI tonalita porfídica/ tonalite porphyrytic
82	27-jul-04	139	ciz-N145E/80E	1706082	7236630	GIII cizallado-N145E/80E/ GIII deformed
	27-jul-04	140		1706426	7236647	Granodiorita a monzogranito GIII/ granodiorite to monzogranite GIII
	27-jul-04	141		1706607	7236478	Granodiorita a monzogranito GIII/ granodiorite to monzogranite GIII
	27-jul-04	142		1706760	7236355	Granodiorita a monzogranito GIII/ granodiorite to monzogranite GIII
83*Gq	27-jul-04	143		1706834	7236331	GII
	27-jul-04	144		1706967	7236285	Granodiorita a monzogranito GIII/ granodiorite to monzogranite GIII
	27-jul-04	145		1707194	7236313	Granodiorita a monzogranito GIII/ granodiorite to monzogranite GIII
	28-jul-04	146		1704240	7221175	GI
84	28-jul-04	147		1704013	7221590	GI tonalita/ tonalite
85	28-jul-04	148		1704480	7221675	GI tonalita/ tonalite
86*Gq	28-jul-04	149		1704600	7221615	GI tonalita/ tonalite
	28-jul-04	150	ciz-N-S	1709775	7226485	GI tonalita, suave deformación/ tonalite, slightly deformed
87	28-jul-04	151		1709680	7226387	GI tonalita/ tonalite
88*Gq	28-jul-04	152		1709570	7226455	GI tonalita/ tonalite
89	28-jul-04	153		1703892	7229805	GI tonalita porfídica/ tonalite porphyrytic
90	28-jul-04	154	diq-N75E	1703970	7229819	GI tonalita y dique máfico/tonalite and mafic dike

JO04-	Fecha	Stop n°	Estructuras	E-coord	N-coord	Comentario
91	29-jul-04	155		1697888	7213050	GI tonalita porfídica/ tonalite porphyrytic Råberget
	29-jul-04	156		1698165	7213160	GI tonalita porfídica/ tonalite porphyrytic Råberget
	29-jul-04	157		1698280	7213102	GI tonalita porfídica/ tonalite porphyrytic Råberget
92	29-jul-04	158		1698333	7213205	GI tonalita porfídica/ tonalite porphyrytic Råberget
	29-jul-04	159	contacto	1698105	7213030	GI tonalita/ tonalite
93	29-jul-04	160	contacto	1699125	7215770	GI tonalita/ tonalite
94*Gq	29-jul-04	161		1699278	7215565	GI tonalita, suave deformación/ tonalite slightly deformed
95	29-jul-04	162		1699376	7215725	GI tonalita/ tonalite
96	29-jul-04	163		1698757	7213220	GI tonalita/ tonalite
97	29-jul-04	164		1692580	7224070	GI tonalita/ tonalite
98	29-jul-04	165		1692300	7225770	GI tonalita/ tonalite
99	30-jul-04	166		1688596	7227165	GI tonalita/ tonalite
	30-jul-04	167		1688130	7227757	GI tonalita/ tonalite
100*Gq	30-jul-04	168		1688105	7227773	GII
	30-jul-04	169		1688520	7223193	GI tonalita/ tonalite
101*Gq	30-jul-04	170		1688600	7223140	Dacita sin-intrusiva/syn-intrusive dacite, GII?
	30-jul-04	171	Contacto	1693464	7218614	GI brechificado por máfica porfídica/ tonalite breccia and basalt
	30-jul-04	172	Contacto	1693374	7218506	GI brechificado por máfica porfídica/ tonalite breccia and basalt
102	31-jul-04	173	Bedrock?	1682693	7226343	roca félsica microgranuda brechificada por tonalita/felsic breccia, tonalite veins
	31-jul-04	174		1677460	7230980	basalto andesítico porfídico pl+px/andeseite basalt porphyrytic pl+px
103	31-jul-04	175	Dik-N130E	1677423	7231020	GI tonalita intruido por basalto porfídico/ tonalite intruded by porphyrytic basalt
	31-jul-04	176		1677386	7231049	GI tonalita/ tonalite
104	31-jul-04	177		1682720	7228628	GI tonalita porfídica/qz + plg porphyritic rock
105	31-jul-04	178		1682166	7230405	GI tonalita/ tonalite; idem to 23J40
106	31-jul-04	179		1679037	7235370	basalto andesítico porfídico, cantos de GI/andesite porphyrytic basalt, GI fragments
107*Gq	5-ago-04	204	dique máfico	1683768	7234447	GI tonalita/ tonalite
108	5-ago-04	205		1685423	7242615	GI tonalita, facies porfídica de borde/ tonalite, qz+pl porphyrytic border facies
109*Gq	5-ago-04	206		1688038	7242145	GI tonalita porfídica/ tonalite porphyrytic
110	5-ago-04	207		1689602	7244382	GI tonalita/ tonalite
111	5-ago-04	208		1694097	7249732	GI tonalita, facies porfídica de borde/ tonalite, qz+pl porphyrytic border facies
112*Gq	5-ago-04	209		1695395	7249993	GII
113	7-ago-04	210	N130E/75SW	1702646	7252061	GII foliación/foliated
114*Gq	7-ago-04	211		1702825	7254584	GII
115*Gq	7-ago-04	212		1702688	7255023	Näsberget gabro/gabbro
116	7-ago-04	213		1702200	7255185	Idem JO04-114
	7-ago-04	214		1702589	7255039	Idem stop -211, -213
	7-ago-04	215		1702995	7254320	Idem stop-211, -213, -214
117	7-ago-04	216		1701189	7250861	gabro/gabbro; ol+qz poor
	7-ago-04	217		1701230	7250950	gabro/gabbro
118	7-ago-04	218	dik-N60E	1701422	7251190	GIIa granodiorita y dique máfico/ granodiorite and mafic dike
	7-ago-04	219	ori-N30E	1701264	7251234	GIIa granodiorita y dique máfico/ granodiorite and mafic dike
119*Gq	7-ago-04	220		1701333	7251284	GIIa
	8-ago-04	221		1707014	7227788	GI tonalita/ tonalite
120*Gq	8-ago-04	222		1707066	7227795	GI tonalita/ tonalite
121	8-ago-04	223	def-N130E	1709147	7229330	GI tonalita, fuerte deformación/ tonalite; intense deformation
	8-ago-04	224	dik-N60E	1702150	7225762	GI tonalita/ tonalite
122*Gq	8-ago-04	225		1702132	7225725	GIIa
123	17-ago-04	226		1699158	7208655	Diorita a gabro/diorite-Gabbro
124*Gq	17-ago-04	227		1699776	7208502	Rengård tonalita/tonalite
1258	17-ago-04	228	def?	1701709	7206656	Rengård tonalita, ligera deformación/tonalite; slightly deformed
126	17-ago-04	229	def?	1701655	7206650	Rengård tonalita, ligera deformación/tonalite; slightly deformed
127*Gq	17-ago-04	230		1697180	7213930	GI tonalita porfídica/qz + plg porphyritic rock
128*Gq	18-ago-04	231		1700381	7222353	GII
129	18-ago-04	232		1700766	7223164	GI tonalita/ tonalite
	18-ago-04	233		1700754	7223103	GI tonalita/ tonalite
130*Gq	18-ago-04	234		1696165	7219375	GI tonalita/ tonalite
	18-ago-04	235		1696180	7219430	Diorita a gabro/diorite-Gabbro
	18-ago-04	236		1696134	7219435	Diorita a gabro/diorite-Gabbro
131	18-ago-04	237		1696155	7219475	Diorita a gabro/diorite-Gabbro
132	18-ago-04	238	N120E/85S	1696133	7219438	GI tonalita y dique máfico/tonalite and mafic dike
133	18-ago-04	239		1696121	7219423	GI tonalita/ tonalite
	18-ago-04	240		1692145	7220632	GI tonalita/ tonalite
134	18-ago-04	241	fol-N135E/65N	1693020	7218843	zonas masivas, acumulados y foliadas/foliated, massive and cummulates
	18-ago-04	242	fol-N115E/65N	1689737	7220144	zonas masivas, acumulados y foliadas/foliated, massive and cummulates
135*Gq	18-ago-04	243		1683510	7226363	GI tonalita/ tonalite
Gq-07	19-ago-04	244		1707754	7244764	GIII-Hobergsliden
136*Gq	19-ago-04	245		1705649	7248480	GII
137	19-ago-04	246	cnt-N35E/70SE	1702897	7247949	GII
23a*Gq	19-ago-04	247	cnt-N20E	1702888	7247958	GI tonalita/ tonalite
	20-ago-04	248		1712106	7248710	Diorita a gabro/diorite-Gabbro
138*Gq	20-ago-04	249		1712144	7248698	GII
Gq-34	20-ago-04	250	dik-N40E	1710192	7251600	GII
Gq-40	20-ago-04	251		1707694	7258145	GII
139*Gq	20-ago-04	252		1702957	7259567	GII
140	20-ago-04	253		1702954	7259560	GII
141	21-ago-04	254	charn-60_N175	1711453	7255080	Metasedimentos/sediments
142*Gq	21-ago-04	255		1711458	7255113	GIIa
143	21-ago-04	256	def-N200E	1713502	7254563	GIIa
Gq-24a	21-ago-04	257		1705320	7250550	GII
Gq-51	21-ago-04	258		1698142	7255292	GI tonalita/ tonalite
Gq-67	21-ago-04	259		1698440	7252679	GI tonalita/ tonalite

JO04-	Fecha	Stop n°	Estructuras	E-coord	N-coord	Comentario
144*Gq	22-ago-04	260		1708579	7212435	GI-Klokträsk /qz-porphyrytic tonalite
145*Gq	22-ago-04	261		1715795	7223625	Stavaträsk, granodiorita de grano medio/medium grain granodiorite
146*Gq	22-ago-04	262		1698785	7213335	GI Brännliden, tonalita textura granitica/granitic tonalite
147*Gq	22-ago-04	263	contacto	1700632	7227111	contacto GI-GII + dique máfico N40E/GII-GI contact ans mafic dike
148	22-ago-04	264		1704585	7219395	gabronorita de grano medio/medium grain gabbronorite
	22-ago-04	265		1704409	7219468	gabro de grano fino/fine grain gabbro
149*Gq	22-ago-04	266		1704473	7219448	gabro de grano fino/fine grain gabbro
150	18-sep-04	267	Contacto	1693464	7218614	GI intruido por basalto porfídico/basalt porphyrytic rock intrusive on GI tonalite
151-152	18-sep-04	268				brecha polimictica GI-basalto, falla?/ basalt-GI polimictic fault? Breccia
153	18-sep-04	269	fol-N140E	1693350	7218340	becha de basalto, clastos de GI y basalto/basaltic breccia, GI and auto-clasts
154*Gp	18-sep-04	270	Venas	1693130	7218420	basalto andesítico porfídico/andesite porphyrytic basalt
155	18-sep-04	271				GI tonalita/ tonalite
156	18-sep-04	272	N120E/80S			basalto porfídico (auto?)brecha/andesite porphyrytic basalt (auto?)breccia

VIC04-	Fecha	Stop n°	Estructuras	E-coord	N-coord	Comentario
1	2-ago-04	180	def-N20E	1637240	7220282	"Hbl-tonalite"/tonalita algo deformada
2	2-ago-04	181		1632911	7222806	"Mine Prophyry"/trondhjemita grano fino
03A-B	2-ago-04	182	plGN100E	1632953	7221125	"High strain..."/tonalita y zonas máficas, muy plegadas
	2-ago-04	183		1633167	7220917	"Xenolithic trond??"/tonalita y zonas máficas, muy plegadas
4	2-ago-04	184		1633205	7220938	"Xenolithic trond??"/tonalita poco deformada+pirrotita
5	2-ago-04	185	def-N60E	1633250	7220933	"Xenolithic trond??"/tonalita y zonas máficas, muy deformadas
6	2-ago-04	186	fol-N45E	1633175	7220685	Granitoide rico en filosil. secundarios, idem a "bandas máficas"
7	2-ago-04	187		1633336	7220602	"Hbl tonalite"/tonalita rica en máficos
	2-ago-04	188	fol-N100E/85N	1632168	7220982	"High strain..."/tonalita y zonas máficas, muy plegadas
8	2-ago-04	189	fol-N100E/85N	1632180	7220966	"High strain..."/tonalita y zonas máficas, muy plegadas
9	2-ago-04	190		1631135	7221072	"Mine Prophyry"/idem a dikes en Stop-182
	2-ago-04	191	fol-N95E/75S	1631115	7221061	"Mine Prophyry"/idem Stop-182, qz-diorita en zona no deformada
10	2-ago-04	192		1630985	7220981	"Mine Prophyry"/idem Stop-182, qz-diorita en zona no deformada
11	2-ago-04	193		1631550	7221260	"Xenolitic trond??"/tonalita como en Stop-187
12	3-ago-04	194		1642477	7220270	Revsund type-granite
13	3-ago-04	195		1632290	7218801	"Hbl-tonalite"/tonalita grano medio-fino
	3-ago-04	196	fol-N60E/80SE	1632323	7218824	"Hbl-tonalite"/tonalita def. Con bandas máficas
14	3-ago-04	197		1632376	7218965	"Hbl-tonalite"/tonalita de grano fino
15	3-ago-04	198		1632432	7219052	"Mine porphyry"/idem a Stop-181, trondhjemite grano fino
	3-ago-04	199	def	1632446	7219166	"Mine porphyry"/idem a Stop-181, trondhjemite grano fino
	3-ago-04	200	def	1633806	7217070	"Hbl-tonalite"/muy alterada y deformada en esta zona
16	3-ago-04	201		1634870	7214909	"Hbl-tonalite"/muy alterada y deformada en esta zona
17	3-ago-04	202		1629410	7218000	Metavolcánicas Grupo Skellefte
18	3-ago-04	203		1629230	7217435	Metavolcánicas Grupo Skellefte

ANEXO VIII. FOTOS PETROGRAFÍA

PETROGRAPHY MICROPHOTOGRAPHS

Nr.	muestra	N-coord	E-coord	
1	23J15	7224000	1692750	Cuarzo recristalizado a agregado microcristalino de cuarzo poligonal en muestras de GI *GI: Recrystallized quartz to microgranular polygonal quartz aggregate*
2a	JO04-135	7226363	1683510	En verde chl que sustituye a bi_1 y posterior bi_2 de menor tamaño en centro y bordes de chl *Igneous biotite (bi_1) substituted by chlorite (green) and late smaller biotite (bi_2) in core and rim of chlorite*
2b	23J30	7227900	1688100	Chl por alteración de bi_1 y posteriores bi_2 con textura decusada y grano muy fino *Chl by alteration of bi_1 and late decussate very fine bi_2*
3	JO03-31	7215600	1699360	Cristales de epidota generados en el centro y borde de cristal de plagioclasa *Epidote crystals in rim and core of plagioclase*
4a	23J28	7226850	1682350	Biotita cristalizada en los planos de exfoliación de anfíbol parcialmente alterado *Recrystallized bi_2 in the oblique cleavage system of amphiboles*
4b	JO04-135	7226363	1683510	Biotita metamórfica que sustituye parcialmente cristales de anfíbol *Metamorphic biotite (bi_2) substituting some amphiboles*
5	23J11	7224900	1686150	Bi_2 decusada cristalizadas sobre cristal de bi_1 alterado, qz y tit como productos de alteración *Bi_2 decussate crystals on altered bi_1, qz and tit as alteration products*
6	JO03-110	7207443	1700946	Microcristales de cuarzo poligonales en borde de fenocristal de cuarzo *Polygonal quartz microcrystals in the rim of igneous quartz*

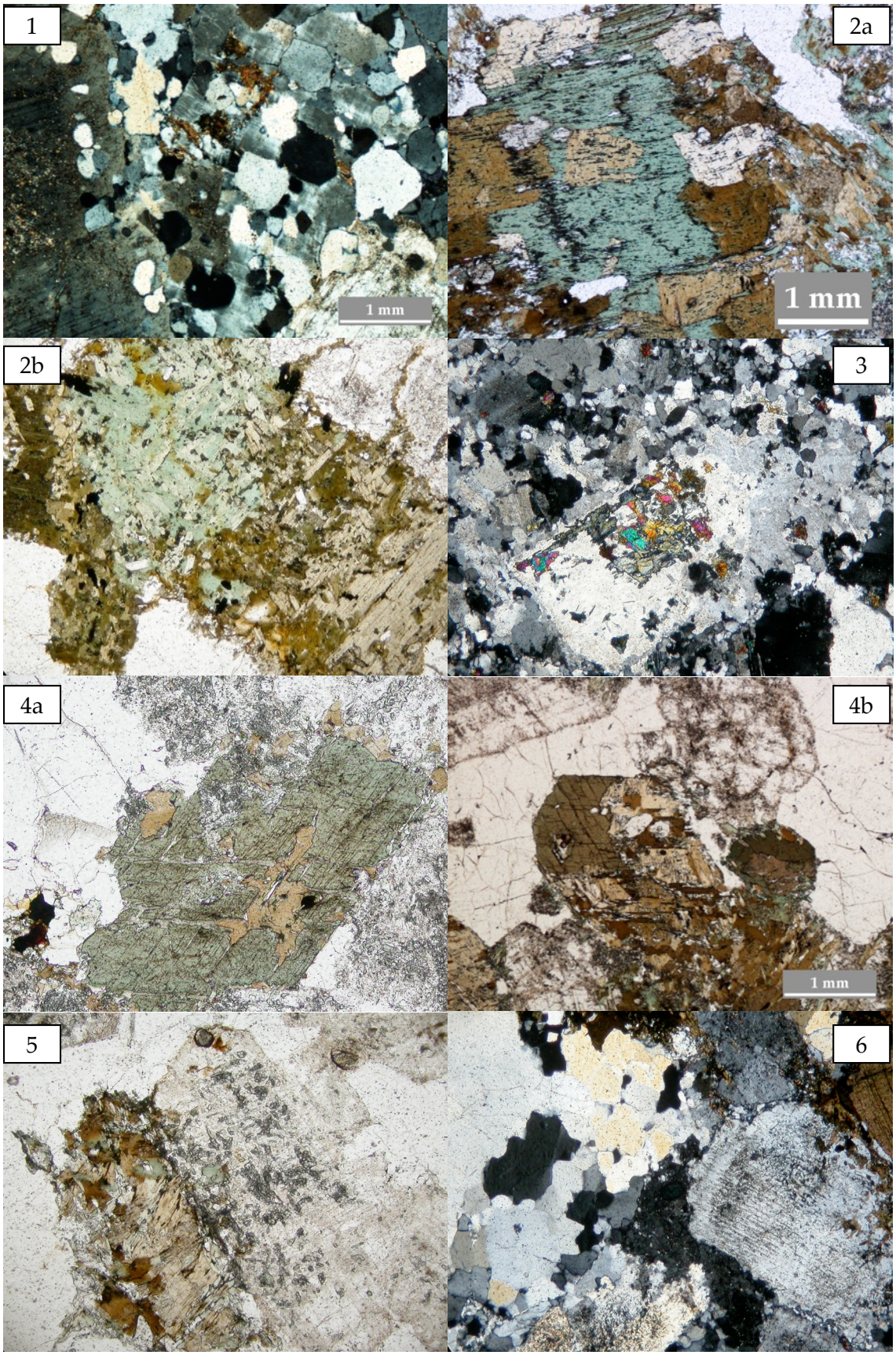
1
1 mm
2a
1 mm
2b
3
4a
4b
1 mm
5
6

Nr.	muestra	N-coord	E-coord	
7	JO03-110	7207443	1700946	Cristal de biotita y titanita (cristal rómbico) opaco de Rengård *Biotite and opaque titanite crystals in Rengård*
8	JO03-110	7207443	1700946	Anfíboles tipo hastingsita y tschermakita posdatan la biotita y anfíbol ígneos *Hastingsite and tschermakite amphiboles postdating igneous biotite and amphibole*
9	JO03-80	7214607	1704441	Detalle de la textura de tonalitas de Klockträsk granudas, anfíbol poiquilítico *Texture of Klockträsk tonalite, poikilitic amphibole*
10	JO03-81	7215099	1704252	Coexistencia entre chl y bi_2 sustituyendo a cristales de bi_1 y anfíbol ígneo (hornblenda) *Chl and bi_2 coexisting on altered igneous bi_1 and amphibole (hornblende)*
11	23J14	7224400	1690850	Porfirocristales de cuarzo y plagioclasa en textura milonítica ocelar *Porphyrocrystls of plagioclase and quartz. Ocelar milonite*
12	JO04-120	7227795	1707066	Bending de relicto biotita ígnea (bi_1) y microcristales de bi_2 en borde *Bending of biotite relict (bi_1) and bi_2 microcrystals in the rim*
13	JO03-106	7219452	1704349	Cuarzo con límites aserrados-dentados, recristalización dinámica *Quartz with serrated limits, dynamic recrystallization*
14	23K23	7222700	1703300	Recristalización de fenocristal de plagioclasa y flexión de cristales resultantes *Recrystallization of plagioclase and bending of the new formed crystals*

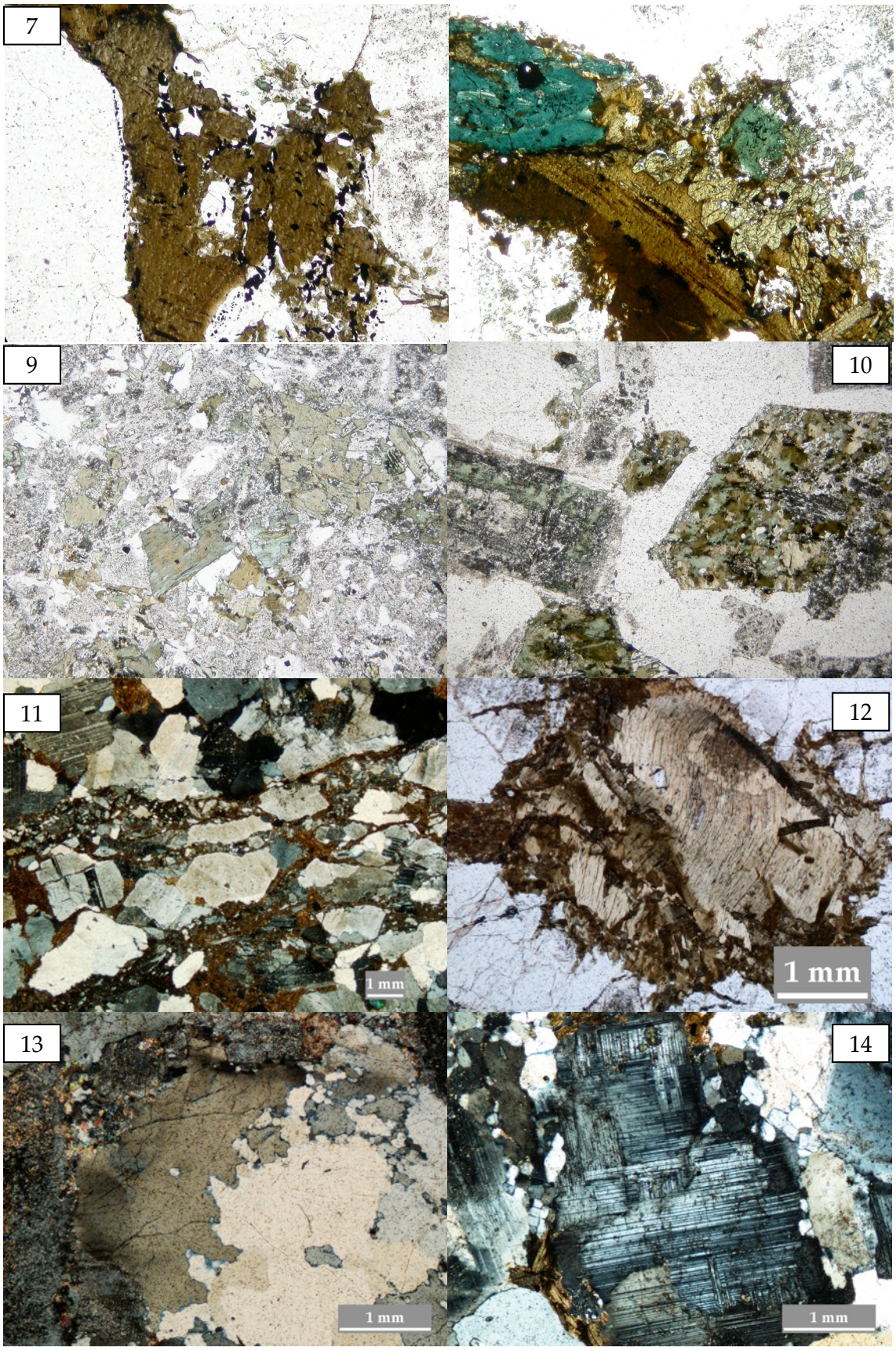
7
9
10
11
1 mm
12
1 mm
13
1 mm
14
1 mm

Nr.	muestra	N-coord	E-coord	
15	23J28	7226850	1682350	Plagioclasa albitizada en bordes y zonas internas, progradación según planos de exfoliación *Albitized plagioclase in rim and cores, progradation of alteration across cleavage*
16	JO03-61	7242310	1697050	Albitización de borde de plagioclasa con núcleo sericitizado. Ancho de foto 4 mm *Albitized rim and sericitized core of plagioclase. Picture 4 mm wide*
17a	JO03-35B	7219520	1696170	Sustitución de cristales de plagioclasa por epidota. Ancho de foto 4 mm *Plagioclase substitution by epidote. Picture 4 mm wide*
17b	23K10	7215300	1705350	Núcleos de plagioclasa alterados y sustituidos por clorita en textura decusada, borde albítico. Ancho de foto 2 mm *Decussated chlorite in core of altered plagioclase, albitized rim. Picture 2 mm wide*
18	JO03-114	7223676	1615670	Sustitución de núcleo de pl por sericita y epidota, borde albitizado. *Plagioclase core substitution by epidote and sericite, albitized rim*
19	JO03-94	7238203	1677930	Epidota sustituyendo parcialmente parte de cristal de pl, progradación a través del doble sistema de planos de exfoliación *Partially substitution of plagioclase by epidote, progradation of alteration across cleavage*

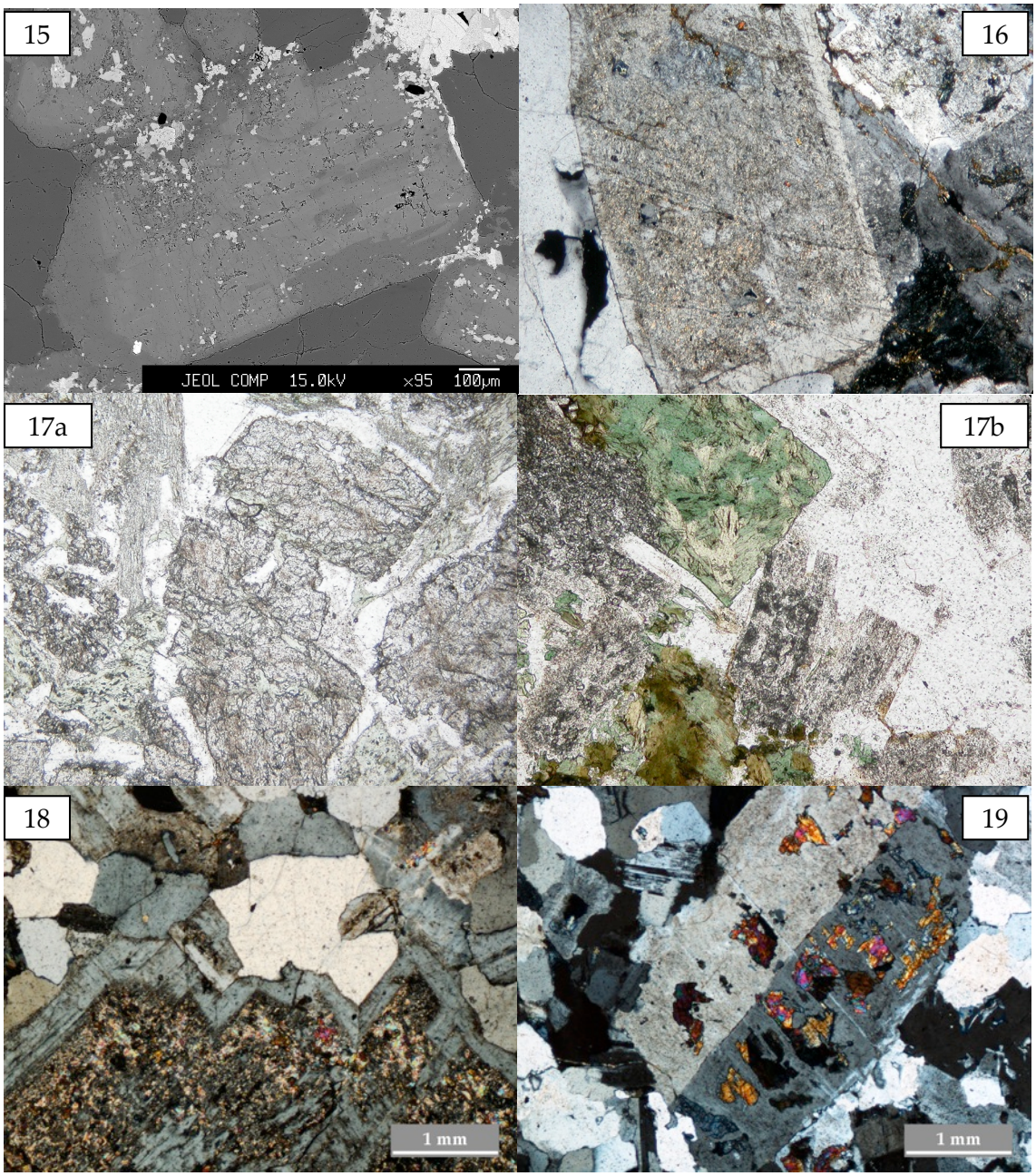
15
JEOL COMP 15.0kV ×95 100µm
16
17a
17b
18
1 mm
19
1 mm

Nr.	muestra	N-coord	E-coord	
20	JO03-79	7212420	1708590	Cristal aislado de epidota formado por alteración de pl y bi. Ancho de foto 2 mm *Epidote crystal from altered plagioclase and biotite. Picture 2 mm wide*
21	23J31	7227200	1688500	Cristales de epidota formados en contacto entre cristales de pl y bi. Ancho de foto 2 mm *Epidote crystals in pl-bi boundary. Picture 2 mm wide*
22	JO03-56	7225700	1682100	Banda de calcita y borde de clorita en contactos con minerales máficos. Ancho de foto 2 mm *Calcite vein with chlorite in the opaque alteration. Picture 2 mm wide*
23	JO03-29	7215600	1699360	Chl de grano muy fino y textura decusada rellenando huecos. Ancho de foto 4 mm *Fine grain decussated chlorite. Picture 4 mm wide*
24	JO04-128	7222353	1700381	Sustitución parcial de bi_1 por chl. Textura de sándwich de bi y chl *Partially substituted bi_1 by chl. Sandwich texture of bi and chl layers*
25	JO03-35B	7219520	1696170	Alteración clorítica de cristales de anfíbol. Textura decusada. Ancho de foto 2 mm *Amphibole altered to decussated chlorite. Picture 2 mm wide*

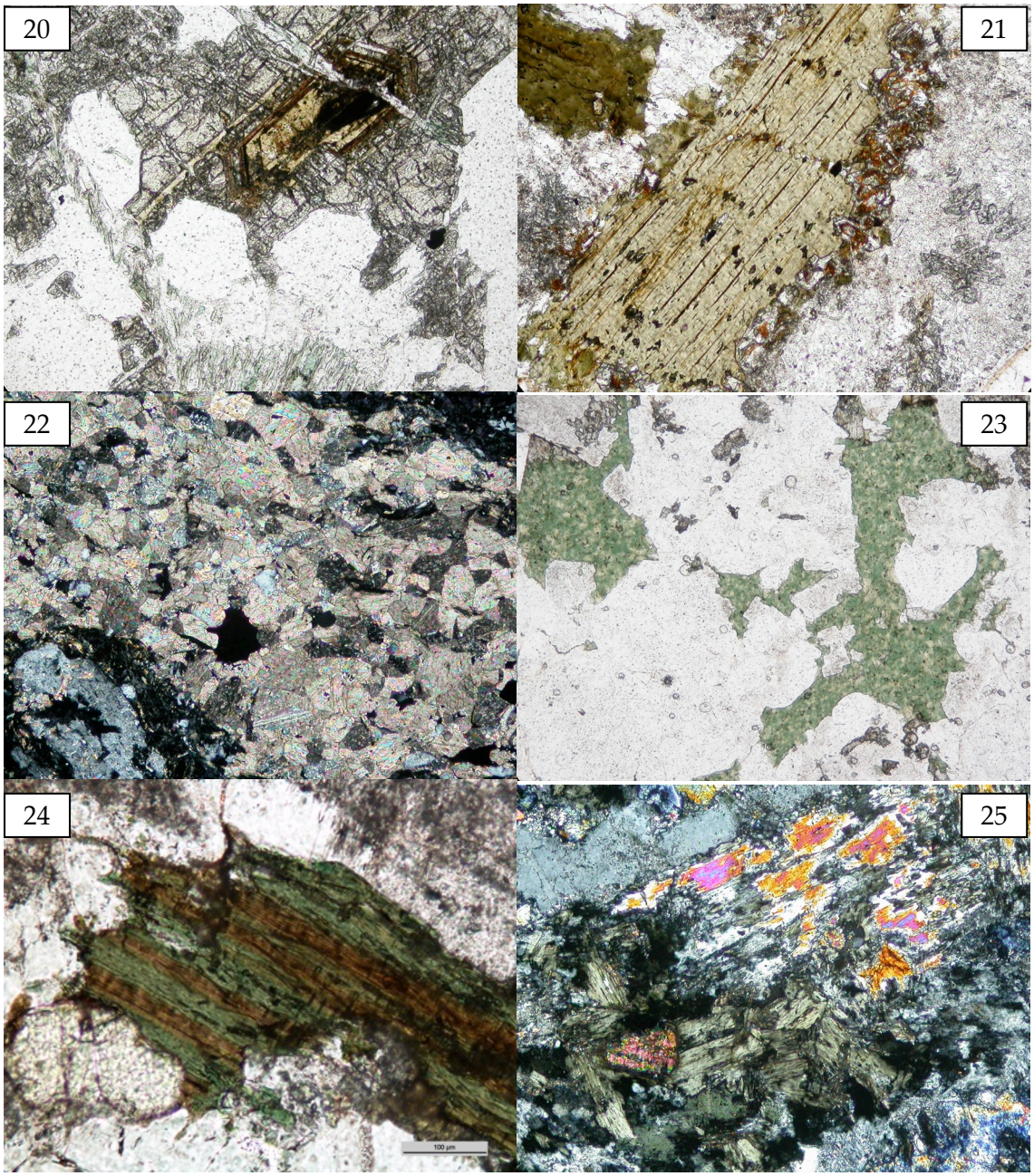
20
21
22
23
24
25

Nr.	muestra	N-coord	E-coord	
27	23J28	7226850	1682350	Generación de cuarzo y titanita por alteración de bi_1. Ocurrencia de bi_2. Ancho de foto 2 mm *Secondary quartz and titanite as bi_1 alteration products. Picture 2 mm wide*
28	JO04-135	7226363	1683510	Generación de bi_2 posdatando chl+tit y deformación que han afectado a bi_1 *Bi_2 postdating chl+tit and deformation on bi_1*
29	23K37	7226650	1701150	Biotita sustituida por cristales de bi_2 decusada y ep posdatando a bi_1 y tit *Biotite substituted by decussated bi_2 and epidote postdating bi_1 and tit*
30	JO03-109	7207839	1700777	Detalle de microcristales de biotita (bi_2) decusada *Decussated bi_2 detail*
31	JO04-120	7227795	1707066	Cristales de bi_2 en borde y zonas flexionadas de bi_1 *Crystals of bi_2 in rim and bended areas of bi_1*
32	JO04-100	7227773	1688105	Pseudomorfo de biotita sustituido por cristales de bi_2 decusada *Bi pseudomorph substituted by decussated bi_2*
33a	JO03-81	7215099	1704252	Orientación de tit y qz liberados por alteración de bi_1 diferente a bi_2 neoformada *Tit and quartz crystals oriented in bi_1 original cleavage and later bi_2*
33b	JO03-81	7215099	1704252	Idem a 73a con nicoles cruzados *73a crossed polars*

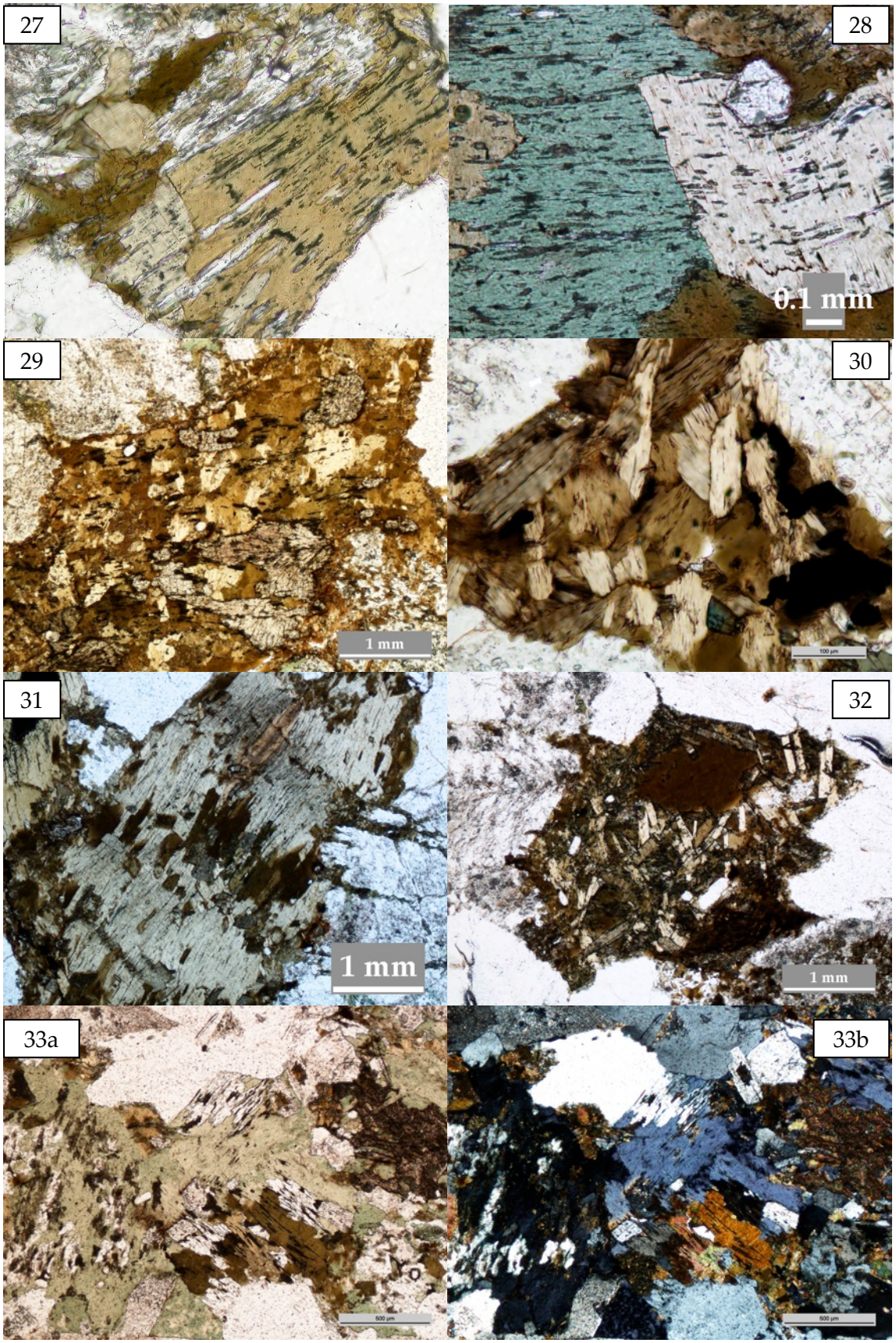
27
28
0.1 mm
29
1 mm
30
31
1 mm
32
1 mm
33a
33b

Nr.	muestra	N-coord	E-coord	
34	JO04-135	7226363	1683510	Bi_2 sustituyendo a anfíbol según orientación de planos de exfoliación *Bi_2 substituting amphibole in the cleavage system*
35	JO03-59	7242130	1697080	Fenocristales de anfíbol sustituidos por bi_2, óxidos y actinolita. Ancho de foto 4 mm *Amphibole phenocrystals substituted by bi_2, opaque and actinolite. Picture 4 mm wide*
36	JO03-109	7207839	1700777	Cristal de biotita y titanita (cristal rómbico) opaco de Rengård *Opaque titanite and biotite of Rengård*
37	JO03-109	7207839	1700777	Sustitución de fenocristal de anfíbol ígneo por $amph_1$ metamórfico en Rengård *Matrix and fragments of southern dike with igneous amphibole substituted by metamorphic $amph_1$*
38	JO03-110	7207443	1700946	Anfíbol metamórfico ($amph_2$) posdata a biotita ígnea en Rengård *Metamorphic amphibole ($amph_2$) postdating igneous biotite in Rengård*
39	JO04-124	7288502	1699776	Anfíbol metamórfico ($amph_2$) sin orientación cristalográfica preferente *Metamorphic amphibole ($amph_2$) not oriented in the matrix*
40	JO03-109	7207839	1700777	Esquina superior izquierda con $amph_3$ tipo pargasita *Pargasite type metamorphic amphibole ($amph_3$) in left upper corner*
41	JO04-84	7221590	1704013	Anfíbol metamórfico en la muestra de Nörd-Jörnsberget *Metamorphic amphibole in Nörd-Jörnsberget area*

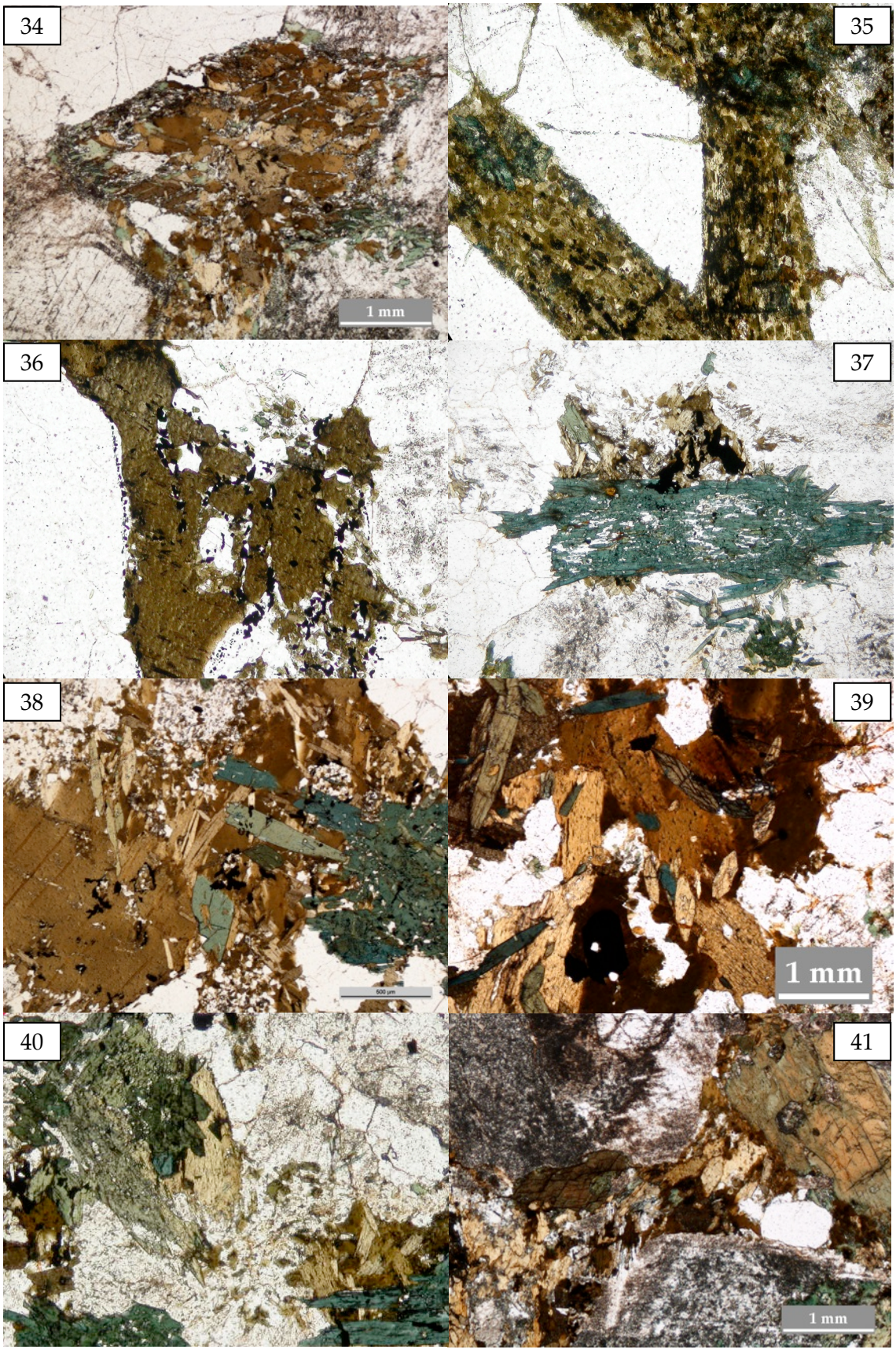
34
1 mm
35
36
37
38
500 µm
39
1 mm
40
41
1 mm

Nr.	muestra	N-coord	E-coord	
44	JO03-57	7222730	1700340	Clot de cristales de anfíboles comunes en las muestras de GIIa *Amphibole clots in GIIa*
45	JO04-28	7248891	1712439	Abundantes cristales de titanita asociados a los anfíboles característicos de GII *Characteristic titanite crystals in association with amphibole of GII*
46	JO04-34	7251600	1710192	Relicto de cpx uralitizado a anfíbol en las muestras de GIIb *Clinopyroxene relict uralitized to amphibole in GIIb*
47	JO04-147	7227111	1700632	A izquierda: enclave microgranudo de GII con mayor abundancia de máficos que roca huésped *(left) microgranular enclave of GII, abundant amphibole and biotite*
48	JO03-67	7252679	1698440	Detalle de borde de enclave microgranudo de GII, no existe textura de reacción o borde frío *Detail of microgranular enclave, no quenching or mineral reaction is observed*
49	Stop-45 2003	7227120	1700620	Afloramiento de GIIb intruyendo a GIIa, abundancia de enclaves microgranudos en GIIb y fragmentos de GIIa además de otras rocas máficas (diques) en la zona *GIIb-GIIa outcrop, GIIb hosting microgranular enclaves and mafic and GIIa xenoliths*
50a	JO04-34	7251600	1710192	Uralitización de cpx (augita) a amph (hornblenda) en GIIb *Cpx uralitized to hornblende in GIIb*
50b	JO04-147	7227111	1700632	Uralitización de cpx (augita) a amph (hornblenda) en enclave microgranudo de GIIb. *Cpx uralitized to hornblende in microgranular enclave of GIIb*

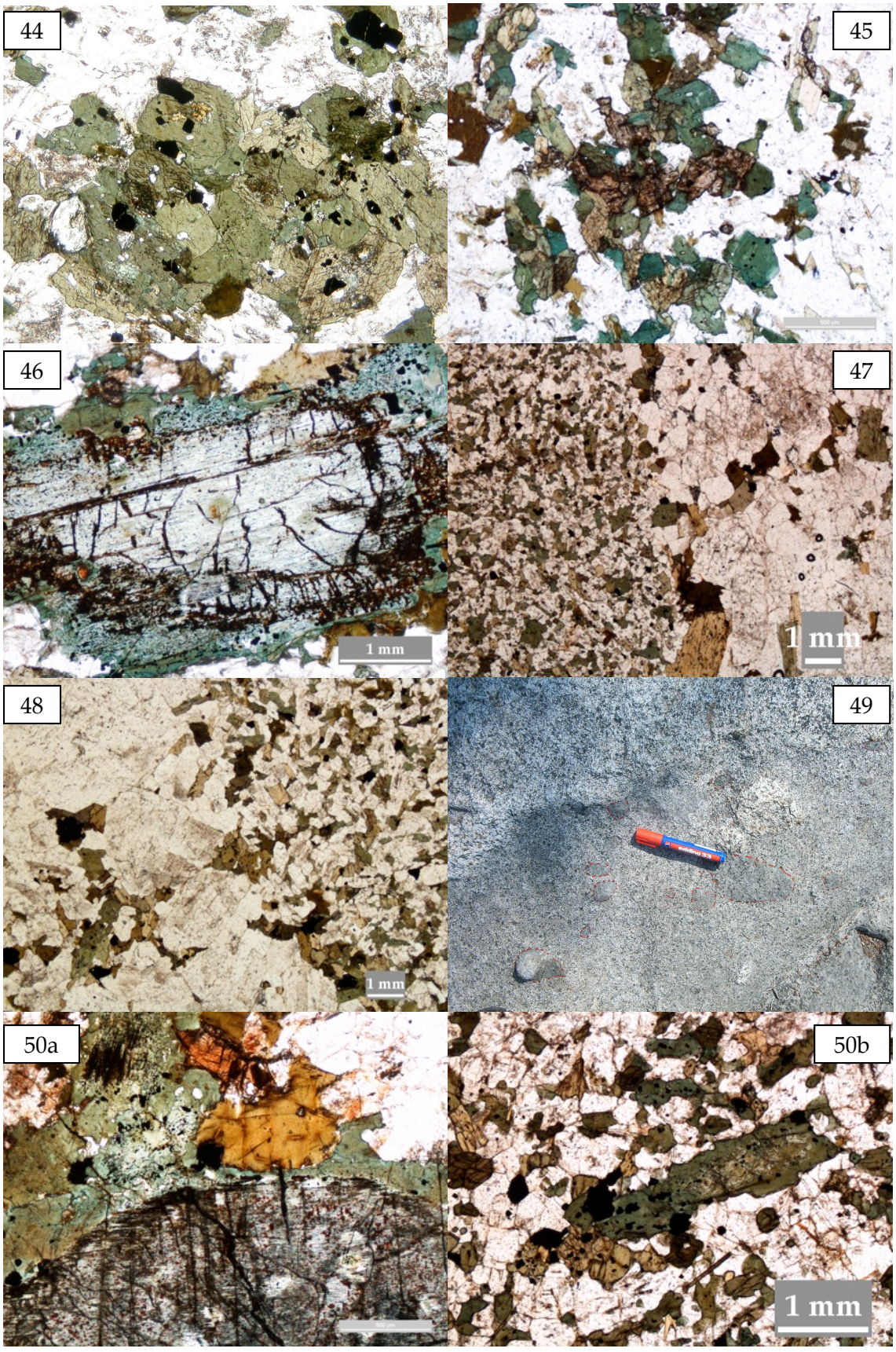
44
45
46
1 mm
47
1 mm
48
1 mm
49
50a
50b
1 mm

Nr.	muestra	N-coord	E-coord	
51	JO03-45	7238490	1704500	Pertitas características de los feldespatos de GIII, kfs de tallas mucho mayores a pl *GIII alkali feldspar pertite*
52	JO04-07	7244764	1707754	Textura general de las muestras de Hobergsliden, minerales máficos casi inexistentes *General view of Hobergsliden granite, mafic mineral absent*
53	23J58	7239300	1693900	Textura esqueletal de plagioclasa en kfs de la fase GIV, centro de JGC *Skeletal plagioclase in alkali feldspar in GIV, core of the JGC*
54	23J82	7250000	1697200	Cpx con exsoluciones de opx, cristales de opx parcialmente alterados. Ancho de foto 2 mm *Opx exsolutions on cpx, opx partially altered. Picture 2 mm wide*
55	JO03-51	7249830	1697230	Textura de reacción de magnetita con pl, borde de cpx alrededor de pl o en borde de pl en contacto con cristales de magnetita. Ancho de foto 2 mm *Reaction of magnetite with plagioclase, cpx rim in pl*
56	23J81	7249300	1697000	Cpx poiquilítico englobando cristales de pl. Ancho de foto 4 mm *Poikilitic cpx hosting plagioclase. Picture 4 mm wide*

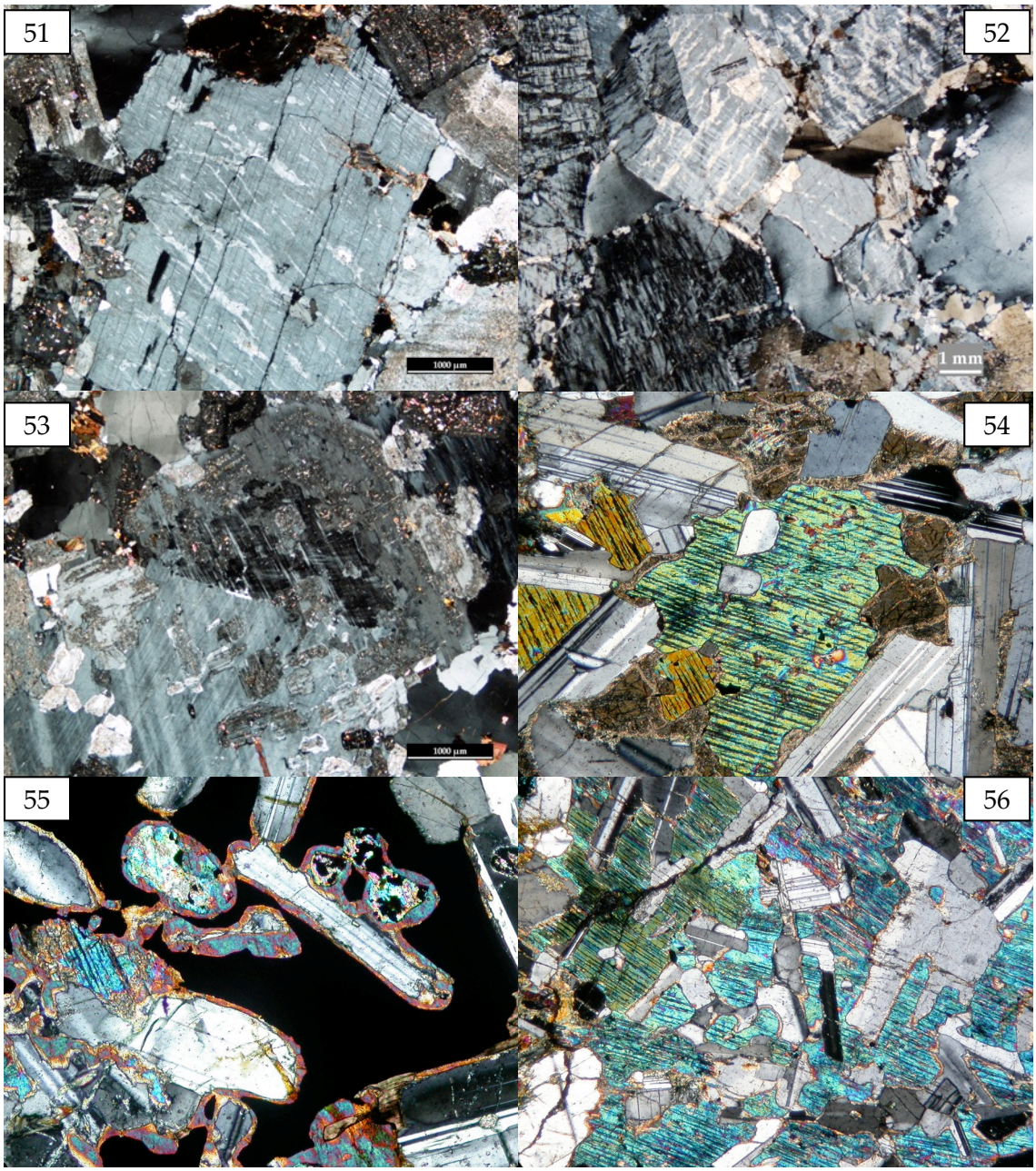
51
1000 µm
52
1 mm
53
1000 µm
54
55
56

Nr.	muestra	N-coord	E-coord	
57	JO03-69	7253132	1701681	Detalle de simplectitas de opx y olivino en gabronoritas olivínicas de Näsberget *Olivine-opx simplectite in olivine gabbronorite of Näsberget*
58	JO03-105	7219468	1704409	Ejemplo de textura ofítica de rocas máficas indiferenciadas en JGC. Ancho de foto 4 mm *Ofitic texture in the undifferentiated mafic of JGC. Picture 4 mm wide*
59	JO03-119	7233161	1711571	Ejemplo de textura poiquilítica de rocas máficas indiferenciadas en JGC. Ancho de foto 4 mm *Poikilitic texture in the undifferentiated mafic of JGC. Picture 4 mm wide*
60a	JO04-43	7256365	1701585	Texturas de matriz en basaltos andesíticos. Compuestas por cpx, pl y mt *Matrix in the porphyrytic andesite basalts. Cpx+pl+mt*
60b	JO04-44	7256500	1701259	Textura general en basaltos andesíticos porfídicos. Compuestas por cpx, pl y mt *General view of andesite basalts. Cpx+pl+mt*
61a	JO03-103B	7228954	1670724	Ejemplo de fenocristales de opx en basaltos andesíticos *Opx phenocrystals in the andesite basalts*
61b	JO03-93	7238430	1677933	Ejemplo de fenocristales de opx en basaltos andesíticos. Ancho de foto 4 mm *Opx phenocrystals in the andesite basalts. Picture 4 mm wide*
62	JO03-103B	7228954	1670724	Detalle de pl parcialmente alterada en basaltos andesíticos. Ancho de foto 2 mm *Partially altered plagioclase in andesite basalts. Picture 2 mm wide*

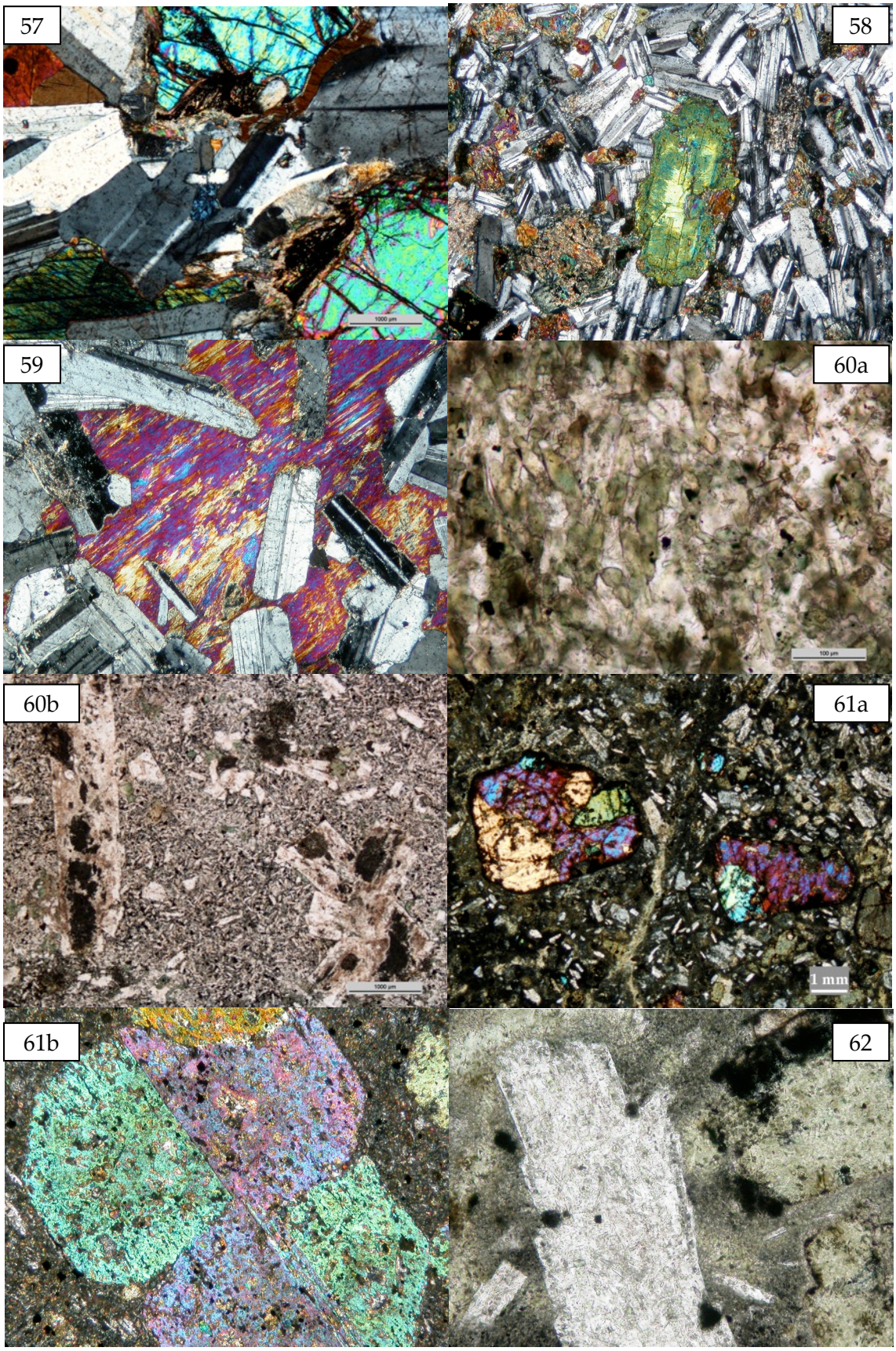
57
58
59
60a
60b
61a
1 mm
61b
62

Nr.	muestra	N-coord	E-coord	
63	JO03-07(f)	7219000	1691790	Detalle de contacto entre fragmento y matriz de brecha de basalto andesítico. Ancho de foto 4 mm *Fragment and matrix detail in the andesite basalt (breccia). Picture 4 mm wide*
64	JO03-07(f)	7219000	1691790	Fenocristales de piroxeno fuertemente alterados a chl y ep. Ancho de foto 2 mm *Pyroxene phenocrytals altered to chl and ep. Picture 2 mm wide*
65	JO03-07(m)	7219000	1691790	Detalle de matriz de basalto andesítico en zona foliada: pl, cpx, amph, ep, chl. Ancho de foto 2 mm *Foliation in the andesite basalt matrix: pl, cpx, amph, ep and chl. Picture 2 mm wide*
66	Stop-201 2003	7220170	1689718	Detalle de afloramiento de (auto?) brecha de los basaltos andesíticos Dique Sur de JGC *Outcrop of (auto?)breccia of andesite basalts, Southern dike of JGC*
67	JO03-124	7220170	1689718	Fenocristales máficos de Dique Sur estirados por la deformación. Ancho de foto 2 mm *Foliation of mafic phenocrystals of the southern dike. Picture 2 mm wide*
68	JO03-09	7219310	1690800	Matriz y fragmentos en Dique Sur con fenocristales poco deformados y alterados. Ancho de foto 4 mm *Matrix and fragments of southern dike with fenocrystals slightly altered and deformed*
69	Stop-268 2004	7213380	1698980	Detalle de afloramiento con fragmentos de GI englobados en Dique Sur, zona con intensa foliación *GI fragments in foliated southern dike andesite basalt, strongly deformed*
70	JO03-85	7231989	1674657	Biotita y amph con texturas radiales en monzonita junto a diseminado de mt. Ancho de foto 2 mm *Radial crystals of biotite and amphibole in monzonite of Gallejaur, mt dissemination. Picture 2 mm wide*


63
64
65
66
67
68
69
70

Nr.	muestra	N-coord	E-coord	
71	JO03-85	7231989	1674657	Bandas y diseminado de mt en monzonita, epidota y cpx. Ancho de foto 4 mm *Bands and dissemination of mt in the Gallejaur monzonite, ep and cpx. Picture 4 mm wide*
72	JO03-86	7234738	1674485	Simplectitas comunes en monzonita, fenocristales de plagioclasa. Ancho de foto 4 mm *Simplectite in the Gallejaur monzonite, plagioclase phenocrystals. Picture 4 mm wide*
73	Stop-139 2003	7234738	1674485	Afloramiento de monzonita de Gallejaur con multitud de enclaves microgranudos *Microgranular enclaves in the Gallejaur monzonite.*
74	VIC04-01	7220282	1637240	Bandeado metamórfico en tonalitas de VIC. Amph+bi frente pl+qz *Metamorphic bands of VIC hornblende tonalite. Amph+bi and pl+qz*
75	VIC04-01	7220282	1637240	Granoblastos de plagioclasa parcialmente rotados en banda leucocrática de tonalita de VIC *Plagioclase granoblast in leucocratic band of VIC hornblende tonalite*
76	VIC04-02	7228806	1632911	Detalle de textura general de trondhjemitas de VIC. Fenocristal de plagioclasa en el centro *VIC trondhjemite, plagioclase phenocrystal*
77	Stop-182 2004	7221125	1632953	Detalle de afloramiento de monte Viterliden con pliegues tipo chevron *Chevron folds in the Viterliden*
78	Stop-182 2004	7221125	1632953	Detalle de afloramiento de monte Viterliden con crenulación de pliegues y foliación *Foliation and crenulation of folds in Viterliden*

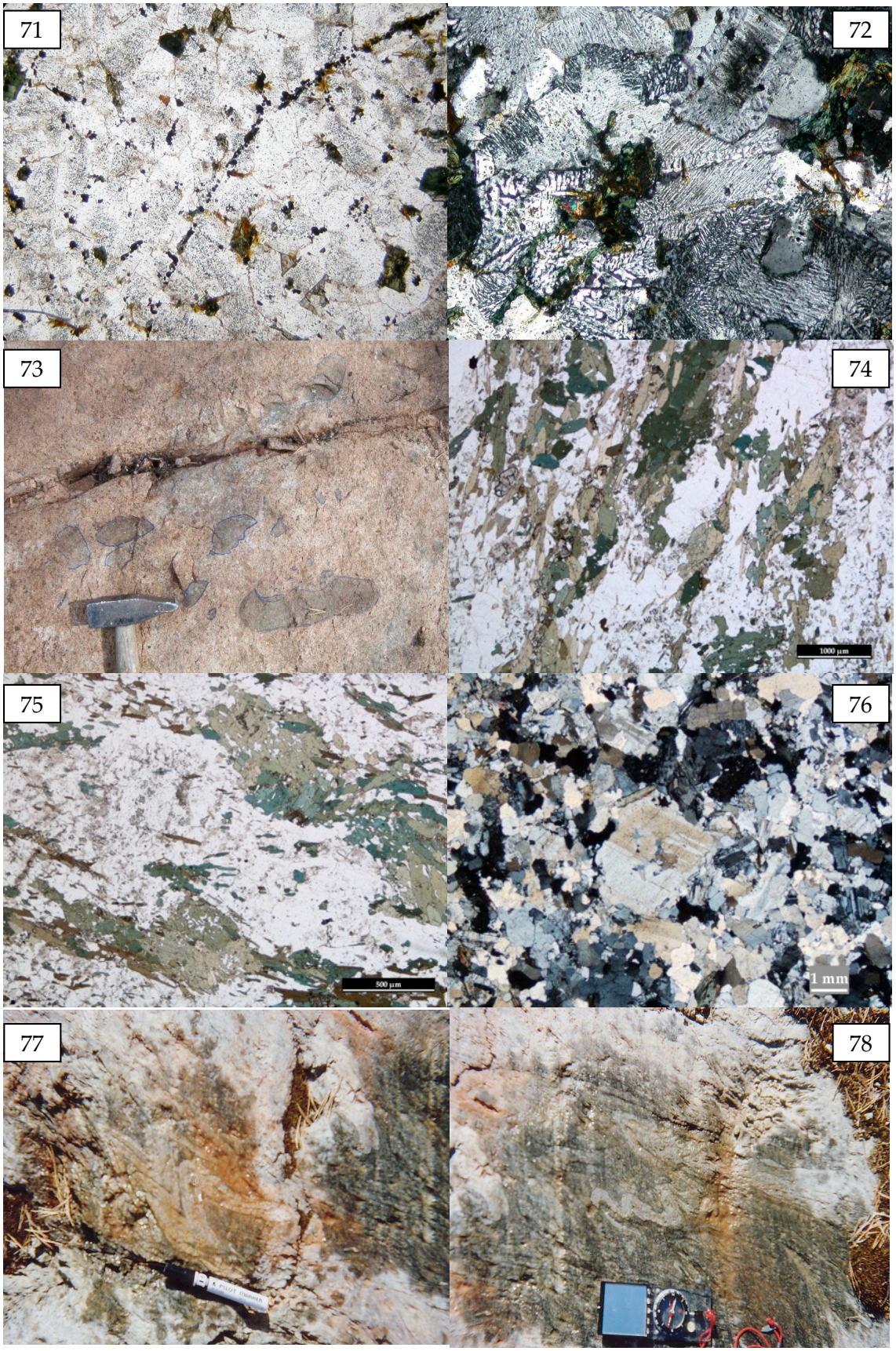
71
72
73
74
1000 µm
75
500 µm
76
1 mm
77
78

Nr.	muestra	N-coord	E-coord	
79	JO03-114	7223676	1715670	Porfiroblasto de anfíbol en tonalitas (cuarzo anfibolitas) de VIC. Ep+amph+bi metamórficos *Amphibole porphyroclast in VIC tonalite (quartz amphibolite). Ep+amph+bi*
80	VIC04-07	7220602	1633336	Inclusiones de biotita en bandas melanocráticas de amph + bi en cuarzo anfibolitas de VIC *Biotite inclusions in melanocratic bands of amph+bi in VIC quartz amphibolite*
81	VIC04-16	7214909	1634870	Textura general de roca metavolcánica con moscovita, bi, distena, cuarzo y cordierita *Metavolcanic rock with muscovite, bi, kyanite, quartz and cordierite*
82	Stop-142 2003	7205848	1706604	Detalle de enclave microganudo medio en granitos de Revsund *Microgranular enclave in the Revsund granite*
83	VIC04-12	7220270	1642477	Textura de granitos de Revsund en la zona de VIC, con dos micas (moscovita y biotita) *Revsund granite in the VIC are (two micas granite: muscovite and biotite)*
84	Stop-143 2003	7205530	1707226	Detalle de enclave microganudo de gran tamaño en granitos de Revsund *Microgranular enclave in Revsund granite*
85	Stop-147 2003	7206784	1705008	Zona de abundancia de enclaves microganudos y xenolitos en granitos de Revsund *Xenoliths and microgranular enclaves zone in the Revsund granite*
86	JO03-108	7208010	1700692	Cristal de andalucita (quiastolito) en roca metasedimentaria en zona de metamorfismo de contacto (Stavaträsk) *Andalusite (kyastolite) in metasedimentary contact aureole (Stavaträsk)*

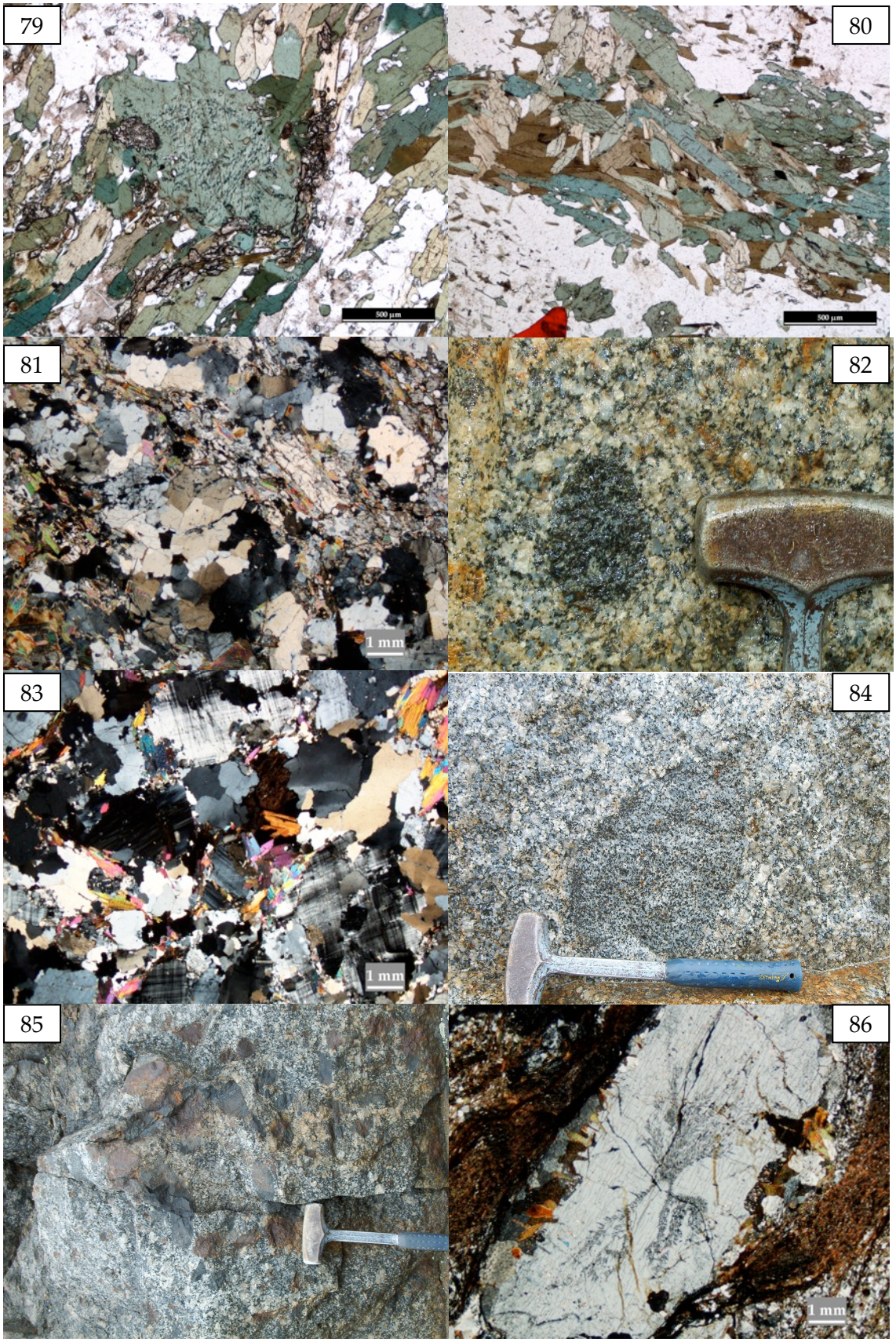
79
500 µm
80
500 µm
81
1 mm
82
83
1 mm
84
85
86
1 mm

ANEXO IX. FOTOS QUÍMICA MINERAL

MINERAL CHEMISTRY MICROPHOTOGRAPHS

Nr.	muestra/sample	N-coord	E-coord	
1	23J28	7226850	1682350	Ep: 1; chl: 2; bi: 3; tit: 4
2	23J28	7226850	1682350	Pl: 5-6
3	23J28	7226850	1682350	Bi: 11, 15; chl: 12; tit: 14; amph: 16
4	23J28	7226850	1682350	Amph: 17, bi: 18; chl: 19
5	23J29	7226600	1683400	Bi: 1-5
6	23J29	7226600	1683400	Bi: 6-8, 10; chl: 9
7	23J31	7227200	1688500	Bi: 1, 5; pl: 3, 6, 7, 9; ep: 2, 4
8	23J31	7227200	1688500	Chl: 11, 14; bi: 13, 15; pl: 16-18
9	23J84	7249500	1699200	Px: 1, 2; amph: 4, 5
10	23J84	7249500	1699200	Px: 14-16, 21; bi: 20
11	23K09	7215200	1704700	Bi: 1, 2, 4; amph: 3
12	23K09	7215200	1704700	Bi: 8
13	23K37	7226650	1701150	Bi: 5-7
14	23K37	7226650	1701150	Chl: 1; bi: 2, 6; ep: 3, 4
15	24K104	7255100	1702500	Bi: 10-12; amph: 13, 14; chl: 15, 16
16	24K104	7255100	1702500	Allanita: 23-28
17	JO03-35a	7219520	1696170	Bi: 8; ep: 9; chl: 10
18	JO03-35a	7219520	1696170	Bi: 18, 20; chl: 19; ep: 21
19	JO03-38B	7227120	1700620	Amph: 1-3; pl: 4, 5
20	JO03-38B	7227120	1700620	Amph: 8, 9; px: 6, 7, 10, 11
21	JO03-67	7227111	1700632	Amph: 1, 2; bi: 3; pl: 4, 5
22	JO03-67	7227111	1700632	Pl: 10, 11; bi: 12; amph: 13, 14
23	JO03-80	7214607	1704441	Bi: 1-4
24	JO03-80	7214607	1704441	Bi: 11; chl: 12; ep: 13
25	JO03-87	7234387	1683748	Bi: 1-6
26	JO03-87	7234387	1683748	Bi: 8-12
27	JO03-87	7234387	1683748	Bi: 4, 6; chl: 5
28	JO03-87	7234387	1683748	Bi: 9-11; chl: 12
29	JO03-103B	7228954	1670724	Px: 1-4
30	JO03-103B	7228954	1670724	Px: 5, 11: ep: 6; pl: 7-10
31	JO03-103B	7228954	1670724	Px: 15-19
32	JO03-103B	7228954	1670724	Px: 22-24
33	JO03-109	7207839	1700777	Bi: 8, 9; amph: 4-7, 10, 11
34	JO03-109	7207839	1700777	Amph: 26-28
35	JO03-109	7207839	1700777	Bi: 35, 36; amph: 33, 34
36	JO03-110	7207443	1700946	Amph: 5, 8; bi: 6, 7
37	JO03-110	7207443	1700946	Bi: 12; amph: 14; pl: 13
38	JO03-110	7207443	1700946	Amph: 15-17, 23, 26, 28; bi: 18-20, 24, 27; chl: 25
39	JO03-110	7207443	1700946	Idem 38
40	JO03-110	7207443	1700946	Bi: 34; amph: 35 (12, 14, 15 SEM-EDS)
41	JO03-45	7238490	1704500	Pl: 23, 24; kfs: 22; bi: 25
42	JO03-45	7238490	1704500	Bi: 26, 27, 29; chl: 28
43	JO03-58	7234200	1691900	Pl: 8-12
44	JO03-58	7234200	1691900	Pl: 16-20; kfs: 21
45	JO03-67	7227111	1700632	Px: 12, 13; amph: 14-21, 24, 25; pl: 22, 23; bi: 26
46	JO03-67	7227111	1700632	Bi: 39, 40, 47, 48; Amph: 41, 45, 50, 51, 55; pl: 44, 49, 52, 53, 56, 58
47	JO03-124	7220170	1689718	Bi: 2, 5; amph: 1, 3; chl: 4; pl: 6
48	JO03-124	7220170	1689718	Bi: 12; chl: 13; amph: 15
49	JO04-34	7251600	1710192	Px: 21, 23, 25, 30; amph: 22, 24, 26, 28; bi: 27, 29
50	JO04-34	7251600	1710192	Pl: 31-34, 36; amph: 35
51	JO04-42	7259346	1703097	Pl: 16-19, 21, 22; kfs: 23, 24
52	JO04-42	7259346	1703097	Amph: 31-34, 36, 39; bi: 35, 37, 38, 40
53	JO04-128	7222353	1700381	Bi: 107; chl: 106; pl: 102-104; kfs: 105
54	JO04-128	7222353	1700381	Pl: 132-135; amph: 123, 126, 127; bi: 129-131
55	JO04-75	7214030	1704438	Amph: 47-49; bi: 42, 44-46,
56	JO04-75	7214030	1704438	Pl: 58-64
57	JO04-86	7221615	1704600	Bi: 19, 21; ep: 18; pl: 16, 17
58	JO04-86	7221615	1704600	Bi: 24, 25, 29; amph: 23, 27, 28; ep: 26
59	JO04-86	7221615	1704600	Idem 58
60	JO04-86	7221615	1704600	Bi: 31, 33, 37; amph: 32, 34-36, 38
61	JO04-110	7244382	1689602	Pl: 74-77; amph: 73; bi: 65-69, 71, 72,
62	JO04-110	7244382	1689602	Bi: 94; pl: 89-91; kfs: 92
63	VIC04-11	7221260	1631550	Pl: 5-10; chl: 1, 4; bi: 2, 3, 11
64	VIC04-11	7221260	1631550	Bi: 12, 14, 19; chl: 13; pl: 15-17, 20
65	23J58	7239300	1693900	Kfs: 25, 26; pl: 23, 24
66	23J58	7239300	1693900	Bi: 29; pl: 27, 28; kfs: 30
67	23J58	7239300	1693900	Bi: 31-34; apt: 35, 36
68	VIC04-01	7220282	1637240	Amph: 2, 8, 10; bi: 3, 7, 9; pl: 4, 5
69	VIC04-01	7220282	1637240	Amph: 15; pl: 11-14, 16-18
70	VIC04-01	7220282	1637240	Amph: 20-25, 28; bi: 26, 27
71	VIC04-07	7220602	1633336	Amph: 33-36; bi: 37
72	VIC04-07	7220602	1633336	Amph: 38, 40, 42, 44; bi: 39, 43, 45, 46; chl: 41

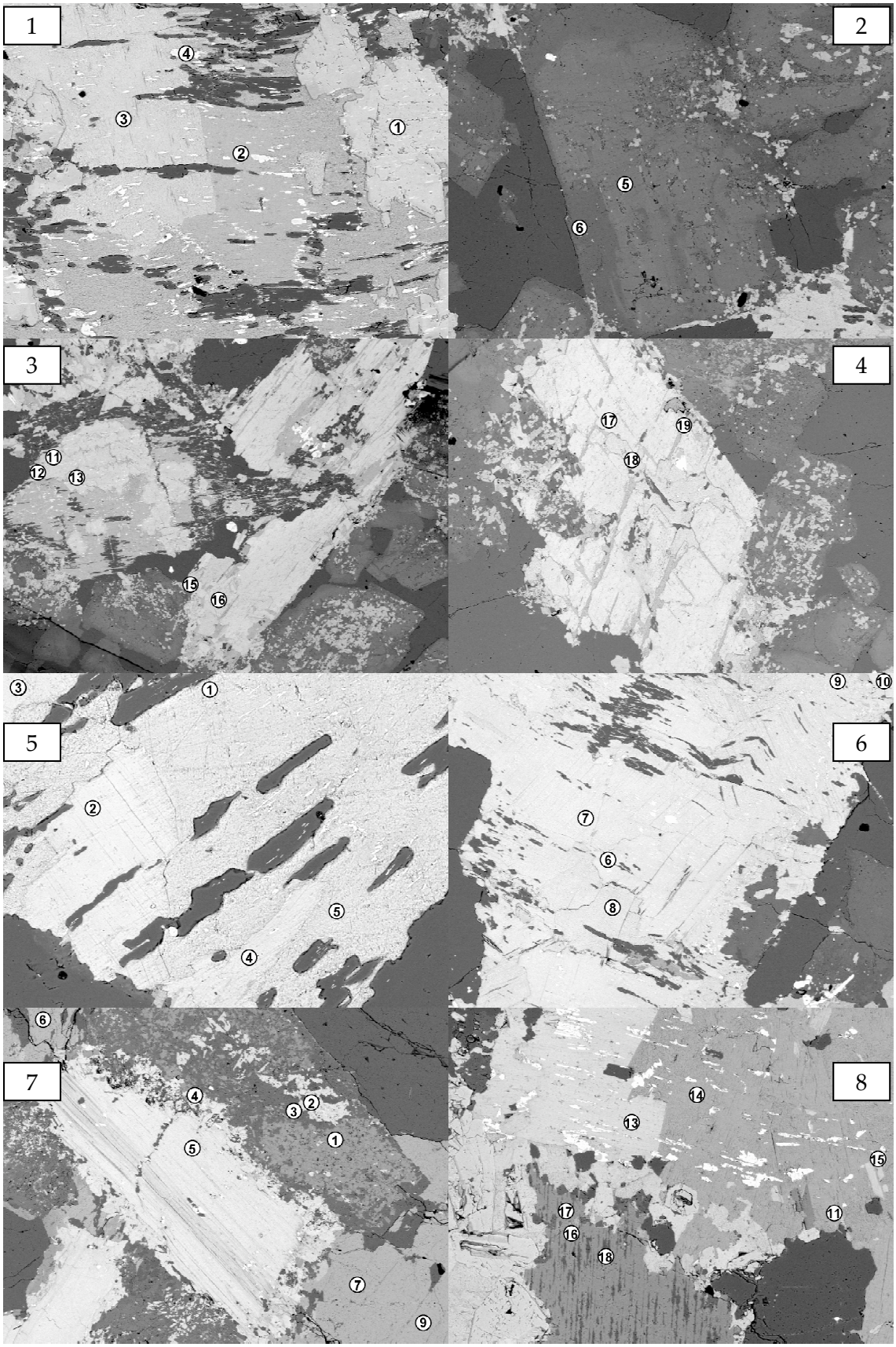
1
2
3
4
5
6
7
8

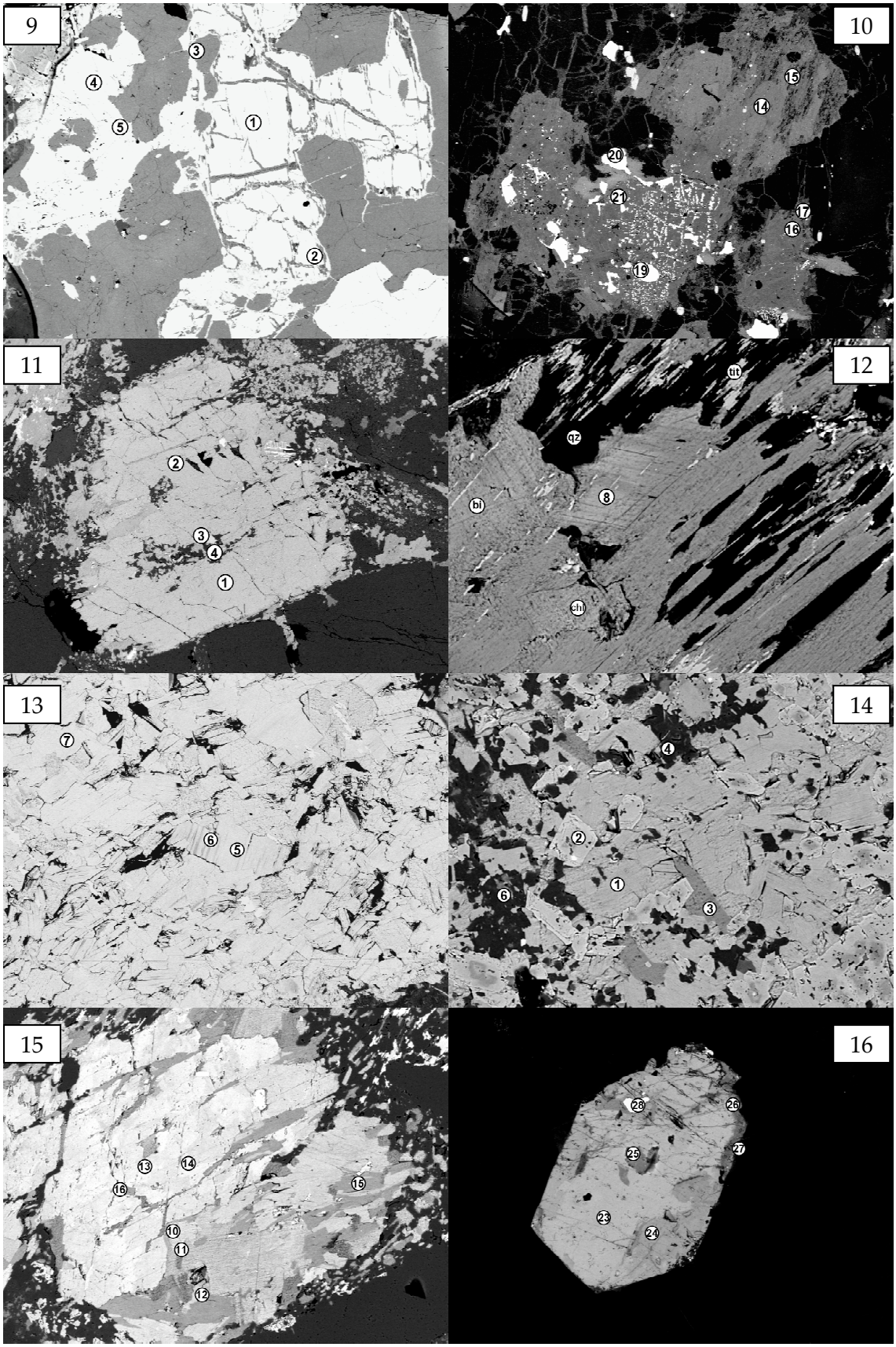
9
3
4
5
1
2
10
15
14
20
21
17
16
19
11
2
3
4
1
12
tit
qz
bi
8
chl
13
7
6
5
14
4
2
1
6
3
15
13
14
16
15
10
11
12
16
28
26
25
27
23
24

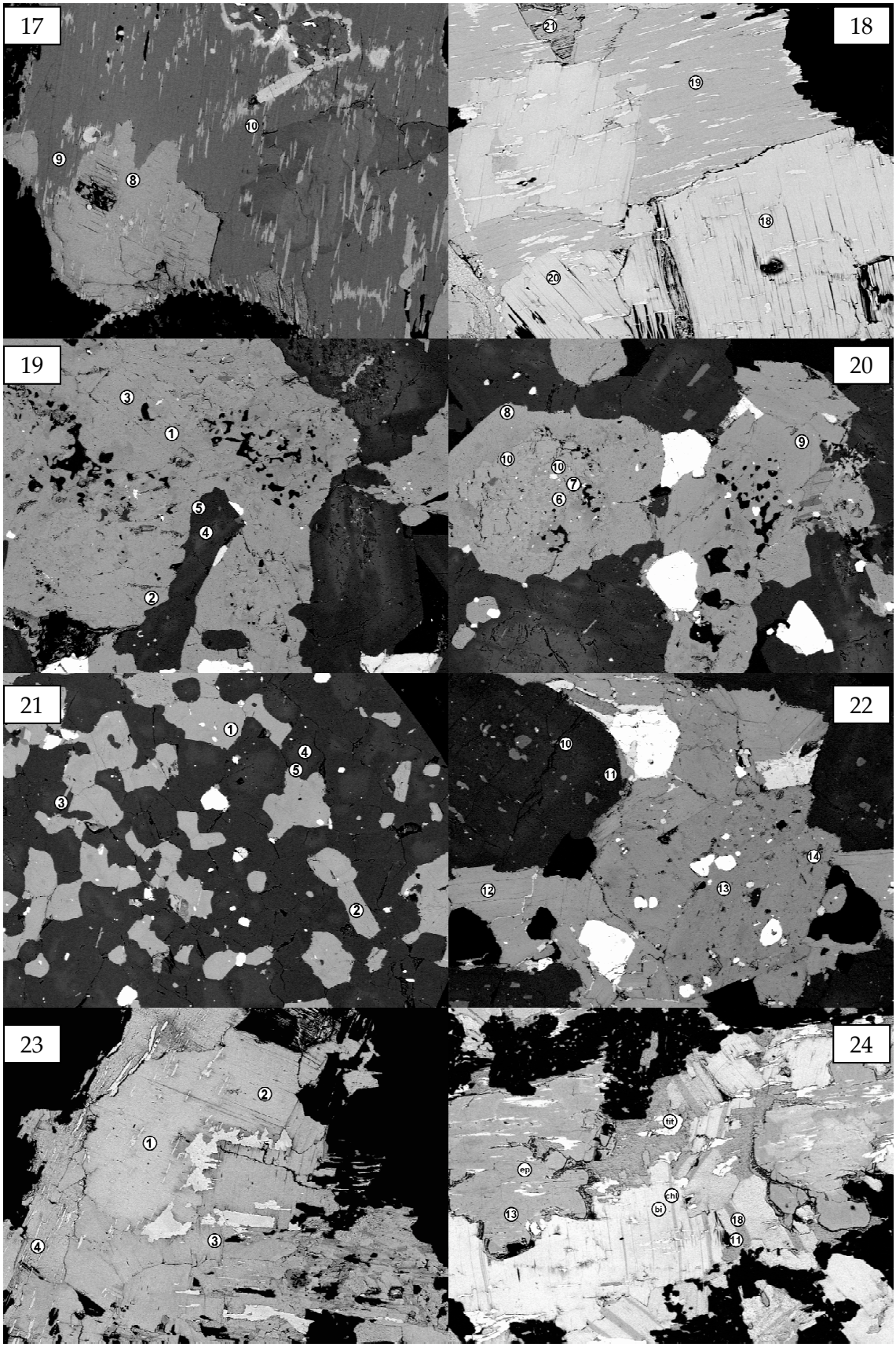
17
10
9
8
18
21
19
18
20
19
3
1
5
4
2
20
8
9
10
10
7
6
21
1
4
5
3
2
22
10
11
14
12
13
23
2
1
4
3
24
wt
ep
chl
bi
13
18
11

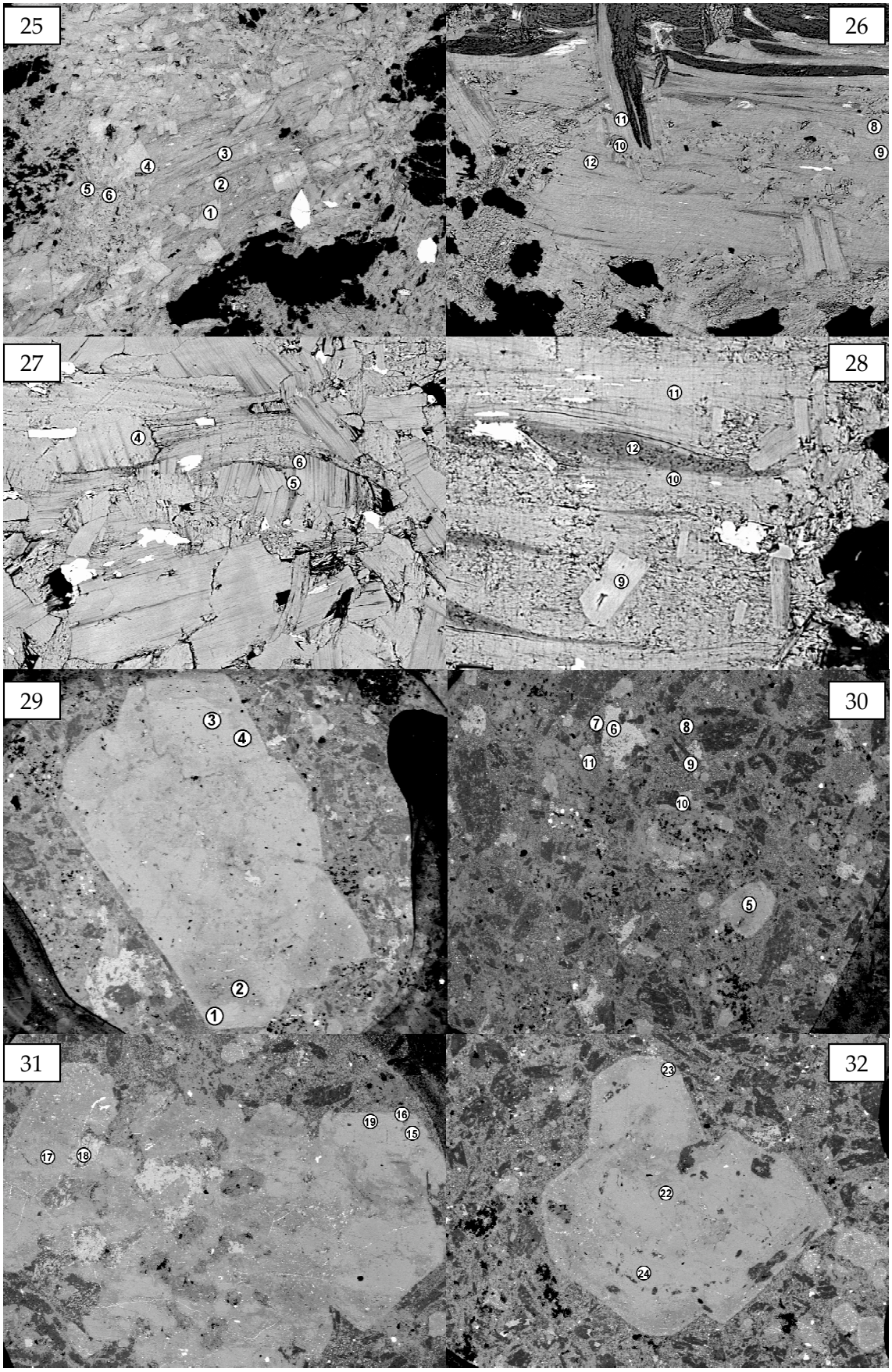
25
26
27
28
29
30
31
32

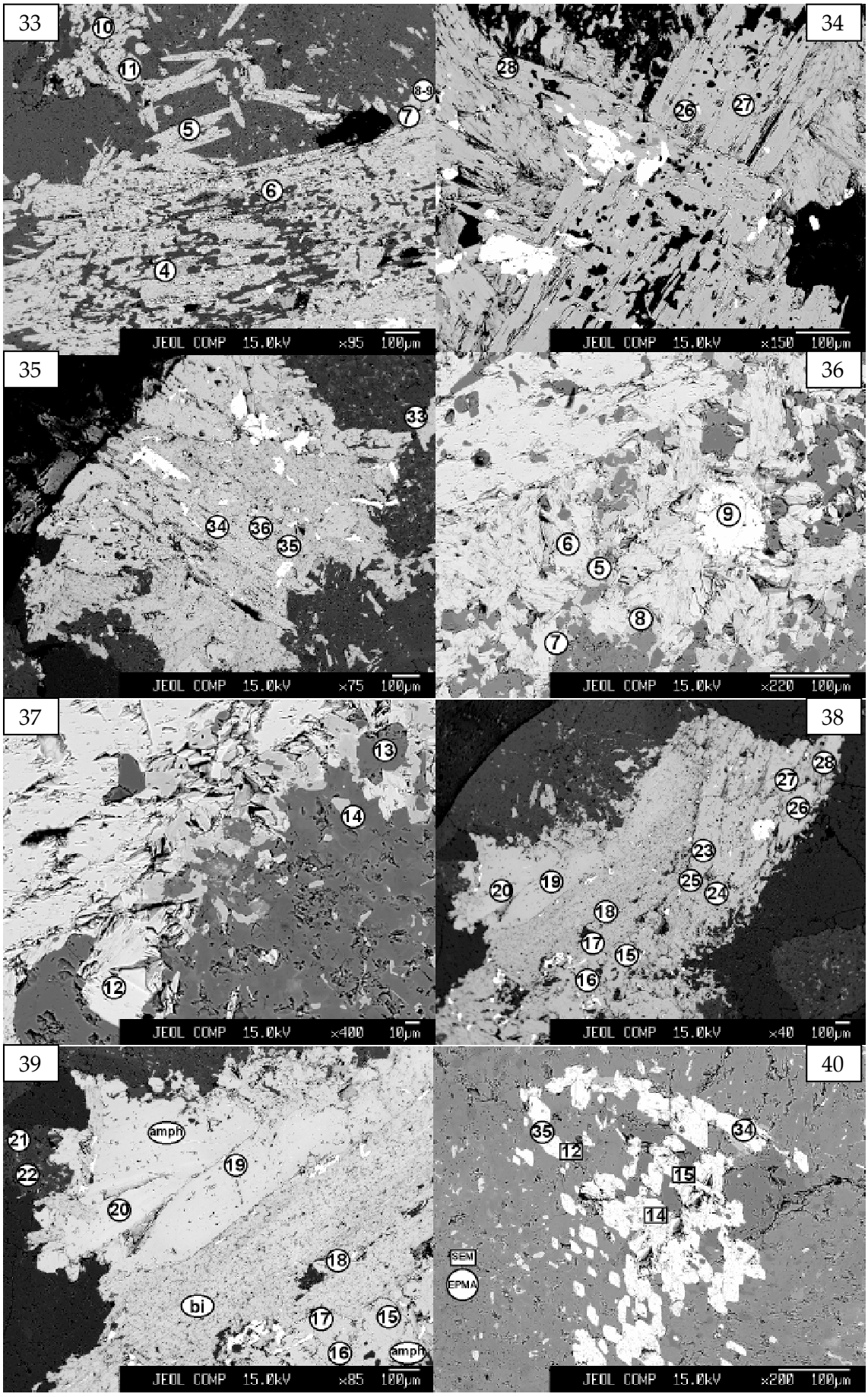
33
10
11
8-9
7
5
6
4
JEOL COMP 15.0kV ×95 100μm
34
28
26
27
JEOL COMP 15.0kV ×150 100μm
35
33
34
36
35
JEOL COMP 15.0kV ×75 100μm
36
9
6
5
8
7
JEOL COMP 15.0kV ×220 100μm
37
13
14
12
JEOL COMP 15.0kV ×400 10μm
38
28
27
26
23
20
19
25
24
18
17
15
16
JEOL COMP 15.0kV ×40 100μm
39
amph
21
22
19
20
18
bi
17
15
16
amph
JEOL COMP 15.0kV ×85 100μm
40
35
34
12
15
14
SEM
EPMA
JEOL COMP 15.0kV ×200 100μm

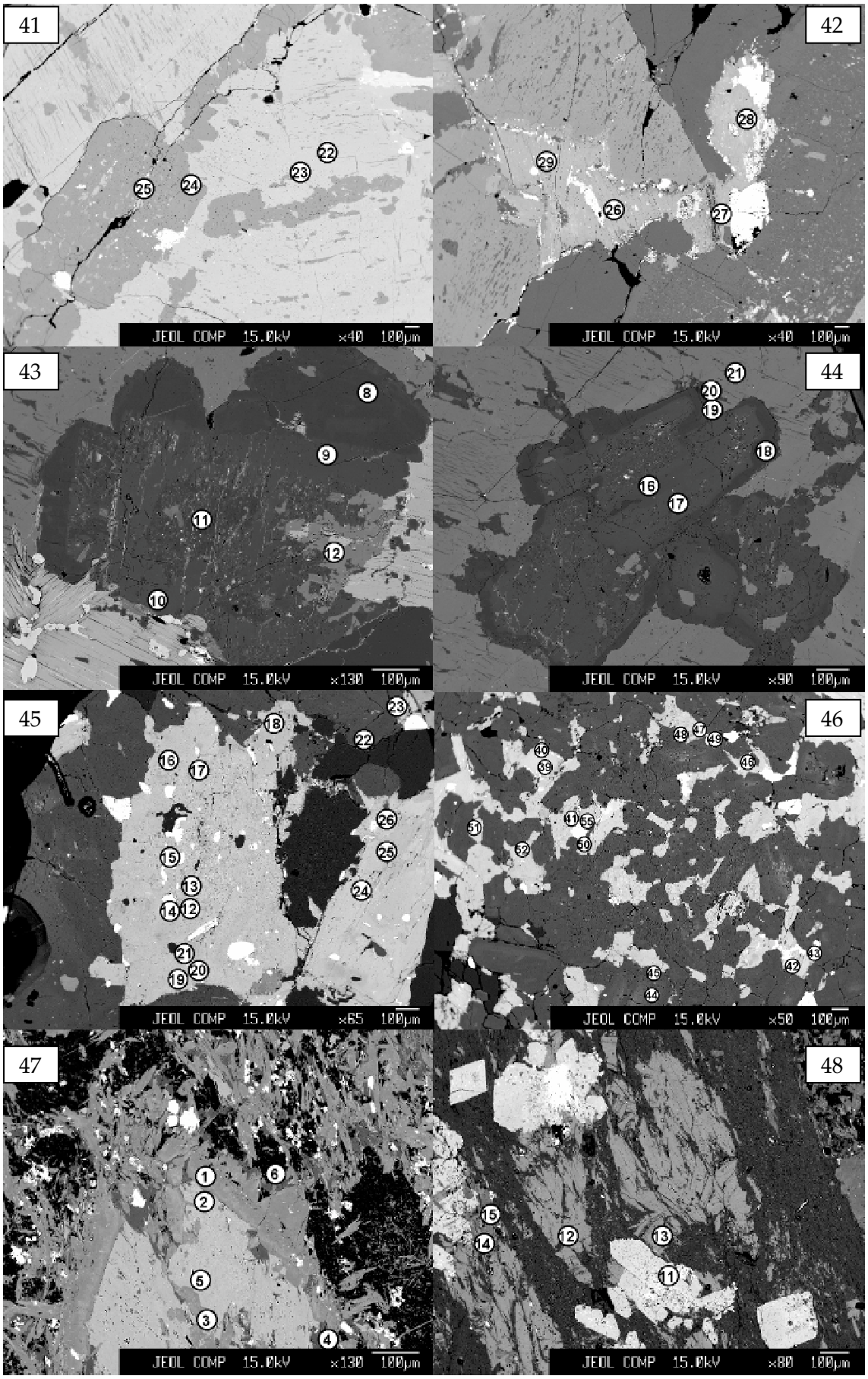
41
JEOL COMP 15.0kV ×40 100μm
42
JEOL COMP 15.0kV ×40 100μm
43
JEOL COMP 15.0kV ×130 100μm
44
JEOL COMP 15.0kV ×90 100μm
45
JEOL COMP 15.0kV ×65 100μm
46
JEOL COMP 15.0kV ×50 100μm
47
JEOL COMP 15.0kV ×130 100μm
48
JEOL COMP 15.0kV ×80 100μm

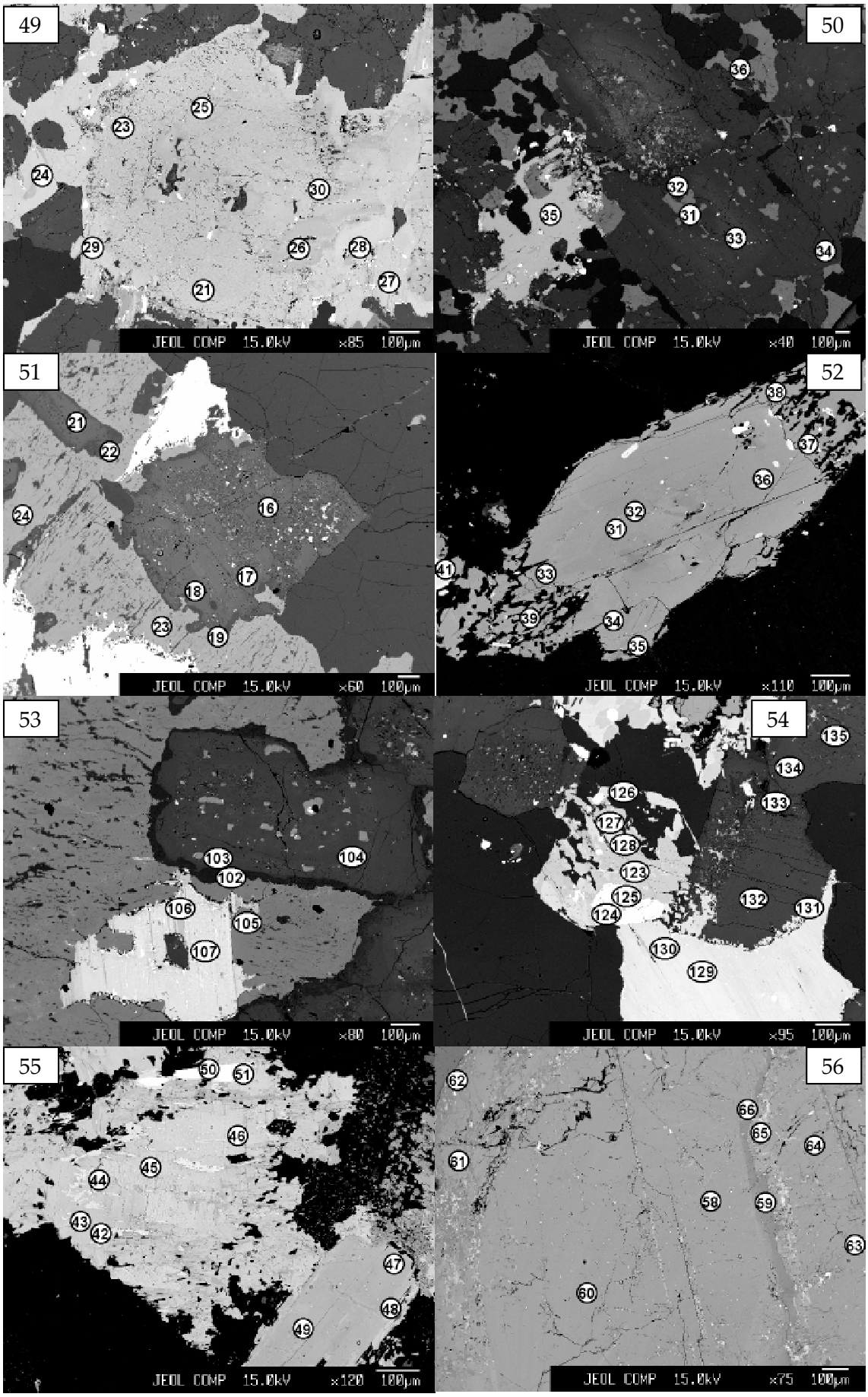
49
25
23
24
30
29
26
28
27
21
JEOL COMP 15.0kV ×85 100μm
50
36
32
35
31
33
34
JEOL COMP 15.0kV ×40 100μm
51
21
22
24
16
17
18
23
19
JEOL COMP 15.0kV ×60 100μm
52
38
37
36
32
31
41
33
39
34
35
JEOL COMP 15.0kV ×110 100μm
53
103
104
102
106
105
107
JEOL COMP 15.0kV ×80 100μm
54
135
134
126
133
127
128
123
125
132
131
124
130
129
JEOL COMP 15.0kV ×95 100μm
55
50
51
46
45
44
43
42
47
48
49
JEOL COMP 15.0kV ×120 100μm
56
62
66
65
64
61
58
59
63
60
JEOL COMP 15.0kV ×75 100μm

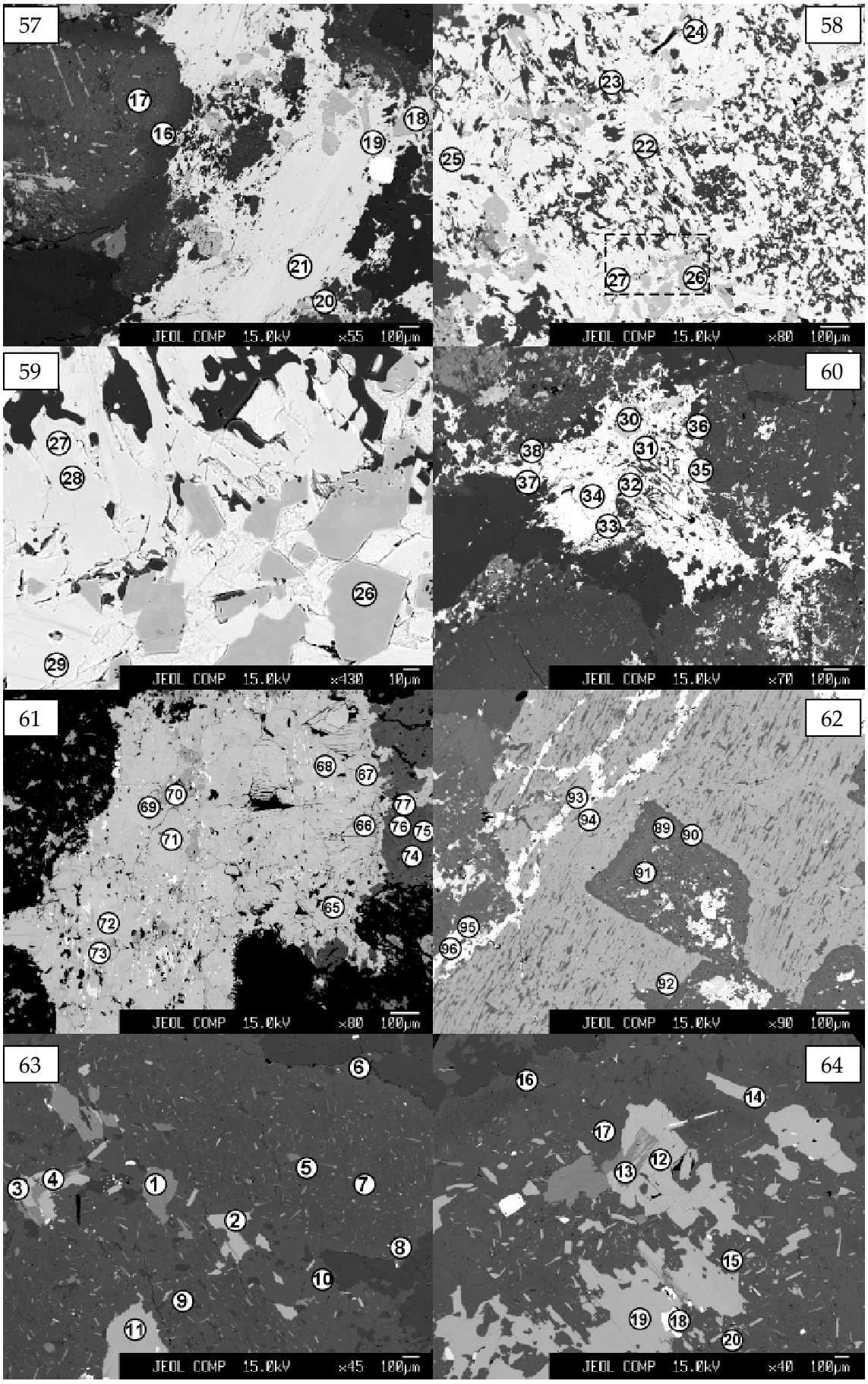
57
17
16
18
19
21
20
JEOL COMP 15.0kV ×55 100μm
58
24
23
22
25
27
26
JEOL COMP 15.0kV ×80 100μm
59
27
28
26
29
JEOL COMP 15.0kV ×130 10μm
60
30
36
38
31
35
37
34
32
33
JEOL COMP 15.0kV ×70 100μm
61
68
67
70
69
77
66
76
75
71
74
65
72
73
JEOL COMP 15.0kV ×80 100μm
62
93
94
89
90
91
95
96
92
JEOL COMP 15.0kV ×90 100μm
63
6
5
7
3
4
1
2
8
10
9
11
JEOL COMP 15.0kV ×45 100μm
64
16
14
17
12
13
15
19
18
20
JEOL COMP 15.0kV ×40 100μm

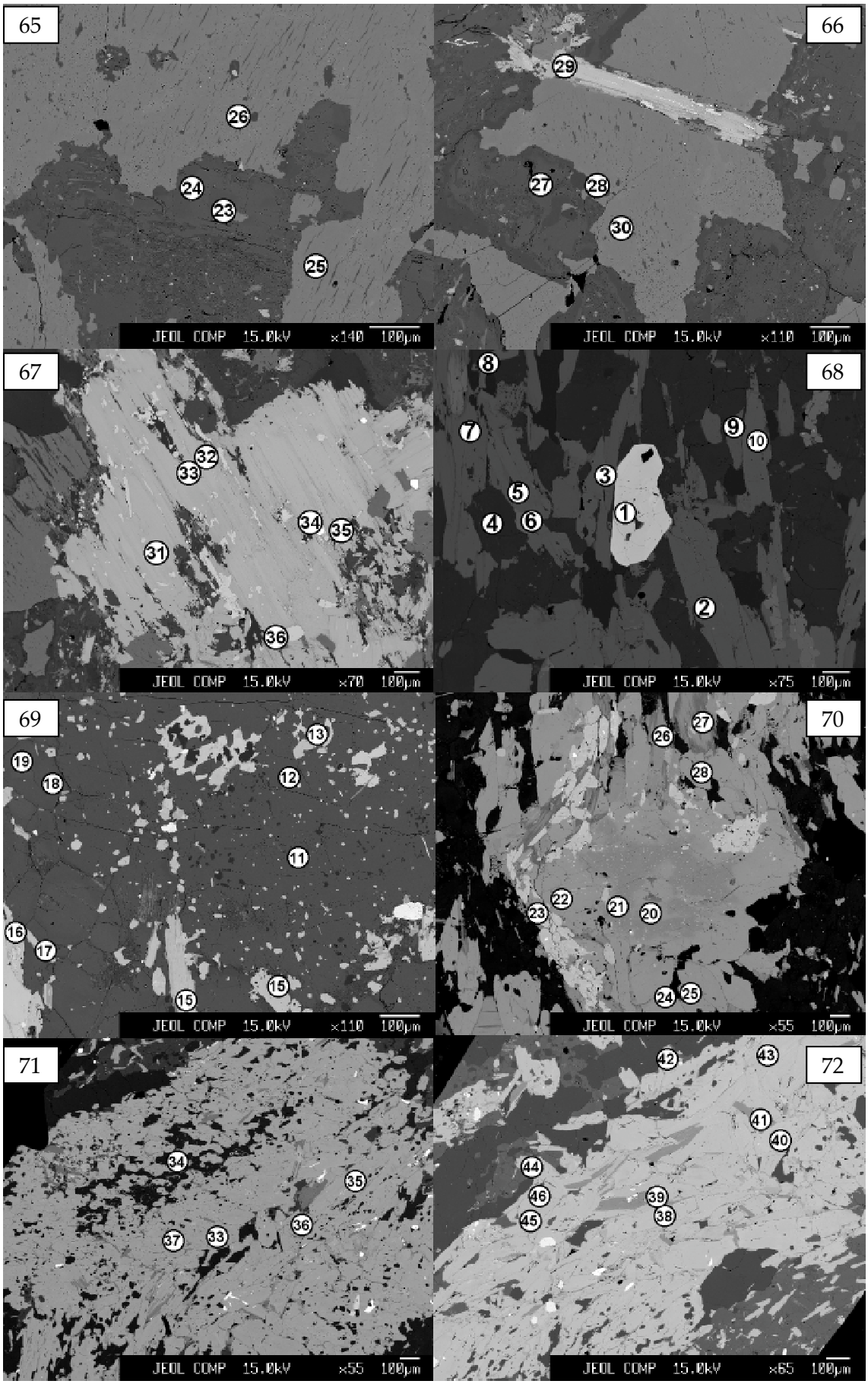
65
26
24
23
25
JEOL COMP 15.0kV ×140 100μm
66
29
27
28
30
JEOL COMP 15.0kV ×110 100μm
67
32
33
34
35
31
36
JEOL COMP 15.0kV ×70 100μm
68
8
7
9
10
3
5
1
4
6
2
JEOL COMP 15.0kV ×75 100μm
69
13
19
18
12
11
16
17
15
15
JEOL COMP 15.0kV ×110 100μm
70
27
26
28
22
23
21
20
24
25
JEOL COMP 15.0kV ×55 100μm
71
34
35
36
37
33
JEOL COMP 15.0kV ×55 100μm
72
42
43
41
40
44
46
45
39
38
JEOL COMP 15.0kV ×65 100μm

ANEXO X. MAPAS GEOLÓGICOS
GEOLOGICAL MAPS

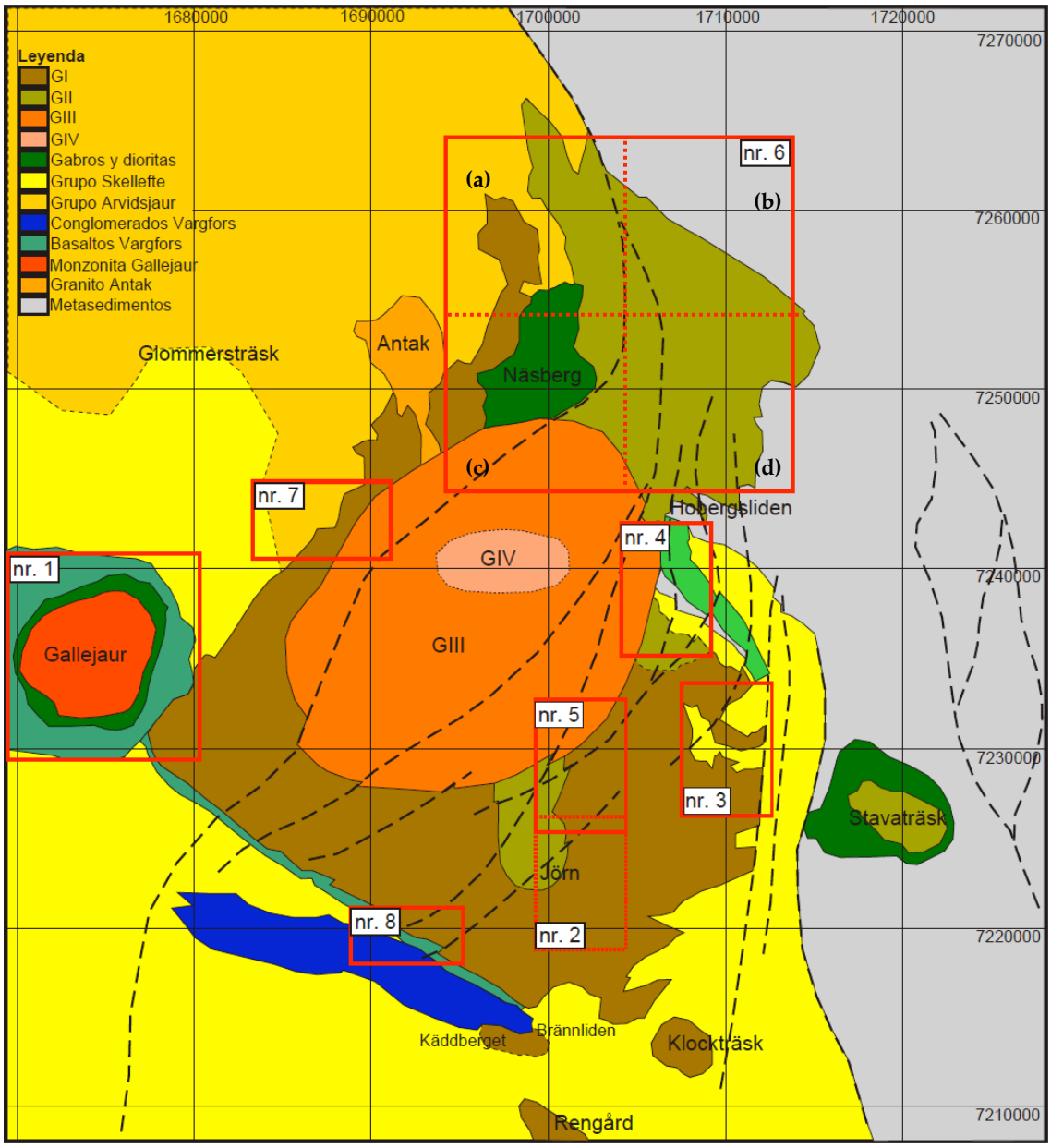

Mapa geológico regional de JGC con la localización de los mapas de detalle. En negro las descripciones de muestras y afloramientos de 2003, en rojo las de 2004.

Regional Geological Map of JGC with the location of the detailed maps. Labeled in black descriptions of samples and outcrops of 2003; in red samples of 2004 fieldwork.
Leyenda: Legend
Gabros y dioritas: Gabbros and diorites
Grupo Skellefte: Skellefte Group
Grupo Arvidsjaur: Arvidsjaur Group
Conglomerados Vargfors: Vargfors conglomerate
Basaltos Vargfors: Vargfors basalts
Monzonita Gallejaur: Gallejaur monzonite
Granito Antak: Antak granite
Metasedimentos: Metasediments

Nr. 1: Gallejaur

5 agosto de 2003, Stop 119-120:
119: afloramiento de tonalitas tipo GI de grano medio
120: GI intruido por dique de basalto porfídico con orientación N130E. Muestra JO03-71.

6 de agosto de 2003, Stop 121-130:
121: basalto porfídico con fenocristales de piroxeno y algo de plagioclasa, zonas brecificadas (autobrecha?) con cantos de 1-10 cm de la misma litología que la matriz.
122: ídem a 121 brechificado.
123: tonalita GI moderadamente alterada (plagioclasa a epidota)
124: serie de pequeños afloramientos de tonalita de GI, numerosas zonas afectadas por venas (ricas en clorita?), foliación con orientación N130E/85S.
125: tonalita GI de grano medio muy alterada y afectada por dique de pórfido de cuarzo de grano medio, intensa foliación N110E/80N.
126: tonalita GI con textura cuarzo porfídica de grano medio. Muestra JO03-72.
127: dique máfico sobre tonalita GI, orientación de dique en N15E/70E. Muestra JO03-73.
128: tonalita cuarzo porfídica de grano medio tipo GI, moderada deformación en matriz. Dique máfico N50E. Muestra de tonalita JO03-74.
129: Tonalita GI intruye a roca félsica (Grupo Skellefte?) porfídica de grano fino (**Foto 1-1**).
130: tonalita GI porfídica de grano medio, fracturación N150E/55N.

7 de agosto de 2003, Stop 131-135:
131: contacto neto intrusivo entre gabros/dioritas y basaltos, orientación N90E/80S. Al sur del contacto están los basaltos porfídicos con foliación N140E/76SW. Muestra del basalto JO03-75.
132: contacto intrusivo de diorita sobre basaltos, la diorita contiene fragmentos (1-50 cm) de los basaltos porfídicos. Muestra del gabro/diorita JO03-76.
133: conjunto de afloramientos donde aparecen diorita y basaltos porfídicos pero no se encuentra la zona de contacto, pero el contacto continua aproximadamente en orientación E-W.
134-135: afloramientos de diorita/gabro, muestra JO03-77.

9 de agosto de 2003, Stop 136-140:
136: zona sur de monzonita de Gallejaur. Monzonita de grano medio con plagioclasa, anfíbol y biotita, y poco contenido en feldespato alcalino y cuarzo. Muestra JO03-85.
137-138: ídem a Stop 136, presencia de enclaves microgranulares de grano muy fino.
139: zona central de monzonita de Gallejaur. Abundantes enclaves microgranulares (10-15 % de la roca). Texturas de simplectita. Muestra JO03-86.
140: ídem a Stop 139, zonas con menor contenido de enclaves.

17 de agosto de 2003, Stop 155-156:
155: bloque desplazado de monzonita con enclaves.
156: monzonita de Gallejaur de grano medio. Muestra JO03-91.

18 de agosto de 2003, Stop 157-163:
157: subida a los afloramientos de monte Vithatten desde la falda noreste. Basalto porfídico con escasos fenocristales (< 5 %) de grano medio. Muestra JO03-92.
158-159: ídem a Stop 157.
160: basalto porfídico brechificado (autobrecha) con 10-15 % de clastos 1-10 cm (**Foto 1-2**).
161: ídem a Stop157.
162: basalto porfídico con mayor contenido en fenocristales de feldespato y piroxeno que muestras anteriores y de tamaño de grano grueso. Muestra JO03-93.
163: Vithatten, basalto porfídico con fenocristales de piroxeno. Muestra JO03-94.

19 de agosto de 2003, Stop 164-167:
164: monzonita de grano medio a fino en ladera de Bredträskliden. Textura de simplectita, no se observan enclaves. Muestra JO03-95.
165: gabro textura ofítica de grano medio, zonas con moderada alteración. Bandeado mineralógico de plagioclasa y piroxeno. Dique de monzonita N70E/52N.
166: gabro moderadamente alterado y basaltos porfídicos hacia la zona sur de afloramientos, venas félsicas. Gabro de grano medio y fino, foliación E-W.
167: basalto porfídico, posible falla N80E?. Al norte de la falla están los gabros y al sur los basaltos. Muestras JO03-98 (basalto porfídico), JO03-99 (gabro).

22 de agosto de 2003, Stop 175:
175: basaltos porfídicos de Grupo Vargfors. Muestra JO03-103. Sobre este basalto de Vargfors aparecen conglomerados de GI (Grupo Vargfors) e ignimbrita datada en 1875±4 Ma (Billström and Weihed, 1996).

24 de agosto de 2003, Stop 185-188:
185: zona de Stop 167. Basalto porfídico con fenocristales de plagioclasa y feldespato de grano medio. Contacto con gabro según N50E similar Stop 166. Muestra JO03-111

186: basaltos porfídicos muy alterados con venas similares a monzonita de Gallejaur.
187: basaltos porfídicos con fluidos similares a monzonita, intensa foliación N75E/75N.
188: basaltos porfídicos con alto contenido de fenocristales. Muestra JO03-112.

Nr. 1: Gallejaur

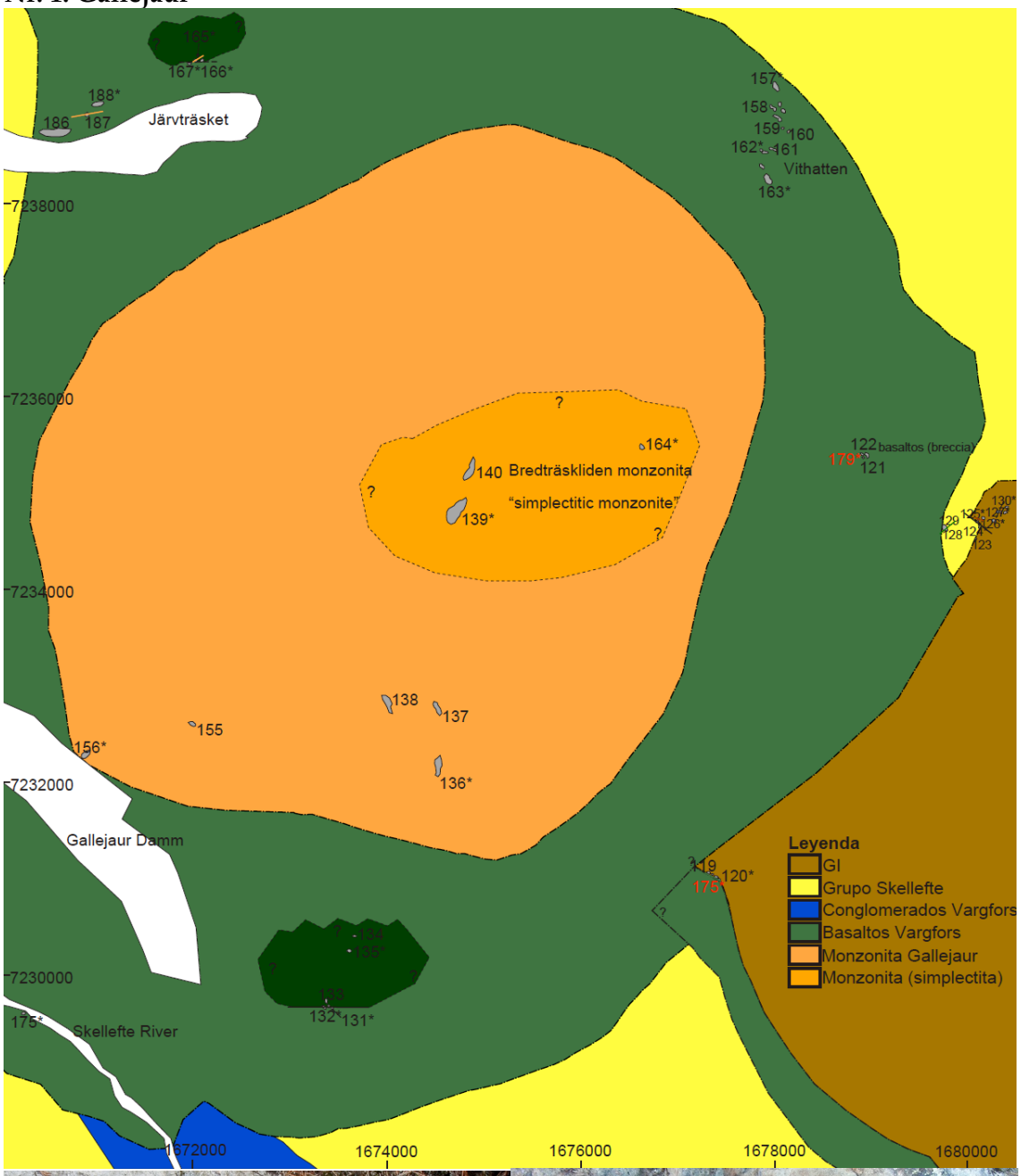



Foto 1-1: tonalita GI intruye sobre volcánica félsica.



Foto 1-2: (auto?) brecha de basalto porfídico.

Nr. 2: Zona de Jörn

19 de julio de 2003; Stop 55:
55: granodiorita tipo GIIa? Con fenocristales de plagioclasa y cuarzo de tamaño de grano medio, diques máficos con orientaciones N30-50E.

25 de julio de 2003; Stop 84:
84: granodiorita inequigranular de tamaño de grano medio con plagioclasa, cuarzo ahumado, feldespato alcalino, anfíbol y biotita. Muestra JO04-57.

8 de agosto de 2003; Stop 5H-6H.
5H: inmediaciones del contacto sur de JGC. Muestra de tonalita de GI porfídica con fenocristales de cuarzo azulado de tamaño de grano medio con matriz de cuarzo, plagioclasa y biotita. Muestra JO03-83.
6H: tonalita de GI inequigranular con cuarzo y plagioclasa de tamaño de grano medioa a grueso.

23 de agosto de 2003; Stop 177.
177: gabronorita de tamaño de grano medio a fino con fenocristales de piroxeno. Muestra JO04-105.

26 de julio de 2004; Stop 133-138.
133: ídem a Stop 5H de 2003. Muestra JO04-78.
134: tonalita GI porfídica con fenocristales de cuarzo de tamaño de grano medio y matriz de qz, pl y bi de grano fino. Muestra JO04-79.
135: dique? (no se observan bordes) de GII sobre la tonalita GI. Granodiorita de tamaño de grano medio a fino. Muestra JO04-80.
136-138: tonalita GI inequigranular de tamaño de grano grueso con pl, qz y bi. Muestra JO04-81.

28 de julio de 2004; Stop 147-149.
147: tonalita GI inequigranular de tamaño de grano medio a grueso compuesto por pl, qz y bi. Muestra JO04-84.
148: tonalita GI inequigranular de tamaño de grano medio a grueso compuesto por pl, qz y bi. Muestra JO04-85.
149: tonalita GI inequigranular de tamaño de grano medio a grueso compuesto por pl, qz y bi. Muestra JO04-86.

8 de agosto de 2004; Stop 225.
225: (ídem a Stop 55 de 2003) granodiorita de tamaño de grano medio.
Muestra JO04-122.

18 de agosto de 2004; Stop 231-232.
231: granodiorita porfídica con fenocristales de anfíbol y plagioclasa, matriz de qz, pl, kfs, amph y bi de tamaño de grano fino. Contiene enclaves microgranudos de grano fino. Muestra JO04-128 y Gq-128.
232: tonalita GI inequigranular de tamaño de grano medio compuesto por pl, qz y bi. Muestra JO04-129.

22 de agosto de 2004; Stop 264-266.
264: gabronorita de tamaño de grano medio. Muestra JO04-148.
265: ídem a Stop 177 en 2003.
266: gabronorita de tamaño de grano fino. Muestra JO04-149.

Nr. 2: Zona de Jörn

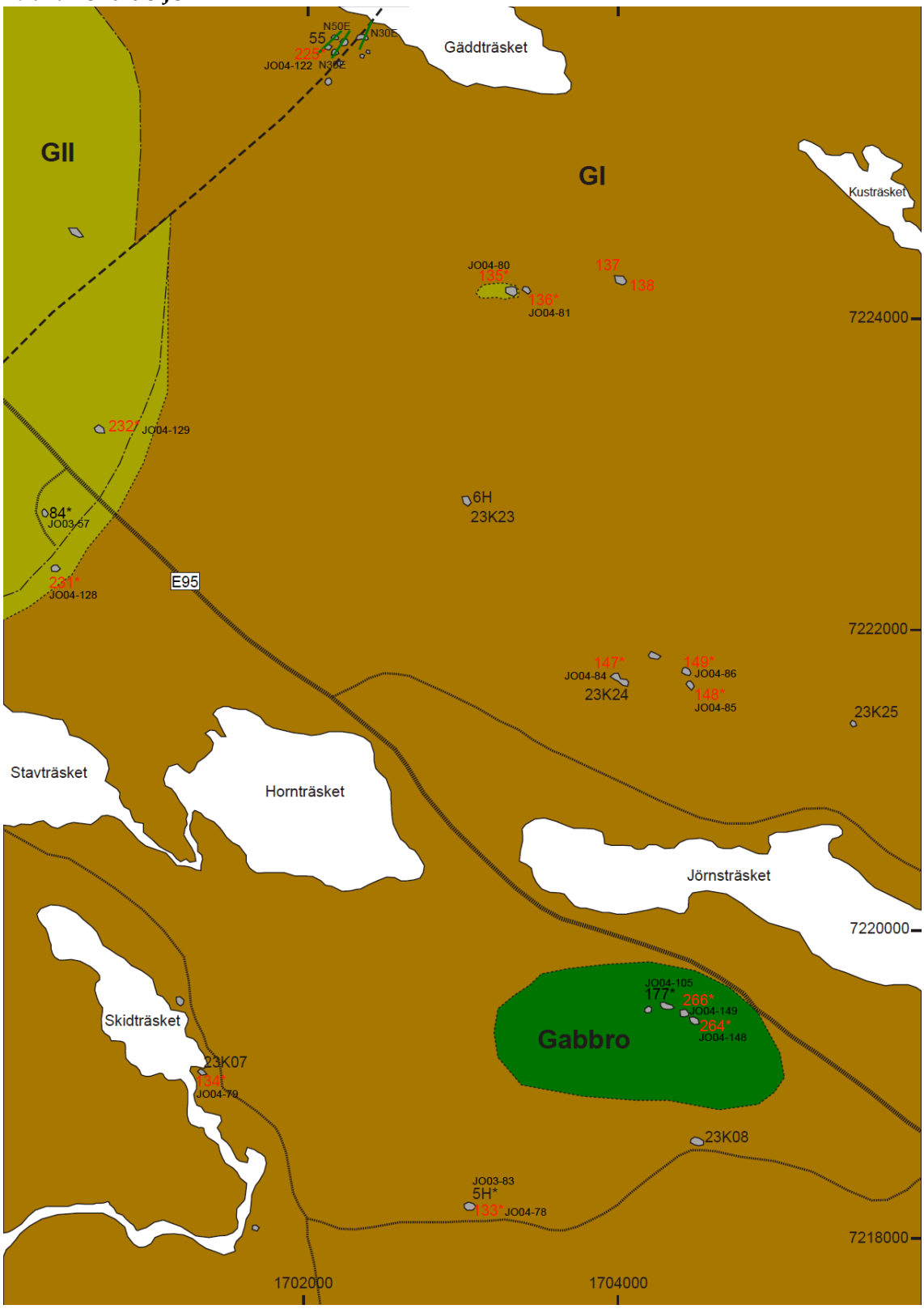

Nr. 3: Zona Este.

25 de agosto de 2003, Stop 189-197.
189: tonalita GI porfídica con fenoristales de plagioclasa idiomorfos de tamaño de grano medio, matriz de cuarzo, plagioclasa y biotita (bi reemplaza amph). Muestra JO03-113.
192-194: gabronorita hornbléndica-piroxenítica de tamaño de grano medio. Muestra JO03-114.
195: cuarzo diorita de tamaño de grano medio a fino. Muestra JO03-115.
196: gabronorita, muestra JO03-116
197: gabronorita hornbléndica-piroxenítica con anfíboles poiquilíticos de tamaño de grano grueso.

28 de julio de 2004, Stop 150-152.
150: tonalita de GI porfídica con fenocristales de plagioclasa y cuarzo de tamaño de grano medio, cizalla frágil N-S.
151: tonalita de GI porfídica con fenocristales de cuarzo de tamaño de grano fino con matriz muy fina, apariencia de dacita subvolcánica. Muestra JO04-87.
152: tonalita GI equigranular con plagioclasa, cuarzo y biotita de tamaño de grano medio. Muestra JO04-88 y Gq-88.

8 de agosto de 2004, Stop 222.
222: tonalita de GI de tamaño de grano medio con cuarzo, plagioclasa y biotita hipidiomorfos. Muestra JO04-120 y Gq-120.

Nr. 3: Zona E de JGC

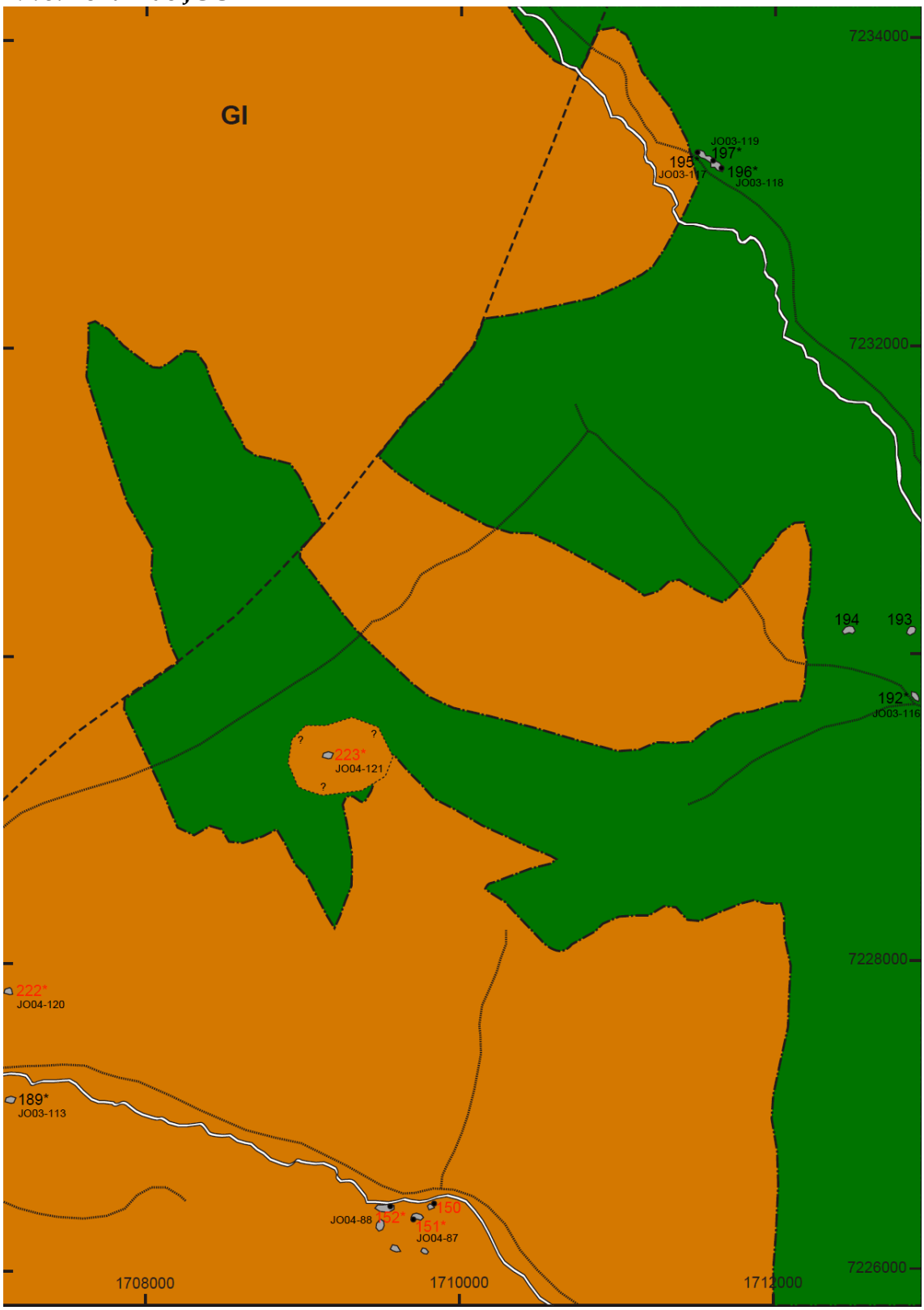

Nr. 4: Zona ENE

22 de julio de 2003, Stop 67-70.
67: granito de GIII porfídico con fenocristales de plagioclasa y cuarzo de tamaño de grano grueso y matriz de pl, qz, kfs y bi de tamaño de grano medio a fino. Cuarzo azulado
68: ídem a Stop 67. Muestra JO03-45.
70: ídem a Stop 67 con variaciones a tamaño de grano medio de fencristales y fino de matriz. Muestra JO03-46.

27 de julio de 2004, Stop 139-143.
139: granito de GIII porfídico con fenocristales de plagioclasa y cuarzo de tamaño de grano grueso. Zonas con cizalla N145E/80SE. Muestra JO04-82.
140-142: serie de afloramientos de granito de GIII ídem a Stop 139.
143: granodiorita de GIIa. Muestra de JO04-83 y Gq-83.

Muestreo de Boliden Mineral por U. Svenson en 1976.
23K53: cuarzo monzodiorita de GIIb.
23K61: granito de GIII.
23K62: granito de GIII.
23K63: cuarzo monzodiorita de GIIb.
23K64: cuarzo monzodiorita de GIIb.
23K74: granito de GIII.
23K76: cuarzo monzodiorita de GIIb.
23K77: cuarzo monzodiorita de GIIb.

Nr. 4: Zona ENE de JGC

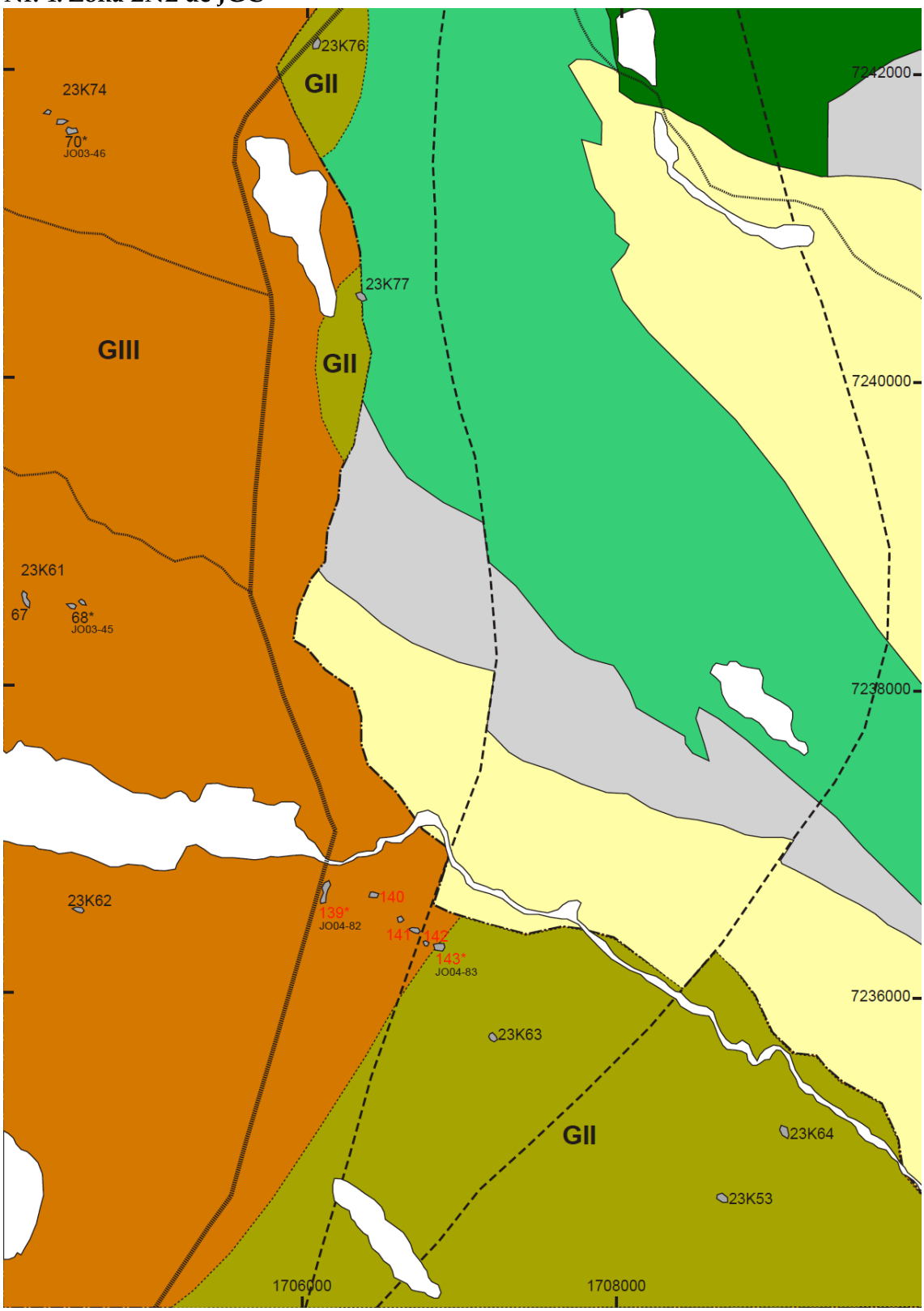

Nr. 5: Contacto GI-GII-GIII

18 de julio de 2003; Stop 42-50:
42: revisar!!. Tonalita de GI porfídica con fenocristales de cuarzo y plagioclasa de tamaño de grano medio y matriz de grano medio a fino de pl, qz y bi. Muestra JO03-36.
43: granodiorita de GIIa inequigranular porfídica con fenocristales de plagioclasa y cuarzo de tamaño de grano medio con matriz de amph, qz, pl y bi. La roca está intruida por dique máfico porfídico con orientación N110E. Muestra JO03-37.
44: ídem a Stop 42.
45: afloramiento con contacto entre las muestras de GIIa y GIIb con enclaves microgranulares. Zona central con granodiorita con fenocristales de cuarzo y plagioclasa de grano medio. Al oeste contacto con cuarzo monzodiorita de GIIb con enclaves microgranulares, contacto orientado N-S (**Foto 5-1**). La cuarzo monzodiorita contiene fragmentos de GIIa y de muestra máfica. En el extremo este del afloramiento está dique máfico porfídico con fenocristales de plagioclasa y piroxeno orientado N40E/84SE, el dique presenta borde frío con la granodiorita de la zona central (**Foto 5-2**). Muestra JO03-38
46-48: tonalita de GI porfídico con fenocristales de cuarzo y plagioclasa de tamaño de grano medio con numerosos diques máficos (< 1 m ancho) con orientaciones N40E. Muestras JO04-39 y -40.
49: dique sin intrusivo porfídico (aspecto de dacita) con fenocristales de cuarzo xenomorfo y plagioclasa subidiomorfa de tamaño de grano medio con matriz microcristalina de qz, pl, bi y amph de tamaño de grano fino. Posible muestra de GII intruyendo a GI?. Muestra JO03-41.
50: ídem a Stop 42 (GI).

19 de julio de 2003; Stop 51-55:
51: ídem a Stop 42.
52: continuación de dique de GII de Stop 49. Muestra JO03-42.
53: ídem a Stop 42.
54: ídem a Stop 42.
55: granodiorita tipo GIIa? Con numerosos diques máficos con orientaciones N30-50E.

21 de julio de 2003; Stop 56-64:
56: tonalita de GI en las inmediaciones del contacto con GIII, multitud de venas y bandeado mineralógico aparecen en estos afloramientos. Diques máficos porfídicos con fenocristales de plagioclasa y anfíbol de tamaño de grano medio abundan en la zona (similar a muestras de GIIb). Muestra JO03-43.
57: granito de GIII porfídico con fenocristales de cuarzo y plagioclasa de tamaño de grano grueso y matriz de kfs, qz, pl y bi; zona muy meteorizada. Muestra JO03-44.
58-64: afloramientos de GIII ídem a Stop 57.



Foto 5-1: detalle de enclaves microgranulares.



Foto 5-2: detalle de dique máfico en granodiorita.

Nr. 5: GI-GII-GIII

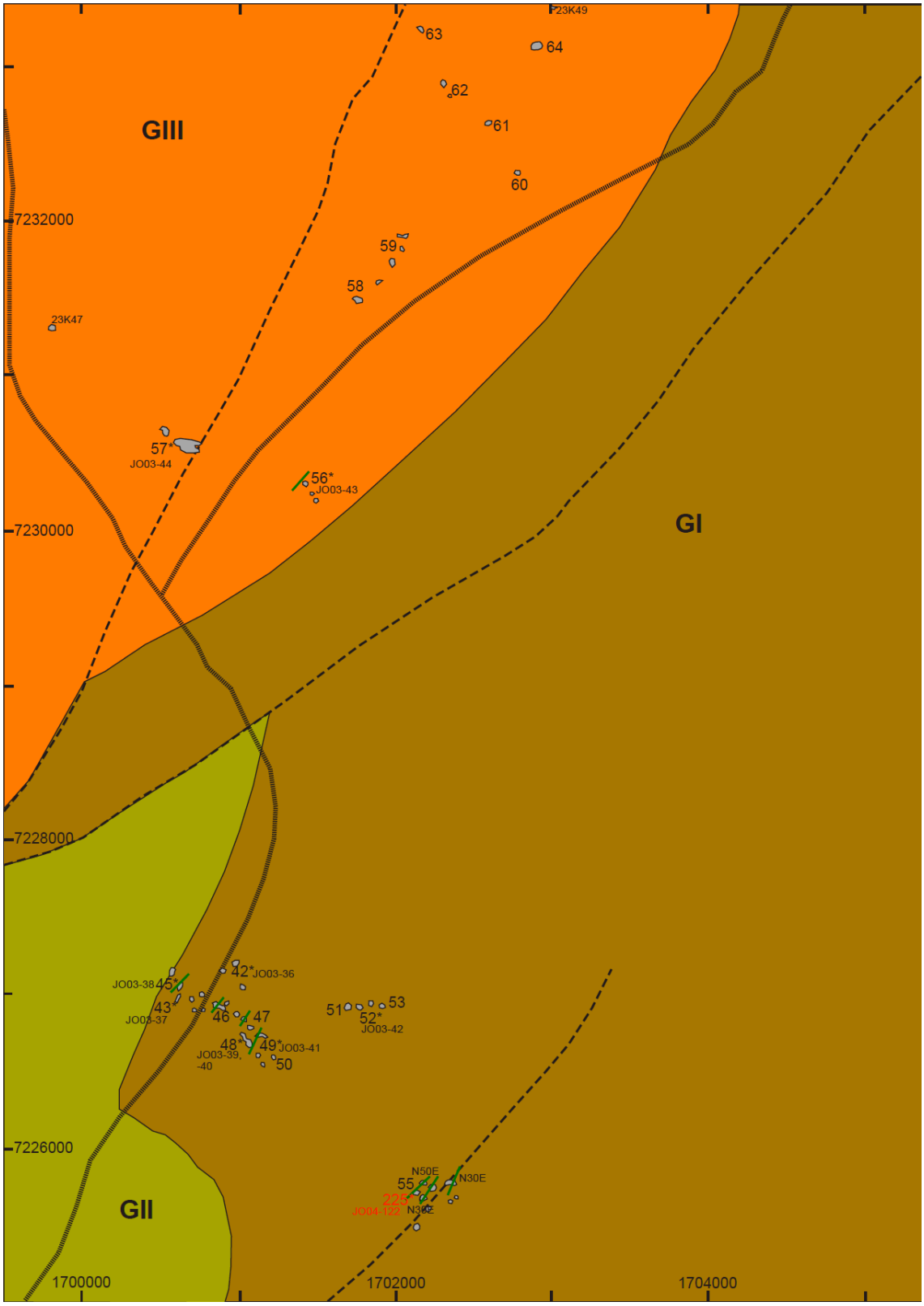

Nr. 6: Zona norte de JGC y Näsberget (cuatro partes):

24 de julio de 2003, Stop 71-78:
71: muestra de gabronorita de grano medio (0.5-2 mm) con textura subofítica con pl, opx, cpx y óxidos. Los minerales máficos están moderadamente alterados, la plagioclasa se conserva inalterada. Zona cruzada por numerosas venas y diques félsicos (feldespato fundamentalmente) con orientación N40E. Muestra JO03-47.
72: gabronorita de grano medio ídem a JO03-47. Diques máficos orientados N50E/80SE similares a aquellos presentes en los granitoides (**Foto 6-1**). Muestra JO03-48.
73: gabronoritas con fenocristales de cpx de tamaño de grano grueso con texturas poiquilíticas. Muestra JO03-49.
74: gabronorita ídem a Stop 71 con presencia de diques máficos N50E y cizalla con venas félsicas N140E.
75: ídem a Stop 72 con varios diques máficos N50E.
76: gabronorita a leucogabronorita de tamaño de grano grueso y textura subofítica.
77: gabronorita olivínica de tamaño de grano grueso y textura ofítica. Muestra JO03-50.
78: gabronorita de tamaño de grano medio a fino con cristales poiquilíticos de cpx. Muestra JO03-51.

2 de agosto de 2003, Stop 109-114:
109: granodiorita GII hipidiomorfa inequigranular de tamaño de grano grueso en el rio Byske. Diques máficos con orientación N40E85SE. Muestra JO03-68.
110-111: ídem a Stop 109, presencia de enclaves microgranudos (geometría redondeada) de 5-30 cm.
112: gabronorita olivínica con clastos de granitoide (tonalita tipo GI?). lineación mineral en N120E con la presencia de posible falla destral con misma orientación
113-114: gabronoritas con variaciones en textura desde diorita de grano medio-fino a gabros con cpx poiquilítico de tamaño de grano grueso. Presencia de venas y diques félsicos (pegmatíticos) orientación N-S, además de pórfido de cuarzo y plagioclasa con foliación N120E. (cerca del borde con granitoides).

3 de julio de 2004, Stop 1-5:
1: ídem a Stop 109 en 2003, granitoide GII. Muestra JO04-01.
2: ídem a Stop 112 en 2003, muestra de canto de tonalita en el gabro olivínico. Muestra JO04-02.
3: gabro olivínico de tamaño de grano medio con microenclaves, zona de contacto con granitoides?. Muestra JO04-03 y Gq-03.
4: gabronorita con pirrotina de tamaño de grano medio. Muestra JO04-04.
5: gabronorita de tamaño de grano medio a fino en contacto con diorita/gabro porfídicos.

7 de julio de 2004, Stop 7-22:
7: subfase de Hobergsliden; muestra de granito hipidiomorfa inequigranular de tamaño de grano medio, ligera deformación frágil con lineaciones en N20E.
8: ídem a anterior sin deformar, color rosado en muestra de mano. Muestra JO04-07 y Gq-07.
9: dique de diorita (bloque?) en granito de Hobergsliden. Muestra JO04-08.
10: afloramiento diorita (bloque?) en granito de Hobergsliden. Muestra JO04-09.
11-12: afloramientos de granitos tipo Hobergsliden vs. GIII de tamaño de grano medio. Muestra JO04-10.
13: granitos de feldespato alcalino de tamaño de grano medio, muy pobres en biotita. Muestra JO04-11.
14-15: muestra de granitoide (granodiorita GII?) de grano medio a fino con dique máfico porfídico con fenocristales de anfíbol y plagioclasa de tamaño de grano medio a fino y enclaves microgranulares (ambos lados de puente carretera sobre río Ålsån). Probablemente relacionado con la generación de GIIb. Muestra JO04-12.
16: ídem a Stop 15 2004.

Nr. 6a:

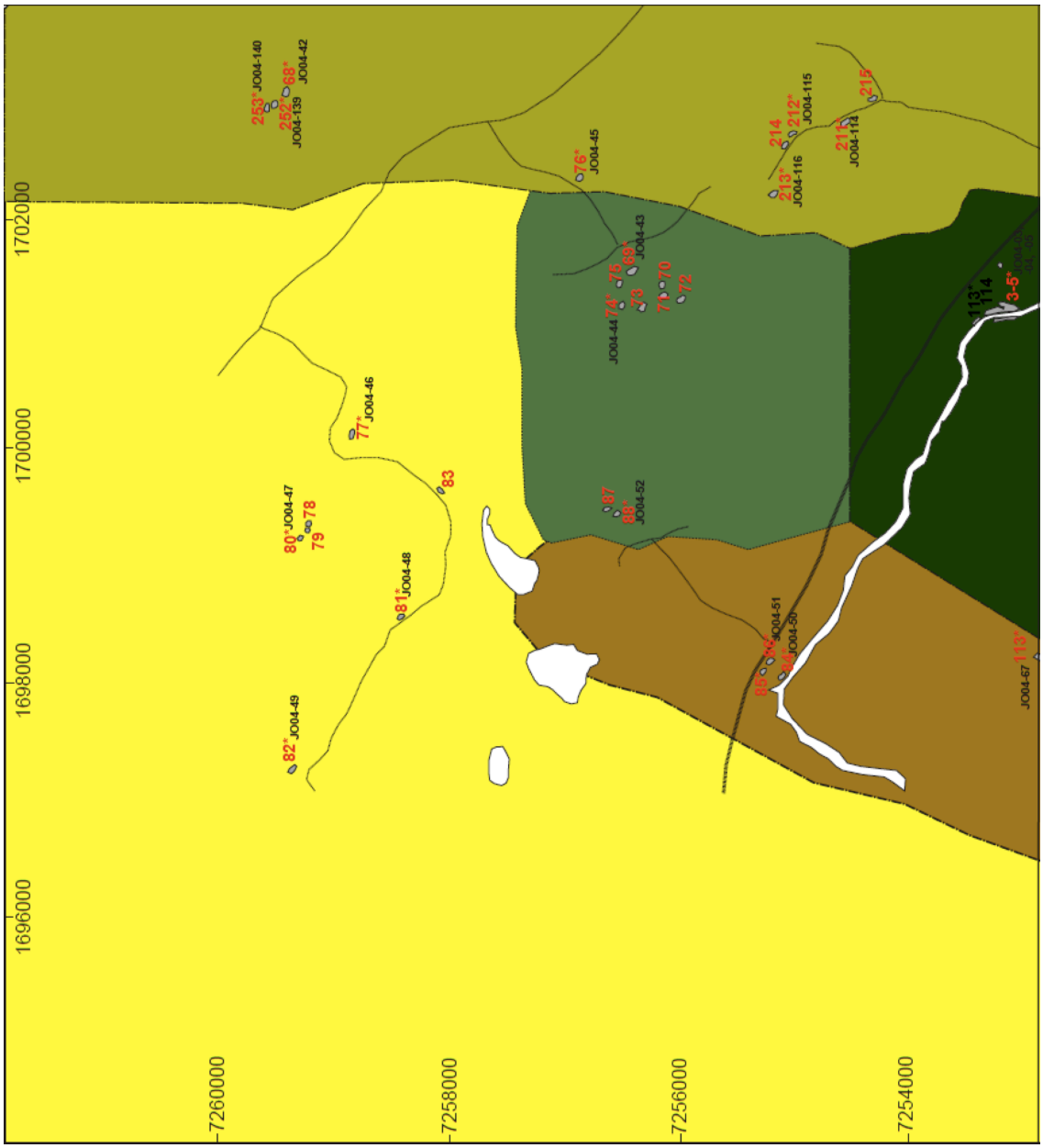



Foto 6-1: detalle de dique básico sobre gabro.

17: serie de afloramientos de granitoides tipo granodiorita de GII de grano medio asociados a numerosos diques máficos.
18: máfica porfídica de grano medio a fino similar a Stop 14 de 2004. Probable dique.
19: muestra de granodiorita de GII con textura hipidiomorfa equigranular de tamaño de grano medio. Muestra JO04-13.
20: muestra de máfica porfídica intrusiva sobre granodiorita de tamaño de grano medio tipo GII. Parece dique sin intrusivo con la muestra de granitoide GIIb. Muestra JO04-14.
21: granodiorita GIIa inequigranular con kfs porfídico de tamaño de grano medio a grueso, qz+pl+kfs+bi. Muestra JO04-15.
22: granodiorita GIIa inequigranular de tamaño de grano medio a grueso (pl, qz, kfs, bi).

8 de julio de 2004, Stop 23-34:
23: granitoide tipo GIIb de tamaño de grano medio a fino, continuación de los afloramientos Stop 15 y 22 de 2004.
24: en las inmediaciones de la anterior Stop 23 se encuentra granitoide (posiblemente GIIa sin anfíbol). Varios diques máficos porfídicos con orientación N20E.
25-27: ídem a Stop 24, granitoide de grano medio a fino. Varios diques máficos.
28: granodiorita de tamaño de grano medio tipo GIIa (sin anfíbol), presencia de diques máficos (30 cm ancho) con orientación N60E/65NW. Muestra JO04-16.
29: granitoide rico en feldespato alcalino (posiblemente Hobergsliden) con numerosos diques máficos de grano fino. Muestra JO04-17.
30: ídem a Stop 29, muestras de Hobergsliden.
31: zona límite entre gabro de Näsberg con GII. Gabronorita con variaciones texturales de gabro ofítico de grano medio a fino, presencia de diques sin-intrusivos de gabro.
32: ídem a Stop 31 pero con predominancia de las fases de grano fino sobre las de grano medio, estas rocas se corresponden con dique de GIIb. Muestra JO04-18.
33: bandas de granodioritas de GIIa atraviesan al gabro. Muestra JO04-19.
34: muestra de cuarzo monzodioritas tipo GIIb que se generan sobre el gabro de Näsberg (megabloque o fundido diferenciado desde gabro?). Muestra JO04-20.

9 de julio de 2004, Stop 35-41:
35-37: (antiguo puente sobre río Byske) granodioritas de GIIa de tamaño de grano medio con ligera alteración de las plagioclasas, muestra de GIIa JO04-21a. Varios diques máficos porfídicos de tamaño de grano medio a fino (15 m anchura), muestra de dique JO04-21b.
38-39: (nuevo puente sobre río Byske) diorita a cuarzo diorita con fenocristales de plagioclasa y anfíbol de grano medio y matriz de pl y qz, posee enclaves, diques microgranulares y una zona con gran abundancia de ambas, lo que sugiere posible mezcla de fundidos. La roca es similar a GIIb pero con ausencia de kfs y zonas con textura gráfica de feldespato con cuarzo y ligera alteración de la plagioclasa. Muestra JO04-22. Ambas rocas muestran bordes lobulados (ambas fundidas) y similitudes mineralógicas (**Foto 6-2**).
40: zona de contacto entre GIIa y GIII. Al margen norte de río Ålsån aparece GII (W) en contacto con GIII (E) separados por zona de cizalla dominada por dique máfico. En el margen sur de río Ålsån GIII (W) entra en contacto con dique máfico con orientación N35E/70SE. GIII presenta zonas dominadas por simplectita de qz y feldespato (**Foto 6-3**). Muestra JO04-23 y Gq-23 (GIIa).
41: afloramiento de tonalita de GI como posible megabloque de GI dentro de las muestras de GIIa?. Muestra JO04-24.

10 de julio de 2004, Stop 42-51:
42-46: serie de afloramientos de granodioritas a tonalitas-granodioritas de grano medio a fino (GIIa?) con enclaves microgranulares porfídicos (GIIb). Los enclaves no se observan en todas las localizaciones y son relativamente poco abundantes. Muestras JO04-25 y JO04-26.

Nr. 6b:

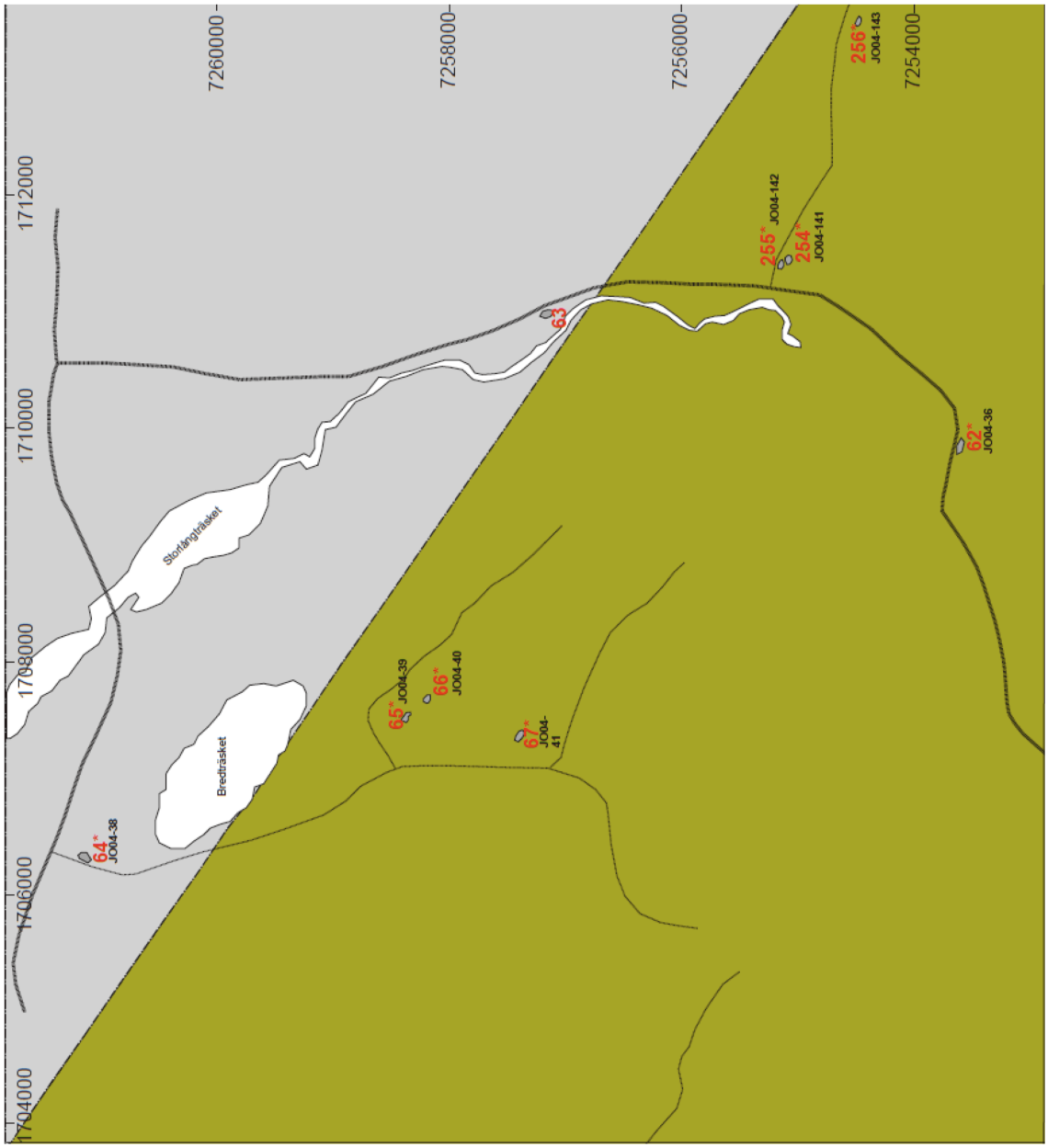



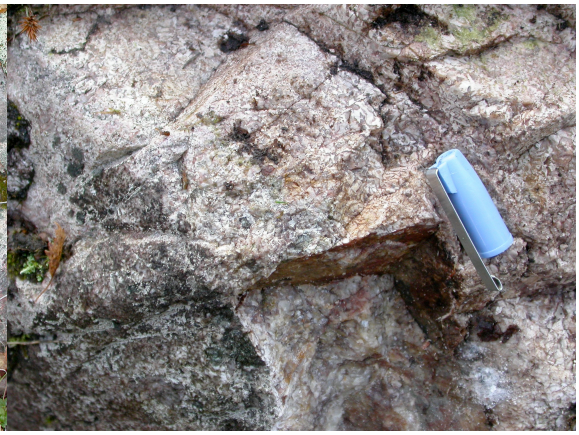

Foto 6-2: detalle de GIIb con gabro (borde lobulado). **Foto 6-3:** detalle de simplectita en GIII.

47-49: serie de afloramientos similares a Stop 42-46. Leuco granodioritas porfídicas con fenocristales de plagioclasa de tamaño de grano medio y matriz de pl, qz, kfs y bi de tamaño de grano fino, posible GIIa (similar a fases de borde de GII). Muestra JO04-27.
50: GIIb, cuarzo monzodiorita porfídica con fenocristales de anfíbol (anterior cpx) de grano medio a fino. Muestra JO04-28.
51: ídem a Stop 42-46 y Stop 47-49, granodiorita posible GIIa. Muestra JO04-29.

11 de julio de 2004, Stop 52-59:
52: leuco granodiorita porfídica con fenocristales de plagioclasa de tamaño de grano medio, GIIa. Muestra JO04-30.
53: leuco granodiorita con variaciones de porfídica a equigranular de tamaño de grano medio (qz, pl, kfs y bi). Muestra JO03-31.
54: ídem a muestras Stop 52 y 53.
55-56: leuco granodiorita (facies de borde de GIIa en borde noreste de JGC) brechificando rocas máficas porfídicas en posición casi *in situ* (encaje de fragmentos).
57: ídem a Stop 55-56 con presencia de fluidos y venas de granitoides.
58-59: leuco granodiorita ídem a Stop 55-57 de tamaño de grano medio a grueso sin presencia de rocas máficas. Muestras JO04-32 y JO04-33.

13 de julio de 2004, Stop 60-61:
60: GIIb, cuarzo monzodiorita porfídica con fenocristales de clinopiroxeno de tamaño de grano medio, matriz de kfs, pl, qz, bi y amph. Muestra JO04-34 y Gq-34.
61: GIIb, cuarzo monzodiorita porfídica con fenocristales de clinopiroxeno de tamaño de grano medio, matriz de kfs, pl, qz, bi y amph de grano fino. JO04-35.

14 de julio de 2004, Stop 62-67:
62: gabronorita de tamaño de grano medio (pl, opx, cpx, bi, opq y algo de cuarzo), similar a algunas zonas de Näsberg. Muestra JO04-36.
63: metasedimentos cerca del borde GII-sedimentos en el extremo noreste de JGC. Muestra JO04-37.
64: gabronorita en el extremo norte de JGC, zona exterior. Muestra JO04-38.
65-67: grupo de afloramientos de granodiorita de GIIa al norte de JGC. muestras JO04-39, -40, -41 y Gq-40.

15 de julio de 2004, Stop 68-76:
68: GIIa, granodiorita de grano medio. Muestra JO04-42.
69-75: basalto porfídico con fenocristales de plagioclasa y piroxeno de tamaño de grano medio y matriz afanítica. Muestras JO04-43 y -44.
76: dos tipos de granodioritas. GIIa inequigranular de tamaño de grano grueso, muestra JO04-45a. Granodiorita GIIa de tamaño de grano medio a fino ídem a facies de borde de GIIa, muestra JO04-45b.

16 de julio de 2004, Stop 77-89:
77-80: muestras de riolitas a dacitas del Grupo Arvidsjaur con fenocristales xenomorfos de cuarzo y alguna plagioclasa de tamaño de grano grueso con matriz afanítica. Esferulitos en matriz y carbonatos dispersos. Muestras JO04-46 y -47.
81-83: dacita porfídica moderadamente deformada con fenocristales hipidiomorfos de plagioclasa de tamaño de grano medio y matriz afanítica. Intensa alteración a carbonatos de la matriz y fenocristales. Muestras JO04-48 y -49.
84: afloramiento de roca máfica porfídica en contacto con tonalita de GI intensamente alterada. Muestra JO04-50.
85: GI, tonalita con fenocristales de cuarzo y feldespato de tamaño de grano medio intensamente alterada. Diques máficos (1 m ancho) con orientación N45E.
86: tonalita GI con fenocristales de cuarzo y feldespato de tamaño de grano medio intensamente alterada. Muestra JO04-51 y Gq-51.
87-89: basalto porfídico con fenocristales de pl y px de tamaño de grano medio y matriz afanítica. Muestra JO04-52.

Nr. 6c:

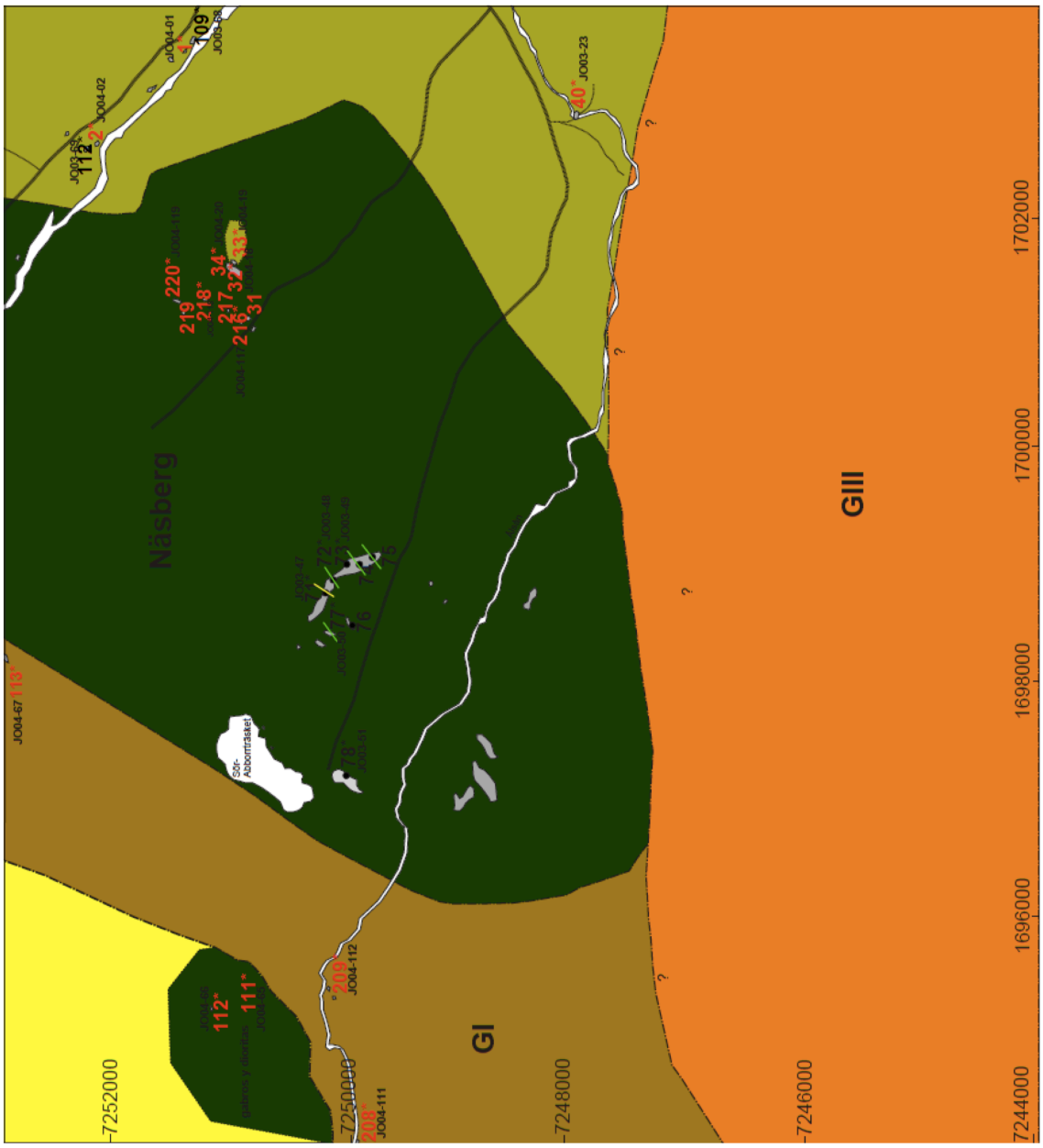
Näsberg
GI
GIII
7252000
7250000
7248000
7246000
7244000
1696000
1698000
1700000
1702000
J004-67
J004-112
J004-111
J003-23

21 de julio de 2004, Stop 111-112:
111-112: gabronoritas con texturas ofíticas con fenocritales de plagioclasa de tamaño de grano medio. Muestras JO04-65 y -66.
113: tonalita GI. Muestra JO04-67 y Gq-67.

5 de agosto de 2004, Stop 208-209:
208-209: tonalitas porfídicas con fenocristales de cuarzo similares a las facies de GI de borde en Stop 205 de 2004. Muestras JO04-111, JO04-112 y Gq-112.

7 de agosto de 2004, Stop 210-220:
210: granodiorita de GIIa cercana a borde con gabro de Näsberg. Foliación con orientación N130E/75SW, muestra JO04-113.
211: granodioritas tipo GIIa de tamaño de grano medio. Muestra JO04-114.
212: gabro de grano medio, muestra JO04-115 y Gq-115.
213-215: ídem a Stop 211. Muestra JO04-116.
216-217: gabro piroxenítico similar a muestra 23K95. Muestra JO04117.
218-220: afloramientos de muestra GIIa de tamaño de grano medio con presencia de diques máficos N30E. Muestras JO04-118 y -119.

20 de agosto de 2004, Stop 248-253:
248: misma que Stop 42.
249: misma que Stop 47. Muestras JO04-138 y Gq-138.
250: misma que Stop 60. Gq-34
251: misma que Stop 66, mustra Gq-40.
252: cuarzo monzodiorita de tamaño de grano medio a fino de GIIb. Muestra JO04-139 y Gq-139.
253: ídem a Stop 252, zona con intensa alteración. Muestra JO04-140.

21 de agosto de 2004, Stop 254-258:
254: metasedimentos plegados contenidos en el interior de GII en la zona norte, probable constituya megabloque. Líneas de charnela inclinadas 60º hacia N175E. Muestra JO04-141.
255: metasedimentos deformados como megabloque en GII. Muestra JO04-142.
256: granodiorita GIIa hipidiomorfa inequigranular con pl, qz, kfs, bi y amph. Muestra JO04-143.
257: equivale a Stop 41, muestra Gq-24a.
258: equivale a Stop 86, muestra Gq-51

Nr. 6d:

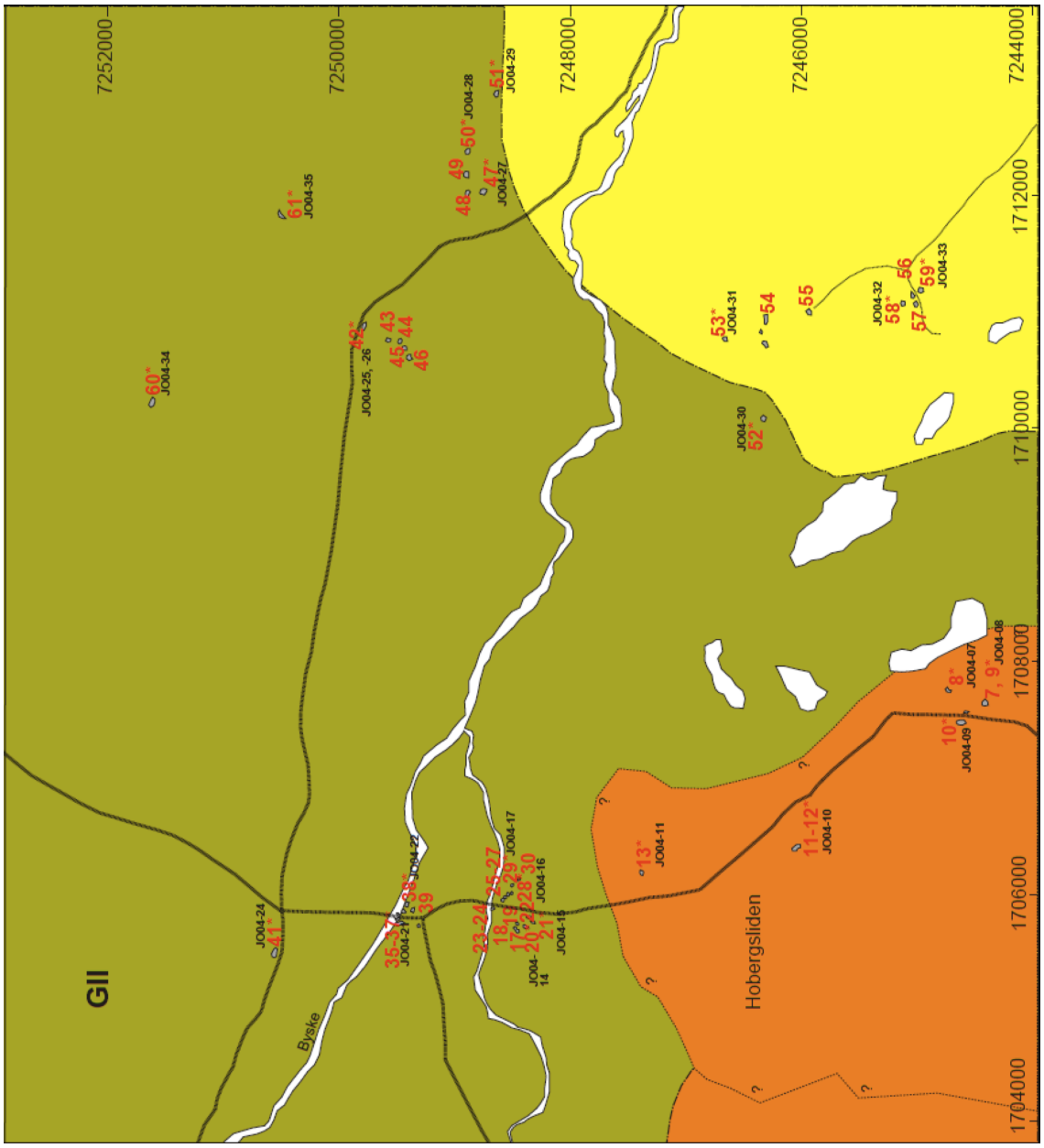
7252000
7250000
7248000
7246000
7244000
1712000
1710000
1708000
1706000
1704000
GII
Hobergsliden
Byske
JO04-24
JO04-25, -26
JO04-27
JO04-28
JO04-29
JO04-30
JO04-31
JO04-32
JO04-33
JO04-34
JO04-35
JO04-07
JO04-08
JO04-09
JO04-10
JO04-11
JO04-15
JO04-16
JO04-17
41*
42*
43
44
45
46
47*
48
49
50*
51*
52*
53*
54
55
56
57
58*
59*
60*
61*
7, 9*
8*
10*
11-12*
13*
18
19
20
21
22
23-24
25-27
28
29
30
35-37
38*
39

Nr. 7: Ullbergsträsket:

29 de julio de 2003, Stop 91-99:
91: cima del Järpkullen. Tonalita GI textura hipidiomorfa equigranular de grano medio (qz, pl, amph y bi) con variaciones a porfídica con fenocristales de qz de tamaño de grano grueso y matriz de grano medio con amph, bi y pl. Matriz con algún feldespato alcalino probablemente secundario. Muestra JO03-59.
92: variación porfídica de tonalita de GI con fenocristales de cuarzo de tamaño de grano medio y matriz de grano fino (similar a dacita). Muestra JO03-60.
93: tonalita GI textura hipidiomorfa equigranular de grano medio (qz, pl, amph y bi), presencia de kfs secundario?. Dique máfico orientación N50E, anchura métrica. Muestra JO03-61.
94: tonalita GI textura hipidiomorfa equigranular de grano medio (qz, pl, amph y bi). Numerosos diques máficos N50E de anchura inferior a 50 cm.
95: probable monzonita hipidiomorfa inequigranular de grano fino (color rosado en muestra de mano) similar a las muestras de monzonita de la zona central de Gallejaur. Texturas de simplectita como en las muestras JO03-86 y -95. Probable dique N100E de unos 30-40 m de anchura aunque no se observan los bordes. Muestra JO03-62.
96: ídem a Stop 92.
97: tonalita GI hipidiomorfa equigranular de tamaño de grano medio. Numerosos diques similares a dacita sobre tonalita GI.
98: tonalita de GI hipidiomorfa inequigranular de tamaño de grano medio. Dique de dacita? porfídico con fenocristales de qz y pl y matriz afanítica de tamaño de grano muy fino, orientación N100E. Muestra de dique JO03-63.
99: tonalita de GI hipidiomorfa inequigranular (variación a porfídica) de tamaño de grano medio. Dique félsico (dacita-riolita) similar a muestra JO03-63 con orientación N90E/70S.

1 de agosto de 2003, Stop 107-108:
107-108: afloramientos de GI hipidiomorfa inequigranular de grano medio porfídica con fenocristales de qz de tamaño de grano grueso y matriz de grano medio con amph, bi y pl (ídem a Stop 91).

21 de julio de 2004, Stop 107-108:
107: tonalita tipo GI hipidiomorfa inequigranular de grano medio, zonas de la roca muestran textura poligonal de cristales (metamorfismo). Muestra JO04-62.
108: granodiorita a granito hipidiomorfa porfídica de grano grueso con fenocristales de qz y kfs, matriz de qz, pl y poca bi de tamaño de grano medio. Afloramiento afectado por meteorización. Muestra JO04-63.

5 de agosto de 2004, Stop 107-108:
205: tonalita de GI (?). roca hipidiomorfa porfídica con fenocristales de qz de tamaño de grano medio y matriz de qz+pl de tamaño de grano medio a fino. Posible facies de borde de GI. Muestra JO04-108.
206: cima de Järpkullen (ídem a Stop 91 de 2003). Muestra JO04-109 y Gq-109 para geoquímica.
207: villa de Högbrännas, tonalita de GI hipidiomorfa inequigranular de tamaño de grano medio con qz, pl y bi. Muestra JO04-110.

Nr. 7: Ullbergträsket

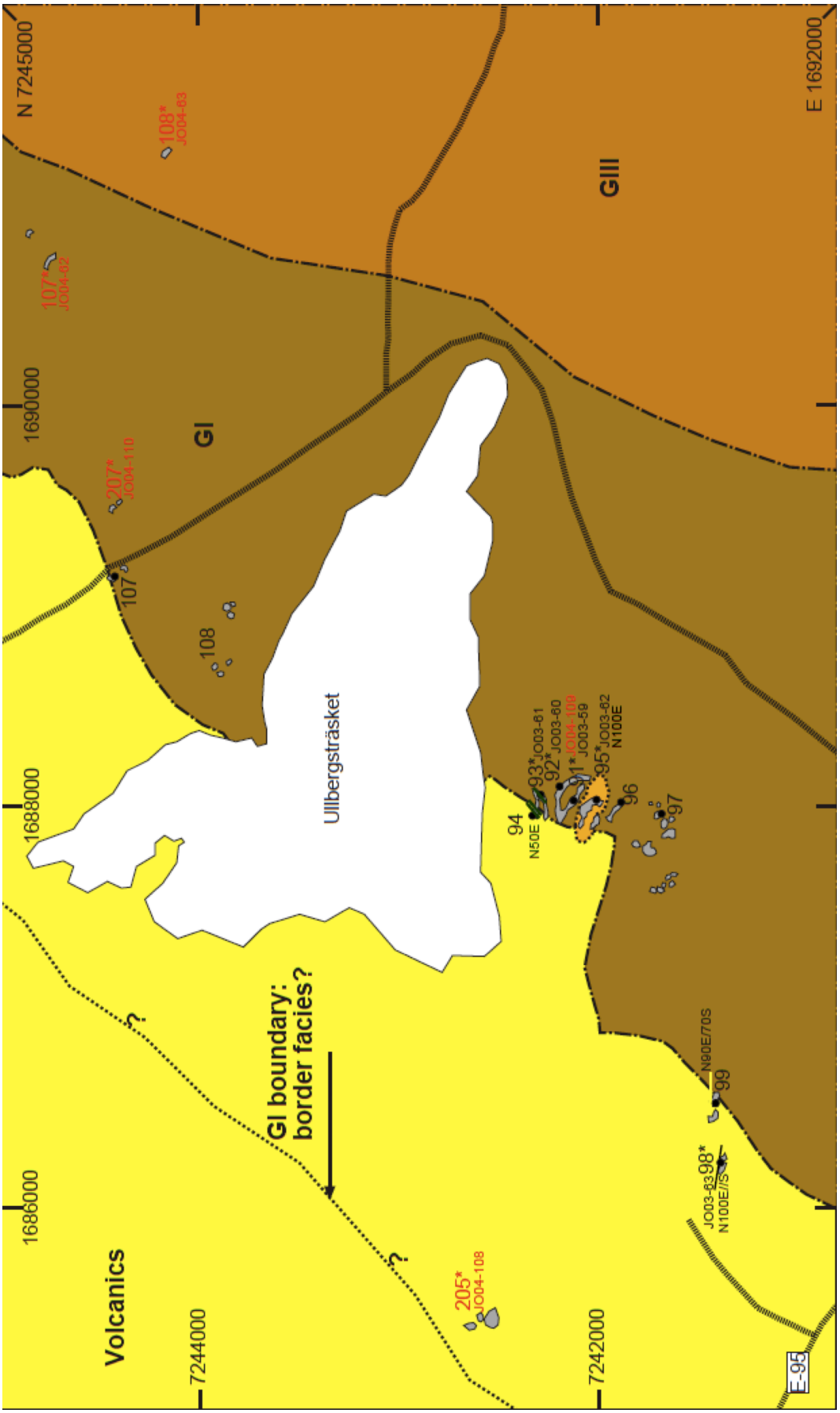

Nr. 8: Dique Sur

6 de julio de 2003; Stop 1-5:
1: basalto porfídico con fenocristales de piroxeno (pocos de plagioclasa) de tamaño de grano medio y matriz afanítica. Foliación intensa con orientación N110E. Muestras JO03-01: zona foliada; JO03-02: zona masiva con fragmento y JO03-03: zona con mayor contenido de fenocristales.
2: ídem a Stop 1, zona con menos deformación.
3: tonalita fragmentada por fluidos máficos, textura de fragmentos en jigsaw-fit. Muestra JO03-04.
4: metabasita rica en anfíbol, posible superficie de falla. Muestra JO03-05.
5: tonalita de GI con fenocristales de cuarzo de tamaño de grano medio a grueso y matríz rica en qz, pl y bi de grano fino. Muestra JO03-06.

7 de julio de 2003; Stop 6-11:
6: basalto equivalente a Stop 1 con numerosos fragmentos monomícticos del mismo basalto porfídico, posibles autoclastos?. Clastos milimétricos a 20 cm de media, generalmente angulosos. Estos fragmentos poseen la misma variedad textural que se observa en los basaltos (porfídicos, afaníticos y acumulados de fenocristales).
7: ídem a Stop 6. Muestra de fragmento de basalto porfídico JO03-07.
8: tramo masivo de los basaltos al este de afloramiento y zona con fragmentos al oeste. Clastos de basalto superior a 50 cm. Muestra JO03-08.
9: basalto porfídico intensamente deformado, foliación con orientación N110E. Muestra JO03-09.
10: tonalita de GI inequigranular hipidiomorfa con plagioclasa, cuarzo y poca biotita de tamaño de grano medio. Muestra JO03-10.
11: leuco tonalita de GI de grano medio. Muestra JO03-11.

8 de julio de 2003; Stop 12-16:
12: basalto porfídico masivo con fenocristales de piroxeno y plagioclasa de tamaño de grano medio y matriz afanítica. JO03-12.
13: ídem a Stop 12 con deformación, foliación N115E/76NE.
14: tonalita GI con fenocristales de plagioclasa y cuarzo de tamaño de grano medio y matriz de cuarzo, plagioclasa y biotita de grano fino. Muestra JO03-12.
15: ídem a Stop 12 y 13.
16: tonalita de GI inequigranular hipidiomorfa de tamaño de grano medio con cuarzo, plagioclasa y biotita. Muestra JO03-13.

11 de julio de 2003; Stop 25-29:
25: tonalita de GI porfídica con fenocristales de cuarzo de tamaño de grano medio a grueso y matriz con pl, qz y bi de tamaño de grano medio. Muestra JO03-18.
26: dolerita con plagioclasa y minerales máficos intensamente alterados, poco cuarzo. Muestra JO03-19 y -20.
27: roca compuesta por fragmentos de tonalita GI y basaltos porfídicos con matriz de basalto. Posible roca de falla o zona de contacto entre dique sur (basalto) con tonalitas de GI. Muestra JO03-21 de fragmento de basalto porfídico con fenocristales de plagioclasa y piroxeno (**Foto 8-1**).
28: basalto porfídico masivo. Muestra JO03-22.
29: dolerita de tamaño de grano medio con pl y px. Muestra JO03-23.

1 de agosto de 2003; Stop 104:
104: afloramiento de tonalita de GI porfídico con fenocristales de cuarzo de tamaño de grano medio. En la zona sur de afloramiento la tonalita es intruida por basalto porfídico (ídem a basalto porfídico masivo de anteriores Stop), los fragmentos de GI están *in situ* (**Foto 8-2**).



Foto 8-1 (izq): posible roca de falla polimíctica con fragmentos de GI, basaltos porfídicos y bandeados.
Foto 8-2 (dcha): textura jigsaw de fragmentos de tonalita intruidos por basalto porfídico.

Nr. 8: Contacto dique sur

